U.S. Geological Survey Office of Groundwater
U.S. Geological Survey National Water-Quality Assessment Program

Prepared in cooperation with the Bureau of Reclamation

Geophysics- and Geochemistry-Based Assessment of the Geochemical Characteristics and Groundwater-Flow System of the U.S. Part of the Mesilla Basin/Conejos-Médanos Aquifer System in Doña Ana County, New Mexico, and El Paso County, Texas, 2010–12

Scientific Investigations Report 2017–5028

U.S. Department of the Interior
U.S. Geological Survey

Front cover.

Background, Sun setting on the Mesilla Valley in the Mesilla Basin study area in Doña Ana County, New Mexico, and El Paso County, Texas, November 2010.

Upper left photograph, U.S. Geological Survey scientist making a water-level measurement in the Mesilla Basin study area in Doña Ana County, New Mexico, and El Paso County, Texas, November 2010.

Middle photographs, U.S. Geological Survey scientists collecting and processing water-quality samples in the Mesilla Basin study area in Doña Ana County, New Mexico, and El Paso County, Texas, November 2010.

Lower right photograph, U.S. Geological Survey scientist making field notes, Mesilla Basin study area in Doña Ana County, New Mexico, and El Paso County, Texas, November 2010.

Back cover.

Background, Ruins of an abandoned homestead in the Mesilla Basin study area in Doña Ana County, New Mexico, and El Paso County, Texas, November 2010.

Geophysics- and Geochemistry-Based Assessment of the Geochemical Characteristics and Groundwater-Flow System of the U.S. Part of the Mesilla Basin/Conejos-Médanos Aquifer System in Doña Ana County, New Mexico, and El Paso County, Texas, 2010–12

By Andrew P. Teeple

U.S. Geological Survey Office of Groundwater
U.S. Geological Survey National Water-Quality Assessment Program

Prepared in cooperation with the Bureau of Reclamation

Scientific Investigations Report 2017–5028

U.S. Department of the Interior
U.S. Geological Survey

U.S. Department of the Interior
RYAN ZINKE, Secretary

U.S. Geological Survey
William H. Werkheiser, Acting Director

U.S. Geological Survey, Reston, Virginia: 2017

For more information on the USGS—the Federal source for science about the Earth, its natural and living resources, natural hazards, and the environment—visit https://www.usgs.gov or call 1–888–ASK–USGS.

For an overview of USGS information products, including maps, imagery, and publications, visit https://store.usgs.gov.

Any use of trade, firm, or product names is for descriptive purposes only and does not imply endorsement by the U.S. Government.

Although this information product, for the most part, is in the public domain, it also may contain copyrighted materials as noted in the text. Permission to reproduce copyrighted items must be secured from the copyright owner.

Suggested citation:
Teeple, A.P., 2017, Geophysics- and geochemistry-based assessment of the geochemical characteristics and groundwater-flow system of the U.S. part of the Mesilla Basin/Conejos-Médanos aquifer system in Doña Ana County, New Mexico, and El Paso County, Texas, 2010–12: U.S. Geological Survey Scientific Investigations Report 2017–5028, 183 p., https://doi.org/10.3133/sir20175028.

ISSN 2328-0328 (online)

Contents

Abstract 1
Introduction 3
Previous Investigations 6
Purpose and Scope 9
Description of the Study Area 9
Geologic Setting 14
Hydrogeologic Setting 17
Geophysics 18
Airborne Geophysical Resistivity Methods 18
Direct-Current Resistivity 21
Time-Domain Electromagnetic Surveys 22
Geophysical Integration 23
Comparison of Geophysical Results to Historical Dissolved-Solids Concentrations 29
Geochemistry 36
Sample Collection and Analysis 36
Field Procedures 36
Analytical Methods 38
Environmental Tracer Methods 38
Hydrogen and Oxygen Isotopic Ratios 38
Strontium-87 39
Tritium 39
Carbon-14 40
Quality-Assurance and Quality-Control Procedures 40
Equipment and Field Blanks 41
Sequential-Replicate Analyses 41
Matrix Spikes 42
Geochemical Characteristics 43
Physicochemical Properties 43
Major-Ion Chemistry 45
Anions 45
Chloride 46
Sulfate 47
Bicarbonate 48
Fluoride 48
Bromide 50
Nitrate Plus Nitrite 50
Cations 52
Sodium 52
Calcium 52
Magnesium 53
Silica 53
Potassium 55
Ammonia 55

Water Types 56
Trace-Element Chemistry 59
Isotopes 64
Hydrogen-2/Hydrogen-1 (Deuterium) and Oxygen-18/Oxygen-16 64
Strontium-87 67
Tritium 67
Carbon-14 69
Geochemical Groups 73
Groundwater-Flow System 76
Regional Groundwater Flow 77
Water Sources, Geochemical Evolution, and Groundwater Mixing 81
Summary 91
References Cited 97
Appendixes
1. Previously Published Data from United States Geological Survey Seepage Investigations 175
2. Methods for Constructing the Probability Plots of Groundwater Chemistry and Isotopes 182
3. Methods for Constructing the Boxplots of Groundwater Chemistry and Isotopes 183

Figures

1. Map showing location of the Mesilla Basin study area in Doña Ana County, New Mexico, and El Paso County, Texas 4
2. Chart showing geologic and hydrogeologic units of the Mesilla Basin study area in Doña Ana County, New Mexico, and El Paso County, Texas 5
3. Map showing physiography of the Mesilla Basin study area in Doña Ana County, New Mexico, and El Paso County, Texas 8
4. Map showing land cover in the Mesilla Basin study area in Doña Ana County, New Mexico, and El Paso County, Texas, 2011 11
5. Map showing surface water features and seepage measurement stations of the Mesilla Basin study area in Doña Ana County, New Mexico, and El Paso County, Texas 12
6. Graphs showing discharge of the Rio Grande between 1950 and 2011 at International Boundary and Water Commission streamflow-gaging station 08364000 Rio Grande at El Paso, Tex. 13
7. Graph showing relative median gain or loss at seepage measurement stations along the Rio Grande in the Mesilla Basin study area in Doña Ana County, New Mexico, and El Paso County, Texas, from 20 seepage investigations conducted between 1988 and 2013 14
8. Map showing generalized boundaries of subbasins and uplifts of the Mesilla Basin study area in Doña Ana County, New Mexico, and El Paso County, Texas 16
9. Map showing location of geophysical surveys in the surface geophysical subset area of the Mesilla Basin study area in Doña Ana County, New Mexico, and El Paso County, Texas, 2012 19
10. Schematic showing the helicopter frequency domain electromagnetic method 21
11. Schematic showing the direct-current resistivity method 21

12. Schematic showing the time-domain electromagnetic method 22
13. Map showing gridded resistivity values from the helicopter frequency domain electromagnetic survey data in the Mesilla Basin study area in Doña Ana County, New Mexico, and El Paso County, Texas 24
14. Three-dimensional representation of resistivity values less than or equal to 10 ohm-meters from the combined inverse modeling results of the direct-current resistivity and time-domain electromagnetic soundings in the surface geophysical subset area of the Mesilla Basin study area in Doña Ana County, New Mexico, and El Paso County, Texas https://doi.org/10.3133/sir20175028
15. Maps showing gridded resistivity values from the combined inverse modeling results of the direct-current resistivity and time-domain electromagnetic soundings at various depths below land surface in the surface geophysical subset area of the Mesilla Basin study area in Doña Ana County, New Mexico, and El Paso County, Texas 25
16. Map showing locations of wells where historical (1922–2007) dissolved-solids-concentration data were collected in the surface geophysical subset area of the Mesilla Basin study area in Doña Ana County, New Mexico, and El Paso County, Texas 30
17. Historical (1922–2007) dissolved-solids-concentration data spatially plotted with a three-dimensional representation of resistivity values less than or equal to 10 ohm-meters from the combined inverse modeling results of the direct-current resistivity and time-domain electromagnetic soundings in the surface geophysical subset area of the Mesilla Basin study area in Doña Ana County, New Mexico, and El Paso County, Texas, 2012 .....https://doi.org/10.3133/sir20175028
18. Graph showing resistivity relative to historical (1922–2007) dissolved-solids concentrations in the surface geophysical subset area of the Mesilla Basin study area in Doña Ana County, New Mexico, and El Paso, Texas 31
19. Maps showing historical dissolved-solids concentrations projected to the nearest depth of the gridded resistivity values from the combined inverse modeling results of the direct-current resistivity and time-domain electromagnetic soundings at various depths in the surface geophysical subset area of the Mesilla Basin study area in Doña Ana County, New Mexico, and El Paso County, Texas 32
20. Map showing locations of wells from which geochemical data were collected in the Mesilla Basin study area in Doña Ana County, New Mexico, and El Paso County, Texas, 2010 37
21. Probability plots showing selected constituent concentrations measured in groundwater samples collected in the Mesilla Basin study area in Doña Ana County, New Mexico, and El Paso County, Texas, 2010, grouped by hydrogeologic unit 164
22. Boxplots showing selected constituent concentrations measured in groundwater samples collected in the Mesilla Basin study area in Doña Ana County, New Mexico, and El Paso County, Texas, 2010, grouped by hydrogeologic unit 169
23. Graph showing relation between the molar concentrations of chloride and sodium measured in groundwater samples collected in the Mesilla Basin study area in Doña Ana County, New Mexico, and El Paso County, Texas, 2010 46
24. Graph showing relation between the molar concentrations of calcium and sulfate measured in groundwater samples collected in the Mesilla Basin study area in Doña Ana County, New Mexico, and El Paso County, Texas, 2010 47
25. Boxplot showing molar ratios of sulfate to chloride measured in groundwater samples collected in the Mesilla Basin study area in Doña Ana County, New Mexico, and El Paso County, Texas, 2010 48

26. Map showing spatial variations in the ratio of molar concentrations of sulfate to chloride measured in groundwater samples collected in the Mesilla Basin study area in Doña Ana County, New Mexico, and El Paso County, Texas, 2010 49
27. Map showing spatial variations in the mass ratios of chloride to bromide concentrations measured in groundwater samples collected in the Mesilla Basin study area in Doña Ana County, New Mexico, and El Paso County, Texas, 2010 51
28. Boxplot showing molar ratios of calcium to sodium measured in groundwater samples collected in the Mesilla Basin study area in Doña Ana County, New Mexico, and El Paso County, Texas, 2010 53
29. Map showing spatial variations in the molar ratios of calcium to sodium measured in groundwater samples collected in the Mesilla Basin study area in Doña Ana County, New Mexico, and El Paso County, Texas, 2010 54
30. Graph showing relation between bicarbonate and silica concentrations measured in groundwater samples collected in the Mesilla Basin study area in Doña Ana County, New Mexico, and El Paso County, Texas, 2010 55
31. Trilinear diagram showing relations between major cations and anions measured in groundwater samples collected in the Mesilla Basin study area in Doña Ana County, New Mexico, and El Paso County, Texas, 2010 56
32. Trilinear diagram showing water type based on the percent milliequivalents of major cations and anions 57
33. Map showing general spatial distribution of water types from analysis of major cations and anions measured in groundwater samples collected in the Mesilla Basin study area in Doña Ana County, New Mexico, and El Paso County, Texas, 2010 58
34. Graph showing relation between the molar concentrations of silica and aluminum measured in groundwater samples collected in the Mesilla Basin study area in Doña Ana County, New Mexico, and El Paso County, Texas, 2010 59
35. Map showing locations of wells from which groundwater samples containing relatively low silica concentrations and variable aluminum concentrations (indicated by the solid red well symbols) were collected in the Mesilla Basin study area in Doña Ana County, New Mexico, and El Paso County, Texas, 2010 60
36. Graph showing relation between arsenic concentration and temperature measured in groundwater samples collected in the Mesilla Basin study area in Doña Ana County, New Mexico, and El Paso County, Texas, 2010 61
37. Graph showing relation between iron concentration and pH measured in groundwater samples collected in the Mesilla Basin study area in Doña Ana County, New Mexico, and El Paso County, Texas, 2010 62
38. Map showing locations of wells from which groundwater samples containing relatively low pH (less than 7.8) and relatively high iron concentrations (greater than 177 micrograms per liter) were collected in the Mesilla Basin study area in Doña Ana County, New Mexico, and El Paso County, Texas, 2010 63
39. Graph showing relation between delta deuterium and delta oxygen-18 measured in groundwater samples collected in the Mesilla Basin study area in Doña Ana County, New Mexico, and El Paso County, Texas, 2010 65
40. Map showing locations of wells from which groundwater samples that plotted near the shifted global meteoric water line and the Rio Grande evaporation line were collected in the Mesilla Basin study area in Doña Ana County, New Mexico, and El Paso County, Texas, 2010 66

41. Mixing plot showing chloride and bromide ratios (mass chloride/mass bromide) and delta deuterium isotopic ratios measured in groundwater samples collected in the Mesilla Basin study area in Doña Ana County, New Mexico, and El Paso County, Texas, 2010 68
42. Graph showing relation between tritium concentration and apparent groundwater age measured in groundwater samples collected in the Mesilla Basin study area in Doña Ana County, New Mexico, and El Paso County, Texas, 2010 70
43. Graph showing relation between delta deuterium and delta oxygen-18 measured in groundwater samples and apparent groundwater ages, Mesilla Basin study area in Doña Ana County, New Mexico, and El Paso County, Texas, 2010 71
44. Map showing locations of wells from which groundwater samples with lighter stable isotopes and apparent ages of less than 10,000 carbon-14 years before 1950 and with heavier stable isotopes and apparent ages of greater than 10,000 carbon-14 years before 1950 were collected in the Mesilla Basin study area in Doña Ana County, New Mexico, and El Paso County, Texas, 2010 72
45. Map showing groundwater sampling locations categorized by geochemical groups, Mesilla Basin study area in Doña Ana County, New Mexico, and El Paso County, Texas, 2010 74
46. Map showing potentiometric surface developed from mean winter water-level altitudes (November 2010 through April 2011) measured in wells completed in the Rio Grande alluvium in the Mesilla Basin study area in Doña Ana County, New Mexico, and El Paso County, Texas 78
47. Map showing potentiometric surface developed from mean winter water-level altitudes (November 2010 through April 2011) measured in wells completed in the Santa Fe Group in the Mesilla Basin study area in Doña Ana County, New Mexico, and El Paso County, Texas 79
48. Map showing potentiometric surface and hydraulic gradient developed from mean winter water-level altitudes (November 2010 through April 2011) measured in wells completed in the Santa Fe Group, Mesilla Basin study area in Doña Ana County, New Mexico, and El Paso County, Texas 80
49. Map showing water-level-altitude differences between the Rio Grande alluvium and the Santa Fe Group developed by using the 2010–11 potentiometric-surface maps for each hydrogeologic group, locations of wells in proximity of each other, and the helicopter frequency domain electromagnetic data obtained at a depth of 50 feet along the Rio Grande in the Mesilla Basin study area in Doña Ana County, New Mexico, and El Paso County, Texas 82
50. Graphs showing water-level altitudes depicting the vertical hydraulic gradient at wells in proximity of each other in the Mesilla Basin study area in Doña Ana County, New Mexico, and El Paso County, Texas 83

Tables

1. Direct-current resistivity and time-domain electromagnetic sounding locations in the surface geophysical subset area of the Mesilla Basin study area in Doña Ana County, New Mexico, and El Paso County, Texas, October 2012 20
2. Fresh and saline water classified by dissolved-solids concentration 29
3. Wells where historical (1922–2007) dissolved-solids-concentration data were collected in the surface geophysical subset area of the Mesilla Basin study area in Doña Ana County, New Mexico, and El Paso County, Texas 106

4. Historical (1922–2007) dissolved-solids concentrations and resistivity values from the three-dimensional model of the combined inverse modeling results of the direct-current resistivity and time-domain electromagnetic soundings in the surface geophysical subset area of the Mesilla Basin study area in Doña Ana County, New Mexico, and El Paso County, Texas 112
5. Wells from which geochemical data were collected in the Mesilla Basin study area in Doña Ana County, New Mexico, and El Paso, Texas, 2010 122
6. Major-ion, nutrient, trace-element, and selected pesticide analyses for equipment-blank samples and field-blank samples collected in association with groundwater samples in the Mesilla Basin study area in Doña Ana County, New Mexico, and El Paso County, Texas, 2010 123
7. Relative percent differences between environmental and sequential-replicate samples analyzed for physicochemical properties, dissolved solids, major ions, nutrients, trace elements, and selected pesticides measured in groundwater samples collected from wells in the Mesilla Basin study area in Doña Ana County, New Mexico, and El Paso County, Texas, 2010 129
8. Concentrations of selected pesticides in unspiked and spiked environmental samples and percent recovery of selected pesticide compounds added to spiked environmental samples, Mesilla Basin study area in Doña Ana County, New Mexico, and El Paso County, Texas, 2010 134
9. Major-ion balances and saturation indexes calculated from constituent concentrations measured in groundwater samples collected in the Mesilla Basin study area in Doña Ana County, New Mexico, and El Paso County, Texas, 2010 140
10. Summary of selected physicochemical properties measured in groundwater samples collected in the Mesilla Basin study area in Doña Ana County, New Mexico, and El Paso County, Texas, 2010 142
11. Summary of water types and selected constituents measured in groundwater samples collected in the Mesilla Basin study area in Doña Ana County, New Mexico, and El Paso County, Texas, 2010 144
12. Summary of water types from the analysis of major cations and anions measured in groundwater samples collected in the Mesilla Basin study area in Doña Ana County, New Mexico, and El Paso County, Texas, 2010 148
13. Summary of isotopic results measured in groundwater samples collected in the Mesilla Basin study area in Doña Ana County, New Mexico, and El Paso County, Texas, 2010 150
14. Summary statistics for selected physicochemical properties, constituents, and isotopes measured in groundwater samples within each geochemical group determined in the Mesilla Basin study area in Doña Ana County, New Mexico, and El Paso County, Texas, 2010 152
15. Mean winter water-level altitudes (November 2010 through April 2011) used for constructing potentiometric-surface maps of the Rio Grande alluvium and Santa Fe Group hydrogeologic units in the Mesilla Basin study area in Doña Ana County, New Mexico, and El Paso County, Texas 155
16. Differences in water-level altitudes (Rio Grande alluvium minus Santa Fe Group) based on data collected between 1985 and 2012 for different well groups in the Mesilla Basin study area in Doña Ana County, New Mexico, and El Paso County, Texas 161

Conversion Factors

U.S. customary units to International System of Units

Multiply	By	To obtain
	Length	
inch (in.)	2.54	centimeter (cm)
inch (in.)	25.4	millimeter (mm)
foot (ft)	0.3048	meter (m)
mile (mi)	1.609	kilometer (km)
	Area	
square mile (mi^2)	259.0	hectare (ha)
square mile (mi^2)	2.590	square kilometer (km^2)
	Flow rate	
cubic foot per second (ft^3/s)	0.02832	cubic meter per second (m^3/s)
	Radioactivity	
picocurie per liter (pCi/L)	0.037	becquerel per liter (Bq/L)
	Specific capacity	
gallon per minute per foot [(gal/min)/ft)]	0.2070	liter per second per meter [(L/s)/m]
	Hydraulic conductivity	
foot per day (ft/d)	0.3048	meter per day (m/d)
	Transmissivity*	
foot squared per day (ft^2/d)	0.09290	meter squared per day (m^2/d)

Water-Quality Units

Chemical concentration is given in units of milligrams per liter (mg/L), micrograms per liter (µg/L), moles per liter (mol/L), millimoles per liter (mmol/L), or milliequivalents per liter. Milligrams per liter are units expressing the mass of the solute per unit volume (liter) of water; milligrams per liter is equivalent to “parts per million.” A mole is the mass in grams numerically equal to the atomic mass of a given element; concentrations in moles per liter (mol/L) were determined by dividing the concentration of a given constituent reported in milligrams per liter by the atomic weight of the constituent. Milliequivalents are units expressing the number of electron-moles of a solute per unit volume (liter).

Temperature in degrees Celsius (°C) may be converted to degrees Fahrenheit (°F) as follows:

$°F = (1.8 \times °C) + 32.$

Frequency is given in hertz (Hz) and may be converted to seconds (s) as follows:

$s = 1/Hz$

Vertical coordinate information is referenced to the North American Vertical Datum of 1988 (NAVD 88).

Horizontal coordinate information is referenced to the North American Datum of 1983 (NAD 83).

Altitude, as used in this report, refers to distance above the vertical datum.

Elevation, as used in this report, refers to uplift.

*Transmissivity: The standard unit for transmissivity is cubic foot per day per square foot times foot of aquifer thickness [(ft^3/d)/ft^2]ft. In this report, the mathematically reduced form, foot squared per day (ft^2/d), is used for convenience.

Specific conductance is given in microsiemens per centimeter at 25 degrees Celsius (µS/cm at 25 °C).

Resistivity is given in ohm-meters (ohm-m).

Tritium concentrations are discussed in tritium units (TU). Based upon a tritium half-life of 12.32 years (Lucas and Unterweger, 2000), 1 TU is equal to 3.22 picocuries per liter.

Isotope Unit Explanations

Per mil: A unit expressing the ratio of stable-isotope abundances of an element in a sample to those of a standard material. Per mil units are equivalent to parts per thousand. Stable-isotope ratios are computed as follows (Kendall and McDonnell, 1998):

$\delta X = \{(R_{sample} - R_{standard}) / R_{standard}\} \times 1{,}000$

where

- δ is the “delta” notation,
- X is the heavier stable isotope, and
- R is the ratio of the heavier, less abundant isotope to the lighter, stable isotope in a sample or standard.

The δ values for stable-isotope ratios discussed in this report are referenced to the following standard materials:

Element	R	Standard identity and reference
Hydrogen	Hydrogen-2/hydrogen-1 (δD)	Vienna Standard Mean Ocean Water (Fritz and Fontes, 1980)
Oxygen	Oxygen-18/oxygen-16 ($\delta^{18}O$)	Vienna Standard Mean Ocean Water (Fritz and Fontes, 1980)
Carbon	Carbon-13/carbon-12 ($\delta^{13}C$)	Vienna PeeDee Belemnite (Fritz and Fontes, 1980)

Geophysics- and Geochemistry-Based Assessment of the Geochemical Characteristics and Groundwater-Flow System of the U.S. Part of the Mesilla Basin/Conejos-Médanos Aquifer System in Doña Ana County, New Mexico, and El Paso County, Texas, 2010–12

By Andrew P. Teeple

Abstract

One of the largest rechargeable groundwater systems by total available volume in the Rio Grande/Río Bravo Basin (hereinafter referred to as the "Rio Grande") region of the United States and Mexico, the Mesilla Basin/Conejos-Médanos aquifer system, supplies water for irrigation as well as for cities of El Paso, Texas; Las Cruces, New Mexico; and Ciudad Juárez, Chihuahua, Mexico. The U.S. Geological Survey in cooperation with the Bureau of Reclamation assessed the groundwater resources in the Mesilla Basin and surrounding areas in Doña Ana County, N. Mex., and El Paso County, Tex., by using a combination of geophysical and geochemical methods. The study area consists of approximately 1,400 square miles in Doña Ana County, N. Mex., and 100 square miles in El Paso County, Tex. The Mesilla Basin composes most of the study area and can be divided into three parts: the Mesilla Valley, the West Mesa, and the East Bench. The Mesilla Valley is the part of the Mesilla Basin that was incised by the Rio Grande between Selden Canyon to the north and by a narrow valley (about 4 miles wide) to the southeast near El Paso, Tex., named the Paso del Norte, which is sometimes referred to in the literature as the "El Paso Narrows."

Previously published geophysical data for the study area were compiled and these data were augmented by collecting additional geophysical and geochemical data. Geophysical resistivity measurements from previously published helicopter frequency domain electromagnetic data, previously published direct-current resistivity soundings, and newly collected (2012) time-domain electromagnetic soundings were used in the study to detect spatial changes in the electrical properties of the subsurface, which reflect changes that occur within the hydrogeology. The geochemistry of the groundwater system was evaluated by analyzing groundwater samples collected in November 2010 for physicochemical properties, major ions, trace elements, nutrients, pesticides (reported but not used in the assessment), and environmental tracers. The data obtained from these samples (with the exception of the pesticide data) were used to gain insights into processes controlling the groundwater movement through the groundwater system in the study area. Results from the geophysical and geochemical assessments facilitated the interpretation of the geochemical characteristics of the groundwater sources and geochemical groups within the groundwater system.

The groundwater-flow system in the study area consists primarily of the Mesilla Basin aquifer system, which can be divided into four hydrogeologic units by using an informal classification scheme based on basin-fill stratigraphy and sedimentology with an emphasis on aquifer characteristics. The four hydrogeologic units are (1) the Rio Grande alluvium, which is the shallow aquifer of the Mesilla Basin within the confines of the Mesilla Valley, and the three hydrogeologic units that compose the Santa Fe Group: (2) the lower part of the Santa Fe Group, which is the least productive zone, (3) the middle part of the Santa Fe Group, which is the primary water-bearing hydrogeologic unit in the basin and is generally saturated, and (4) the upper part of the Santa Fe Group, which is the most productive water-bearing unit within the Santa Fe Group but is only partially saturated in the north and largely unsaturated in the south and western parts of the Mesilla Basin.

The helicopter frequency domain electromagnetic survey results indicated that approximately half of the resistivity values were less than 10 ohm-meters at depths of 50 and 100 feet with a transition where the resistivity values changed from relatively high values (greater than 20 ohm-meters) to relatively low resistivity values (less than 10 ohm-meters) near Vado, New Mexico. Slightly more than 25 percent of the gridded resistivity values from the three-dimensional grid of the combined inverse modeling results of the direct-current resistivity and time-domain electromagnetic soundings were equal to or less than 10 ohm-meters with large regions of low resistivity becoming apparent in the southernmost part of the study area near the Paso Del Norte where these low resistivity features are spatially the widest at or below the top of the

bedrock. These low resistivity values might represent clayey deposits, sediments composed largely of sand and gravel saturated with saline water, or both. Historical dissolved-solids-concentration data within the surface geophysical subset area of the study area were compiled and compared to the inverse modeling results of the combined direct-current resistivity and time-domain soundings; this comparison was done to strengthen the interpretation made from the combined inverse modeling results that the low resistivity features were representative of sand and gravel deposits saturated with saline water and not clayey deposits.

Water-level altitudes within the Rio Grande alluvium generally decreased from north to south, with a west to east decrease in water-level altitudes near Las Cruces, New Mexico, as a result of groundwater pumping. Groundwater flow within the Santa Fe Group is more complex than the groundwater flow within the Rio Grande alluvium because of the larger lateral and vertical extent of the Santa Fe Group compared to the Rio Grande alluvium. Groundwater from the Organ Mountains flows directly south towards the Paso del Norte. Groundwater from the Robledo Mountains, the Rough and Ready Hills, and the Sleeping Lady Hills generally flows to the southeast. Groundwater flowing near the north end of the midbasin uplift generally continues east towards the Rio Grande and then flows south on the east side of the midbasin uplift. Groundwater flowing near the west side of the midbasin uplift generally continues south parallel to the faults that make up the midbasin uplift and then flows east towards the Paso del Norte when it reaches the south end of the midbasin uplift. Groundwater from the Aden Hills and the East and West Potrillo Mountains flows to the south end of the midbasin uplift and then continues east towards the Paso del Norte. Throughout most of the Mesilla Valley, the vertical hydraulic gradient was downward because the water-level altitude in the Rio Grande alluvium was higher than it was in the Santa Fe Group, but in some areas (typically in the middle and southern parts of the Mesilla Valley), the vertical hydraulic gradient was substantially reduced or even reversed to an upward hydraulic gradient.

The geochemistry data indicate that there was a complex system of multiple geochemical endmembers and mixing between these endmembers with recharge to the Rio Grande alluvium and Santa Fe Group composed mostly of seepage from the Rio Grande, inflows from deeper or neighboring water systems, and mountain-front recharge. Five distinct geochemical groups were identified in the Mesilla Basin study area: (1) ancestral Rio Grande (pre-Pleistocene) geochemical group, (2) modern Rio Grande (Pleistocene to present) geochemical group, (3) mountain-front geochemical group, (4) deep groundwater upwelling geochemical group, and (5) unknown freshwater geochemical group. The ancestral Rio Grande groundwater was water that recharged into the system as seepage losses from the ancestral Rio Grande; this groundwater generally flows from north to south-southeast towards the Paso del Norte. Groundwater on the west side of the midbasin uplift generally flows south until it reaches the southern part of the study area; from the southern part of the study area, the groundwater flows east towards the Paso del Norte. Groundwater on the east side of the midbasin uplift flows south-southeast towards the Paso del Norte where it mixes with groundwater from the modern Rio Grande, uplifted areas in the west, and the deep saline source. The water type of the modern Rio Grande geochemical group ranged from calcium-sulfate water type in the northern part of the study area to sodium-chloride-sulfate water type in the southern part of the study area; from north to south there was a substantial increase in specific conductance, strontium-87/strontium-86 ratio, potassium, and the trace metals of iron and lithium, changing the water chemistry such that it became similar to the water chemistry of the deep groundwater upwelling geochemical group. From age-dating results, water in the modern Rio Grande geochemical group was recharged to the Rio Grande alluvium within the past 10 years. The mountain-front geochemical group was generally old water (apparent age was greater than 10,000 carbon-14 years before present) that was somewhat mineralized and has relatively high concentrations of fluoride and silica, which might indicate longer exposure to volcanic and siliciclastic rocks or aluminosilicate minerals. There were five different locations of recharge determined from the groundwater geochemistry within the mountain-front geochemical group, all having a slightly different geochemical signature: (1) the Rough and Ready Hills, Robledo Mountains, and the Sleeping Lady Hills, (2) the Doña Ana Mountains, (3) the Aden Hills and West Potrillo Mountains, (4) the East Potrillo Mountains, and (5) the Sierra Juárez in Mexico. The groundwater from the Rough and Ready Hills, Robledo Mountains, the Sleeping Lady Hills, and the Doña Ana Mountains generally flows toward the Rio Grande and eventually mixes together and with the modern Rio Grande groundwater. The groundwater originating from the Aden Hills and East and West Potrillo Mountains generally flows east to southeast at a slow rate and eventually mixes and continues east, where it mixes with groundwater from the ancestral Rio Grande geochemical group and with the groundwater from the Sierra Juárez. The groundwater from the Sierra Juárez flows north and then east towards the Paso del Norte where it mixes with groundwater from the uplifted areas in the west, ancestral and modern Rio Grande groundwater, and the upwelling groundwater from a deep saline source. The deep groundwater upwelling geochemical group had the highest concentrations of bicarbonate, potassium, silica, aluminum, iron, and lithium within the study area, indicating that it had been in contact with carbonate and siliciclastic rocks for a much longer period of time and at higher temperatures compared to the other geochemical groups, and was most likely ancient marine groundwater originating from the Paleozoic and Cretaceous carbonate rocks which was upwelling into the Mesilla Basin aquifer system in the southeastern part of the study area through the extensive fault systems. Direct-current resistivity and time-domain electromagnetic soundings support the interpretation of ancient marine groundwater upwelling into the Mesilla Basin

aquifer system, as do the analytical results from wells, and the helicopter frequency domain electromagnetic data collected along the Rio Grande. The hydrogen-2/hydrogen-1 ratio and oxygen-18/oxygen-16 ratio isotopic results for samples in the unknown freshwater geochemical group did not plot on the Rio Grande evaporation line, indicating this group did not have a Rio Grande signature (that is, there was no isotopic evidence of a component of Rio Grande water) and it also had the lowest mineralized content of any geochemical group in the study area.

Introduction

Developing a thorough understanding of water resources by using a comprehensive, integrated analysis of available scientific data enables water managers to make better informed decisions. A thorough understanding of water resources is especially valuable for binational waters, where managers from each country need to make informed decisions as to not violate any water treaties between the countries. The 2006 United States-Mexico Transboundary Aquifer Assessment Act (hereinafter referred to as "the act") authorized "the Secretary of the Interior to cooperate with the States on the international border with Mexico and other appropriate entities in conducting a hydrogeologic characterization, mapping, and modeling program for priority transboundary aquifers, and for other purposes" (United States-Mexico Transboundary Aquifer Assessment Act, Public Law 109–448). One objective of the act was to develop and implement a systematic process to prioritize the transboundary aquifers for further analysis. The transboundary Mesilla Basin/Conejos-Médanos aquifer system (fig. 1) was one of the priority transboundary aquifer systems identified for additional study under the act (Alley, 2013).

The U.S. part of the Mesilla Basin/Conejos-Médanos aquifer system, bisected by the Rio Grande/Río Bravo (hereinafter referred to as the "Rio Grande"), was the focus of this assessment. The hydrogeologic units of the U.S. part of the aquifer system consist of the Rio Grande alluvium and the underlying hydrogeologic units of the Santa Fe Group in and near the Mesilla Basin in Doña Ana County, New Mexico, and El Paso County, Texas (figs. 1 and 2). The Mesilla Basin aquifer system in the United States and the Conejos-Médanos aquifer system in Chihuahua, Mexico, are hydrologically one aquifer system with no natural boundaries separating them (fig. 1). Different names and management policies are among the consequences of an aquifer system bisected by the U.S.-Mexico international border. The U.S. part of the Mesilla Basin/Conejos-Médanos aquifer system is hereinafter referred to as the Mesilla Basin aquifer system.

The Mesilla Basin/Conejos-Médanos aquifer system is one of the largest rechargeable groundwater systems by total available volume in the Rio Grande Basin region of the United States and Mexico (Alley, 2013), and the aquifer system is relied on for irrigation and as a source of municipal and domestic supplies for several cities in or near the study area including the large adjoining cities of El Paso, Tex., and Ciudad Juárez, Mexico (fig. 1). The Rio Grande has been identified as a major source of recharge to the aquifer system in the form of seepage losses from the river-bed to the Rio Grande alluvium in parts of the Mesilla Valley (fig. 1) in New Mexico (Peterson and others, 1984; Crilley and others, 2013; U.S. Geological Survey, 2017). The sustainability of the aquifer system taking into account irrigation needs and increasing water demands of rapidly growing cities in or near the study area that rely extensively on groundwater is an ongoing concern. In his description of the aquifer system near El Paso, Ryder (1996) noted that annual groundwater pumping near El Paso was already exceeding annual recharge in 1985, when the population of the city was 464,000. By 2014, the population of El Paso had increased by about 50 percent compared to the population in 1985, to 679,000 (U.S. Census Bureau, 2015). The population of Ciudad Juárez, El Paso's twin city in Mexico, also increased rapidly, from about 1 million in 1995 to about 1.3 million in 2010 (Instituto Nacional de Estadística y Geografía, 2010). The third largest city in the study area, Las Cruces, N. Mex., also relies extensively on the Mesilla Basin aquifer system as a water supply (City of Las Cruces, 2016); its population in 2014 was 101,000 (U.S. Census Bureau, 2015) (fig. 1).

The "Previous Investigations" section of this report documents the long history of multiagency water-resource investigations of the hydrogeology of the Mesilla Basin aquifer system. The existence of a good knowledge base upon which to build and the need for a better understanding of the availability, use, and quality of the groundwater in the Mesilla Basin aquifer system resulted in the prioritization of the aquifer system for further evaluation (Alley, 2013). For the prioritized aquifers, the act specifies that an evaluation of all available data and publications, development or enhancement of a geographic information system (GIS) database, and an establishment of field studies (including ongoing monitoring and metering) and groundwater models need to be done in order to fully assess the aquifer. In cooperation with the Bureau of Reclamation (Reclamation), the U.S. Geological Survey (USGS) focused their contribution to this large effort on the evaluation of previously published and newly collected geophysical and groundwater geochemical data for the Mesilla Basin aquifer system (fig. 1). The work by the USGS in cooperation with Reclamation is part of a larger collaborative effort to develop high-quality, comprehensive groundwater-quantity and -quality information for the Mesilla Basin aquifer system involving scientists from Mexico through the International Boundary and Water Commission (IBWC), scientists from numerous institutes and universities including New Mexico Water Resources Research Institute, New Mexico State University, Texas AgriLife Research, Texas Water Research Institute, Texas A&M University System, and scientists from other State agencies and organizations.

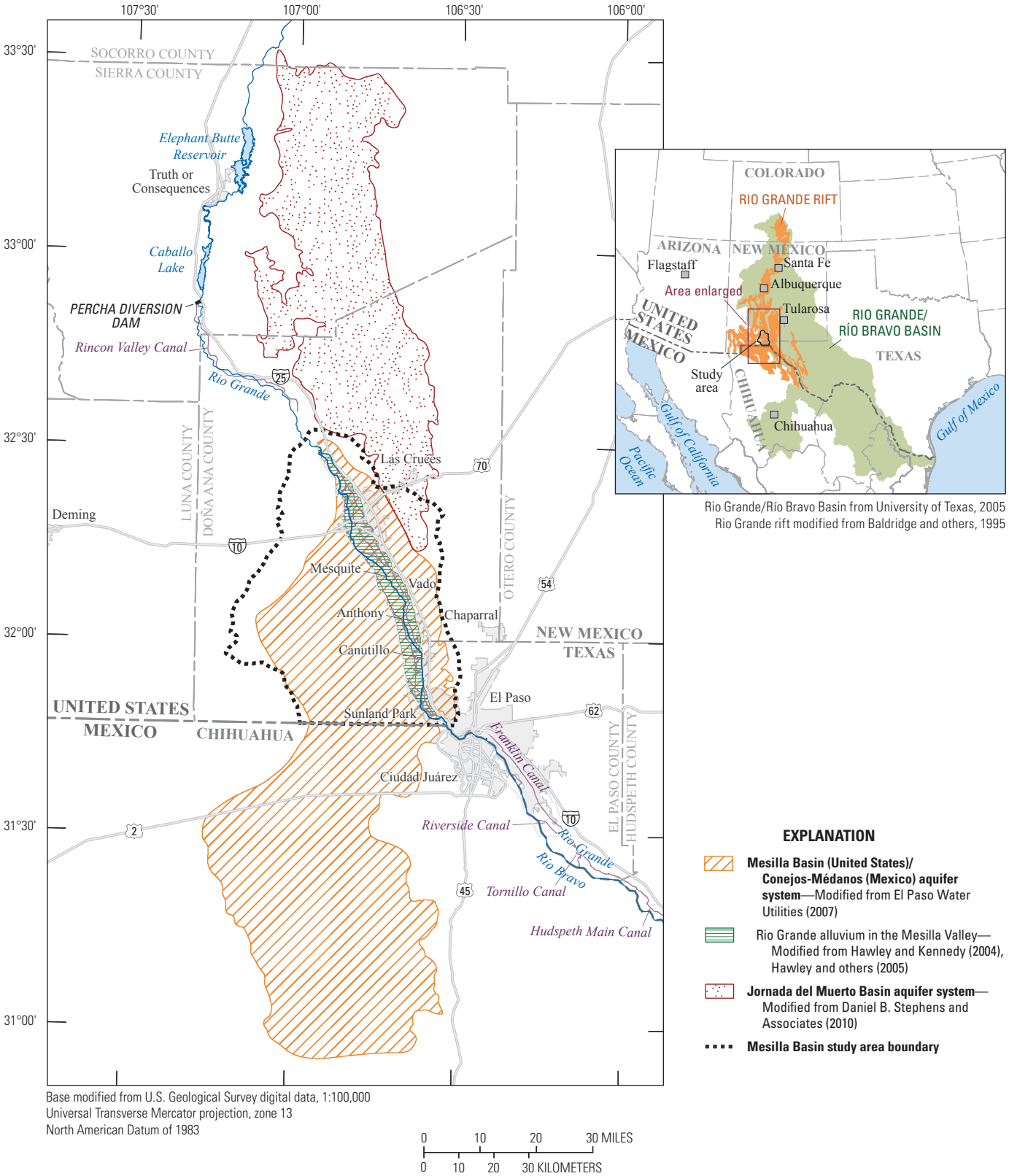

Rio Grande/Río Bravo Basin from University of Texas, 2005
Rio Grande rift modified from Baldridge and others, 1995

Figure 1. Location of the Mesilla Basin study area in Doña Ana County, New Mexico, and El Paso County, Texas.

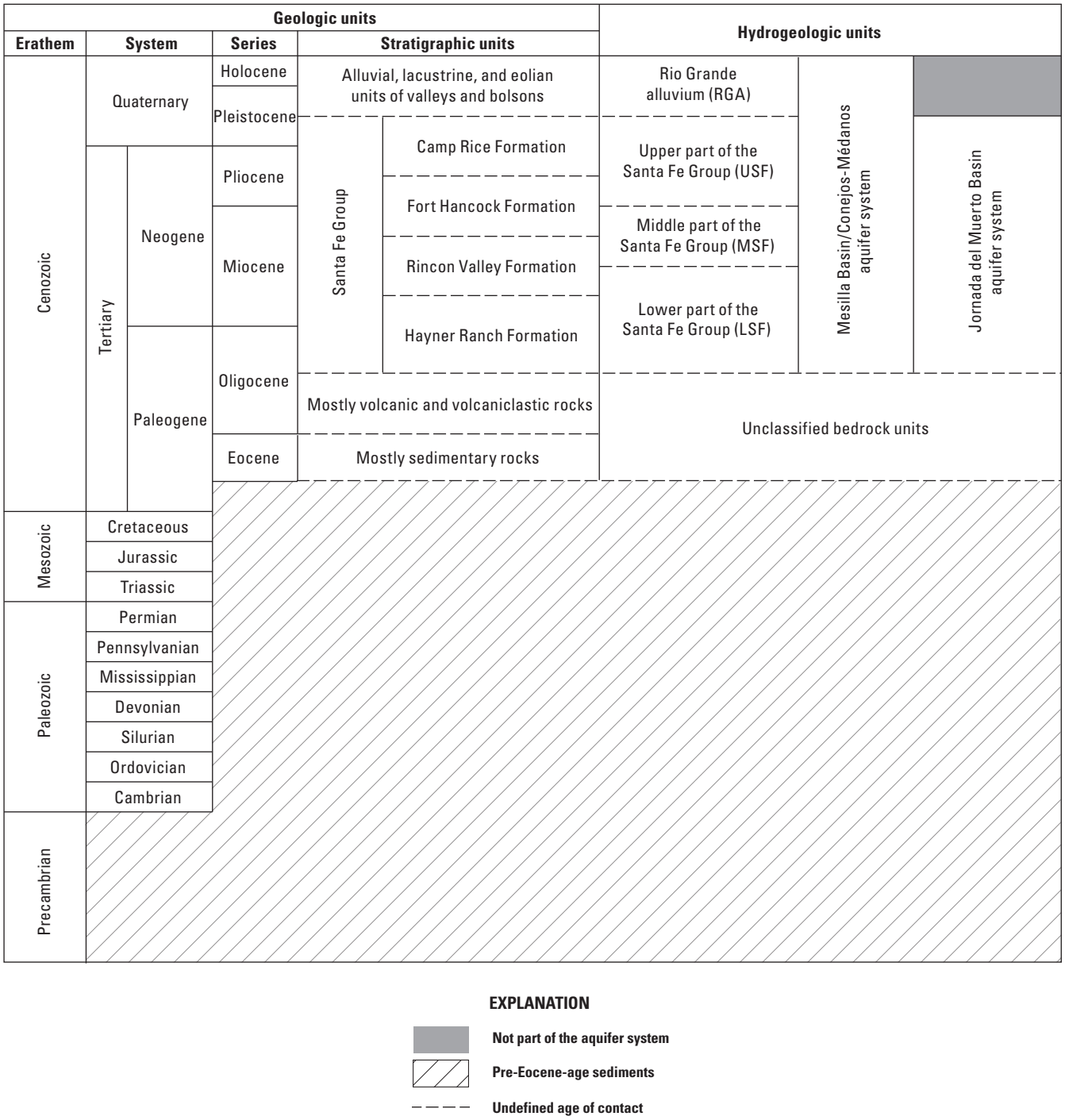

Figure 2. Geologic and hydrogeologic units of the Mesilla Basin study area in Doña Ana County, New Mexico, and El Paso County, Texas (modified from Nickerson and Myers, 1993; Hawley and Kennedy, 2004; Hawley and others, 2005).

Changes in water quality (particularly the long-term spatial and temporal increases of salinity in the Mesilla Basin aquifer system) are a concern to water managers in the United States and Mexico tasked with meeting increasing demands for potable water in and near the Mesilla Basin (Alley, 2013) (fig. 1). For more than 100 years, relatively elevated salinity values (dissolved-solids concentrations of more than 1,000 milligrams per liter [mg/L]) in the Rio Grande near the Texas-New Mexico border area have been known to exist, with salinity values increasing as the river flows downstream from Elephant Butte Reservoir, N. Mex. (Doremus and Michelsen, 2008). Use of water for irrigation, increasing urban growth, and subsequently increasing demand of potable water create additional water concerns as regulation of the potable supply increases, and the quantity and quality of the potable supply decreases because of increases in salinity within the Rio Grande and the shallow aquifer in the Rio Grande alluvium (New Mexico Environment Department, 2012). Natural sources of salinity such as upwelling of sedimentary brine and geothermal waters have been identified as major contributors to the elevated salinity concentrations in the Rio Grande near where the river exits the Mesilla Basin (fig. 1) (Doremus and Michelsen, 2008). Evaluation of the groundwater quality within the Mesilla Basin aquifer system can aid in defining the extent of available freshwater resources, identifying natural and anthropogenic sources of salinity, and determining the source and movement of groundwater.

To address groundwater-quantity and -quality concerns, as well as fulfill the requirements of the act, the USGS in cooperation with Reclamation completed a comprehensive hydrogeologic assessment of the groundwater resources within the study area (fig. 1). The collection and analysis of previously published and newly collected geophysical data were a key part of the interpretation of geochemical characteristics. Geophysical resistivity methods can be used to detect spatial changes in the electrical properties of the subsurface (Zohdy and others, 1974). The electrical properties of soil and rock are determined by water content, porosity, clay content, and conductivity (reciprocal of electrical resistivity) of the pore water (Lucius and others, 2007). Typically, the resistivity of the water, which can be affected by the type and concentration of dissolved constituents, has a large effect on the bulk resistivity of the subsurface (Teeple and others, 2009). Electrical changes detected within the subsurface also reflect changes that occur within the hydrogeology. Geophysical methods (which are relatively non-invasive) are therefore valuable for interpreting hydrogeologic characteristics in areas between wells where typically little to no information is available. The geophysical resistivity data assessed for this report included (1) helicopter frequency domain electromagnetic (HFEM), (2) direct-current (DC) resistivity, and (3) time-domain electromagnetic (TDEM). All of the HFEM data and DC resistivity soundings were compiled from previously published surveys (Cain, 2002; Dunbar and others, 2004; Zohdy and others, 1976; Al-Garni, 1996), whereas TDEM soundings were collected by the USGS in October 2012 (Teeple, 2017). In November 2010, the USGS collected groundwater samples from 44 wells and analyzed them for major ions, trace elements, nutrients, and environmental tracers, to better understand the geochemical processes controlling the groundwater movement through the Mesilla Basin aquifer system. Pesticides were also analyzed in the samples collected in November 2010; the results of these analyses are included but are not discussed in this report.

Previous Investigations

Geophysical studies of subsurface resistivity have been completed within the Mesilla Basin to provide information about the condition of the levees along the Rio Grande (Cain, 2002; Dunbar and others, 2004); these studies and others (Zohdy and others, 1976; Al-Garni, 1996) provide information about the subsurface in the southern part of the Mesilla Valley in New Mexico (fig. 1). Airborne geophysical resistivity methods produce high-quality vertical resolution of the resistive properties of the subsurface over extensive horizontal profiles. The application of airborne geophysical resistivity methods in this report is similar to other applications where airborne geophysical resistivity methods have been used successfully, including a study in Nebraska to improve the understanding of the relation between surface-water and groundwater systems (Smith and others, 2008; Smith and others, 2011), a study in Florida to map water quality related to saltwater intrusion (Fitterman and Deszcz-Pan, 2002), and studies in Berrien County, Michigan (Duval and others, 2002), and Fort Huachuca, Ariz. (Bultman and others, 1999), to map the geology of these areas for input to hydrogeologic and three-dimensional (3-D) geologic models.

Cain (2002) outlined the geophysical resistivity data-collection methods and results from about 677.5 flight miles (mi) of HFEM data flown along the levee system near the Rio Grande in September 2002. Cain (2002) provides technical information on the collection methods and quality assurance for HFEM data collected within the Mesilla Basin. Dunbar and others (2004) provided additional information concerning the HFEM survey and ground-truthing results for the assessment that Cain (2002) performed on the Rio Grande levees. Dunbar and others (2004) also identified and mapped reaches of levees that would benefit from additional geophysical evaluations. Dunbar and others (2004) provided detailed files of HFEM data collected along the Rio Grande within the Mesilla Basin. Zohdy and others (1976) presented survey results of DC resistivity soundings collected in the southeastern part of the Mesilla Basin. The data from that study were reprocessed by Al-Garni (1996) using an automated data-interpretation program, which yielded robust and realistic results. The reprocessed DC resistivity soundings were used to identify areas of low resistivity, less than 10 ohm-meters (ohm-m), that could be associated with sediments composed largely of clay (clayey deposits) or high concentrations of dissolved solids in the pore water. The Zohdy and others (1976) and Al-Garni (1996) reports provided the DC resistivity sounding results

used to aid the interpretation of the geochemistry in this report.

Results from Harbour (1972), Hoffer (1976), and Drewes (1991) were used in the development of the geologic understanding of the study area. Harbour (1972) detailed an in-depth investigation of the geology of the Franklin Mountains (fig. 3) and nearby areas with an emphasis on the Paleozoic rocks (fig. 2). Hoffer (1976) described the basalt field (fig. 3) in southwestern Doña Ana County, indicating that the fractures through which the basalt flowed were created by the same early Tertiary extensional forces as was the Rio Grande rift (fig. 1). The investigation into the Doña Ana County basalt field by Hoffer (1976) was done in the context of preparing detailed geologic maps of the area emphasizing locations of volcanic units. The geologic maps by Hoffer (1976) are accompanied by descriptions of the geology and the formation of the Aden Hills, West Potrillo Mountains, and the western part of the East Potrillo Mountains near the southwestern boundary of the Mesilla Basin in the United States (fig. 3). Drewes (1991) investigated the orogeny and geology in and near the southern part of the study area, concluding that the East Potrillo Mountains (United States) and Sierra Juárez (Mexico) (fig. 3) most likely formed about 55–63 million years ago during the Laramide orogeny within the Cordilleran orogenic belt. Drewes (1991) also describes the geology of the East Potrillo Mountains and Sierra Juárez.

Previous hydrogeologic studies of the Mesilla Basin include Frenzel and Kaehler (1992), Nickerson and Myers (1993), Hawley and Kennedy (2004), Hawley and others (2005), Creel and others (2006), and S.S. Papadopulos and Associates, Inc. (2007). Results from these studies provide insights into the hydrology and basic geochemistry of the Mesilla Basin study area (fig. 1). Frenzel and Kaehler (1992) developed a groundwater-flow model of the Mesilla Basin aquifer system as part of an assessment of alluvial basins in Colorado, New Mexico, and Texas. The model approximated hydraulic heads, drain discharges, and river depletions. The following hydrogeologic description of the Mesilla Basin is provided by Frenzel and Kaehler (1992, p. C–1):

> The Mesilla Basin [is] hydrologically representative of many alluvial basins * * *. The basin fill [of the Mesilla Basin], composed of Santa Fe Group and younger deposits, forms a three-dimensional groundwater-flow system whose lateral extent and depth are defined by bedrock that has a much smaller hydraulic conductivity than the basin fill. Near Las Cruces, groundwater flow generally is away from the Mesilla Valley and is toward the valley in the southern part of the basin. Most flow into and out of the groundwater system occurs at or near land surface in the Mesilla Valley and is the result of interaction of the Rio Grande, drains, canals, evapotranspiration, and groundwater withdrawals. These flows fluctuate in the short and intermediate term (as much as about 5 years) with the availability of surface water, but in the long term, they do not change much. The general direction of groundwater flow is southeastward along the Mesilla Valley. Some recharge results from torrential surface runoff, mainly near mountain fronts. Recharge over most of the West Mesa area is unlikely but occasionally may occur in places.

Nickerson and Myers (1993) studied the hydrogeology of the Mesilla Basin aquifer system to evaluate recharge and discharge mechanisms, describe aquifer characteristics, document water-level altitudes, determine groundwater-flow direction, characterize interactions between surface water and groundwater (relations between streams and aquifers), and measure water-quality properties at selected wells. Nickerson and Myers (1993) provided some general information on the geology and water quality of the aquifer system, along with in-depth information on groundwater gradients and relations between streams and aquifers such as identifying losing stream reaches and recharge to the shallow aquifer adjacent to and under the Rio Grande near Las Cruces and Mesquite, N. Mex., and Canutillo, Tex. (fig. 1). Hawley and Kennedy (2004) created a hydrogeologic framework model for the Mesilla Basin by using GIS methods. In addition to detailed geologic maps pertaining to the Mesilla Basin study area, Hawley and Kennedy (2004) prepared multiple hydrogeologic cross sections delineating the altitude of the tops and bases of stratigraphic subdivisions with an emphasis on the hydrologic properties of the stratigraphic units. A detailed interpretation of the hydrogeologic units in the Mesilla Basin was developed as well (Hawley and Kennedy, 2004). Hawley and others (2005) extended the study area in Hawley and Kennedy (2004) into adjacent counties to Doña Ana County, N. Mex. Creel and others (2006) wrote about the water resources along the international border between New Mexico and Mexico. Contributions by Creel and others (2006) include detailed descriptions of seven transboundary aquifer systems between El Paso, Tex., and the New Mexico-Arizona border (one of which is the Mesilla Basin aquifer system), a discussion of water issues pertaining to each of these aquifer systems, and a preliminary reconnaissance of the geology and hydrology of the Mesilla Basin aquifer system. S.S. Papadopulos and Associates, Inc. (2007) developed a groundwater-flow model of the Mesilla Basin aquifer system and provided insights into the interaction between surface water and groundwater in the Rio Grande Basin.

Anderholm (1992), Witcher and others (2004), and Hogan and others (2007) described the geochemistry of the Mesilla Basin study area depicted in figure 1. Anderholm (1992) (a chapter in Frenzel and Kaehler, 1992) detailed the water quality and the geochemistry of the Mesilla Basin aquifer system (fig. 1). Anderholm (1992) indicated that there is inflow of geothermal groundwater in the eastern part of the Mesilla Basin aquifer system. Witcher and others (2004) performed a chemical analysis within the Mesilla Basin to identify sources of salinity; their results indicated that mixing between geothermal and nongeothermal groundwater and surface water, dissolution reactions, and ion exchange are the

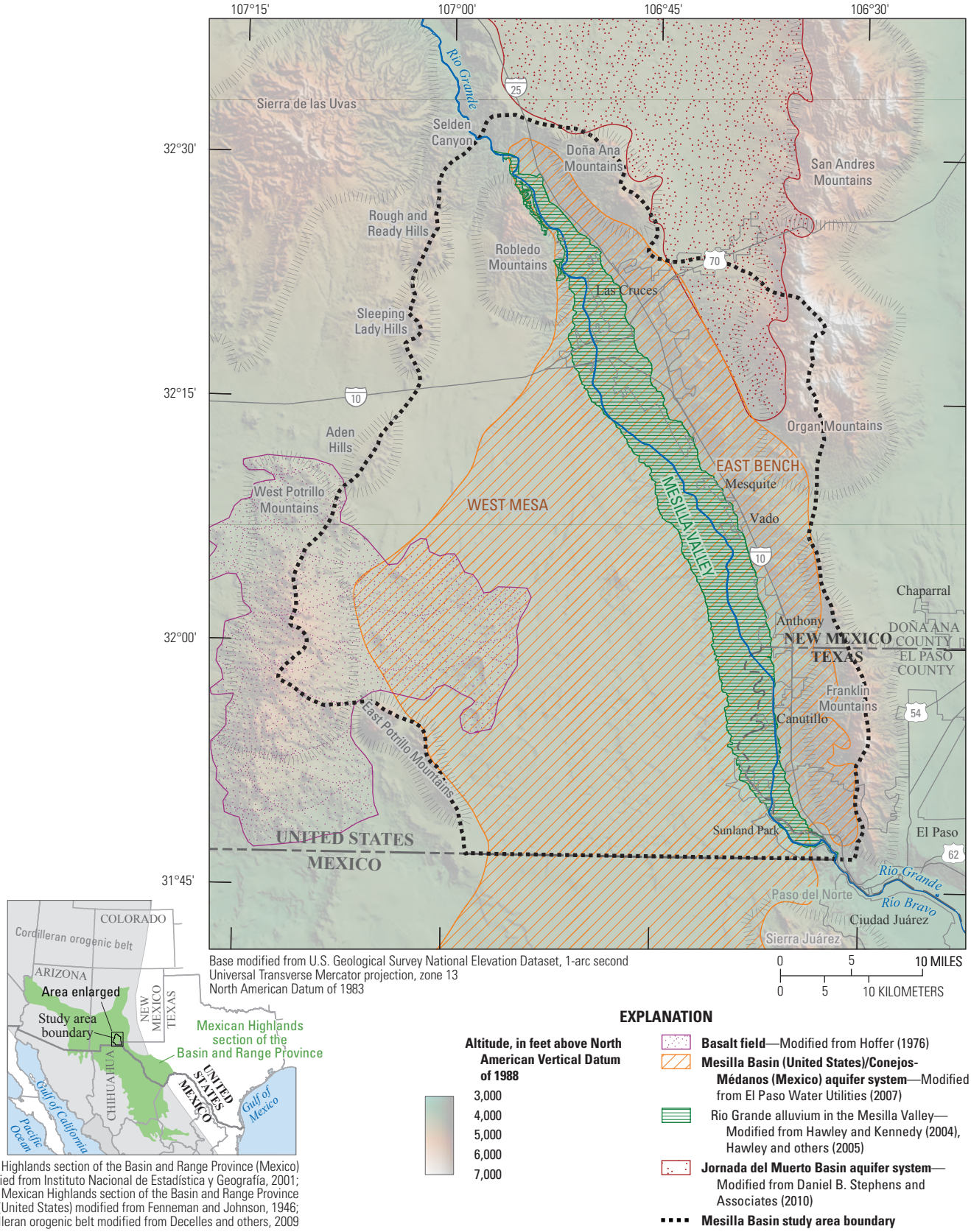

Figure 3. Physiography of the Mesilla Basin study area in Doña Ana County, New Mexico, and El Paso County, Texas.

driving forces of the geochemistry in the Mesilla Basin, where evaporative concentrations of salts play an important role in the water quality of surface water and shallow groundwater. Deeper groundwater and geothermal mixing of deeper groundwater with groundwater in the shallow aquifer play a more dominant role in governing geochemistry in the southern and eastern parts of the Mesilla Basin study area (Witcher and others, 2004). Hogan and others (2007) explored the origins of water in the Rio Grande by studying the movement of environmental tracers in Rio Grande streamflow from its headwaters to east of El Paso County, Tex. (fig. 1). Hogan and others (2007) concluded that water in the Rio Grande had one of two primary endmember signatures: Rio Grande headwaters composed of atmospheric deposition plus mineral weathering or saline groundwater of sedimentary brine origin; they also concluded that natural saline groundwater discharges to the river affected salinity in groundwater more than the recharge of irrigation return flows. In a related finding, Hogan and others (2007) reported that the largest fluxes of saline groundwater occurred in large alluvial basins and in smaller basins with appreciable geothermal activity such as the Mesilla Basin.

Purpose and Scope

This report describes a geophysics- and geochemistry-based assessment of the geochemical characteristics and groundwater-flow system of the Mesilla Basin aquifer system (fig. 1) in Doña Ana County, N. Mex., and El Paso County, Tex., completed during 2010–12. Previously published and newly collected geophysical and geochemical data were augmented by the use of other hydrologic data that were compiled or collected, including historical salinity-related data and water-level-altitude data. Geophysical data (previously published HFEM data and DC resistivity soundings, and TDEM data collected during 2012) supplemented previously published and newly collected geochemical data in the evaluation of the hydrogeology in the southeastern part of the Mesilla Basin study area, as well as along the Rio Grande throughout the entire study area. Geochemical data consisted of historical (1922–2007) dissolved-solids-concentration data and a large suite of constituents (physicochemical properties, major ions, nutrients, trace elements, pesticides, and environmental tracers [tritium, chlorofluorocarbons, and selected stable isotopes]) measured in samples collected from wells throughout the Mesilla Basin study area during 2010. Historical dissolved-solids-concentration data within the surface geophysical subset area (see “Geophysics” section of this report) of the Mesilla Basin study area were compared to the inverse modeling results of the combined DC resistivity and TDEM soundings. Differences in water quality and water-level altitudes were assessed to gain insights regarding sources of salinity and movement of groundwater in the Mesilla Basin study area. The different water types within the Mesilla Basin study area were characterized and delineated; water types were determined from major-ion concentrations by using trilinear diagrams. Probability plots and boxplots were prepared to explore differences in the spatial patterns of geochemical data. Trace-element chemistry provided information that aided in the interpretation of potential water sources or processes within the different hydrogeologic units found in the Mesilla Basin study area. Differences in water quality were related to differences in the geology in the Mesilla Basin study area. Environmental tracers were used to aid in identifying sources, processes, and ages of groundwater. The chemical properties of water are described in context of the geologic and hydrogeologic setting of the Mesilla Basin study area, along with regional groundwater-flow patterns, aquifer recharge, and mixing of water from different sources. Selected pesticides were reported but were not used in this assessment of the groundwater system in the study area.

Description of the Study Area

The study area consists mostly of the Mesilla Basin, which is underlain by the Mesilla Basin aquifer system. Orographic features (uplift areas, hills, and mountains) surround and form part of the study area. A small part of the Jornada del Muerto Basin (hereinafter referred to as the “Jornada Basin”) forms the northeast part of the study area. The different areas that compose the study area are collectively referred to as the “Mesilla Basin study area.” The alluvial aquifer system underlying the Jornada Basin is referred to as the “Jornada Basin aquifer system” in this report. Groundwater flow in this part of the Jornada Basin is westward, towards the Mesilla Valley, so the potential exists for interbasin flow between the Jornada Basin and the Mesilla Basin in buried ancient arroyo (paleoflow) channels (Peterson and others, 1984; Nickerson and Myers, 1993). The study area covers about 1,400 square miles (mi^2) in Doña Ana County, N. Mex., and about 100 mi^2 in El Paso County, Tex., all in the Mexican Highlands section of the Basin and Range physiographic province (figs. 1 and 3) (Hawley and Kennedy, 2004; Hawley and others, 2005). The surface-water drainage area of the Mesilla Basin was used to delineate much of the study area in order to include all of the drainage sources to the Mesilla Basin aquifer system. The eastern, western, and northern boundaries of the study area were delineated as the watershed divides associated with the East and West Potrillo Mountains, the Aden Hills, the Sleeping Lady Hills, the Rough and Ready Hills, the Robledo and Doña Ana Mountains, and the Organ and Franklin Mountains (fig. 3). The international border between the United States and Mexico forms the southern boundary of the study area. Higher amounts of precipitation in the mountains compared to the basins and valleys account for a minor source of groundwater recharge referred to as “mountain-front water” (Robson and Banta, 1995). The altitude within the study area ranges from about 9,000 feet (ft) to the east in the Organ Mountains to about 3,700 ft to the south in the Mesilla Valley. The Sierra Juárez, about 5 mi south of the international border between the

United States and Mexico, near the southeastern part of the study area, are another possible source of mountain-front recharge because these mountains are in the same structural basin as the West Mesa area (Anderholm, 1992).

The Mesilla Basin can be divided into three parts in the study area: the Mesilla Valley, the West Mesa, and the East Bench (fig. 3). The Mesilla Valley is the part of the Mesilla Basin that was incised by the Rio Grande between Selden Canyon to the north and by a narrow valley (about 4 mi wide) to the southeast near El Paso, Tex., named the Paso del Norte, which is sometimes referred to in the literature as the "El Paso Narrows" (Frenzel and Kaehler, 1992; Hawley and Kennedy, 2004). The Mesilla Valley contains the majority of the population and greatest water use within the Mesilla Basin (Nickerson and Myers, 1993; Hawley and Kennedy, 2004; Hawley and others, 2005). The altitude of the Mesilla Valley decreases slightly from 3,980 ft at Selden Canyon to 3,730 ft at the Paso del Norte (Frenzel and Kaehler, 1992). The average width of the Mesilla Valley is about 5 mi, with more narrow widths near the Rio Grande's entry and exit points into and out of the basin at Selden Canyon and the Paso del Norte, respectively. The West Mesa is west of the Mesilla Valley and is bounded by the East and West Potrillo Mountains, the Aden Hills, the Sleeping Lady Hills, and the Rough and Ready Hills (fig. 3). The West Mesa is relatively flat, with closed drainage basins gradually sloping towards the southeast (Frenzel and Kaehler, 1992). The mean altitude of the West Mesa is about 300–350 ft higher than the Rio Grande and contains scattered remnants of volcanic activity (Frenzel and Kaehler, 1992; Nickerson and Myers, 1993). The West Mesa is as wide as 30 mi from the West Potrillo Mountains to the Mesilla Valley. The uplifted and gently sloping area east of the Mesilla Valley that is bounded by the Doña Ana, Organ, and Franklin Mountains is referred to in this report as the "East Bench" (fig. 3). The East Bench roughly coincides to the "piedmont slope of the Franklin Mountains" described by Frenzel and Kaehler (1992, p. C12). The East Bench increases in altitude towards the Doña Ana, Organ, and Franklin Mountains (Frenzel and Kaehler, 1992). The altitude of the East Bench ranges from about 4,000 ft near the Paso del Norte to about 4,700 ft at the base of the Organ Mountains east of Las Cruces. The mean width of the East Bench is about 6 mi, with the widest part near the Organ Mountains reaching about 9 mi in width.

The Jornada Basin is separated from the Mesilla Basin by a fault zone and is bounded within the study area by the Doña Ana Mountains to the west and the Organ Mountains to the east (fig. 3) (Nickerson and Myers, 1993). The small section of the Jornada Basin within the study area is primarily composed of the uplifts that form the Organ Mountains. The altitudes in this part of the Jornada Basin range from about 4,350 ft in the west to more than 9,000 ft in the east in the Organ Mountains. The width of the Jornada Basin within the study area increases from about 2 mi in the south to about 8 mi in the north.

Leggat and others (1963) describe the climate in the lower Mesilla Valley as arid, characterized by a wide range in temperature, low humidity, high evaporation, and low precipitation—a description that applies to the entire study area. Compared to the mountainous parts of the study area, precipitation amounts are lower and temperatures are higher in the basin and valley lowlands. Climatological records from 1981 through 2010 indicate that about 10 inches (in.) of precipitation falls annually in the basins and valleys in the study area, compared to more than 17 in. at the higher altitudes of the Franklin and Organ Mountains (fig. 3) (Parameter-elevation Regressions on Independent Slopes Model [PRISM] Climate Group, 2004; National Oceanic and Atmospheric Administration, 2014). Monthly high temperatures for the Mesilla Valley range from about 14 degrees Celsius (°C) (57 degrees Fahrenheit [°F]) in December to 35 °C (95 °F) in June and July, and monthly low temperatures range from -1 °C (30 °F) in January and December to 20 °C (69 °F) in July (National Oceanic and Atmospheric Administration, 2014).

Land cover within the study area is mostly shrub and scrub vegetation (80.6 percent) (fig. 4) (U.S. Geological Survey, 2013). The other predominant land-cover types within the study area are cultivated crops (8.9 percent) and developed areas (6.2 percent) in and near the Mesilla Valley. Water for crops is primarily obtained from the Rio Grande by a system of irrigation canals; groundwater is used to supplement the irrigation water obtained from the Rio Grande (Frenzel and Kaehler, 1992). Developed areas include Las Cruces and part of the greater metropolitan area of El Paso, as well as numerous small communities such as Mesquite, Vado, Anthony, and Sunland Park, N. Mex., and Canutillo, Tex. Developed areas rely primarily on groundwater for domestic, municipal, and industrial use (Frenzel and Kaehler, 1992).

In addition to the Rio Grande, the surface-water features of the study area include an intricate network of arroyos, canals, drains, laterals, and irrigation diversions (fig. 5). All of these surface-water features directly or indirectly contribute recharge to the shallow aquifer in the Rio Grande alluvium (Frenzel and Kaehler, 1992; Hawley and Kennedy, 2004; Hawley and others, 2005). A series of canals, laterals, and irrigation diversions were dug in the 1840s and improved in the late 1890s to supply water from the Rio Grande to irrigation fields (Frenzel and Kaehler, 1992).

Discharge of the Rio Grande was greatly altered by the Rio Grande Project, an irrigation, hydroelectricity (after 1940), flood-control, and interbasin water-transfer project (Bureau of Reclamation, 2011). The Rio Grande Project included the impoundment of Elephant Butte Reservoir beginning in 1915 (fig. 1); the enlargement of Franklin Canal during 1914–15 (fig. 1); construction of Mesilla Diversion Dam during 1914–19 (fig. 5), which diverts water into the East Side and West Side Canals (fig. 5), and construction of Percha Diversion Dam (fig. 1), which diverts water to Rincon Valley Main Canal (fig. 1). The Rio Grande Project also included the development and improvement of a lateral and drainage system in the Mesilla Valley from 1916 to 1930 (Bureau of Reclamation, 2011).

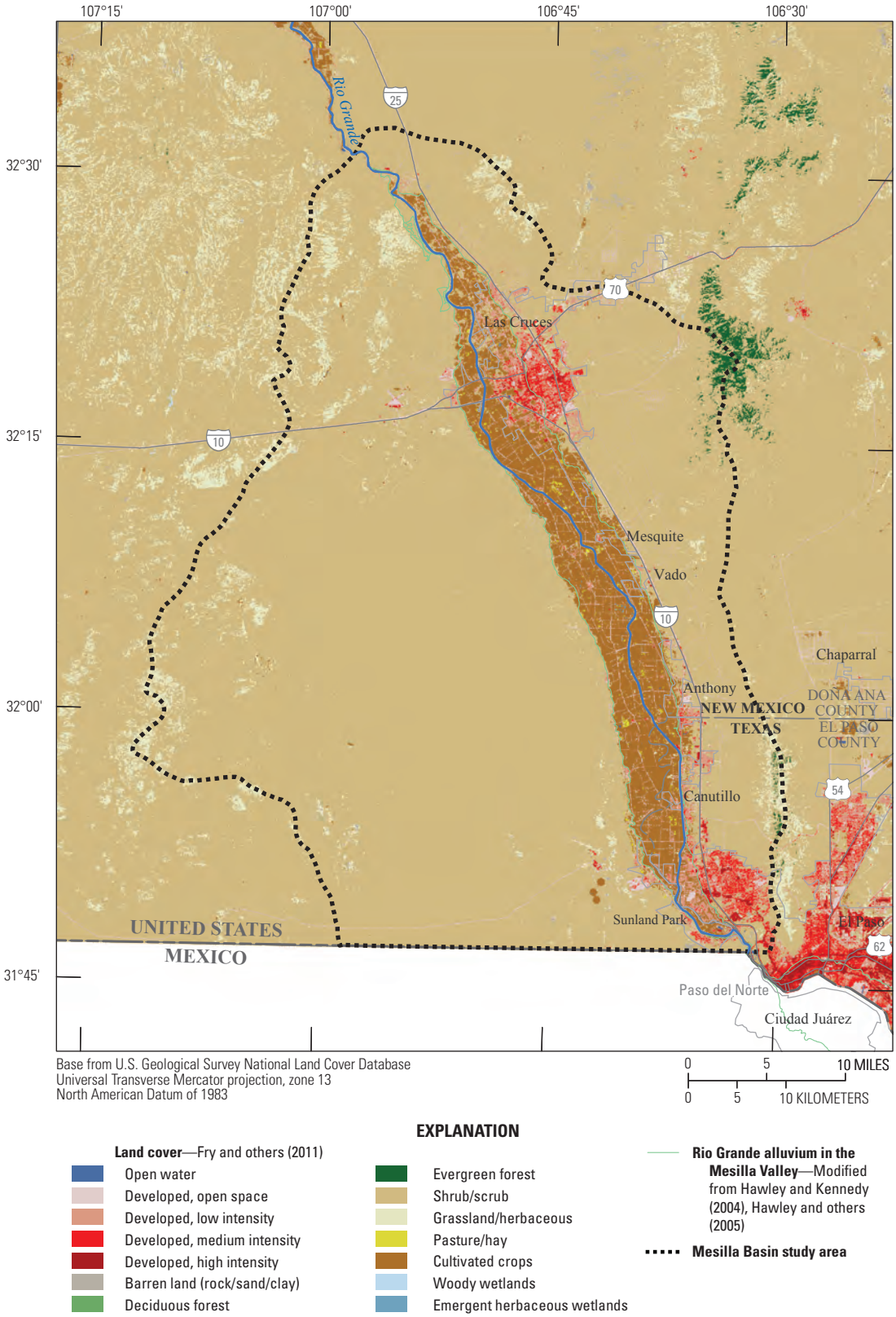

Figure 4. Land cover in the Mesilla Basin study area in Doña Ana County, New Mexico, and El Paso County, Texas, 2011.

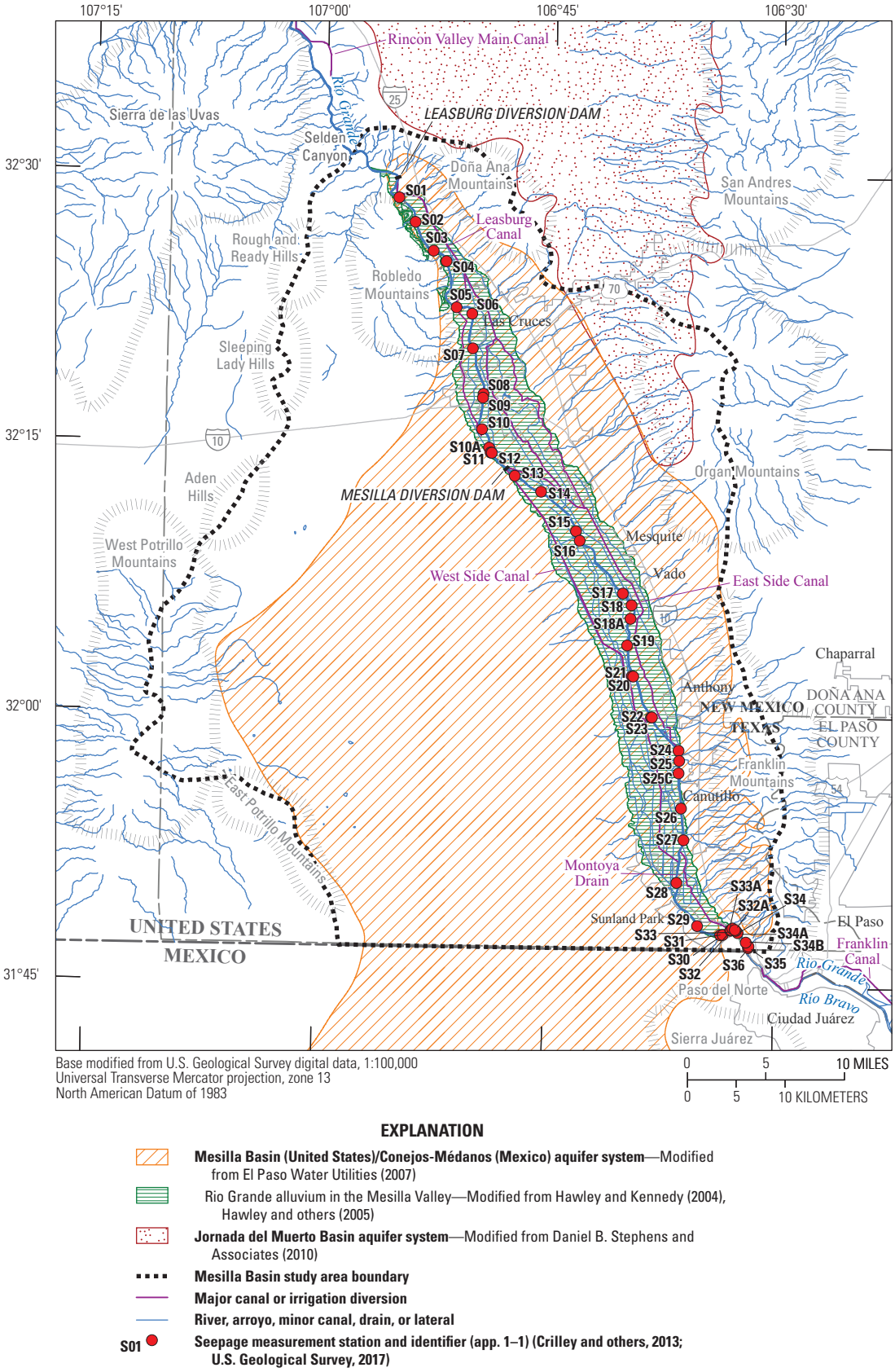

Figure 5. Surface water features and seepage measurement stations of the Mesilla Basin study area in Doña Ana County, New Mexico, and El Paso County, Texas.

Discharge of the Rio Grande in the study area fluctuates from almost no flow to several thousand cubic feet per second (ft^3/s). Some annual peak discharges of more than 15,000 ft^3/s were recorded before 1915 (fig. 6*A*) (International Boundary and Water Commission, 2013). Since 1915, the annual peak discharge has not exceeded 9,150 ft^3/s, which is less than the pre-1915 mean annual peak discharge of 9,830 ft^3/s. The reduction in peak discharge was a result of modifications made to the river as part of the Rio Grande Project.

The arroyos in the study area (fig. 5) flow only in response to intense rainfall. Some water from arroyos originating from the Franklin and Organ Mountains will flow into the Rio Grande during periods of runoff (Frenzel and Kaehler, 1992). These arroyos likely contribute water to the shallow groundwater system during runoff events. In addition to varying annually, discharge in the Rio Grande varies seasonally, with relatively higher discharges during warmer months of the year (March through September) compared to cooler months (October through February) (fig. 6*B*) (International Boundary and Water Commission, 2013).

To better understand the interaction between groundwater and surface water along the reach of the Rio Grande that traverses the study area, the USGS completed 20 seepage investigations between 1988 and 2013 (Crilley and others, 2013; U.S. Geological Survey, 2017) (app. 1). Figure 7 depicts the relative median streamflow gain or loss at each measurement station relative to the previous (upstream) measurement station along the reach of Rio Grande in the

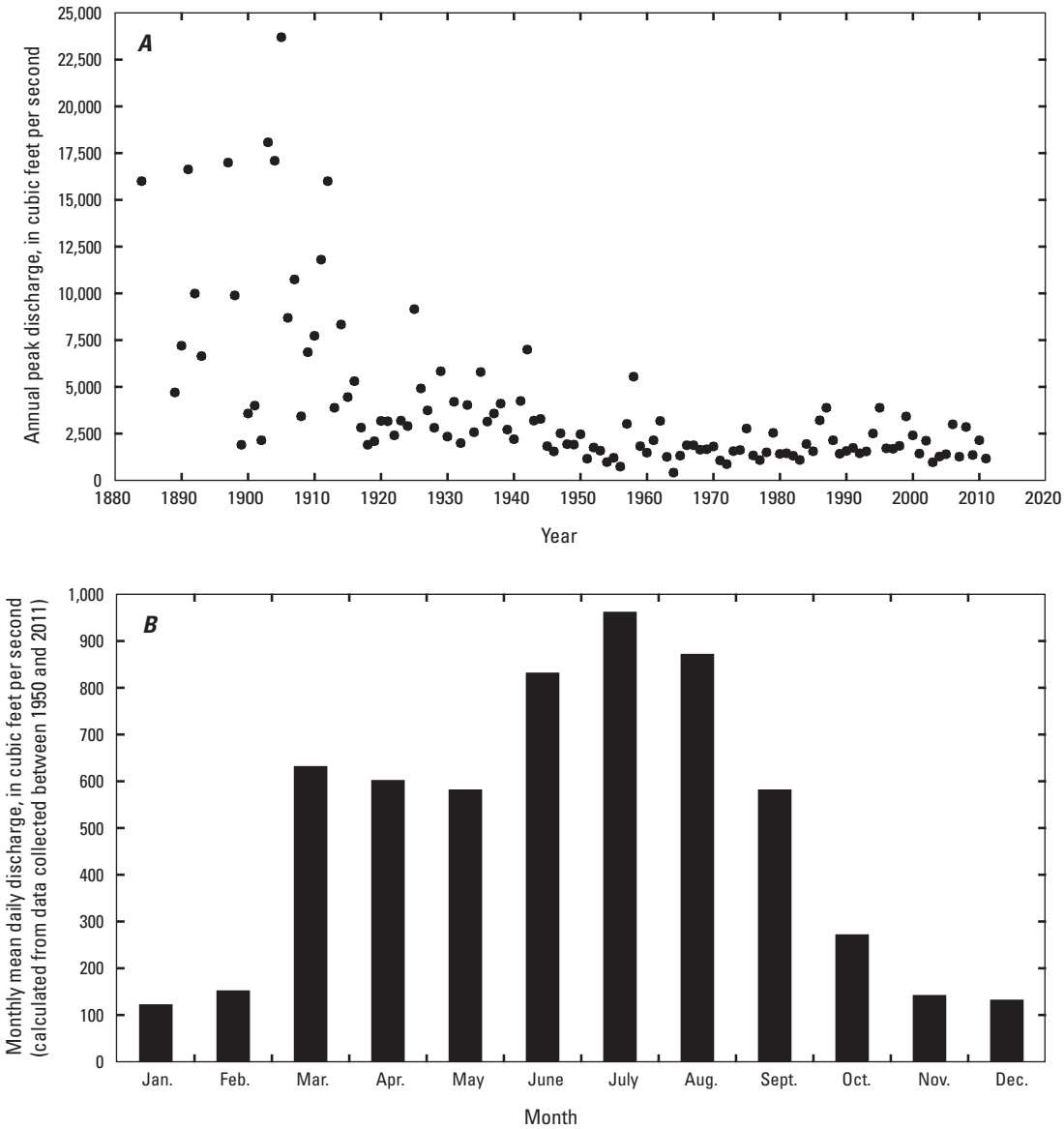

Figure 6. Discharge of the Rio Grande between 1950 and 2011 at International Boundary and Water Commission streamflow-gaging station 08364000 Rio Grande at El Paso, Tex. *A*, Annual peak discharge. *B*, Monthly mean daily discharge.

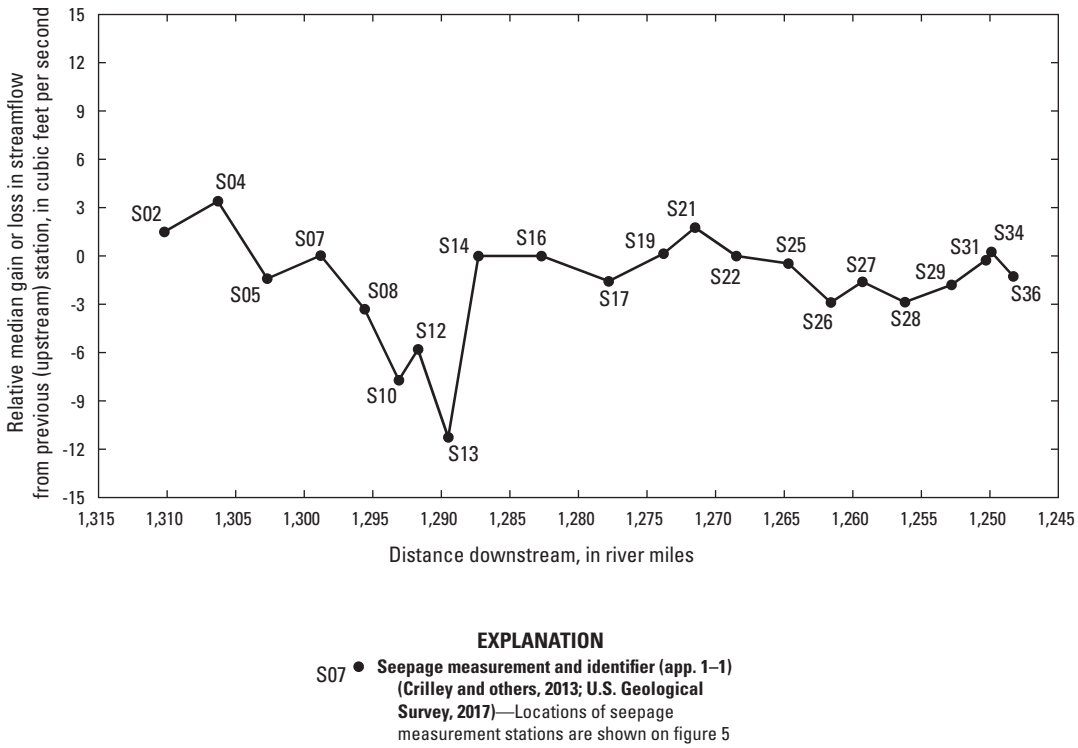

Figure 7. Relative median gain or loss at seepage measurement stations along the Rio Grande in the Mesilla Basin study area in Doña Ana County, New Mexico, and El Paso County, Texas, from 20 seepage investigations conducted between 1988 and 2013 (modified from Crilley and others, 2013; U.S. Geological Survey, 2017).

study area. The results from these previous investigations indicate that the Rio Grande is a losing stream throughout much of the study area but that there are several reaches where there is a relative gain in streamflow between the upstream and downstream measuring stations that define each reach. Along with these gaining reaches, there are some reaches where the median value indicates that overall there is little gain or loss (fig. 7). Reaches with little gain or loss include a shorter reach of about 7 mi located west of Las Cruces between S05 and S08 and a longer reach of about 9 mi between Las Cruces and Vado, N. Mex., between S14 and S17 (figs. 5 and 7). As stated in Peterson and others (1984), areas along the Rio Grande where the water table is above or within a foot or two from the river bed can be considered hydraulically connected, which means that there is the potential for seepage to and from the river depending on the water-table altitude and river-bed conditions.

Increased irrigation in the late 1910s resulted in more irrigation water recharging the shallow groundwater system, causing the water table to rise and salts to accumulate in the soils (Frenzel and Kaehler, 1992). As these salts were subsequently leached from the soils by the application of excess irrigation water that seeped past the root zone, the salinity of the shallow groundwater system increased (Anderholm, 1992). A drainage system was constructed to keep the water table below the altitude of the irrigated fields, allowing the salts within the soil to be leached out with excess irrigation water (Anderholm, 1992; Frenzel and Kaehler, 1992). The excess irrigation created downward flow, resulting in the leached water mixing with the shallow groundwater system (Anderholm, 1992). Because of this process, drains within the study area have been of concern because they might contribute to the problem of increasing salinity within the Rio Grande and the shallow groundwater system (Doremus and Michelsen, 2008).

The following sections describe the geologic and hydrogeologic settings. The majority of the geologic and hydrogeologic background information presented in this report is summarized from Hawley and Kennedy (2004).

Geologic Setting

Most of the study area is in the Rio Grande rift (fig. 1). The Rio Grande rift is characterized by north-south trending basins located between mountain ranges originating from tilted fault-blocks and uplifted areas resulting from volcanic activity, including uplifted areas formed by relatively young (Quaternary) volcanism (fig. 2) (Hawley and Kennedy, 2004; Hawley and others, 2005). Except for the exposed bedrock formations of the mountain ranges and uplifted areas from volcanic activity, most of the study area is buried by deep alluvium deposits (Hoffer, 1976). Basin subsidence began

in the late Oligocene with the majority of the displacement most likely occurring within the late Miocene and early Pliocene (fig. 2) (Hawley and Kennedy, 2004; Hawley and others, 2005). Half-grabens, which are basin blocks sinking relative to an adjacent uplift (Stewart, 1998), formed as a result of extensional forces caused by rifting. Multiple half-grabens within the Mesilla Basin resulted in smaller basins, or subbasins, which were subsequently filled by the deposition of eroded sediments. As erosion and deposition continued through the middle Pliocene and early Pleistocene, individual subbasins began to fill up, and the basin-fill material covered the subbasins and the uplifts that separated the subbasins. This collection of subbasins and fill has come to be identified as the Mesilla Basin (fig. 1). Basin filling ended in the middle Pleistocene (fig. 2) as the modern Rio Grande (Pleistocene to present) began to entrench the Mesilla Valley into the basin.

High-angle normal faulting accounts for almost all of the boundary features between subbasins and uplifts (Hawley and Kennedy, 2004; Hawley and others, 2005). From west to east, the major subbasins (all of which generally trend north to south) are the Southwestern and Northwestern subbasins, the South-central subbasin, and the La Union-Mesquite and Southeastern subbasins (fig. 8). The La Union-Mesquite subbasin is the deepest (maximum depth of about 3,000 ft), followed by Northwestern and Southwestern subbasins, which each have maximum depths of about 2,000 ft (Hawley and Kennedy, 2004; Hawley and others, 2005). The midbasin uplift (informally named by Hawley and Lozinsky, 1992) separates the Northwestern and Southwestern subbasins from the La Union-Mesquite, South-central, and Southeastern subbasins. Flanking the western boundary of the study area are the Robledo and East Potrillo uplifts, on either side of which there are major, bounding fault zones (the East and West Robledo Fault zones to the northwest and the East and West Potrillo Fault zones to the southwest). Near the eastern boundary of the study area are the Doña Ana, Tortuga, Organ, Franklin, and Cristo Rey-Juárez uplifts, which jointly act as the eastern boundary of the basin (Hawley and Kennedy, 2004; Hawley and others, 2005).

The majority of the uplifts within the study area are composed of Paleozoic- and early Cretaceous-age carbonate and siliciclastic rocks, which are sedimentary rocks containing almost exclusively silicate-bearing clasts such as quartz, feldspars, and other silicate minerals (fig. 2) (Hawley and Kennedy, 2004; Hawley and others, 2005). The two major uplifts that do not contain these lithologies are the Organ and Doña Ana Mountains, which are mainly composed of Tertiary-age igneous rocks (granite, monzonite, rhyolite, and andesite). Deposits from the Organ and Doña Ana Mountains include trace metals, which can act as replacements in the chemical substitution of ions with a similarly sized and charged element within select minerals such as feldspars (Klein and Hurlbut, 1998). All uplifts within the study area include Tertiary igneous intrusions such as sills, dikes, or plugs (Frenzel and Kaehler, 1992). During the middle to late Quaternary, alkali olivine basalt flowed from the Fitzgerald, East and West Robledo, and Aden Fault zones (fig. 8) (Hoffer, 1976). East Potrillo and Franklin Mountains and the Sierra Juárez are composed of mostly lower Cretaceous limestone and dolomite; limestone and dolomite consist primarily of calcium carbonate ($CaCO_3$) and calcium magnesium carbonate ($CaMg[CO_3]_2$), respectively (Harbour, 1972; Drewes, 1991). Some Pennsylvanian-age beds of gypsite or gypsum, which are both composed mostly of calcium and sulfate ($CaSO_4 \cdot 2H_2O$) mixed with other trace elements, are present between the Organ and Franklin Mountains (Hawley and Kennedy, 2004; Hawley and others, 2005). Near the southeastern border of the study area there are substantial amounts of Paleozoic- and Cretaceous-age carbonate rocks near the surface that have the potential to locally form conduits for the upwelling of deep groundwater from sources below the bedrock (Hawley and Kennedy, 2004; Hawley and others, 2005). The probability of groundwater upwelling is supported by the local occurrence of dissolution features in carbonate and gypsiferous rocks in the area and the presence of an extensive fracture network (Hawley and Kennedy, 2004; Hawley and others, 2005).

The base of the Mesilla Basin study area (the bedrock) is composed mainly of lower to middle Tertiary volcanic and volcaniclastic rocks; lower Tertiary sedimentary units are exposed in a few areas in the northern and eastern parts of the study area (fig. 2) (Hawley and Kennedy, 2004; Hawley and others, 2005). These Tertiary-age rocks are underlain mostly by Cretaceous and upper Paleozoic-age rocks but in some areas are directly underlain by lower Paleozoic- and Precambrian-age rocks. Directly overlying the base of the Mesilla Basin are late Oligocene to Quaternary sedimentary deposits, of which almost all are characterized as belonging to the Santa Fe Group (fig. 2). The Santa Fe Group is basin fill composed mainly of alluvium from adjacent uplifts, eolian sediments, and some fluvial sediments from the ancestral Rio Grande (pre-Pleistocene) (Hawley and Kennedy, 2004; Hawley and others, 2005). The lower part of the Santa Fe Group is associated with the Hayner Ranch Formation and the lower part of the Rincon Valley Formation (fig. 2) and is predominantly fine-grained, basin-floor sediments with some calcium-sulfate ($Ca\text{-}SO_4$) and sodium-sulfate ($Na\text{-}SO_4$) evaporites and cementation. Sheets of eolian sediments are interbedded with the basin-floor sediments in the southern part of the study area. The middle part of the Santa Fe Group corresponds to the upper part of the Rincon Valley Formation and the lower part of the Fort Hancock Formation and is composed of alternating beds of sand, silty sand, and silty clay along with some eolian sediment along the eastern boundary of the study area. The upper part of the Santa Fe Group corresponds to the upper part of the Fort Hancock Formation and the Camp Rice Formation and is mostly composed of fluvial sand deposited by the ancestral Rio Grande along with some interbedded fine-grained basin fill. Basalt and andesite flows from dikes, sills, and plugs are interbedded within the basin fill. Repeated incision and backfill from the Rio Grande and other tributary systems create a valley-filled unit of the middle to late Quaternary age, referred to as the “Rio Grande

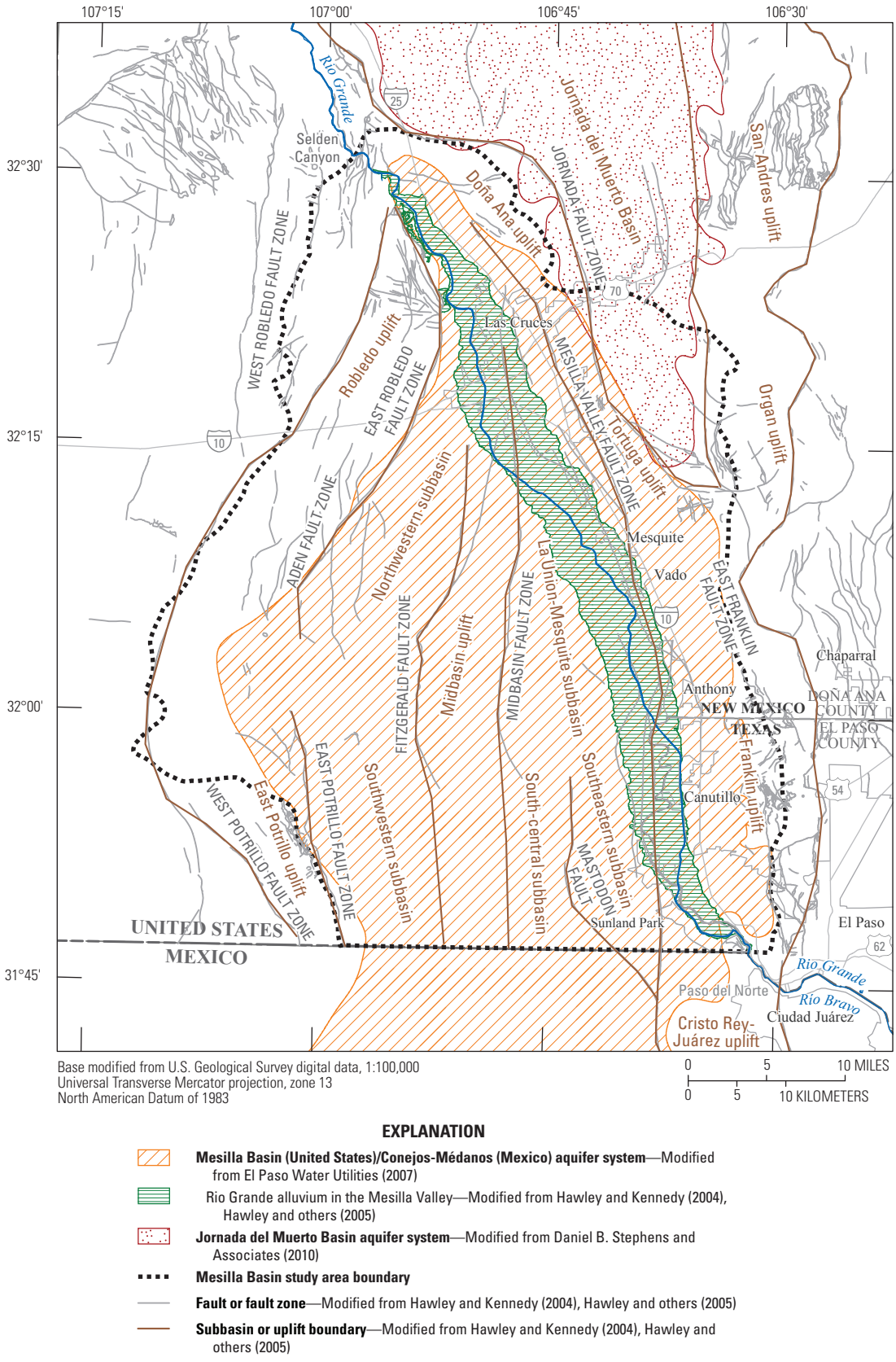

Figure 8. Generalized boundaries of subbasins and uplifts of the Mesilla Basin study area in Doña Ana County, New Mexico, and El Paso County, Texas.

alluvium" (fig. 2). The Rio Grande alluvium is composed of a range of sediments from sand and gravel to silts and clays (Hawley and Kennedy, 2004; Hawley and others, 2005).

Sand in the Santa Fe Group is derived from more than one fault-bounded area (source terrane) (Hawley and Kennedy, 2004; Hawley and others, 2005). Summarizing petrographic interpretations of rock fragments and mineral grains by other investigators, Hawley and Kennedy (2004) reported that most of the sand in the Santa Fe Group is from volcanic, sedimentary, or granitic source terranes. An intermediate composition volcanic source terrane is likely the origin of the majority of the sand grains, as indicated by an abundance of plagioclase (a series of feldspar with varying compositions of Ca and Na) and andesitic lithic fragments. Presence of an abundance of quartz, chert, and chalcedony indicates a sedimentary source terrane. Microcline, strained quartz, and granite rock fragments indicate a source terrane that was likely granitic.

Clay minerals within the Santa Fe Group include illite, smectite, kaolinite, and montmorillonite. In addition to clay minerals, secondary mineral groups associated with feldspar alteration such as zeolites also occur primarily near uplift areas, likely from silicic-volcanic source terrane. Determination of the exact source for these deposits is difficult because of the lack of paleoflow indicators (Hawley and Kennedy, 2004; Hawley and others, 2005).

Hydrogeologic Setting

The Mesilla Basin aquifer system (Rio Grande alluvium and Santa Fe Group) is the predominant aquifer system in the study area; a small part of Jornada Basin aquifer system is included in the study area because of the possibility of interbasin groundwater flow (fig. 1). Groundwater flow in the Mesilla Basin aquifer system generally is from the north to the south-southeast with the majority of the groundwater discharging at the Paso del Norte (fig. 8) (Hawley and Kennedy, 2004; Hawley and others, 2005). Hydrogeologic boundaries for deep groundwater flow in the Mesilla Basin consist of the East Robledo and East Potrillo Fault zones to the west and the Mesilla Valley Fault zone to the east. Interbasin groundwater flow from the Jornada Basin into the Mesilla Basin might exist through zones of higher permeability, such as buried ancient arroyo (paleoflow) channels, even with the existence of normally effective barriers to flow such as faults perpendicular to flow or fault zones composed of impermeable rock units such as unfractured bedrock (Peterson and others, 1984; Nickerson and Myers, 1993).

An informal classification scheme based on basin-fill stratigraphy and sedimentology with an emphasis on aquifer characteristics has been developed to identify unique hydrogeologic units (HGUs) for most of the basins in the southeastern part of the Mexican Highlands section of the Basin and Range physiographic province (fig. 3) (Witcher and others, 2004). This report follows the convention of previous investigators who divided the Mesilla Basin aquifer system into four informal HGUs within the study area—the Rio Grande alluvium and the three HGUs that compose the Santa Fe Group (Hawley and Kennedy, 2004; Hawley and others, 2005).

The uppermost water-bearing formation of the Mesilla Basin aquifer system is the Rio Grande alluvium, which consists of a thin layer (generally about 80 ft thick) of upper Quaternary fluvial deposits in the Mesilla Valley (fig. 2). The Rio Grande alluvium includes river-valley fluvial deposits and valley-border alluvial deposits. River-valley fluvial deposits were laid down by the ancestral and modern Rio Grande (Hawley and Kennedy, 2004). Erosion of "older valley fills of the tributary arroyo system and deposits of the ancestral river * * * preserved in terrace remnants on valley borders" (Hawley and Kennedy, 2004, p. 48) produced the valley-border alluvial deposits, which were laid down between the valley walls and the river-valley fluvial deposits (Hawley and Kennedy, 2004; Hawley and others, 2005). The river-valley fluvial deposits are composed of silts, clays, sands, and gravels. Sand and gravel basal channels as thick as 40 ft extend laterally beyond the present floodplain. Underlying the Rio Grande alluvium is the Santa Fe Group, which predates river-valley alluvium and consists of sedimentary basin fill. In numerous publications, the Santa Fe Group has informally been considered as consisting of upper, middle, and lower HGUs, all of which are water bearing (for example, Hawley and Kennedy, 2004; Witcher and others, 2004; Hawley and others, 2005; Creel and others 2006; S.S. Papadopulos and Associates, Inc. 2007). The three HGUs that compose the Santa Fe Group are the upper part of the Santa Fe Group (hereinafter referred to as the "upper Santa Fe"), the middle part of the Santa Fe Group (hereinafter referred to as the "middle Santa Fe"), and the lower part of the Santa Fe Group (hereinafter referred to as the "lower Santa Fe"). The upper Santa Fe is the most productive HGU within the Santa Fe Group and is composed of mostly unconsolidated sand and gravel basin fill deposited by the ancestral Rio Grande; however, it is only partially saturated in the northern and eastern parts and is largely unsaturated in the southern and western parts of the Mesilla Basin. The middle Santa Fe is generally saturated and includes fine-grained unconsolidated basin fill with interbedded sand layers. The saturated thickness within the middle Santa Fe can be as much as 2,000 ft; the middle Santa Fe is the primary aquifer within the basin. The lower Santa Fe is the least productive zone, with the majority of the unit composed of fine-grained and partly consolidated basin fill (Hawley and Kennedy, 2004; Hawley and others, 2005). Similar to the Mesilla Basin aquifer system, the Jornada Basin aquifer system also is primarily composed of the Santa Fe Group.

The specific capacity of wells within the Mesilla Valley decreases with depth, ranging from 10–217 gallons per minute per foot ([gal/min]/ft) (mean of 69 [gal/min]/ft) measured in wells completed near the surface (saturation thickness of less than 200 ft) to 5–75 (gal/min)/ft (mean 25 [gal/min]/ft) in

wells completed deeper in the subsurface (saturation thickness of more than 200 ft) (Hawley and Kennedy, 2004; Hawley and others, 2005). Wells completed 200–600 ft below land surface (bls) (typically corresponding to either the upper Santa Fe or middle Santa Fe) had specific capacity values of less than 40 (gal/min)/ft, and wells completed greater than 600 ft bls (typically corresponding to either middle Santa Fe or lower Santa Fe) generally had specific capacity values between 1 and 10 (gal/min)/ft (Hawley and Kennedy, 2004; Hawley and others, 2005). Most published estimates of transmissivity values (reported from pumping test results) from all units in the Mesilla Valley generally range from 10,000 to 40,000 square feet per day (ft^2/d), but were as high as 50,000 ft^2/d in some parts of the valley. The estimated transmissivity values within the Rio Grande alluvium generally range from 10,000 to 20,000 ft^2/d with some values exceeding 30,000 ft^2/d (Hawley and Kennedy, 2004; Hawley and others, 2005).

Mean estimated transmissivity for the entire Mesilla Basin is about 10,000 ft^2/d (Hawley and Kennedy, 2004; Hawley and others, 2005). Mean horizontal hydraulic conductivity is higher (as much as 70 feet per day [ft/d]) near the surface and decreases with depth. Mean horizontal hydraulic conductivity values measured in wells with completed depths less than 600 ft bls (typically corresponding to either the upper Santa Fe or middle Santa Fe) range from 9 to 43 ft/d (Hawley and Kennedy, 2004; Hawley and others, 2005). Mean horizontal hydraulic conductivity values measured in wells with completed depths greater than 600 ft bls (typically corresponding to either the middle Santa Fe or lower Santa Fe) range from 2 to 14 ft/d (Hawley and Kennedy, 2004; Hawley and others, 2005).

Geophysics

Resistivity measurements were used to construct two-dimensional (2-D) and 3-D grids of the spatial distribution of electrical properties of the subsurface, which were then used to describe variations in the subsurface hydrogeology. The three geophysical resistivity methods used to evaluate the hydrogeology along the Rio Grande and within the surface geophysical subset area (in the southeastern part of the study area; fig. 9) were HFEM, DC resistivity, and TDEM. Comprehensive descriptions of the theory and application of geophysical resistivity methods, as well as tables of the electrical properties of earth materials, are presented in Keller and Frischknecht (1966), Cain (2002), and Lucius and others (2007) and are not presented in this report. Interpretation of the DC resistivity and TDEM soundings was limited to the surface geophysical subset area (table 1, fig. 9).

Airborne Geophysical Resistivity Methods

By using airborne geophysical resistivity methods, previous investigators assessed the bulk resistive properties of the subsurface along the Rio Grande and in the southeastern part of the study area for this report, obtaining data that provide a 3-D grid of the inferred geologic properties to a depth of about 100 ft (Cain, 2002; Dunbar and others, 2004). The airborne geophysical resistivity profiles that were obtained by Dunbar and others (2004) provide data that can also be used to infer hydrogeologic characteristics in the study area.

The HFEM method uses multiple frequencies to measure bulk conductivity values (the inverse of resistivity values) of the subsurface at different depths. These measurements are made by producing an alternating electrical current into a transmitter (Tx) coil at a known frequency (fig. 10) (Lucius and others, 2007). This time-varying electrical current produces a primary magnetic field. The primary magnetic field propagates into the subsurface, where it induces electrical currents that are proportional to the electrical conductivity of the material. These electrical currents, in turn, produce secondary magnetic fields that propagate back to the surface, where they induce a current in the receiver (Rx) coil; the magnitudes of the primary magnetic field and secondary magnetic field are measured by using the Rx coil (fig. 10). In-phase and quadrature (the portion of the secondary magnetic field 90 degrees out of phase with the primary field) responses are calculated as the ratio of the magnitudes of the secondary to the primary magnetic field. These responses are then used to calculate the apparent resistivity of the subsurface. Apparent resistivity represents the resistivity of completely uniform (homogenous and isotropic) earth material (Keller and Frischknecht, 1966). Further explanation of how apparent resistivity values are calculated from the in-phase and quadrature responses is provided by Cain (2002).

The HFEM data used in this report were collected by Fugro Airborne Surveys in cooperation with the IBWC in September 2002 to assess the conditions of the levees along the Rio Grande by interpreting changes in resistivity (Dunbar and others, 2004). The data were collected by a helicopter towing a RESOLVE electromagnetic sensor (Fugro Airborne Surveys, 2013) about 100 ft below the helicopter and at a height of about 100 ft above the ground in three passes along the Rio Grande levees: one pass along the center of the levee and additional passes on each side of the center line at a spacing of 164 ft from the center (fig. 9). Data were collected at five frequencies (100, 25, 6.2, 1.5, and 0.4 kilohertz) along with power line noise and magnetometer data. The rate of collection was set so that a data point was measured at about every 10 ft (about 10 samples per second). The collected data were leveled, or corrected to account for equipment drift (drift corrected), and processed by Fugro Airborne Surveys. Measured conductivity values were converted to apparent conductivity values to remove variations in the data caused by changes in transmitter-receiver separations, frequency, or time. The Sengpiel conductivity-depth method (Cain, 2002) was used to obtain the depths associated with the apparent conductivity values. A detailed description of the data collection and processing can be found in the Fugro

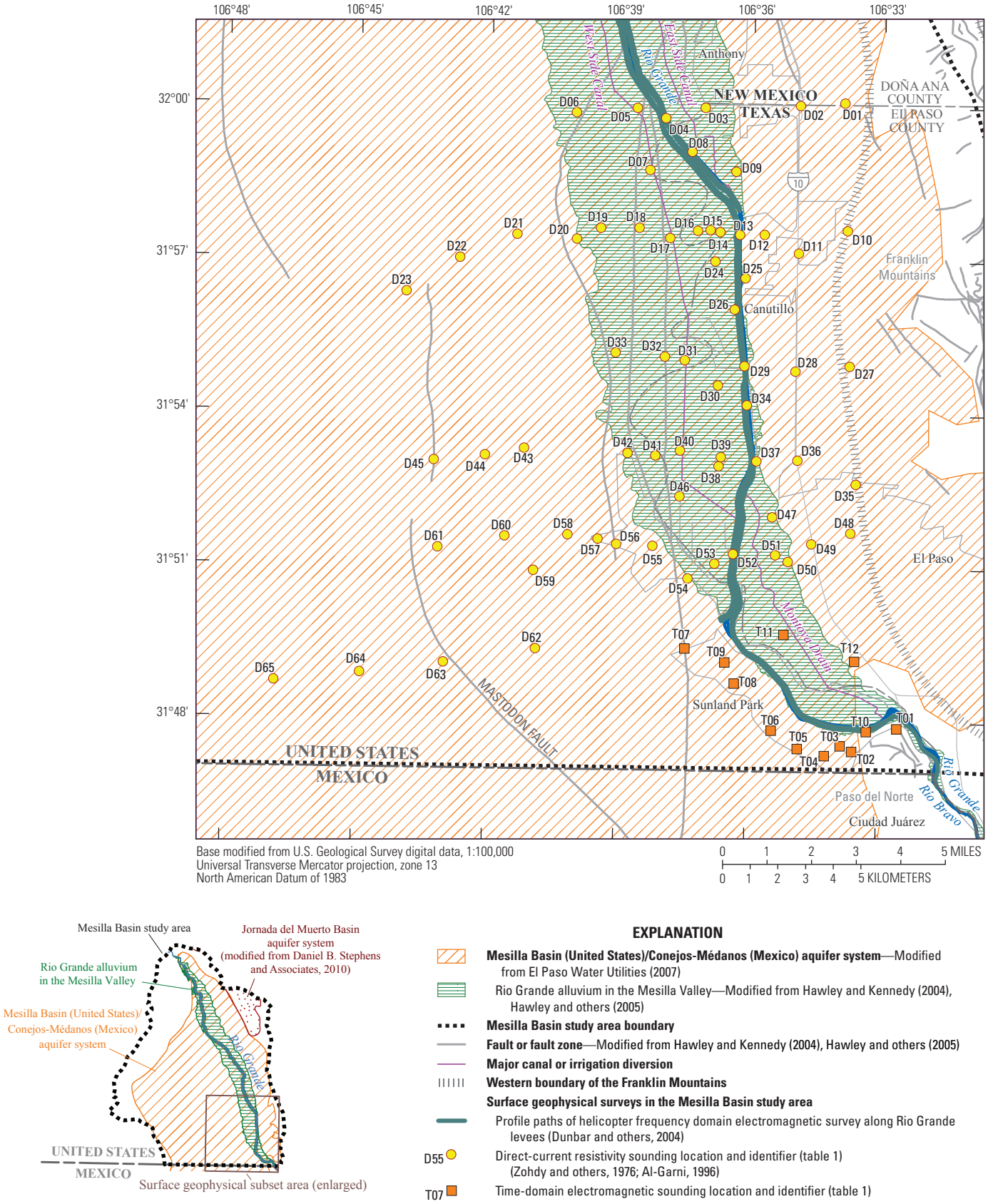

Figure 9. Location of geophysical surveys in the surface geophysical subset area of the Mesilla Basin study area in Doña Ana County, New Mexico, and El Paso County, Texas, 2012.

Table 1. Direct-current resistivity and time-domain electromagnetic sounding locations in the surface geophysical subset area of the Mesilla Basin study area in Doña Ana County, New Mexico, and El Paso County, Texas, October 2012.

[ft, foot; NAVD 88, North American Vertical Datum of 1988; DC, direct-current; TDEM, time-domain electromagnetic]

Site identifier (fig. 9)	Latitude (decimal degrees)	Longitude (decimal degrees)	Land-surface altitude (ft) (NAVD 88)	Geophysical method
D01	32.00167	106.56518	4,042	DC
D02	32.00068	106.58218	3,912	DC
D03	31.99963	106.61851	3,792	DC
D04	31.99610	106.63359	3,784	DC
D05	31.99930	106.64450	3,794	DC
D06	31.99762	106.66770	3,791	DC
D07	31.97917	106.63931	3,788	DC
D08	31.98526	106.62332	3,789	DC
D09	31.97901	106.60642	3,796	DC
D10	31.96014	106.56355	4,111	DC
D11	31.95264	106.58210	3,933	DC
D12	31.95856	106.59526	3,824	DC
D13	31.95845	106.60468	3,782	DC
D14	31.95929	106.61224	3,781	DC
D15	31.95987	106.61597	3,781	DC
D16	31.95961	106.62080	3,782	DC
D17	31.95713	106.63133	3,783	DC
D18	31.96031	106.64311	3,784	DC
D19	31.96011	106.65783	3,787	DC
D20	31.95647	106.66696	3,792	DC
D21	31.95773	106.68974	4,048	DC
D22	31.94999	106.71144	4,106	DC
D23	31.93879	106.73171	4,124	DC
D24	31.94970	106.61396	3,778	DC
D25	31.94436	106.60237	3,788	DC
D26	31.93412	106.60633	3,773	DC
D27	31.91605	106.56212	4,085	DC
D28	31.91422	106.58277	3,890	DC
D29	31.91574	106.60233	3,771	DC
D30	31.90934	106.61233	3,766	DC
D31	31.91741	106.62511	3,769	DC
D32	31.91849	106.63272	3,773	DC
D33	31.91962	106.65158	3,776	DC
D34	31.90301	106.60119	3,762	DC
D35	31.87766	106.55917	4,048	DC
D36	31.88523	106.58159	3,853	DC
D37	31.88483	106.59720	3,768	DC
D38	31.88308	106.61164	3,760	DC
D39	31.88604	106.61078	3,761	DC
D40	31.88799	106.62643	3,761	DC
D41	31.88630	106.63582	3,763	DC
D42	31.88695	106.64640	3,771	DC
D43	31.88820	106.68594	4,067	DC
D44	31.88584	106.70083	4,109	DC
D45	31.88401	106.72033	4,111	DC
D46	31.87309	106.62640	3,759	DC
D47	31.86668	106.59092	3,759	DC
D48	31.86176	106.56097	4,052	DC
D49	31.85805	106.57584	3,835	DC
D50	31.85225	106.58470	3,756	DC
D51	31.85435	106.58956	3,755	DC
D52	31.85454	106.60564	3,752	DC
D53	31.85131	106.61270	3,752	DC
D54	31.84639	106.62285	3,757	DC
D55	31.85689	106.63645	3,776	DC
D56	31.85730	106.65024	3,839	DC
D57	31.85897	106.65739	3,867	DC
D58	31.86019	106.66890	3,904	DC
D59	31.84846	106.68177	4,084	DC
D60	31.85953	106.69292	4,108	DC
D61	31.85561	106.71842	4,112	DC
D62	31.82299	106.68062	4,113	DC
D63	31.81821	106.71566	4,093	DC
D64	31.81464	106.74751	4,096	DC
D65	31.81176	106.78020	4,111	DC
T01	31.79828	106.54236	3,821	TDEM
T02	31.79069	106.55946	3,780	TDEM
T03	31.79250	106.56389	3,784	TDEM
T04	31.78923	106.56986	3,844	TDEM
T05	31.79141	106.58021	3,858	TDEM
T06	31.79726	106.59025	3,867	TDEM
T07	31.82361	106.62361	3,921	TDEM
T08	31.81241	106.60460	3,861	TDEM
T09	31.81924	106.60831	3,852	TDEM
T10	31.79721	106.55401	3,738	TDEM
T11	31.82847	106.58592	3,746	TDEM
T12	31.82004	106.55882	3,752	TDEM

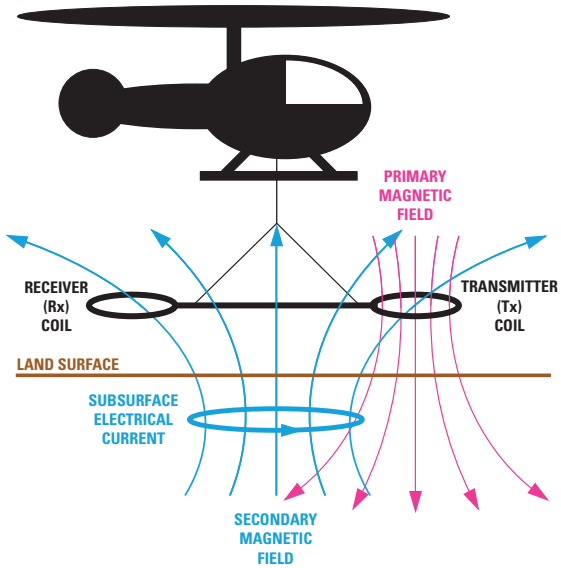

Figure 10. The helicopter frequency domain electromagnetic method (modified from Teeple and others, 2009).

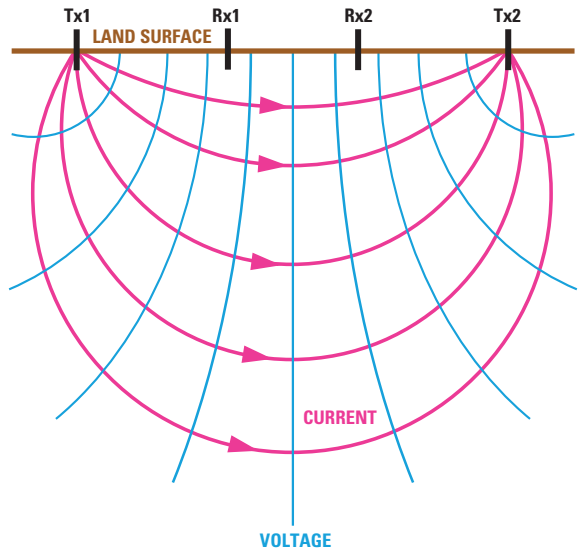

EXPLANATION

Tx1	Transmitting electrode 1
Tx2	Transmitting electrode 2
Rx1	Receiving electrode 1
Rx2	Receiving electrode 2

Figure 11. The direct-current resistivity method.

Airborne Surveys report by Cain (2002). The HFEM data published by Cain (2002) were used by the USGS to identify electrical changes within the subsurface that could be related to geochemical changes. For this study, the 121 mi of HFEM data were converted from apparent conductivity values to apparent resistivity values and gridded in 3-D by using a kriging method with a horizontal grid spacing of 330 by 330 ft (100 by 100 meters [m]) and a vertical spacing of 10 ft. The spacing of the horizontal and vertical grids for the HFEM data was large compared to the actual data collection because of the need for a direct comparison between the HFEM grid and the DC resistivity and TDEM sounding grid. Two-dimensional grid data were extracted from the 3-D grid for viewing on surface maps. The kriging method used to create this 3-D grid is described in Geosoft, Inc. (2012).

Direct-Current Resistivity

The previously published DC resistivity soundings used in this assessment were obtained from an array of four electrodes (two Tx electrodes and two Rx electrodes) inserted into the soil to measure bulk electrical resistivity in the subsurface for a given point on the Earth's surface (fig. 11). A known current was transmitted into the subsurface through the Tx electrodes, and the resulting electrical potential was measured as a voltage change between the two Rx electrodes. Using the known current and the measured voltage values, a resistance (the relative ability of earth material to transmit a current) was calculated by using Ohm's law. The apparent resistivity of the subsurface was obtained by multiplying the resistance by a geometric factor dependent on the array geometry (Zohdy and others, 1974). By increasing the distance between electrodes, the Tx current flows deeper into the subsurface, with the resulting voltage potential measured at the Rx electrodes representative of bulk electrical characteristics at greater depth. The typical simplified model used to calculate apparent resistivity is based on the assumption of a completely uniform (homogenous and isotropic) earth material (Keller and Frischknecht, 1966). A more realistic representation of the subsurface resistivity is obtained through inverse modeling, which is the iterative optimization of a series of forward models to compute the resistivity of an equivalent non-uniform earth material. A description of the DC resistivity method and tables of the electrical properties of earth materials can be found in Zohdy and others (1974), Sumner (1976), and Sharma (1997).

Zohdy and others (1976) published results from 65 DC resistivity soundings collected within the study area to analyze hydrogeology within the lower Mesilla Valley. These data were later reprocessed by using sophisticated inversion techniques and published by Al-Garni (1996). The reprocessed DC resistivity soundings (table 1, fig. 9) were used to identify areas of low bulk resistivity (less than 10 ohm-m) that could be associated with sediments having either a large amount of clayey deposits or high concentration of dissolved solids in the pore water. Detailed descriptions of the data collection, processing, and analysis can be found in Zohdy and others (1976) and Al-Garni (1996).

Time-Domain Electromagnetic Surveys

TDEM instruments measure the bulk resistivity of the subsurface by producing an alternating electrical current in a Tx loop deployed on the land surface. The Tx signal of most systems consists of equal periods of time when current is turned on or off, commonly referred to as "on-time" and "off-time" (North Carolina Division of Water Resources, 2004). Termination of the current is not instantaneous but occurs over a period of a few microseconds, known as the ramp time, during which a time-varying magnetic field is produced. This time-varying primary field propagates in a largely diffusive manner and induces eddy currents in the ground beneath the Rx coil (fig. 12). As the eddy currents subsequently decay, they produce secondary electromagnetic fields, and a portion of the secondary fields propagates back to the surface. The secondary electromagnetic fields are measured by using the Rx coil during the off-time period. The depth of investigation, therefore, depends not only on the size of the Tx loop and the magnitude of the Tx current but also on the time interval after current shutoff; as the time interval lengthens, the Rx measures eddy currents at progressively greater depths. The intensity of the eddy currents at specific times and depths is determined by the combined electrical conductivity of the subsurface lithology and pore fluid (Stewart and Gay, 1986). An apparent resistivity value can be calculated by using the magnitude of the eddy current strength at specific times. Multiple TDEM measurements, where a single measurement is a "stack" (the compilation of datasets collected during the integration time), are averaged to obtain a final mean TDEM sounding (Teeple and others, 2009).

In October 2012, 12 TDEM soundings (Teeple, 2017) were collected near the southeastern part of the study area (in the surface geophysical subset area) by the USGS to provide more information on the area south of where the DC resistivity soundings had been collected (table 1, fig. 9). TDEM soundings were collected by using the Zonge GDP-32^{II} Rx and the ZeroTEM Tx (Zonge International, 2013). The ZeroTEM setup uses a multiturn Rx coil to measure electromagnetic fields in the center of the Tx loop (fig. 12). At each sounding location, data were collected at 2 hertz (Hz), and 20 stacks were collected using an integration time of 64 seconds. A trimmed mean (Helsel and Hirsch, 2002) was calculated for all of the 20 stacks, and the resulting mean was stored in one sounding. The trimmed mean represents the central tendency of a dataset after a selected percentage of the highest and lowest values have been removed. In our application, 5 percent of the data from each end of the distribution were removed, and a mean of the central 90 percent of the data was computed. The means of each time gate (discrete voltages measured at increasingly later times after shutoff of the current) were saved as processed data files for use in the inversion software (Interpex Limited, 1996).

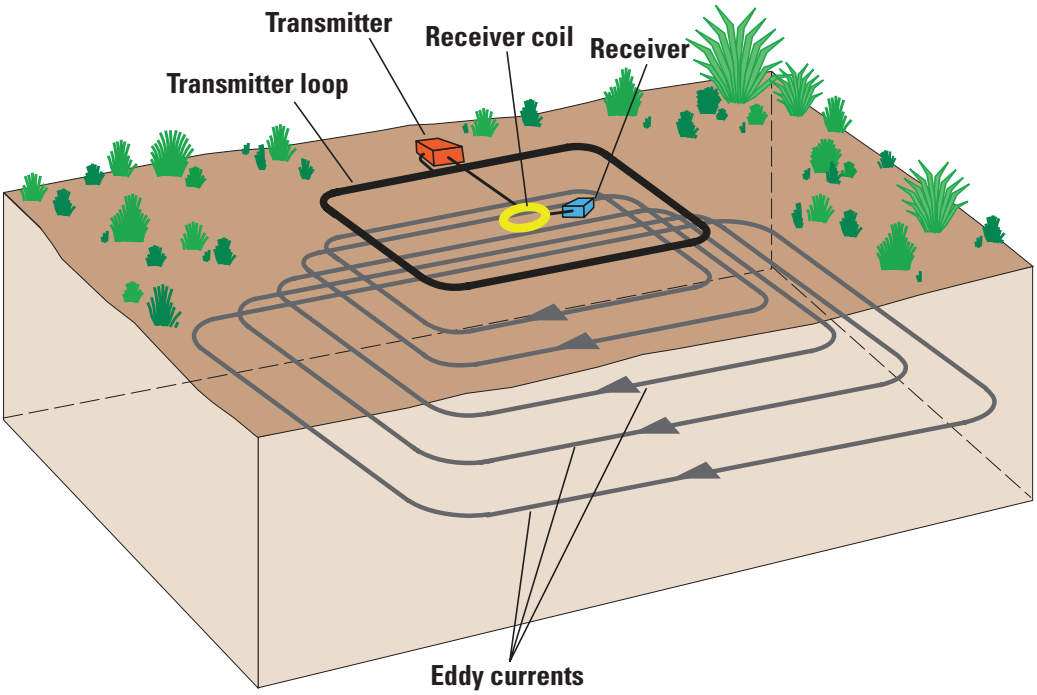

Figure 12. The time-domain electromagnetic method (modified from North Carolina Division of Water Resources, 2004).

Inverse modeling is the process of estimating the spatial distribution of subsurface resistivity from the measured voltage. The IX1D v3 program, developed by Interpex Limited (1996), was used for inverse modeling of the TDEM soundings. A smooth inverse model (a multilayered model that holds the depth values fixed and allows the resistivity values to vary during inversion) was fit to the data by using Occam's inversion principle, a preferred-homogeneity regularization condition (Constable and others, 1987). After inversion, data points that substantially deviated from the smooth-model curve, generally near the noise threshold in the area, were removed on a case-per-case basis. For this report, root mean square errors (RMSEs) between the measured apparent resistivity and the calculated apparent resistivity of 10 percent or less were considered acceptable. The RMSE is derived from the residuals between the measured apparent resistivity and the calculated apparent resistivity, as given in the following equation:

$$RMSE = \sqrt{\frac{1}{n}\sum_{i=1}^{n}(M_i - C_i)^2} \qquad (1)$$

where

RMSE is root mean square error,
n is the number of observations,
i is the given time step,
M is the measured apparent resistivity at the given time step, and
C is the calculated apparent resistivity at the given time step.

The inverse modeling results of the final processed TDEM data collected throughout the geophysical subset area had RMSEs of less than 10 percent for all soundings collected. Because of the similar depth and resistivity response by the DC resistivity and TDEM soundings, the data were gridded together into a 3-D grid by using a 3-D-kriging method using the default kriging parameters with a horizontal grid spacing of 330 by 330 ft (100 by 100 m) and a vertical spacing of 10 ft. Two-dimensional grids can be extracted from the 3-D grid for viewing on surface maps.

Geophysical Integration

Zohdy and others (1976) and Al-Garni (1996) discussed the use of geophysical methods to assess the hydrogeology, referred to herein as "geophysical integration." Zohdy and others (1976) and Al-Garni (1996) state that resistivity values less than 10 ohm-m can represent sediments composed largely of clay (clayey deposits), sediments composed largely of sand and gravel deposits saturated with saline water, or both. For this report, resistivity values of 10 ohm-m or less were used to help identify areas in the subsurface where saline water might be present in the interstitial pore-space of sand and gravel deposits.

Near the land surface (that is, at or about 0 ft bls), the HFEM profiles indicated that the resistivity was generally greater than 20 ohm-m along the reach of the Rio Grande corresponding to the location of the levees that were the target of the HFEM investigation (fig. 13) (Dunbar and others, 2004). Near-surface resistivity values were less than 10 ohm-m in some reaches along the Rio Grande west of Anthony, N. Mex., and near the Paso del Norte. With increasing depth, resistivity values less than 10 ohm-m were increasingly measured; about half of the resistivity values were less than 10 ohm-m at depths of 50 and 100 ft. Near Vado, N. Mex., there were transitions at 50 and 100 ft bls where the resistivity values changed from relatively high resistivity values (greater than 20 ohm-m) to relatively low resistivity values (less than 10 ohm-m).

Slightly more than 25 percent of the gridded resistivity values from the 3-D grid of the combined inverse modeling results of the DC resistivity and TDEM soundings were low, less than or equal to 10 ohm-m. When the 3-D resistivity grid was clipped (that is, grid cells with values larger than 10 ohm-m were omitted), depth-dependent regions of low resistivity are apparent in the southernmost part of the study area near the Paso del Norte (fig. 14, a 3-D figure in an interactive Portable Document Format [PDF] file, available at https://doi.org/10.3133/sir20175028). These regions of low resistivity are spatially the widest at or below the top of the bedrock. Although low resistivity can be indicative of clayey deposits, from the 3-D depictions of the resistivity data, it appears there are sand and gravel deposits saturated with saline water. There is likely a plume of groundwater emanating as dense, highly saline water upwelling through fractures within the bedrock. It is unlikely that clayey deposits would be embedded in the shape and orientation of the region of low resistivity observed from the 3-D depictions of the alluvial-fluvial environment in which the Santa Fe group was formed (Frenzel and Kaehler (1992). The change in gridded resistivity values with depth indicates that the low resistivity zones penetrated the land surface to the east of the Rio Grande near the base of the Franklin Mountains and continued to the south to the Paso del Norte (fig. 15). The length of the low resistivity zone expanded northward with depth.

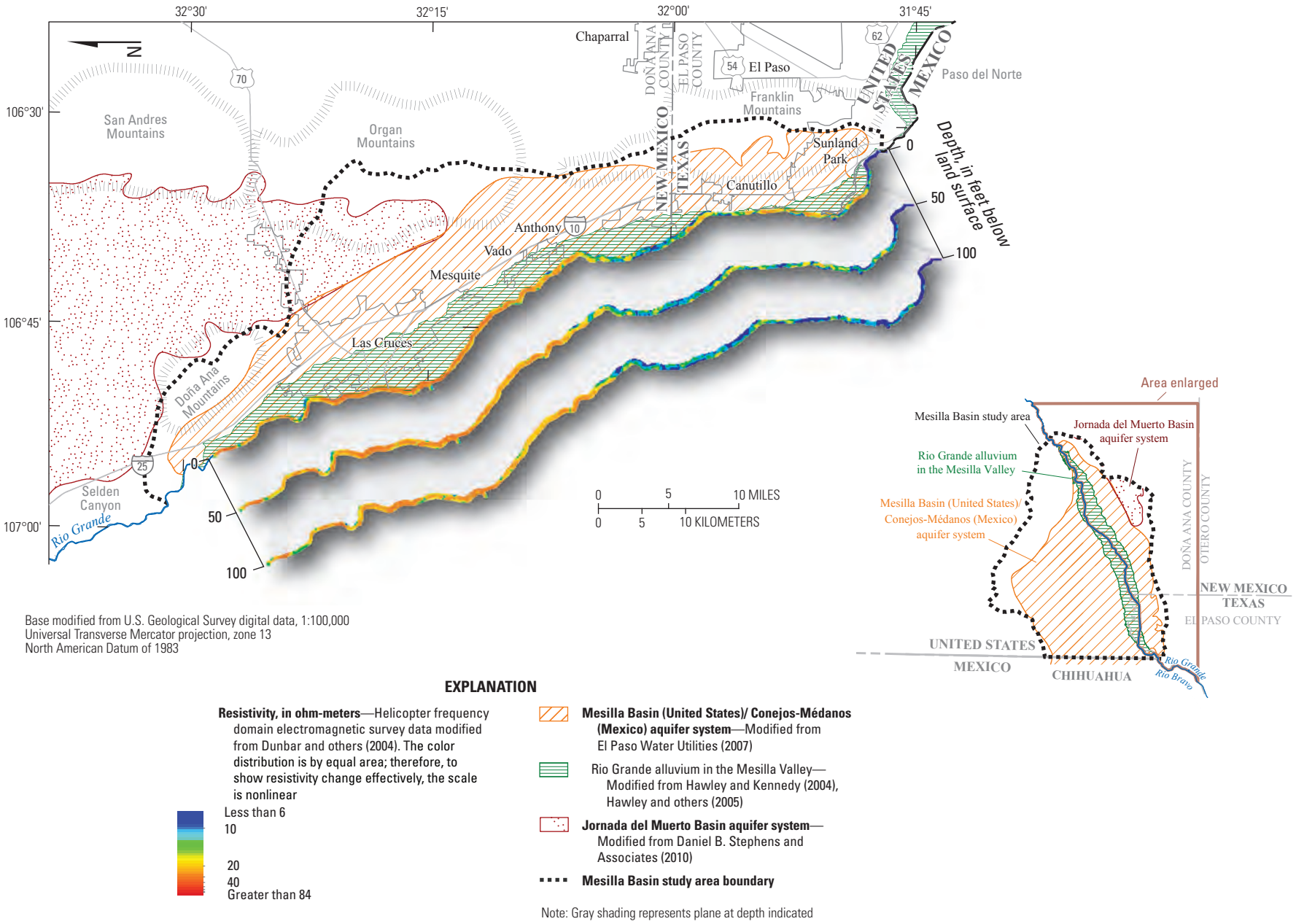

Figure 13. Gridded resistivity values from the helicopter frequency domain electromagnetic survey data (from Dunbar and others, 2004) in the Mesilla Basin study area in Doña Ana County, New Mexico, and El Paso County, Texas.

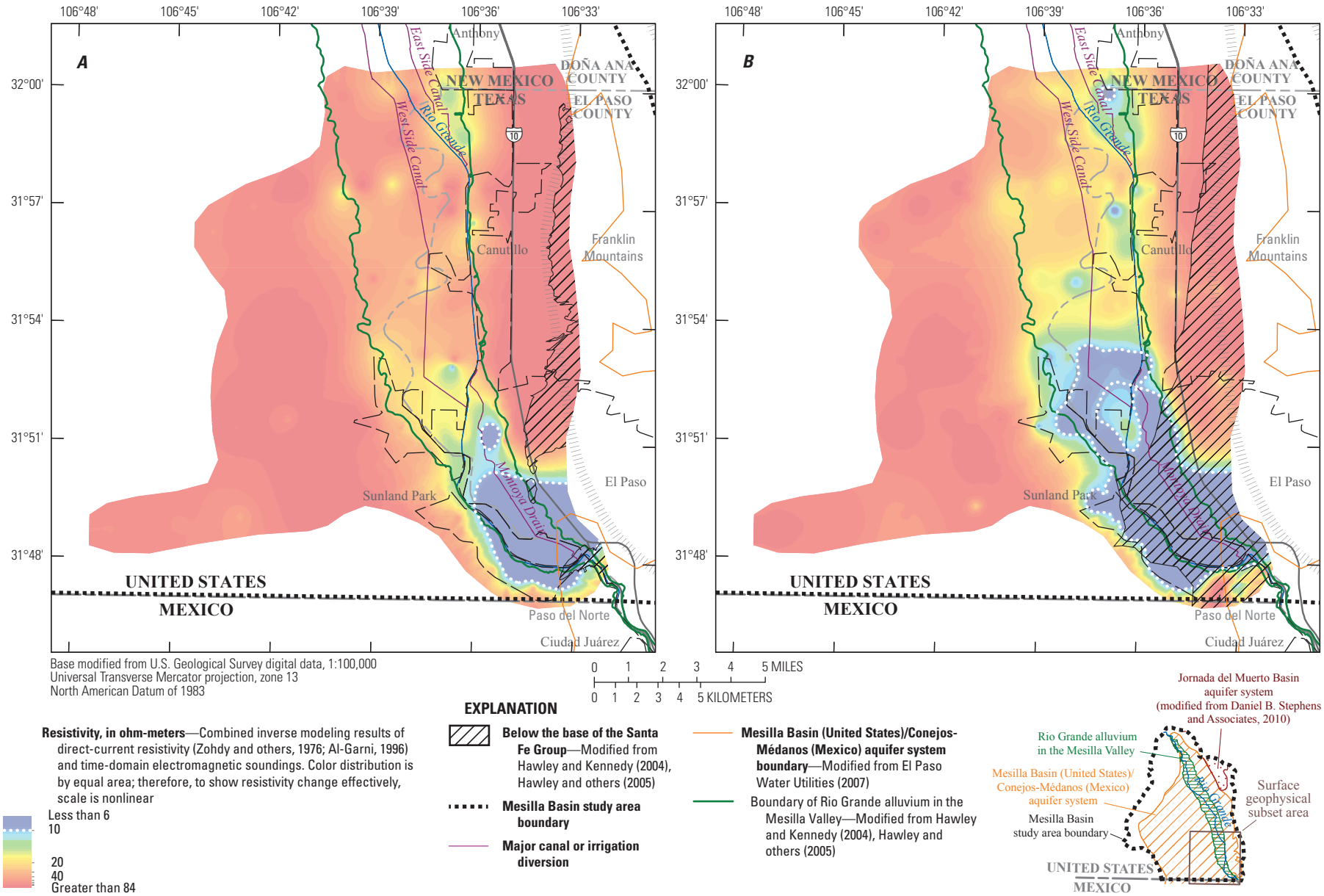

Figure 15. Gridded resistivity values from the combined inverse modeling results of the direct-current resistivity and time-domain electromagnetic soundings at various depths below land surface in the surface geophysical subset area of the Mesilla Basin study area in Doña Ana County, New Mexico, and El Paso County, Texas. *A*, 0 feet. *B*, 250 feet. *C*, 500 feet. *D*, 750 feet. *E*, 1,000 feet. *F*, 1,250 feet. *G*, 1,500 feet. *H*, 1,750 feet.

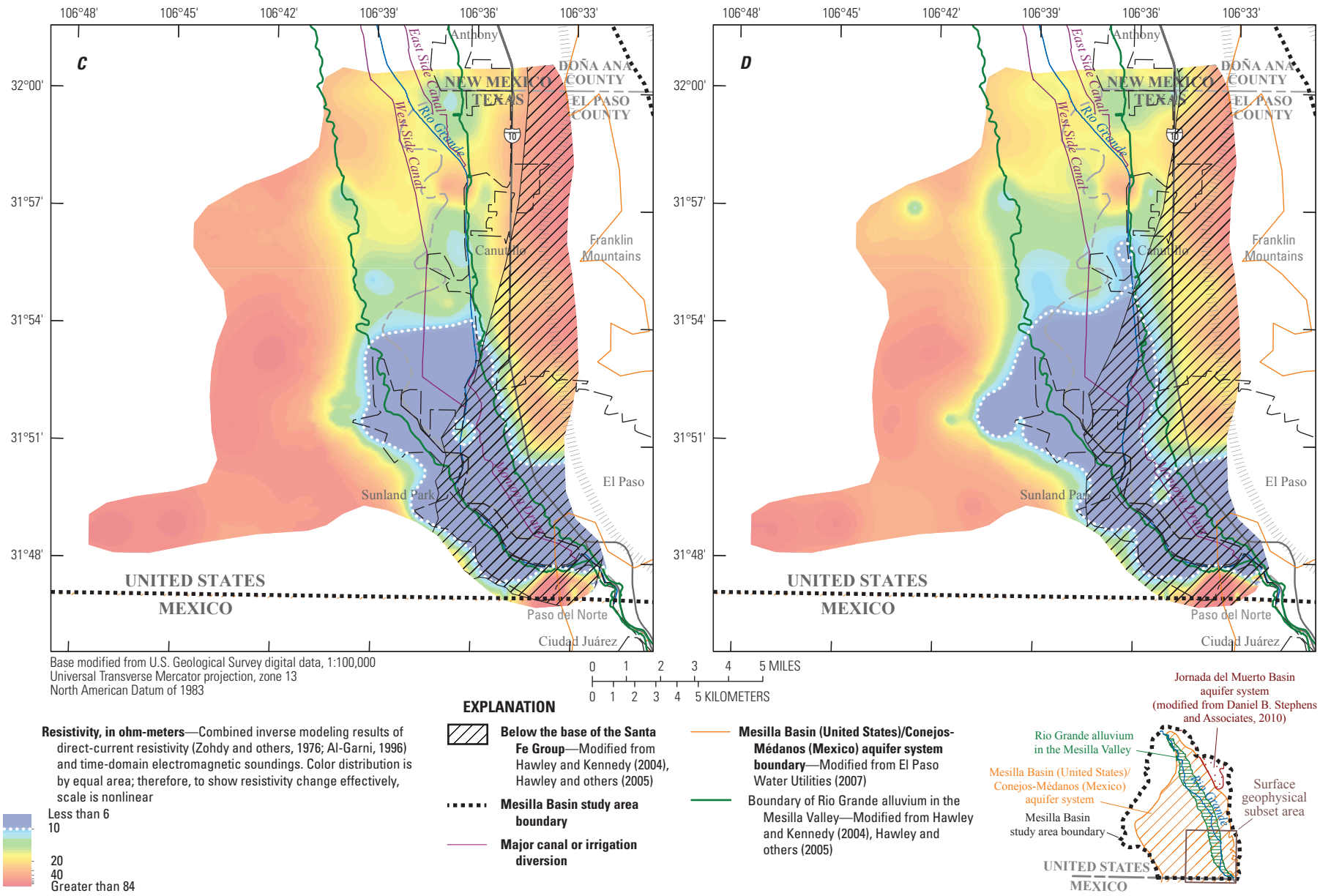

Figure 15. Gridded resistivity values from the combined inverse modeling results of the direct-current resistivity and time-domain electromagnetic soundings at various depths below land surface in the surface geophysical subset area of the Mesilla Basin study area in Doña Ana County, New Mexico, and El Paso County, Texas. *A*, 0 feet. *B*, 250 feet. *C*, 500 feet. *D*, 750 feet. *E*, 1,000 feet. *F*, 1,250 feet. *G*, 1,500 feet. *H*, 1,750 feet.—Continued

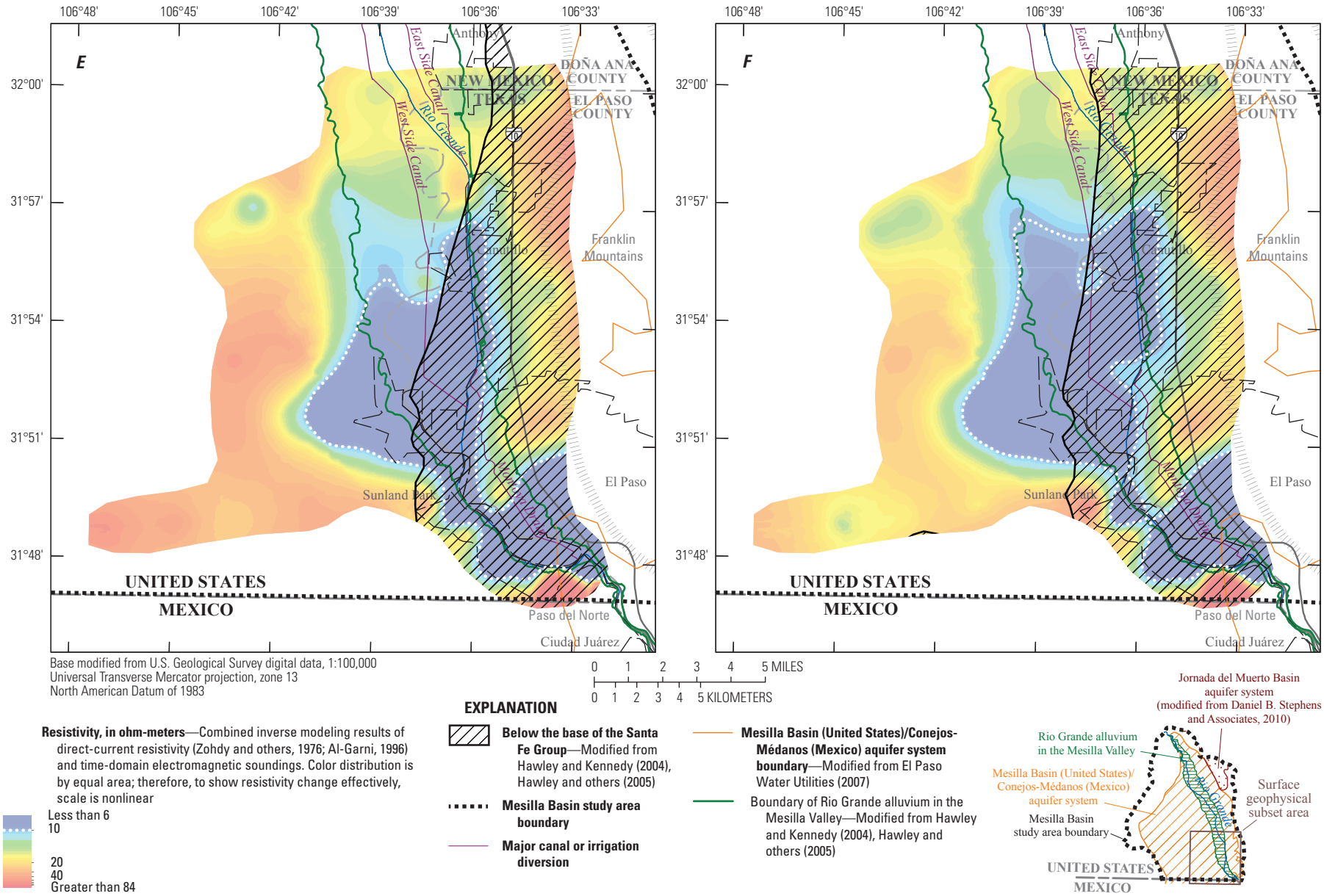

Figure 15. Gridded resistivity values from the combined inverse modeling results of the direct-current resistivity and time-domain electromagnetic soundings at various depths below land surface in the surface geophysical subset area of the Mesilla Basin study area in Doña Ana County, New Mexico, and El Paso County, Texas. *A*, 0 feet. *B*, 250 feet. *C*, 500 feet. *D*, 750 feet. *E*, 1,000 feet. *F*, 1,250 feet. *G*, 1,500 feet. *H*, 1,750 feet.—Continued

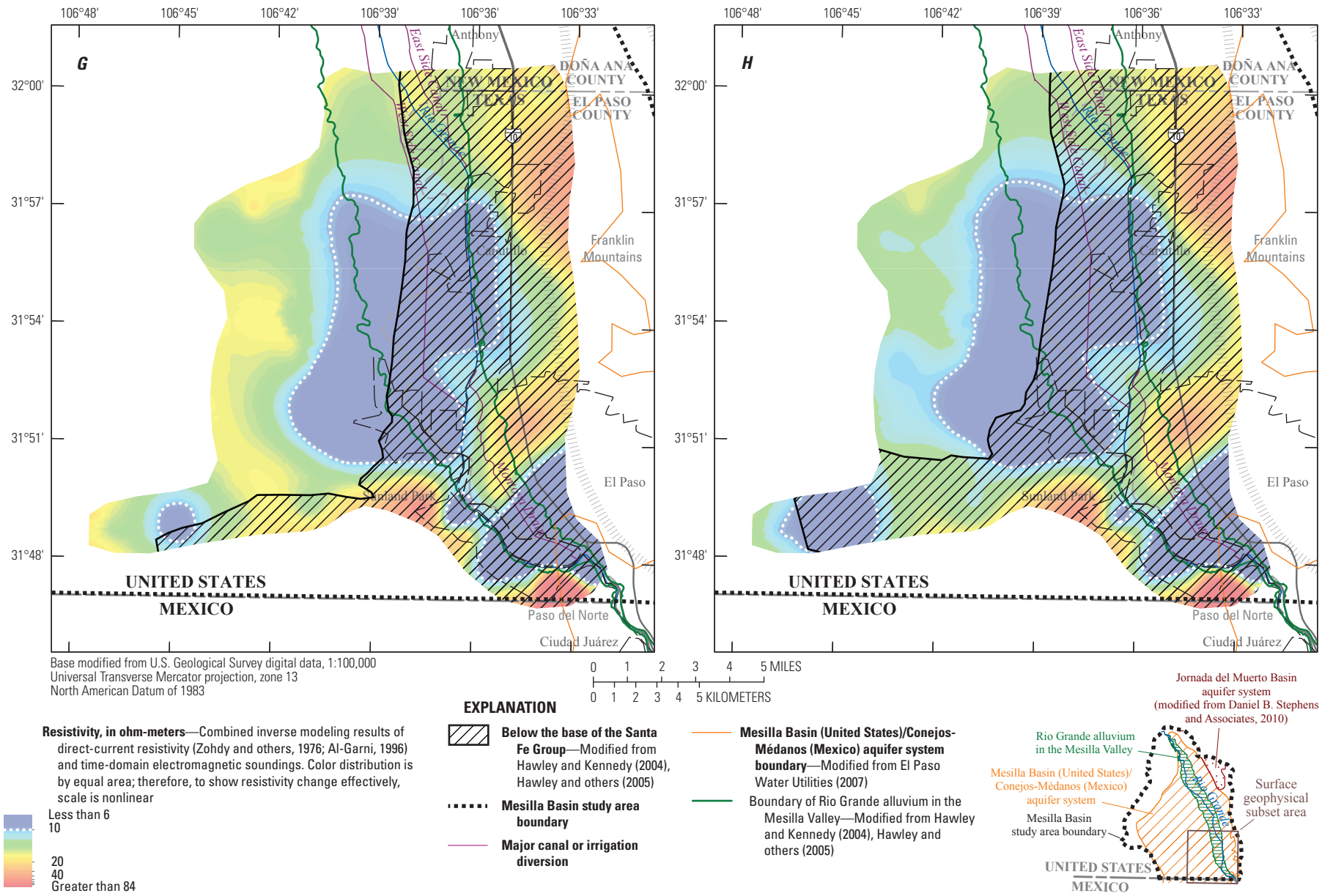

Figure 15. Gridded resistivity values from the combined inverse modeling results of the direct-current resistivity and time-domain electromagnetic soundings at various depths below land surface in the surface geophysical subset area of the Mesilla Basin study area in Doña Ana County, New Mexico, and El Paso County, Texas. *A*, 0 feet. *B*, 250 feet. *C*, 500 feet. *D*, 750 feet. *E*, 1,000 feet. *F*, 1,250 feet. *G*, 1,500 feet. *H*, 1,750 feet.—Continued

Comparison of Geophysical Results to Historical Dissolved-Solids Concentrations

Historical dissolved-solids-concentration data within the surface geophysical subset area of the study area were compiled and compared to the inverse modeling results of the combined DC resistivity and TDEM soundings. This comparison was done to strengthen the interpretation made from the combined inverse modeling results that the low resistivity features were representative of sand and gravel deposits saturated with saline water and not clayey deposits. Dissolved-solids concentrations are a common measure used to identify salinity of water. Winslow and Kister (1956) identified ranges of dissolved-solids concentrations that represent certain classifications in salinity of water. These dissolved-solids-concentration ranges were used to separate the historical dissolved-solids concentrations into salinity groups (table 2). Conductivity (the inverse of resistivity) has a strong correlation to salinity in that a greater salt concentration causes greater conductivity; therefore, when salinity decreases, the resistivity increases (Kemker, 2014). With a correlation between salinity and dissolved solids, a decrease in dissolved solids would indicate greater resistivity values. In general, the resistivity in freshwater streams ranges from 5 to 100 ohm-m depending on the degree to which the freshwater is influenced by saltwater—100-ohm-m resistivity values indicate little saltwater influence, and 5-ohm-m resistivity values indicate appreciable saltwater influence. Where the inflows of saltwater are extreme, freshwater resistivity values of less than 5 ohm-m are possible (Kemker, 2014). The exact conductivity values are not universally consistent but are related to the ionic composition of the water, the formation resistivity, and the temperature of the medium (Ken E. Davis Associates, 1988).

Historical dissolved-solids-concentration data were compiled from readily available sources such as databases from the USGS National Water Information System (NWIS) (U.S. Geological Survey, 2017), Texas Water Development Board (2012), New Mexico Office of the State Engineer (2014), New Mexico Office of Border Health (2014), and El Paso Water Utilities (2007), as well as from published reports such as Wilson and others (1981) and Witcher and others (2004). The focus of the compilation was obtaining dissolved-solids-concentration data that could be referenced spatially in the subsurface on the basis of reported sampling depths or could be referenced on the basis of sampling depths estimated from reported screened intervals, open-hole intervals, or total well depths (open holes and completed wells are both referred to as “wells” in this report).

Dissolved-solids-concentration data collected during 1922–2007 were compiled from 239 wells (table 3, at back of report); on occasion, two or more values were compiled for a given well (table 4, at back of report; fig. 16). Sample depths were reported for most of the dissolved-solids-concentration data (table 4, at back of report). For dissolved-solids-concentration data that did not have a reported sampling depth, the sampling depth was estimated as the midpoint of the screened or open-hole interval of the well (tables 3 and 4, at back of report). If multiple screened or open-hole intervals were associated with the well, the midpoint between the top of the uppermost screened or open-hole interval and the bottom of the lowermost screened or open-hole interval was used to estimate the sampling depth of the screened or open-hole sections of the well. This estimation was done under the assumption that the sampled groundwater came from each of the screened or open-hole intervals. If no screened or open-hole interval was reported for a well, the total depth of the well was used for the sampling depth, with the assumption that the well is cased to the bottom and the opening to the well is at the base of the well.

The dissolved-solids concentrations were plotted spatially with the 3-D resistivity grid to depict where high and low extremes of the dissolved-solids concentrations were located with respect to the low resistivity zones interpreted as sediments composed largely of sand and gravel deposits saturated with saline water (fig. 17, a 3-D figure in an interactive PDF file, available at https://doi.org/10.3133/sir20175028). The dissolved-solids concentrations in the northern part of the surface geophysical subset area were generally less than 1,000 mg/L, representing freshwater (table 2), especially with increasing depth. There were some dissolved-solids concentrations near the surface in the northern part of the surface geophysical subset area within the slightly saline classification (table 2). Those concentrations were most likely slightly saline because of localized seepage of relatively saline water with dissolved-solids concentrations of more than 1,000 mg/L from the Rio Grande into the Rio Grande alluvium. In the southern part of the surface geophysical subset area, where low resistivity was often measured in the subsurface, dissolved-solids concentrations of more than 1,000 mg/L were common, especially with increasing depth (fig. 17, a 3-D figure in an interactive PDF file, available at https://doi.org/10.3133/sir20175028). Some dissolved-solids concentrations were greater than 3,000 mg/L in the southern part of the surface geophysical subset area, representing moderately to very saline water (table 2).

Table 2. Fresh and saline water classified by dissolved-solids concentration (modified from Winslow and Kister, 1956).

Classifications of fresh and saline water	Dissolved-solids concentration (milligrams per liter)
Freshwater	Less than 1,000
Slightly saline	1,000 to 3,000
Moderately saline	3,000 to 10,000
Very saline	10,000 to 35,000

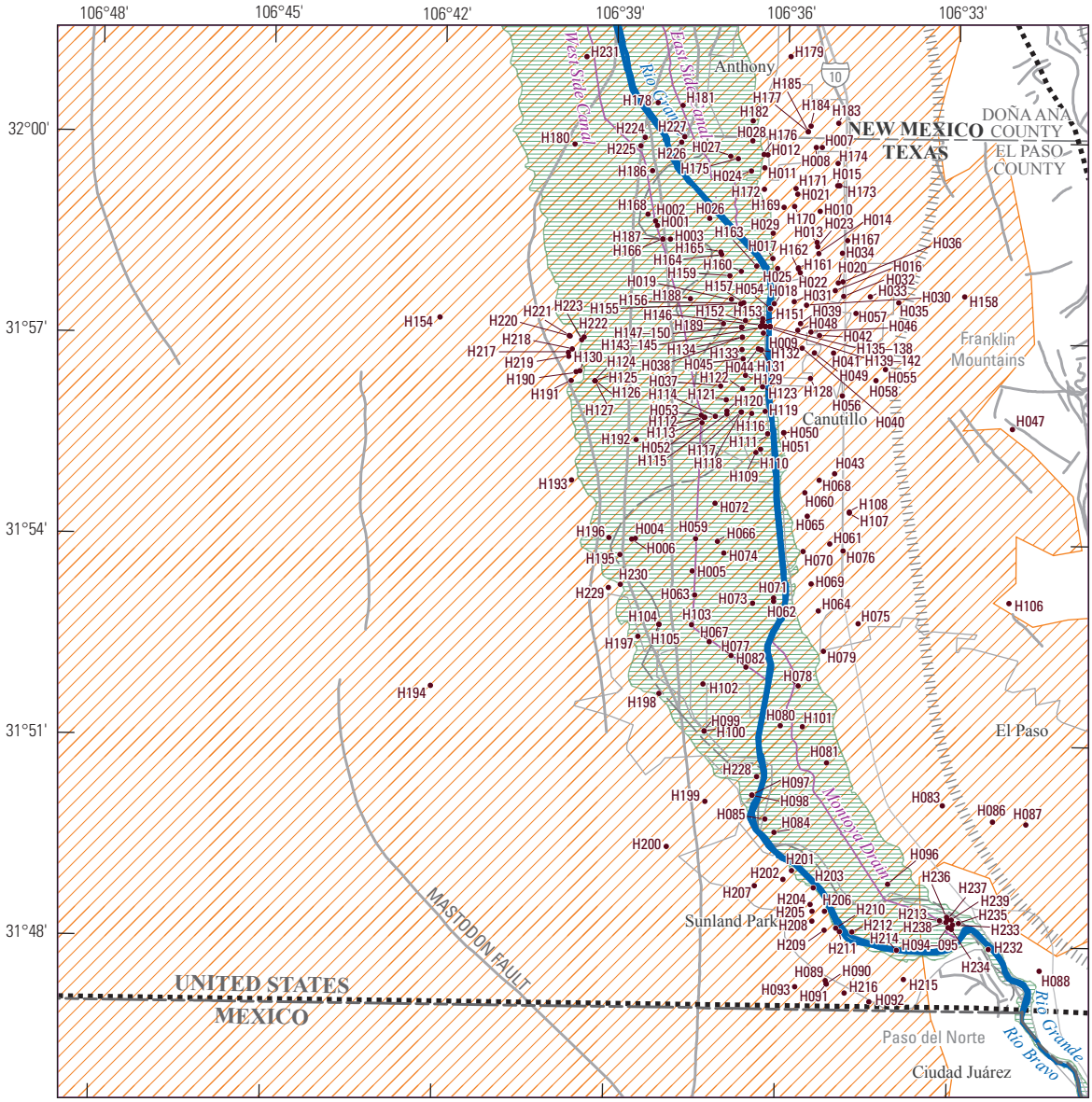

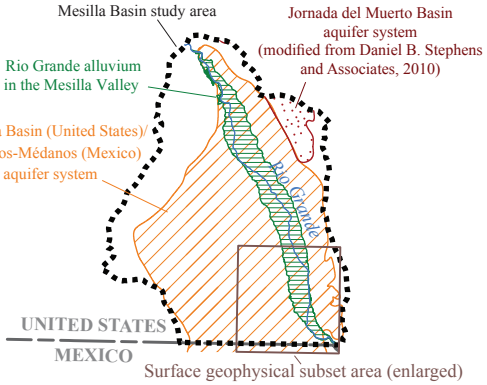

EXPLANATION

- **Mesilla Basin (United States)/Conejos-Médanos (Mexico) aquifer system**—Modified from El Paso Water Utilities (2007)
- Rio Grande alluvium in the Mesilla Valley—Modified from Hawley and Kennedy (2004), Hawley and others (2005)
- **Mesilla Basin study area boundary**
- **Fault or fault zone**—Modified from Hawley and Kennedy (2004), Hawley and others (2005)
- **Major canal or irrigation diversion**
- **Western boundary of the Franklin Mountains**
- H055 **Historical (1922–2007) geochemical dissolved-solids sampling site and identifier (table 3)**

Figure 16. Locations of wells where historical (1922–2007) dissolved-solids-concentration data were collected in the surface geophysical subset area of the Mesilla Basin study area in Doña Ana County, New Mexico, and El Paso County, Texas.

The resistivity was obtained from the 3-D model of DC resistivity and TDEM soundings at the depth the sample was collected (table 4, at back of report). These resistivity values were plotted against the dissolved-solids concentrations to determine if there was a correlation between dissolved-solids concentration and resistivity (fig. 18). Higher dissolved-solids concentrations were generally associated with lower resistivity values (less than or equal 10 ohm-m), and lower dissolved-solids concentrations were generally associated with higher resistivity values (greater than 10 ohm-m). Despite this general pattern, there was too much variability to fit a regression line to the data. This variability might be caused by different amounts of clayey deposits in the sediments.

The dissolved-solids concentrations were separated into depth ranges to plot with the gridded resistivity values at depth increments of 250 ft ranging from 0 to 1,750 bls referred to as "depth slices" to provide a more direct visual comparison between the dissolved-solids concentrations and the resistivity data (fig. 19). The midpoints of these ranges were where the resistivity depth slices were plotted in figure 15. The dissolved-solids concentrations were projected, therefore, to the midpoint depth within the respective ranges and were plotted with the appropriate resistivity depth slice (for example, concentrations representing depths between 125 and 375 ft bls were projected onto the 250-ft resistivity depth slice). All of the dissolved-solids concentrations with a sampling depth less than 125 ft bls were projected to a depth of 0 ft.

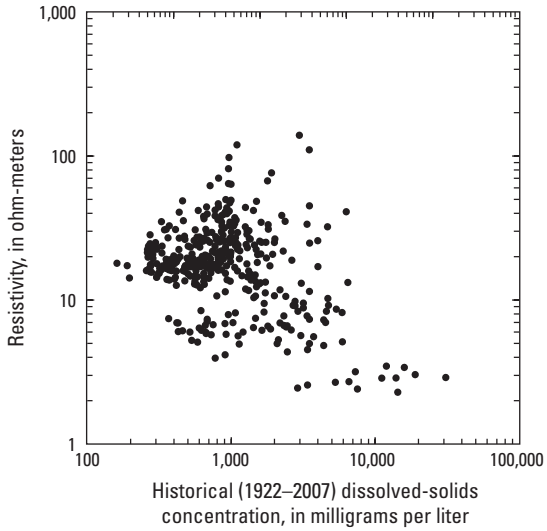

Note: Resistivity data are from the combined inverse modeling results of the direct-current resistivity (Zohdy and others, 1976; Al-Garni, 1996) and time-domain electromagnetic soundings that were collected in the study area.

Figure 18. Resistivity relative to historical (1922–2007) dissolved-solids concentrations in the surface geophysical subset area of the Mesilla Basin study area in Doña Ana County, New Mexico, and El Paso, Texas.

Comparing the dissolved-solids concentrations to the resistivity values with increasing depth, the wells from which samples with dissolved-solids concentrations greater than 1,000 mg/L were collected tended to be within or near areas of low resistivity (fig. 19) except for the depth slice of 0 ft (fig. 19*A*). In the depth slice at 0 ft, there were multiple samples that had dissolved-solids concentrations of greater than 1,000 mg/L that were within or near areas of high resistivity, but most of these samples were in areas where the resistivity was not within the extreme highs of greater than 52 ohm-m. The relatively low resistivity values (less than 52 ohm-m) in these areas indicated that there may be water present with appreciable amounts of dissolved solids. In the depth slice of 250 ft bls (fig. 19*B*), there were some low resistivity features in the northern part of the surface geophysical subset area that correlate with the dissolved-solids concentrations in this area, indicating that there was some slightly saline (1,000–3,000 mg/L) water in the area. The low resistive feature in the northern part of the surface geophysical subset area was more resistive at a depth of 500 ft, and the dissolved-solids concentrations were less than 1,000 mg/L, indicating more freshwater at that depth (fig. 19*C*). The differences observed in resistivity and dissolved-solids concentrations indicated that the source for the salinity in the northern part of the surface geophysical subset area was most likely seepage of relatively saline surface water from the Rio Grande into the Rio Grande alluvium. A low resistivity feature was larger in the southern part of the surface geophysical subset area compared to other parts of the surface geophysical subset area. The increasing dissolved-solids concentrations with increasing depth within this low resistivity feature were generally representative of slightly saline to very saline water (1,000 to 35,000 mg/L), whereas the dissolved-solids concentrations of freshwater (less than 1,000 mg/L) were generally outside of the low resistivity feature. As stated in the "Geophysical Integration" section of this report, this low resistivity feature was interpreted as a plume of saline groundwater upwelling through fractures within the bedrock (the plume makes the highly resistive bedrock conductive); groundwater is likely more saline near the upwelling plume compared to the surrounding groundwater. The comparison between the dissolved-solids concentrations and the resistivity data indicated a good correlation between low resistivity values and high dissolved-solids concentrations. The correlation observed between resistivity and dissolved-solids concentrations helped to strengthen the interpretation that the low resistivity values in the geophysical subset area were most likely caused by more saline water than by a greater amount of clayey deposits in the sediments.

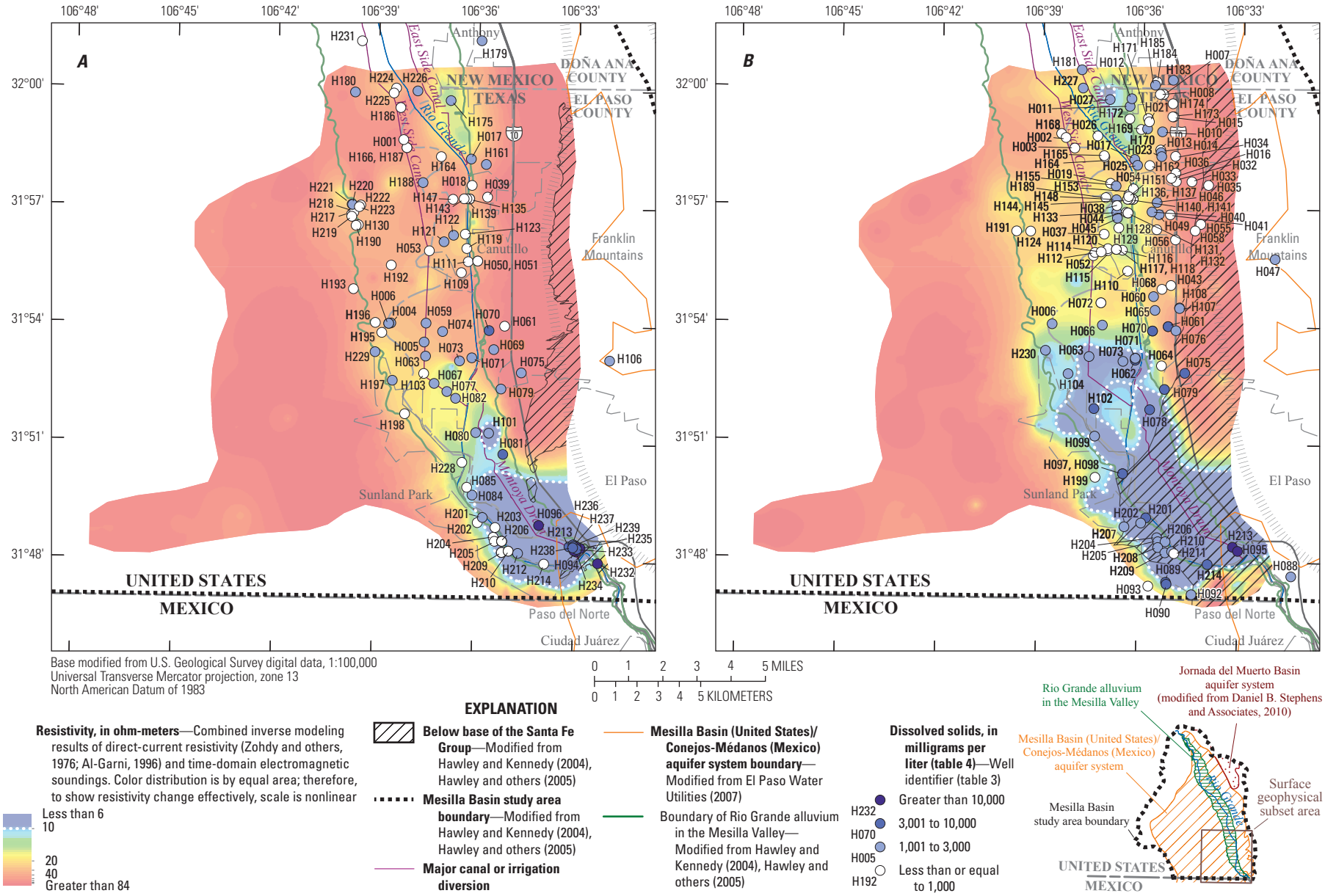

Figure 19. Historical dissolved-solids concentrations projected to the nearest depth of the gridded resistivity values from the combined inverse modeling results of the direct-current resistivity and time-domain electromagnetic soundings at various depths in the surface geophysical subset area of the Mesilla Basin study area in Doña Ana County, New Mexico, and El Paso County, Texas. *A*, 0 feet. *B*, 250 feet. *C*, 500 feet. *D*, 750 feet. *E*, 1,000 feet. *F*, 1,250 feet. *G*, 1,500 feet. *H*, 1,750 feet.

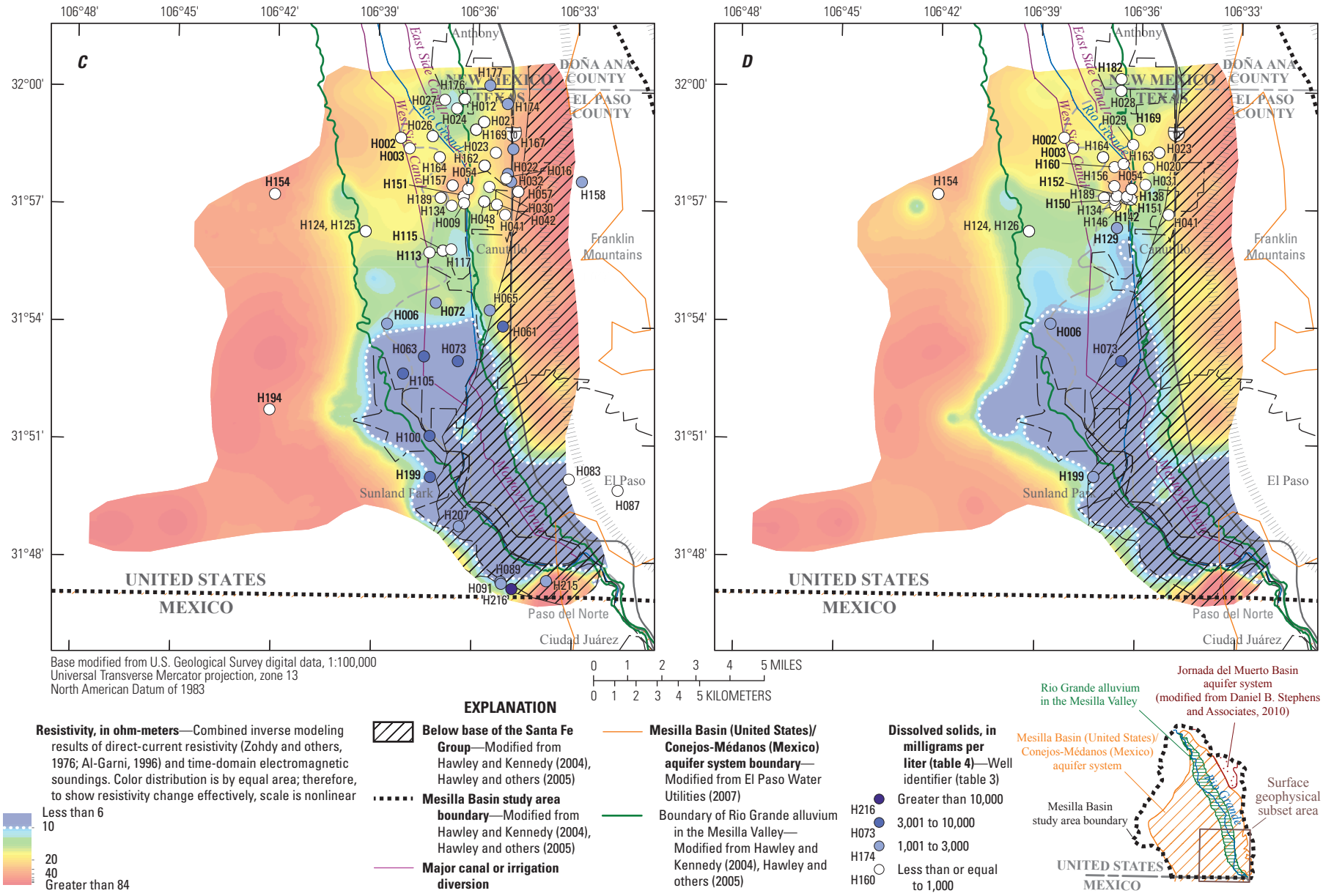

Figure 19. Historical dissolved-solids concentrations projected to the nearest depth of the gridded resistivity values from the combined inverse modeling results of the direct-current resistivity and time-domain electromagnetic soundings at various depths in the surface geophysical subset area of the Mesilla Basin study area in Doña Ana County, New Mexico, and El Paso County, Texas. *A*, 0 feet. *B*, 250 feet. *C*, 500 feet. *D*, 750 feet. *E*, 1,000 feet. *F*, 1,250 feet. *G*, 1,500 feet. *H*, 1,750 feet.—Continued

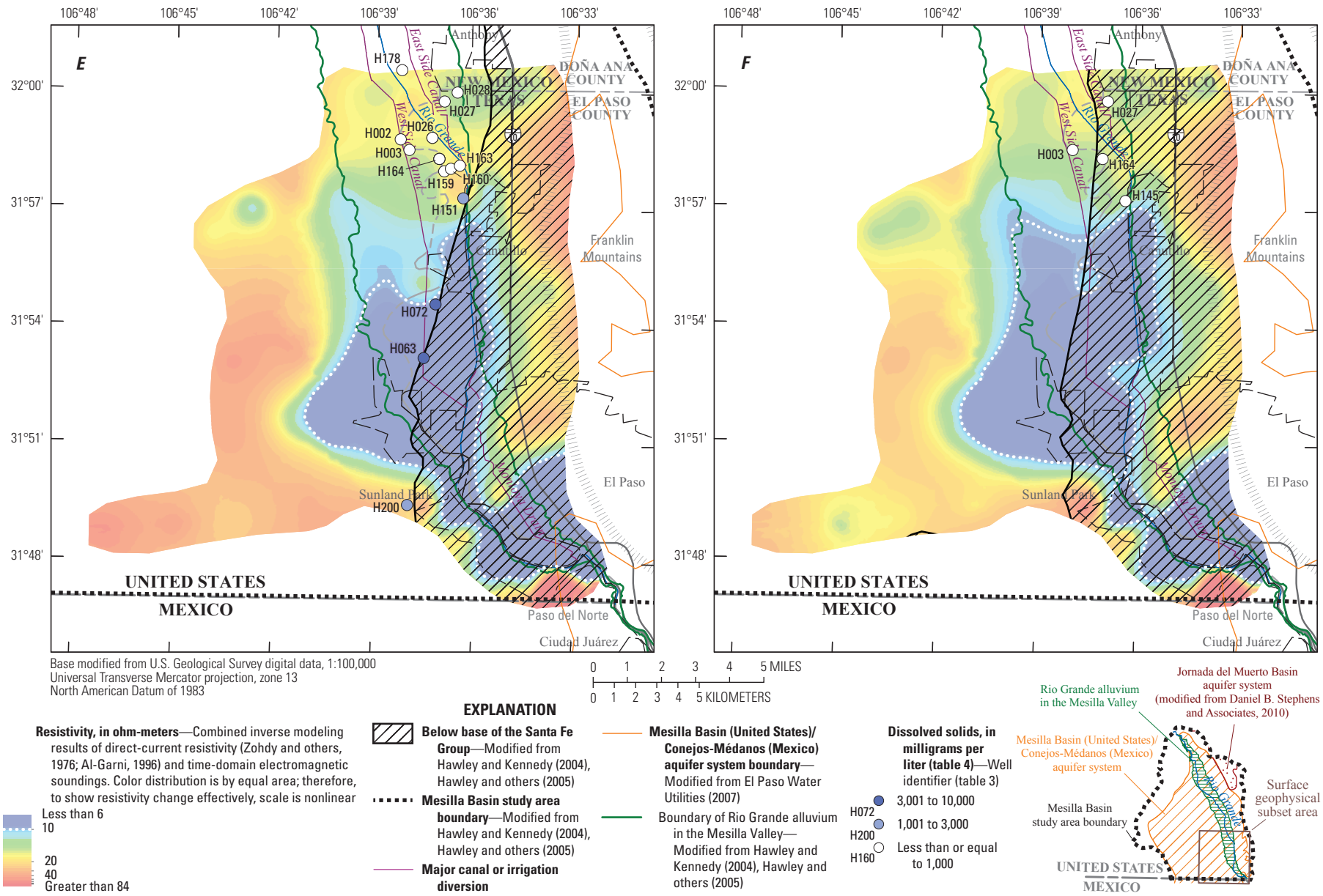

Figure 19. Historical dissolved-solids concentrations projected to the nearest depth of the gridded resistivity values from the combined inverse modeling results of the direct-current resistivity and time-domain electromagnetic soundings at various depths in the surface geophysical subset area of the Mesilla Basin study area in Doña Ana County, New Mexico, and El Paso County, Texas. *A*, 0 feet. *B*, 250 feet. *C*, 500 feet. *D*, 750 feet. *E*, 1,000 feet. *F*, 1,250 feet. *G*, 1,500 feet. *H*, 1,750 feet.—Continued

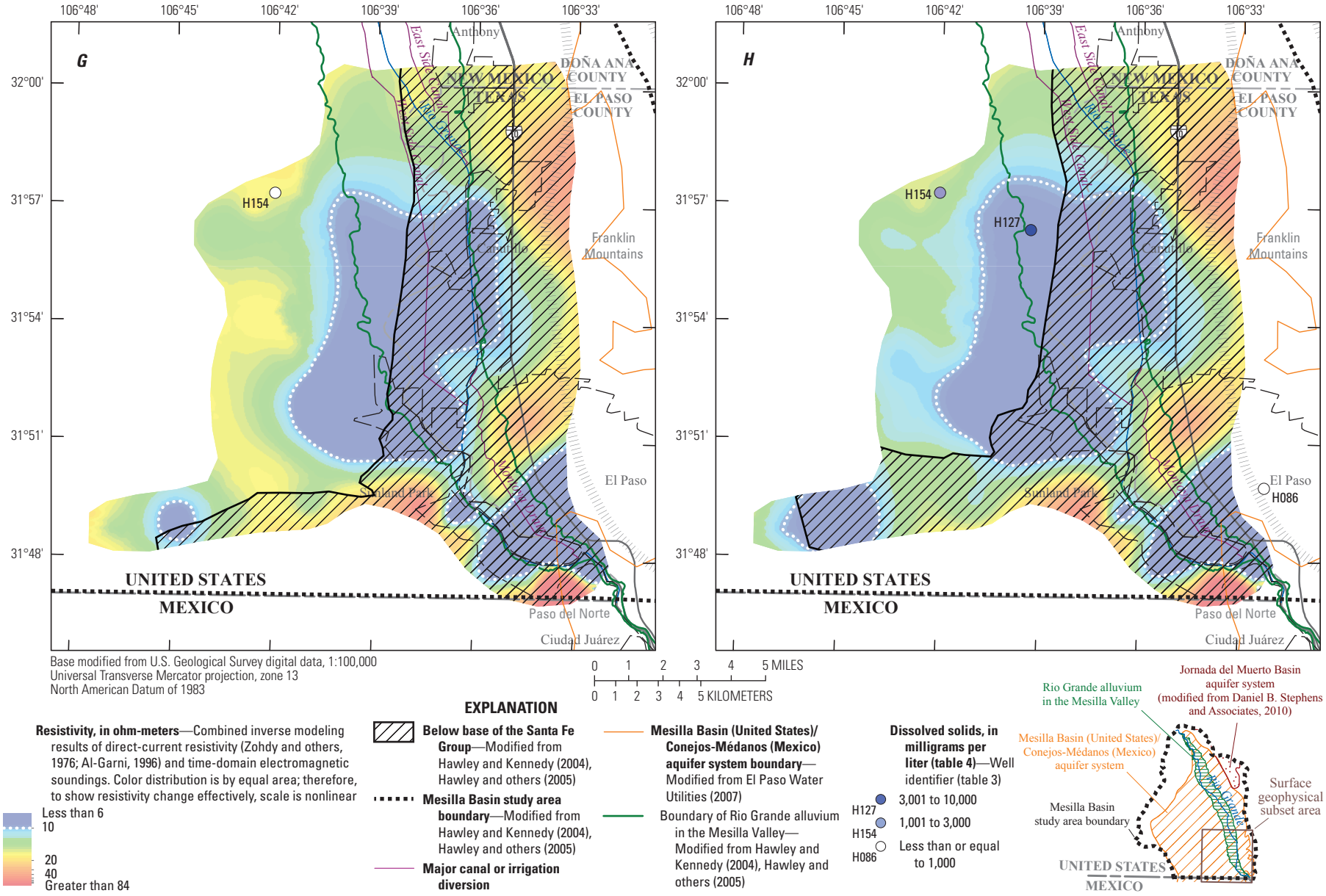

Figure 19. Historical dissolved-solids concentrations projected to the nearest depth of the gridded resistivity values from the combined inverse modeling results of the direct-current resistivity and time-domain electromagnetic soundings at various depths in the surface geophysical subset area of the Mesilla Basin study area in Doña Ana County, New Mexico, and El Paso County, Texas. *A*, 0 feet. *B*, 250 feet. *C*, 500 feet. *D*, 750 feet. *E*, 1,000 feet. *F*, 1,250 feet. *G*, 1,500 feet. *H*, 1,750 feet.—Continued

Geochemistry

Groundwater samples were collected in November 2010 from 44 wells completed in either the Rio Grande alluvium or in the upper, middle, or lower part of the Santa Fe Group (table 5, at back of report; fig. 20). Physicochemical properties (pH, specific conductance [SpC], dissolved oxygen [DO], water temperature [T], turbidity, and alkalinity) along with barometric pressure, groundwater pumping rates, and depth to water were measured in the field at the time of sample collection. Samples also were collected and shipped for laboratory analysis of major ions, nutrients, trace elements, pesticides, tritium (^{3}H), chlorofluorocarbons, carbon-14, (^{14}C, a radioactive isotope of carbon), and selected stable isotopes. Stable isotopes are measured as the ratio of the two most abundant isotopes of a given element. For example, the most abundant and stable isotopes of oxygen are oxygen-18 (^{18}O) and oxygen-16 (^{16}O) (Clark and Fritz, 1997), and the ratio these stable isotopes (ratio of ^{18}O to ^{16}O) is referred to as $\delta^{18}O$. The other stable isotopes that were measured were hydrogen (hydrogen-2/hydrogen-1 [δD]), strontium (strontium-87/strontium-86 [$^{87}Sr/^{86}Sr$]), and carbon-13/carbon-12 ($\delta^{13}C$). All water-quality results were reviewed for completeness and accuracy and stored in NWIS (U.S. Geological Survey, 2017).

Sample Collection and Analysis

This section provides descriptions of the field procedures used to collect groundwater samples during 2010, and of the methods used to analyze these samples for major ions, nutrients, trace elements, and pesticides. The environmental tracer methods that were used to assess the age of groundwater (that is, when rainwater infiltrated the land surface, reached the water table, and became groundwater) are also described.

Probability plots and boxplots were prepared to explore differences in the spatial patterns of physicochemical properties. The methods used to construct probability plots and boxplots are described (apps. 2 and 3, respectively). The discussion on boxplot construction methods also describes how outliers were determined for all constituents (app. 3). Concentrations reported as less than the laboratory reporting limit (censored data) were incorporated into the statistical analyses based on specific criteria (Helsel and Hirsch, 2002). The Kaplan-Meier estimate was used if less than 80 percent of the data were censored (Bauch and others, 2014). If 80 percent or more of the data were censored, only the minimum and maximum statistics were used for analysis (Bauch and others, 2014).

Field Procedures

In conjunction with the collection of groundwater samples from each of the 44 wells (table 5, at back of report; fig. 20), measurements were made of physicochemical properties, groundwater-pumping rates, and water-level altitudes. The field procedures used to collect most groundwater samples are described in the USGS “National Field Manual for the Collection of Water-Quality Data” (U.S. Geological Survey, variously dated). Samples for isotope analyses were collected in accordance with procedures from the USGS Chlorofluorocarbon Laboratory in Reston, Virginia (U.S. Geological Survey, 2012a), and the USGS Stable Isotope Laboratory in Reston, Va. (U.S. Geological Survey, 2012b).

Prior to sample collection, each well was pumped until one to three casing volumes was purged in order to remove stagnant water. Water-level-altitude measurements were acquired prior to pumping each well by using an electric tape or steel tape following methods described in Cunningham and Schalk (2011). The amount of water that was purged depended on the type of well and the frequency of pumping performed at that well. For wells that are continuously pumped, such as public supply, domestic supply, or industrial wells, purging less than three casing volumes was sometimes done, which is permissible (U.S. Geological Survey, variously dated, chapter A4). Wells that are not continuously pumped were purged to remove a minimum of three casing volumes. Observation wells were pumped by using an electric, portable, submersible, positive displacement pump constructed of stainless steel and Teflon (Grundfos Redi-Flo2 or Redi-Flo3). For wells with pumps already installed, these existing pumps were used to purge the water when necessary, and samples were collected at the wellhead prior to any pressure tanks or filtering or other treatment devices. Connections were made for purging and sampling by installing a brass connector with compression fitting to refrigeration-grade copper tubing.

After the required casing volumes were purged, the wells were pumped continually until a steady state for all of the physicochemical properties was reached (U.S. Geological Survey, variously dated). When the system reached equilibrium, water samples were collected through Teflon tubes and stored in new, precleaned bottles. Samples were processed onsite to minimize chemical changes or contamination. Laboratory protocols were followed for sample preparation and shipping, which involved preservation with appropriate acid (when required) or chilling to 4 °C to help prevent sample degradation and maintain the initial concentration of compounds from the time of collection to the time the laboratory analyzed the sample. All samples were stored on ice in coolers and shipped overnight to the analyzing laboratories. After sample collection and processing, the sampling equipment was cleaned according to the established protocols prior to use at the next sampling well (Wilde, 2004).

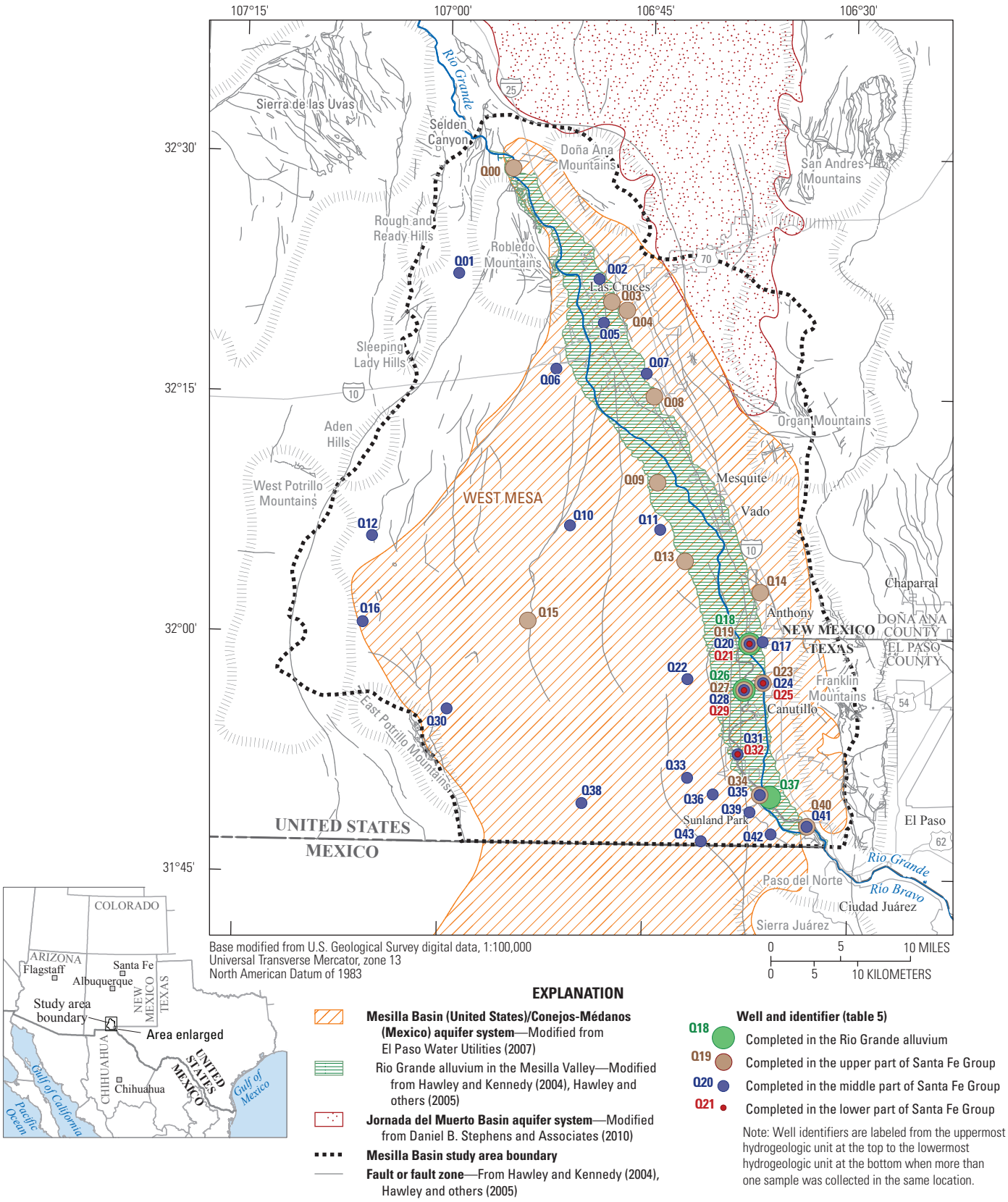

Figure 20. Locations of wells from which geochemical data were collected in the Mesilla Basin study area in Doña Ana County, New Mexico, and El Paso County, Texas, 2010.

Analytical Methods

Major ions, nutrients, trace elements, and pesticides were analyzed by the USGS National Water Quality Laboratory (NWQL), Denver, Colo., by using published methods. Methods for major ions are published in Fishman and Friedman (1989), Fishman (1993), and American Public Health Association (1998). Nutrients methods are published in Fishman (1993) and Patton and Kryskalla (2003). Trace-element methods are published in Fishman and Friedman (1989), Garbarino (1999), and Garbarino and others (2006). Pesticide analysis methods are published in Zaugg and others (1995), Lindley and others (1996), Sandstrom and others (2001), and Madsen and others (2003). Samples for the analysis of chlorofluorocarbons were shipped to the USGS Dissolved Gas Laboratory in Reston, Va., and analyzed by using methods described in Busenberg and others (1993, 2001).

The USGS uses two reporting conventions for the analytical data from the NWQL, the laboratory reporting level (LRL) and the long-term method detection level (LT-MDL) (Childress and others, 1999). The LT-MDL is a modified method detection limit (MDL) that serves as a censoring limit for most analytical methods at the NWQL. The LT-MDL is the minimum concentration of a constituent that can be measured and reported with a 99-percent confidence that the concentration is greater than zero. This limit helps to reduce the occurrence of a false positive (reporting a sample concentration equal to or greater than the LT-MDL when the actual concentration is less than the LT-MDL) to less than 1 percent. The LRL is set at two times the LT-MDL to reduce the occurrence of a false negative (reporting a sample concentration as less than the LT-MDL when the actual concentration is equal to or greater than the LT-MDL). Any samples that had concentrations measured between the LRL and LT-MDL are reported as estimated (E) concentrations. Childress and others (1999) provide additional information on MDLs, LRLs, and LT-MDLs.

Environmental Tracer Methods

To help define areas of groundwater recharge and discharge, water-rock interactions along flow paths, and determine potential mixing of groundwater derived from multiple sources, isotopic analyses of δD, $\delta^{18}O$, $^{87}Sr/^{86}Sr$, ^{3}H, $\delta^{13}C$, and ^{14}C were completed. Analysis for δD and $\delta^{18}O$ was done at the USGS Stable Isotope Laboratory in Reston, Va. δD methods are described in Révész and Coplen (2008a), and $\delta^{18}O$ analytical methods are described in Révész and Coplen (2008b). ^{87}Sr and ^{86}Sr isotopes were analyzed at the Menlo Park Isotope Laboratory in Menlo Park, California, in accordance with methods described by Kendall and McDonnell (1998). ^{3}H was analyzed at the Menlo Park Tritium Laboratory in Menlo Park, Calif. Analytical methods for ^{3}H are documented in Östlund and Werner (1962) and Thatcher and others (1977). $\delta^{13}C$ and ^{14}C were analyzed at the National Ocean Sciences Accelerator Mass Spectrometry Facility (NOSAMS) at the Woods Hole Oceanographic Institution in Woods Hole, Massachusetts (Woods Hole Oceanographic Institution, 2016). $\delta^{13}C$ was analyzed by stable isotope ratio mass spectrometry (SIRMS), whereas ^{14}C was analyzed by accelerator mass spectrometry (AMS). Methods for analyzing SIRMS results are described by Vogel and others (1987), Donahue and others (1990), McNichol and others (1992), Gagnon and Jones (1993), McNichol and others (1994), and Schneider and others (1994). Methods for analyzing AMS results are described by Roberts and others (2010) and are reported in the standard ^{14}C format (Stuiver and Polach 1977). The experimental uncertainty, estimated from ^{14}C ion counting statistics, comparison of replicate seawater samples, and reproducibility of primary and secondary standards, is 3–4 per mil for radiocarbon analysis and 0.03–0.05‰ for stable isotope analysis (Elder and others, 1998). Methods for determining and reporting ^{14}C ages are described in Karlen and others (1964), Olsson and Klasson (1970), Stuiver and Polach (1977), and Stuiver (1980). The age of groundwater is qualified as "apparent age" in this report because chemical processes affect the environmental tracers used to determine age. Musgrove and others (2010, p. 42) explain that "because it is not possible to identify and account for all physical and chemical processes that might affect groundwater age-tracer results, the apparent age of groundwater is most appropriately reported."

Hydrogen and Oxygen Isotopic Ratios

Ratios of the stable isotopes of the water molecule (hydrogen and oxygen) can yield isotopic signatures that are useful indicators of the regional recharge regimes of a hydrogeologic system. Plotting the ratio of δD to $\delta^{18}O$ ($\delta D/\delta^{18}O$) can aid in analyzing when and from where the groundwater was initially recharged into the system (Faure, 1986; Uliana and others, 2007; Bumgarner and others, 2012). For comparison purposes with published $\delta D/\delta^{18}O$ ratios for precipitation, the $\delta D/\delta^{18}O$ ratios from the two nearest Global Network of Isotopes in Precipitation (GNIP) stations (International Atomic Energy Agency, 2016) where δD and $\delta^{18}O$ are measured on a regular basis within multiple years are also plotted. The nearest GNIP stations where $\delta D/\delta^{18}O$ ratios were measured were in Chihuahua, Mexico (about 250 mi south of the study area), and Flagstaff, Arizona (about 350 mi northwest of the study area) (fig. 20). At the Chihuahua, Mexico, GNIP station, there were 126 and 131 δD and $\delta^{18}O$ samples, respectively, collected from June 1962 to November 1988 resulting in a mean annual δD value of -44.13 per mil and a mean annual $\delta^{18}O$ value of -6.57 per mil. At the Flagstaff, Ariz., GNIP station, 97 and 110 δD and $\delta^{18}O$ samples were respectively collected from December 1961 to July 1974, resulting in a mean annual δD value of -63.23 per mil and a mean annual $\delta^{18}O$ value of -8.04 per mil. The $\delta D/\delta^{18}O$ ratios for these GNIP stations were calculated from their mean annual δD and $\delta^{18}O$ values (International Atomic Energy Agency, 2016).

Craig (1961) used δD and $\delta^{18}O$ isotopic analysis from multiple rainfall samples collected around the world to create the "Global Meteoric Water Line" (GMWL), a linear regression line calculated as $\delta D = 8 \times \delta^{18}O + 10$. Changes along this line can be attributed to multiple factors including altitude, storm intensity, latitude, seasons, and continental climate (Fontes, 1980). Precipitation with relatively larger amounts of the heavier isotopes generally occurs in lower altitudes, lower latitudes, warmer weather, and closer to the coasts (Witcher and others, 2004). Values that deviate from the GMWL can be a result of two processes: (1) evaporation prior to recharge and (2) oxygen isotope exchange with rocks (Witcher and others, 2004). Evaporation can cause preferential loss of water molecules containing the lighter stable isotopes of hydrogen and oxygen. Multiple samples collected over time in various environmental conditions (location, temperature, humidity, wind speed, and other factors) are used to develop a linear regression line referred to as the "evaporation line." The Rio Grande evaporation line was computed by previous researchers as $\delta D = 5.1 \times \delta^{18}O - 28$ by using samples of water collected from the Rio Grande at intervals of 1,200 ft starting from the headwaters in Colorado and ending about 80 mi south of El Paso, Tex. (Phillips and others, 2003). Samples that indicate gains or losses of oxygen atoms from interaction with rocks tend to deviate from the GMWL in the lateral position since there is the gain or loss of only the oxygen element.

A study by Adams and others (1995) documented a substantial range of δD (-138.8 to -25.4 per mil) and $\delta^{18}O$ (-18.25 to -0.29 per mil) within the precipitation throughout 4 years of data collection near Santa Fe, N. Mex. (about 250 mi north of the study area) (fig. 20). This large range was most likely a result of the seasonal variations of the isotopically lighter, cooler precipitation from the Pacific Ocean and the isotopically heavier, warmer precipitation from the Gulf of Mexico (Adams and others, 1995). The stable isotopic signatures in the Mesilla Basin may reflect cooler and warmer water recharged during different recharge regimes. Because of this, the apparent groundwater age (Plummer and Busenberg, 2000) as determined by other isotopic techniques (tritium and ^{14}C) aids in determining if groundwater of a lower temperature and lighter isotopic signature was recharged into the aquifer system during the wet and cool climate of the late Pleistocene (Bumgarner and others, 2012) or from recent recharge from precipitation occurring during the winter and early spring months.

Strontium-87

Because Sr commonly replaces Ca within minerals and is common within carbonate rocks, it is useful in evaluating sources of dissolved constituents and water-rock interaction along groundwater-flow paths (Banner, 2004; Musgrove and others, 2010; Bumgarner and others, 2012). The ratio of strontium ($^{87}Sr/^{86}Sr$) undergoes negligible fractionation during chemical or physical reactions (that is, the $^{87}Sr/^{86}Sr$ ratio is set at the time of mineral formation), so the value is indicative of the mineral that the groundwater has been in contact with the longest (Witcher and others, 2004). ^{87}Sr is a beta decay product of rubidium-87 (^{87}Rb), and rubidium (Rb) readily replaces potassium (K) within minerals. Witcher and others (2004, p. 92) explain that "because Rb has an ionic radius similar to K, K-rich rocks may be enriched in ^{87}Rb. With sufficient time, a rock with high K content may have high ^{87}Sr contents as a result of ^{87}Rb beta decay."

Precambrian granites within the study area had initial $^{87}Sr/^{86}Sr$ ratios between 0.70000 and 0.72800 (Witcher and others, 2004). Values have increased over geologic time with the decay of ^{87}Rb into ^{87}Sr, such that $^{87}Sr/^{86}Sr$ ratios values may range as large as 0.81000 (Witcher and others, 2004). Initial $^{87}Sr/^{86}Sr$ ratios of other rocks within the study area range from 0.70800 to 0.70850 for the carbonate rocks of the Pennsylvanian age, 0.70300 to 0.70400 for Tertiary and Quaternary basalts, 0.70700 to 0.70800 for mid-Tertiary basaltic andesite, and 0.71000 to 0.73000 for Tertiary silicic volcanics. Because of low K and relatively high Ca within most of these rocks (except for the Tertiary volcaniclastic and siliciclastic rock), the initial $^{87}Sr/^{86}Sr$ ratios will have changed little over geologic time (Witcher and others, 2004). The modern $^{87}Sr/^{86}Sr$ ratios for the Tertiary volcaniclastic and siliciclastic rocks will be higher compared to their initial $^{87}Sr/^{86}Sr$ ratios because of the relatively high Rb content within these rocks (Witcher and others, 2004).

Tritium

The use of ^{3}H to analyze groundwater is qualitative in that apparent ages of groundwater cannot be determined, but rather, differences in ^{3}H concentrations can potentially distinguish if the groundwater was recharged before, during, or after widespread atomic bomb testing began in the 1950s. As noted by Hinkle (1996, p. 5) "the definition of modern water is a function of the dating tool used. Although different dating tools rely on different dates in defining the boundary between modern and old water, the range of these dates is small." For the purpose of this report, the term "prebomb" is used when at least some water was recharged prior to 1950, and the term "postbomb water" is used when at least some water was recharged since 1950. The determination of groundwater age by using ^{3}H is relative to ^{3}H concentrations in the area when samples were collected in 2010. ^{3}H is commonly measured in picocuries per liter (pCi/L) or in tritium units (TU), where 3.22 pCi/L is equivalent to 1 TU or 1 part ^{3}H in 10^{18} parts hydrogen (Lucas and Unterweger, 2000). Before atomic bomb testing, the naturally occurring concentration of ^{3}H in the atmosphere ranged from about 2 to 8 TU (Motzer, 2008). From about 1950 to 1970, widespread atomic bomb testing resulted in a substantial increase (more than 1.1×10^{9} TU) of ^{3}H in the atmosphere of the Northern Hemisphere (Motzer, 2008). Concentrations of ^{3}H have declined appreciably since the cessation of atmospheric atomic bomb testing. For example, concentrations of ^{3}H measured

in precipitation samples collected during 2000–2005 at the GNIP station near Albuquerque, N. Mex. (fig. 20), ranged from 4 to 10 TU (International Atomic Energy Agency, 2016). The elevated ^{3}H concentrations in the atmosphere beginning in about 1950 resulted in groundwater recharge containing appreciably higher ^{3}H concentrations compared to groundwater recharged before 1950. Consequently, ^{3}H is a good tracer for groundwater that was recharged during the 60 years prior to when samples were collected for this study (1950–2010). As a tracer, ^{3}H offers additional advantages, including a short half-life of about 12.3 years and the relative ease with which it can be measured in precipitation samples (Clark and Fritz, 1997). Because ^{3}H decay continues to occur after groundwater recharges into an aquifer, groundwater samples can have ^{3}H concentrations less than the naturally occurring concentration in the atmosphere, which is generally representative of older water. By using the ^{3}H concentration measured in precipitation samples collected at a GNIP station in Albuquerque, N. Mex. (about 200 mi north of the study area), the lowest adjusted ^{3}H concentration (adjusted for radioactive decay from the time of sample collection [2010] done for this study) recorded at that location after the beginning of widespread atomic bomb testing was determined to be 1.6 TU. The adjusted value of 1.6 TU is calculated from the initial, undecayed 5.4 TU concentration measured in December 1989 (International Atomic Energy Agency, 2016).

For this analysis, it was assumed that prebomb ^{3}H concentrations measured in the atmosphere before 1950 were not greater than 16 TU, two times the assumed maximum prebomb atmospheric concentration of 8 TU reported by Motzer (2008). When adjusted for radioactive decay during 1950–2010, the 16 TU value decreases to about 0.6 TU, which means that any ^{3}H concentrations of less than 0.6 TU are likely indicative of prebomb water. Solomon and Cook (2000) reported a similar prebomb ^{3}H concentration, indicating that groundwater recharged prior to 1950 contains less than 0.5 TU. Tritium values of less than zero are possible in prebomb water. As explained in Kay and Buszka (2016, p. 40), “a negative tritium concentration is equivalent to zero for reporting purposes; a negative value originates from tritium derived decay counts yielded from analysis of the sample that was less than the analytical background.”

Because the lowest adjusted concentration measured in precipitation after widespread atomic bomb testing began is 1.6 TU, any groundwater ^{3}H concentrations between 0.6 and 1.6 TU are indicative of a mixture of prebomb and postbomb recharge. The 2000–2005 ^{3}H concentrations measured in precipitation samples collected at the Albuquerque, N. Mex., GNIP station were as large as about 10 TU, so groundwater ^{3}H concentrations between 1.6 and 10 TU are indicative of postbomb water. Any groundwater ^{3}H concentrations of greater than 10 TU are indicative of a mixture of water recharged during the peak of widespread atomic bomb testing.

Carbon-14

^{14}C is the radioactive isotope of carbon with a (Libby) half-life of 5,568 years and is naturally produced in the upper atmosphere (Plummer and others, 1994). Because ^{14}C has a relatively long radioactive half-life, it is useful for dating groundwater that is thousands to tens of thousands of years old (Oden and Truini, 2013). Citing the work of Kalin (2000), Nishikawa and others (2004, p. 39) explain “carbon-14 data are expressed as percent modern carbon (pmc) by comparing ^{14}C activities to the specific activity of National Bureau of Standards [now the National Institute of Standards and Technology] oxalic acid: 13.56 disintegrations per minute per gram of carbon in the year 1950 equals 100 pmc (Kalin, 2000).”

Groundwater recharged after 1950 likely results in a ^{14}C activity value of 100 pmc or greater because atmospheric ^{14}C concentrations increased by as much as 20 percent from atomic bomb testing in the 1950s and 1960s (Plummer and others, 1994). ^{14}C typically moves into groundwater tied up in the carbon dioxide (CO_2) dissolved in precipitation or in organic carbon dissolved in surface water and soil pore water (Ingebritsen and Sanford, 1999; Raymond and Bauer, 2001). ^{14}C can enter surface water directly as water flows over the land towards stream channels (overland flow) or indirectly as the result of soil-pore water moving through the soil zone and discharging to a surface-water body (Linsley and others, 1982). Surface water in turn can provide a source of groundwater recharge through surface water/groundwater interactions. Carbon released in various forms by living plants and decaying organic material is dissolved in water as dissolved inorganic and organic carbon (Raymond and Bauer, 2001). Along the water’s flow path, ^{14}C concentrations begin to decrease as ^{14}C decays to nitrogen-14 (^{14}N). Dilution of ^{14}C through geochemical processes, such as the dissolution of carbonates, can substantially alter the original ^{14}C concentration (Lemay, 2002). ^{14}C concentrations in groundwater may be altered, therefore, by the introduction of nonradioactive carbon-12 (^{12}C) from exchange with carbon in rocks that are millions of years old, resulting in apparent ^{14}C groundwater ages that are falsely old. Various types of geochemical modeling can be used to correct for these effects to obtain better estimates of groundwater age (Plummer and others, 1994). All groundwater sample results for the ^{14}C age-dating method presented in this report are reported in pmc for ^{14}C activity and Libby half-life uncorrected radiocarbon years before 1950 (^{14}C years before present [BP]) for the apparent age of groundwater.

Quality-Assurance and Quality-Control Procedures

Quality-control data were collected in October and November 2010 to assess the variability and bias that may exist within the sample-collection procedures and laboratory

analyses (U.S. Geological Survey, variously dated). To test for bias, two equipment-blank samples and six field-blank samples were collected; to test for variability, four sequential-replicate samples were collected; and to test for bias and variability, two matrix-spiked environmental samples were collected. The term "environmental sample" refers to the portion of the groundwater sample collected for analysis from a well during a specific date and time or a range of dates (Dupré and others, 2012).

Equipment and Field Blanks

Equipment-blank samples were collected and processed in a controlled environment to determine if the procedures used to clean the sampling equipment and containers were sufficient to produce unbiased analytical results from the environmental samples. Equipment-blank samples were collected by passing ultra-pure water through the collection and processing equipment used for environmental samples. The analysis procedures for equipment-blank samples are the same as those for environmental samples. Equipment-blank results indicated that the sampling equipment and containers did not introduce appreciable amounts of bias (table 6, at back of report). In the equipment-blank sample collected on October 7, 2010 (about 1 month before the environmental sampling began), small concentrations of the following trace elements were detected: barium (Ba) (presence verified but not quantified), chromium (Cr) (0.08 micrograms per liter [µg/L]), cobalt (Co) (0.07 µg/L), lead (Pb) (0.06 µg/L), manganese (Mn) (0.9 µg/L), molybdenum (Mo) (0.10 µg/L), nickel (Ni) (1.8 µg/L), and silver (Ag) (presence verified but not quantified). Only aluminum (Al) (3.3 µg/L) and Co (0.05 µg/L) were detected in the equipment-blank sample collected on October 15, 2010. The results for the equipment-blank samples indicate that the cleaning procedures were generally effective in removing contaminants from sampling equipment and containers. There may be some slight bias in the environmental results for the trace elements detected in either equipment-blank sample (from October 7, 2010, or from October 15, 2010). Relatively large values (more than an order of magnitude larger than the LRL) were considered meaningful, so these slight amounts of bias did not affect the interpretation of the environmental results.

Field-blank samples were collected and processed at six randomly selected sampling wells prior to the collection of environmental samples to ensure that equipment cleaning conducted in the field between the collection of samples from different wells was adequate and that the collection, processing, or transporting procedures in the field did not contaminate the environmental samples. Field-blank results indicate that the sample collection and handling procedures did not introduce appreciable amounts of bias to the environmental samples, with possible exceptions for Pb, selenium (Se), uranium (U) and organic carbon—constituents that were not used in this assessment (table 6, at back of report). A Pb concentration of 0.03 µg/L (Q33) (table 6, at back of report; fig. 20) was detected in one field-blank sample. A Se concentration of 0.07 µg/L (Q04) (table 6, at back of report; fig. 20) was detected in one field-blank sample. A U concentration of 0.02 µg/L (Q04) (table 6, at back of report; fig. 20) was detected in one field-blank sample. Organic carbon concentrations of 0.2 and 0.3 mg/L were detected in two of the environmental blanks (0.2 mg/L was measured in the sample from well Q05, and 0.3 mg/L in the sample from well Q36). The detections of arsenic (As) and Co in field-blank samples were considered negligible (table 6, at back of report). An As concentration of 0.04 µg/L (well Q04) (table 6, at back of report; fig. 20) was detected in one field-blank sample, which was negligible compared to all the environmental samples because this value is close to the LT-MDL for this constituent (0.02 µg/L). Co concentrations of 0.01 and 0.02 µg/L (wells Q02 and Q33) were detected in two field blanks, which were also negligible compared to all the environmental samples because these values are less than or the same as the LT-MDL for this constituent (0.02 µg/L). The cause for low-level concentrations of some constituents in the field-blank samples is unknown. To avoid any possible bias from contamination, values for constituents measured in environmental samples at concentrations that were less than or equal to those measured in equipment-blank or field-blank samples were omitted for interpretive purposes.

Sequential-Replicate Analyses

Sequential-replicate samples were collected to measure the variability in results originating from sampling procedures and analytical methods (table 7, at back of report). Inorganic constituents were measured in replicate samples that were collected by using a new, preconditioned capsule filter. Capsule filters were replaced prior to collecting the sequential-replicate sample to prevent the possibility of filter loading, which might reduce the effective pore size of the filter (Horowitz and others, 1996).

To evaluate the potential variability introduced during sample collection, processing, or laboratory analysis, the analytical results measured in an environmental sample were compared with those measured in the associated replicate sample by computing the relative percent difference (RPD) for each constituent. The RPD was computed by using the following equation:

$$RPD = \frac{|C_1 - C_2|}{((C_1 + C_2)/2)} \times 100 \qquad (2)$$

where

C_1 is the concentration from the environmental sample, and

C_2 is the concentration from the replicate sample.

RPDs of 10 percent or less indicate good agreement between the paired results if the concentrations were sufficiently large compared to their associated LRLs

(Oden and others, 2011). An RPD was not computed if either of the paired results was reported as an estimated concentration. There was generally good agreement between the environmental and replicate sample concentrations, with a few exceptions. For the environmental-replicate sample pair collected from well Q31 (fig. 20) on November 9, 2010, RPDs that exceeded 10 percent were measured for the following constituents: Al (13.95 percent), beryllium (Be) (40.00 percent), Cr (125.58 percent), Ni (28.22 percent), antimony (Sb) (28.57 percent), and Co (28.57 percent) (table 7, at back of report). On November 15, 2010, the RPDs exceeded 10 percent for the following environmental-replicate sample pairs collected from well Q17 (fig. 20): Al (14.81 percent), Co (40.00 percent), and organic carbon (50.00 percent) (table 7, at back of report). On November 18, 2010, the constituents with RPDs that exceeded 10 percent for the environmental-replicate sample pair collected from well Q37 were Be (66.67 percent), cadmium (Cd) (10.53 percent), Co (116.67 percent), Ni (12.77 percent), and U (14.01 percent) (table 7, at back of report; fig. 20). Concentrations of the pesticide compounds were less than the LRL in both the environmental and the replicate samples with the two exceptions: 1,2-Dichloropropane (0.14 µg/L) was measured in the environmental and replicate samples collected from well Q03 (fig. 20) on November 8, 2010, and ethyl methyl ketone (0.5 µg/L) was detected in the environmental and replicate samples collected from well Q37 (fig. 20) on November 18, 2010 (table 7, at back of report).

Many of the RPDs that exceeded 10 percent were an artifact of the small concentrations measured in the paired samples—concentrations that were within five times the LT-MDL. Small differences in concentration associated with small concentration values can result in large RPDs. Differences in sample concentration that are sufficiently large might indicate bias introduced during sample collection, processing, or laboratory analysis.

Matrix Spikes

A spiked environmental sample is an environmental replicate sample to which a known volume containing known concentrations of target constituents is added in the field (Wilde and others, 2004). Martin and others (2009, p. 4) provide the following explanation of matrix spikes:

> The term "matrix" indicates that the spiked solution has been added to an environmental water sample (as opposed to a blank/reagent water sample). Water is collected from the stream or well and processed by use of standard procedures to produce two samples (U.S. Geological Survey, variously dated; Shelton, 1994; Koterba and others, 1995). Spike solution is added to only one of the two water samples, resulting in spiked and unspiked samples (the matrix spike and the "background" sample, respectively).

Unspiked and spiked environmental samples were used to assess bias and variability from degradation of pesticide constituent concentrations during sample processing, storage, and analysis. Analytical recoveries of the spiked target constituents are expressed as percentages of expected (theoretical) concentrations. The percent recoveries of constituents in spiked environmental samples were compared to theoretical and laboratory recoveries to evaluate matrix interferences or degradation of pesticides. Percent recovery is computed as follows:

$$\text{Percent recovery} = \frac{(C_{\text{spiked}} - C_{\text{unspiked}})}{C_{\text{expected}}} \times 100 \qquad (3)$$

where

C_{spiked} is the measured concentration in the spiked environmental sample, in micrograms per liter,

C_{unspiked} is the measured concentration in the unspiked environmental sample, in micrograms per liter, and

C_{expected} is the theoretical concentration in the spiked environmental sample, in micrograms per liter, and is computed as follows:

$$C_{\text{expected}} = \frac{(C_{\text{solution}} \times V_{\text{spike}})}{V_{\text{sample}}} \qquad (4)$$

where

C_{solution} is the concentration of constituent in the spiked environmental sample, in micrograms per liter,

V_{spike} is the volume of spike added to the environmental sample, in milliliters, and

V_{sample} is the volume of the environmental sample, in liters.

Constituent concentrations less than the LRL were set to zero for the purpose of calculating percent recovery.

A mixture of target constituents was added to two of the replicate environmental samples (the samples collected from well Q33 on November 3, 2010, and from well Q14 on November 15, 2010) (table 8, at back of report; fig. 20). The calculated spike recoveries in this report were compared to a time-series graph of groundwater spike recoveries depicted in appendix 4 of Martin and Eberle (2011). The spike recoveries for the samples analyzed in this report were generally within the range of spike recoveries provided by Martin and Eberle (2011). For constituents that were not discussed by Martin and Eberle (2011), the spike recoveries of these constituents added to reagent water by the NWQL (laboratory-matrix spike samples) were reviewed to assess method performance, with methods appearing to be operating normally (U.S. Geological Survey, 2012c). Concentrations of selected pesticides measured in the unspiked environmental samples

were consistently less than the LRL and are reported for completeness (table 8, at back of report) but are not discussed further.

Geochemical Characteristics

The relations between and spatial patterns of groundwater chemical data and isotopic data are useful for determining recharge sources, direction of flow, and geochemical processes (Plummer and others, 2004). The spatial extent and coverage of the groundwater samples relative to the study area were constrained by where wells were available for sampling and by suitability for sample collection on the basis of the screened or open intervals of available wells. There were only three samples collected from wells completed in the Rio Grande alluvium and four from wells completed in the lower Santa Fe, resulting in a relative lack of geochemical information for these HGUs—the remainder of the samples were collected from wells completed in either the upper or middle Santa Fe. Aside from this sampling bias, the overall spatial extent and coverage of the study area were deemed sufficient by the authors to make a meaningful interpretation of the complete aquifer system.

Various geochemical and salinization processes within the study area that have previously been documented were further explored by analyzing the groundwater samples collected in November 2010. These processes include gypsum dissolution and reprecipitation, cation exchange with partly authigenic clay minerals and zeolites, diagenetic alteration of sand and silt grains, some halite dissolution, and evapotranspiration where the water table is near the surface (Witcher and others, 2004).

Saturation indexes for selected minerals aid in the interpretation of dissolution processes and were calculated by using the geochemical software PHREEQC (table 9, at back of report) (Parkhurst, 1995). As explained in Tribble (1997, p. 10), “a saturation index of zero occurs when the solution is at equilibrium with the mineral. A positive saturation index indicates thermodynamic oversaturation and a tendency for the mineral to precipitate. A negative saturation index indicates undersaturation and a tendency for the mineral to dissolve.”

PHREEQC calculates the distribution of aqueous species, along with the state of saturation of each water sample with respect to a variety of commonly occurring rock-forming minerals. The saturation index is calculated by using the following equation:

$$\mathrm{SI} = \log(IAP/K_{sp}) \tag{5}$$

where

SI	is the saturation index,
log	is the base 10 logarithm,
IAP	is the ion activity product, and
K_{sp}	is the solubility product.

Physicochemical Properties

The pH of groundwater samples collected in the study area ranged from 6.8 to 9.1 standard units (table 10, at back of report; fig. 21*A*, at back of report). About 75 percent of the groundwater samples can be characterized as slightly alkaline, with pH values greater than 7.5 standard units (the first quartile value of the entire dataset for pH) (fig. 21*A*, at back of report). Mean pH values (excluding outliers) in samples collected from the Rio Grande alluvium, upper Santa Fe, middle Santa Fe, and lower Santa Fe were about 7.4, 7.5, 8.0, and 8.4 standard units, respectively (fig. 22*A*, at back of report).

In general, pH values increased with depth (fig. 22*A*, at back of report). Groundwater samples collected from wells in the southeastern and western parts of the study area typically had higher pH values (greater than 8.2 standard units, the third quartile value of the entire dataset for pH) (fig. 21*A*, at back of report) compared to groundwater samples collected in other parts of the study area (table 10, at back of report; fig. 20). Higher pH values in the groundwater may be attributable to relatively elevated concentrations of bicarbonate (HCO_3), CO_3, and carbon dioxide that result from dissolution of carbonate rocks (Domenico and Schwartz, 1998).

Specific conductance (SpC) values within the Mesilla Basin ranged from 399 to 42,800 microsiemens per centimeter at 25 °C (µS/cm at 25 °C) (table 10, at back of report; fig. 21*B*, at back of report). The mean SpC values (excluding outliers) in groundwater samples collected from the Rio Grande alluvium, upper Santa Fe, middle Santa Fe, and lower Santa Fe were about 3,970, 1,510, 1,050, and 2,430 µS/cm at 25 °C, respectively (table 10, at back of report; fig. 22*B,* at back of report). SpC is an indicator of ion concentration and is related to the amount of dissolved solids within the water: higher SpC values indicate higher dissolved-solids concentrations (Hem, 1985). Because SpC is a conservative property (the value should not change as the water moves downgradient unless it mixes with water from a different source or interacts with a different rock or sediment type), it can be useful in locating areas of similar water types and can provide evidence pertaining to groundwater flow and mixing (Plummer and others, 2004). Boxplots were prepared to depict the SpC values measured in samples collected from wells completed in the different hydrogeologic units (fig. 22*B*, at back of report). In general, SpC values were higher in the samples representing the Rio Grande alluvium or lower Santa Fe compared to the SpC values measured in samples representing the upper Santa Fe or middle Santa Fe. The higher SpC values measured in lower Santa Fe samples were attributed to groundwater upwelling from deeper aquifers, whereas the higher SpC values measured in Rio Grande alluvium samples were from several different sources. Based solely on the SpC data, there does not appear to be a direct link between the higher SpC values in the lower Santa Fe and the higher SpC values in the Rio Grande alluvium—compared to SpC values measured in samples collected from wells completed in the Rio Grande alluvium or lower Santa Fe, lower SpC values were measured in samples collected from wells completed in the upper Santa Fe or middle Santa Fe, the HGUs between the Rio Grande alluvium and lower Santa Fe. Additional data within the area, such as geophysical, other geochemical constituents, and interpretation of the groundwater-flow system, indicated that the major source for the elevated SpC values measured in groundwater samples collected from the Rio Grande alluvium was likely a deep groundwater source interacting with the Rio Grande, increasing the salinity in the river. The relatively saline groundwater contributed inflow to the Rio Grande, which in turn contributed to recharge to the Rio Grande alluvium as the river flowed downstream through the rest of the study area. The hydrogeologic connection between the Rio Grande, deep upwelling saline waters, and the Rio Grande alluvium is discussed in detail in the "Regional Groundwater Flow" section of this report. The SpC measurements in groundwater samples collected from wells completed in the upper Santa Fe in the Mesilla Valley generally increased from north to south, with the highest values measured in groundwater samples collected at the Paso del Norte (table 10, at back of report; fig. 20). Four SpC values greater than 2,100 µS/cm at 25 °C (the third quartile value of the entire dataset for SpC) (fig. 21*B*, at back of report) were measured in groundwater samples collected from wells completed in the middle Santa Fe in the southeastern part of the study area, near the Paso del Norte (fig. 20). These four samples with these higher SpC values were collected from wells Q31 (2,260 µS/cm at 25 °C), Q35 (7,020 µS/cm at 25 °C), Q41 (26,500 µS/cm at 25 °C), and Q42 (42,800 µS/cm at 25 °C) (table 10, at back of report; fig. 20). Near Las Cruces, groundwater samples collected from wells completed in the upper Santa Fe and middle Santa Fe had SpC values were lower compared to the SpC values in groundwater samples collected from wells completed in the middle Santa Fe in the southeastern part of the study area (table 10, at back of report; fig. 20). Wilson and others (1981) stated that there was a freshwater zone present throughout most of the Mesilla Valley. The measurements of relatively low SpC in the groundwater samples collected near Las Cruces were likely from this freshwater zone. Additional geochemical constituents for these samples indicated that the source of groundwater for these samples was not attributable to the Rio Grande and may possibly be groundwater underflow from the Jornada Basin. There is a bedrock high to the northeast of Las Cruces that restricts the flow of groundwater from the Jornada Basin to the Mesilla Basin but may not completely prevent flow through shallow structural saddles in the bedrock (Hawley and Kennedy, 2004; Hawley and others, 2005; Witcher and others, 2004).

Dissolved oxygen (DO) values within the study area ranged from 0.1 to 5.2 mg/L (table 10, at back of report; fig. 21*C*, at back of report). Mean DO concentrations (excluding outliers) measured in groundwater samples collected from the Rio Grande alluvium, upper Santa Fe, middle Santa Fe, and lower Santa Fe were about 0.2, 0.2, 0.5, and 0.2 mg/L, respectively (fig. 22*C*, at back of report). DO concentrations in groundwater samples collected in the study area were generally less than 0.5 mg/L (the third quartile value of the entire dataset for DO) (fig. 21*C*, at back of report) indicating most of the groundwater was likely under reducing conditions (McMahon and Chapelle, 2008). There were 11 groundwater samples with DO concentrations greater than or equal to 0.5 mg/L within the study area (table 10, at back of report). Eight of those groundwater samples with DO concentrations greater than or equal to 0.5 mg/L were measured in groundwater samples collected from wells completed in the middle Santa Fe (wells Q01 [4.2 mg/L], Q02 [1.1 mg/L], Q11 [2.6 mg/L], Q12 [5.2 mg/L], Q30 [1.6 mg/L], Q36 [1.2 mg/L], Q39 [1.4 mg/L], and Q43 [0.6 mg/L]) (table 10, at back of report; fig. 20). The remaining three groundwater samples with DO concentrations greater than or equal to 0.5 mg/L were collected from wells completed in the upper Santa Fe (wells Q00 [0.6 mg/L] and Q40 [0.5 mg/L]) or from the lower Santa Fe (well Q32 [0.6 mg/L]) (table 10, at back of report; fig. 20). The two measurements from groundwater with the highest DO concentrations were collected near the Aden Hills (well Q12 [5.2 mg/L]) and between the Rough and Ready Hills and the Robledo Mountains (well Q01 [4.2 mg/L]) (table 10, at back of report;

fig. 20). An additional measurement from groundwater with a relatively high DO concentration (well Q30 [1.6 mg/L]) was collected directly east of the East Potrillo Mountains (table 10, at back of report; fig. 20). The remaining eight measurements from groundwater with DO concentrations greater than or equal to 0.5 mg/L were collected near the Mesilla Valley (wells Q00 [0.6 mg/L], Q02 [1.1 mg/L], Q11 [2.6 mg/L], Q32 [0.6 mg/L], Q36 [1.2 mg/L], Q39 [1.4 mg/L], Q40 [0.5 mg/L], and Q43 [0.6 mg/L]). The measurements from groundwater with higher DO concentrations were indicative of recharge areas, areas containing little or no oxidizable materials in the subsurface, or areas of short residence times compared to the rate of oxygen consumption (Boghici, 2003)

Groundwater temperatures in the study area ranged from 16.6 to 34.5 °C; the mean water temperature of the entire dataset was 24.1 °C (table 10, at back of report; fig. 21*D*, at back of report). Compared to temperatures measured in samples collected from shallower depths, temperatures were generally higher in groundwater collected from deeper within the subsurface. The mean groundwater temperatures (excluding outliers) gradually increased with depth in samples collected from the Rio Grande alluvium (19.3 °C), upper Santa Fe (20.7 °C), middle Santa Fe (25.4 °C), and lower Santa Fe (26.7 °C) (table 10, at back of report; fig. 22*D*, at back of report). The temperature of groundwater was generally less than 24 °C in the upper Santa Fe but often was greater than 24 °C in the middle Santa Fe (fig. 22*D*, at back of report). These results are consistent with the apparent geothermal gradient reported by Witcher and others (2004). For the purpose of our investigation, groundwater warmer than 24 °C was classified as geothermal groundwater. Conversely, groundwater with a temperature of 24 °C or cooler was classified as "nongeothermal groundwater." Wells completed within the upper Santa Fe where geothermal groundwater was evident (Q14 [24.8 °C], Q15 [34.5 °C], Q27 [24.0 °C], and Q34 [24.2 °C]) were either outside of the Mesilla Valley or near the southern part of the Mesilla Valley (table 10, at back of report; fig. 20). The presence of geothermal groundwater may be a result of a localized inflow to a well from the upwelling of deeper, geothermal groundwater. The groundwater surrounding wells from which the samples that were obtained were classified as nongeothermal groundwater may have indirectly interacted with deeper, geothermal groundwater but was cooler than 24 °C (and therefore lacked a geothermal signature) because the warmer water cools as it moves away from its heat source and mixes with cooler groundwater (Witcher and others, 2004). As a result of this cooling and mixing of different sources of water, some groundwater had chemical characteristics of deeper, geothermal groundwater but was classified as nongeothermal.

Major-Ion Chemistry

The ionic composition of water can be determined by measuring the concentrations of major ions (anions and cations). Bartos and Ogle (2002) provide an overview on the use of anion and cation concentrations to characterize and describe the chemical quality of water. The major-ion balance was calculated and examined for each groundwater sample as a quality-assurance check of the chemical analyses. Anion and cation concentrations were used to calculate major-ion balances by using the following equation:

$$\text{Major-ion balance} = (\Sigma\text{cations} - \Sigma\text{anions}) \times 100/(\Sigma\text{cations} + \Sigma\text{anions}) \quad (6)$$

where

Σcations is the sum of the concentrations of dissolved cations (in milliequivalents per liter), and

Σanions is the sum of the concentrations of dissolved anions (in milliequivalents per liter).

The absolute values of major-ion-balance differences were less than 6 percent in 43 of the 44 groundwater samples (table 9, at back of report). The only sample with an absolute major-ion balance difference greater than 6 percent was collected from well Q31; this sample contained relatively high concentrations (greater than the third quartile value for the entire dataset of the constituent) of HCO_3 (1,060 mg/L), sodium (Na) (436 mg/L), magnesium (Mg) (37.5 mg/L), silica (Si) (63.8 mg/L), As (116 µg/L), lithium (Li) (547 µg/L), and uranium (U) (18.6 µg/L) (table 11, at back of report). The high concentrations of bicarbonate and Si measured in the sample from well Q31 are consistent with the relatively high saturation indexes of dolomite, strontianite, carbon dioxide gas, quartz, and chalcedony for this sample (table 9, at back of report).

Anions

Some of the most abundant anions in groundwater include Cl, SO_4, HCO_3, and CO_3. Less abundant anions include fluoride (F), bromide (Br), nitrate (NO_3), and nitrite (NO_2) (Hem, 1985; Freeze and Cherry, 1979). The concentrations of anions measured in groundwater samples collected in the study area are listed (table 11, at back of report). When considered together with cation concentrations, anion concentrations are useful for interpreting the chemical quality of groundwater and for determining water types based on ionic composition, also referred to as hydrochemical facies (Freeze and Cherry, 1979; Bartos and Ogle, 2002) (see "Water Types" section of this report). Anions also play an important role in determining whether groundwater is acidic or alkaline. In aqueous solutions, Cl and SO_4 are protonated to form hydrochloric acid (HCl) and sulfuric acid (H_2SO_4), respectively, both of which are strong acids. Weak acids and solutes derived from weak acids can be considered as contributing to acidity, alkalinity, or both, depending on the pH at which dissociation occurs. Through deprotonation, the weak acid carbonic acid (H_2CO_3) disassociates to HCO_3^- and water (H_2O); HCO_3^- can be further deprotonated to CO_3^{2-}; the additional proton added to solution also contributes to the acidity (Hem, 1985).

Chloride

Within the study area, Cl concentrations spanned four orders of magnitude, from 14.2 to 15,300 mg/L (table 10, at back of report; fig. 21*E*, at back of report). Mean Cl concentrations (excluding outliers) measured in groundwater samples collected from wells completed in the Rio Grande alluvium, upper Santa Fe, middle Santa Fe, and lower Santa Fe HGUs were 663, 170, 95.7, and 377 mg/L, respectively (table 11, at back of report; fig. 22*E*, at back of report). Cl concentrations were compared to the secondary drinking-water standard for Cl of 250 mg/L established by the U.S. Environmental Protection Agency (EPA) (U.S. Environmental Protection Agency, 2013). Comparisons to the EPA secondary drinking-water standard for Cl were done only as a point of reference for informational purposes; groundwater samples are not finished drinking water, so concentrations measured in untreated groundwater are not necessarily representative of the concentrations that would be measured in finished drinking water. Cl concentrations were greater than 250 mg/L in the samples collected from the following wells: Q14 (397 mg/L), Q18 (745 mg/L), Q19 (296 mg/L), Q25 (320 mg/L), Q26 (613 mg/L), Q29 (377 mg/L), Q32 (769 mg/L), Q34 (836 mg/L), Q35 (1,960 mg/L), Q37 (631 mg/L), Q40 (7,630 mg/L), Q41 (15,300 mg/L), and Q42 (305 mg/L) (table 11, at back of report; fig. 20). The Cl concentration values greater than 250 mg/L were all measured in groundwater samples collected in or near the southern part of the Mesilla Valley, near the Paso del Norte (table 11, at back of report; fig. 20). Cl concentrations in the three samples collected from wells completed in the Rio Grande alluvium ranged from 613 to 745 mg/L. A boxplot (fig. 22*E*, at back of report) depicts that Cl concentrations in the groundwater samples tended to decrease from the Rio Grande alluvium to the middle Santa Fe but then increased again in the lower Santa Fe, but generally not to the concentrations measured in the samples from the Rio Grande alluvium. Whereas Cl concentrations were greater than 250 mg/L in three of the four groundwater samples collected from wells completed in the lower Santa Fe, the majority of Cl concentrations measured in groundwater samples collected from wells completed in the upper Santa Fe and the middle Santa Fe were less than 250 mg/L (table 11, at back of report; fig. 22*E*, at back of report).

Sources of Cl in the Rio Grande alluvium, upper Santa Fe, middle Santa Fe, and lower Santa Fe were investigated. A comparison of Cl to Na molar concentrations helped to determine whether the Cl originated from rock-water interactions or from anthropogenic sources (Indiana Department of Natural Resources, 2002). When halite (NaCl) dissolves, a 1:1 correlation between Cl and Na results, representing equal amounts of Cl and Na. Many of the groundwater samples plotted below the 1:1 molar ratio line, indicating an apparent excess of Na in the groundwater system relative to Cl (fig. 23). The elevated concentrations of Na could be derived from the dissolution of silicate minerals such as plagioclase feldspar, cation exchange processes, or both (Plummer and others, 2004).

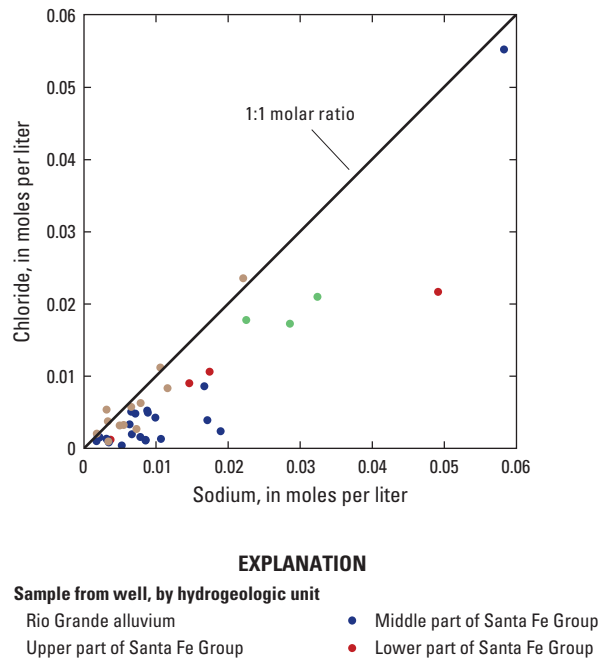

Figure 23. Relation between the molar concentrations of chloride and sodium measured in groundwater samples collected in the Mesilla Basin study area in Doña Ana County, New Mexico, and El Paso County, Texas, 2010.

The elevated Cl concentrations measured in groundwater samples collected from wells completed in the lower Santa Fe relative to the concentrations of Cl measured in samples collected from wells completed in the upper or middle Santa Fe resulted from the dissolution of halite within the deep subsurface (Witcher and others, 2004), whereas the relatively elevated Cl concentrations measured in groundwater samples collected from wells completed in the Rio Grande alluvium compared to the concentrations of these constituents measured in samples collected from wells completed in the upper and middle Santa Fe were likely from water recharging the system from the Rio Grande. A previous study indicated that Cl concentrations within the Rio Grande were similar to Cl concentrations within the Rio Grande alluvium; during periods of large flow, the Cl concentrations were lower in stream samples compared to the Cl concentrations measured in groundwater samples collected from the Rio Grande alluvium (Leggat and others, 1963). As explained in the “Description of the Study Area” section of this report, after 1915, the modifications made to the Rio Grande caused the amount of flow in the river to appreciably decrease on an overall basis. This decrease in flow reduces the dilution of inflows of relatively saline water from drains and saline groundwater, resulting in higher Cl concentrations in the Rio Grande than would have occurred if the streamflow were unregulated (Moyer and others, 2013). Because the Rio Grande is typically a losing stream within the study area, high concentrations of Cl in the river raise the concentrations of Cl in the underlying

groundwater system, which is reflected in the Cl concentrations measured in samples collected from the Rio Grande alluvium. The sources of Cl include leaching of salts from the soils by irrigation (excess water drains from the fields and becomes inflow to the Rio Grande) and groundwater from a deep groundwater source discharging higher salinity water to the river with subsequent downstream transport and recharge into the Rio Grande alluvium. This process is discussed in detail in the "Regional Groundwater Flow" section of this report.

Sulfate

Mean SO_4 concentrations (excluding outliers) measured in groundwater samples collected from wells completed in the Rio Grande alluvium, upper Santa Fe, middle Santa Fe, and lower Santa Fe HGUs were 978, 254, 139, and 424 mg/L, respectively (table 11, at back of report; fig. 22*F*, at back of report). Similar to the analytical results from the groundwater samples for Cl concentration, SO_4 concentrations were generally higher in groundwater samples collected from wells completed in the Rio Grande alluvium or the lower Santa Fe compared to SO_4 concentrations measured in groundwater samples collected from wells completed in the upper Santa Fe or the middle Santa Fe (table 11, at back of report; fig. 22*F*, at back of report). The concentration of SO_4 exceeded the secondary drinking water standard of 250 mg/L established by the EPA for this constituent (U.S. Environmental Protection Agency, 2013) in 18 of the 44 groundwater samples collected in the study area. With exception of the SO_4 concentration of 544 mg/L measured in the sample collected from well Q01 located between the Rough and Ready Hills and the Robledo Mountains, all of SO_4 concentrations greater than 250 mg/L were measured in samples collected from wells in or near the Mesilla Valley: Q03 (469 mg/L), Q09 (441 mg/L), Q13 (639 mg/L), Q18 (938 mg/L), Q25 (412 mg/L), Q26 (1,380 mg/L), Q29 (296 mg/L), Q31 (256 mg/L), Q32 (912 mg/L), Q34 (331 mg/L), Q35 (1,090 mg/L), Q36 (357 mg/L), Q37 (616 mg/L), Q39 (268 mg/L), Q40 (4,600 mg/L), Q41 (4,970 mg/L), and Q42 (735 mg/L) (table 11, at back of report; fig. 20).

Potential sources of SO_4 in the groundwater system may be dissolution of gypsum and anhydrite (anhydrous $CaSO_4$) (Witcher and others, 2004). The weathering of sulfide materials such as pyrite (FeS_2) might be another source of SO_4 through complex oxidation processes (Nordstrom and others, 2007), but the oxidation of these sulfide materials likely contribute only a minor amount of SO_4 to the groundwater system (Witcher and others, 2004). A comparison of the molar ratios of Ca and SO_4 (moles per liter [mol/L] Ca per mol/L SO_4) measured in the groundwater samples collected in the study area indicated whether the Ca and SO_4 originated from the dissolution of gypsum and anhydrite or from another source. If gypsum and anhydrite were dissolved proportionally, there should be a 1:1 correlation between molar ratios of Ca and SO_4. The chemical composition of many of the groundwater samples collected in the study area was representative of gypsum and anhydrite dissolution, but there was likely slightly more SO_4 in the groundwater system than Ca because many of the groundwater samples plotted below the 1:1 line (fig. 24). Other potential sources of SO_4 within the system might be the dissolution of celestite ($SrSO_4$). Calcite ($CaCO_3$), dolomite, and aragonite ($CaCO_3$) all had saturation indexes of about zero, which indicated that those minerals were in equilibrium in the groundwater (table 9, at back of report). There was generally a negative saturation index for gypsum, anhydrite, and celestite (table 9, at back of report), indicating that these minerals were readily dissolved in the groundwater system, that most of the Ca in the groundwater likely originates from the dissolution of gypsum and anhydrite, and that most of the SO_4 likely originates from the dissolution of gypsum, anhydrite, and celestite.

Whereas the differences in SO_4 to Cl molar ratios by hydrogeologic unit were generally small (fig. 25), spatial variations were evident (fig. 26). Groundwater samples with SO_4 to Cl molar ratios greater than 0.85 (the third quartile value for the entire dataset of SO_4 to Cl molar ratios) were generally collected from wells in uplifted areas in the western part of the study area, where concentrations of SO_4 and Cl were relatively low (table 11, at back of report; fig. 26). Even though the concentrations of SO_4 and Cl were relatively low (less than 242 and 139 mg/L, respectively) (table 11, at back of report) in the western part of the study area, SO_4 to Cl molar ratios were greater than 0.85, which is indicative of slightly more dissolution of gypsum and anhydrite and less dissolution of halite.

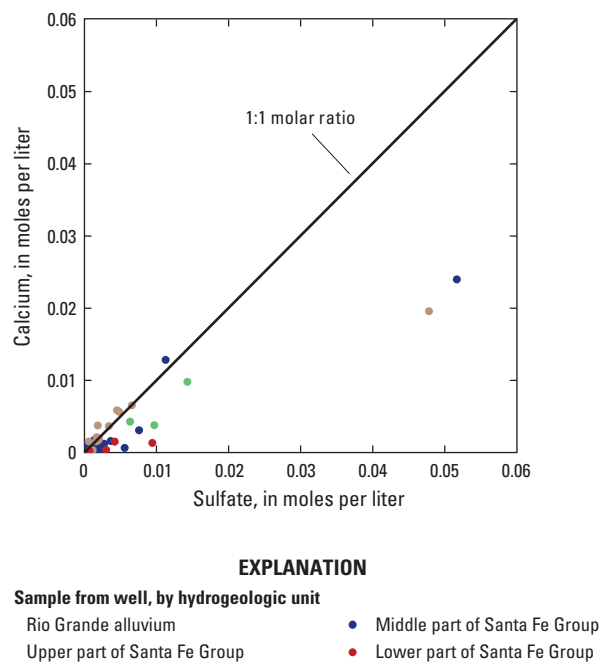

Figure 24. Relation between the molar concentrations of calcium and sulfate measured in groundwater samples collected in the Mesilla Basin study area in Doña Ana County, New Mexico, and El Paso County, Texas, 2010.

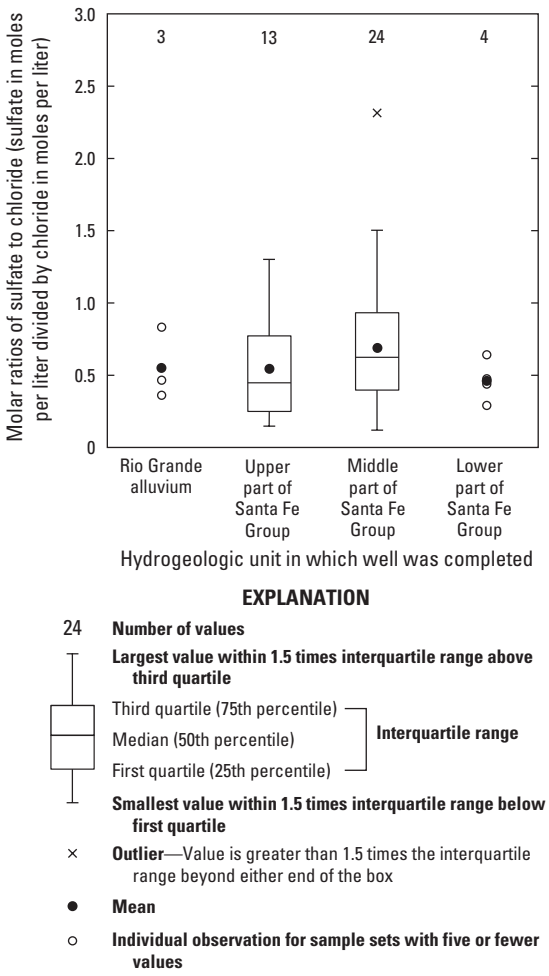

Figure 25. Molar ratios of sulfate to chloride measured in groundwater samples collected in the Mesilla Basin study area in Doña Ana County, New Mexico, and El Paso County, Texas, 2010.

Bicarbonate

For the entire dataset, HCO_3 concentrations ranged from 18.5 to 1,970 mg/L, and the mean was 289 mg/L (table 11, at back of report; fig. 21*G*, at back of report). Mean HCO_3 concentrations (excluding outliers) measured in groundwater samples collected from wells completed in the Rio Grande alluvium, upper Santa Fe, middle Santa Fe, and lower Santa Fe HGUs were about 516, 279, 180, and 527 mg/L, respectively (fig. 22*G*, at back of report). The mean HCO_3 concentration for the lower Santa Fe is greater than the mean HCO_3 concentrations for the other HGUs because the sample collected from well Q32 yielded a HCO_3 concentration of 1,970 mg/L, which is two orders of magnitude larger than the HCO_3 concentrations measured in the other three samples collected from wells completed in the lower Santa Fe (wells Q21 [79.9 mg/L], Q25 [18.5 mg/L], and Q29 [40.7 mg/L]) (table 11, at back of report). Because the lower Santa Fe had a small sample set, none of the values were considered outliers, but the mean without the value from well Q32 included is 46.4 mg/L, which would result in the lower Santa Fe having the smallest mean HCO_3 concentrations of all of the HGUs. Compared to groundwater samples collected from the other HGUs in the study area, groundwater samples collected from the Rio Grande alluvium generally had the highest HCO_3 concentrations. A total of 30 of the 39 HCO_3 concentrations measured samples collected from wells completed in the upper Santa Fe, middle Santa Fe, or lower Santa Fe were less than 358 mg/L (the third quartile value of the entire dataset for HCO_3) (table 11, at back of report; fig. 21*G*, at back of report). Most of the HCO_3 concentrations greater than 358 mg/L were measured in samples collected from the southeastern part of the study area, in or near the Mesilla Valley, or from the southwestern part of the study area, near the East and West Potrillo Mountains (table 11, at back of report; fig. 20). A few relatively high HCO_3 concentrations of more than 358 mg/L were measured in samples from the upper Santa Fe, particularly in samples collected in southern part of the Mesilla Valley. Concentrations of HCO_3 may be higher where feldspar-rich sands are common. Feldspar-rich sands are prevalent in the Camp Rice Formation (upper part of the upper Santa Fe) (fig. 2) and facilitate dissolution of aluminosilicate minerals such as potassium feldspar (Witcher and others, 2004). The highest concentrations of HCO_3 were measured in two groundwater samples collected at the same location in the southern part of the Mesilla Valley (one sample collected from a well completed in the middle Santa Fe [well Q31, 1,060 mg/L] and the other from the lower Santa Fe [well Q32, 1,970 mg/L]) (table 11, at back of report; fig. 20). The samples with high concentrations of HCO_3 collected from deeper in the subsurface (middle Santa Fe and lower Santa Fe) may represent water that had prolonged exposure to the Paleozoic- and early Cretaceous-age carbonate and siliciclastic rocks found in the uplifts in the area (Witcher and others, 2004).

Fluoride

The concentrations of F were relatively low in the groundwater samples collected throughout the study area, with the highest concentrations generally measured in samples collected from wells completed in the middle Santa Fe (table 11, at back of report; fig. 21*H*, at back of report). Mean F concentrations (excluding outliers) measured in samples collected from wells completed in the Rio Grande alluvium, upper Santa Fe, middle Santa Fe, and lower Santa Fe HGUs were about 0.42, 0.48, 0.92, and 1.61 mg/L, respectively (fig. 22*H*, at back of report). The F concentration measured in the sample collected from well Q29 (4.73 mg/L) is an order of magnitude larger than F concentrations measured in the other samples collected from wells completed in the lower Santa Fe (wells Q21 [0.68 mg/L], Q25 [0.28 mg/L], and Q32 [0.73 mg/L]) (table 11, at back of report). Because of the small number of samples collected from wells completed in the lower Santa Fe, the F concentration measured in the

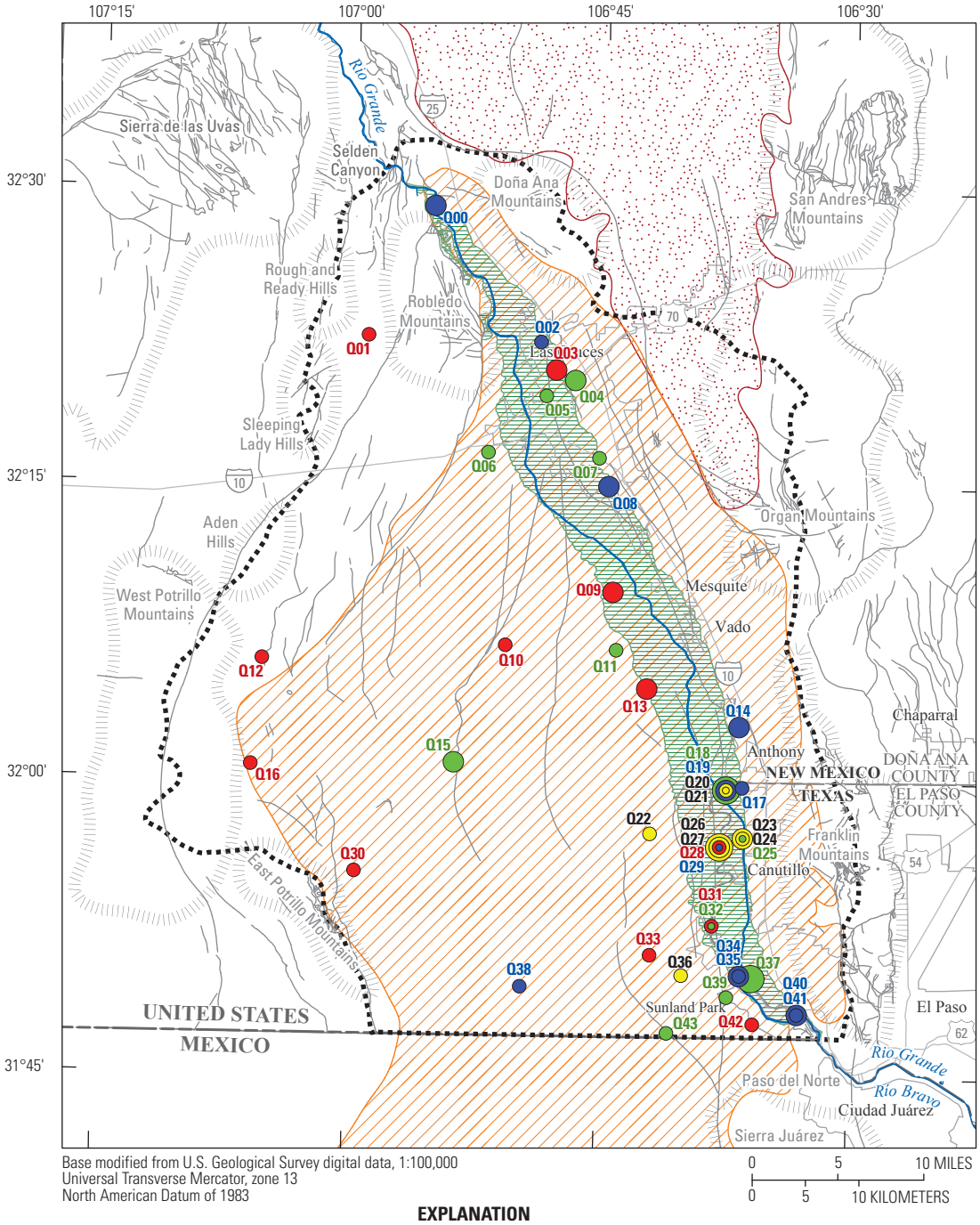

Figure 26. Spatial variations in the ratio of molar concentrations of sulfate to chloride measured in groundwater samples collected in the Mesilla Basin study area in Doña Ana County, New Mexico, and El Paso County, Texas, 2010.

sampled collected from well Q29 was not considered an outlier. All of the other samples collected in the study area with F concentrations greater than 1.10 mg/L (the third quartile value of the entire dataset for F) were collected from wells completed in the middle Santa Fe, with the exceptions of one sample collected from a well completed in the upper Santa Fe (well Q15 [1.33 mg/L]) in the center of the West Mesa and one sample collected from a well completed in the lower Santa Fe (well Q29 [4.73 mg/L]) near the southern part of the Mesilla Valley (table 11, at back of report; fig. 20). Groundwater samples collected from wells completed in the middle Santa Fe with F concentrations greater than 1.10 mg/L were generally collected in the southern and southwestern parts of the study area. The volcanic highlands in the western part of the study area can be a potential source of F to the groundwater system; weathering of volcanic rocks can cause F concentrations in groundwater to increase (Plummer and others, 2004).

Bromide

In 33 of the 44 groundwater samples collected, Br concentrations were less than 0.547 mg/L (the third quartile value of the entire dataset for Br) (table 11, at back of report; fig. 21*I*, at back of report). Mean Br concentrations (excluding outliers) measured in groundwater samples collected from wells completed in the Rio Grande alluvium, upper Santa Fe, middle Santa Fe, and lower Santa Fe HGUs were 0.818, 0.235, 0.281, and 0.364 mg/L, respectively (fig. 22*I*, at back of report). Groundwater samples with elevated concentrations of Br (greater than the third quartile of the entire dataset for Br) were distributed among the different HGUs as follows: three Rio Grande alluvium samples (wells Q18 [0.753 mg/L], Q26 [1.11 mg/L], and Q37 [0.590 mg/L]), two upper Santa Fe samples (wells Q34 [0.776 mg/L] and Q40 [4.82 mg/L]), five middle Santa Fe samples (wells Q01 [1.72 mg/L], Q16 [0.666 mg/L], Q35 [0.776 mg/L], Q36 [0.913 mg/L], and Q41 [7.92 mg/L]), and one lower Santa Fe sample (well Q32 [0.597 mg/L]) (table 11, at back of report; fig. 20). The highest mean Br concentrations were generally measured in groundwater samples collected from the Rio Grande alluvium. Compared to Br concentrations measured in other samples from the same HGU, outliers were identified among the samples collected from wells completed in the upper Santa Fe (wells Q34 [0.776 mg/L] and Q40 [4.82 mg/L]) and the middle Santa Fe (wells Q01 [1.72 mg/L] and Q41 [7.92 mg/L]) (table 11, at back of report; fig. 20). The mean Br values for upper and Middle Santa Fe would have been higher had the outliers from those HGUs not been excluded from analysis. All of the groundwater samples with Br concentrations greater than 0.547 mg/L were collected from the southern part of the Mesilla Valley except for two groundwater samples collected from uplifted areas in the western part of the Mesilla Basin (wells Q01 [1.72 mg/L] and Q16 [0.666 mg/L]).

Br is a conservative ion, and is less abundant in natural groundwater than Cl (Witcher and others, 2004). Ratios of Cl to Br (Cl in mg/L divided by Br in mg/L) can indicate potential sources of Br into the system. Low ratios of Cl to Br (Cl/Br) are typical in natural water systems. Witcher and others (2004) reported the following Cl/Br ratios: seawater (290), meteoric water (50–180), organic materials (20–200), and igneous and metamorphic rocks (100–500). Compared to these relatively low Cl/Br ratios for seawater, meteoric water, organic materials, and igneous and metamorphic rocks, higher Cl/Br ratios can be associated with anthropogenic sources such as road salt, sewage, industrial waste, and agricultural processes or with dissolution of evaporite minerals such as halite or the release of salts during other water-rock interactions (Witcher and others, 2004). Davis and others (1998) reported that Cl/Br ratios in subsurface saline water can range from a mean of about 60 to as high as 5,700, and that differences in the ratio can indicate the source and type of water, predominant water-rock interactions, or both. According to Davis and others (1998), the presence of seawater in the subsurface is indicated when the Cl/Br ratio is about 290, that water influenced by dissolution of halite is indicated when the Cl/Br ratio is about 4,000, and that water with a Cl/Br ratio of about 125 likely represents static water within ancient igneous rocks. Davis and others (1998) also determined that geothermal water has a mean Cl/Br ratio of 1,237, and that in subsurface fresh and brackish water, the mean Cl/Br ratios range from about 40 to about 300.

Cl/Br ratios measured in the 44 samples collected in the study area ranged from 70.3 to 2,530 (table 11, at back of report). Cl/Br ratios between 467 and 997 (the first and third quartiles, respectively, of the entire dataset of Cl/Br ratios) were representative of groundwater mixing with dissolution of evaporite minerals contained in basin deposits or mixing with geothermal waters (fig. 27) (Witcher and others, 2004). The Cl/Br ratios in this range for some of the samples collected in or near Las Cruces (wells Q02 [874], Q04 [657], Q05 [642], Q06 [646], Q07 [584], and Q08 [782]) (fig. 27) might be an artifact of Cl inputs from anthropogenic sources such as road salts, sewage, and industrial waste within the city and leachate from agricultural processes near the city (fig. 27). Samples with Cl/Br ratios greater than 997 were representative of geothermal water in which geochemical processes such as dissolution of evaporite minerals from the Paleozoic marine rocks may have occurred (Witcher and others, 2004).

Nitrate Plus Nitrite

Combined nitrate plus nitrite (NO_3+NO_2) concentrations in groundwater samples collected from wells completed in the Rio Grande alluvium, upper Santa Fe, and lower Santa Fe HGUs were less than the LRL of 0.02 mg/L with the exception of one sample collected from a well completed in the upper Santa Fe (well Q00). In contrast, the NO_3+NO_2 concentration exceeded the LRL in 10 of the 24 samples collected from wells completed in the middle Santa Fe (the LRL was exceeded in the samples from wells Q01, Q02, Q12, Q16, Q30, Q33, Q36, Q39, Q42, and Q43) (table 11, at back of report). Groundwater samples with measurable

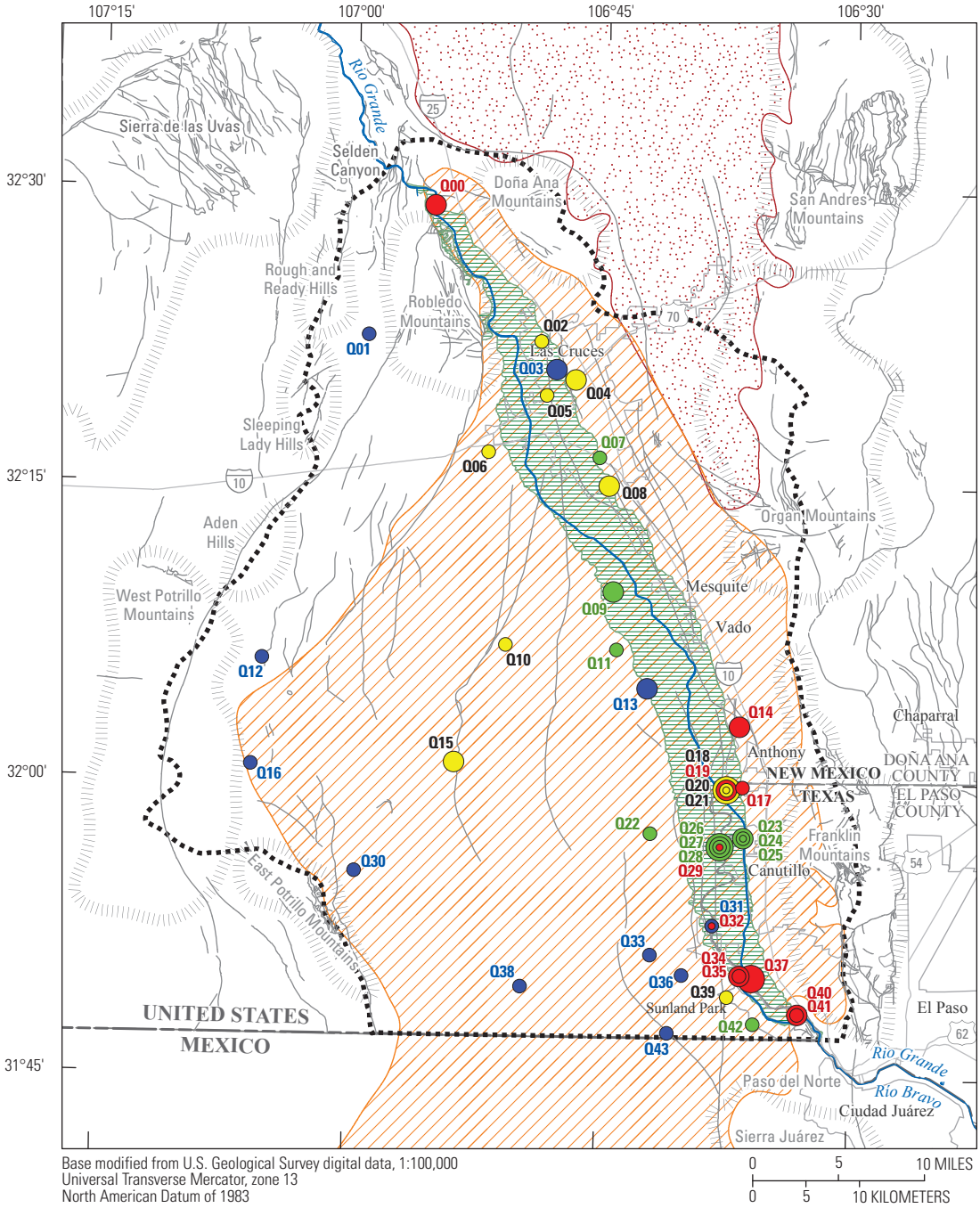

EXPLANATION

Mesilla Basin (United States)/Conejos-Médanos (Mexico) aquifer system—Modified from El Paso Water Utilities (2007)

Rio Grande alluvium in the Mesilla Valley—Modified from Hawley and Kennedy (2004), Hawley and others (2005)

Jornada del Muerto Basin aquifer system—Modified from Daniel B. Stephens and Associates (2010)

Mesilla Basin study area boundary

Fault or fault zone—From Hawley and Kennedy (2004), Hawley and others (2005)

Well sampled, by ratio of chloride, in milligrams per liter, to bromide, in milligrams per liter (table 11), and identifier (table 5)

Q41 Greater than the third quartile value of 997 (fourth quartile)

Q10 Greater than the median value of 637 and less than or equal to 997 (third quartile)

Q07 Greater than the first quartile value of 467 and less than or equal to 637 (second quartile)

Q43 Less than or equal to 467 (first quartile)

Well sampled—Symbol size represents hydrogeologic unit in which well was completed

Completed in the Rio Grande alluvium

Completed in the upper part of Santa Fe Group

Completed in the middle part of Santa Fe Group

Completed in the lower part of Santa Fe Group

Note: Well identifiers are labeled from the uppermost hydrogeologic unit at the top to the lowermost hydrogeologic unit at the bottom when more than one sample was collected in the same location.

Figure 27. Spatial variations in the mass ratios of chloride to bromide concentrations measured in groundwater samples collected in the Mesilla Basin study area in Doña Ana County, New Mexico, and El Paso County, Texas, 2010.

concentrations of NO_3+NO_2 tended to have relatively high DO concentrations (more than 0.5 mg/L, the third quartile of the entire dataset for DO) (fig. 21*C*, at back of report). All but 3 of the 11 groundwater samples with NO_3+NO_2 concentrations above the LRL also had DO concentrations greater than 0.5 mg/L (table 10, at back of report). Sources of NO_3 include the dissolution and recharge of accumulations of NO_3 (from fertilizer, atmospheric deposition, or natural sources) on the land surface during periodic wet periods and discharges from septic tanks or other domestic sources (Plummer and others, 2004; U.S. Geological Survey, 1999). The highest and second highest NO_3+NO_2 concentrations were measured in a groundwater sample collected in the Aden Hills (well Q12 [8.38 mg/L]) and in a groundwater sample collected from a well between the Rough and Ready Hills and the Robledo Mountains (well Q01 [6.34 mg/L]) (table 11, at back of report; fig. 20). Another groundwater sample with a relatively high NO_3+NO_2 concentration was collected east of the East Potrillo Mountains (well Q30 [3.41 mg/L]) (table 11, at back of report; fig. 20). The wells from which these samples were collected were all in areas where runoff from mountains and uplifted area recharged into the groundwater system, indicating these locations likely have aerobic conditions causing the oxidation of ammonia (NH_3) into NO_2 and further oxidation of NO_2 into NO_3. Concentrations of NH_3 were less than or equal to the LRL in all but two of the groundwater samples (well Q00 [0.086 mg/L as nitrogen] and Q42 [0.010 mg/L as nitrogen, equivalent to the LRL for reporting purposes]) collected in the study area with concentration of NO_3+NO_2 greater than the LRL (table 11, at back of report). The lack of NH_3 in samples with measurable concentrations of NO_3+NO_2, with the exceptions of well Q00 and Q42, is consistent with the hypothesis of NH_3 oxidation.

Cations

Some of the most abundant cations in groundwater are Na, Ca, Mg, and K; concentrations of these and other less abundant cations such as Si and ammonia (as nitrogen) (NH_3-N) can provide insights regarding the chemical quality of groundwater (Hem, 1985; Freeze and Cherry, 1979). The concentrations of cations and water types for each groundwater sample collected in the study area are provided (table 11, at back of report).

Sodium

The majority of Na concentrations measured in groundwater samples were less than 387 mg/L (the third quartile of the entire dataset for Na); concentrations less than 387 mg/L were measured in most samples collected from wells completed within the Santa Fe Group (upper Santa Fe, middle Santa Fe or lower Santa Fe) (table 11, at back of report; fig. 21*K*, at back of report). Mean Na concentrations (excluding outliers) measured in groundwater samples collected from wells completed in the Rio Grande alluvium, upper Santa Fe, middle Santa Fe, and lower Santa Fe HGUs were about 640, 138, 173, and 488 mg/L, respectively (fig. 22*K*, at back of report). The Na concentrations decreased from the Rio Grande alluvium to the upper Santa Fe but then gradually increased from the upper Santa Fe to the lower Santa Fe. Groundwater samples with the highest Na concentrations (those greater than the third quartile of the entire dataset for Na) were collected from three wells completed in the Rio Grande alluvium (wells Q18 [745 mg/L], Q26 [657 mg/L], and Q37 [518 mg/L]), two wells completed in the upper Santa Fe (wells Q34 [508 mg/L] and Q40 [5,230 mg/L]), four wells completed in the middle Santa Fe (wells Q01 [394 mg/L], Q31 [436 mg/L], Q35 [1,340 mg/L], and Q41 [8,590 mg/L]), and two wells completed in the lower Santa Fe (Q29 [401 mg/L] and Q32 [1,130 mg/L]) (table 11, at back of report; fig. 20). Samples with Na concentrations greater than 387 mg/L were collected from wells in the southern part of the Mesilla Valley near the Paso del Norte except for well Q01, which is between the Rough and Ready Hills and the Robledo Mountains.

Calcium

In general, the groundwater samples with the highest Ca concentrations were collected from wells completed in the Rio Grande alluvium (table 11, at back of report; fig. 21*L*, at back of report). Mean Ca concentrations (excluding outliers) measured in groundwater samples collected from wells completed in the Rio Grande alluvium, upper Santa Fe, middle Santa Fe, and lower Santa Fe HGUs were about 239, 117, 31.7, and 34.7 mg/L, respectively (fig. 22*L*, at back of report). Ca concentrations decreased with depth and were lower in samples collected from wells completed in the upper Santa Fe compared to wells completed in the Rio Grande alluvium and decreased further in samples collected from wells completed in the middle Santa Fe and the lower Santa Fe. Groundwater samples with elevated concentrations of Ca (greater than the third quartile of the entire dataset for Ca) were collected from three wells completed in the Rio Grande alluvium (wells Q18 [152 mg/L], Q26 [393 mg/L], and Q37 [172 mg/L]), six wells completed in the upper Santa Fe (wells Q03 [227 mg/L], Q09 [235 mg/L], Q13 [263 mg/L], Q14 [151 mg/L], Q34 [147 mg/L], and Q40 [785 mg/L]), and two wells completed in the middle Santa Fe (wells Q35 [515 mg/L] and Q41 [962 mg/L]) (table 11, at back of report; fig. 20). All of these wells are in the Mesilla Valley.

A comparison of Ca to Na molar ratios across the study area reveals that most were less than 1, indicating there was less Ca than Na in most of the groundwater samples (fig. 28). The highest Ca to Na molar ratio values were measured in groundwater samples collected from wells completed in the upper Santa Fe near the middle part of the Mesilla Valley (fig. 29). These relatively high Ca to Na molar ratios might be related to spatial differences in the molar concentrations Ca and Na and mineral dissolution (table 11, at back of report; fig. 20). As discussed in the “Sulfate” section of this report, groundwater samples with relatively high SO_4 to Cl molar ratios (greater than 0.85) were typically collected in the uplifted areas (fig. 26), and high molar ratios of SO_4 relative

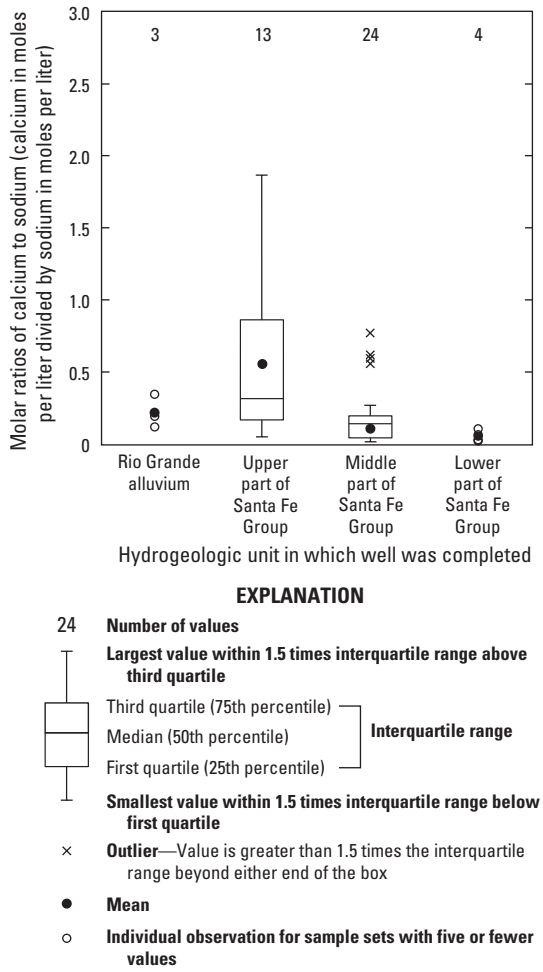

Figure 28. Molar ratios of calcium to sodium measured in groundwater samples collected in the Mesilla Basin study area in Doña Ana County, New Mexico, and El Paso County, Texas, 2010.

to Cl imply slightly more dissolution of gypsum and anhydrite and less dissolution of halite in the uplifted areas. High SO_4 molar concentrations relative to Cl were also manifested in the saturation indexes for calcite, dolomite, gypsum, anhydrite, and aragonite; calcite, dolomite, and aragonite had saturation indexes close to zero, and there were generally negative saturation indexes for gypsum and anhydrite (table 9, at back of report). The negative saturation indexes indicated that gypsum and anhydrite were readily dissolved, with most of the Ca in the groundwater originating from the dissolution of these minerals. Comparisons of the molar ratios of Ca to Na (figs. 28 and 29), Ca to SO_4 (fig. 24), SO_4 to Cl (figs. 25 and 26), and Cl to Na (fig. 23) indicated that there was dissolution of halite, celestite, gypsum, and anhydrite within the groundwater system, and that there appeared to be more halite dissolution than gypsum dissolution.

Magnesium

Mean Mg concentrations (excluding outliers) in groundwater samples collected from wells completed in the Rio Grande alluvium, upper Santa Fe, middle Santa Fe, and lower Santa Fe were about 51.0, 23.0, 5.90, and 5.47 mg/L, respectively (fig. 22*M*, at back of report). The mean value for the lower Santa Fe is likely skewed to a high value because there is one value (well Q32 [21.4 mg/L]) that is two orders of magnitude larger than the other three samples in that HGU (wells Q21 [0.166 mg/L], Q25 [0.172 mg/L], and Q29 [0.149 mg/L]) (table 11, at back of report). Because the small sample set collected from wells completed in lower Santa Fe was small, none of the values were considered outliers, but the mean without the value from well Q32 included is 0.162 mg/L, which would result in the lower Santa Fe having an appreciably lower mean value than the other HGUs by at least an order of magnitude. With the exception of most of the samples collected from wells completed in the lower Santa Fe, the Mg concentrations generally decreased with depth. All but three of the Mg concentrations measured in samples collected from wells completed in the middle Santa Fe and lower Santa Fe were less than 22.0 mg/L (the third quartile value of the entire dataset for Mg) (table 11, at back of report; fig. 20; fig. 21*M*, at back of report). The three elevated (greater than 22.0 mg/L) Mg concentrations from the middle Santa Fe (wells Q31 [37.5 mg/L], Q35 [28.1 mg/L], and Q41 [728 mg/L]), along with a Mg concentration of 360 mg/L measured at well Q40 completed in the upper Santa Fe, were all measured in samples collected in the southern part of the Mesilla Valley. The highest and second highest concentrations from this subset of groundwater samples (wells Q40 [360 mg/L] and Q41 [728 mg/L]) were measured in groundwater samples collected at the Paso del Norte. Groundwater exposure to dolomite found within the Paleozoic and Cretaceous rocks, which were shallowly buried in the area, might be the source of the relatively high Mg concentrations in the samples collected at the Paso del Norte (Witcher and others, 2004; Plummer and others, 2004). For the samples with elevated Mg concentrations that were collected from the Rio Grande alluvium or the upper Santa Fe, evaporation was the likely source of the Mg, not the Paleozoic and Cretaceous rocks (Plummer and others, 2004).

Silica

Among the four HGUs, groundwater samples collected from wells completed in the middle Santa Fe had the most variable Si concentrations, ranging from a minimum of 14.5 mg/L (well Q41) to a maximum of 85.1 mg/L (well Q30) (table 11, at back of report; fig. 20; fig. 21*N*, at back of report). Mean Si concentrations (excluding outliers) for samples collected from wells completed in the Rio Grande alluvium, upper Santa Fe, middle Santa Fe, and lower Santa Fe, were about 37.2 mg/L, 33.2 mg/L, 36.3 mg/L, and 31.7 mg/L, respectively (table 11, at back of report; fig. 22*N*, at back of report). The higher Si concentrations (greater than 41.1 mg/L,

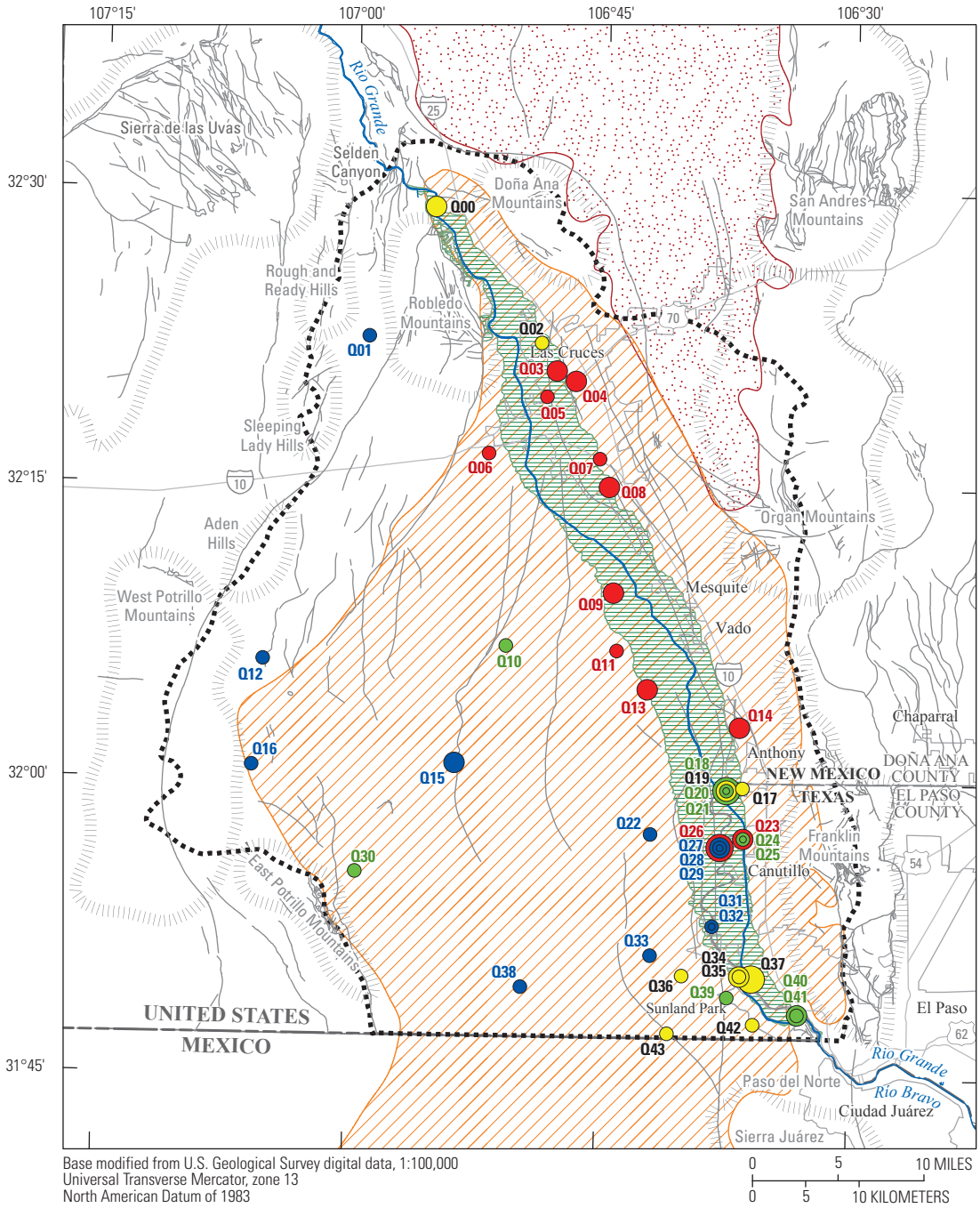

EXPLANATION

Mesilla Basin (United States)/Conejos-Médanos (Mexico) aquifer system—Modified from El Paso Water Utilities (2007)

Rio Grande alluvium in the Mesilla Valley—Modified from Hawley and Kennedy (2004), Hawley and others (2005)

Jornada del Muerto Basin aquifer system—Modified from Daniel B. Stephens and Associates (2010)

Mesilla Basin study area boundary

Fault or fault zone—From Hawley and Kennedy (2004), Hawley and others (2005)

Well sampled, by ratio of calcium, in moles per liter, to sodium, in moles per liter (table 11), and identifier (table 5)

Q05 Greater than the third quartile value of 0.31 (fourth quartile)

Q17 Greater than the median value of 0.15 and less than or equal to 0.31 (third quartile)

Q41 Greater than the first quartile value of 0.06 and less than or equal to 0.15 (second quartile)

Q22 Less than or equal to 0.06 (first quartile)

Well sampled—Symbol size represents hydrogeologic unit in which well was completed

Completed in the Rio Grande alluvium

Completed in the upper part of Santa Fe Group

Completed in the middle part of Santa Fe Group

Completed in the lower part of Santa Fe Group

Note: Well identifiers are labeled from the uppermost hydrogeologic unit at the top to the lowermost hydrogeologic unit at the bottom when more than one sample was collected in the same location.

Figure 29. Spatial variations in the molar ratios of calcium to sodium measured in groundwater samples collected in the Mesilla Basin study area in Doña Ana County, New Mexico, and El Paso County, Texas, 2010.

the third quartile value of the entire dataset for Si) were generally measured in groundwater samples collected in the southern part of the study area except for one groundwater sample with a concentration of 72.1 mg/L (well Q01) collected between the Rough and Ready Hills and the Robledo Mountains. Witcher and others (2004) noted that high Si concentrations might indicate geothermal waters or mixtures of geothermal and nongeothermal waters within the study area, but that there may be other processes involved.

As stated in the "Bicarbonate" section of this report, the high concentrations of HCO_3 within the upper units (Rio Grande alluvium and upper Santa Fe) in the Mesilla Valley may have been a result of dissolution of aluminosilicate minerals (Witcher and others, 2004); in addition to releasing HCO_3, dissolution of aluminosilicate minerals would have also released Si and K into solution, increasing the concentrations of Si and K in the groundwater. Comparison of HCO_3 to Si (mass HCO_3/mass Si) indicated that samples that had higher concentrations of HCO_3 generally had higher concentrations of Si (fig. 30). The dissolution of aluminosilicate minerals was a result of low-temperature irreversible feldspar-dissolution processes and not temperature-dependent geothermal processes (Witcher and others, 2004).

Potassium

Mean K concentrations (excluding outliers) in groundwater samples collected from the Rio Grande alluvium, upper Santa Fe, middle Santa Fe, and lower Santa Fe were about 15.8, 10.8, 5.58, and 3.40 mg/L, respectively

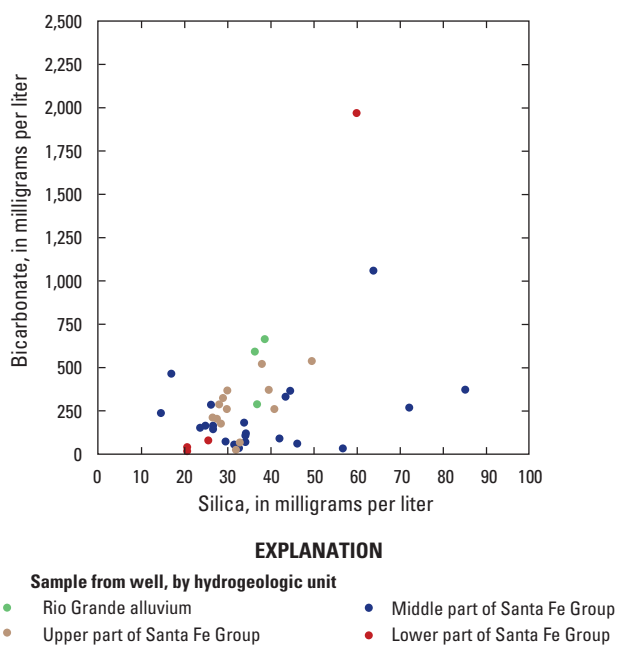

Figure 30. Relation between bicarbonate and silica concentrations measured in groundwater samples collected in the Mesilla Basin study area in Doña Ana County, New Mexico, and El Paso County, Texas, 2010.

(fig. 22*O*, at back of report). Groundwater sample results for concentrations of K within the study area generally decreased with depth: the highest mean concentrations of K were generally measured in groundwater samples collected from wells completed in the Rio Grande alluvium, and the lowest mean concentrations of K were generally measured in groundwater samples collected from wells completed in the lower Santa Fe. All but four of the groundwater samples with K concentrations greater than 11.1 mg/L (the third quartile of the entire dataset for K) were collected from wells in and near the Mesilla Valley (table 11, at back of report; fig. 20; fig. 21*O*, at back of report). Three of the four remaining groundwater samples with elevated K concentrations (greater than 11.1 mg/L) were collected from wells in the southwestern part of the study area (wells Q15 [11.5 mg/L], Q30 [20.4 mg/L], and Q38 [13.3 mg/L]); the other was collected in the northwestern part of the study area from a well between the Rough and Ready Hills and the Robledo Mountains (well Q01 [27.6 mg/L]) (table 11, at back of report; fig. 20). When analytical results from groundwater sample concentrations of Si to concentrations of K were compared, elevated concentrations for these constituents were often measured in samples collected from the same well (table 11, at back of report; fig. 20). In addition to high Si concentrations, high K concentrations can result from the dissolution of aluminosilicate minerals (Witcher and others, 2004).

Ammonia

Mean concentrations (excluding outliers) of ammonia (as nitrogen) (NH_3-N) in groundwater samples collected from wells completed in the Rio Grande alluvium, upper Santa Fe, middle Santa Fe, and lower Santa Fe were about 0.398, 0.049, 0.017, and 0.045 mg/L, respectively (fig. 22*P*, at back of report). NH_3-N concentrations were generally higher in samples collected from wells completed in the Rio Grande alluvium compared to samples collected from wells completed in one of the HGUs composing the Santa Fe Group (upper Santa Fe, middle Santa Fe, or lower Santa Fe). There were eight NH_3-N concentrations of more than 0.089 mg/L (the third quartile value of the entire dataset for NH_3-N) (table 11, at back of report; fig. 21*P*, at back of report) measured in samples collected from wells completed in one of the HGUs composing the Santa Fe Group in the middle and southern parts of the Mesilla Valley (wells Q09 [0.290 mg/L], Q13 [0.186 mg/L], and Q40 [1.39 mg/L] completed in the upper Santa Fe; wells Q06 [0.132 mg/L], Q31 [0.097 mg/L], Q35 [0.111 mg/L], and Q41 [1.11 mg/L] completed in the middle Santa Fe; and well Q32 [0.101 mg/L] completed in the lower Santa Fe) (table 11, at back of report; fig. 20). Irrigation return flows might account for the high concentrations of NH_3-N found in some samples; nutrient-laden irrigation water containing NH_3-N can run off from agricultural fields and drain into the surface-water system or directly recharge into the groundwater system. The transition from surface water and groundwater must take place quickly within the Mesilla Valley because NH_3 oxidizes rapidly into NO_2 and NO_3 (Ward, 1996).

Rapid isolation of the surface water from the atmosphere as it becomes groundwater recharge would curtail the oxidation of NH_3 into NO_2 and NO_3 (Buss and others, 2004).

Water Types

As explained in Freeze and Cherry (1979), methods for referring to different water compositions by identifiable groups or categories (water types) were expounded upon in the 1960s by several authors (Back, 1961, 1966; Morgan and Winner, 1962; Seaber, 1962). Water types were depicted by plotting the percent milliequivalents of the major ions measured in the groundwater samples on a trilinear (Piper) diagram (Piper, 1944) (fig. 31). Each of the two triangles on either side of the Piper diagram are separated into four subdivisions, and the middle diamond is separated into six subdivisions (Singhal and Gupta, 2010) (fig. 32). Samples plotting within the subdivision represent that type of groundwater (table 11).

Of the 44 groundwater samples collected, 36 (81.8 percent) represented Na-dominated water types, specifically Na-Cl-SO_4 or Na-HCO_3 water types, with the Na-Cl-SO_4 water type being the most common (70.5 percent of the Na-dominated samples were of this water type) (table 12, at back of report). Eight of the 44 groundwater samples (18.2 percent) were collected from wells near the Mesilla Valley Fault zone and represented Ca-Cl-SO_4 or Ca-HCO_3 water types (fig. 33). The eight samples representing Ca-dominated water were collected from wells completed in the upper Santa Fe (wells Q03, Q08, Q09, and Q13) or wells completed in the middle Santa Fe (wells Q05, Q06, Q07, and Q11) (table 11, at back of report).

The predominant water types can be characterized as anions of strong or weak acids (as demonstrated by the upper right diamond in fig. 32) and as cations of alkaline earth or alkali metals (as demonstrated by the upper left diamond in fig. 32). The upper left and upper right diamonds in figure 32 represent the same ion range as the diamond in the middle. There were two groundwater samples collected from the center of the study area (wells Q10 and Q11), two collected near the uplifted areas in the southwestern part of the study area (wells Q16 and Q30), and two collected in the southeastern part of the study area (wells Q31 and Q33) that were predominantly anions of weak acids (HCO_3 water type), but the majority of the groundwater samples (86.4 percent) were predominantly composed of water containing anions of strong acids (Ca-Cl-SO_4 or Na-Cl-SO_4 water types (table 12, at back of report; fig. 33).

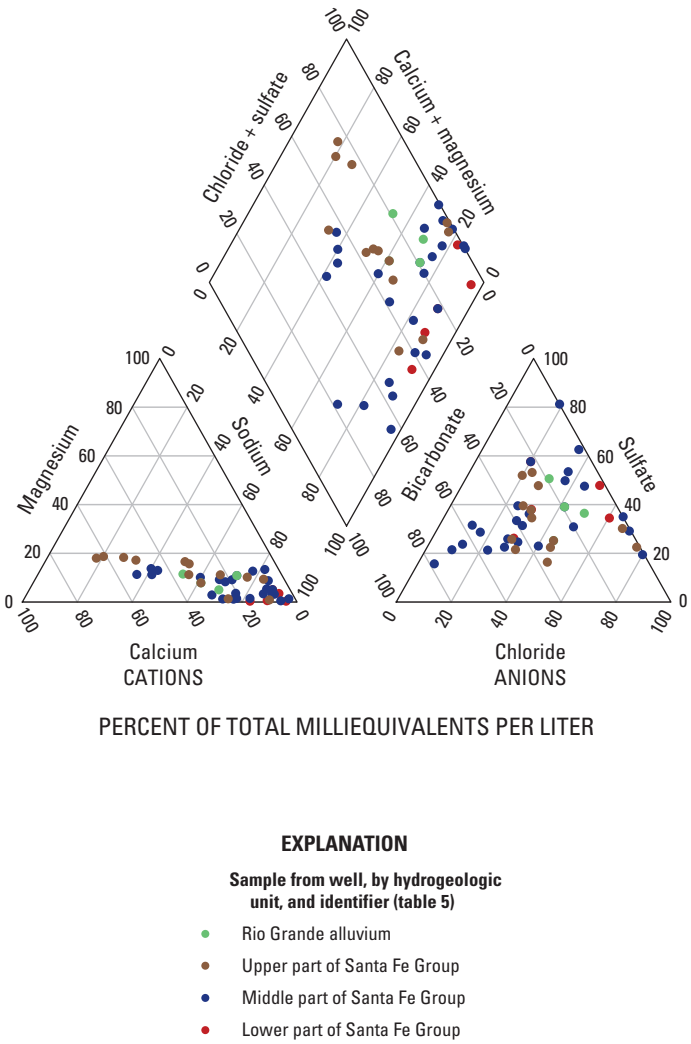

Figure 31. Relations between major cations and anions measured in groundwater samples collected in the Mesilla Basin study area in Doña Ana County, New Mexico, and El Paso County, Texas, 2010.

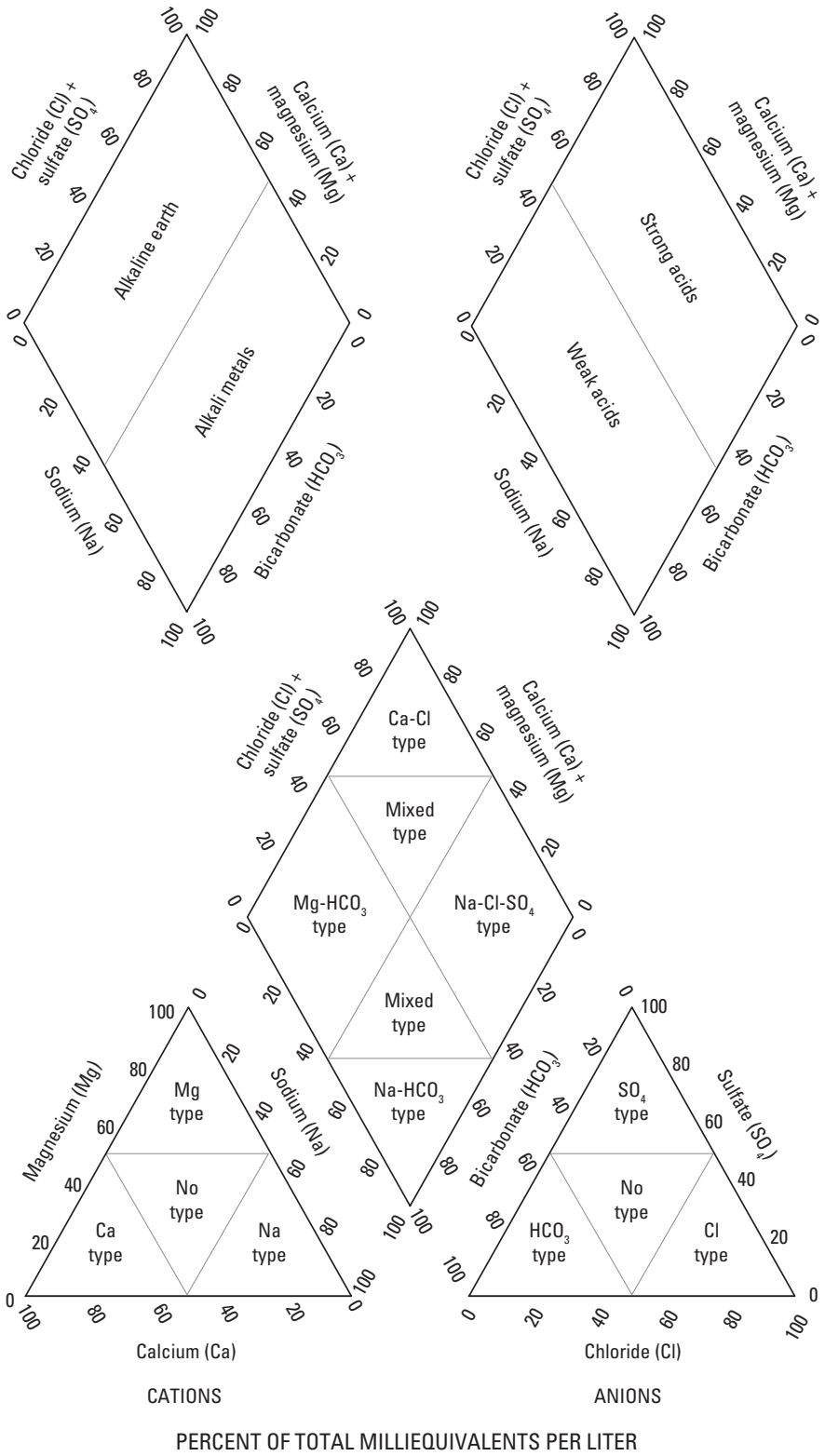

Figure 32. Water type based on the percent milliequivalents of major cations and anions.

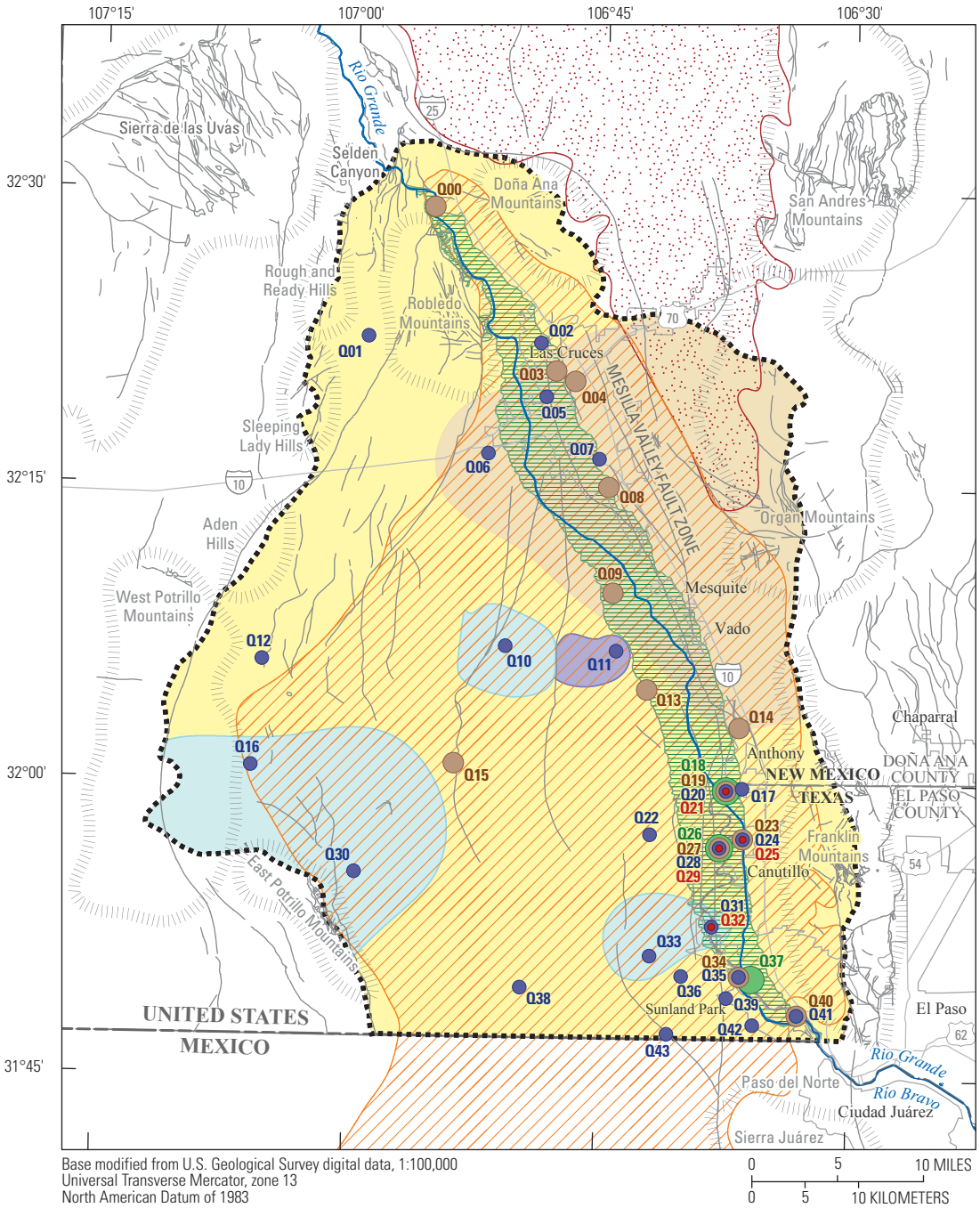

EXPLANATION

Water type from analysis of major cations and anions—Spatial interpolation from samples collected from wells Q00 through Q40

- Sodium-chloride-sulfate
- Sodium-bicarbonate
- Calcium-chloride-sulfate
- Calcium-bicarbonate

- **Mesilla Basin (United States)/Conejos-Médanos (Mexico) aquifer system**—Modified from El Paso Water Utilities (2007)
- Rio Grande alluvium in the Mesilla Valley—Modified from Hawley and Kennedy (2004), Hawley and others (2005)
- **Jornada del Muerto Basin aquifer system**—Modified from Daniel B. Stephens and Associates (2010)
- **Mesilla Basin study area boundary**
- **Fault or fault zone**—From Hawley and Kennedy (2004), Hawley and others (2005)

Well and identifier (table 5)

- Q18 Completed in the Rio Grande alluvium
- Q19 Completed in the upper part of Santa Fe Group
- Q20 Completed in the middle part of Santa Fe Group
- Q21 Completed in the lower part of Santa Fe Group

Note: Well identifiers are labeled from the uppermost hydrogeologic unit at the top to the lowermost hydrogeologic unit at the bottom when more than one sample was collected in the same location.

Figure 33. General spatial distribution of water types from analysis of major cations and anions measured in groundwater samples collected in the Mesilla Basin study area in Doña Ana County, New Mexico, and El Paso County, Texas, 2010.

Trace-Element Chemistry

Trace-element chemistry provided information that aided in the interpretation of potential water sources or processes within the HGUs. Trace elements analyzed for in this study were Al, Sb, As, Ba, Be, B, Cd, Cr, Co, copper (Cu), iron (Fe), Pb, Li, Mn, Mo, Ni, Se, Ag, Sr, thallium (Tl), U, vanadium (V), and zinc (Zn). Results for Sb, Be, B, Cd, Cr, Co, Cu, Pb, Mo, Ni, Se, Ag, Tl, V, and Zn were not used in this assessment because of either low concentrations or blank-contamination concerns.

About 25 percent of all Al values were greater than 4.9 µg/L, the third quartile value of the entire dataset for Al concentrations (table 11, at back of report; fig. 21*Q*, at back of report). All of the Al concentrations in groundwater samples collected from wells completed in the lower Santa Fe were greater than 4.9 µg/L (table 11, at back of report). Al concentrations greater than 4.9 µg/L were also measured in four samples collected from wells completed in the upper Santa Fe (wells Q14 [5.2 µg/L], Q23 [5.3 µg/L], Q27 [8.7 µg/L], and Q40 [32.5 µg/L]) and in three samples collected from wells completed in the middle Santa Fe (wells Q28 [42.8 µg/L] and Q35 [6.8 µg/L], and possibly from well Q41 [less than 25.5 µg/L], where the value was qualified because of matrix effects). The Al concentrations greater than 4.9 µg/L were all measured in groundwater samples collected from wells in or near the southern part of the Mesilla Valley (table 11, at back of report; fig. 20). Mean Al concentrations (excluding outliers) in groundwater samples collected from wells completed in the Rio Grande alluvium, upper Santa Fe, middle Santa Fe, and lower Santa Fe were about 3.4, 2.7, 2.2, and 8.9 µg/L, respectively (fig. 22*Q*, at back of report).

Molar concentrations of Si were compared to molar concentrations of Al, and there appeared to be two distinct groups of groundwater samples: one group with relatively low Al concentrations (less than or equal to 0.00025 millimoles per liter [mmol/L]) and variable Si concentrations and a second group with relatively low Si concentrations (less than 1.64 mmol/L) and variable Al concentrations (fig. 34). Eight samples collected in the southern part of the Mesilla Valley from wells Q21 (12.1 µg/L), Q23 (5.3 µg/L), Q25 (6.1 µg/L), Q27 (8.7 µg/L), Q28 (42.8 µg/L), Q29 (12.4 µg/L), Q40 (32.5 µg/L), and Q41 (less than 25.5 µg/L) were in the group with relatively low Si concentrations and variable Al concentrations (fig. 34). As discussed in the "Silica" section of this report, the abundance of Si within the system is likely from the dissolution of aluminosilicate minerals—the same process that likely accounts for the abundance of Al. The groundwater samples containing relatively low Si concentration and variable Al concentration were collected from wells near the southern part of the study area (fig. 35).

Groundwater samples with elevated concentrations of As (greater than 16.3 µg/L, the third quartile of the entire dataset for As) (fig. 21*R*, at back of report) were collected in the southern part of the study area. These elevated As concentrations were mainly found in groundwater samples collected from the deep HGUs, including one sample collected from a well completed in the upper Santa Fe (well Q27 [25.0 µg/L]), eight samples collected from wells completed in the middle Santa Fe (wells Q10 [18.4 µg/L], Q22 [20.0 µg/L], Q28 [24.0 µg/L], Q30 [25.5 µg/L], Q31 [116 µg/L], Q33 [34.6 µg/L], Q35 [16.7 µg/L], and Q38 [21.1 µg/L]), and two samples collected from wells completed in the lower Santa Fe (wells Q29 [64.7 µg/L] and Q32 [71.5 µg/L]) (table 11, at back of report; fig. 20). Mean As concentrations (excluding outliers) in groundwater samples collected from the Rio Grande alluvium, upper Santa Fe, middle Santa Fe, and lower Santa Fe were about 2.7, 7.4, 12.8, and 35.3 µg/L, respectively (fig. 22*R*, at back of report). Water temperatures in groundwater samples generally increased with increasing As concentrations (fig. 36). Groundwater with elevated As concentrations is typically found in areas with geothermal activity (LennTech, 2012a). Naturally occurring As is commonly found in volcanic rocks, adsorbed to and co-precipitated with the metal oxides in those rocks—especially iron oxides (Hinkle and Polette, 1998). Potential sources of As in groundwater samples collected in the study area were the dissolution of the iron oxides found in the volcanic rocks or basin fill derived from the volcanic rocks or the upwelling of deep, circulating geothermal groundwater rich in iron oxides (Welch and others, 1999).

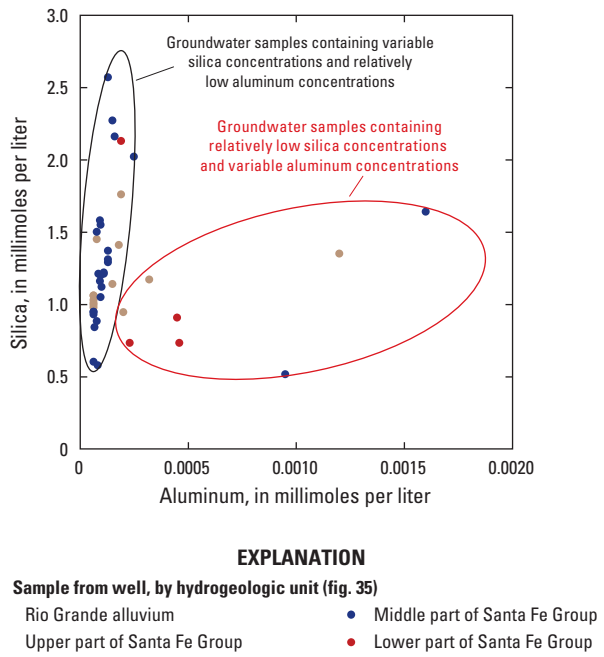

Figure 34. Relation between the molar concentrations of silica and aluminum measured in groundwater samples collected in the Mesilla Basin study area in Doña Ana County, New Mexico, and El Paso County, Texas, 2010.

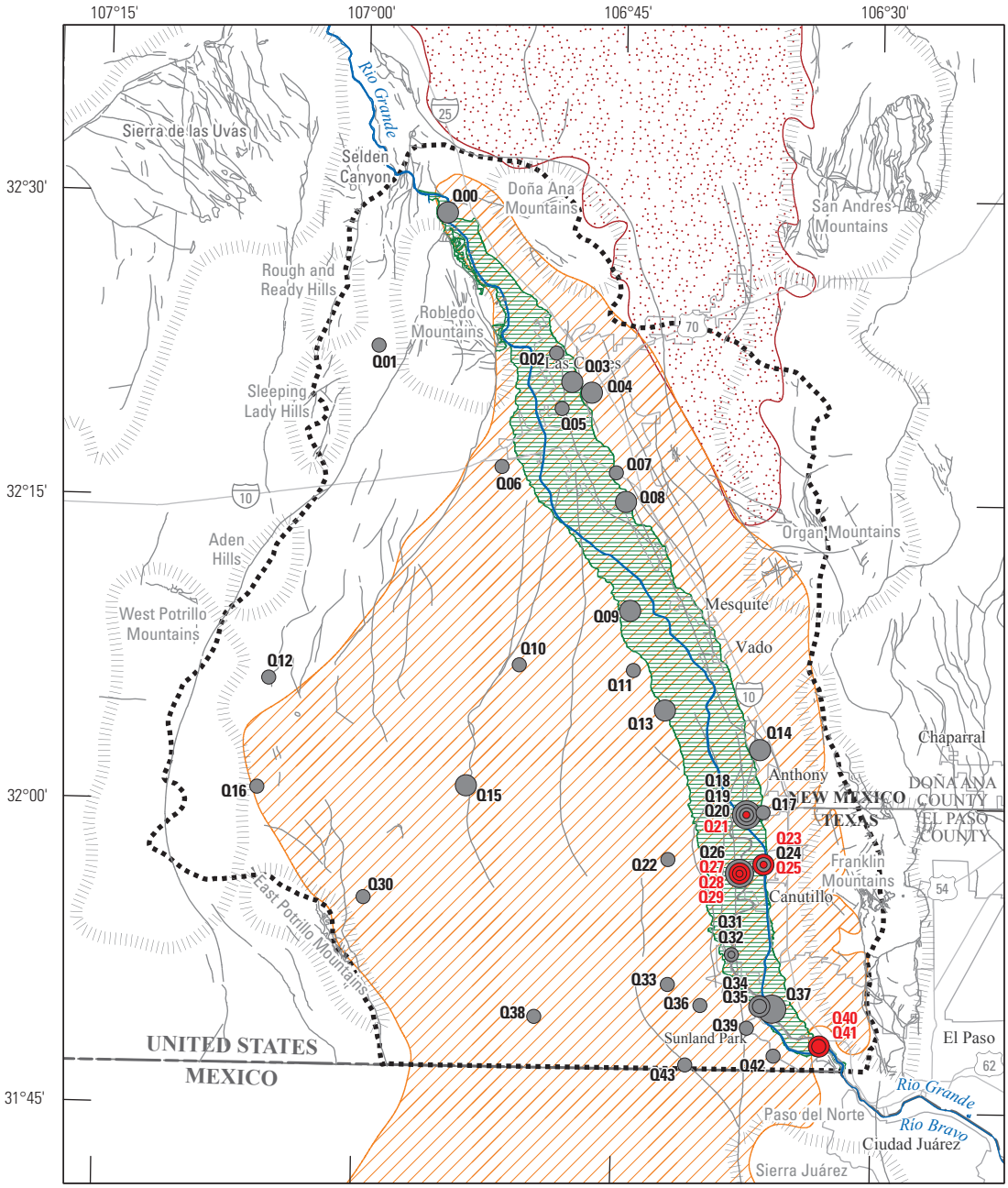

EXPLANATION

Mesilla Basin (United States)/Conejos-Médanos (Mexico) aquifer system—Modified from El Paso Water Utilities (2007)

Rio Grande alluvium in the Mesilla Valley—Modified from Hawley and Kennedy (2004), Hawley and others (2005)

Jornada del Muerto Basin aquifer system—Modified from Daniel B. Stephens and Associates (2010)

Mesilla Basin study area boundary

Fault or fault zone—From Hawley and Kennedy (2004), Hawley and others (2005)

Q41 **Well with groundwater sample containing relatively low silica concentration and variable aluminum concentration (fig. 34) and identifier (table 5)**

Q07 **Well with groundwater sample containing variable silica concentration and relatively low aluminum concentration (fig. 34) and identifier (table 5)**

Well sampled—Symbol size represents hydrogeologic unit in which well was completed

Completed in the Rio Grande alluvium

Completed in the upper part of Santa Fe Group

Completed in the middle part of Santa Fe Group

Completed in the lower part of Santa Fe Group

Note: Well identifiers are labeled from the uppermost hydrogeologic unit at the top to the lowermost hydrogeologic unit at the bottom when more than one sample was collected in the same location.

Figure 35. Locations of wells from which groundwater samples containing relatively low silica concentrations and variable aluminum concentrations (indicated by the solid red well symbols) were collected in the Mesilla Basin study area in Doña Ana County, New Mexico, and El Paso County, Texas, 2010.

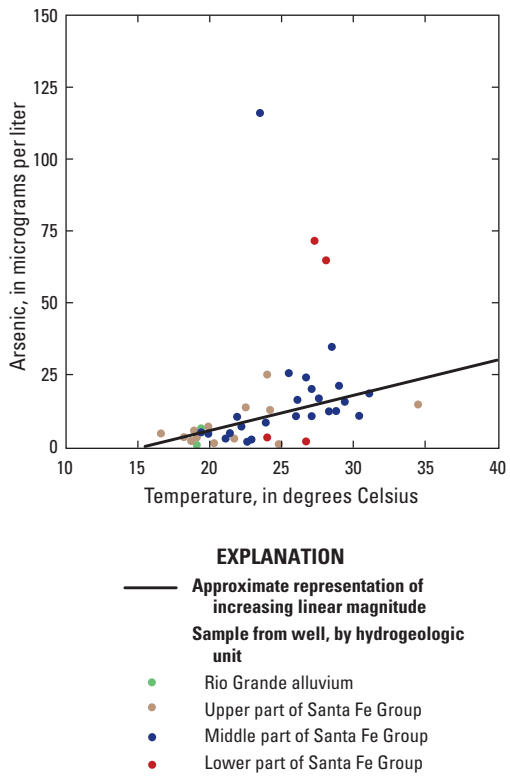

Figure 36. Relation between arsenic concentration and temperature measured in groundwater samples collected in the Mesilla Basin study area in Doña Ana County, New Mexico, and El Paso County, Texas, 2010.

Mean Ba concentrations in groundwater samples collected from the Rio Grande alluvium, upper Santa Fe, middle Santa Fe, and lower Santa Fe were about 44.4, 55.5, 38.1, and 27.8 µg/L, respectively (fig. 22*S*, at back of report). Most of the groundwater samples with concentrations of Ba less than 23.7 µg/L (the first quartile value of the entire dataset for Ba) were collected from wells completed within the middle Santa Fe or lower Santa Fe, with two samples collected from wells completed in the upper Santa Fe (Q27 [18.9 µg/L] and Q40 [18.1 µg/L]) (table 11, at back of report; fig. 20; fig. 21*S*, at back of report). All of the groundwater samples with concentrations of Ba that were less than the first quartile value of the entire dataset for Ba were collected in the southern part of the study area in and near the Mesilla Valley with the exception of the sample collected from well Q01. A potential source of Ba in groundwater in the study area may be potassium feldspar because Ba can substitute for K in the crystalline potassium-feldspar matrix (Plummer and others, 2004).

Mean Fe concentrations (excluding outliers) in groundwater samples collected from the Rio Grande alluvium, upper Santa Fe, middle Santa Fe, and lower Santa Fe were about 876, 48.6, 31.9, and 55.9 µg/L, respectively (fig. 22*T*, at back of report). The mean value for the lower Santa Fe is likely skewed to a high value because of one sample with a high concentration (well Q32 [212 µg/L]) that was not excluded as an outlier; among the samples from the lower Santa Fe, there also were two samples with concentrations below the LRL (wells Q25 and Q29) and one sample with a concentration of 5.2 µg/L (well Q21) (table 11, at back of report). Because the lower Santa Fe was represented by a small sample set, none of the Fe values were considered outliers. Had the Fe concentration of 212 µg/L measured in the sample from well Q32 been excluded, the mean for the Lower Santa Fe would have been more than an order of magnitude smaller compared to the mean Fe values for the other HGUs. For the entire dataset of groundwater samples collected in the study area, the third quartile of Fe concentrations was 109 µg/L (table 11, at back of report; fig. 21*T*, at back of report). Fe concentrations greater than 109 µg/L were measured in the three groundwater samples collected from wells completed in the Rio Grande alluvium (table 11, at back of report; fig. 21*T*, at back of report). Fe concentrations greater than 109 µg/L also were measured in 3 of the 13 samples collected from wells completed in the upper Santa Fe (wells Q04 [112 µg/L], Q08 [177 µg/L], and Q40 [2,580 µg/L]) (table 11, at back of report; fig. 20). The remaining samples with Fe concentrations greater than 109 µg/L were collected from wells completed in the middle Santa Fe at wells Q01 (319 µg/L), Q28 (110 µg/L), Q38 (294 µg/L), and Q41 (433 µg/L), and from one well completed in the lower Santa Fe at well Q32 (212 µg/L) (table 11, at back of report; fig. 20). Except for wells Q01, Q04, Q08, and Q38, all of the wells with Fe concentrations greater than 109 µg/L were in the southern part of the Mesilla Valley (table 11, at back of report; fig. 20).

When the pH and Fe concentration were compared in each groundwater sample, there appeared to be two distinct groups: one group of groundwater samples with relatively low pH (less than 7.8) with a variable but generally high Fe concentration (greater than 177 µg/L) and a second group of samples that had a variable pH with a relatively low Fe concentration (less than 177 µg/L) (fig. 37). Fe is more soluble in acidic groundwater, which corresponds to the group with relatively low pH and a variable but generally high Fe concentration (LennTech, 2012b). With the exception of the groundwater sample collected from well Q01, the groundwater samples with this type of pH and Fe signature were collected from wells near the southern part of the study area where relatively higher concentrations of metals were generally measured compared to other parts of the study area (fig. 38).

Mean Li concentrations (excluding outliers) in groundwater samples collected from the Rio Grande alluvium, upper Santa Fe, middle Santa Fe, and lower Santa Fe were about 425, 127, 87.1, and 334 µg/L, respectively (fig. 22*U*, at back of report). For most of the study area, Li concentrations were relatively low, with a concentration less than 183 µg/L (the third quartile value of the entire dataset for Li) (table 11, at back of report; fig. 21*U*, at back of report). There were 11 groundwater samples with Li concentrations greater

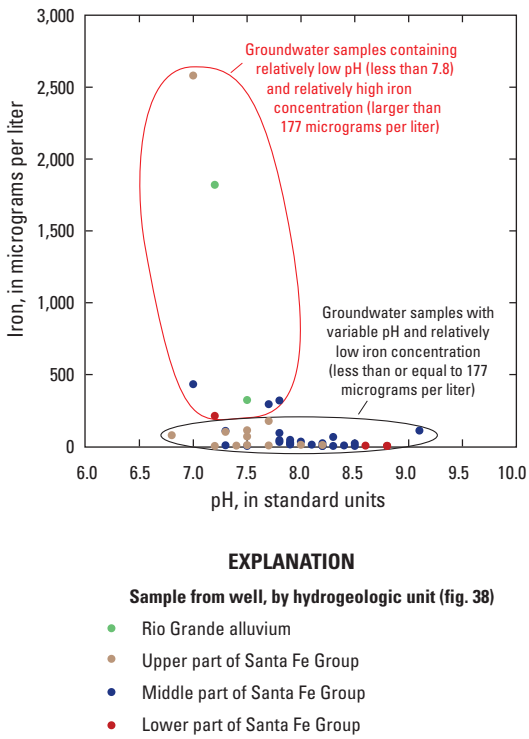

Note: A pH measurement was not made for the sample collected from well Q18 that is screened in the Rio Grande alluvium.

Figure 37. Relation between iron concentration and pH measured in groundwater samples collected in the Mesilla Basin study area in Doña Ana County, New Mexico, and El Paso County, Texas, 2010.

than 183 µg/L—all three groundwater samples collected from the Rio Grande alluvium (wells Q18 [610 µg/L], Q26 [457 µg/L], and Q37 [207 µg/L]), three groundwater samples collected from wells completed in the upper Santa Fe (wells Q14 [265 µg/L], Q19 [251 µg/L], and Q40 [897 µg/L]), four groundwater samples collected from wells completed in the middle Santa Fe (wells Q10 [194 µg/L], Q31 [547 µg/L], Q35 [522 µg/L], and Q41 [1,270 µg/L]), and one groundwater sample collected from a well completed in the lower Santa Fe (well Q32 [998 µg/L]) (table 11, at back of report; fig. 20). These groundwater samples were all collected in and near the southern part of the Mesilla Valley except for one sample (well Q10) collected near the center of the Mesilla Basin (fig. 20). Potential sources of Li in the study area could be from diagenesis of volcanic glass into lithium-rich clays and zeolites or from lithium-rich geothermal brines flowing into the system where the geothermal brines became enriched with lithium through leaching of older volcanic rocks (Brenner-Tourtelot and Machette, 1979).

Mean Mn concentrations (excluding outliers) in groundwater samples collected from the Rio Grande alluvium, upper Santa Fe, middle Santa Fe, and lower Santa Fe were about 1,030, 239, 8.72, and 16.0 µg/L, respectively (fig. 22*V*, at back of report). For all Mn concentrations, the third quartile was 89.9 µg/L (table 11, at back of report; fig. 21*V*, at back of report). Mn concentrations greater than 89.9 µg/L were measured in 11 samples: in the three groundwater samples collected from the Rio Grande Alluvium (wells Q18 [390 µg/L], Q26 [2,170 µg/L], and Q37 [531 µg/L]), in six groundwater samples collected from wells completed in the upper Santa Fe (wells Q00 [606 µg/L], Q03 [915 µg/L], Q08 [262 µg/L], Q09 [105 µg/L], Q13 [796 µg/L], and Q40 [1,950 µg/L]), and in two groundwater samples collected from wells completed in the middle Santa Fe (Q05 [186 µg/L] and Q41 [2,350 µg/L]) (table 11, at back of report; fig. 20). These 11 groundwater samples with relatively high concentrations of Mn were collected in the Mesilla Valley, with the highest concentrations generally measured in samples collected in the southern part of the valley. Elevated concentrations of Mn might indicate discharges from geothermal springs, return flows from irrigation water, or urban land-use discharges (Levings and others, 1998).

Mean Sr concentrations (excluding outliers) measured in groundwater samples collected from the Rio Grande alluvium, upper Santa Fe, middle Santa Fe, and lower Santa Fe were about 3,650, 1,930, 579, and 495 µg/L, respectively (fig. 22*W*, at back of report). Sr concentrations tended to decrease with increasing sampling depth. All groundwater samples with Sr concentrations greater than 1,750 µg/L (the third quartile value of the entire dataset for Sr) were collected from wells completed in either the Rio Grande alluvium or upper Santa Fe, except for two samples with relatively high Sr concentrations collected from wells completed in the middle Santa Fe (wells Q35 [2,410 µg/L] and Q41 [19,600 µg/L]) (table 11, at back of report; fig. 20). All groundwater samples with Sr concentrations of 1,750 µg/L or higher were collected in or near the Mesilla Valley.

Saturation indexes for celestite and strontianite ($SrCO_3$) were mostly negative for the study area (table 9, at back of report), indicating the potential for high dissolution of these minerals, increasing the amount of Sr in the groundwater. Sr commonly replaces Ca in minerals; other sources of Sr within the study area might include dissolution of carbonate rocks, plagioclase feldspars, or gypsum and anhydrite, resulting in Sr substitution for Ca (Plummer and others, 2004).

Mean U concentrations (excluding outliers) in groundwater samples collected from the Rio Grande alluvium, upper Santa Fe, middle Santa Fe, and lower Santa Fe were about 1.24, 2.49, 3.76, and 7.67 µg/L, respectively (fig. 22*X*, at back of report). The third quartile for all U concentrations was 7.60 µg/L (table 11, at back of report; fig. 21*X*, at back of report). There were 11 groundwater samples that had U concentrations greater than 7.60 µg/L—three groundwater samples collected from wells completed in the upper Santa Fe (wells Q03 [62.4 µg/L], Q13 [23.0 µg/L], and Q14 [30.6 µg/L]), seven groundwater samples collected from wells completed in the middle Santa Fe (wells Q01 [16.0 µg/L], Q02 [10.4 µg/L], Q07 [8.79 µg/L], Q31 [18.6 µg/L], Q33 [23.5 µg/L], Q38 [29.3 µg/L], and Q41 [107 µg/L]), and

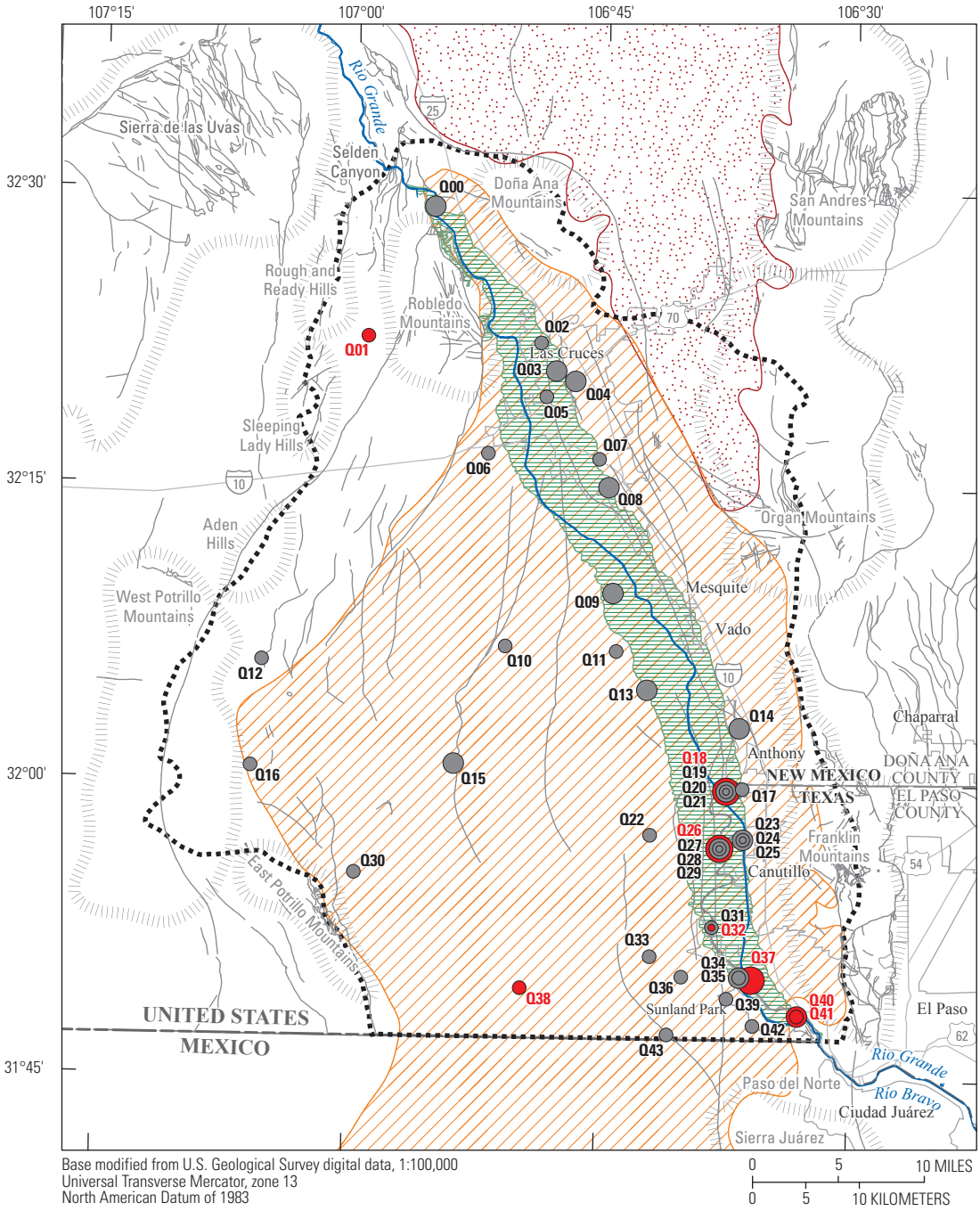

EXPLANATION

Mesilla Basin (United States)/Conejos-Médanos (Mexico) aquifer system—Modified from El Paso Water Utilities (2007)

Rio Grande alluvium in the Mesilla Valley—Modified from Hawley and Kennedy (2004), Hawley and others (2005)

Jornada del Muerto Basin aquifer system—Modified from Daniel B. Stephens and Associates (2010)

Mesilla Basin study area boundary

Fault or fault zone—From Hawley and Kennedy (2004), Hawley and others (2005)

Q21 **Well with groundwater sample containing relatively low pH (less than 7.8) and relatively high iron concentration (larger than 177 micrograms per liter) (fig. 37) and identifier**

Q14 **Well with groundwater sample containing variable pH and relatively low iron concentration (less than or equal to 177 micrograms per liter) (fig. 37) and identifier (table 5)**

Well sampled—Symbol size represents hydrogeologic unit in which well was completed

Completed in the Rio Grande alluvium

Completed in the upper part of Santa Fe Group

Completed in the middle part of Santa Fe Group

Completed in the lower part of Santa Fe Group

Note: Well identifiers are labeled from the uppermost hydrogeologic unit at the top to the lowermost hydrogeologic unit at the bottom when more than one sample was collected in the same location.

Figure 38. Locations of wells from which groundwater samples containing relatively low pH (less than 7.8) and relatively high iron concentrations (greater than 177 micrograms per liter) were collected in the Mesilla Basin study area in Doña Ana County, New Mexico, and El Paso County, Texas, 2010.

one groundwater sample collected from a well completed in the lower Santa Fe (Q32 [30.4 µg/L]) (table 11, at back of report; fig. 20). Groundwater samples with these higher U concentrations were collected in or near the Mesilla Valley, except for one groundwater sample collected in the southwestern part of the study area (well Q38) and one groundwater sample collected from well Q01 in the northwestern part of the study area between the Rough and Ready Hills and the Robledo Mountains.

Isotopes

Isotopic data aid in identifying sources, processes, and age of groundwater (Witcher and others, 2004). Table 13 (at back of report) contains the isotopic results for groundwater samples collected in the study area.

Hydrogen-2/Hydrogen-1 (Deuterium) and Oxygen-18/Oxygen-16

Mean δD values (excluding outliers) in groundwater samples collected from the Rio Grande alluvium, upper Santa Fe, middle Santa Fe, and lower Santa Fe were about -68.65, -77.23, -78.68, and -83.46 per mil, respectively (fig. 22*Y*, at back of report). Mean $\delta^{18}O$ values (excluding outliers) measured in groundwater samples collected from the Rio Grande alluvium, upper Santa Fe, middle Santa Fe, and lower Santa Fe HGUs were about -8.09, -9.70, -10.21, and -11.05 per mil, respectively (fig. 22*Z*, at back of report). The normal probability plots (Helsel and Hirsch, 2002) for both δD (fig. 21*Y*, at back of report) and $\delta^{18}O$ (fig. 21*Z*, at back of report) indicated two fairly distinct groups of isotopic data. The groups were separated by an abrupt change in values at the 50th percentile of the normal probability distribution (50 percent mark) for δD and $\delta^{18}O$. For example, at the 50 percent mark for δD values, there was an abrupt change in δD values from -82.65 per mil to -75.16 per mil, resulting in one group of isotope results having δD values greater than -75.16 per mil (isotopically heavier; greater than 50 percent in the probability plot) and another group of isotope results having δD values less than -82.65 per mil (isotopically lighter; less than 50 percent in the probability plot) (fig. 21*Y*, at back of report). For the $\delta^{18}O$ isotopic results, at the 50 percent mark, there was an abrupt change in $\delta^{18}O$ values from -10.93 per mil to -10.10 per mil and even further to -9.46 per mil at 53 percent, resulting in one group of isotope results having $\delta^{18}O$ values greater than -10.10 per mil (isotopically heavier; greater than 50 percent in the probability plot) and another group of isotope results having $\delta^{18}O$ values less than -10.93 per mil (isotopically lighter; less than 50 percent in the probability plot) (fig. 21*Z*, at back of report). These two groups were labeled as isotopically heavier groundwater (values greater than -80.00 and -10.50 per mil δD and $\delta^{18}O$, respectively) and isotopically lighter groundwater (values less than -80.00 and -10.50 per mil δD and $\delta^{18}O$, respectively). On the basis of their isotopic chemistry, groundwater samples collected from wells completed in the Rio Grande alluvium or upper Santa Fe can be characterized as predominantly belonging to the isotopically heavier group (table 13, at back of report; figs. 22*Y* and 22*Z*, at back of report). Groundwater samples collected from wells completed in the middle Santa Fe or lower Santa Fe can be characterized as predominately belonging to the isotopically lighter group (table 13, at back of report; figs. 22*Y* and 22*Z*, at back of report). Compared to other parts of the study area, relatively heavier isotopic signatures were observed in groundwater analytical results from the southern part of the study area, as well as from a few locations in the Mesilla Valley (table 13, at back of report; fig. 20).

Two fairly distinct groups of isotopically heavier and lighter water signatures were also evident when δD and $\delta^{18}O$ (δD/ $\delta^{18}O$) were plotted (fig. 39). The water composing samples collected from wells completed in the middle Santa Fe and lower Santa Fe tended to plot in the isotopically lighter group, whereas samples collected from wells completed in the Rio Grande alluvium or upper Santa Fe tended to plot in the isotopically heavier group. There was a fair amount of variability in samples collected from wells completed in the upper Santa Fe and middle Santa Fe, but the overall pattern is consistent with there being generally isotopically heavier water in the Rio Grande alluvium and upper Santa Fe compared to the water in the middle Santa Fe and lower Santa Fe (fig. 39).

Along with the two fairly distinct groups of isotopically heavier and lighter groundwater, there were linear patterns in the relation between δD and $\delta^{18}O$. About 50 percent of the groundwater samples collected plotted along the Rio Grande evaporation line of $\delta D = 5.1 \times \delta^{18}O - 28$ (fig. 39) (Phillips and others, 2003). Where the groundwater samples plotted in relation to the Rio Grande evaporation line demonstrates that the Rio Grande is a major source of groundwater within the area (fig. 40). In studies by Adams and others (1995) and Eastoe and others (2007), isotopes in precipitation near Santa Fe, N. Mex.; El Paso, Tex.; and Ciudad Juárez, Chihuahua, plotted relatively close to the GMWL. As stated in the "Environmental Tracer Methods" section of this report, "samples that indicate gains or losses of oxygen atoms from interaction with rocks tend to deviate from the GMWL in the lateral position since there is the gain or loss of only the oxygen element." About 25 percent of the groundwater samples plotted along a parallel shift of the GMWL that has an equation of $\delta D = 8.0 \times \delta^{18}O + 3$ (fig. 39). The addition of ^{18}O through dissolution processes, which may increase with geothermal activity, may have caused a shift away from the GMWL to the right, indicating a shift to relatively more ^{18}O and less ^{16}O. A shift to relatively more ^{18}O and less ^{16}O results in an isotopically heavier $\delta^{18}O$ signature without any change in the $\delta^{2}H$ signature. The shifted GMWL for the study area represents old groundwater and geothermal groundwater that have gained ^{18}O from rocks by exchange processes associated with water-rock interaction and hydrothermal alteration

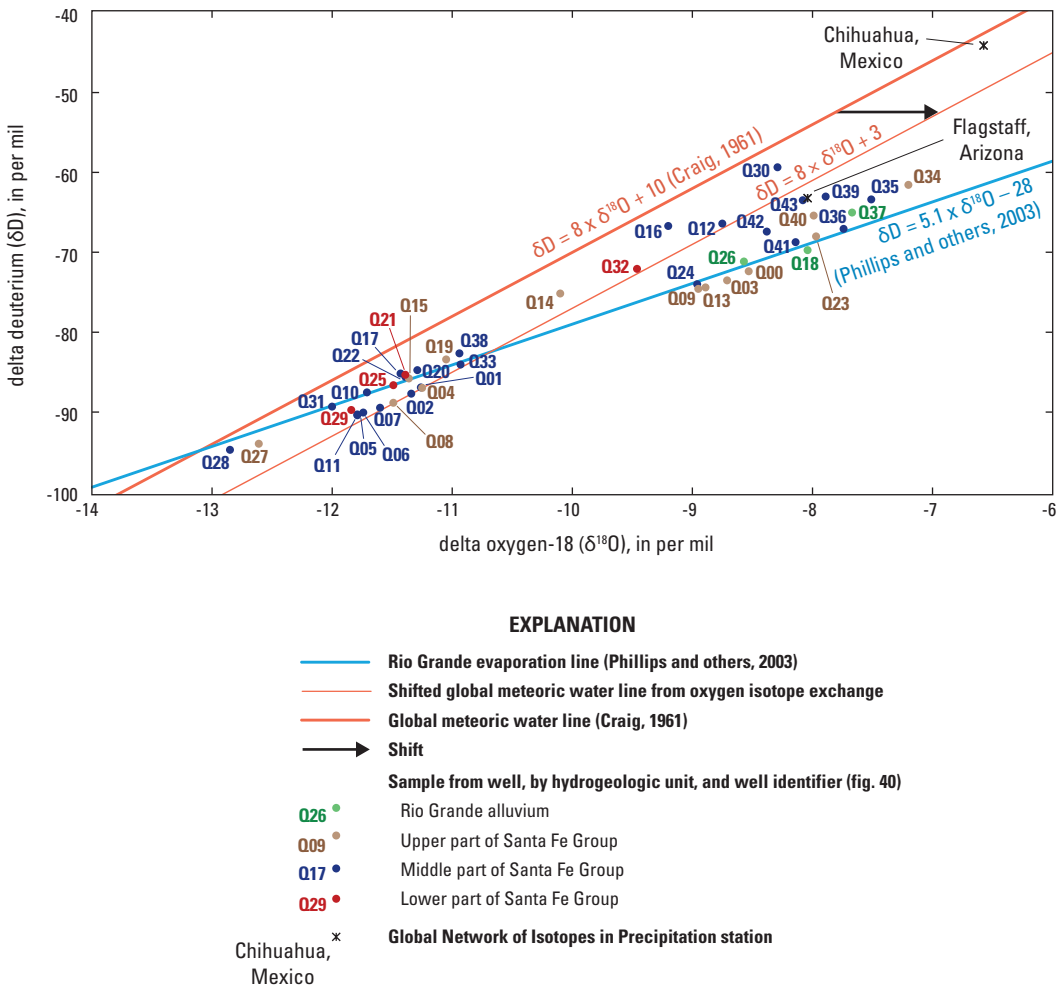

Figure 39. Relation between delta deuterium and delta oxygen-18 measured in groundwater samples collected in the Mesilla Basin study area in Doña Ana County, New Mexico, and El Paso County, Texas, 2010.

where the amount of oxygen exchanged or changed in $\delta^{18}O$ is a function of rock composition, texture, temperature, and length of contact (Witcher and others, 2004). Most of the groundwater samples that plot along the shifted GMWL represent isotopically lighter water, with δD values less than -80.00 per mil and $\delta^{18}O$ values less than -10.50 per mil. This lighter isotopic signature indicates that these samples most likely represent water recharged during the relatively wet and cool Pleistocene climate (Bumgarner and others, 2012). This groundwater was likely relatively old and had obtained its isotopically heavier ^{18}O signature through extended contact with soluble materials. Groundwater samples that plotted between the Rio Grande evaporation line and the shifted GMWL were most likely a mixture of the two water types in the southeastern part of the study area near the Paso del Norte (fig. 40)—an area where Witcher and others (2004) indicated that mixing was likely to occur. The wells representing mixing in this area were Q29, Q34, Q35, Q37, Q39, Q40, Q42, and Q43 (fig. 40). There were several groundwater samples that plotted above both the Rio Grande evaporation line and the shifted GMWL, including the samples collected from wells Q14, Q16, and Q30 (fig. 39). On the basis of the locations of wells Q14, Q16, and Q30, the stable isotopic signatures of these groundwater samples might reflect inflows of recent recharge from uplifted areas. Two of these sampling wells are in the southwestern part of the study area near the West and East Potrillo Mountains (wells Q16 and Q30, respectively), and the third is near the Franklin Mountains (well Q14) (fig. 40). When compared, the δD and $\delta^{18}O$ values from well Q14 were similar to the δD and $\delta^{18}O$ values reported by Eastoe and others (2007) for samples collected from the “Organ and Franklin Mountain group” discussed in their report.

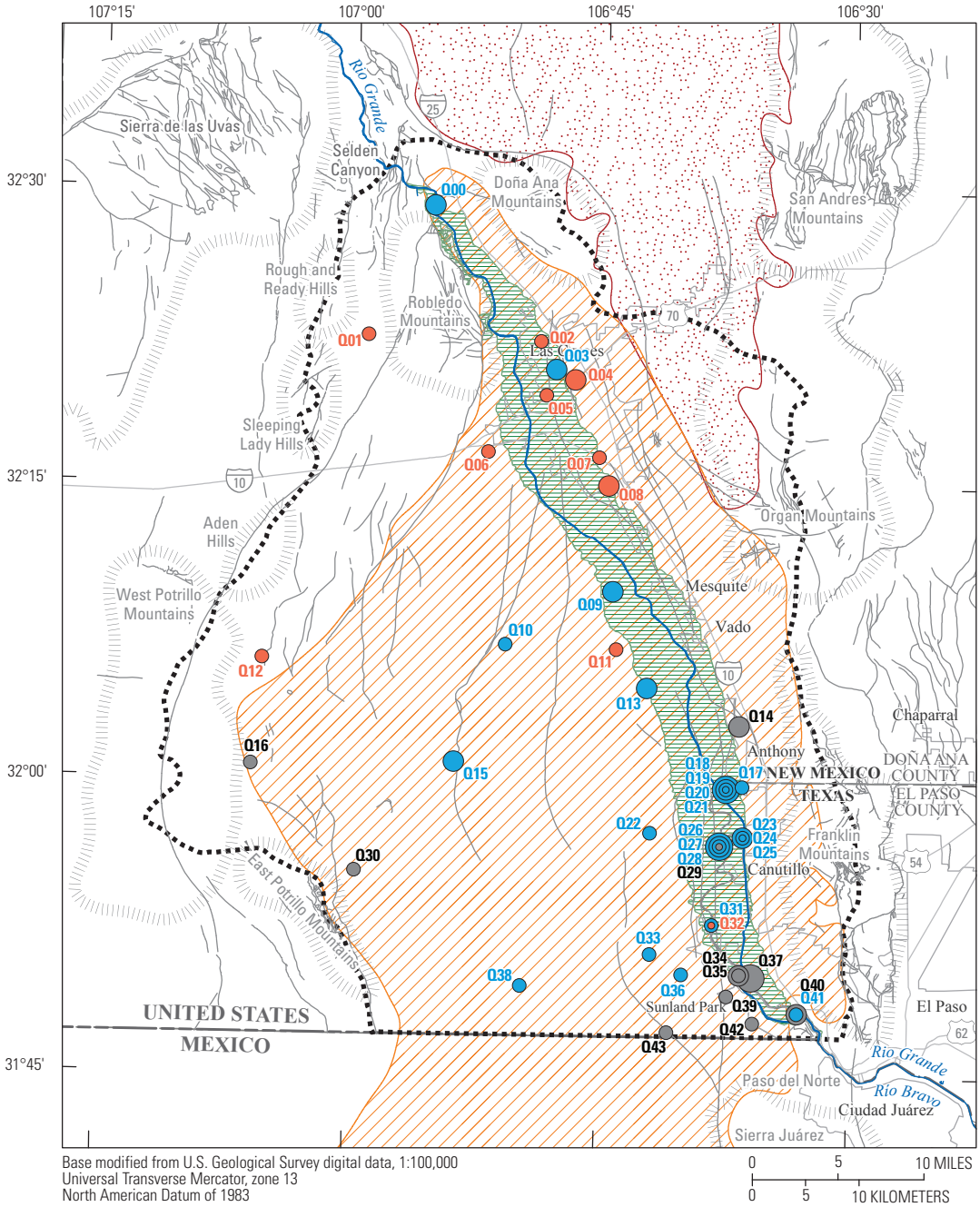

Figure 40. Locations of wells from which groundwater samples that plotted near the shifted global meteoric water line and the Rio Grande evaporation line were collected in the Mesilla Basin study area in Doña Ana County, New Mexico, and El Paso County, Texas, 2010.

The relation of Cl/Br ratios to δD values provides insight into different geochemical characteristics (signatures) of different water types (endmembers) and mixing between endmembers (fig. 41) (Witcher and others, 2004). Three endmembers were identified. Each endmember was uniquely modified by evaporation and dissolution processes, resulting in a different geochemical signature. The three endmembers were (1) groundwater with no geothermal or evaporative processes (low Cl/Br and low δD), (2) geothermal groundwater (medium Cl/Br and high δD), and (3) evaporative groundwater (water that has had some evaporation associated with it but no geothermal processes). Compared to groundwater with no geothermal processes (endmembers 1 and 3), geothermal groundwater (endmember 2) typically has a higher Cl/Br ratio. In contrast to groundwater with no geothermal or evaporative processes (endmember 1), in evaporative groundwater the Cl/Br ratio will remain constant and δD will increase. Evaporative water is indicative of recharge from a surface-water feature where water can evaporate into the atmosphere, near-surface groundwater where evaporation may still occur, or evaporation of rain during infiltration (all resulting in recharge from water with a heavy isotopic signature) (Kendall and others, 2004). Compared to groundwater with geothermal or evaporative processes (endmembers 2 and 3, respectively), groundwater with no geothermal or evaporative processes (endmember 1) has low Cl/Br ratios and a light δD isotopic signature. Values in between the endmembers resulted in mixing between two or all three endmembers.

The samples collected within the study area were separated into four groundwater-mixing groups on the basis of water quality: (1) a general groundwater group in which there was little or no mixing of the groundwater with geothermal groundwater and little or no mixing with evaporative groundwater (group 1), (2) an evaporative groundwater group in which there was some evaporation associated with the groundwater and no mixing of the groundwater with geothermal groundwater (group 2), (3) a geothermal groundwater group in which there was some mixing of the groundwater with geothermal groundwater (group 3), and (4) a blended groundwater group in which the groundwater had attributes of all three endmembers (group 4) (fig. 41). Groundwater samples in the general groundwater group (group 1) represented groundwater collected from the deeper HGUs (upper Santa Fe, middle Santa Fe, and lower Santa Fe) throughout the study area. Groundwater samples in the evaporative groundwater group (group 2) represented groundwater collected from wells completed in the middle Santa Fe and were generally from wells near uplifted areas of the study area, with Q12, Q16, and Q30 near the Aden Hills and West and East Potrillo Mountains, respectively, and Q36 and Q43 near the Sierra Juárez (fig. 20). Groundwater samples in the geothermal groundwater group (group 3) represented all of the different HGUs and were collected from wells in the southern part of the Mesilla Valley. Groundwater samples in the blended groundwater group (group 4) represented groundwater collected from near-surface HGUs (Rio Grande alluvium, upper Santa Fe, and middle Santa Fe) from wells in or near the Mesilla Valley.

Strontium-87

Groundwater that was in equilibrium with Sr-bearing carbonate minerals in the aquifer will have a $^{87}Sr/^{86}Sr$ signature reflecting the isotopic ratio of the minerals in the rocks (Banner and Kaufman, 1994; Uliana and others, 2007; Bumgarner and others, 2012). As a result, Sr isotopes are useful in determining groundwater-flow paths and identifying areas of groundwater mixing (Banner and Kaufman, 1994). The $^{87}Sr/^{86}Sr$ ratios ranged from 0.70790 to 0.71227 in groundwater samples collected in the study area (fig. 21*AA*, at back of report), and the mean $^{87}Sr/^{86}Sr$ ratios (excluding outliers) in groundwater samples collected from the Rio Grande alluvium, upper Santa Fe, middle Santa Fe, and lower Santa Fe were about 0.71019, 0.70989, 0.70955, and 0.71003, respectively (table 13, at back of report; fig. 22*AA*, at back of report). Groundwater samples with relatively high $^{87}Sr/^{86}Sr$ ratios were collected in the northern and northwestern parts of the study area or in the southeastern part of the study area, near the base of the Franklin Mountains (table 13, at back of report; fig. 20). These samples with relatively high $^{87}Sr/^{86}Sr$ ratios may represent groundwater residing in or near uplift areas that were formed from Tertiary volcanics; such groundwater tends to have higher $^{87}Sr/^{86}Sr$ ratios compared to groundwater in other parts of the study area (Witcher and others, 2004). Groundwater samples with relatively low $^{87}Sr/^{86}Sr$ ratios were collected in the center and southeastern parts of the study area (table 13, at back of report; fig. 20). Groundwater samples with relatively low $^{87}Sr/^{86}Sr$ ratios collected from the center of the study area are consistent with groundwater residing in basin-fill sediments (Witcher and others, 2004). The groundwater samples with the low $^{87}Sr/^{86}Sr$ ratios in the southeastern part of the study area may represent deep groundwater that has been in contact with the bedrock for an extended period (Witcher and others, 2004).

Tritium

Analyzing groundwater for ^{3}H concentration was useful for distinguishing if the groundwater was recharged into the system before, during, or after widespread atomic bomb testing began in the 1950s. Mean ^{3}H concentrations (excluding outliers) in groundwater samples collected from the Rio Grande alluvium, upper Santa Fe, middle Santa Fe, and lower Santa Fe were about 6.0, 2.6, 0.0, and 0.3 TU, respectively (fig. 22*BB*, at back of report).

Among the results for samples representing the four HGUs in the study area, ^{3}H concentrations were generally the highest in groundwater samples collected from wells completed in the Rio Grande alluvium or the upper Santa Fe. In the two samples collected from wells completed in the Rio Grande alluvium for which ^{3}H concentrations were measured, the TU values were 4.6 TU (well Q18) and 7.5 TU (well Q26).

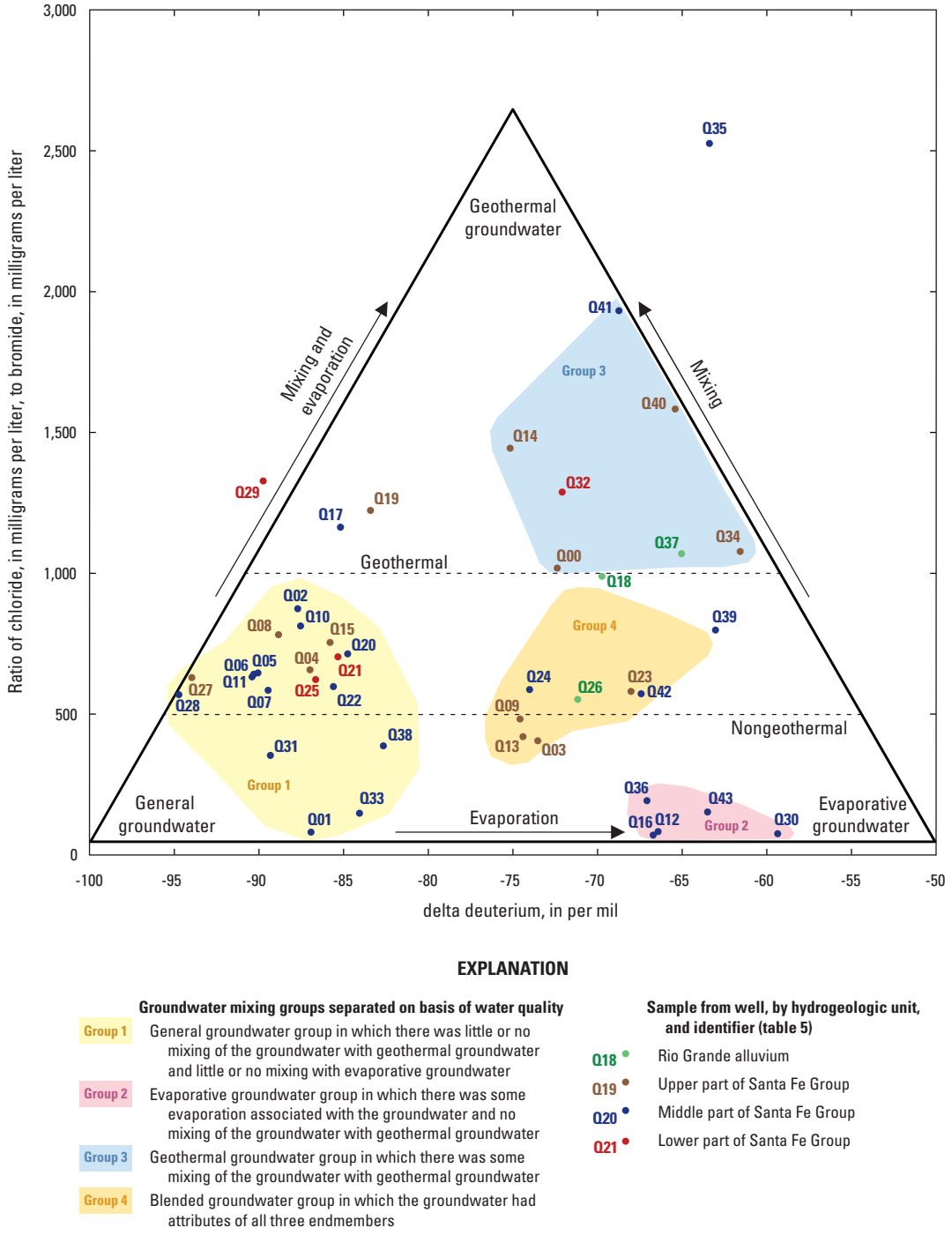

EXPLANATION

Groundwater mixing groups separated on basis of water quality

- Group 1 — General groundwater group in which there was little or no mixing of the groundwater with geothermal groundwater and little or no mixing with evaporative groundwater
- Group 2 — Evaporative groundwater group in which there was some evaporation associated with the groundwater and no mixing of the groundwater with geothermal groundwater
- Group 3 — Geothermal groundwater group in which there was some mixing of the groundwater with geothermal groundwater
- Group 4 — Blended groundwater group in which the groundwater had attributes of all three endmembers

Sample from well, by hydrogeologic unit, and identifier (table 5)

- Q18 — Rio Grande alluvium
- Q19 — Upper part of Santa Fe Group
- Q20 — Middle part of Santa Fe Group
- Q21 — Lower part of Santa Fe Group

Figure 41. Chloride and bromide ratios (mass chloride/mass bromide) and delta deuterium isotopic ratios measured in groundwater samples collected in the Mesilla Basin study area in Doña Ana County, New Mexico, and El Paso County, Texas, 2010.

The concentrations of ^{3}H were generally negative to extremely low (less than 0.6 TU, the concentration value used to define prebomb water in the study area) in groundwater samples collected from wells completed in the middle Santa Fe and lower Santa Fe.

The TU values were greater than 0.6 TU in only two of the groundwater samples that were collected from wells completed in either the middle Santa Fe or lower Santa Fe (well Q24 completed in the middle Santa Fe [10.3 TU] and well Q25 completed in the lower Santa Fe [0.9 TU]) (table 13, at back of report; fig. 20). There were six groundwater samples collected from wells completed in the upper Santa Fe with ^{3}H concentrations less than 0.6 TU (wells Q08 [0.1 TU], Q14 [0.1 TU], Q15 [0.0 TU], Q19 [0.2 TU], Q27 [-0.1 TU], and Q34 [-0.1 TU]) indicating prebomb groundwater, two groundwater samples with ^{3}H concentrations between 0.6 and 1.6 TU (wells Q04 [1.3 TU] and Q40 [1.3 TU]) indicating a mixture of prebomb and postbomb groundwater, and five groundwater samples with ^{3}H concentrations between 1.6 and 10 TU (wells Q00 [3.6 TU], Q03 [8.1 TU], Q09 [8.8 TU], Q13 [6.2 TU], and Q23 [4.2 TU]) indicating postbomb water. On the basis of the classification of analytical results for ^{3}H concentrations outlined in the "Environmental Tracer Methods" section of this report, the TU values measured in groundwater samples collected from the Rio Grande alluvium were indicative of recent postbomb recharge into the groundwater system (water recharged between 5 and 10 years prior to sampling). The TU values measured in samples collected from wells completed in the upper Santa Fe were indicative of a mixture of prebomb and postbomb water. Most TU values measured in samples collected from wells completed in the middle Santa Fe and lower Santa Fe were indicative of recharge into the system before atomic bomb testing (prebomb water). The groundwater sample from the middle Santa Fe with the high ^{3}H concentration (well Q24 [10.3 TU]) was collected near the Rio Grande, indicating that there might be a hydrologic connection between the middle Santa Fe and surface water, which may affect groundwater recharge at this location.

Carbon-14

^{14}C activity values (mean pmc values excluding outliers) used to determine ^{14}C apparent ages in years BP in groundwater samples collected from the Rio Grande alluvium, upper Santa Fe, middle Santa Fe, and lower Santa Fe were about 102.46 pmc (modern), 60.10 pmc (10,000 ^{14}C years BP), 20.02 pmc (19,000 ^{14}C years BP), and 5.70 pmc (29,000 ^{14}C years BP), respectively (figs. 22*CC* and 22*DD*, at back of report). These ^{14}C age-dating results indicate that the Rio Grande alluvium contained the youngest water and that the middle Santa Fe and lower Santa Fe contained the oldest water, results consistent with apparent groundwater age increasing with depth. From the probability plot for ^{14}C apparent ages in years BP, an abrupt change in sample ages from 5,800 ^{14}C years BP to 15,000 ^{14}C years BP is evident at about 38 percent of the normal probability distribution (fig. 21*DD*, at back of report). Groundwater samples with ^{14}C apparent ages greater than 10,000 ^{14}C years BP were designated as representing old water. There were some groundwater samples collected from wells completed in the Rio Grande alluvium or upper Santa Fe that had ^{14}C activity values greater than 100 pmc (table 13 at back of report; fig. 21*CC*, at back of report). These same groundwater samples had greater counting errors associated with the ^{14}C results. As stated in the "Environmental Tracer Methods" section of this report ^{14}C activity values greater than 100 pmc were likely recharged after 1950 because atmospheric ^{14}C concentrations increased from atomic bomb testing (Plummer and others, 1994); for this report, groundwater samples with ^{14}C activity values greater than 99 pmc were considered modern water. The ^{14}C activity values for groundwater samples collected from the Rio Grande alluvium were all greater than 99 pmc; groundwater in the Rio Grande alluvium was therefore classified as modern recharge. Similar to the groundwater sample results for ^{3}H, groundwater samples collected from wells completed in the upper Santa Fe indicate a mix of young (less than 1,000 ^{14}C years BP) and old (greater than 10,000 ^{14}C years BP) water. The ^{14}C activity values in groundwater samples collected from wells completed in the upper Santa Fe ranged from 2.61 to 141.50 pmc (table 13, at back of report), which equates to apparent ages ranging from about 29,000 ^{14}C years BP to modern within this HGU (figs. 22*CC* and 22*DD*, at back of report). Groundwater samples collected from five wells completed in the upper Santa Fe had apparent ^{14}C ages greater than 10,000 ^{14}C years BP (wells Q14 [29,000 ^{14}C years BP], Q15 [20,000 ^{14}C years BP], Q19 [18,000 ^{14}C years BP], Q27 [26,000 ^{14}C years BP], and Q34 [24,000 ^{14}C years BP]) (table 13, at back of report; fig. 20). Three of these groundwater samples were collected from wells in the southern part of the Mesilla Valley (wells Q19, Q27, and Q34) (fig. 20). The remaining groundwater samples collected from wells completed in the upper Santa Fe had apparent ^{14}C ages less than 10,000 ^{14}C years BP, with most of these groundwater samples collected from the northern part of the Mesilla Valley. The ^{14}C activity values in groundwater samples collected from wells completed in the middle Santa Fe ranged from 1.21 to 70.41 pmc, which equates to apparent ^{14}C age-dates of about 35,000 to 2,800 ^{14}C years BP (table 13, at back of report; figs. 22*CC* and 22*DD*, at back of report). Most of the apparent ages for groundwater obtained from the middle Santa Fe were greater than 10,000 ^{14}C years BP. Six of the groundwater samples collected from wells completed in the middle Santa Fe had apparent ages that were less than 10,000 ^{14}C years BP (wells Q02 [5,700 ^{14}C years BP], Q05 [3,500 ^{14}C years BP], Q06 [3,900 ^{14}C years BP], Q07 [2,900 ^{14}C years BP], Q11 [2,800 ^{14}C years BP], and Q24 [5,500 ^{14}C years BP]); these groundwater samples were collected from wells located in or near the Mesilla Valley (table 13, at back of report; fig. 20). Groundwater samples collected from wells completed in the lower Santa Fe had pmc values ranging

from 0.26 to 12.64 pmc, which equates to the apparent age of the groundwater being about 48,000 to 17,000 ^{14}C years BP (table 13, at back of report; figs. 22*CC* and 22*DD*, at back of report). These groundwater samples were all considered old groundwater.

The groundwater sample results for ^{3}H compared favorably to the apparent ^{14}C age-dates. Most of the groundwater samples with ^{3}H concentrations that were greater than 1.6 TU (postbomb water) had modern ^{14}C apparent ages (table 13, at back of report; fig. 42). The one groundwater sample that had an elevated ^{3}H concentration of 10.3 TU (well Q24) (table 13, at back of report) was labeled as groundwater with a mix of prebomb and postbomb water. This groundwater sample had an apparent ^{14}C age date of about 5,500 ^{14}C years BP (table 13, at back of report), indicating that there could potentially be mixing with postbomb water, prebomb water, and water recharged during the peak of atomic bomb testing. This mixing was corroborated by a groundwater sample collected from a well completed in the lower Santa Fe (well Q25) at the same location, where ^{3}H concentration was 0.9 TU and the ^{14}C age dating was calculated as about 17,000 ^{14}C years BP, which is younger than the age of the groundwater from the lower Santa Fe in the two nearest wells (wells Q21 [20,000 ^{14}C years BP] and Q29 [33,000 ^{14}C years BP]) (table 13, at back of report; fig. 20). The elevated ^{3}H concentration of 0.9 TU and the younger apparent age than nearby groundwater samples collected from wells completed in the lower Santa Fe indicated some mixing at the location of well Q25 between postbomb water and prebomb water. The two other groundwater sample results for ^{3}H that fall within the mixing range of 0.6 to 1.6 TU had groundwater sample results for apparent ^{14}C age dates of 700 (well Q40) and 5,800 (well Q04) ^{14}C years BP, which supported the possibility that groundwater mixing may also be occurring at the locations of wells Q40 and Q04. All of the groundwater samples with ^{3}H concentrations of less than 0.6 TU were classified as older water with apparent ages of ^{14}C ranging from about 2,800 to 35,000 ^{14}C years BP.

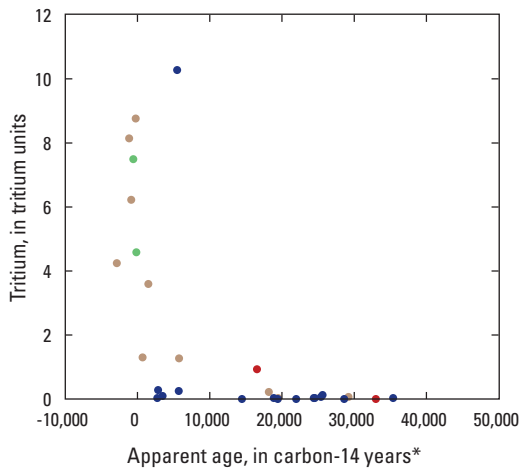

EXPLANATION

Sample from well, by hydrogeologic unit

- Rio Grande alluvium
- Upper part of Santa Fe Group
- Middle part of Santa Fe Group
- Lower part of Santa Fe Group

*Apparent groundwater age in carbon-14 years is from Libby half-life uncorrected radiocarbon years before 1950.

Figure 42. Relation between tritium concentration and apparent groundwater age measured in groundwater samples collected in the Mesilla Basin study area in Doña Ana County, New Mexico, and El Paso County, Texas, 2010.

When groundwater sample results of δD and $\delta^{18}O$ were compared with the groundwater sample results of ^{14}C age dating, most of the groundwater samples classified as old groundwater (greater than 10,000 ^{14}C years BP) were also classified as isotopically lighter (table 13, at back of report; fig. 43), supporting the hypothesis that this water was recharged during the wet and cool climate of the Pleistocene. There were six groundwater samples that had a lighter stable isotopic signature and apparent groundwater ages less than 10,000 ^{14}C years BP (collected from wells Q02, Q04, Q05, Q06, Q07, and Q11) (table 13, at back of report; figs. 43 and 44). These six groundwater samples were collected from wells in and near the northern part of the Mesilla Valley and may indicate some interbasin mixing with isotopically lighter water from the Jornada Basin. Eleven groundwater samples had a heavier stable isotopic signature and apparent ages of greater than 10,000 ^{14}C years BP (collected from wells Q12, Q14, Q16, Q30, Q32, Q34, Q35, Q36, Q39, Q42, and Q43) (table 13, at back of report; figs. 43 and 44). These 11 groundwater samples were collected from wells that were generally either in the southeastern or southwestern part of the study area (fig. 44). Since the isotopic signature of these groundwater samples more closely followed the shifted GMWL than the Rio Grande evaporation line, and because these samples had a heavy stable isotopic signature with older apparent ages, the groundwater may have been subjected to geothermal activity, a long residence time, mixing with a more modern source of water, or a combination of these processes.

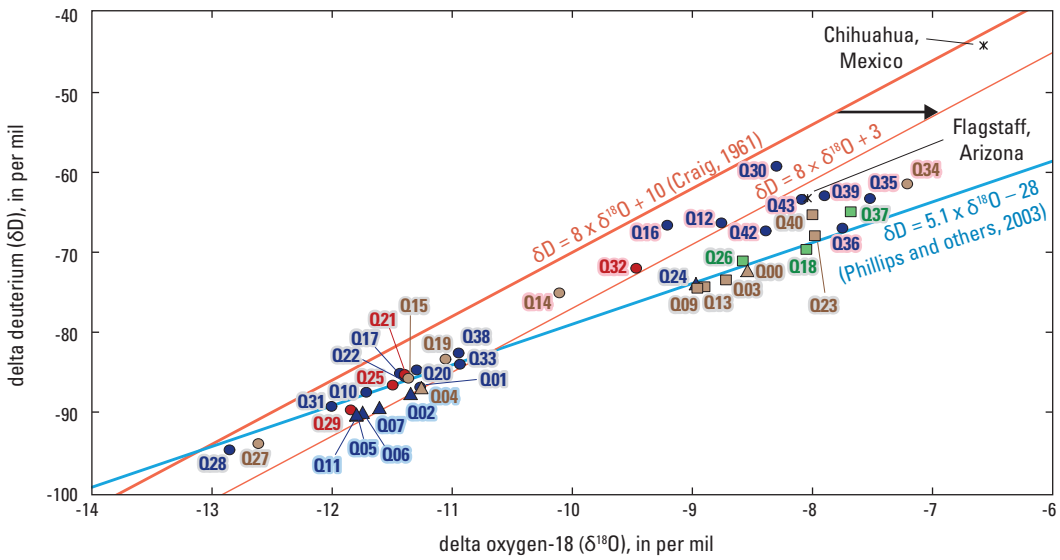

EXPLANATION

Rio Grande evaporation line (Phillips and others, 2003)

Shifted global meteoric water line from oxygen isotopic exchange

Global meteoric water line (Craig, 1961)

Shift

Sample from well, by hydrogeologic unit—Symbol color represents hydrogeologic unit

- Rio Grande alluvium
- Upper part of Santa Fe
- Middle part of Santa Fe
- Lower part of Santa Fe

Sample from well, by apparent age, in carbon-14 years before present (1950)—Symbol shape represents apparent age of groundwater

- Less than 1,001 } Younger
- 1,001 to 10,000 } Younger
- Greater than 10,000 Older

Well identifier—Outline color of well identifier indicates isotopic signature and apparent age of groundwater sample (fig. 44)

- Q34 Sample from well yields isotopically heavier groundwater with older apparent age
- Q05 Sample from well yields isotopically lighter groundwater with younger apparent age
- Q29 Sample from well yields isotopically heavier groundwater with younger apparent age or isotopically lighter groundwater with older apparent age

Chihuahua, Mexico **Global Network of Isotopes in Precipitation station**

Note: Wells Q08 and Q41 are not plotted because carbon-14 results are not available.

Figure 43. Relation between delta deuterium and delta oxygen-18 measured in groundwater samples and apparent groundwater ages, Mesilla Basin study area in Doña Ana County, New Mexico, and El Paso County, Texas, 2010.

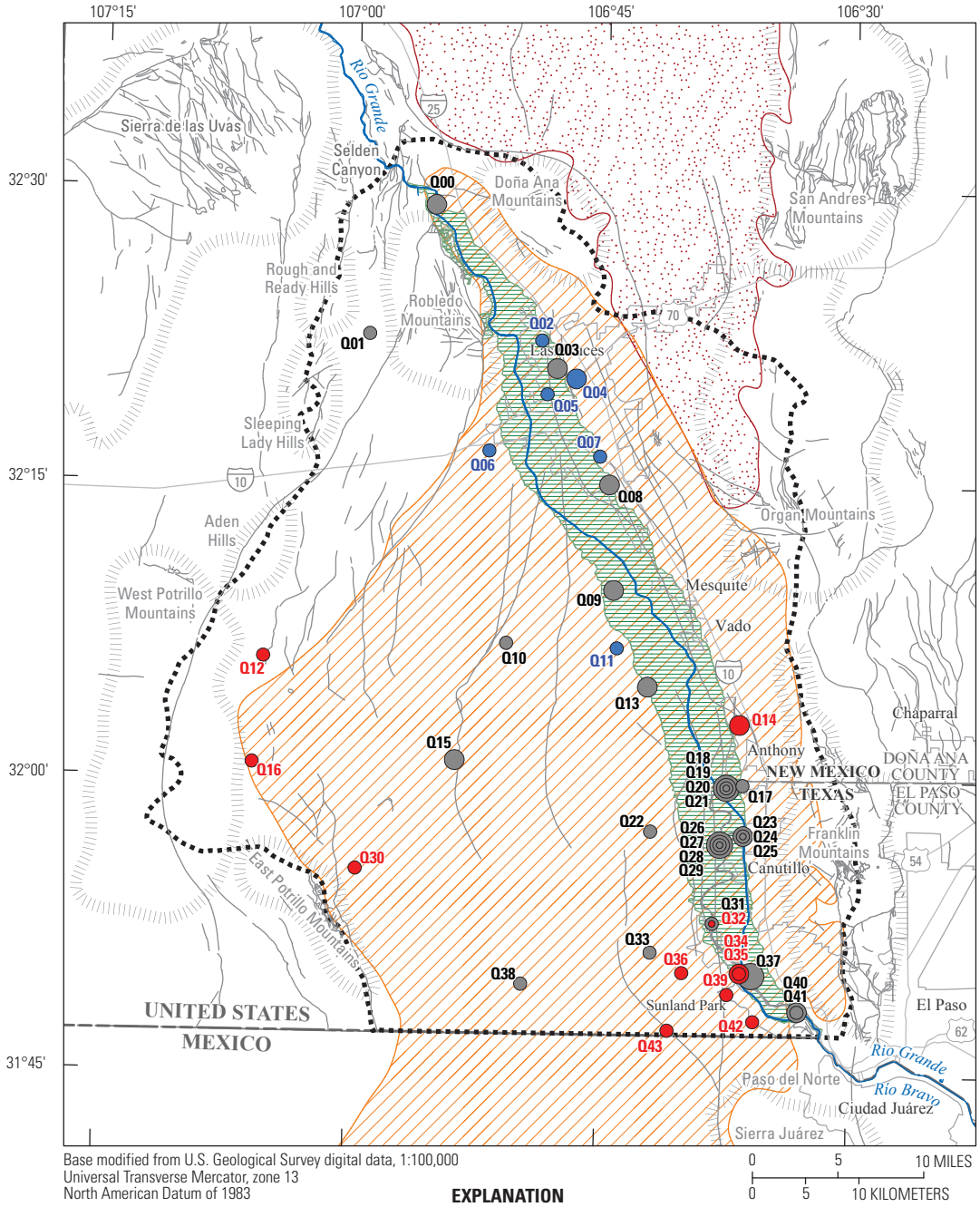

Base modified from U.S. Geological Survey digital data, 1:100,000
Universal Transverse Mercator, zone 13
North American Datum of 1983

0 5 10 MILES
0 5 10 KILOMETERS

EXPLANATION

Mesilla Basin (United States)/Conejos-Médanos (Mexico) aquifer system—Modified from El Paso Water Utilities (2007)

Rio Grande alluvium in the Mesilla Valley—Modified from Hawley and Kennedy (2004), Hawley and others (2005)

Jornada del Muerto Basin aquifer system—Modified from Daniel B. Stephens and Associates (2010)

Mesilla Basin study area boundary

Fault or fault zone—From Hawley and Kennedy (2004), Hawley and others (2005)

Q14 **Well with isotopically heavier groundwater with values greater than -80.00 and -10.50 per mil δD and $\delta^{18}O$, respectively, and an older apparent age of greater than 10,000 carbon-14 years before present (1950) (fig. 43, table 13) and identifier (table 5)**

Q06 **Well with isotopically lighter groundwater with values less than -80.00 and -10.50 per mil δD and $\delta^{18}O$, respectively, and a younger apparent age of less than 10,000 carbon-14 years before present (1950) (fig. 43, table 13) and identifier (table 5)**

Q13 **Well with groundwater sample that had a lighter stable isotopic signature and apparent groundwater age of more than 10,000 carbon-14 years before present (1950) or well with groundwater sample that had a heavier stable isotopic signature and apparent groundwater age of less than 10,000 carbon-14 years before present (1950) (table 5)**

Well sampled—Symbol size represents hydrogeologic unit in which well was completed

Completed in the Rio Grande alluvium

Completed in the upper part of Santa Fe Group

Completed in the middle part of Santa Fe Group

Completed in the lower part of Santa Fe Group

Note: Well identifiers are labeled from the uppermost hydrogeologic unit at the top to the lowermost hydrogeologic unit at the bottom when more than one sample was collected in the same location.

δD, delta deuterium
$\delta^{18}O$, delta oxygen-18

Figure 44. Locations of wells from which groundwater samples with lighter stable isotopes and apparent ages of less than 10,000 carbon-14 years before 1950 and with heavier stable isotopes and apparent ages of greater than 10,000 carbon-14 years before 1950 were collected in the Mesilla Basin study area in Doña Ana County, New Mexico, and El Paso County, Texas, 2010.

Geochemical Groups

The geochemistry data indicate that there was a complex system of geochemical endmembers and mixing between these endmembers. All of the groundwater analytical results indicated mixing or localized processes and conditions, but there were enough similarities between certain groundwater analytical results that the following distinct geochemical groups could be identified: (1) seepage from the ancestral Rio Grande—groundwater older than 10,000 ^{14}C years BP (hereinafter referred to as the "ancestral Rio Grande geochemical group"); (2) seepage from the modern Rio Grande—groundwater younger than 10,000 ^{14}C years BP (hereinafter referred to as the "modern Rio Grande geochemical group"); (3) mountain-front recharge from the Organ and Robledo Mountains and from the highlands to the southwest (hereinafter referred to as the "mountain-front geochemical group"); (4) deep groundwater upwelling, which would be from a deep saline source (hereinafter referred to as the "deep groundwater upwelling geochemical group"); and (5) unidentifiable source of freshwater, which could contain interbasin flow from the Jornada Basin (hereinafter referred to as the "unknown freshwater geochemical group"). The sources of water to these geochemical groups were (1) seepage from the Rio Grande, (2) mountain-front recharge, and (3) inflow from deeper or neighboring water systems. The groundwater samples not represented in one of the five distinct geochemical groups were combined into a "mixed water" geochemical group.

The groundwater samples in the ancestral Rio Grande geochemical group (collected from wells Q10, Q15, Q17, Q20, Q21, Q22, Q27, Q28, and Q33) (fig. 45) predominantly were of a Na-HCO_3 or a Na-SO_4-HCO_3 water type and were characterized by relatively high mean temperature and pH values, relatively low mean concentrations of DO, Ca, Mg, K, Mn, Sr, and ^3H, and relatively low mean $^{87}Sr/^{86}Sr$ ratios (table 14, at back of report) compared to samples from the other geochemical groups. There were some outlying values for a few of the groundwater sample constituents within the ancestral Rio Grande geochemical group. Cl concentrations of 95.8 and 171 mg/L were measured in the groundwater samples collected from wells Q15 and Q17, respectively, whereas the remaining Cl concentrations measured in groundwater samples in this geochemical group ranged from 29.6 to 69.9 mg/L (with a mean concentration of about 45 mg/L) (table 11, at back of report). The Mg concentration of 10.1 mg/L measured in the groundwater sample collected from well Q15 was greater than the Mg concentrations measured in any of the other groundwater samples in this geochemical group, which were all less than 3.50 mg/L. Al concentrations measured in the samples from this geochemical group ranged from about 2 to 3 µg/L except for those measured in groundwater samples collected from wells Q21 (12.1 µg/L), Q27 (8.7 µg/L), and Q28 (42.8 µg/L). Fe concentrations of 43.7 and 110 µg/L were measured in the groundwater samples collected from wells Q10 and Q28, respectively, whereas the Fe concentrations ranged from about 5 to 14 µg/L in most of the groundwater samples in this geochemical group. A U concentration of 23.5 µg/L was measured in the groundwater sample collected from well Q33, which was substantially higher compared to the U concentrations measured in the other groundwater samples within this geochemical group, which were less than 2.00 µg/L. The ancestral Rio Grande geochemical group represented old groundwater, with a mean apparent groundwater age of 24,000 ^{14}C years BP (table 14, at back of report), and had the second least mineralized water (water with dissolved minerals such as salts and other compounds) (as indicated by a mean SpC value of 725 µS/cm at 25 °C) within the study area after the unknown freshwater geochemical group (mean SpC value of 568 µS/cm at 25 °C) (table 14, at back of report). The ancestral Rio Grande geochemical group had a Rio Grande isotopic signature because the samples plotted along the Rio Grande evaporation line (fig. 39) and was composed of water from deep within the subsurface, where geothermal energy can be transferred without geothermal water mixing. The lack of geothermal water mixing was evidenced by the high temperature values and low amount of water mineralization.

The groundwater samples in the modern Rio Grande geochemical group (collected from wells Q03, Q09, Q13, Q18, Q23, Q26, and Q37) generally were of the Ca-SO_4, Na-Cl-SO_4, or Na-Ca-SO_4 water type, with the water transitioning from a Ca-SO_4 water type in the northern part of the study area to a Na-Cl-SO_4 water type near the southern end of the study area (table 14, at back of report; fig. 45). Among the different geochemical groups, this geochemical group was characterized as having the lowest mean water temperature and pH values, the youngest apparent ^{14}C ages, the lowest concentrations of F and As, and relatively low concentrations of NO_3+NO_2. This geochemical group was also characterized by having relatively high mean concentrations of Ba, Mn, δD, $\delta^{18}O$, and tritium compared to the other geochemical groups (table 14, at back of report). There were some outlying values for a few of the groundwater sample constituents within the modern Rio Grande geochemical group. The K concentration of 31.4 mg/L measured in the groundwater sample collected from well Q18 was about twice as large as the next highest K concentration of 15.9 mg/L measured in the groundwater sample collected from well Q03 (table 11, at back of report). The concentrations of NH_3-N (0.805 mg/L), Fe (1,820 µg/L), and Mn (2,170 µg/L) measured in the groundwater sample collected from well Q26 were substantially higher than the concentrations of these constituents measured in the other groundwater samples in this geochemical group, for which the next highest concentrations of NH_3-N, Fe, and Mn were 0.186 mg/L (well Q13), 485 µg/L (well Q18), and 915 µg/L (well Q03), respectively. The U concentrations of 62.4 and 23.0 µg/L measured in the groundwater samples collected from wells Q03 and Q13 respectively, were substantially greater than the next highest concentration of 4.61 µg/L measured in the groundwater sample collected from well Q23. The groundwater in the modern Rio Grande

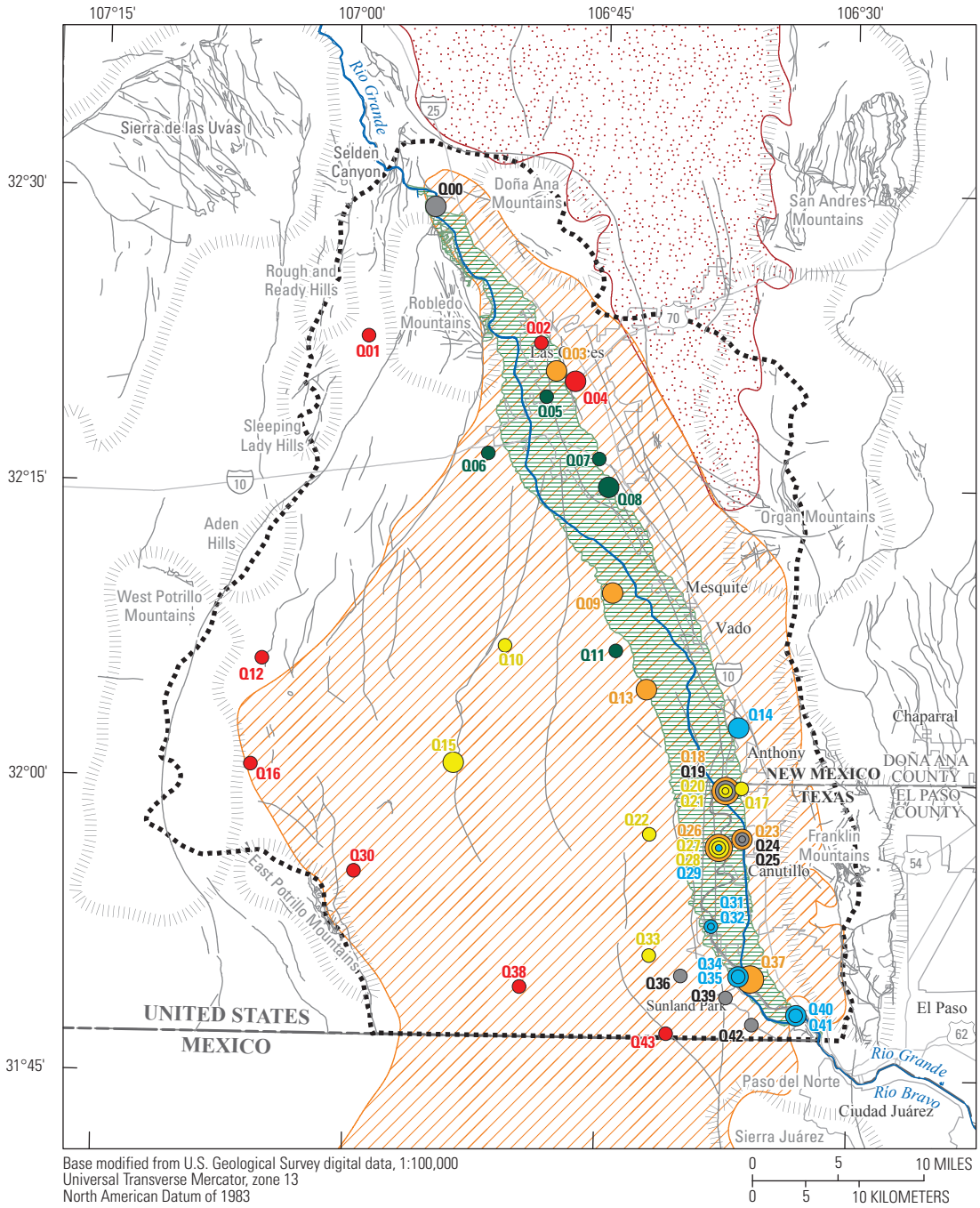

EXPLANATION

Mesilla Basin (United States)/Conejos-Médanos (Mexico) aquifer system—Modified from El Paso Water Utilities (2007)

Rio Grande alluvium in the Mesilla Valley—Modified from Hawley and Kennedy (2004), Hawley and others (2005)

Jornada del Muerto Basin aquifer system—Modified from Daniel B. Stephens and Associates (2010)

Mesilla Basin study area boundary

Fault or fault zone—From Hawley and Kennedy (2004), Hawley and others (2005)

Well sampled and identifier (table 5), by geochemical group (table 14)

- Q15 Ancestral Rio Grande
- Q09 Modern Rio Grande
- Q01 Mountain-front
- Q41 Deep groundwater upwelling
- Q06 Unknown freshwater
- Q00 Mixed water

Well sampled—Symbol size represents hydrogeologic unit in which well was completed

- Completed in the Rio Grande alluvium
- Completed in the upper part of Santa Fe Group
- Completed in the middle part of Santa Fe Group
- Completed in the lower part of Santa Fe Group

Note: Well identifiers are labeled from the uppermost hydrogeologic unit at the top to the lowermost hydrogeologic unit at the bottom when more than one sample was collected in the same location.

Figure 45. Groundwater sampling locations categorized by geochemical groups, Mesilla Basin study area in Doña Ana County, New Mexico, and El Paso County, Texas, 2010.

geochemical group was recharged after 1950 (based on tritium values, table 14, at back of report), was the second most mineralized water (as indicated by a mean SpC value of 2,400 µS/cm at 25 °C) within the study area after the deep groundwater upwelling geochemical group (mean SpC value of 11,400 µS/cm at 25 °C), and had a Rio Grande isotopic signature because the samples plotted along the Rio Grande evaporation line (table 14, at back of report) (fig. 39).

The groundwater samples in the mountain-front geochemical group (collected from wells Q01, Q02, Q04, Q12, Q16, Q30, Q38, and Q43) generally had some of the highest mean DO, F, NO_3+NO_2, and Si concentrations, and the lowest mean NH_3-N concentration among the different geochemical groups (table 14, at back of report; fig. 45). The mountain-front geochemical group represented recharge from the uplifted areas surrounding the study area (fig. 45). The groundwater samples in this group were a mix of the Na water types (Na-HCO_3, Na-SO_4, Na-SO_4-HCO_3, Na-Cl-SO_4, and Na-Cl-HCO_3) (table 12, at back of report). There were some outlying values for a few of the groundwater sample constituents within this geochemical group. The concentration of SO_4 measured in the groundwater sample collected from well Q01 was 544 mg/L, which was more than two times the concentration measured in the groundwater sample with the next highest SO_4 concentration of 242 mg/L (well Q12). The groundwater sample collected from well Q01 also had a Br concentration of 1.72 mg/L; the next highest Br concentration was 0.666 mg/L (well Q16). The groundwater samples collected from wells Q02 and Q04 had Ca concentrations of 70.5 and 62.4 mg/L, respectively, which were more than two times the next highest Ca concentration of 31.0 mg/L (well Q30). The groundwater sample collected from well Q38 had a substantially higher Mn concentration (84.8 µg/L) than did the other groundwater samples in this group—more than an order of magnitude larger than the next highest Mn concentration of 4.89 µg/L (well Q16). The groundwater sample collected from well Q38 also had a substantially higher U concentration of 29.3 µg/L compared to the next highest concentration among samples in this group of 16.0 µg/L (well Q01). The groundwater samples in the mountain-front geochemical group represented old groundwater with a mean apparent age of 18,000 ^{14}C years BP. The geochemistry of the samples in this group indicates that the groundwater moves slowly through areas with low concentrations of reducing agents such as aluminum or iron, indicated by the high mean concentrations of DO and NO_3+NO_2 and low mean concentration of NH_3-N, and that the groundwater had prolonged exposure to aluminosilicate minerals, indicated by the high mean concentrations of F and Si (table 14, at back of report).

The groundwater samples in the deep groundwater upwelling geochemical group were collected from wells Q14, Q29, Q31, Q32, Q34, Q35, Q40, and Q41 (fig. 45). Compared to the other geochemical groups, the deep groundwater upwelling geochemical group had the highest mean SpC value, some of the highest mean concentrations of Cl, SO_4, HCO_3, Br, Na, Ca, Mg, K, NH_3-N, Al, As, Fe, Li, Sr, and U, and the oldest apparent age date (table 14, at back of report). Wells Q40 and Q41 were likely indicative of the deep groundwater upwelling endmember, as samples collected from these wells yielded extreme values for many of the constituents used to characterize the deep groundwater upwelling geochemical group, whereas the other samples represented a slight dilution of the deep groundwater upwelling endmember with another endmember in the study area (table 11, at back of report). To observe the subset of samples representing this diluted mixture, wells Q40 and Q41 were excluded when calculating the mean of the deep groundwater upwelling geochemical group. When the mean values from this subset of samples were compared to the mean values for other geochemical groups, the groundwater samples in the modern Rio Grande geochemical group had the highest mean concentrations for SO_4, Br, Ca, Mg, NH_3-N, Fe, Sr, and U, and the groundwater samples that had a composition consistent with that of the ancestral Rio Grande geochemical group had the highest concentration of Al of any group of samples. The groundwater samples of the deep groundwater upwelling geochemical group were mostly a Na-Cl water type (Na-Cl, Na-Cl-SO_4, or Na-Cl-HCO_3) with two of the wells yielding a Na-HCO_3 water type, which may be a result of some mixing with groundwater from the ancestral Rio Grande geochemical group; there were some outlying values for a few of the groundwater sample constituents within this geochemical group. Within a geochemical group, there often was a large difference between the highest concentration of a constituent and the second highest concentration. For example, the sample collected from well Q35 had a Cl concentration of 1,960 mg/L; the next highest Cl concentration was 836 mg/L, which was measured in a sample collected from well Q34 (table 11, at back of report). The highest concentration of F (4.73 mg/L) was measured in the sample collected from well Q29, compared to the next highest F concentration of 1.23 mg/L (well Q35). The highest Ca concentration (515 mg/L) was measured in groundwater sample collected from well Q35, compared to the next highest Ca concentration of 147 mg/L, which was measured in the groundwater sample collected from well Q34. The groundwater sample collected from well Q14 had the highest concentrations of K and Sr, 45.5 mg/L and 5,080 µg/L, respectively; the next highest concentrations of K and Sr were 11.0 mg/L and 2,410 µg/L, respectively, which were measured in the groundwater sample collected from well Q35. The groundwater in the deep groundwater upwelling geochemical group was the oldest groundwater sampled within the study area (mean apparent groundwater age of 26,000 ^{14}C years BP) and was the most mineralized water (as indicated by a mean SpC value of 11,400 µS/cm at 25 °C) (table 14, at back of report), which was representative of the ancient marine groundwater located within the Paleozoic and Cretaceous carbonate rocks (Hawley and Kennedy, 2004; Hawley and others, 2005).

The groundwater samples in the unknown freshwater geochemical group (wells Q05, Q06, Q07, Q08, and Q11) (fig. 45) generally were of the Ca-Na-HCO_3 water type. Of all

the geochemical groups, the unknown freshwater geochemical group had the lowest mean SpC values and the lowest mean concentrations of Cl, SO_4, Br, Na, Si, Al, and Li (table 14, at back of report). There were some outlying values for a few of the groundwater sample constituents within this geochemical group. A DO concentration of 2.6 mg/L was measured in the groundwater sample collected from well Q11; the groundwater sample collected from well Q11 was the only groundwater sample in the unknown freshwater geochemical group with a DO concentration greater than 0.10 mg/L (table 10, at back of report). The highest U concentration was 8.79 µg/L in this geochemical group, which was measured in the sample collected from well Q07. The next highest U concentration of 0.552 µg/L was measured in the sample collected from well Q11 (table 11, at back of report).

The samples composing the unknown freshwater geochemical group represented moderately old groundwater with a mean apparent age of 3,300 ^{14}C years BP and the least mineralized water of any geochemical group (as indicated by a mean SpC value of 568 µS/cm at 25 °C) (table 14, at back of report). The source for this geochemical group was unknown because the groundwater does not have a Rio Grande isotopic signature (fig. 39) and because the low concentrations of minerals in the groundwater samples that compose this group made this water unlike the water of any other geochemical group within the study area. This geochemical group may represent groundwater affected by interbasin flow from the Jornada Basin (Hawley and Kennedy, 2004; Witcher and others, 2004; Hawley and others, 2005).

Within the study area, the remaining groundwater samples characterized as the "mixed water" geochemical group (collected from wells Q00, Q19, Q24, Q25, Q36, Q39, and Q42) generally were of the Na-SO_4-Cl water type and had the lowest mean concentrations of HCO_3, Fe, and U (table 14, at back of report; fig. 45). There were some outlying values for a few of the groundwater sample constituents within this geochemical group. Within the "mixed water" geochemical group, the groundwater sample with the highest SO_4 concentration (735 mg/L) was collected from well Q42, whereas the groundwater sample with the next highest concentration (412 mg/L) was collected from well Q25 (table 11, at back of report; fig. 45). The groundwater samples collected from wells Q00 and Q19 had HCO_3 concentrations of 261 and 372 mg/L, respectively, whereas the remaining groundwater samples had HCO_3 concentrations less than 100 mg/L. The groundwater sample collected from well Q36 had a NO_3+NO_2 concentration of 1.16 mg/L, which was almost an order of magnitude larger than that in the groundwater sample with the next highest concentration of 0.26 mg/L (well Q42). The groundwater sample collected from well Q00 had a K concentration of 21.6 mg/L, which was almost three times greater than that in the groundwater sample with the next highest concentration of 8.82 mg/L (well Q19). The groundwater sample collected from well Q19 had an Fe concentration of 69.0 µg/L, whereas the groundwater sample with the next highest concentration was 22.3 µg/L (well Q42). The groundwater sample collected from well Q00 had a substantially higher concentration of Mn (606 µg/L) than did the groundwater sample with the next highest concentration, 36.6 µg/L (well Q19). The groundwater sample collected from well Q36 had a U concentration of 4.51 µg/L, which was more than twice as large as next highest U concentration of 2.22 µg/L (well Q19). The groundwater samples collected from wells Q00 (3.6 TU) and Q24 (10.3 TU) had ^3H concentrations greater than 1.6 TU, whereas all of the remaining groundwater samples were less than 1.6 TU (table 13, at back of report; fig. 45). The groundwater samples in the "mixed water" geochemical group lacked definitive geochemistry characteristics.

Groundwater-Flow System

Geophysical and geochemical data were used in conjunction with water-level-altitude data to investigate regional groundwater-flow paths, recharge sources, discharge zones, and areas of groundwater mixing. The geophysical data also provided insights into potential groundwater upwelling and groundwater flow in the surface geophysical subset area, which is hydrogeologically the most complex part of the study area. The geochemical data were used to identify potential groundwater sources and the mixing between these sources, as well as the groundwater-flow paths and the chemical changes along these flow paths. Water-level-altitude data were used to create potentiometric-surface maps and evaluate vertical hydraulic gradients between the Rio Grande alluvium and the Santa Fe HGUs. Groundwater preferentially flows horizontally and vertically in the direction of decreasing water-level altitude (Heath, 1983). The direction of the vertical hydraulic gradient indicates the potential direction of flow in an aquifer system. High pressures within lower HGUs may result in an upward vertical flow. For example, an upward vertical hydraulic gradient from the Santa Fe HGUs to the Rio Grande alluvium would indicate the potential for upward movement of water. The potentiometric-surface maps and the vertical hydraulic gradient analysis aided in the interpretation of the geochemical data by providing preferential groundwater-flow paths and estimated locations of vertical mixing between the Rio Grande alluvium and the Santa Fe HGUs (upper Santa Fe, middle Santa Fe, and lower Santa Fe).

Water-level-altitude data were used to create potentiometric-surface maps and evaluate vertical hydraulic gradients between the Rio Grande alluvium and the Santa Fe HGUs. Water-level altitude data were compiled for wells in and near the study area by using data obtained from NWIS (U.S. Geological Survey, 2017) and TWDB (Texas Water Development Board, 2012) databases. Overall, there were 526 wells in or near the study area with available water-level-altitude data. Each well was categorized in one of two hydrogeologic groups depending on whether the well was

completed in the Rio Grande alluvium or in the Santa Fe Group, which is a combination of the aforementioned upper Santa Fe, middle Santa Fe, and lower Santa Fe. The upper Santa Fe, middle Santa Fe, and lower Santa Fe were combined into one hydrogeologic group (Santa Fe Group) because the number of wells with available water-level-altitude data was much larger compared to the number of wells for the water-quality analysis and because many of the wells lacked detailed information about their screened intervals or geologic descriptions—information that would have made it feasible to assign all 526 wells to individual HGUs. The wells with water-quality data and water-level-altitude data were separated into the hydrogeologic groups according to their NWIS aquifer code. If the well record did not specify an aquifer code, the total depth of the well was compared to the depth of surrounding wells, and the well was assigned an aquifer code based on the NWIS aquifer code information of nearby wells. After completing this process, there were water-level-altitude data available for 221 wells completed in the Rio Grande alluvium and 286 wells completed in the Santa Fe Group. Potentiometric-surface maps for the Rio Grande alluvium and the Santa Fe Group were prepared from the mean water-level altitudes during the 2010 winter season (November 1, 2010, through April 30, 2011) (table 15, at back of report; figs. 46–48). Because there is little irrigation during the winter season, water-level altitudes are less affected by drawdown caused by groundwater pumping compared to the rest of the year. On March 23, 2011, several wells near the New Mexico-Texas state line in the northwestern part of the study area recorded water-level altitudes that were anomalously low. These anomalously low water-level altitudes (compared to other water-level altitudes in this area) were likely caused by groundwater pumping in the surrounding well field at the time of the measurement and were not used in the creation of the potentiometric-surface maps. The potentiometric-surface grids were generated by using minimum-curvature interpolation techniques along with professional judgment to adjust for gridding errors near the study area boundaries where data were sparse. The minimum-curvature methods used for grid generation are described in Geosoft, Inc. (2012). Minimum-curvature interpolation techniques are ideal for randomly distributed datasets, helping to produce realistic potentiometric grids between data points (Geosoft, Inc., 2012). The water-level-altitude data were contoured from these potentiometric grids. Water-level altitudes did not change appreciably except in pumping areas, resulting in relatively smooth potentiometric-surface map contours (fig. 46). The spatial distribution of wells with water-level altitude data representing the Santa Fe Group was relatively sparse throughout the study area except for high densities of wells near Las Cruces, Sunland Park, and Canutillo, N. Mex. Because of a scarcity of data representing the Santa Fe Group for the remainder of the study area, the potentiometric-surface maps have some uncertainty associated with them but still represent general patterns.

Regional Groundwater Flow

Water-level altitudes within the Rio Grande alluvium generally decreased from north (greater than 3,920 ft) to south (less than 3,730 ft) (fig. 46). There was a west to east decrease in water-level altitudes near Las Cruces, N. Mex. associated with drawdown related to a cone of depression in the underlying Santa Fe Group (fig. 47) as a result of groundwater pumping by the City of Las Cruces for municipal supply purposes (McCoy and Peery, 2008). Groundwater flow within the Rio Grande alluvium was from north to south except near Las Cruces, where groundwater pumping resulted in a northwest to southeast hydraulic gradient near the city.

Water-level altitudes within the Santa Fe Group generally decreased from the north and northwest to the south and southeast (figs. 47 and 48). The highest groundwater altitudes (greater than 4,300 ft) were measured northwest of the study area near the Sleeping Lady Hills. The lowest groundwater altitudes (less than 3,720 ft) were located to the southeast near the Paso del Norte. There were two cones of depression in the potentiometric surface for the Santa Fe Group, one near Las Cruces and one near Canutillo, Tex. Groundwater movement within the Santa Fe Group appeared to be affected by the faults within the area. There were multiple locations where the magnitude of the hydraulic gradient decreased or substantially flattened while crossing a fault boundary, specifically, along the Fitzgerald Fault zone (figs. 47 and 48) to the southwest of Las Cruces (south of wells L022, L023, and L024) and along the southern part of the East Robledo Fault zone (figs. 47 and 48) towards the western part of the study area (near wells L068 and L076) (figs. 47 and 48). Areas of relatively steep horizontal hydraulic gradients with relatively high rates of water movement (compared to horizontal hydraulic gradients typically found in the basins and valleys) were located in the northern and northwestern parts of the study area (in the Organ Mountains to the north and the Robledo Mountains, Rough and Ready Hills, and Sleeping Lady Hills to the northwest). There were also some areas of steeper horizontal hydraulic gradients in the southeastern part of the study area. The highest water-level altitudes in the southeastern part of the study area were south of Canutillo, Tex., indicating a locally higher rate of water movement that was likely caused by groundwater pumping in this area. There were some relatively lower horizontal hydraulic gradient zones north of Canutillo, Tex. (north of wells L084, L088, L089, and L090), south of Las Cruces (south of wells L049–L053 and L055–L060), and near the Paso del Norte (fig. 48). These lower hydraulic gradients were likely a result of the upwelling of deep groundwater as discussed in the "Geophysical Integration" and "Geochemical Groups" sections of this report describing geophysical and geochemical data. The upwelling of deep groundwater restricted groundwater movement within the Santa Fe at these locations by introducing more water into the system, causing a slight increase in water-level altitudes. Groundwater flow decreased or changed direction in areas where the upwelling of deep groundwater restricted groundwater movement.

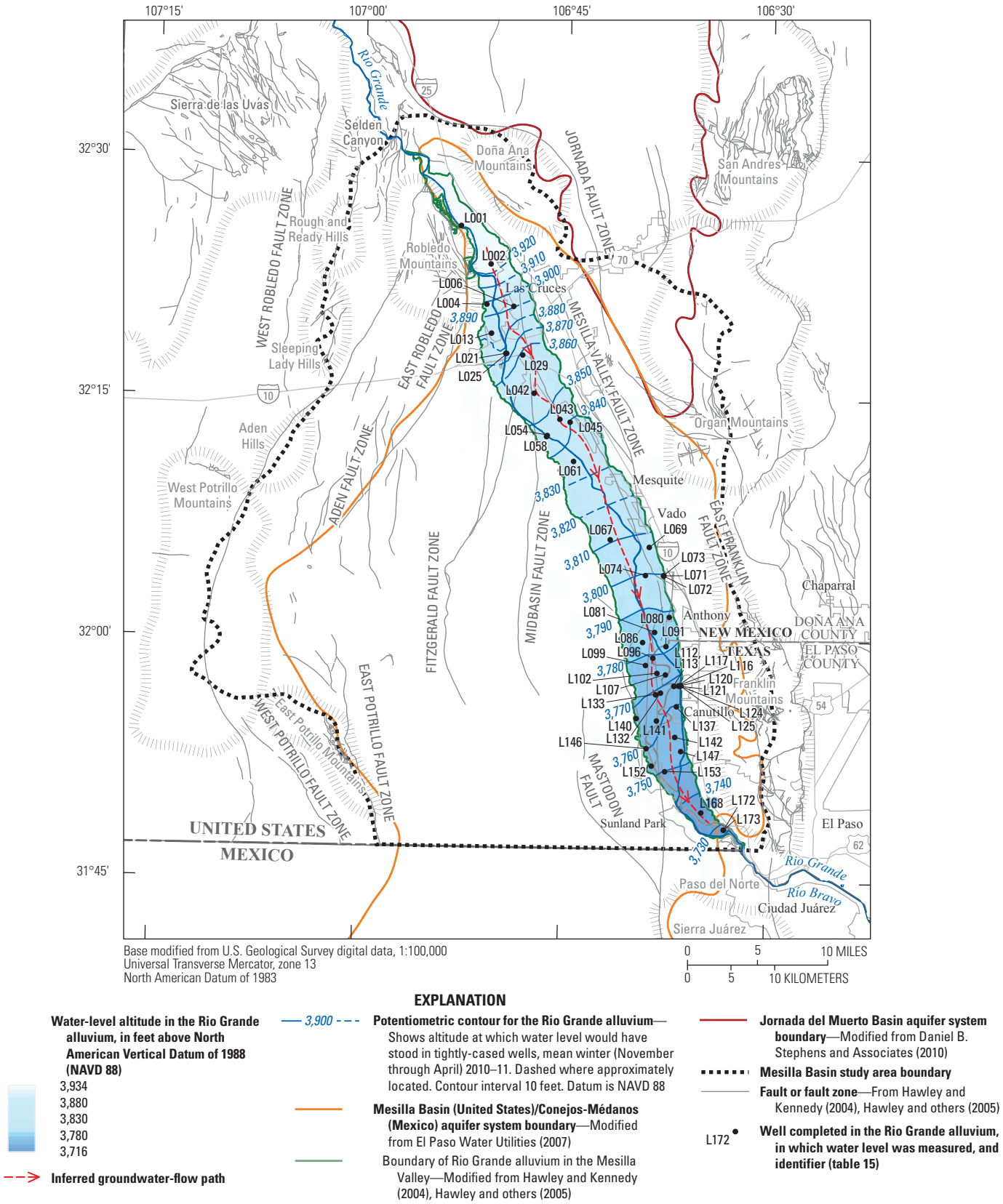

Base modified from U.S. Geological Survey digital data, 1:100,000
Universal Transverse Mercator, zone 13
North American Datum of 1983

0 5 10 MILES
0 5 10 KILOMETERS

EXPLANATION

Water-level altitude in the Rio Grande alluvium, in feet above North American Vertical Datum of 1988 (NAVD 88)
3,934
3,880
3,830
3,780
3,716

Inferred groundwater-flow path

3,900 **Potentiometric contour for the Rio Grande alluvium**—Shows altitude at which water level would have stood in tightly-cased wells, mean winter (November through April) 2010–11. Dashed where approximately located. Contour interval 10 feet. Datum is NAVD 88

Mesilla Basin (United States)/Conejos-Médanos (Mexico) aquifer system boundary—Modified from El Paso Water Utilities (2007)

Boundary of Rio Grande alluvium in the Mesilla Valley—Modified from Hawley and Kennedy (2004), Hawley and others (2005)

Jornada del Muerto Basin aquifer system boundary—Modified from Daniel B. Stephens and Associates (2010)

Mesilla Basin study area boundary

Fault or fault zone—From Hawley and Kennedy (2004), Hawley and others (2005)

L172 **Well completed in the Rio Grande alluvium, in which water level was measured, and identifier (table 15)**

Figure 46. Potentiometric surface developed from mean winter water-level altitudes (November 2010 through April 2011) measured in wells completed in the Rio Grande alluvium in the Mesilla Basin study area in Doña Ana County, New Mexico, and El Paso County, Texas.

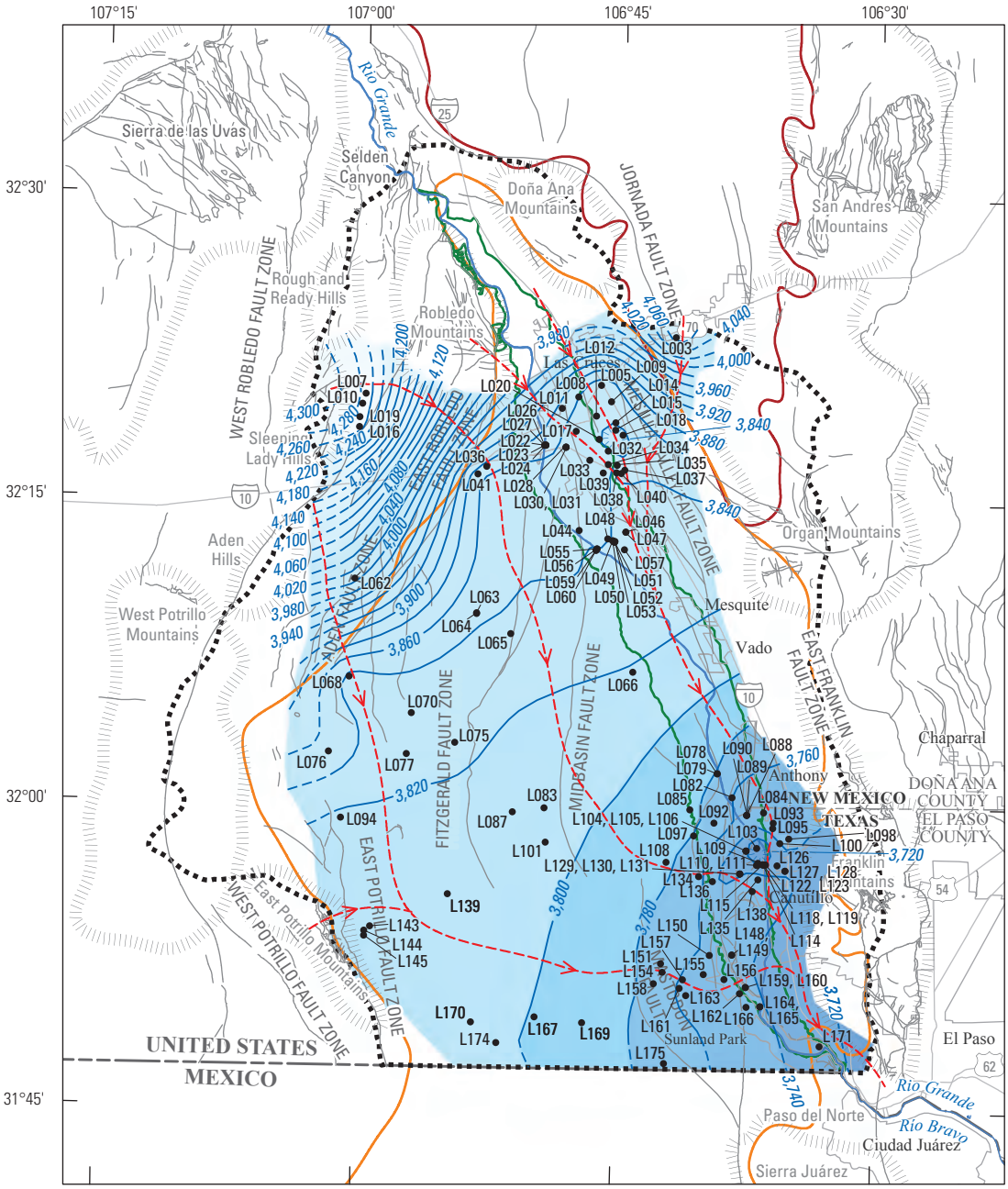

Base modified from U.S. Geological Survey digital data, 1:100,000
Universal Transverse Mercator, zone 13
North American Datum of 1983

0 5 10 MILES
0 5 10 KILOMETERS

EXPLANATION

Water-level altitude in the Santa Fe Group, in feet above North American Vertical Datum of 1988 (NAVD 88)
4,315
4,150
4,000
3,850
3,696

Inferred groundwater-flow path

3,900 **Potentiometric contour for the Santa Fe Group**—Shows altitude at which water level would have stood in tightly-cased wells, mean winter (November through April) 2010–11. Dashed where approximately located. Hachures indicate depression. Contour interval 20 feet. Datum is NAVD 88

Mesilla Basin (United States)/Conejos-Médanos (Mexico) aquifer system boundary—Modified from El Paso Water Utilities (2007)

Boundary of Rio Grande alluvium in the Mesilla Valley—Modified from Hawley and Kennedy (2004), Hawley and others (2005)

Jornada del Muerto Basin aquifer system boundary—Modified from Daniel B. Stephens and Associates (2010)

Mesilla Basin study area boundary

Fault or fault zone—From Hawley and Kennedy (2004), Hawley and others (2005)

L155 **Well completed in the Santa Fe Group, in which water level was measured, and identifier (table 15)**

Figure 47. Potentiometric surface developed from mean winter water-level altitudes (November 2010 through April 2011) measured in wells completed in the Santa Fe Group in the Mesilla Basin study area in Doña Ana County, New Mexico, and El Paso County, Texas.

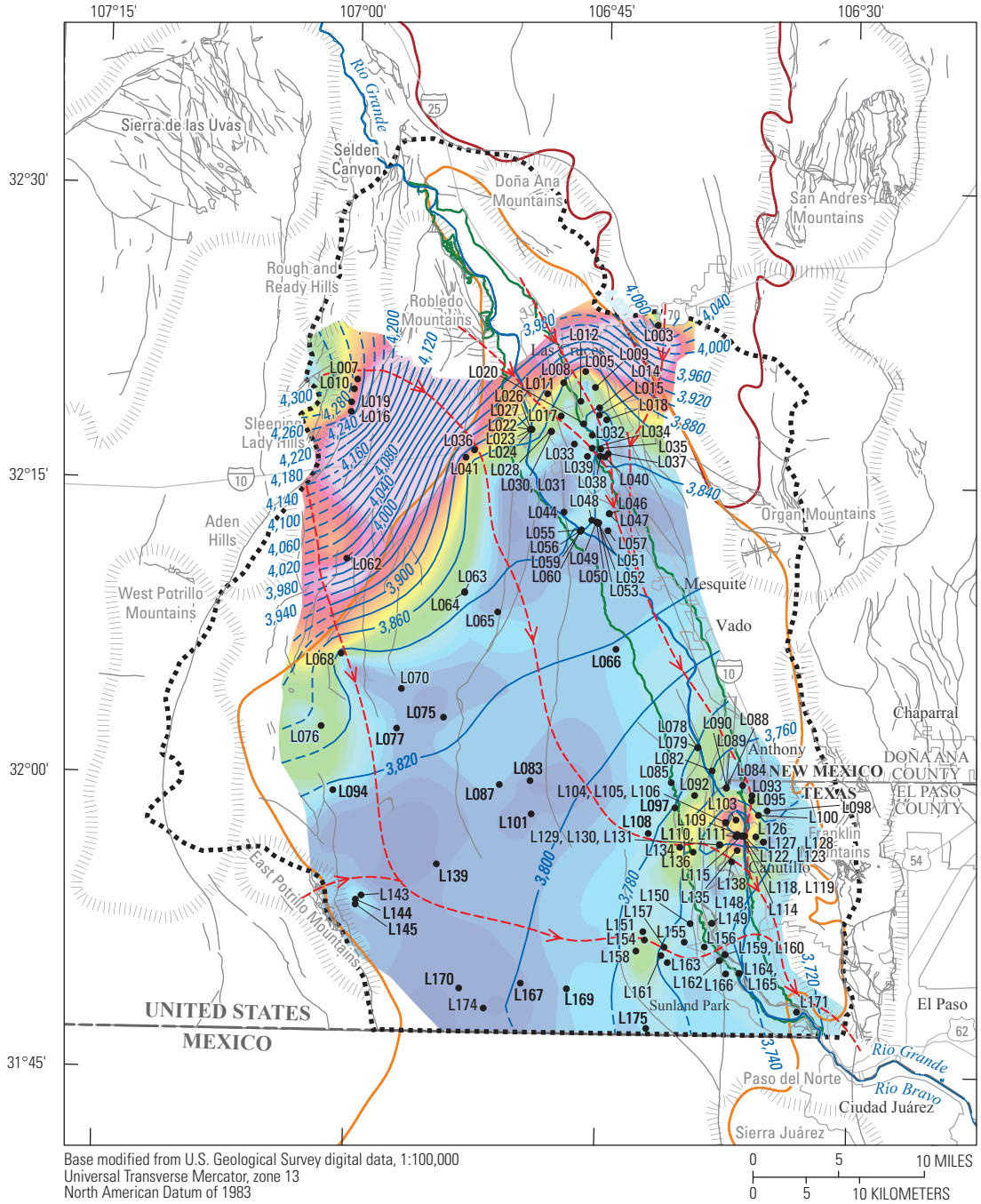

Base modified from U.S. Geological Survey digital data, 1:100,000
Universal Transverse Mercator, zone 13
North American Datum of 1983

0 5 10 MILES
0 5 10 KILOMETERS

EXPLANATION

Horizontal gradient, in feet per foot

- 0
- 0.005
- 0.010
- 0.015
- 0.020
- Greater than 0.025

Inferred groundwater-flow path

3,900 **Potentiometric contour for the Santa Fe Group**—Shows altitude at which water level would have stood in tightly-cased wells, mean winter (November through April) 2010–11. Dashed where approximately located. Contour interval 20 feet. Datum is North American Vertical Datum of 1988

Mesilla Basin (United States)/Conejos-Médanos (Mexico) aquifer system boundary—Modified from El Paso Water Utilities (2007)

Boundary of Rio Grande alluvium in the Mesilla Valley—Modified from Hawley and Kennedy (2004), Hawley and others (2005)

Jornada del Muerto Basin aquifer system boundary—Modified from Daniel B. Stephens and Associates (2010)

Mesilla Basin study area boundary

Fault or fault zone—From Hawley and Kennedy (2004), Hawley and others (2005)

L155 **Well completed in the Santa Fe Group, in which water level was measured, and identifier (table 15)**

Figure 48. Potentiometric surface and hydraulic gradient developed from mean winter water-level altitudes (November 2010 through April 2011) measured in wells completed in the Santa Fe Group, Mesilla Basin study area in Doña Ana County, New Mexico, and El Paso County, Texas.

Groundwater flow within the Santa Fe Group is more complex than the groundwater flow within the Rio Grande alluvium because of the larger lateral and vertical extent of the Santa Fe Group compared to the Rio Grande alluvium. Groundwater from the Organ Mountains flows directly south towards the Paso del Norte. Groundwater from the Robledo Mountains, the Rough and Ready Hills, and the Sleeping Lady Hills generally flows to the southeast. Groundwater flowing near the north end of the midbasin uplift generally continues east towards the Rio Grande and then flows south on the east side of the midbasin uplift. Groundwater flowing near the west side of the midbasin uplift generally continues south parallel to the faults that make up the midbasin uplift and then flows east towards the Paso del Norte when it reaches the south end of the midbasin uplift. Groundwater from the Aden Hills and the East and West Potrillo Mountains flows to the south end of the midbasin uplift and then continues east towards the Paso del Norte (fig. 48).

Wells completed in the Rio Grande alluvium or Santa Fe Group were assigned to different well groups on the basis of how close the wells were to one another (table 16, at back of report). The maximum distance between wells in a well group was 315 ft, which was the maximum distance between the different wells assigned to group M–3. Wells were assigned to these different groups to facilitate a vertical hydraulic gradient analysis between the Rio Grande alluvium and the Santa Fe Group (table 16, at back of report; figs. 49 and 50). A potential for interaction between groundwater in the Rio Grande alluvium and the Santa Fe Group was identified by evaluating the vertical hydraulic gradient within each group. Throughout most of the Mesilla Valley, the vertical hydraulic gradient was downward because the water-level altitude in the Rio Grande alluvium was generally higher than it was in the Santa Fe Group (figs. 49 and 50). In some areas, the vertical hydraulic gradient was substantially reduced or even reversed from a downward to an upward hydraulic gradient. The reduced or reversed groundwater hydraulic gradient occurred in well groups ISC-4 (about 1.00 ft), ISC-5 (about -0.06 ft), ISC-6 (about -2.65 ft), ISC-7 (about -2.00 ft), M-3 (about 1.00 ft), LC-3 (about 2.80 ft) and NM344 (about 1.00 ft), located in the middle and southern parts of the Mesilla Valley (table 16, at back of report; figs. 49 and 50). A conceptual grid depicting locations in which the Rio Grande alluvium had a lower potentiometric surface than the Santa Fe Group was created by calculating the difference between the Rio Grande alluvium and the Santa Fe Group potentiometric-surface grids (Rio Grande alluvium minus Santa Fe Group) (fig. 49). This conceptual grid corresponded closely to the vertical hydraulic gradients at the grouped wells (table 16, at back of report; fig. 50).

A comparison between the vertical hydraulic gradient data and the geophysical data indicated two distinct areas where deep salinity sources may be contributing to the Rio Grande alluvium. The HFEM data indicated that there was a resistivity change at depth from relatively high resistivity near the surface to relatively low resistivity at greater depths in the middle part of the Mesilla Valley that corresponded with the low vertical hydraulic gradient (fig. 49). This resistivity change could be attributed to changes in lithology, such as a large amount of clayey deposits and silts within this reach of the Rio Grande alluvium; however, the USGS seepage investigations, historical dissolved-solids-concentration analysis, and geochemical analyses indicated that this reach of the river has the potential to be a gaining reach (implying that there were sands and gravels instead of clayey deposits and silts in this location). These lines of evidence indicate that upwelling from deep salinity sources may be the cause of the decrease in resistivity. The upwelling of relatively saline groundwater would increase the salinity within the Rio Grande alluvium in the middle part of the Mesilla Valley. This saline groundwater then discharges from the Rio Grande alluvium to the Rio Grande in the middle part of the Mesilla Valley. Downstream from the middle part of the Mesilla Valley, the Rio Grande becomes a losing stream, resulting in saline water seeping into the Rio Grande alluvium and increasing the deposition of salts within the subsurface. A second area where deep salinity sources may be contributing to the Rio Grande alluvium is near the Paso del Norte. The vertical hydraulic gradient conceptual grid (fig. 49) and the water-level altitudes measured in well groups ISC-5 to ISC-7 (figs. 50*O* to 50*Q*) indicated that there was an upward hydraulic gradient near the Paso del Norte. This upward hydraulic gradient may result in the upwelling of groundwater from a deep saline source. Low resistivity features identified by the DC resistivity and TDEM data provide additional evidence of upwelling in this area (figs. 14 and 15). These geophysical data can be interpreted as plumes of saline water originating below the base of the Santa Fe Group. If this interpretation is correct, these plumes likely eventually rise to land surface to the west of the Rio Grande near the Paso del Norte, potentially affecting the salinity of the drains in the area.

Water Sources, Geochemical Evolution, and Groundwater Mixing

Sources of water for the groundwater system within the study area consist of seepage from the Rio Grande, runoff and recharge within the mountains and uplifted areas, and inflows of upwelling groundwater from deep saline sources or from other aquifer systems. These sources of water were qualitatively analyzed and compared to previously published studies within the area (Frenzel and Kaehler, 1992; Nickerson and Myers, 1993; Witcher and others, 2004; S.S. Papadopulos and Associates, Inc., 2007). The predominant source of water for the groundwater system within the study area was the Rio Grande, with the other water sources contributing a small fraction of the total amount of water. Runoff and recharge within the mountains and uplifted areas (including mountain-front recharge) contributed the least amount, consistent with the local climate and annual rainfall in the area (S.S. Papadopulos and Associates, Inc., 2007).

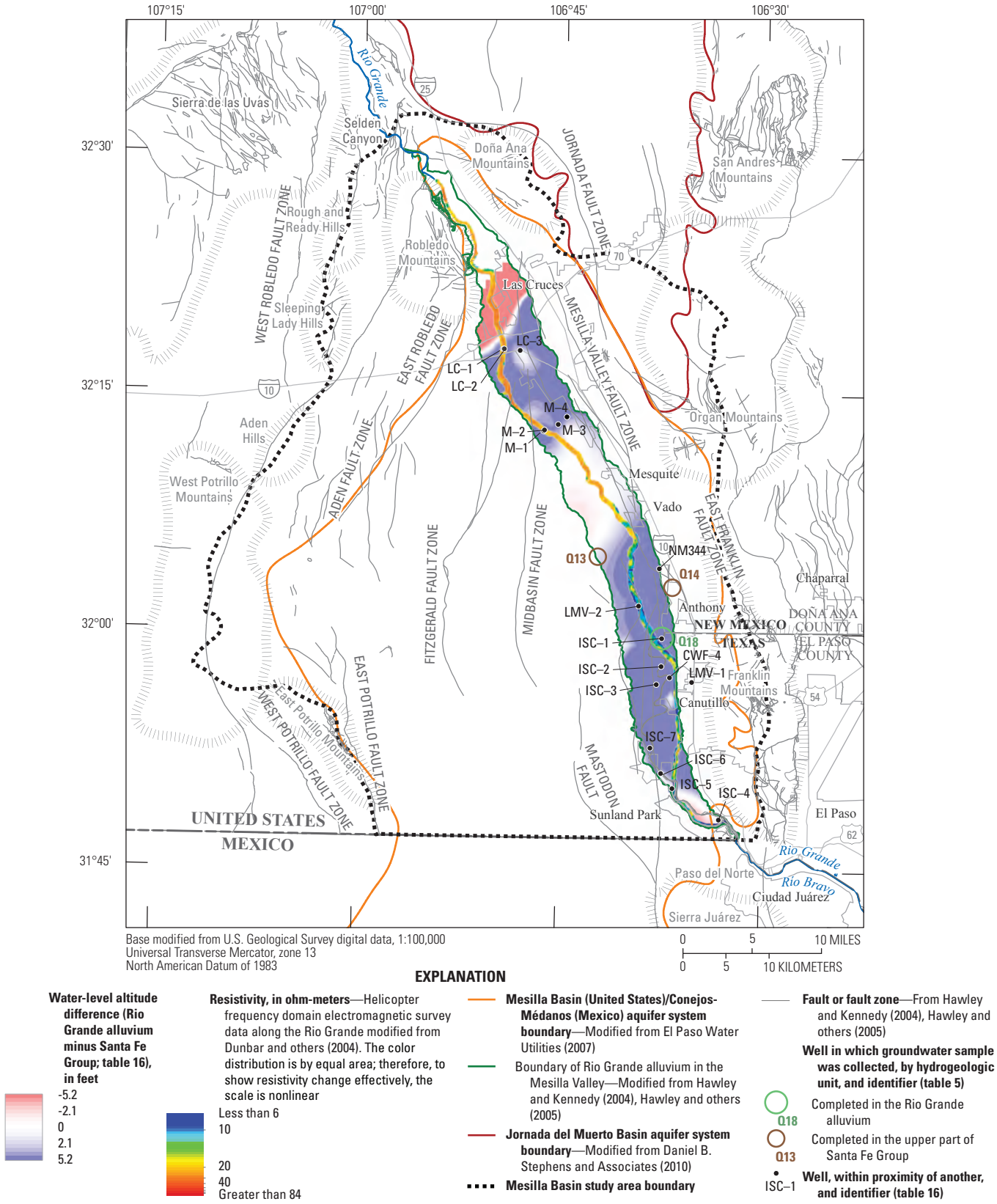

Figure 49. Water-level-altitude differences between the Rio Grande alluvium and the Santa Fe Group developed by using the 2010–11 potentiometric-surface maps for each hydrogeologic group, locations of wells in proximity of each other, and the helicopter frequency domain electromagnetic data obtained at a depth of 50 feet along the Rio Grande in the Mesilla Basin study area in Doña Ana County, New Mexico, and El Paso County, Texas.

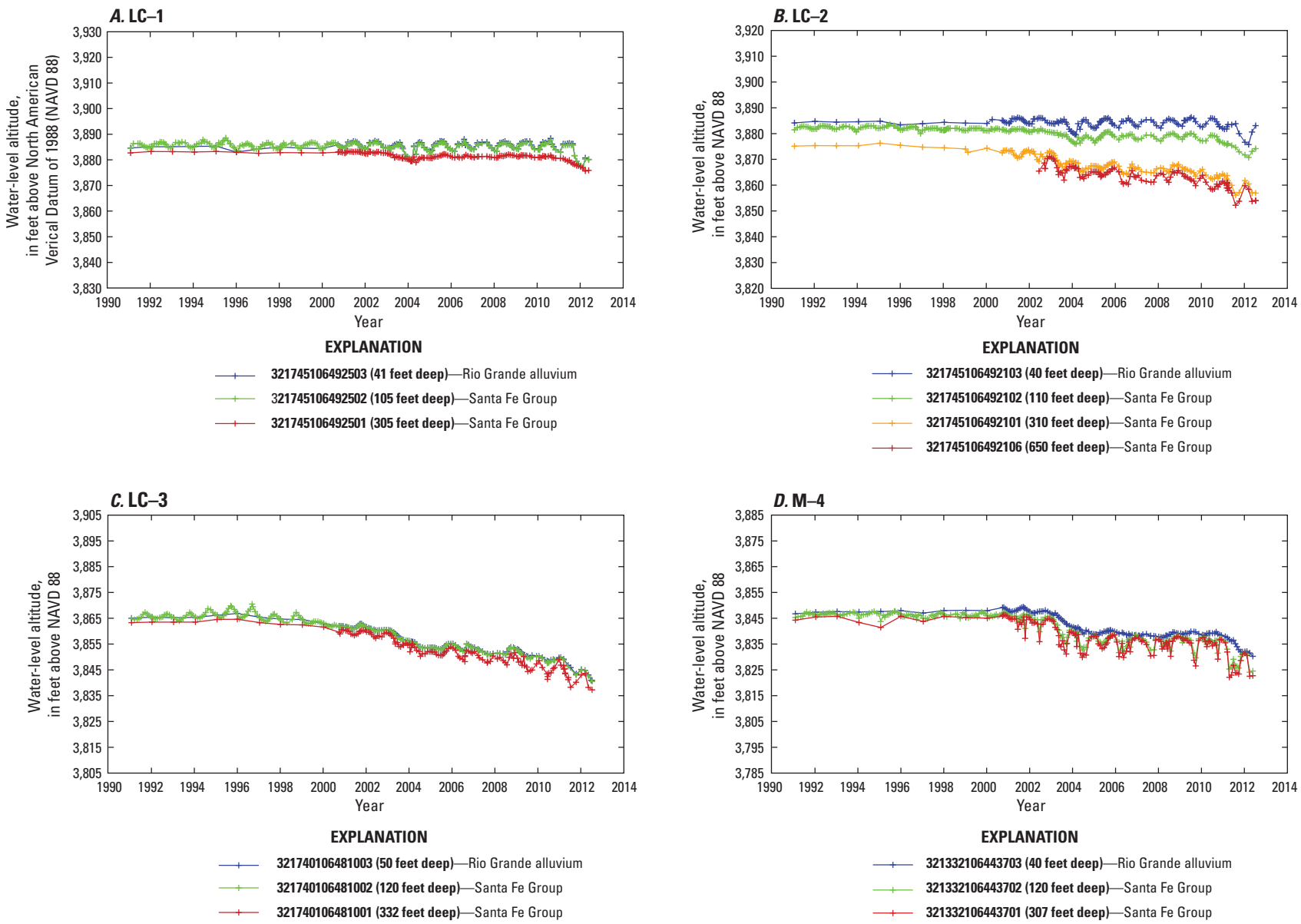

Figure 50. Water-level altitudes depicting the vertical hydraulic gradient at wells in proximity of each other in the Mesilla Basin study area in Doña Ana County, New Mexico, and El Paso County, Texas. *A*, LC–1. *B*, LC–2. *C*, LC–3. *D*, M–4. *E*, M–3. *F*, M–2. *G*, M–1. *H*, NM344. *I*, LMV–2. *J*, ISC–1. *K*, ISC–2. *L*, CWF–4. *M*, LMV–1. *N*, ISC–3. *O*, ISC–7. *P*, ISC–6. *Q*, ISC–5. *R*, ISC–4.

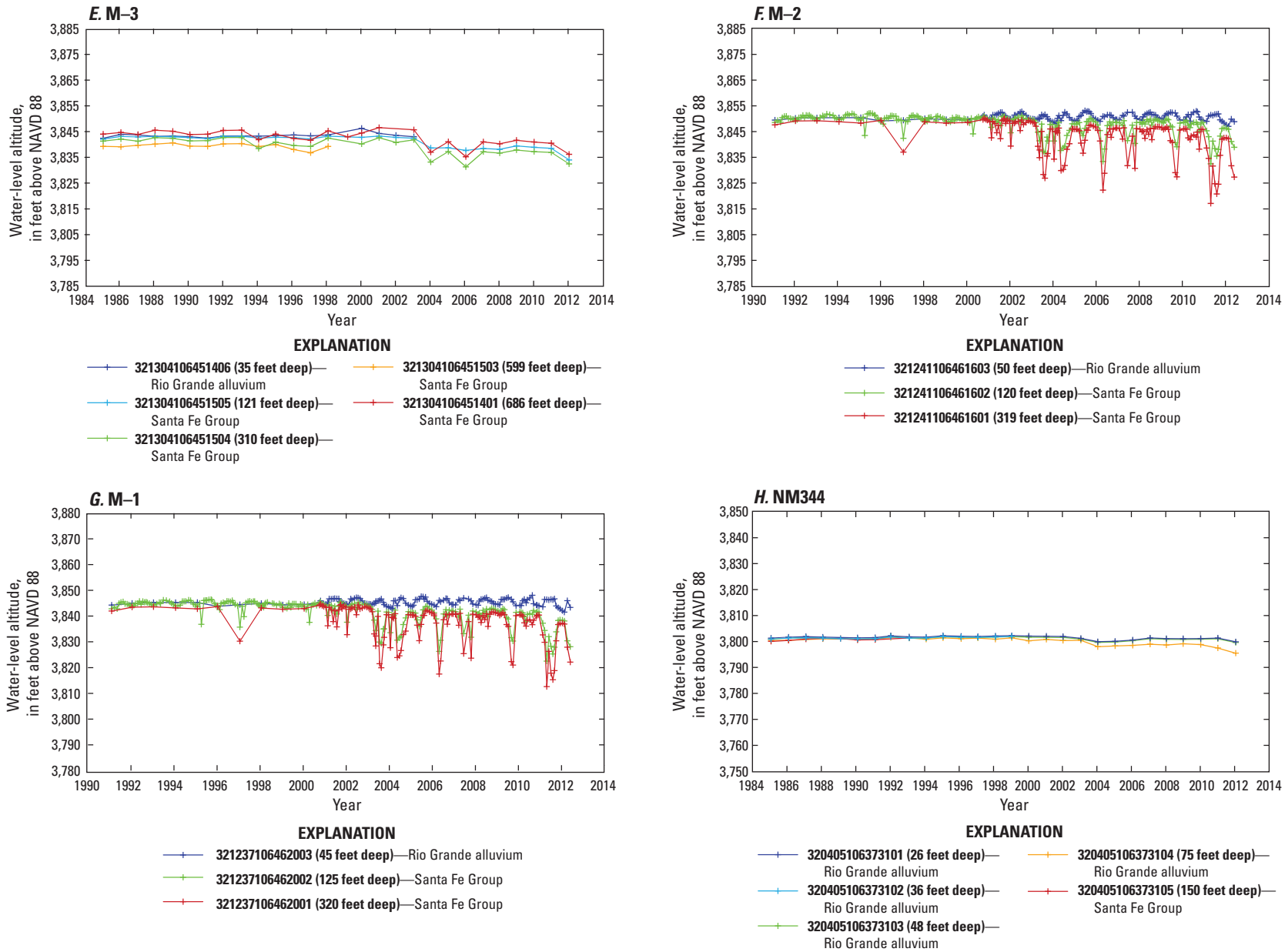

Figure 50. Water-level altitudes depicting the vertical hydraulic gradient at wells in proximity of each other in the Mesilla Basin study area in Doña Ana County, New Mexico, and El Paso County, Texas. *A*, LC–1. *B*, LC–2. *C*, LC–3. *D*, M–4. *E*, M–3. *F*, M–2. *G*, M–1. *H*, NM344. *I*, LMV–2. *J*, ISC–1. *K*, ISC–2. *L*, CWF–4. *M*, LMV–1. *N*, ISC–3. *O*, ISC–7. *P*, ISC–6. *Q*, ISC–5. *R*, ISC–4.—Continued

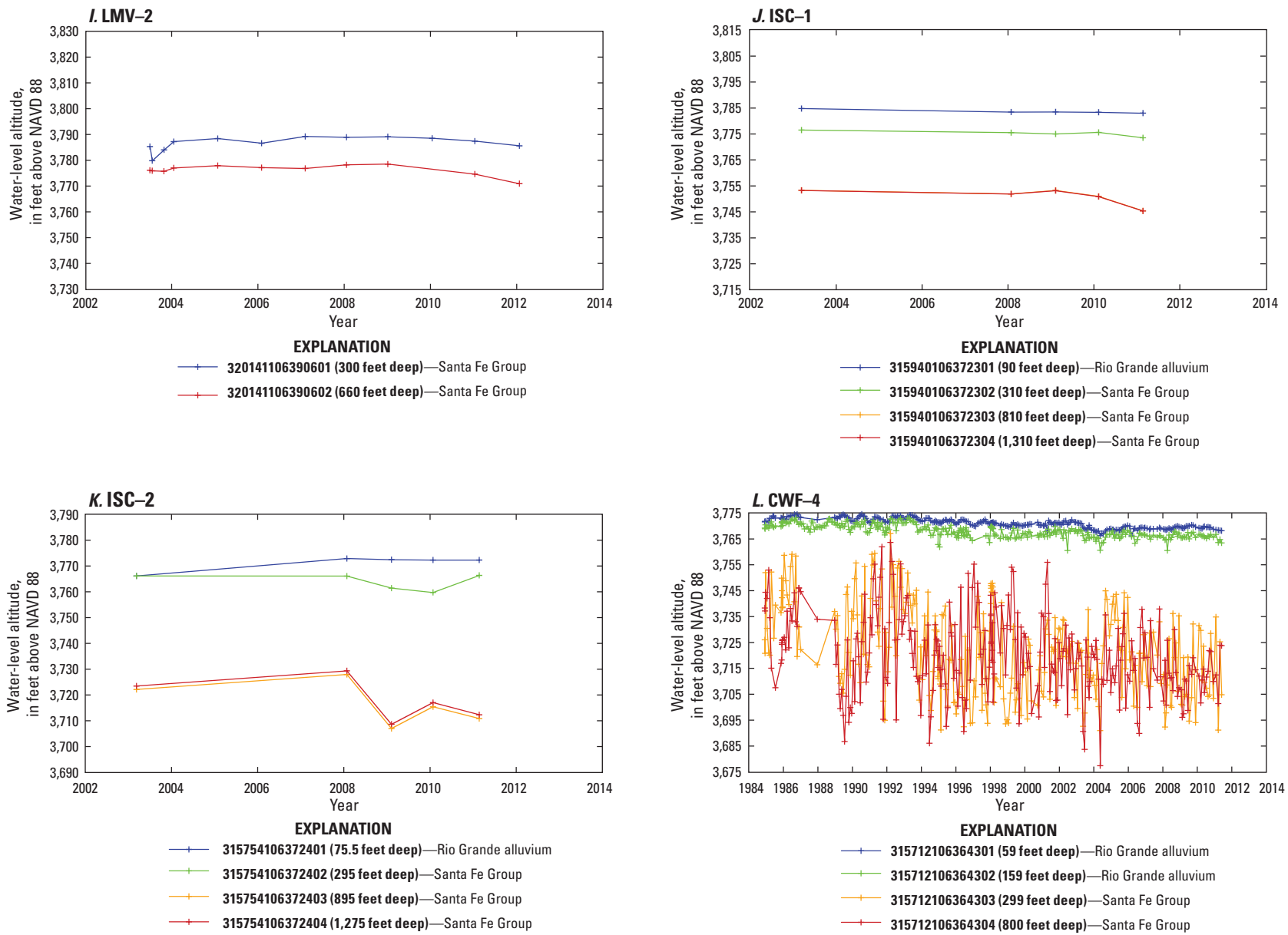

Figure 50. Water-level altitudes depicting the vertical hydraulic gradient at wells in proximity of each other in the Mesilla Basin study area in Doña Ana County, New Mexico, and El Paso County, Texas. *A*, LC–1. *B*, LC–2. *C*, LC–3. *D*, M–4. *E*, M–3. *F*, M–2. *G*, M–1. *H*, NM344. *I*, LMV–2. *J*, ISC–1. *K*, ISC–2. *L*, CWF–4. *M*, LMV–1. *N*, ISC–3. *O*, ISC–7. *P*, ISC–6. *Q*, ISC–5. *R*, ISC–4.—Continued

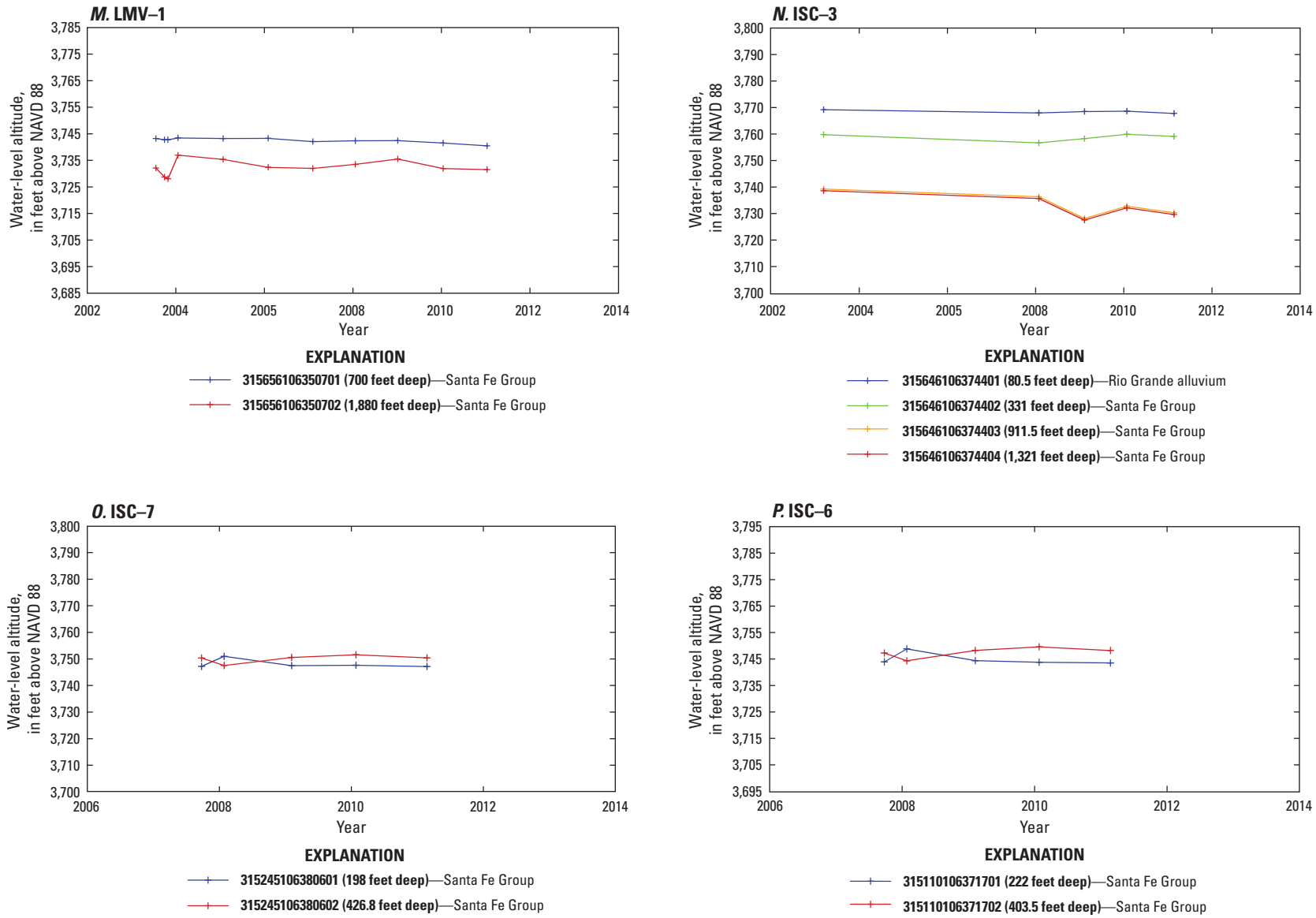

Figure 50. Water-level altitudes depicting the vertical hydraulic gradient at wells in proximity of each other in the Mesilla Basin study area in Doña Ana County, New Mexico, and El Paso County, Texas. *A*, LC–1. *B*, LC–2. *C*, LC–3. *D*, M–4. *E*, M–3. *F*, M–2. *G*, M–1. *H*, NM344. *I*, LMV–2. *J*, ISC–1. *K*, ISC–2. *L*, CWF–4. *M*, LMV–1. *N*, ISC–3. *O*, ISC–7. *P*, ISC–6. *Q*, ISC–5. *R*, ISC–4.—Continued

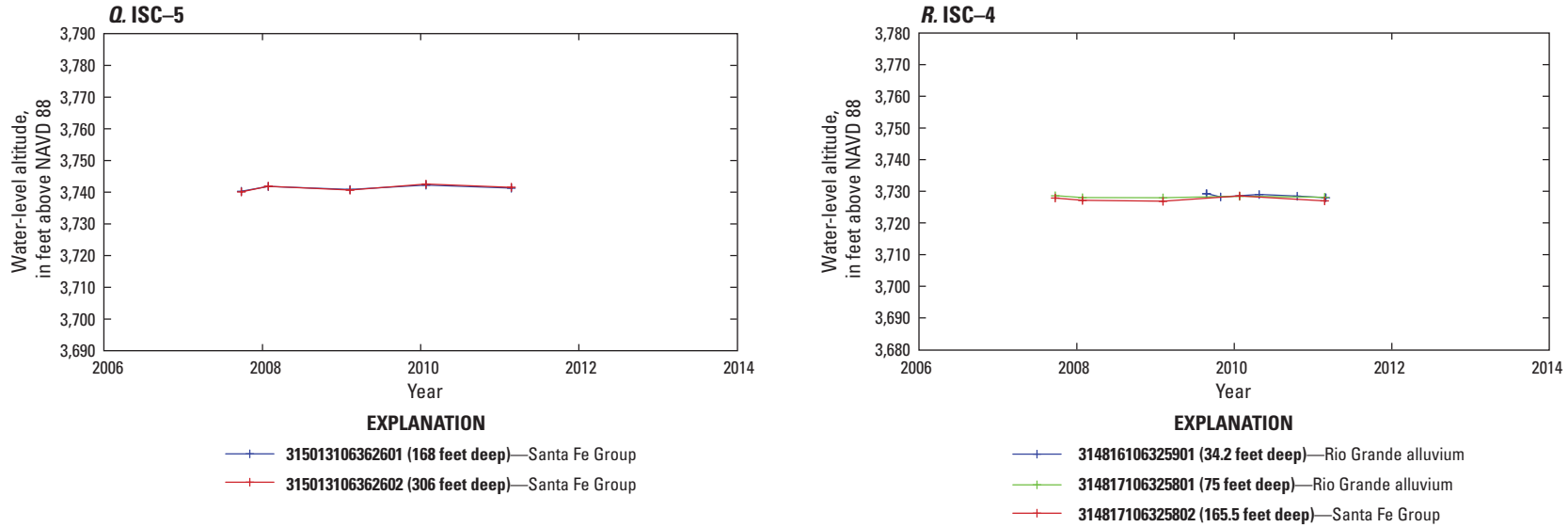

Figure 50. Water-level altitudes depicting the vertical hydraulic gradient at wells in proximity of each other in the Mesilla Basin study area in Doña Ana County, New Mexico, and El Paso County, Texas. *A*, LC–1. *B*, LC–2. *C*, LC–3. *D*, M–4. *E*, M–3. *F*, M–2. *G*, M–1. *H*, NM344. *I*, LMV–2. *J*, ISC–1. *K*, ISC–2. *L*, CWF–4. *M*, LMV–1. *N*, ISC–3. *O*, ISC–7. *P*, ISC–6. *Q*, ISC–5. *R*, ISC–4.—Continued

The ancestral Rio Grande groundwater was water that recharged into the groundwater system as seepage losses from the ancestral Rio Grande. The mean apparent age of this groundwater was estimated as 24,000 ^{14}C years BP, and it flows generally from north to south-southeast towards the Paso del Norte (table 14, at back of report; fig. 45). The midbasin uplift (fig. 8), located in the middle of the study area, did not act as a complete barrier to groundwater flow but did restrict the flow, causing the groundwater to flow preferentially along on either side of the uplift with some groundwater flowing over the uplift (fig. 47). Groundwater on the west side of the midbasin uplift generally flows south until it reaches the southern part of the study area, and then flows east towards the Paso del Norte. Groundwater on the east side of the uplift continued to flow south-southeast towards the Paso del Norte, where it mixes with groundwater from the modern Rio Grande, the uplifted areas in the west, and the deep saline source. The constituent concentrations measured in the groundwater samples collected from wells Q19, Q24, and Q25 indicate mixing between the ancestral and modern Rio Grande waters; most of the constituent concentrations measured in the well Q19, Q24, and Q25 samples were within the range of constituent concentrations measured in samples representing these two sources of water (tables 10, 11, and 13, at back of report; fig. 45). The relation of Cl/Br to δD (fig. 41) also indicated that the samples from well Q19 plotted outside of the general groundwater group (group 1), which is consistent with the interpretation of some mixing or evaporation of water. Recalling the grouping of wells into different geochemical groups on the basis of water quality as described in the "Hydrogen-2/Hydrogen-1 (Deuterium) and Oxygen-18/Oxygen-16" section of this report, constituent concentrations measured in the sample collected from well Q24 plotted within the blended groundwater group (group 4), the same group in which the modern Rio Grande groundwater samples plotted. The groundwater samples collected from wells Q36, Q39, and Q42 indicated more complex mixing, as four geochemical groups (ancestral and modern Rio Grande, mountain front, and deep groundwater upwelling) converge in the southeastern part of the study area where these wells are located. The samples collected from these wells had chemical characteristics similar to the chemical characteristics measured from all of these geochemical groups.

Various sources of inflows to the Rio Grande in the study area (such as inflows from drainages and deep saline groundwater inflows) cause the water chemistry of the river to change appreciably from where it enters to where it exits the study area (Moyer and others, 2013). These changes in water chemistry are evident in water-quality data for the near-surface groundwater-quality samples obtained from the Rio Grande alluvium. The water-quality data for samples collected from the Rio Grande alluvium characterize the modern Rio Grande geochemical group (table 14, at back of report; fig. 45). From the age-dating results, water in the modern Rio Grande geochemical group was recharged to the Rio Grande alluvium within the last 10 years. The variable nature of water chemistry in the modern Rio Grande geochemical group is evident in the relation of Cl/Br to δD (fig. 41)—all of the samples within the geochemical group plotted within the blended groundwater group (group 4) and have different isotopic signatures representing each of the three endmembers depicted (general groundwater, evaporative groundwater, and geothermal groundwater). The water type of the modern Rio Grande geochemical group ranged from a Ca-SO_4 water type in the northern part of the study area (as observed in the sample collected from well Q03) to a Na-Cl-SO_4 water type in the southern part of the study area (as observed in the sample collected from well Q37) (table 11, at back of report; fig. 45). There was also a substantial increase in SpC values from north to south in the study area, from 1,540 µS/cm at 25 °C in the groundwater sample collected from well Q03 to 3,360 µS/cm at 25 °C in the groundwater sample collected from well Q37, which was likely a result of the increase in concentration in five dissolved solids (Cl, SO_4, F, Br, and Na) from north to south (tables 10 and 11, at back of report; fig. 45). The constituent concentrations in the samples collected from wells Q03 and Q37 were compared further. The Ca concentration in the well Q37 sample was slightly lower than the Ca concentration measured in the well Q03 sample, whereas Na and Cl concentrations were appreciably higher in the well Q37 sample compared to the concentrations of Na and Cl measured in the Q03 sample. The differences in Ca, Na, and Cl concentrations correspond to changes in Rio Grande water chemistry. The change in the groundwater chemistry of the modern Rio Grande geochemical group samples is first evident in the groundwater samples collected from wells Q09, Q13, and Q18, where the concentrations of Cl, SO_4, F, Br, and Na increase between wells Q09 and Q13 and then again between wells Q13 and Q18 (table 11, at back of report; fig. 45). Another observation from the groundwater samples collected from these wells was that after gradually decreasing from north to south $^{87}Sr/^{86}Sr$ ratios increased between wells Q09 and Q18 (table 13, at back of report; fig. 45). This increase was likely related to the increase in K between these two wells (table 11, at back of report; fig. 45) because minerals with high K content can be enriched with ^{87}Rb. The mineral exchange of K together with ^{87}Rb enrichment results in more K in the groundwater and more ^{87}Rb in the rocks, which eventually leads to higher $^{87}Sr/^{86}Sr$ ratios after beta decay. Increases in selected trace metal concentrations were also measured (Fe and Li) (table 11, at back of report; fig. 45). When the water-quality results obtained from the wells are considered in upgradient to downgradient order, the chemical characteristics of the groundwater samples in the modern Rio Grande geochemical group become similar to those of the deep groundwater upwelling geochemical group (table 14, at back of report). The sample from well Q18 (which contained elevated concentrations for many constituents) plots near the thermal boundary line in a graph depicting the relation of Cl/Br to δD (fig. 41), likely because some geothermal groundwater mixes with the groundwater near well Q18. From the HFEM resistivity data obtained at a depth of 50 ft,

a change from high resistivity to low resistivity was evident near Vado, N. Mex., in an area hydrologically upgradient from wells Q13 and Q18 (fig. 49). The change in chemical characteristics causing the modern Rio Grande geochemical group to become similar to the deep groundwater upwelling group might be caused by deep, highly saline groundwater with dissolved siliciclastic materials coming to or near the surface at or near this resistivity change. Such inflows have been interpreted to exist from evidence provided by Hogan and others (2007).

The mountain-front geochemical group was generally old water (apparent age was greater than 10,000 ^{14}C years BP) that was somewhat mineralized, with most of the dissolved major-ion concentrations measured in the samples in this geochemical group among the three highest concentrations measured in all of the five groups of samples collected in the study area. The mountain-front geochemical group had relatively high mean concentrations of F and Si as compared to the other geochemical groups (table 14, at back of report), which might indicate a longer period of exposure to volcanic and siliciclastic rocks or aluminosilicate minerals. There were five different locations of recharge determined from the groundwater geochemistry within the mountain-front geochemical group, all having a slightly different geochemical signature: (1) the Rough and Ready Hills, the Robledo Mountains, and the Sleeping Lady Hills, (2) the Doña Ana Mountains, (3) the Aden Hills and the West Potrillo Mountains, (4) the East Potrillo Mountains, and (5) the Sierra Juárez in Mexico (fig. 45). None of the groundwater samples had a direct geochemical signature of eastern mountain-front water (the Organ and Franklin Mountains), but it was assumed that there was some mixing of water originating from these mountain fronts with one of the other geochemical groups in the study area. Groundwater collected from well Q14 had isotopic signatures that were similar to those of groundwater samples collected from the Organ and Franklin Mountains as documented by Eastoe and others (2007), but overall the groundwater from this well had a signature more similar to the deep groundwater upwelling geochemical group, indicating that there may have been some mixing between the mountain-front geochemical group and the deep groundwater upwelling geochemical group (tables 13 and 14, at back of report; fig. 45).

Among the samples in the mountain-front geochemical group, the groundwater from the Rough and Ready Hills, the Robledo Mountains, and the Sleeping Lady Hills (well Q01) had the highest SpC value and generally had higher mineral concentrations (highest SO_4, Na, and K) (tables 10 and 11, at back of report; fig. 45). Compared to other samples from wells in the mountain-front geochemical group (wells Q02, Q04, Q12, Q16, Q30, Q38, Q43), the sample from (well Q01) also had higher concentrations of Br, Si, Al, Fe, Mn, Li, and Sr, which might indicate that the water had prolonged exposure to the siliciclastic rocks found in the uplift areas. Within the mountain-front geochemical group, the groundwater from the Doña Ana Mountains (wells Q02 and Q04) was the youngest (less than 10,000 ^{14}C years BP) and had the highest concentrations of Ca, Mg, and Sr and some of the higher concentrations of Cl, Li, and U (tables 11 and 13, at back of report; fig. 45). Some of the lowest concentrations of F, Si, and As also were measured in groundwater from the Doña Ana Mountains (wells Q02 and Q04) (tables 10 and 11, at back of report; fig. 45). These results correspond with the composition of the Doña Ana Mountains, which are composed mostly of volcanic rocks (monzonite and andesite) and clastic sediments (Frenzel and Kaehler, 1992). It was determined that the groundwater near the Rough and Ready Hills, the Robledo Mountains, and the Sleeping Lady Hills and near the Doña Ana Mountains generally flows toward the Rio Grande (fig. 47). The groundwater from these mountains eventually mixes together and with modern Rio Grande groundwater as illustrated by the results from the groundwater sample collected from well Q00. With a few exceptions, most constituent concentrations measured in the sample collected from well Q00 were similar to the constituent concentrations measured in groundwater samples collected from well Q01 and wells Q02 and Q04 (tables 10, 11, and 13, at back of report; fig. 45). Compared to the concentrations measured in samples from wells Q01, Q02, and Q04, higher concentrations of Cl, Mn, and Li and a lower concentration of U were measured in the sample from well Q00, differences which can all be attributed to some mixing with the groundwater recharged from the modern Rio Grande.

Compared to all of the other samples in the mountain-front geochemistry group, the groundwater near the Aden Hills (well Q12) and the West Potrillo Mountains (well Q16) had the lowest concentrations of Ca and Si and had low concentrations of Cl, Mg, K, Al, Ba, and Li (table 11, at back of report; fig. 45). This groundwater also had relatively higher concentrations of SO_4, F, and Br. Although the groundwater at these two wells (wells Q12 and Q16) was fairly similar, there were some differences. The sample from the West Potrillo Mountains (well Q16) had substantially higher concentrations of Na, Fe, and Mn, whereas the sample from the Aden Hills (well Q12) had substantially higher concentrations of Mg, SO_4, and Sr. The elevated concentrations of Fe in the sample from well Q16, the elevated concentrations of Mg in the sample from well Q12, and the low concentrations of Si in the samples from both of these wells indicated that the groundwater near the Aden Hills and Potrillo Mountains had a geochemical signature similar to that of alkali olivine basalt (Haldar and Tišljar, 2013). This alkali olivine basalt originated as lava flows from basaltic fissures southeast of Aden Hills and in the West Potrillo Mountains; these lava flows were relatively high in Na, Mg, K, and Fe and relatively low in Si (Hoffer, 1976). Because it has relatively high concentrations of Na and K, this basalt is characterized as having an alkali signature (Haldar and Tišljar, 2013). Groundwater samples from the West Potrillo Mountains tended to have slightly higher trace-element concentrations compared to groundwater samples from the Aden Hills, likely because there are more siliciclastic rocks present in the West Potrillo Mountains than

there are in the Aden Hills. The highest concentrations of Si and As measured in samples from wells in the mountain-front geochemical group (along with relatively high concentrations of HCO_3, Ca, K, Al, and Ba) were measured in the groundwater sample from the East Potrillo Mountains (well Q30), which also had relatively low concentrations of Cl, SO_4, Na, Fe, Mn, Sr, Li, U, and Br (table 11, at back of report). This slightly mineralized groundwater with relatively high concentrations of HCO_3 and Ca was indicative of water flowing through the limestone and dolomite rocks found in the East Potrillo Mountains. The groundwater originating from the Aden Hills and the East and West Potrillo Mountains generally flows southeast and then east (indicated by the potentiometric surface developed from water-level altitudes measured in wells completed in the Santa Fe Group) (fig. 47), at a slow rate (indicated by the apparent age (22,000 ^{14}C years BP measured in the sample collected from well Q30) (table 13, at back of report). Groundwater originating from these uplifted areas eventually mixes and continues east, where it mixes with the ancestral Rio Grande groundwater and with the groundwater from the Sierra Juárez. The relation of Cl/Br to δD (fig. 41) indicated there was some mixing of groundwater originating from mountains and uplifted areas with the ancestral Rio Grande; the general groundwater group (group 1) contained results from wells representing the mountain front and ancestral Rio Grande geochemical groups (table 14, at back of report; fig. 45). The geochemistry results for the sample collected from well Q38 were consistent with this mixing of groundwater originating from the Aden Hills and the East and West Potrillo Mountains with the ancient Rio Grande groundwater—most of the constituent concentrations measured in the sample collected from well Q38 were similar to the range of concentrations measured in the samples collected from wells Q12 (Aden Hills), Q16 (West Potrillo Mountains), and Q30 (East Potrillo Mountains) (tables 10, 11, and 13, at back of report; fig. 45). The groundwater sample collected from well Q38 did have higher concentrations of Cl, Fe, Mn, Al, Li, and U compared to other groundwater samples collected in the uplifted areas in the west (wells Q12, Q16, and Q30) (tables 10, 11, and 13, at back of report; fig. 45), a difference that might result from a longer exposure of the groundwater to volcaniclastic and siliciclastic bedrock as the groundwater flows east (Witcher and others, 2004).

Groundwater that originated from the Sierra Juárez might affect the groundwater quality near well Q43. Of the 44 samples collected in the study area in 2010, (tables 10 and 11, at back of report) the sample collected from well Q43 had a relatively low SpC value (501 µS/cm at 25 °C), and relatively low or non-detected concentrations of SO_4, HCO_3, Na, Mg, K, Fe, Li, Mn, Sr, and U (tables 10 and 11, at back of report; fig. 45). The sample from well Q43 also had relatively high concentrations of As and Ba. The slightly mineralized groundwater characterized by the sample from well Q43 was indicative of water flowing through limestone and dolomite rocks, which are found in the Sierra Juárez (Plummer and others, 2004; Witcher and others, 2004). There was some dissolution of volcanic rocks as indicated by the relatively high concentration of As. This groundwater likely flows north from the Sierra Juárez and then east towards the Paso del Norte, where it mixes with groundwater from the mountains and uplifted areas in the west, ancestral and modern Rio Grande groundwater, and deep saline source groundwater (fig. 47). Evidence of this mixing was provided by groundwater samples from wells Q36, Q39, and Q42, which were not consistent with any of the five distinct geochemical groups, indicating a mixture of water representing two or more geochemical groups. Wells Q36, Q39, and Q42 are downgradient from well Q43 and represent locations where water from the mountain-front, ancestral and modern Rio Grande, and deep groundwater upwelling geochemical groups mixes (figs. 45 and 47).

The groundwater samples in the deep groundwater upwelling geochemical group had some of the highest mineralized content of any samples collected in the study area (table 14, at back of report). This groundwater likely slowly originates from a deep source. The relation of Cl/Br to δD indicated that some of the samples in the deep groundwater upwelling geochemical group also were within the geothermal groundwater group, (group 3; fig. 41), further indicating that the water likely had been mixing with geothermal groundwater or was predominantly geothermal groundwater. This deep groundwater upwelling geochemical group had the highest concentrations of HCO_3, K, Si, Al, Fe, and Li within the study area, indicating that the groundwater had been in contact with carbonate and siliciclastic rocks for a much longer period of time and at higher temperatures than the groundwater represented by the other samples in the other geochemical groups (table 14, at back of report). The collective traits of the deep groundwater upwelling geochemical group indicated that this water was most likely ancient marine groundwater originating from Paleozoic and Cretaceous carbonate rocks; the water had most likely upwelled into the U.S. part of the Mesilla Basin aquifer system in the southeastern part of the study area through the extensive fault systems. This interpretation is consistent with previous interpretations of extensive saline groundwater resources in the study area (Hawley and Kennedy, 2004) and of saline groundwater inflows to the Rio Grande (Hogan and others, 2007). The DC resistivity and TDEM soundings also supported this interpretation by indicating low resistive zones, interpreted to represent highly saline water (SpC value greater than 10,000 µS/cm at 25 °C) upwelling from below the bedrock to the surface (figs. 14 and 15) in areas of potential upward vertical hydraulic gradients, known fault systems, or both (figs. 49, 50*P*, and 50*Q*).

The analytical results from the well Q14 sample indicated an elevated mineralized signature with relatively high concentrations of HCO_3, Si, Al, Fe, and Li (tables 11 and 13, at back of report). The sample collected from well Q14 had a Cl/Br ratio of 1,440 (table 11, at back of report), which plots it in the geothermal groundwater section of the mixing plot of Cl/Br ratios and δD values (fig. 41). The HFEM data

collected along the Rio Grande (fig. 49) to the west of the well indicated that there was a change in resistivity from high to low northwest of well Q14, indicating a potential inflow of deep groundwater near that location.

The source of water for samples in the unknown freshwater geochemical group could not be determined. The δD and $\delta^{18}O$ isotopic results for samples in the unknown freshwater geochemical group (samples collected from wells Q05, Q06, Q07, Q08, and Q11) did not plot on the Rio Grande evaporation line, indicating that this group did not have a Rio Grande isotopic signature (that is, there was no isotopic evidence of a component of Rio Grande water) (table 13, at back of report; fig. 39). All of the groundwater samples in this geochemical group were part of the general groundwater group (group 1) based on their Cl/Br ratios and δD values, indicating there was no evidence of geothermal mixing or evaporative processes (fig. 41). Although the source of water for this geochemical group was unknown, most of these samples were collected from wells near the boundary between the Jornada Basin and the Mesilla Basin (fig. 45), indicating that the source of the groundwater could be interbasin flow from the Jornada Basin as discussed in the "Geologic Setting" section of this report. From the potentiometric surface map (fig. 47), it is evident that groundwater characterized as unknown freshwater flows south until it mixes with groundwater from the Rio Grande geochemical group and deep saline groundwater geochemical group.

Summary

The 2006 United States-Mexico Transboundary Aquifer Assessment Act authorized the Secretary of the Interior to cooperate with the States on the international border with Mexico and other appropriate entities in conducting a hydrogeologic characterization, mapping, and modeling program for priority transboundary aquifers, and for other purposes. The transboundary Mesilla Basin/Conejos-Médanos aquifer system, which is bisected by the Rio Grande/Río Bravo (hereinafter referred to as the "Rio Grande"), was one of the priority transboundary aquifer systems identified for additional study. In cooperation with the Bureau of Reclamation, the U.S. Geological Survey assessed the U.S. part of the Mesilla Basin/Conejos-Médanos aquifer system (hereinafter referred to as the "Mesilla Basin aquifer system") by using a combination of previously published and newly collected geophysical and groundwater geochemical data.

The geophysical resistivity data assessed for this report included (1) helicopter frequency domain electromagnetic (HFEM), (2) direct-current (DC) resistivity, and (3) time-domain electromagnetic (TDEM). All of the HFEM data and DC resistivity soundings were compiled from previously published surveys, whereas TDEM soundings were collected by the USGS in October 2012. In November 2010, the USGS collected groundwater samples from 44 wells and analyzed them for major ions, trace elements, nutrients, and pesticides (reported by not used in the assessment), along with environmental tracers, to better understand the geochemical processes controlling the groundwater movement through the Mesilla Basin aquifer system.

The study area consists mostly of the Mesilla Basin, which is underlain by the Mesilla Basin aquifer system. Orographic features (uplift areas, hills, and mountains) surround and form part of the study area, including the East and West Potrillo Mountains, Aden Hills, Sleeping Lady Hills, Rough and Ready Hills, and the Robledo, Doña Ana, Organ, and Franklin Mountains. A small part of the Jornada del Muerto Basin (hereinafter referred to as the "Jornada Basin") forms the northeast part of the study area. The alluvial aquifer system underlying the Jornada Basin is referred to as the "Jornada Basin aquifer system" in this report. The study area covers about 1,400 square miles (mi^2) in Doña Ana County, New Mexico, and about 100 mi^2 in El Paso County, Texas, all in the Mexican Highlands section of the Basin and Range physiographic province. The Mesilla Basin can be divided into three parts in the study area: the Mesilla Valley, the West Mesa, and the East Bench. The Mesilla Valley is the part of the Mesilla Basin that was incised by the Rio Grande between Selden Canyon to the north and by a narrow valley (about 4 miles [mi] wide) to the southeast near El Paso, Tex., named the Paso del Norte. Most of the study area is in the Rio Grande rift, which is characterized by north-south trending basins between mountain ranges originating from tilted fault-blocks and uplifted areas resulting from volcanic activity, including uplifted areas formed by relatively young (Quaternary) volcanism.

Groundwater flow in the Mesilla Basin aquifer system generally is from the north to the south-southeast with the majority of the groundwater discharging at the Paso del Norte. Hydrogeologic boundaries for deep groundwater flow in the Mesilla Basin consist of the East Robledo and East Potrillo Fault zones to the west and the Mesilla Valley Fault zone to the east. The uppermost water-bearing formation of the Mesilla Basin aquifer system is the Rio Grande alluvium, which consists of a thin layer (generally about 80 feet [ft] thick) of upper Quaternary fluvial deposits in the Mesilla Valley. Underlying the Rio Grande alluvium is the Santa Fe Group, which predates river valley alluvium and consists of sedimentary basin fill. In numerous publications, the Santa Fe Group has informally been considered as consisting of three hydrogeologic units (HGUs), all of which are water bearing: the upper part of the Santa Fe Group (hereinafter referred to as the "upper Santa Fe"), the middle part of the Santa Fe Group (hereinafter referred to as the "middle Santa Fe"), and the lower part of the Santa Fe Group (hereinafter referred to as the "lower Santa Fe"). The upper Santa Fe is the most productive HGU within the Santa Fe Group and is composed of mostly unconsolidated sand and gravel basin fill deposited by the ancestral Rio Grande; however, it is only partially saturated in the northern and eastern parts and is largely unsaturated in the southern and western parts of the Mesilla Basin. The middle

Santa Fe is generally saturated and includes fine-grained unconsolidated basin fill with interbedded sand layers. The saturated thickness within the middle Santa Fe can be as much as 2,000 ft; the middle Santa Fe is the primary aquifer within the Mesilla Basin. The lower Santa Fe is the least productive zone, with the majority of the unit composed of fine-grained and partly consolidated basin fill. Similar to the Mesilla Basin aquifer system, the Jornada Basin aquifer system also is primarily composed of the Santa Fe Group.

Airborne (HFEM), DC, and TDEM geophysical resistivity methods were used to evaluate the hydrogeology along the Rio Grande and within the southeastern part of the study area. For this study, the 121 mi of previously published HFEM data were converted from apparent conductivity values to apparent resistivity values and gridded in three dimensions (3-D) by using a kriging method with a horizontal grid spacing of 330 by 330 ft (100 by 100 meters [m]) and a vertical spacing of 10 ft.

Previously published results from 65 DC resistivity soundings collected within the study area were used to analyze hydrogeology within the lower Mesilla Valley. Reprocessed DC resistivity soundings (were used to identify areas of low bulk resistivity (less than 10 ohm-meters [ohm-m]) that could be associated with sediments having either a large amount of clayey deposits or high concentration of dissolved solids in the pore water. The 65 compiled DC resistivity soundings and the 12 TDEM soundings collected by the USGS in October 2012 were gridded in 3-D by using a kriging method with the same horizontal and vertical grid spacing used to grid the HFEM data in 3-D.

Near the land surface (that is, at or about 0 ft below land surface [bls]), the HFEM profiles indicated that the resistivity was generally greater than 20 ohm-m along the reach of the Rio Grande corresponding to the location of the levees that were the target of the HFEM investigation. With increasing depth, resistivity values less than 10 ohm-m were increasingly measured; about half of the resistivity values were less than 10 ohm-m at depths of 50 and 100 ft. Near Vado, N. Mex., there were transitions at 50 and 100 ft bls where the resistivity values changed from relatively high resistivity values (greater than 20 ohm-m) to relatively low resistivity values (less than 10 ohm-m).

Slightly more than 25 percent of the gridded resistivity values from the 3-D grid of the combined inverse modeling results of the DC resistivity and TDEM soundings were low, less than or equal to 10 ohm-m. Depth-dependent regions of low resistivity are apparent in the southernmost part of the study area near the Paso del Norte. These regions of low resistivity are spatially the widest at or below the top of the bedrock. Although low resistivity can be indicative of clayey deposits, from the 3-D depictions of the resistivity data, it appears there are sand and gravel deposits saturated with saline water. There is likely a plume of groundwater emanating as dense, highly saline water upwelling through fractures within the bedrock. It is unlikely that clayey deposits would be embedded in the shape and orientation of the region of low resistivity observed from the 3-D depictions of the alluvial-fluvial environment in which the Santa Fe Group was formed. The change in gridded resistivity values with depth indicates that the low resistivity zones penetrated the land surface to the east of the Rio Grande near the base of the Franklin Mountains and continued to the south to the Paso del Norte. The length of the low resistivity zone expanded northward with depth.

Historical dissolved-solids-concentration data within the surface geophysical subset area of the study area were compiled and compared to the inverse modeling results of the combined DC resistivity and TDEM soundings; this comparison was done to strengthen the interpretation made from the combined inverse modeling results that the low resistivity features were representative of sand and gravel deposits saturated with saline water and not clayey deposits. Conductivity (the inverse of resistivity) has a strong correlation to salinity in that a greater salt concentration causes greater conductivity; therefore, when salinity decreases, the resistivity increases. With a correlation between salinity and dissolved solids, a decrease in dissolved solids would indicate greater resistivity values. In general, the resistivity in freshwater streams ranges from 5 to 100 ohm-m depending on the degree to which the freshwater is influenced by saltwater—100-ohm-m resistivity values indicate little saltwater influence, and 5-ohm-m resistivity values indicate appreciable saltwater influence. Where the inflows of saltwater are extreme, freshwater resistivity values of less than 5 ohm-m are possible. The exact conductivity values are not universally consistent but are related to the ionic composition of the water, the formation resistivity, and the temperature of the medium.

The dissolved-solids concentrations in the northern part of the surface geophysical subset area were generally less than 1,000 milligrams per liter (mg/L), representing freshwater, especially with increasing depth. In the southern part of the surface geophysical subset area, where low resistivity was often measured in the subsurface, dissolved-solids concentrations of more than 1,000 mg/L were common, especially with increasing depth. Some dissolved-solids concentrations were greater than 3,000 mg/L in the southern part of the surface geophysical subset area, representing moderately to very saline water. The comparison between the dissolved-solids concentrations and the resistivity data indicated a good correlation between low resistivity values and high dissolved-solids concentrations, which helped to strengthen the interpretation that the low resistivity values in the surface geophysical subset area were most likely caused by more saline water than by a greater amount of clayey deposits in the sediments.

The relations between and spatial patterns of groundwater chemical data and isotopic data are useful for determining recharge sources, direction of flow, and geochemical processes. Groundwater samples were collected in November 2010 from 44 wells completed in either the Rio Grande alluvium or in the upper, middle, or lower part of the Santa Fe Group. Physicochemical properties (pH, specific conductance [SpC], dissolved oxygen [DO], water temperature, turbidity,

and alkalinity) were measured in the field at the time of sample collection. Samples also were collected and shipped for laboratory analysis of major ions, nutrients, trace elements, pesticides, tritium (^3H), chlorofluorocarbons, carbon-14, and selected stable isotopes (hydrogen-2/hydrogen-1 [δD], oxygen-18/oxygen-16 [$\delta^{18}O$], strontium-87/strontium-86 [$^{87}Sr/^{86}Sr$], and carbon-13/carbon-12 [$\delta^{13}C$]).

The pH ranged from 6.8 to 9.1 standard units in the groundwater samples collected in November 2010. About 75 percent of the groundwater samples can be characterized as slightly alkaline because their pH values were greater than 7.5 standard units. SpC values ranged from 399 to 42,800 microsiemens per centimeter at 25 degrees Celsius (µS/cm at 25 °C). In general, SpC values were higher in the samples representing either the Rio Grande alluvium or lower Santa Fe compared to the SpC values measured in samples representing the upper Santa Fe or middle Santa Fe. The higher SpC values measured in lower Santa Fe samples were attributed to groundwater upwelling from deeper aquifers, whereas the higher SpC values measured in Rio Grande alluvium samples were from several different sources. DO concentrations ranged from 0.1 to 5.2 mg/L, and were generally less than 0.5 mg/L (the third quartile value of the entire dataset for DO) indicating that the most of the groundwater was likely under reducing conditions. Groundwater temperatures in the study area ranged from 16.6 to 34.5 °C and generally increased with sampling depth; the mean water temperature of the entire dataset was 24.1 °C.

Some of the most abundant anions in groundwater include Cl, SO_4, HCO_3, and CO_3. Less abundant anions include fluoride (F), bromide (Br), nitrate (NO_3), and nitrite (NO_2). When considered together with cation concentrations, anion concentrations are useful for interpreting the chemical quality of groundwater and for determining water types based on ionic composition. The Cl concentration was greater than 250 mg/L in 13 groundwater samples collected in or near the southern part of the Mesilla Valley near the Paso del Norte. Many of the groundwater samples collected in study area indicated an apparent excess of Na in the groundwater system relative to Cl, which could be derived from the dissolution of silicate materials such as plagioclase feldspars, cation exchange, or both. The Cl concentrations in the three samples collected from wells completed in the Rio Grande alluvium ranged from 613 to 745 mg/L. Whereas Cl concentrations were greater than 250 mg/L in three of the four groundwater samples collected from wells completed in the lower Santa Fe, the majority of Cl concentrations measured in groundwater samples collected from wells completed in the upper Santa Fe and the middle Santa Fe were less than 250 mg/L. The elevated Cl concentrations measured in groundwater samples collected from wells completed in the lower Santa Fe resulted from the dissolution of halite within the deep subsurface, whereas the elevated Cl concentrations measured in groundwater samples collected from the Rio Grande alluvium were likely from water recharging the system from the Rio Grande. The concentration of SO_4 was greater than 250 mg/L in 18 of the 44 the groundwater samples collected in the study area. With one exception, all of the SO_4 concentrations greater than 250 mg/L were measured in samples collected from wells in or near the Mesilla Valley. The chemical composition of many of the groundwater samples collected in the study area was representative of gypsum and anhydrite dissolution, but there was likely slightly more SO_4 in the groundwater system than Ca. A total of 30 of the 39 HCO_3 concentrations measured in groundwater samples collected from wells completed in the upper Santa Fe, middle Santa Fe, or lower Santa Fe were less than 358 mg/L (the third quartile value of the entire dataset for HCO_3). Most of the HCO_3 concentrations greater than 358 mg/L were measured in samples collected from the southeastern part of the study area, in or near the Mesilla Valley, or from the southwestern part of the study area, near the East and West Potrillo Mountains.

Groundwater samples with Cl/Br ratios between 467 and 997 (the second and third quartiles of the entire Cl/Br ratio dataset) were representative of groundwater mixing with dissolution of evaporite minerals contained in basin deposits or mixing with geothermal waters, whereas samples with Cl/Br ratios greater than 997 (the third quartile value of the entire Cl/Br ratio dataset) were representative of geothermal water where geochemical processes such as dissolution of evaporite minerals may have occurred. Combined nitrate plus nitrite (NO_3+NO_2) concentrations in groundwater samples collected from wells completed in the Rio Grande alluvium, upper Santa Fe, and lower Santa Fe HGUs were less than the laboratory reporting level (LRL) with the exception of one sample collected from a well completed in the upper Santa Fe. In contrast, the NO_3+NO_2 concentration exceeded the LRL in 10 of the 24 samples collected from wells completed in the middle Santa Fe. All but 3 of the 11 groundwater samples with NO_3+NO_2 concentrations above the LRL also had DO concentrations greater than 0.5 mg/L. The majority of Na concentrations measured in groundwater samples were less than 387 mg/L (the third quartile of the entire dataset for Na); concentration less than 387 mg/L were measured in most samples collected from wells completed within the Santa Fe Group (upper Santa Fe, middle Santa Fe, or lower Santa Fe). Samples with Na concentrations greater than 387 mg/L were collected from wells in the southern part of the Mesilla Valley near the Paso del Norte except for the sample collected from well Q01, which is between the Rough and Ready Hills and the Robledo Mountains. Excluding outliers, groundwater samples with the highest concentrations of Ca, Mg, and K were for the most part collected from wells completed in the Rio Grande alluvium and the concentrations of these constituents tended to decrease with depth. Groundwater samples with higher Si concentrations (greater than 41.1 mg/L, the third quartile value of the entire dataset for Si) were generally measured in groundwater samples collected in the southern part of the study area. NH_3-N concentrations were generally higher in samples collected from wells completed in the Rio Grande alluvium compared to samples collected from wells completed in one of the HGUs composing the

Santa Fe Group (upper Santa Fe, middle Santa Fe, or lower Santa Fe). Irrigation return flows might account for the high concentrations of NH_3-N found in some samples.

Water types were determined by plotting the major ions measured in the groundwater samples on a trilinear (Piper) diagram. Of the 44 groundwater samples collected, 36 (81.8 percent) represented Na-dominated water samples. The remaining eight groundwater samples (18.2 percent) were collected from wells near the Mesilla Valley Fault zone and represented Ca-Cl-SO_4 or Ca-HCO_3 water types. The majority of the groundwater samples (86.4 percent) are predominantly composed of water containing anions of strong acids (Ca-Cl-SO_4 or Na-Cl-SO_4 water types).

Trace elements collected for this study were aluminum (Al), antimony (Sb), arsenic (As), barium (Ba), beryllium (Be), boron (B), cadmium (Cd), chromium (Cr), cobalt (Co), copper (Cu), iron (Fe), lead (Pb), lithium (Li), manganese (Mn), molybdenum (Mo), nickel (Ni), selenium (Se), silver (Ag), Sr, thallium (Tl), uranium (U), vanadium (V), and zinc (Zn), but Sb, Be, B, Cd, Cr, Co, Cu, Pb, Mo, Ni, Se, Ag, Tl, V, and Zn were not used in this assessment because of either low concentrations or blank-contamination concerns. All of the Al concentrations in groundwater samples collected from wells completed in the lower Santa Fe were greater than 4.9 micrograms per liter (µg/L) (the third quartile value of the entire Al dataset). The Al concentrations greater than 4.9 µg/L were all measured in groundwater samples collected from wells in or near the southern part of the Mesilla Valley. Groundwater samples with elevated concentrations of As (greater than 16.3 µg/L, the third quartile of the entire dataset for As) were collected in the southern part of the study area and were mainly found in groundwater samples collected from the deep HGUs with one sample collected from a well completed in the upper Santa Fe, eight samples collected from wells completed in the middle Santa Fe, and two samples collected from wells completed in the lower Santa Fe. Mean Ba concentrations in groundwater samples collected from the Rio Grande alluvium, upper Santa Fe, middle Santa Fe, and lower Santa Fe were about 44.4, 55.5, 38.1, and 27.8 µg/L, respectively. Most of the groundwater samples with concentrations of Ba less than 23.7 µg/L (the first quartile value of the entire dataset for Ba) were collected from wells completed within the middle Santa Fe or lower Santa Fe.

Most Fe concentrations measured in groundwater samples were less than 109 µg/L (the third quartile value of the entire Fe dataset). Fe concentrations greater than 109 µg/L were measured in the three groundwater samples collected from wells completed in the Rio Grande alluvium. In most of the study area, Li concentrations were relatively low, generally less than 183 µg/L (the third quartile value of the entire dataset for Li). Eleven groundwater samples with Li concentrations greater than 183 µg/L were collected in the southern part of the Mesilla Valley—all three groundwater samples collected from the Rio Grande alluvium, three groundwater samples collected from wells completed in the upper Santa Fe, four groundwater samples collected from wells completed in the middle Santa Fe, and one groundwater sample collected from a well completed in the lower Santa Fe. The third quartile of all Mn concentrations was 89.9 µg/L. Mn concentrations greater than 89.9 µg/L were measured in the three groundwater samples collected from the Rio Grande Alluvium, in six groundwater samples collected from wells completed in the upper Santa Fe), and in two groundwater samples collected from wells completed in the middle Santa Fe. All of these groundwater samples with relatively high concentrations of Mn were collected in the Mesilla Valley, with the highest concentrations generally measured in samples collected in the southern part of the valley. Mean Sr concentrations (excluding outliers) measured in groundwater samples collected from the Rio Grande alluvium, upper Santa Fe, middle Santa Fe, and lower Santa Fe were about 3,650, 1,930, 579, and 495 µg/L, respectively. Sr concentrations tended to decrease with increasing sampling depth. All groundwater samples with Sr concentrations of 1,750 µg/L or higher (the third quartile value of the entire dataset for Sr) were collected in or near the Mesilla Valley. Of the 11 groundwater samples with U concentrations greater than 7.60 µg/L (the third quartile value of the entire dataset for U), three were collected from wells completed in the upper Santa Fe, seven were collected from wells completed in the middle Santa Fe, and one was collected from a well completed in the lower Santa Fe.

When the δD and $\delta^{18}O$ (δD/$\delta^{18}O$) values measured in the 44 groundwater samples collected in the study area were compared, two fairly distinct groups of isotopically heavier and lighter water signatures were evident. The δD and $\delta^{18}O$ results were used to identify isotopically heavier groundwater (values greater than -80.00 and -10.50 per mil δD and $\delta^{18}O$, respectively) and isotopically lighter groundwater (values less than -80.00 and -10.50 per mil δD and $\delta^{18}O$, respectively). Groundwater samples collected from wells completed in the Rio Grande alluvium or upper Santa Fe can be characterized as predominantly belonging to the isotopically heavier group. Groundwater samples collected from wells completed in the middle Santa Fe or lower Santa Fe can be characterized as predominately belonging to the isotopically lighter group.

Along with the two fairly distinct groups of isotopically heavier and light groundwater, there were linear patterns in the relation between δD and $\delta^{18}O$: a Rio Grande evaporation line that about 50 percent of the groundwater samples collected plotted along, and a parallel shift of the Global Meteoric Water Line (GMWL) that about 25 percent of the groundwater samples plotted along. Most of the groundwater samples that plot along the shifted GMWL likely represent water recharged during the relatively wet and cool Pleistocene climate.

The relation between Cl/Br ratios to δD values ([Cl/Br]/δD), provides insight into different geochemical characteristics (signatures) of different water types (endmembers) and mixing between endmembers. The following endmembers were identified: (1) groundwater with no geothermal or evaporative processes (low Cl/Br ratios and low δD), (2) geothermal groundwater (medium Cl/Br ratios and high δD), and (3) evaporative groundwater (water that has

had some evaporation associated with it but no geothermal processes). The samples collected within the study area were separated into four groundwater-mixing groups: (1) a general groundwater group in which there was little or no mixing of the groundwater with geothermal groundwater and little or no mixing with evaporative groundwater (group 1) generally representing groundwater collected from deep HGUs (upper Santa Fe, middle Santa Fe, lower Santa Fe), (2) an evaporative groundwater group in which there was some evaporation associated with the groundwater and no mixing of the groundwater with geothermal groundwater (group 2) generally representing groundwater collected near uplifted areas, (3) a geothermal groundwater group in which there was some mixing of the groundwater with geothermal groundwater (group 3) generally representing groundwater collected from the southeast part of the Mesilla Valley, and (4) a blended groundwater group in which the groundwater had attributes of all three endmembers (group 4) generally representing groundwater collected from near surface HGUs (Rio Grande alluvium, upper Santa Fe, and middle Santa Fe).

The $^{87}Sr/^{86}Sr$ ratios range from 0.70790 to 0.71227 in groundwater collected from within the study area. The mean $^{87}Sr/^{86}Sr$ ratios (excluding outliers) in groundwater samples collected from the Rio Grande alluvium, upper Santa Fe, middle Santa Fe, and lower Santa Fe were about 0.71019, 0.70989, 0.70955, and 0.71003, respectively. Relatively high $^{87}Sr/^{86}Sr$ ratios may be indicative of groundwater residing in or near uplift areas that were formed from Tertiary volcanics. Relatively low $^{87}Sr/^{86}Sr$ ratios may be indicative of groundwater residing in basin-fill sediments or deep groundwater that had been in contact with the bedrock for an extended period.

Among the results for samples representing the four HGUs in the study area, ^{3}H concentrations were generally the highest in groundwater samples collected from wells completed in the Rio Grande alluvium or the upper Santa Fe. The concentrations of ^{3}H were generally negative to extremely low (less than 0.6 tritium units [TU], the concentration value used to define prebomb water in the study area) in groundwater samples collected from wells completed in the middle Santa Fe and lower Santa Fe. The TU values measured in groundwater samples collected from the Rio Grande alluvium were indicative of recent postbomb recharge into the groundwater system (water recharged between 5 and 10 years prior to sampling). The TU values measured in samples collected from wells completed in the upper Santa Fe were indicative of a mixture of prebomb and postbomb water. Most TU values measured in samples collected from wells completed in the middle Santa Fe and lower Santa Fe were indicative of recharge into the system before atomic bomb testing (prebomb water).

The ^{14}C age-dating results indicate the Rio Grande alluvium contained the youngest water and that the middle Santa Fe and lower Santa Fe contained the oldest water, results consistent with apparent groundwater age increasing with increasing depth. The groundwater sample results for ^{3}H compared favorably to the apparent ^{14}C age-dates; most of the groundwater samples with ^{3}H concentrations that were greater than 1.6 TU (postbomb water) had modern ^{14}C apparent ages. All of the groundwater samples with ^{3}H concentrations of less than 0.6 TU were classified as older water with apparent ages of ^{14}C ranging from about 2,800 to 35,000 ^{14}C years before present [BP].

The groundwater sample results of δD and $\delta^{18}O$ were compared with the groundwater sample results of ^{14}C age dating. Most of the groundwater samples classified as old groundwater (greater than 10,000 ^{14}C years BP) were also classified as isotopically lighter (δD values of less than -82.65 per mil), supporting the hypothesis that this water was recharged during the wet and cool climate of the Pleistocene.

The geochemistry data indicate that there was a complex system of multiple geochemical endmembers and mixing between these endmembers with recharge to the Rio Grande alluvium and Santa Fe HGUs composed mostly of seepage from the Rio Grande, inflows from deeper or neighboring water systems, and mountain-front recharge. The following distinct geochemical groups were determined in the study area: (1) seepage from the ancestral Rio Grande—groundwater older than 10,000 ^{14}C years BP (hereinafter referred to as the "ancestral Rio Grande geochemical group"), (2) seepage from the modern Rio Grande—groundwater younger than 10,000 ^{14}C years BP (hereinafter referred to as the "modern Rio Grande geochemical group"), (3) mountain-front recharge from the Organ and Robledo Mountains and from the highlands to the southwest (hereinafter referred to as the "mountain-front geochemical group"), (4) deep groundwater upwelling (hereinafter referred to as the "deep groundwater upwelling geochemical group"), and (5) unidentifiable source of freshwater, which could contain interbasin flow from the Jornada Basin (hereinafter referred to as the "unknown freshwater geochemical group"). The groundwater samples not represented in one of the five distinct geochemical groups were combined into a "mixed water" geochemical group. The ancestral Rio Grande geochemical group represented old groundwater, with a mean apparent groundwater age of 24,000 ^{14}C years BP. As indicated by a mean SpC value of 725 µS/cm at 25 °C, ancestral Rio Grande geochemical group had the second least mineralized water within the study area behind the unknown freshwater geochemical group (568 µS/cm at 25 °C). The ancestral Rio Grande geochemical group had a Rio Grande isotopic signature and was composed of water from deep within the subsurface where geothermal energy can be transferred without geothermal water mixing. The groundwater in the modern Rio Grande geochemical group was recharged after 1950, was the second most mineralized water (as indicated by a mean SpC value of 2,400 µS/cm at 25 °C) within the study area after the deep groundwater upwelling geochemical group (mean SpC value of 11,400 µS/cm at 25 °C), and had a Rio Grande isotopic signature because the samples plotted along the Rio Grande evaporation line. The mountain-front geochemical group represented old groundwater with a mean apparent age of

18,000 ^{14}C years BP; the geochemistry of the samples in this group was indicative of groundwater moving slowly through areas with relatively low concentrations of reducing agents such as aluminum or iron and prolonged exposure to aluminosilicate minerals. The groundwater in the deep groundwater upwelling geochemical group was the oldest groundwater sampled within the study area (mean apparent groundwater age of 26,000 ^{14}C years BP) and was the most mineralized water (as indicated by a mean SpC value of 11,400 µS/cm at 25 °C), which was representative of the ancient marine groundwater located within the Paleozoic and Cretaceous carbonate rocks. The deep groundwater upwelling geochemical group also had the highest concentrations of HCO_3, K, Si, Al, Fe, and Li of all the geochemical groups within the study area, indicating that the groundwater samples in the deep groundwater upwelling group had been in contact with carbonate and siliciclastic rocks for a much longer period of time and at higher temperatures than the rest of the groundwater samples and was most likely ancient marine groundwater originating from the Paleozoic and Cretaceous carbonate rocks. Water in the deep groundwater upwelling geochemical group had most likely upwelled into the U.S. part of the Mesilla Basin aquifer system through the extensive faults in the southeast part of the study area; this interpretation was supported by the DC resistivity and TDEM soundings, the analytical results from wells, and the HFEM data collected along the Rio Grande. The samples composing the unknown freshwater geochemical group represented moderately old groundwater with a mean apparent age of 3,300 ^{14}C years BP and the least mineralized water (as indicated by a mean SpC value of 568 µS/cm at 25 °C). The source for this geochemical group was unknown because the groundwater does not have a Rio Grande isotopic signature and because the low concentrations of minerals in the groundwater samples that compose this group made this water unlike the water of any other geochemical group within the study area. This geochemical group may represent groundwater affected by interbasin flow from the Jornada Basin.

Mean water-level altitudes measured during the 2010 winter season (November 2010 through April 2011) were used to make potentiometric-surface maps for the Rio Grande alluvium and the Santa Fe Group. Water-level altitudes within the Rio Grande alluvium generally decreased from north (greater than 3,920 ft) to south (less than 3,730 ft), with a west to east decrease in groundwater altitudes near Las Cruces, N. Mex., as a result of groundwater pumping. Water-level altitudes within the Santa Fe Group generally decreased from the northwest and north to the southeast and east with the highest water-level altitudes (greater than 4,300 ft) northwest of the study area near the Sleeping Lady Hills and the lowest water-level altitudes (lower than 3,720 ft) near the Paso del Norte. Groundwater flow within the Santa Fe Group is more complex than the groundwater flow within the Rio Grande alluvium, which may be a result of the larger lateral and vertical extent of the Santa Fe Group compared to the Rio Grande alluvium. Groundwater from the Organ Mountains flows directly south towards the Paso del Norte; groundwater from the Robledo Mountains, the Rough and Ready Hills, and the Sleeping Lady Hills generally flows to the southeast; and groundwater flowing near the north end of the midbasin uplift would generally continue east towards the Rio Grande and then flow south on the east side of the midbasin uplift. Groundwater flowing near the west end of the midbasin uplift would generally continue south parallel to the faults that made up the midbasin uplift and then flow east towards the Paso del Norte when it reached the southern boundary of the midbasin uplift, and groundwater from the Aden Hills and East and West Potrillo Mountains flows to the southern boundary of the midbasin uplift and then continues east towards the Paso del Norte. Throughout most of the Mesilla Valley, the vertical hydraulic gradient was downward because the water-level altitude in the Rio Grande alluvium was generally higher than it was in the Santa Fe Group, but in some areas, the vertical hydraulic gradient was substantially reduced or even reversed to an upward hydraulic gradient. The reduced or reversed hydraulic gradient was generally located in the middle and southern parts of the Mesilla Valley. A comparison between the vertical hydraulic gradient data and the geophysical data indicated two distinct areas where deep salinity sources may be contributing to the Rio Grande alluvium. The HFEM data indicated that there was a resistivity change at depth from relatively high resistivity near the surface to relatively low resistivity at greater depths in the middle part of the Mesilla Valley which corresponded with the low vertical hydraulic gradient. The USGS seepage investigations, historical dissolved solids concentration analysis, and geochemical analyses indicated that this reach of the river has the potential to be a gaining reach (implying that there were sands and gravels instead of clayey deposits and silts in this location), and these lines of evidence indicate that upwelling from a deep saline source may be the cause of the decrease in resistivity. The upwelling of relatively saline groundwater would increase the salinity within the Rio Grande alluvium in the middle part of the Mesilla Valley. The second area where deep salinity sources may be contributing to the Rio Grande alluvium is near the Paso del Norte as indicated by an upward hydraulic gradient from the vertical hydraulic gradient conceptual grid and well groups ISC-5 to 7. Low resistivity features identified by the DC resistivity and TDEM data provide additional evidence of upwelling in this area; the geophysical data can be interpreted as plumes of saline water originating below the base of the Santa Fe Group and eventually reaching the surface to the west of the Rio Grande near the Paso del Norte, potentially affecting the salinity of the drains in the area.

Sources of water for the groundwater system within the study area consist of seepage from the Rio Grande, runoff and recharge within the mountains and uplifted areas, and inflows of upwelling groundwater from deep saline sources or from other aquifer systems. The predominant source of water for the groundwater system within the study area was the Rio Grande, with the other water sources contributing a small fraction of the total amount of water. Runoff and recharge within

the mountains and uplifted areas (including mountain-front recharge) contributed the least amount.

From the age-dating results, water in the modern Rio Grande geochemical group was recharged to the Rio Grande alluvium within the last 10 years. The variable nature of water chemistry in the modern Rio Grande geochemical group is evident in the relation of Cl/Br to δD. The water type of the modern Rio Grande geochemical group ranged from a Ca-SO_4 water type in the northern part of the study area to a Na-Cl-SO_4 water type in the southern part of the study area. The north to south change in water type in the modern Rio Grande geochemical group was accompanied by a substantial increase in SpC [likely a result of the increase in concentration in five dissolved solids (Cl, SO_4, F, Br, and Na)], $^{87}Sr/^{86}Sr$, K, and in the concentrations of the trace metals of Fe and Li. When the water-quality results obtained from the wells are considered in upgradient to downgradient order, the chemical characteristics of the groundwater samples in the modern Rio Grande geochemical group become similar to those of the deep groundwater upwelling geochemical group. The mountain-front geochemical group was generally old water (apparent age was greater than 10,000 ^{14}C years BP) that was somewhat mineralized and characterized by relatively high concentrations of F and Si, which might indicate longer exposure to volcanic and siliciclastic rocks or aluminosilicate minerals compared to the water of other geochemical groups. There were five different locations of recharge determined from the groundwater geochemistry within the mountain-front geochemical group, all having a slightly different geochemical signature: (1) the Rough and Ready Hills, the Robledo Mountains, and the Sleeping Lady Hills, (2) the Doña Ana Mountains, (3) the Aden Hills and the West Potrillo Mountains, (4) the East Potrillo Mountains, and (5) the Sierra Juárez in Mexico. The groundwater from these mountains eventually mixes together and with modern Rio Grande groundwater. The groundwater originating from the Aden Hills and the East and West Potrillo Mountains generally flows southeast and then east at a slow rate (indicated by the apparent age (22,000 ^{14}C years BP measured in the sample collected from well Q30), where it mixes with the ancestral Rio Grande groundwater and with the groundwater from the Sierra Juárez. The groundwater from the Sierra Juárez flows north and then east towards the Paso del Norte where it mixes with groundwater from the uplifted areas in the west, ancestral and modern Rio Grande groundwater, and the deep saline source groundwater.

References Cited

Adams, A.I., Goff, Fraser, and Counce, Dale, 1995, Chemical and isotopic variations of precipitation in the Los Alamos region, New Mexico: Los Alamos National Laboratory, 39 p.

Al-Garni, M.A., 1996, Direct current resistivity investigation of groundwater in the lower Mesilla Valley, New Mexico and Texas: Colorado School of Mines, master's thesis, 126 p.

Alley, W.M., ed., 2013, Five-year interim report of the United States-Mexico Transboundary Aquifer Assessment Program—2007–2012: U.S. Geological Survey Open-File Report 2013–1059, 31 p.

American Public Health Association, 1998, Standard methods for the examination of water and wastewater (20th ed.): Washington, D.C., American Public Health Association, American Water Works Association, and Water Environment Federation, p. 3-37–3-43.

Anderholm, S.K., 1992, Water quality and geochemistry of the Mesilla Basin, *in* Frenzel, P.F., and Kaehler, C.A., 1992, Geohydrology and simulation of ground-water flow in the Mesilla Basin, Doña Ana County, New Mexico and El Paso County, Texas: U.S. Geological Survey Professional Paper 1407–C, 105 p.

Back, William, 1961, Techniques for mapping hydrochemical facies: U.S. Geological Survey Professional Paper 424–D, p. 380–382.

Back, William, 1966, Hydrochemical facies and groundwater flow patterns in northern part of Atlantic Coastal Plain: U.S. Geological Survey Professional Paper 498–A, 42 p., accessed October 22, 2015, at http://pubs.usgs.gov/pp/0498a/report.pdf.

Baldridge, W.S., Keller, G.R., Haak V., Wendlandt, E., Jiracek, G.R., and Olsen, K.H., 1995, The Rio Grande rift in continental rifts—Evolution, structure, tectonics developments, *in* Geotechtonics: Amsterdam, Elsevier, v. 25, p. 233–275.

Banner, J.L., 2004, Radiogenic isotopes—Systematics and applications to earth surface processes and chemical stratigraphy: Earth Science Reviews, v. 65, p. 141–194.

Banner, J.L., and Kaufman, Jonathan, 1994, The isotopic record of ocean chemistry and diagenesis preserved in nonluminescent brachiopods from Mississippian carbonate rocks, Illinois and Missouri: Geological Society of America Bulletin, v. 106, p. 1074–1082.

Bartos, T.T., and Ogle, Kathy Muller, 2002, Water quality and environmental isotopic analyses of ground-water samples collected from Wasatch and Fort Union Formations in areas of coalbed methane development—Implications to recharge and groundwater flow, eastern Powder River Basin, Wyoming: U.S. Geological Survey Water-Resources Investigations Report 02–4045, 96 p., accessed October 17, 2015, at http://pubs.usgs.gov/wri/wri024045/index.html.

Bauch, N.J., Miller, L.D., and Yacob, Sharon, 2014, Analysis of water quality in the Blue River watershed, Colorado, 1984 through 2007: U.S. Geological Survey Scientific Investigations Report 2013–5129, 91 p., http://dx.doi.org/10.3133/sir20135129.

Boghici, P.G., 2003, A field manual for groundwater sampling: Texas Water Development Board User Manual 51, 47 p.

Brenner-Tourtelot, E.F., and Machette, M.N., 1979, The mineralogy and geochemistry of lithium in the Popotosa Formation, Socorro County, New Mexico: U.S. Geological Survey Open-File Report 79–839, 27 p.

Bultman, M.W., Gettings, M.E., Wynn, Jeff, 1999, An interpretation of the 1997 airborne electromagnetic (AEM) survey, Fort Huachuca vicinity, Cochise County, Arizona: U.S. Geological Survey Open-File Report 99–7–B, accessed October 21, 2015, at http://pubs.er.usgs.gov/publication/ofr997B.

Bumgarner, J.R., Stanton, G.P., Teeple, A.P., Thomas, J.V., Houston, N.A., Payne, J.D., and Musgrove, MaryLynn, 2012, A conceptual model of the hydrogeologic framework, geochemistry, and groundwater-flow system of the Edwards-Trinity and related aquifers in the Pecos County region, Texas: U.S. Geological Survey Scientific Investigations Report 2012–5124 (revised July 10, 2012), 74 p.

Bureau of Reclamation, 2011, Reclamation—Managing water in the west—Rio Grande Project: accessed May 15, 2013 at http://www.usbr.gov/projects/Project.jsp?proj_Name=Rio%20Grande%20Project.

Busenberg, Eurybiades, Plummer, L.N., and Bartholomay, R.C., 2001, Estimated age and source of the young fraction of ground water at the Idaho National Engineering and Environmental Laboratory: U.S. Geological Survey Water-Resources Investigations Report 01–4265, 144 p.

Busenberg, Eurybiades, Weeks, E.P., Plummer, L.N., and Bartholomay, R.C., 1993, Age dating groundwater by use of chlorofluorocarbons (CCl3F and CCl2F2) and distribution of chlorofluorocarbons in the unsaturated zone, Snake River Plain aquifer, Idaho National Engineering Laboratory, Idaho: U.S. Geological Survey Water-Resources Investigations Report 93–4054, 47 p.

Buss, S.R., Herbert, A.W., Morgan, P., Thornton, S.F., and Smith, J.W.N., 2004, A review of ammonium attenuation in soil and groundwater: Quarterly Journal of Engineering Geology and Hydrogeology, v. 37, no. 4, p. 347–359.

Cain, M.J., 2002, FUGRO RESOLVE survey for the International Boundary and Water Commission Texas levee survey II: Fugro Airborne Surveys Corp., Mississauga, Ontario, 58 p.

Childress, C.J.O., Foreman, W.T., Connor, B.F., and Maloney, T.J., 1999, New reporting procedures based on long-term method detection levels and some considerations for interpretations of water-quality data provided by the U.S. Geological Survey National Water Quality Laboratory: U.S. Geological Survey Open-File Report 99–193, 24 p.

City of Las Cruces, 2016, Water sources—Where does our water come from?, accessed April 29, 2016, at http://www.las-cruces.org/en/departments/utilities/water-conservation/water-sources.

Clark, I.D., and Fritz, Peter, 1997, Environmental isotopes in hydrogeology: Boca Raton, Fla., Lewis Publishers, 328 p.

Constable, S.C., Parker, R.L., and Constable, C.G., 1987, Occam's inversion—A practical algorithm for generating smooth models from electromagnetic sounding data: Geophysics, v. 52, issue 289.

Craig, Harmon, 1961, Isotopic variations in meteoric waters: Science, v. 133, p. 1702–1703.

Creel, B.J., Hawley, J.W., Kennedy, J.F., and Granados-Olivas, A., 2006, Groundwater resources of the New Mexico-Texas-Chihuahua border region: New Mexico Journal of Science, v. 44. p. 11–29.

Crilley, D.M., Matherne, A.M., Thomas, Nicole, and Falk, S.E., 2013, Seepage investigations of the Rio Grande from below Leasburg Dam, Leasburg, New Mexico, to above American Dam, El Paso, Texas, 2006–13: U.S. Geological Survey Open-File Report 2013–1233, 34 p., accessed October 21, 2015, at http://pubs.usgs.gov/of/2013/1233/.

Cunningham, W.L., and Schalk, C.W., comps., 2011, Groundwater technical procedures of the U.S. Geological Survey: U.S. Geological Survey Techniques and Methods 1–A1, 151 p. [Also available at http://pubs.usgs.gov/tm/1a1/.]

Daniel B. Stephens and Associates, Inc., 2010, Evaluation of Rio Grande salinity San Marcial, New Mexico to El Paso, Texas: Accessed October 18, 2015, at http://www.nmenv.state.nm.us/swqb/documents/swqbdocs/LRG/Program/LRG_Salinity_Rpt_6-30-10.pdf.

Davis, S.N., Whittemore, D.O., and Fabryka-Martin, June, 1998, Uses of chloride/bromide ratios in studies of potable water: Groundwater v. 36, no. 2, p. 338–350, accessed October 21, 2015, at http://onlinelibrary.wiley.com/doi/10.1111/j.1745-6584.1998.tb01099.x/citedby.

Decelles, P.G., Ducea, M.N., Kapp, Paul, and Zandt, George, 2009, Cyclicity in Cordilleran orogenic systems: Nature Geosciences, v. 2, p. 251–257.

Domenico, P.A., and Schwartz, F.W., 1998, Physical and chemical hydrogeology (2d ed.): Hoboken, N.J., Wiley, 528 p.

Donahue, D.J., Linick, T.W., and Jull, A.J.T., 1990, Isotope-ratio and background corrections for accelerator mass spectrometry radiocarbon measurements: Radiocarbon, v. 32, book 2, p. 135–142.

Doremus, Dale, and Michelsen, A.M., 2008, Rio Grande salinity management—First steps towards interstate solutions: Surface Water Opportunities in New Mexico, New Mexico Water Resources Research Institute, 8 p.

Drewes, Harold, 1991, Description and development of the Cordilleran orogenic belt in the southwestern United States and northern Mexico: U.S. Geological Survey Professional Paper 1512, 97 p.

Dunbar, J.B., Murphy, W.L., Ballard, R.F., McGill, T.E., Peyman-Dove, L.D., and Bishop, M.J., 2004, Condition assessment of U.S. International Boundary and Water Commission, Texas and New Mexico levees—Report 2: U.S. Army Corps of Engineers Engineer Research and Development Center, 121 p.

Dupré, D.H., Scott, J.C., Clark, M.L., Canova, M.G., and Stoker, Y.E., 2012, User's manual for the National Water Information System of the U.S. Geological Survey—Water-Quality System, Version 5.0: U.S. Geological Survey Open-File Report 2013–1054, accessed March 17, 2017, at https://pubs.usgs.gov/of/2013/1054/pdf/OFR2013-1054_NWIS_ver5.pdf.

Duval, J.S., Pierce, H.A., Daniels, D.L., Mars, J.C., Webring, M.W., and Hildenbrand, T.G., 2002, Aerial magnetic, electromagnetic, and gamma-ray survey, Berrien County, Michigan: U.S. Geological Survey Open-File Report 02–117, accessed September 2012 at http://pubs.usgs.gov/of/2002/of02-117/.

Eastoe, C.J., Hibbs, B.J., Olivas, A.G., Hogan, J.F., Hawley, John, and Hutchinson, W.R., 2007, Isotopes in the Hueco Bolson aquifer, Texas (USA) and Chihuahua (Mexico)—Local and general implications for recharge sources in alluvial basins: Hydrogeology Journal, v. 16, no. 4, 11 p.

Elder, K.L., McNichol, A.P., and Gagnon, A.R., 1998, Evaluating reproducibility of seawater, inorganic and organic carbon ^{14}C results at the National Ocean Sciences AMS Facility (NOSAMS): Radiocarbon, v. 40, p. 223–230.

El Paso Water Utilities, 2007, Water: Water Resources, accessed August 2014 at http://www.epwu.org/water/water_resources.html.

Faure, Gunter, 1986, Principles of isotope geology: New York, Wiley, 589 p.

Fenneman, N.M., and Johnson, D.W., 1946, Physiographic divisions of the conterminous U.S.—Get this data set: U.S. Geological Survey, accessed June 9, 2016, at http://water.usgs.gov/lookup/getspatial?physio.

Fishman, M.J., ed., 1993, Methods of analysis by the U.S. Geological Survey National Water Quality Laboratory—Determination of inorganic and organic constituents in water and fluvial sediments: U.S. Geological Survey Open-File Report 93–125, 217 p.

Fishman, M.J., and Friedman, L.C., 1989, Methods for determination of inorganic substances in water and fluvial sediments: U.S. Geological Survey Techniques of Water-Resources Investigations, book 5, chap. A1, 545 p.

Fitterman, D.V., and Deszcz-Pan, Maria, 2002, Helicopter electromagnetic data from Everglades National Park and surrounding areas, Florida—Collected 9–14 December 1994: U.S. Geological Survey Open-File Report 02–101, accessed September 2012 at http://sofia.usgs.gov/publications/ofr/02-101/.

Fontes, J., 1980, Environmental isotopes in groundwater hydrology, *in* Fritz, P., and Fontes, J., Handbook of environmental isotope geochemistry, v. 1, The terrestrial environment: New York, Elsevier, p. 75–140.

Freeze, R.A., and Cherry, J.A., 1979, Groundwater: Englewood Cliffs, New Jersey, Prentice-Hall, 604 p.

Frenzel, P.F., and Kaehler, C.A., 1992, Geohydrology and simulation of ground-water flow in the Mesilla Basin, Doña Ana County, New Mexico and El Paso County, Texas: U.S. Geological Survey Professional Paper 1407–C, 114 p.

Fritz, Peter, and Fontes, J.C., eds., 1980, Handbook of environmental isotope geochemistry, v. 1—The terrestrial environment: Amsterdam, Elsevier, 545 p.

Fry, J.A., Xian, George, Jin, Suming, Dewitz, J.A., Homer, C.G., Yang, Limin, Barnes, C.A., Herold, N.D., and Wickham, J.D., 2011, Completion of the 2006 National Land Cover Database for the conterminous United States: Photogrammetric Engineering and Remote Sensing, v. 77, no. 9, p. 858–864.

Fugro Airborne Surveys, 2013, RESOLVE: Accessed January 17, 2013, at http://www.fugroairborne.com/services/geophysicalservices/bysurvey/electromagnetics/helicopter-electromagnetic/resolve.

Gagnon, A.R., and Jones, G.A., 1993, AMS-graphite target production methods at the Woods Hole Oceanographic Institution during 1986–1991: Radiocarbon, v. 35, book 2, p. 301–310.

Garbarino, J.R., 1999, Methods of analysis by the U.S. Geological Survey National Water Quality Laboratory—Determination of dissolved arsenic, boron, lithium, selenium, strontium, thallium, and vanadium using inductively coupled plasma-mass spectrometry: U.S. Geological Survey Open-File Report 99–093, 31 p.

Garbarino, J.R., Kanagy, L.K., and Cree, M.E., 2006, Determination of elements in natural-water, biota, sediment and soil samples using collision/reaction cell inductively coupled plasma-mass spectrometry: U.S. Geological Survey Techniques and Methods, book 5, sec. B, chap. 1, 88 p.

Geosoft, Inc., 2012, Technical workshop—Topics in gridding: Accessed January 18, 2012, at http://geosoft.com/media/uploads/resources/technical-papers/topicsingriddingworkshop.pdf.

Haldar, S.K., and Tišljar, Josip, 2013, Introduction to mineralogy and petrology: New York, Elsevier, 354 p.

Harbour, R.L., 1972, Geology of the northern Franklin Mountains, Texas and New Mexico: Geological Survey Bulletin 1298, 138 p.

Hawley, J.W., and Kennedy, J.F., 2004, Creation of a digital hydrogeologic framework model of the Mesilla Basin and southern Jornada del Muerto Basin: New Mexico Water Resources Research Institute Technical Completion Report no. 332, 105 p., accessed January 18, 2013, at http://wrri.nmsu.edu/publish/techrpt/tr332/downl.html.

Hawley, J.W., Kennedy, J.F., Ortiz, Marquita, and Carrasco, Sean, 2005, Digital hydrogeologic framework model of the Rincon Valley and adjacent areas of Doña Ana, Sierra and Luna Counties, NM: Las Cruces, N. Mex., New Mexico Water Resources Research Institute of New Mexico State University, addendum to Technical Completion Report 332, accessed October 22, 2009, at http://wrri.nmsu.edu/publish/techrpt/tr332/cdrom/addendum.pdf.

Hawley, J.W., and Lozinsky, R.P., 1992, Hydrogeologic framework of the Mesilla Basin in New Mexico and western Texas: New Mexico Bureau of Mines and Mineral Resources Open File Report 323, 55 p.

Heath, R.C., 1983, Basic ground-water hydrology: U.S. Geological Survey Water-Supply Paper 2220, 86 p.

Helsel, D.R., and Hirsch, R.M., 2002, Chapter A3—Statistical methods in water resources: Techniques of Water-Resources Investigations of the U.S. Geological Survey, book 4, Hydrologic Analysis and Interpretation, 524 p.

Hem, J.D., 1985, Study and interpretation of the chemical characteristics of natural water (3d ed.): U.S. Geological Survey Water-Supply Paper 2254, 263 p.

Hinkle, S.R., 1996, Age of ground water in basalt aquifers near Spring Creek National Fish Hatchery, Skamania County, Washington: U.S. Geological Survey Water-Resources Investigations Report 95–4272, 26 p., accessed July 21, 2014, at http://or.water.usgs.gov/pubs_dir/Pdf/95-4272.pdf.

Hinkle, S.R., and Polette, D.J., 1998, Arsenic in ground water of the Willamette Basin, Oregon: U.S. Geological Survey Water-Resources Investigations Report 98–4205, 28 p., 1 pl. [Also available at http://or.water.usgs.gov/pubs_dir/Online/Pdf/98-4205.pdf.]

Hoffer, J.M., 1976, Geology of Potrillo Basalt Field, south-central New Mexico: New Mexico Bureau of Geology and Mineral Resources Circular 149, 30 p.

Hogan, J.F., Phillips, F.M., Mills, S.K., Hendrickx, J.M.H., Ruiz, Joaquin, Chelsey, J.T., and Asmerom, Yamane, 2007, Geologic origins of salinization in a semi-arid river—The role of sedimentary basin brines: Geology, v. 35, p. 1063–1066.

Horowitz, A.J., Lum, K.R., Garbarino, J.R., Hall, G.E.M., LeMieux, C., and Demas, C.R., 1996, Problems associated with using filtration to define dissolved trace element concentrations in natural water samples: Environmental Science Technology, v. 30, no. 3, p. 954–963.

Indiana Department of Natural Resources, 2002, Ground-water resources in the White and West Fork White River Basin, Indiana: Division of Water Resource Assessment 2002–6, 96 p. [Available online at https://www.in.gov/dnr/water/files/WFWR_web1-26.pdf.]

Ingebritsen, S.E., and Sanford, W.E., 1999, Groundwater in geologic processes (2d ed.): New York, Cambridge University Press, 341 p.

Instituto Nacional de Estadística y Geografía, 2001, Subprovincias fisiográficas: Accessed April 2015 at http://www3.inegi.org.mx/sistemas/biblioteca/ficha.aspx?upc=702825267599.

Instituto Nacional de Estadística y Geografía, 2010, Población total, municipio de Juárez, Chihuahua: Accessed September 2014 at http://www.inegi.org.mx/sistemas/mexicocifras/default.aspx?ent=08.

International Atomic Energy Agency, 2016, Global networks of isotopes in precipitation: Accessed May 5, 2016, at http://www-naweb.iaea.org/napc/ih/IHS_resources_gnip.html.

International Boundary and Water Commission, 2013, Rio Grande historical mean daily discharge data: Accessed January 17, 2013, at http://www.ibwc.state.gov/Water_Data/histflo1.htm.

Interpex Limited, 1996, TEMIX XL user's manual, version 4: Golden, Colo., Interpex Limited.

Kalin, R.M., 2000, Radiocarbon dating of groundwater systems, *in* Cook, P.G., and Herczeg, A.L., eds., Chapter 4—Environmental tracers in subsurface hydrology: Boston, Kluwer Academic Publishers, p. 111–144.

Karlen, I., Olsson, I.U., Kallburg, P., and Kilici, S., 1964, Absolute determination of the activity of two ^{14}C dating standards: Arkiv Geofysik, v. 4, p. 465–471.

Kay, R.T., and Buszka, P.M., 2016, Application of hydrogeology and groundwater-age estimates to assess the travel time of groundwater at the site of a landfill to the Mahomet aquifer, near Clinton, Illinois, with a section on regional indications of recharge to the Mahomet aquifer from previously collected tritium and pesticide data, by Buszka, P.M. and Morrow, W.S.: U.S. Geological Survey Scientific Investigations Report 2015–5159, 54 p., accessed February 28, 2017, at http://dx.doi.org/10.3133/sir20155159.

Keller, G.V., and Frischknecht, F.C., 1966, Electrical methods in geophysical prospecting: Oxford, United Kingdom, Pergamon Press, 519 p.

Kemker, Christine, 2014, Conductivity, salinity and total dissolved solids: Fundamentals of Environmental Measurements, Fondriest Environmental, Inc., accessed on January 12, 2015, at http://www.fondriest.com/environmental-measurements/parameters/water-quality/conductivity-salinity-tds/.

Ken E. Davis Associates, 1988, Survey of methods to determine total dissolved solids concentrations: U.S. Environmental Protection Agency Underground Injection Control Program, 87 p.

Kendall, Carol, and McDonnell, J.J., 1998, Isotope tracers in catchment hydrology: Fundamentals of Isotope Geochemistry, Amsterdam, Elsevier, p. 51–86.

Kendall, Carol, Snyder, Dan, and Caldwell, Eric, 2004, Resources on isotopes—Periodic table—Hydrogen: U.S. Geological Survey Isotope Tracers Project, accessed on February 14, 2015, at http://wwwrcamnl.wr.usgs.gov/isoig/period/h_iig.html.

Klein, Cornelis, and Hurlbut, C.S., Jr., 1998, Manual of mineralogy (after James D. Dana) (revised 21st ed.): New York, Wiley, 704 p.

Koterba, M.T., Wilde, F.D., and Lapham, W.W., 1995, Groundwater data-collection protocols and procedures for the National Water-Quality Assessment Program—Collection and documentation of water-quality samples and related data: U.S. Geological Survey Open-File Report 95–399, 113 p. [Also available at http://pubs.usgs.gov/of/1995/ofr-95-399/.]

Leggat, E.R., Lowry, M.E., and Hood, J.W., 1963, Groundwater resources of the lower Mesilla Valley Texas and New Mexico: U.S. Geological Survey Water-Supply Paper 1669–AA, 53 p.

Lemay, T.G., 2002, Carbon-14 dating of groundwater from selected wells in Quaternary and Quaternary-Tertiary sediments, Athabasca Oil Sands (in-situ) area, Alberta: Alberta Geological Survey, 21 p.

LennTech, 2012a, Arsenic and water—reaction mechanisms, environmental impact and health effects: Accessed June 17, 2016, at http://www.lenntech.com/periodic/water/arsenic/arsenic-and-water.htm.

LennTech, 2012b, Iron and water—reaction mechanisms, environmental impact and health effects: Accessed June 17, 2016, at http://www.lenntech.com/periodic/water/iron/iron-and-water.htm.

Levings, G.W., Healy, D.F., Richey, S.F., and Carter, L.F., 1998, Water quality in the Rio Grande Valley, Colorado, New Mexico, and Texas, 1992–95: U.S. Geological Survey Circular 1162, 44 p.

Lindley, C.E., Stewart, J.T., and Sandstrom, M.W., 1996, Determination of low concentrations of acetochlor in water by automated solid-phase extraction and gas chromatography with mass selective detection: Journal of AOAC International, v. 79, no. 4, p. 962–966.

Linsley, R.K., Kohler, M.A., and Paulhus, J.L.H., 1982, Hydrology for engineers (3d ed.): New York, McGraw-Hill, 512 p.

Lucas, L.L., and Unterweger, M.P., 2000, Comprehensive review and critical evaluation of the half-life of tritium: Journal of Research of the National Institute of Standards and Technology, v. 105, no. 4, p. 541–549.

Lucius, J.E., Langer, W.H., and Ellefsen, K.J., 2007, An introduction to using surface geophysics to characterize sand and gravel deposits: U.S. Geological Survey Circular 1310, 33 p.

Madsen, J.E., Sandstrom, M.W., and Zaugg, S.D., 2003, Methods of analysis by the U.S. Geological Survey National Water Quality Laboratory—A method supplement for the determination of fipronil and degradates in water by gas chromatography/mass spectrometry: U.S. Geological Survey Open-File Report 02–462, 11 p.

Martin, J.D., and Eberle, Michael, 2011, Adjustment of pesticide concentrations for temporal changes in analytical recovery, 1992–2010: U.S. Geological Survey Data Series 630, 11 p., 5 apps.

Martin, J.D., Stone, W.W., Wydoski, D.S., and Sandstrom, M.W., 2009, Adjustment of pesticide concentrations for temporal changes in analytical recovery, 1992–2006: U.S. Geological Survey Scientific Investigations Report 2009–5189, 23 p. plus appendixes.

McCoy, A.M. and Peery, R.L., 2008, City of Las Cruces 40–year water development plan: John Shomaker and Associates, Inc. in association with Len Stokes Progressive Environmental Systems, Inc., accessed April 9, 2017, at http://www.las-cruces.org/~/media/lcpublicwebdev2/site%20documents/article%20documents/utilities/water%20resources/40%20year%20plan.ashx?la=en.

McMahon, P.B., and Chapelle, F.H., 2008, Redox processes and water quality of selected principal aquifer systems: Groundwater, v. 46, no. 2, p. 259–271.

McNichol, A.P., Gagnon, A.R., Jones, G.A., and Osborne, E.A., 1992, Illumination of a black box—Analysis of gas composition during graphite target preparation, *in* Long, A., and Kra, R.S., eds., Proceedings of the 14th International ^{14}C Conference: Radiocarbon, v. 34, book 3, p. 321–329.

McNichol, A.P., Jones, G.A., Hutton, D.L. and Gagnon, A.R., 1994, The rapid preparation of seawater ΣC02 for radiocarbon analysis at the National Ocean Sciences AMS Facility: Radiocarbon, v. 36, book 2, p. 237–246.

Morgan, C.O., and Winner, M.D., Jr., 1962, Hydrochemical facies in the 400 foot and 600 foot sands of the Baton Rouge area, Louisiana: U.S. Geological Survey Professional Paper 450–B, p. B120–121.

Motzer, W.E., 2008, Age dating groundwater: Todd Engineers, 4 p.

Moyer, D.L., Anderholm, S.K., Hogan, J.F., Phillips, F.M., Hibbs, B.J., Witcher, J.C., Matherne, A.M., and Falk, S.E., 2013, Knowledge and understanding of dissolved solids in the Rio Grande–San Acacia, New Mexico, to Fort Quitman, Texas, and plan for future studies and monitoring: U.S. Geological Survey Open-File Report 2013–1190, 55 p. [Also available at http://pubs.usgs.gov/of/2013/1190/.]

Musgrove, MaryLynn, Fahlquist, Lynne, Houston, N.A., Lindgren, R.J., and Ging, P.B., 2010, Geochemical evolution processes and water-quality observations based on results of the National Water-Quality Assessment Program in the San Antonio segment of the Edwards aquifer, 1996–2006: U.S. Geological Survey Scientific Investigations Report 2010–5129, 93 p.

National Oceanic and Atmospheric Administration, 2014, Data tools—1981–2010 normals: National Oceanic and Atmospheric Administration National Centers for Environmental Information, accessed November 14, 2014, at https://www.ncdc.noaa.gov/cdo-web/datatools/normals.

New Mexico Environment Department, 2012, Lower Rio Grande Program: Accessed May 14, 2013, at http://www.nmenv.state.nm.us/swqb/LowerRioGrande/.

New Mexico Office of Border Health, 2014, Office of Border Health: Accessed November 14, 2014, at http://archive.nmborderhealth.org/index.shtml.

New Mexico Office of the State Engineer, 2014, Interstate Stream Commission: Accessed November 14, 2014, at http://www.ose.state.nm.us/ISC/index.php.

Nickerson, E.L., and Myers, R.G., 1993, Geohydrology of the Mesilla ground-water basin, Doña Ana County, New Mexico, and El Paso County, Texas: U.S. Geological Survey Water-Resources Investigations Report 92–4156, 96 p.

Nishikawa, Tracy, Izbicki, J.A., Hevesi, J.A., Stamos, C.L., and Martin, Peter, 2004, Evaluation of geohydrologic framework, recharge estimates, and ground-water flow of the Joshua Tree area, San Bernardino County, California: U.S. Geological Survey Scientific Investigations Report 2004–5267, 115 p.

Nordstrom, D.K., Wright, W.G., Mast, M.A., Bove, D.J., and Rye, R.O., 2007, Aqueous-sulfate stable isotopes—A study of mining-affected and undisturbed acidic drainage, chap. E8 *of* Church, S.E., von Guerard, Paul, and Finger, S.E., eds., 2007, Integrated investigations of environmental effects of historical mining in the Animas River watershed, San Juan County, Colorado: U.S. Geological Survey Professional Paper 1651, 1,096 p. plus CD-ROM. [In two volumes.]

North Carolina Division of Water Resources, 2004, Time domain electromagnetic geophysics: North Carolina Department of Environment and Natural Resources, accessed April 27, 2017, at http://www.ncwater.org/?page=562.

Oden, J.H., Brown, D.W., and Oden, T.D., 2011, Groundwater quality of the Gulf Coast aquifer system, Houston, Texas, 2010: U.S. Geological Survey Data Series 598, 64 p.

Oden, T.D., and Truini, Margot, 2013, Estimated rates of groundwater recharge to the Chicot, Evangeline, and Jasper aquifers by using environmental tracers in Montgomery and adjacent counties, Texas, 2008 and 2011: U.S. Geological Survey Scientific Investigations Report 2013–5024, 50 p.

Olsson, I.U., and Klasson, Martin, 1970, Uppsala radiocarbon measurements X: Radiocarbon, v. 12, no. l, p. 281–284.

Östlund, H.G., and Werner, E., 1962, Electrolytic enrichment of tritium and deuterium for natural tritium measurements—Tritium in the physical and biological sciences: Vienna, Austria, International Atomic Energy Agency, v. 1, p. 96–104.

Parameter-elevation Regressions on Independent Slopes Model (PRISM) Climate Group, 2004, PRISM climate data: Oregon State University, accessed November 14, 2014, at http://prism.oregonstate.edu.

Parkhurst, D.L., 1995, User's guide to PHREEQC—A computer program for speciation, reaction-path, advective-transport, and inverse geochemical calculations: U.S. Geological Survey Water-Resources Investigations Report 95–4227, 151 p.

Patton, C.J., and Kryskalla, J.R., 2003, Methods of analysis by the U.S. Geological Survey National Water Quality Laboratory—Evaluation of alkaline persulfate digestion as an alternative to kjeldahl digestion for determination of total and dissolved nitrogen and phosphorus in water: U.S. Geological Survey Water-Resources Investigations Report 03–4174, 33 p.

Peterson, D.M., Khaleel, Raz, and Hawley, J.W., 1984, Quasi three-dimensional modeling of groundwater flow in the Mesilla Bolson, New Mexico and Texas: New Mexico Water Resources Research Institute Report 178, Technical Completion Report, project no. 1–3–45645, accessed May 26, 2017, at https://nmwrri.nmsu.edu/tr178/.

Phillips, F.M., Hogan, J.F., Mills, S.K., and Hendrickx, J.M.H., 2003, Environmental tracers applied to quantifying causes of salinity in arid-region rivers—Preliminary results from the Rio Grande, southwestern USA, *in* Alsharhan, A.S., and Wood, W.W., eds., Water resources perspectives—Evaluation, management, and policy: Amsterdam, Elsevier, Developments in Water Science, v. 50, p. 327–334.

Piper, A.M., 1944, A graphic procedure in the geochemical interpretation of water analyses: Transactions, American Geophysical Union, v. 25, p. 914–923.

Plummer, L.N., Bexfield, L.M., Anderholm, S.K., Sanford, W.E., and Busenberg, Eurybiades, 2004, Geochemical characterization of ground-water flow in the Santa Fe Group aquifer system, Middle Rio Grande Basin, New Mexico: U.S. Geological Survey Water-Resources Investigation Report 03–4131, 414 p.

Plummer, L.N., and Busenberg, Eurybiades, 2000, Chlorofluorocarbons, *in* Cook, P.G., and Herczeg, A.L., eds., Environmental tracers in subsurface hydrology: Boston, Mass., Kluwer Academic Press, chap. 15, p. 441–478.

Plummer, L.N., Prestemon, E.C., and Parkhurst, D.L., 1994, An interactive code (NETPATH) for modeling net geochemical reactions along a flow path version 2.0: U.S. Geological Survey Water-Resources Investigation Report 94–4169, 133 p.

Raymond, P.A., Bauer, J.E., 2001, Use of ^{14}C and ^{13}C natural abundances for evaluating riverine, estuarine, and coastal DOC and POC sources and cycling—A review and synthesis: Organic Geochemistry, v. 32, p. 469–486.

Révész, Kinga, and Coplen, T.B., 2008a, Determination of the δ (2H/1H) of water: RSIL lab code 1574, chap. C1 *of* Révész, Kinga, and Coplen, T.B., eds., Methods of the Reston Stable Isotope Laboratory: U.S. Geological Survey Techniques and Methods, book 10, chap. C1, 27 p.

Révész, Kinga, and Coplen, T.B., 2008b, Determination of the δ(180/160), of water: RSIL lab code 489, chap. C2 *of* Révész, Kinga, and Coplen, T.B., eds., Methods of the Reston Stable Isotope Laboratory: U.S. Geological Survey Techniques and Methods, book 10, chap. C2, 28 p.

Roberts, M.L., Burton, J.R., Elder, K.L., Longsworth, B.E., McIntyre, C.P., von Renden, K.F., Han, B.X., Rosensheim, B.E., Jenkins, W.J., Galutschek, E., and McNichol, A.P., 2010, A high-performance ^{14}C accelerator mass spectrometry system: Radiocarbon, v. 52, p. 228–235.

Robson, S.G., and Banta, E.R., 1995, Ground-water atlas of the United States, segment 2, Arizona, Colorado, New Mexico, and Utah: U.S. Geological Survey Hydrologic Investigations Atlas HA–730C, 32 p.

Ryder, P.D., 1996, Ground water atlas of the United States—Segment 4, Oklahoma, Texas: U.S. Geological Survey Hydrologic Investigations Atlas 730–E, 30 p.

Sandstrom, M.W., Stroppel, M.E., Foreman, W.T., and Schroeder, M.P., 2001, Methods of analysis by the U.S. Geological Survey National Water Quality Laboratory—Determination of moderate-use pesticides and selected degradates in water by C-18 solid-phase extraction and gas chromatography/mass spectrometry: U.S. Geological Survey Water-Resources Investigations Report 01–4098, 70 p.

Schneider, R.J., Jones, G.A., McNichol, A.P., von Reden, K.F., Elder, K.A., Huang, K., and Kessel, E.D., 1994, Methods for data screening, flagging, and error analysis at the National Ocean Sciences AMS Facility: Nuclear Instruments and Methods in Physics Research, book 92, p. 172–175.

Seaber, P.R., 1962, Cation hydrochemical facies of groundwater in the Englishtown Formation, New Jersey: U.S. Geological Professional Paper 627–C, 17 p.

Sharma, P.V., 1997, Environmental and engineering geophysics: Cambridge, United Kingdom, Cambridge University Press.

Shelton, L.R., 1994, Field guide for collecting and processing stream-water samples for the National Water-Quality Assessment Program: U.S. Geological Survey Open-File Report 94–455, 42 p. [Also available at http://pubs.er.usgs.gov/usgspubs/ofr/ofr94455.]

Singhal, B.B.S., and Gupta, R.P., 2010, Applied hydrogeology of fractured rocks—Second edition: New York, Springer, 428 p.

Smith, B.D., Abraham, J.D., Cannia, J.C., Minsley, B.J., Ball, L.B., Steele, G.V., and Deszcz-Pan, Maria, 2011, Helicopter electromagnetic and magnetic geophysical survey data, Swedeburg and Sprague study area, eastern Nebraska, May 2009: U.S. Geological Survey Open-File Report 2010–1288, 37 p.

Smith, B.D., Abraham, J.D., Cannia, J.C., Steele, G.V., and Hill, P.L., 2008, Helicopter electromagnetic and magnetic geophysical survey data, Oakland, Ashland, and Firth study areas, eastern Nebraska, March 2007: U.S. Geological Survey Open-File Report 2008–1018, 20 p.

Solomon, D.K., and Cook, P.G., 2000, ^{3}H and ^{3}He, chap. 13 *of* Cook, P.G., and Herczeg, A.L., eds., Environmental tracers in subsurface hydrology: Boston, Mass., Kluwer Academic Press, p. 397–424.

S.S. Papadopulos and Associates, Inc., 2007, Groundwater flow model for administration and management in the lower Rio Grande Basin: 69 p.

Stewart, J.H., 1998, Regional characteristics, tilt domains, and extensional history of the late Cenozoic Basin and Range province, western North America: Geological Society of America, Special Paper 323, 29 p.

Stewart, Mark, and Gay, M.C., 1986, Evaluation of transient electromagnetic soundings for deep detection of conductive fluids: Ground Water, v. 24, p. 351–356.

Stuiver, Minze, 1980, Workshop on ^{14}C data reporting: Radiocarbon, v. 22, no. 3, p. 964–966.

Stuiver, Minze, and Polach, H.A., 1977, Reporting of ^{14}C data: Radiocarbon, v. 19, no. 3, p. 355–363.

Sumner, J.S., 1976, Principles of induced polarization for geophysical exploration: Amsterdam, Elsevier, 277 p.

Teeple, A.P., 2017, Time-domain electromagnetic data used in the assessment of the U.S. part of the Mesilla Basin/Conejos-Médanos Aquifer System in Doña Ana County, New Mexico, and El Paso County, Texas: U.S. Geological Survey data release, https://doi.org/10.5066/F7PV6HJ3.

Teeple, A.P., Vrabel, Joseph, Kress, W.H., and Cannia, J.C., 2009, Apparent resistivity and estimated interaction potential of surface water and groundwater along selected canals and streams in the Elkhorn-Loup Model study area, north-central Nebraska, 2006–07: U.S. Geological Survey Scientific Investigations Report 2009–5171, 66 p.

Texas Water Development Board, 2012, Groundwater database reports: Accessed September 2012 at http://www.twdb.texas.gov/groundwater/data/gwdbrpt.asp.

Thatcher, L.L., Janzer, V.J., and Edwards, K.W., 1977, Methods for determination of radioactive substances in water and fluvial sediments: U.S. Geological Survey Techniques of Water-Resources Investigations, book 5, chap. A5, 95 p.

Tribble, G.W., 1997, Groundwater geochemistry of Kwajalein Island, Republic of the Marshall Islands, 1991: U.S. Geological Survey Water-Resources Investigations Report 97–4184, 47 p., accessed July 23, 2014, at http://pubs.usgs.gov/wri/wri97-4184/pdf/wri97-4184.pdf.

Uliana, M.M., Banner, J.L., and Sharp, J.M., 2007, Regional groundwater flow paths in Trans-Pecos, Texas inferred from oxygen, hydrogen, and strontium isotopes: Journal of Hydrology, v. 334, p. 334–346.

United States-Mexico Transboundary Aquifer Act, 2006, Public Law no. 109–448, 120 Statute 3328, Cornell University Law School Legal Information Institute, accessed October 22, 2015, at https://www.law.cornell.edu/topn/united_states-mexico_transboundary_aquifer_assessment_act.

University of Texas, 2005, Rio Grande-Río Bravo studies: Center for Research in Water Resources, accessed July 2014 at https://www.census.gov/quickfacts/.

U.S. Census Bureau, 2015, State and county quick facts: Accessed May 26, 2017, at https://www.census.gov/quickfacts/.

U.S. Environmental Protection Agency, 2013, Drinking water contaminants: Accessed May 2014 at http://water.epa.gov/drink/contaminants/.

U.S. Geological Survey, 1999, The quality of our Nation's waters—Nutrients and pesticides: U.S. Geological Survey Circular 1225, 82 p.

U.S. Geological Survey, 2012a, The Reston Chlorofluorocarbon Laboratory: U.S. Geological Survey, accessed September 2012 at http://water.usgs.gov/lab/.

U.S. Geological Survey, 2012b, Reston Stable Isotope Laboratory (RSIL): U.S. Geological Survey, accessed September 2012 at http://isotopes.usgs.gov/.

U.S. Geological Survey, 2012c, National Water Quality Laboratory Quality assurance charts and statistics: U.S. Geological Survey, accessed November 15, 2012, at http://nwql.usgs.gov/Public/PublicQAQC/AggregatedCharts.html.

U.S. Geological Survey, 2013, Multi-Resolution Land Characteristics Consortium: National Land Cover Database, accessed May 14, 2013, at http://www.mrlc.gov/.

U.S. Geological Survey, 2017, U.S. Geological Survey National Water Information System: Accessed March 20, 2017, at http://dx.doi.org/10.5066/F7P55KJN.

U.S. Geological Survey, variously dated, National field manual for the collection of water-quality data: U.S. Geological Survey Techniques of Water-Resources Investigations, book 9, chaps. A1–A9. [Also available at http://pubs.water.usgs.gov/twri9A.]

Vogel, J.S., Nelson, D.E., and Southon, J.R., 1987, ^{14}C background levels in an accelerator mass spectrometry system: Radiocarbon, v. 29, book 3, p. 323–333.

Ward, B.B., 1996, Nitrification and denitrification—Probing the nitrogen cycle in aquatic environments: Microbial Ecology, v. 32, no. 3, p. 247–261.

Welch, A.H., Helsel, D.R., Focazio, M.J., and Watkins, S.A., 1999, Arsenic in ground water supplies of the United States, *in* Chappell, W.R., Abernathy, C.O., and Calderon, R.L., eds., Arsenic exposure and health effects: New York, Elsevier, p. 9–17.

Wilde, F.D., ed., 2004, Cleaning of equipment for water sampling (ver. 2.0): U.S. Geological Survey Techniques of Water-Resources Investigations, book 9, chap. A3, accessed September 2011 at http://pubs.water.usgs.gov/twri9A3/.

Wilde, F.D., Radtke, D.B., Gibs, Jacob, and Iwatsubo, R.T., eds., 2004 with updates through 2009, Processing of water samples (ver. 2.2): U.S. Geological Survey Techniques of Water-Resources Investigations, book 9, chap. A5, April 2004, accessed October 21, 2015, at http://pubs.water.usgs.gov/twri9A5/.

Wilson, C.A., White, R.R., Orr, B.R., and Roybal, R.G., 1981, Water resources of the Rincon and Mesilla Valleys and adjacent areas: New Mexico State Engineer Technical Report 43, 514 p., accessed on October 31, 2016, at https://pubs.er.usgs.gov/publication/70042517.

Winslow, A.G., and Kister, L.R., 1956, Saline-water resources of Texas: U.S. Geological Survey Water-Supply Paper 1365, 114 p.

Witcher, J.C., King, J.P., Hawley, J.W., Kennedy, J.F., Williams, Jerry, Cleary, Michael, and Bothern, L.R., 2004, Sources of salinity in the Rio Grande and Mesilla Basin groundwater: New Mexico Water Resources Research Institute Technical Completion Report no. 330, 184 p.

Woods Hole Oceanographic Institution, 2016, NOSAMS, National Ocean Sciences Accelerator Mass Spectrometry Facility—Radiocarbon data and calculations: Accessed June 20, 2016, at http://www.whoi.edu/nosams/page.do?pid=40146.

Zaugg, S.D., Sandstrom, M.W., Smith, S.G., and Fehlberg, K.M., 1995, Methods of analysis by the U.S. Geological Survey National Water Quality Laboratory—Determination of pesticides in water by C-18 solid-phase extraction and capillary-column gas chromatography/mass spectrometry with selected-ion monitoring: U.S. Geological Survey Open-File Report 95–181, 60 p.

Zohdy, A.A.R., Bisdorf, R.J., and Gates, J.S., 1976, Schlumberger soundings in the lower Mesilla Valley of the Rio Grande, Texas and New Mexico: U.S. Geological Survey Open-File Report 76–324, 77 p.

Zohdy, A.A.R., Eaton, G.P., and Mabey, D.R., 1974, Application of surface geophysics to ground-water investigations: U.S. Geological Survey Techniques of Water-Resources Investigations, book 2, chap. D1, 116 p.

Zonge International, 2013, Equipment: Accessed January 17, 2013, at http://www.zonge.com/Equipment.html.

Table 3. Wells where historical (1922–2007) dissolved-solids-concentration data were collected in the surface geophysical subset area of the Mesilla Basin study area in Doña Ana County, New Mexico, and El Paso County, Texas.

[ft, foot; NAVD 88, North American Vertical Datum of 1988; bls, below land surface; TWDB, Texas Water Development Board; S, screened; --, not available; O, open hole; USGS, U.S. Geological Survey; NMBHO, New Mexico Office of Border Health; EPWU, El Paso Water Utilities]

Well identifier (fig. 16)	Station number	Source of well data	Latitude (decimal degrees)	Longitude (decimal degrees)	Land-surface altitude (ft) (NAVD 88)	Depth of well (ft)	Screened or open hole	Depth to top of open interval (ft bls)	Depth to bottom of open interval (ft bls)	Depth to midpoint of open interval[1] (ft)
H001	4903321	TWDB	31.97844	106.63777	3,788	122	S	42	122	82
H002	4903322	TWDB	31.97955	106.63833	3,789	1,206	--	--	--	--
H003	4903335	TWDB	31.97510	106.63388	3,787	1,550	O	0	1,550	775
H004	4903908	TWDB	31.90056	106.64278	3,768	125	S	74	125	100
H005	4903915	TWDB	31.89260	106.62610	3,763	72	--	--	--	--
H006	4903926	TWDB	31.90038	106.64388	3,768	65	S	30	65	48
H007	4904101	TWDB	31.99843	106.58999	3,866	277	S	145	265	[2]205
H008	4904102	TWDB	31.99843	106.59166	3,858	260	S	147	254	[2]200
H009	4904103	TWDB	31.95205	106.60638	3,781	560	S	274	550	[2]412
H010	4904114	TWDB	31.98260	106.59027	3,886	252	S	158	246	202
H011	4904124	TWDB	31.99316	106.60666	3,802	185	S	85	185	135
H012	4904125	TWDB	31.99639	106.60583	3,802	136	--	--	--	--
H013	4904135	TWDB	31.97482	106.59110	3,840	190	--	--	--	--
H014	4904136	TWDB	31.97205	106.59055	3,854	225	--	--	--	--
H015	4904148	TWDB	31.98899	106.58527	3,901	272	O	189	272	231
H016	4904150	TWDB	31.96288	106.58555	3,899	430	S	209	420	[2]314
H017	4904151	TWDB	31.97066	106.60388	3,786	313	S	165	313	[2]239
H018	4904161	TWDB	31.95944	106.60333	3,786	50	--	--	--	--
H019	4904164	TWDB	31.96038	106.61583	3,782	204	S	141	204	173
H020	4904166	TWDB	31.96722	106.59583	3,820	697	S	654	697	676
H021	4904169	TWDB	31.98677	106.59694	3,827	621	O	0	621	311
H022	4904172	TWDB	31.96482	106.58471	3,907	500	S	260	500	380
H023	4904173	TWDB	31.97371	106.59083	3,846	655	S	490	646	568
H024	4904174	TWDB	31.99232	106.61055	3,798	625	S	355	615	485
H025	4904179	TWDB	31.96816	106.60249	3,795	245	S	155	235	195
H026	4904182	TWDB	31.98038	106.62249	3,787	1,320	O	0	1,320	660
H027	4904183	TWDB	31.99593	106.61666	3,793	1,188	--	--	--	--
H028	4904184	TWDB	31.99982	106.61027	3,794	892	S	532	892	712
H029	4904185	TWDB	31.97694	106.60389	3,796	862	S	510	850	680
H030	4904186	TWDB	31.95917	106.59389	3,835	540	--	--	--	--
H031	4904187	TWDB	31.96000	106.59750	3,804	680	S	640	680	660
H032	4904201	TWDB	31.96149	106.58305	3,917	602	S	200	602	[2]401
H033	4904202	TWDB	31.96149	106.57527	3,993	410	S	220	410	315
H034	4904203	TWDB	31.97222	106.58361	3,899	408	O	325	408	367
H035	4904206	TWDB	31.96010	106.56694	4,077	600	--	--	--	--
H036	4904208	TWDB	31.96510	106.58333	3,916	478	S	200	478	[2]339
H037	4904404	TWDB	31.93871	106.61860	3,773	404	S	220	404	312
H038	4904427	TWDB	31.95094	106.61249	3,779	461	S	230	467	[2]348
H039	4904438	TWDB	31.95455	106.59555	3,829	142	S	40	142	91
H040	4904440	TWDB	31.94844	106.59499	3,836	170	S	90	170	130
H041	4904441	TWDB	31.94733	106.58582	3,907	874	--	--	--	--

Table 3. Wells where historical (1922–2007) dissolved-solids-concentration data were collected in the surface geophysical subset area of the Mesilla Basin study area in Doña Ana County, New Mexico, and El Paso County, Texas.—Continued

[ft, foot; NAVD 88, North American Vertical Datum of 1988; bls, below land surface; TWDB, Texas Water Development Board; S, screened; --, not available; O, open hole; USGS, U.S. Geological Survey; NMBHO, New Mexico Office of Border Health; EPWU, El Paso Water Utilities]

Well identifier (fig. 16)	Station number	Source of well data	Latitude (decimal degrees)	Longitude (decimal degrees)	Land-surface altitude (ft) (NAVD 88)	Depth of well (ft)	Screened or open hole	Depth to top of open interval (ft bls)	Depth to bottom of open interval (ft bls)	Depth to midpoint of open interval[1] (ft)
H042	4904449	TWDB	31.95167	106.59000	3,871	424	--	--	--	--
H043	4904452	TWDB	31.91733	106.58499	3,872	204	S	164	204	184
H044	4904454	TWDB	31.94816	106.60777	3,779	210	S	170	210	190
H045	4904457	TWDB	31.94566	106.61221	3,775	165	S	135	165	150
H046	4904459	TWDB	31.95250	106.59250	3,852	189	--	--	--	--
H047	4904460	TWDB	31.92899	106.53332	4,481	150	--	--	--	--
H048	4904461	TWDB	31.95288	106.59638	3,827	525	S	477	517	497
H049	4904462	TWDB	31.94733	106.59138	3,861	250	S	190	250	220
H050	4904464	TWDB	31.92733	106.59999	3,793	120	S	104	117	111
H051	4904465	TWDB	31.92733	106.59999	3,793	121	S	110	120	115
H052	4904488	TWDB	31.92955	106.62388	3,772	260	S	240	260	250
H053	4904489	TWDB	31.93139	106.62417	3,773	60	--	--	--	--
H054	4904495	TWDB	31.95816	106.60444	3,782	805	S	481	801	641
H055	4904501	TWDB	31.94344	106.57055	4,043	320	--	--	--	--
H056	4904505	TWDB	31.93677	106.58305	3,910	224	--	--	--	--
H057	4904507	TWDB	31.95732	106.57944	3,951	510	S	360	510	435
H058	4904508	TWDB	31.94066	106.57332	3,993	410	S	270	390	330
H059	4904707	TWDB	31.90066	106.62527	3,766	178	S	58	178	[2]118
H060	4904714	TWDB	31.91250	106.59361	3,816	167	--	--	--	--
H061	4904716	TWDB	31.89983	106.58610	3,843	550	--	--	--	--
H062	4904719	TWDB	31.88538	106.60221	3,762	128	--	--	--	--
H063	4904723	TWDB	31.88667	106.62528	3,761	10	--	--	--	--
H064	4904725	TWDB	31.88316	106.58916	3,813	150	--	--	--	--
H065	4904728	TWDB	31.90667	106.59278	3,803	377	S	105	377	[2]241
H066	4904730	TWDB	31.90010	106.61888	3,764	200	--	--	--	--
H067	4904742	TWDB	31.87511	106.62082	3,759	180	S	62	180	[2]121
H068	4904743	TWDB	31.91566	106.58944	3,843	160	--	--	--	--
H069	4904745	TWDB	31.88983	106.59138	3,795	120	--	--	--	--
H070	4904751	TWDB	31.89788	106.59388	3,774	202	--	--	--	--
H071	4904752	TWDB	31.88622	106.60221	3,762	196	S	160	190	175
H072	4904753	TWDB	31.90955	106.61971	3,767	1,062	--	--	--	--
H073	4904754	TWDB	31.88483	106.60832	3,761	65	S	45	65	55
H074	4904755	TWDB	31.89722	106.61694	3,763	60	--	--	--	--
H075	4904802	TWDB	31.88011	106.57749	3,921	320	S	270	310	290
H076	4904805	TWDB	31.89816	106.58221	3,875	236	S	150	230	190
H077	4912102	TWDB	31.87177	106.61444	3,759	123	--	--	--	--
H078	4912103	TWDB	31.86444	106.59472	3,757	130	--	--	--	--
H079	4912106	TWDB	31.87316	106.58749	3,796	407	--	--	--	--
H080	4912115	TWDB	31.85444	106.59972	3,753	92	O	92	92	92
H081	4912122	TWDB	31.84538	106.58610	3,754	65	--	--	--	--
H082	4912123	TWDB	31.86889	106.61000	3,757	120	--	--	--	--

Table 3. Wells where historical (1922–2007) dissolved-solids-concentration data were collected in the surface geophysical subset area of the Mesilla Basin study area in Doña Ana County, New Mexico, and El Paso County, Texas.—Continued

[ft, foot; NAVD 88, North American Vertical Datum of 1988; bls, below land surface; TWDB, Texas Water Development Board; S, screened; --, not available; O, open hole; USGS, U.S. Geological Survey; NMBHO, New Mexico Office of Border Health; EPWU, El Paso Water Utilities]

Well identifier (fig. 16)	Station number	Source of well data	Latitude (decimal degrees)	Longitude (decimal degrees)	Land-surface altitude (ft) (NAVD 88)	Depth of well (ft)	Screened or open hole	Depth to top of open interval (ft bls)	Depth to bottom of open interval (ft bls)	Depth to midpoint of open interval[1] (ft)
H083	4912204	TWDB	31.83511	106.55221	3,952	540	S	310	540	[2]425
H084	4912401	TWDB	31.82788	106.60110	3,747	116	S	103	127	[2]115
H085	4912432	TWDB	31.83122	106.60388	3,757	72	S	44	67	56
H086	4912602	TWDB	31.83122	106.53749	3,992	1,690	S	1,590	1,690	1,640
H087	4912603	TWDB	31.83066	106.52777	4,078	502	O	500	502	501
H088	4912606	TWDB	31.79427	106.52332	3,812	140	--	--	--	--
H089	313505106472301	USGS	31.79122	106.58555	3,905	450	--	--	--	--
H090	313505106472302	USGS	31.79039	106.58527	3,919	--	--	--	--	--
H091	313505106472303	USGS	31.79039	106.58527	3,919	--	--	--	--	--
H092	314710106342201	USGS	31.78611	106.57278	3,876	200	--	--	--	--
H093	314746106353601	USGS	31.78955	106.59443	4,054	190	--	--	--	--
H094	314817106325801	USGS	31.80483	106.54999	3,734	75	S	50	70	60
H095	314817106325802	USGS	31.80483	106.54999	3,734	166	--	--	--	--
H096	314854106340101	USGS	31.81538	106.56777	3,738	20	--	--	--	--
H097	315013106362601	USGS	31.83705	106.60777	3,747	168	S	138	158	148
H098	315013106362602	USGS	31.83705	106.60777	3,747	306	S	276	296	286
H099	315110106371701	USGS	31.85288	106.62194	3,752	223	S	192	212	202
H100	315110106371702	USGS	31.85288	106.62194	3,752	404	S	373	393	383
H101	315115106353401	USGS	31.85427	106.59332	3,754	20	--	--	--	--
H102	315152106371901	USGS	31.86455	106.62249	3,757	128	--	--	--	--
H103	315245106373201	USGS	31.87927	106.62610	3,758	20	--	--	--	--
H104	315245106380601	USGS	31.87927	106.63555	3,761	198	--	--	--	--
H105	315245106380602	USGS	31.87927	106.63555	3,761	427	--	--	--	--
H106	315309106364801	USGS	31.88566	106.53360	4,371	20	--	--	--	--
H107	315427106341801	USGS	31.90760	106.58055	3,893	300	S	200	300	250
H108	315428106344801	USGS	31.90788	106.58055	3,896	315	S	126	315	221
H109	315520106362701	USGS	31.92233	106.60805	3,769	160	S	76	155	116
H110	315523106362201	USGS	31.92316	106.60666	3,769	200	S	64	200	132
H111	315537106361501	USGS	31.92705	106.60471	3,771	122	S	52	122	[2]87
H112	315551106372101	USGS	31.93094	106.62305	3,772	200	S	62	200	131
H113	315551106372201	USGS	31.93094	106.62333	3,772	550	S	356	550	453
H114	315552106371001	USGS	31.93121	106.61999	3,773	200	S	61	200	131
H115	315554106365701	USGS	31.93177	106.61666	3,773	545	S	355	545	450
H116	315556106363101	USGS	31.93205	106.60944	3,772	200	S	100	200	150
H117	315556106364301	USGS	31.93233	106.61249	3,771	452	S	258	452	355
H118	315556106364302	USGS	31.93233	106.61249	3,771	194	S	62	194	128
H119	315557106361801	USGS	31.93260	106.60555	3,772	160	S	59	160	[2]110
H120	315557106365801	USGS	31.93260	106.61666	3,773	202	S	73	202	[2]138
H121	315607106365901	USGS	31.93538	106.61694	3,773	156	S	37	156	97
H122	315617106364201	USGS	31.93816	106.61221	3,772	170	S	53	170	112
H123	315619106362101	USGS	31.93871	106.60638	3,772	152	S	63	152	[2]108

Table 3. Wells where historical (1922–2007) dissolved-solids-concentration data were collected in the surface geophysical subset area of the Mesilla Basin study area in Doña Ana County, New Mexico, and El Paso County, Texas.—Continued

[ft, foot; NAVD 88, North American Vertical Datum of 1988; bls, below land surface; TWDB, Texas Water Development Board; S, screened; --, not available; O, open hole; USGS, U.S. Geological Survey; NMBHO, New Mexico Office of Border Health; EPWU, El Paso Water Utilities]

Well identifier (fig. 16)	Station number	Source of well data	Latitude (decimal degrees)	Longitude (decimal degrees)	Land-surface altitude (ft) (NAVD 88)	Depth of well (ft)	Screened or open hole	Depth to top of open interval (ft bls)	Depth to bottom of open interval (ft bls)	Depth to midpoint of open interval[1] (ft)
H124	315622106391701	USGS	31.93955	106.65527	3,782	706	--	--	--	--
H125	315622106391702	USGS	31.93955	106.65527	3,782	--	--	--	--	--
H126	315622106391703	USGS	31.93955	106.65527	3,782	--	--	--	--	--
H127	315622106391705	USGS	31.93955	106.65527	3,782	1,765	--	1,745	1,755	1,750
H128	315627106353101	USGS	31.94094	106.59249	3,843	235	--	--	--	--
H129	315627106363701	USGS	31.94149	106.61138	3,773	1,013	S	528	1,013	771
H130	315631106393301	USGS	31.94205	106.65972	3,790	--	--	--	--	--
H131	315652106362301	USGS	31.94788	106.60694	3,779	221	S	97	220	[2]158
H132	315652106362302	USGS	31.94788	106.60694	3,779	447	S	242	447	[2]344
H133	315652106364301	USGS	31.94788	106.61249	3,778	219	S	78	219	149
H134	315703106364301	USGS	31.95094	106.61249	3,779	1,060	S	586	1,060	823
H135	315712106361201	USGS	31.95371	106.60444	3,784	52	S	45	50	48
H136	315712106361202	USGS	31.95371	106.60444	3,784	156	S	149	154	152
H137	315712106361203	USGS	31.95371	106.60444	3,784	334	S	327	332	330
H138	315712106361204	USGS	31.95371	106.60444	3,784	803	S	796	801	799
H139	315712106361801	USGS	31.95371	106.60583	3,781	47	S	40	45	43
H140	315712106361802	USGS	31.95371	106.60583	3,781	158	S	151	156	154
H141	315712106361803	USGS	31.95371	106.60583	3,781	300	S	293	298	296
H142	315712106361804	USGS	31.95371	106.60583	3,781	799	S	792	797	795
H143	315712106362301	USGS	31.95371	106.60721	3,782	58	S	51	56	54
H144	315712106362302	USGS	31.95371	106.60721	3,782	158	S	151	156	154
H145	315712106362303	USGS	31.95371	106.60721	3,782	298	S	291	296	294
H146	315712106362304	USGS	31.95399	106.60694	3,782	799	S	792	797	795
H147	315712106364301	USGS	31.95344	106.61277	3,779	59	S	52	57	55
H148	315712106364302	USGS	31.95344	106.61277	3,779	159	S	152	157	155
H149	315712106364303	USGS	31.95344	106.61277	3,779	299	S	292	297	295
H150	315712106364304	USGS	31.95344	106.61277	3,779	800	S	793	798	796
H151	315717106362201	USGS	31.95482	106.60666	3,781	900	S	510	900	705
H152	315717106364001	USGS	31.95510	106.61166	3,780	1,072	S	585	1,050	818
H153	315720106362201	USGS	31.95566	106.60666	3,781	400	S	198	400	299
H154	315720106415601	USGS	31.95482	106.70083	4,101	722	--	--	--	--
H155	315733106364401	USGS	31.95927	106.61305	3,781	202	S	102	202	152
H156	315733106364501	USGS	31.95927	106.61305	3,781	1,090	S	544	1,090	817
H157	315734106364201	USGS	31.95955	106.61221	3,781	550	S	291	550	421
H158	315742106325001	USGS	31.96177	106.54777	4,267	517	O	508	517	513
H159	315758106365701	USGS	31.96621	106.61638	3,782	1,149	S	660	1,149	905
H160	315803106364501	USGS	31.96732	106.61305	3,782	1,063	S	740	1,061	[2]900
H161	315804106354301	USGS	31.96844	106.59638	3,819	190	S	47	190	119
H162	315805106354501	USGS	31.96816	106.59638	3,820	580	S	460	560	510
H163	315807106362901	USGS	31.96871	106.60860	3,784	950	S	543	950	747
H164	315817106370601	USGS	31.97149	106.61888	3,784	1,206	S	630	1,200	915

Table 3. Wells where historical (1922–2007) dissolved-solids-concentration data were collected in the surface geophysical subset area of the Mesilla Basin study area in Doña Ana County, New Mexico, and El Paso County, Texas.—Continued

[ft, foot; NAVD 88, North American Vertical Datum of 1988; bls, below land surface; TWDB, Texas Water Development Board; S, screened; --, not available; O, open hole; USGS, U.S. Geological Survey; NMBHO, New Mexico Office of Border Health; EPWU, El Paso Water Utilities]

Well identifier (fig. 16)	Station number	Source of well data	Latitude (decimal degrees)	Longitude (decimal degrees)	Land-surface altitude (ft) (NAVD 88)	Depth of well (ft)	Screened or open hole	Depth to top of open interval (ft bls)	Depth to bottom of open interval (ft bls)	Depth to midpoint of open interval[1] (ft)
H165	315819106370701	USGS	31.97205	106.61916	3,784	506	S	209	506	358
H166	315830106380801	USGS	31.97510	106.63610	3,787	136	--	55	136	96
H167	315831106345401	USGS	31.97538	106.58221	3,904	500	S	332	492	412
H168	315852106382401	USGS	31.98121	106.64055	3,789	320	--	--	--	--
H169	315900106360101	USGS	31.98344	106.60083	3,805	768	S	437	758	598
H170	315901106355001	USGS	31.98371	106.59777	3,823	264	S	40	264	152
H171	315915106354701	USGS	31.98816	106.59749	3,823	336	S	146	336	241
H172	315916106362201	USGS	31.98788	106.60666	3,800	260	S	90	260	175
H173	315920106350301	USGS	31.98899	106.58471	3,899	230	S	200	230	215
H174	315940106350501	USGS	31.99455	106.58527	3,871	620	--	--	--	--
H175	315943106365001	USGS	31.99538	106.61444	3,794	20	--	--	--	--
H176	315955106362201	USGS	31.99649	106.60694	3,800	600	S	340	600	470
H177	320005106354601	USGS	32.00232	106.59416	3,844	400	--	--	--	--
H178	320032106381101	USGS	32.00899	106.63805	3,793	1,050	--	--	--	--
H179	26S.03E.26.242	Wilson[3]	32.02093	106.59944	3,838	62	--	--	--	--
H180	26S.03E.32.343	Wilson[3]	31.99843	106.66222	3,792	115	--	--	--	--
H181	26S.03E.34.113	Wilson[3]	32.00843	106.63083	3,794	141	--	--	--	--
H182	26S.03E.35.141	Wilson[3]	32.00482	106.61027	3,791	800	--	--	--	--
H183	26S.03E.35.241	Wilson[3]	32.00455	106.58527	3,915	150	--	--	--	--
H184	26S.03E.36.144	Wilson[3]	32.00371	106.59333	3,840	240	--	--	--	--
H185	26S.03E.36.321	Wilson[3]	32.00232	106.59416	3,844	400	--	--	--	--
H186	27S.03E.04.231	Wilson[3]	31.99205	106.63944	3,795	132	--	--	--	--
H187	27S.03E.09.243	Wilson[3]	31.97510	106.63610	3,787	--	--	--	--	--
H188	27S.03E.15.143	Wilson[3]	31.96038	106.62777	3,784	86	--	--	--	--
H189	27S.03E.15.441	Wilson[3]	31.95427	106.61805	3,780	1,200	--	--	--	--
H190	27S.03E.20.324	Wilson[3]	31.94177	106.66083	3,801	60	--	--	--	--
H191	27S.03E.20.333	Wilson[3]	31.93955	106.66222	3,791	146	--	--	--	--
H192	27S.03E.28.341	Wilson[3]	31.92510	106.64305	3,777	136	--	--	--	--
H193	27S.03E.32.321	Wilson[3]	31.91483	106.66166	3,799	178	--	--	--	--
H194	28S.02E.13.333	Wilson[3]	31.86316	106.70194	4,111	481	--	--	--	--
H195	28S.03E.04.322	Wilson[3]	31.89649	106.64721	3,768	103	--	--	--	--
H196	28S.03E.05.422	Wilson[3]	31.90066	106.65055	3,770	122	--	--	--	--
H197	28S.03E.16.124	Wilson[3]	31.87622	106.64166	3,762	148	--	--	--	--
H198	28S.03E.21.224	Wilson[3]	31.86205	106.63527	3,761	87	--	--	--	--
H199	28S.03E.27.111	Wilson[3]	31.83538	106.62138	3,826	1,573	--	--	--	--
H200	28S.03E.34.331	Wilson[3]	31.82400	106.63249	4,001	1,004	--	--	--	--
H201	29S.03E.01.111	Wilson[3]	31.81844	106.59582	3,753	155	--	--	--	--
H202	29S.03E.01.133	Wilson[3]	31.81622	106.59832	3,799	119	--	--	--	--
H203	29S.03E.01.411a	Wilson[3]	31.81427	106.58943	3,741	83	--	--	--	--
H204	29S.03E.01.431	Wilson[3]	31.81011	106.59027	3,792	178	--	--	--	--
H205	29S.03E.01.433	Wilson[3]	31.80844	106.58971	3,797	181	--	--	--	--

Table 3. Wells where historical (1922–2007) dissolved-solids-concentration data were collected in the surface geophysical subset area of the Mesilla Basin study area in Doña Ana County, New Mexico, and El Paso County, Texas.—Continued

[ft, foot; NAVD 88, North American Vertical Datum of 1988; bls, below land surface; TWDB, Texas Water Development Board; S, screened; --, not available; O, open hole; USGS, U.S. Geological Survey; NMBHO, New Mexico Office of Border Health; EPWU, El Paso Water Utilities]

Well identifier (fig. 16)	Station number	Source of well data	Latitude (decimal degrees)	Longitude (decimal degrees)	Land-surface altitude (ft) (NAVD 88)	Depth of well (ft)	Screened or open hole	Depth to top of open interval (ft bls)	Depth to bottom of open interval (ft bls)	Depth to midpoint of open interval[1] (ft)
H206	29S.03E.01.443	Wilson[3]	31.80844	106.58610	3,761	126	--	--	--	--
H207	29S.03E.02.233	Wilson[3]	31.81455	106.60666	3,912	352	--	--	--	--
H208	29S.03E.12.212	Wilson[3]	31.80594	106.58971	3,796	294	--	--	--	--
H209	29S.03E.12.223a	Wilson[3]	31.80372	106.58610	3,784	206	--	--	--	--
H210	29S.03E.12.224	Wilson[3]	31.80427	106.58277	3,745	120	--	--	--	--
H211	29S.04E.07.131a	Wilson[3]	31.80344	106.58166	3,736	274	--	--	--	--
H212	29S.04E.07.141	Wilson[3]	31.80344	106.57805	3,737	281	--	--	--	--
H213	29S.04E.08.221	Wilson[3]	31.80650	106.55249	3,732	20	--	--	--	--
H214	29S.04E.08.311	Wilson[3]	31.79900	106.56499	3,732	246	--	--	--	--
H215	29S.04E.17.112	Wilson[3]	31.79177	106.56277	3,778	420	--	--	--	--
H216	29S.04E.18.132	Wilson[3]	31.78816	106.57999	3,881	393	--	--	--	--
H217	BHO040	NMBHO	31.94656	106.66319	3,806	80	--	--	--	--
H218	BHO041	NMBHO	31.94742	106.66208	3,797	94	--	--	--	--
H219	BHO043	NMBHO	31.94558	106.66311	3,815	100	--	--	--	--
H220	BHO047	NMBHO	31.95064	106.66275	3,807	84	--	--	--	--
H221	BHO048	NMBHO	31.95075	106.66300	3,808	80	--	--	--	--
H222	BHO053	NMBHO	31.95044	106.65864	3,786	118	--	--	--	--
H223	BHO054	NMBHO	31.94972	106.65936	3,786	120	--	--	--	--
H224	BHO073	NMBHO	32.00031	106.64175	3,796	72	--	--	--	--
H225	BHO074	NMBHO	31.99819	106.64294	3,794	108	--	--	--	--
H226	BHO079	NMBHO	31.99922	106.63103	3,789	84	--	--	--	--
H227	BHO090	NMBHO	32.00064	106.63019	3,790	230	--	--	--	--
H228	BHO092	NMBHO	31.84175	106.60644	3,750	40	--	--	--	--
H229	BHO093	NMBHO	31.88822	106.65044	3,786	90	--	--	--	--
H230	BHO116	NMBHO	31.88906	106.64700	3,774	130	--	--	--	--
H231	BHO119	NMBHO	32.02017	106.65908	3,801	60	--	--	--	--
H232	BR-MW-12	EPWU	31.79950	106.53820	3,727	--	S	15	27	21
H233	GW-EPE-MW-09	EPWU	31.80550	106.54870	3,733	26	S	6	26	16
H234	GW-EPE-MW-17	EPWU	31.80440	106.54900	3,734	13	S	1	13	7
H235	GW-EPE-MW-20	EPWU	31.80590	106.54700	3,732	13	S	3	13	8
H236	GW-EPE-MW-21	EPWU	31.80740	106.55050	3,732	17	--	--	--	--
H237	GW-EPE-MW-22	EPWU	31.80670	106.55030	3,732	16	--	--	--	--
H238	GW-EPE-MW-23	EPWU	31.80610	106.55070	3,733	17	--	--	--	--
H239	GW-EPE-MW-AO	EPWU	31.80670	106.54910	3,732	13	S	3	13	8

[1]Multiple openings were treated as one opening from top of first opening interval to bottom of last opening interval.

[2]Well contained multiple opening intervals; top of first opening interval and bottom of last opening interval reported.

[3]Data compiled from Wilson and others (1981).

Table 4. Historical (1922–2007) dissolved-solids concentrations and resistivity values from the three-dimensional model of the combined inverse modeling results of the direct-current resistivity and time-domain electromagnetic soundings in the surface geophysical subset area of the Mesilla Basin study area in Doña Ana County, New Mexico, and El Paso County, Texas.

[mm/dd/yyyy, month/day/year; ft, foot; mg/L, milligram per liter; 3D, three-dimensional; DC, direct-current; TDEM, time-domain electromagnetic; ohm-m, ohm-meter; --, not available; TWDB, Texas Water Development Board; USGS, U.S. Geological Survey; NMOSE, New Mexico Office of the State Engineer; NMBHO, New Mexico Office of Border Health; EPWU, El Paso Water Utilities]

Well identifier (fig. 16)	Sample date (mm/dd/yyyy)	Sample start time	Sample depth (ft)	Explanation of how sample depth was determined	Source of well information	Dissolved solids (mg/L)	Resistivity obtained from 3D model of DC resistivity and TDEM soundings (ohm-m)[1]
H001	06/30/1953	--	82	Middle of open interval	TWDB	676	44
H002	11/12/1953	--	217	Reported	Wilson[2]	400	20
H002	11/12/1953	--	328	Reported	Wilson[2]	356	18
H002	11/13/1953	--	457	Reported	Wilson[2]	374	18
H002	11/13/1953	--	584	Reported	Wilson[2]	603	19
H002	11/14/1953	--	776	Reported	Wilson[2]	384	19
H002	11/16/1953	--	1,037	Reported	Wilson[2]	356	18
H003	07/22/1990	--	269	Reported	TWDB	301	23
H003	07/22/1990	--	494	Reported	TWDB	547	19
H003	07/21/1990	--	769	Reported	TWDB	361	17
H003	07/21/1990	--	1,063	Reported	TWDB	326	16
H003	07/21/1990	--	1,210	Reported	TWDB	317	15
H004	03/26/1952	--	100	Middle of open interval	TWDB	1,108	23
H005	08/31/1952	--	72	Bottom of well[4]	TWDB	2,301	22
H006	02/15/1990	--	48	Middle of open interval	TWDB	1,579	26
H006	02/04/1990	--	55	Reported	TWDB	1,748	25
H006	02/04/1990	--	280	Reported	TWDB	1,326	16
H006	02/01/1990	--	510	Reported	TWDB	1,728	11
H006	02/01/1990	--	860	Reported	TWDB	2,917	8
H007	08/28/1968	--	205	Middle of open interval[3]	TWDB	882	39
H008	08/28/1968	--	201	Middle of open interval[3]	TWDB	982	35
H009	08/17/1966	--	412	Middle of open interval[3]	TWDB	344	17
H010	10/27/1977	--	202	Middle of open interval	TWDB	1,042	33
H011	06/18/1952	--	135	Middle of open interval	TWDB	1,106	16
H012	09/16/1948	--	136	Bottom of well[4]	TWDB	1,059	17
H013	06/18/1952	--	190	Bottom of well[4]	TWDB	971	33
H014	06/18/1952	--	225	Bottom of well[4]	TWDB	1,038	34
H015	08/17/1966	--	231	Middle of open interval	TWDB	774	42
H016	10/06/1970	--	310	Reported	TWDB	972	41
H016	08/14/1975	--	315	Middle of open interval[3]	TWDB	954	41
H016	09/12/1970	--	420	Reported	TWDB	900	32
H017	11/02/1973	--	58	Reported	TWDB	2,017	27
H017	10/31/1973	--	195	Reported	TWDB	1,494	22
H017	10/31/1973	--	250	Reported	TWDB	998	22
H018	10/27/1977	--	50	Bottom of well[4]	TWDB	896	26
H019	05/29/1980	--	173	Middle of open interval	TWDB	986	13
H020	09/02/1975	--	676	Middle of open interval	TWDB	161	18
H021	05/08/1978	--	236	Reported	TWDB	872	21
H021	06/15/1978	--	311	Middle of open interval	TWDB	544	19
H021	05/09/1978	--	364	Reported	TWDB	628	19

Table 4. Historical (1922–2007) dissolved-solids concentrations and resistivity values from the three-dimensional model of the combined inverse modeling results of the direct-current resistivity and time-domain electromagnetic soundings in the surface geophysical subset area of the Mesilla Basin study area in Doña Ana County, New Mexico, and El Paso County, Texas.—Continued

[mm/dd/yyyy, month/day/year; ft, foot; mg/L, milligram per liter; 3D, three-dimensional; DC, direct-current; TDEM, time-domain electromagnetic; ohm-m, ohm-meter; --, not available; TWDB, Texas Water Development Board; USGS, U.S. Geological Survey; NMOSE, New Mexico Office of the State Engineer; NMBHO, New Mexico Office of Border Health; EPWU, El Paso Water Utilities]

Well identifier (fig. 16)	Sample date (mm/dd/yyyy)	Sample start time	Sample depth (ft)	Explanation of how sample depth was determined	Source of well information	Dissolved solids (mg/L)	Resistivity obtained from 3D model of DC resistivity and TDEM soundings (ohm-m)[1]
H021	05/09/1978	--	484	Reported	TWDB	634	18
H021	05/09/1978	--	542	Reported	TWDB	651	17
H021	05/09/1978	--	612	Reported	TWDB	476	17
H022	09/16/1983	--	585	Reported	TWDB	1,072	25
H022	09/16/1983	--	625	Reported	TWDB	1,072	24
H023	10/12/1983	22:00	185	Reported	TWDB	1,619	35
H023	10/12/1983	22:00	508	Reported	TWDB	914	23
H023	10/12/1983	22:00	630	Reported	TWDB	928	21
H023	10/12/1983	11:00	725	Reported	TWDB	989	20
H024	05/20/1988	14:47	485	Middle of open interval	TWDB	580	13
H025	03/26/1987	--	194	Reported	TWDB	1,089	25
H026	08/01/1990	--	240	Reported	TWDB	683	17
H026	08/01/1990	--	405	Reported	TWDB	740	16
H026	08/01/1990	--	530	Reported	TWDB	518	17
H026	07/31/1990	--	880	Reported	TWDB	305	18
H026	07/31/1990	--	1,113	Reported	TWDB	275	17
H027	08/08/1990	--	180	Reported	TWDB	1,437	10
H027	08/07/1990	--	405	Reported	TWDB	911	11
H027	08/07/1990	--	1,035	Reported	TWDB	417	16
H027	08/07/1990	--	1,171	Reported	TWDB	465	16
H028	03/16/1995	--	712	Middle of open interval	TWDB	372	14
H028	11/12/1993	--	765	Reported	TWDB	404	14
H028	11/12/1993	--	885	Reported	TWDB	410	14
H029	01/16/1997	--	680	Middle of open interval	TWDB	287	19
H030	06/04/1998	--	540	Bottom of well[4]	TWDB	645	15
H031	06/04/1998	--	660	Middle of open interval	TWDB	814	16
H032	10/27/1977	--	315	Reported	TWDB	980	47
H032	10/14/1960	--	422	Reported	TWDB	1,085	36
H033	10/16/1972	--	315	Reported	TWDB	819	70
H034	08/17/1966	--	367	Middle of open interval	TWDB	774	38
H035	10/13/1960	--	315	Reported	Wilson[2]	966	97
H036	02/13/1985	--	339	Middle of open interval[3]	TWDB	934	44
H037	02/25/2000	10:06	312	Middle of open interval	TWDB	584	17
H038	11/06/2000	10:40	349	Middle of open interval[3]	TWDB	612	12
H039	06/18/1952	--	91	Middle of open interval	TWDB	436	41
H040	06/10/1980	--	130	Middle of open interval	TWDB	1,816	31
H041	08/28/1953	--	220	Reported	Wilson[2]	999	49
H041	08/17/1953	--	351	Reported	Wilson[2]	860	35
H041	08/20/1953	--	419	Reported	Wilson[2]	860	30
H041	08/21/1953	--	634	Reported	Wilson[2]	992	21

Table 4. Historical (1922–2007) dissolved-solids concentrations and resistivity values from the three-dimensional model of the combined inverse modeling results of the direct-current resistivity and time-domain electromagnetic soundings in the surface geophysical subset area of the Mesilla Basin study area in Doña Ana County, New Mexico, and El Paso County, Texas.—Continued

[mm/dd/yyyy, month/day/year; ft, foot; mg/L, milligram per liter; 3D, three-dimensional; DC, direct-current; TDEM, time-domain electromagnetic; ohm-m, ohm-meter; --, not available; TWDB, Texas Water Development Board; USGS, U.S. Geological Survey; NMOSE, New Mexico Office of the State Engineer; NMBHO, New Mexico Office of Border Health; EPWU, El Paso Water Utilities]

Well identifier (fig. 16)	Sample date (mm/dd/yyyy)	Sample start time	Sample depth (ft)	Explanation of how sample depth was determined	Source of well information	Dissolved solids (mg/L)	Resistivity obtained from 3D model of DC resistivity and TDEM soundings (ohm-m)[1]
H042	06/04/1998	--	424	Bottom of well[4]	TWDB	917	23
H043	07/11/1958	--	184	Middle of open interval	TWDB	826	37
H044	11/09/1976	--	190	Middle of open interval	TWDB	807	17
H045	10/27/1977	--	150	Middle of open interval	TWDB	1,287	18
H046	10/27/1977	--	189	Bottom of well[4]	TWDB	2,375	35
H047	08/29/1979	--	150	Reported	TWDB	1,479	--
H048	07/15/1989	--	497	Middle of open interval	TWDB	258	16
H048	03/15/1980	--	526	Reported	TWDB	274	16
H049	05/29/1980	--	220	Middle of open interval	TWDB	1,256	32
H050	09/22/1966	--	111	Middle of open interval	TWDB	604	27
H051	05/29/1980	--	115	Middle of open interval	TWDB	993	27
H052	03/18/1987	--	250	Middle of open interval	TWDB	494	20
H053	02/23/1990	--	60	Bottom of well[4]	TWDB	879	28
H054	10/21/1992	--	305	Reported	TWDB	649	14
H054	10/21/1992	--	485	Reported	TWDB	372	33
H054	01/15/1998	11:30	641	Middle of open interval	TWDB	466	36
H054	10/20/1992	--	705	Reported	TWDB	328	35
H054	10/20/1992	--	795	Reported	TWDB	355	31
H055	08/31/1953	--	320	Bottom of well[4]	TWDB	959	81
H056	05/18/1974	--	224	Bottom of well[4]	TWDB	815	47
H057	07/17/1986	--	435	Middle of open interval	TWDB	911	41
H057	11/27/1977	--	445	Reported	TWDB	935	40
H058	03/26/1987	--	330	Middle of open interval	TWDB	959	64
H059	02/01/1990	--	118	Middle of open interval[3]	TWDB	1,299	23
H060	01/11/1952	--	167	Bottom of well[4]	TWDB	1,059	34
H061	08/14/1952	--	121	Reported	Wilson[2]	1,000	64
H061	08/09/1952	--	220	Reported	Wilson[2]	3,500	45
H061	08/10/1953	--	313	Reported	Wilson[2]	3,370	34
H061	08/13/1953	--	425	Reported	Wilson[2]	3,510	25
H062	03/30/1951	--	128	Bottom of well[4]	TWDB	6,476	13
H063	01/01/1922	--	10	Reported	Wilson[2]	1,004	30
H063	01/01/1922	--	260	Reported	Wilson[2]	1,800	7
H063	01/01/1922	--	470	Reported	Wilson[2]	3,740	6
H063	01/01/1922	--	1,007	Reported	Wilson[2]	4,542	7
H064	11/16/1977	--	150	Bottom of well[4]	TWDB	811	36
H065	06/06/1970	--	172	Reported	TWDB	864	33
H065	01/30/1989	--	241	Middle of open interval[3]	TWDB	1,340	27
H065	06/09/1970	--	280	Reported	TWDB	1,451	24
H065	06/11/1970	--	382	Reported	TWDB	2,646	19
H066	01/13/1990	--	200	Bottom of well[4]	TWDB	1,142	19

Table 4. Historical (1922–2007) dissolved-solids concentrations and resistivity values from the three-dimensional model of the combined inverse modeling results of the direct-current resistivity and time-domain electromagnetic soundings in the surface geophysical subset area of the Mesilla Basin study area in Doña Ana County, New Mexico, and El Paso County, Texas.—Continued

[mm/dd/yyyy, month/day/year; ft, foot; mg/L, milligram per liter; 3D, three-dimensional; DC, direct-current; TDEM, time-domain electromagnetic; ohm-m, ohm-meter; --, not available; TWDB, Texas Water Development Board; USGS, U.S. Geological Survey; NMOSE, New Mexico Office of the State Engineer; NMBHO, New Mexico Office of Border Health; EPWU, El Paso Water Utilities]

Well identifier (fig. 16)	Sample date (mm/dd/yyyy)	Sample start time	Sample depth (ft)	Explanation of how sample depth was determined	Source of well information	Dissolved solids (mg/L)	Resistivity obtained from 3D model of DC resistivity and TDEM soundings (ohm-m)[1]
H067	03/31/1978	--	112	Reported	TWDB	1,600	13
H068	08/29/1979	--	160	Reported	TWDB	646	38
H069	08/29/1979	--	120	Reported	TWDB	2,250	39
H070	04/13/1987	--	67	Reported	TWDB	6,308	41
H070	04/10/1987	--	134	Reported	TWDB	4,677	32
H070	04/10/1987	--	200	Reported	TWDB	4,002	26
H071	04/08/1987	--	116	Reported	TWDB	1,472	15
H071	04/08/1987	--	179	Reported	TWDB	1,477	11
H071	04/08/1987	8:00	241	Reported	TWDB	1,692	8
H072	12/29/1989	--	135	Reported	TWDB	626	26
H072	12/29/1989	--	335	Reported	TWDB	846	18
H072	12/27/1989	--	585	Reported	TWDB	1,732	13
H072	12/23/1989	--	1,050	Reported	TWDB	5,382	9
H073	01/17/1990	--	50	Reported	TWDB	1,110	22
H073	01/17/1990	--	260	Reported	TWDB	2,327	8
H073	01/16/1990	--	515	Reported	TWDB	4,399	5
H073	01/16/1990	--	650	Reported	TWDB	5,928	5
H074	02/23/1990	--	60	Bottom of well[4]	TWDB	1,073	27
H075	01/25/1982	--	120	Reported	TWDB	2,982	139
H075	01/25/1982	--	160	Reported	TWDB	3,497	110
H076	10/05/1988	--	190	Middle of open interval	TWDB	1,791	67
H077	03/30/1951	--	123	Bottom of well[4]	TWDB	1,568	13
H078	03/26/1952	--	130	Bottom of well[4]	TWDB	3,369	8
H079	11/09/1953	--	120	Reported	TWDB	1,358	26
H079	11/05/1953	--	238	Reported	TWDB	4,012	17
H080	03/14/1952	--	92	Middle of open interval	Wilson[2]	2,190	12
H081	08/08/1972	--	65	Bottom of well[4]	TWDB	3,505	11
H082	01/15/1973	--	120	Bottom of well[4]	TWDB	1,478	13
H083	01/10/1952	--	382	Reported	TWDB	727	6
H084	06/12/1942	--	109	Reported	Wilson[2]	1,070	8
H085	11/16/1977	--	56	Middle of open interval	TWDB	796	11
H086	06/09/1953	--	1,640	Middle of open interval	TWDB	569	--
H087	10/10/1953	--	501	Middle of open interval	TWDB	556	--
H088	06/25/1953	--	140	Bottom of well[4]	Wilson[2]	1,560	--
H089	08/01/1975	12:00	224	Reported	Wilson[2]	1,700	9
H089	08/01/1975	--	310	Reported	Wilson[2]	3,180	9
H089	08/01/1975	--	400	Reported	Wilson[2]	2,780	9
H090	08/01/1975	12:00	310	Reported	NMOSE	3,180	10
H091	08/01/1975	12:00	400	Reported	NMOSE	2,780	10
H092	12/03/1974	--	200	Bottom of well[4]	Wilson[2]	1,210	--

Table 4. Historical (1922–2007) dissolved-solids concentrations and resistivity values from the three-dimensional model of the combined inverse modeling results of the direct-current resistivity and time-domain electromagnetic soundings in the surface geophysical subset area of the Mesilla Basin study area in Doña Ana County, New Mexico, and El Paso County, Texas.—Continued

[mm/dd/yyyy, month/day/year; ft, foot; mg/L, milligram per liter; 3D, three-dimensional; DC, direct-current; TDEM, time-domain electromagnetic; ohm-m, ohm-meter; --, not available; TWDB, Texas Water Development Board; USGS, U.S. Geological Survey; NMOSE, New Mexico Office of the State Engineer; NMBHO, New Mexico Office of Border Health; EPWU, El Paso Water Utilities]

Well identifier (fig. 16)	Sample date (mm/dd/yyyy)	Sample start time	Sample depth (ft)	Explanation of how sample depth was determined	Source of well information	Dissolved solids (mg/L)	Resistivity obtained from 3D model of DC resistivity and TDEM soundings (ohm-m)[1]
H093	12/03/1974	--	190	Bottom of well[4]	Wilson[2]	459	--
H094	02/17/2006	--	60	Middle of open interval	EPWU	19,000	3
H095	02/17/2006	--	166	Bottom of well[4]	EPWU	31,000	3
H096	04/21/1986	--	20	Bottom of well[4]	USGS	11,141	3
H097	02/17/2006	--	148	Middle of open interval	EPWU	4,700	10
H098	08/12/2005	--	286	Middle of open interval	EPWU	4,600	8
H099	08/12/2005	--	202	Middle of open interval	EPWU	2,000	11
H100	08/12/2005	--	383	Middle of open interval	EPWU	4,400	7
H101	04/22/1986	--	20	Bottom of well[4]	USGS	2,456	7
H102	03/30/1951	--	128	Bottom of well[4]	TWDB	3,078	13
H103	05/01/1986	--	20	Bottom of well[4]	USGS	553	19
H104	08/11/2005	--	198	Bottom of well[4]	EPWU	1,500	12
H105	08/12/2005	--	427	Bottom of well[4]	EPWU	3,500	7
H106	04/22/1986	--	20	Bottom of well[4]	USGS	2,042	--
H107	04/21/1988	--	250	Middle of open interval	TWDB	1,260	44
H108	01/15/1976	--	221	Middle of open interval	TWDB	1,502	48
H109	10/28/1997	16:20	116	Middle of open interval	TWDB	975	26
H110	10/05/1995	16:12	132	Middle of open interval	TWDB	983	25
H111	10/28/1997	16:27	87	Middle of open interval[3]	TWDB	713	25
H112	10/24/1995	8:10	131	Middle of open interval	TWDB	572	24
H113	01/22/1998	12:22	453	Middle of open interval	TWDB	313	15
H114	10/24/1995	8:15	131	Middle of open interval	TWDB	522	23
H115	11/04/1987	--	370	Reported	TWDB	502	15
H115	09/21/1983	11:35	400	Reported	TWDB	520	15
H115	07/02/1979	--	450	Middle of open interval	TWDB	358	14
H115	11/15/1984	--	474	Reported	TWDB	477	14
H116	09/19/1983	--	150	Middle of open interval	TWDB	777	18
H116	09/03/1953	--	195	Reported	TWDB	859	16
H117	12/16/1961	--	263	Reported	Wilson[2]	414	16
H117	12/20/1961	--	351	Reported	Wilson[2]	197	14
H117	01/27/2000	10:06	355	Middle of open interval	TWDB	701	14
H117	12/17/1961	--	448	Reported	Wilson[2]	558	13
H118	10/28/1996	11:50	128	Middle of open interval	TWDB	973	20
H119	10/28/1997	16:32	110	Middle of open interval[3]	TWDB	655	18
H120	10/28/1997	16:42	138	Middle of open interval[3]	TWDB	742	22
H121	10/28/1997	16:50	97	Middle of open interval	TWDB	1,117	24
H122	07/02/1986	--	112	Middle of open interval	TWDB	1,529	21
H123	10/28/1996	12:03	108	Middle of open interval[3]	TWDB	655	18
H124	07/24/1975	17:00	205	Reported	Wilson[2]	603	25
H124	07/24/1975	--	460	Reported	Wilson[2]	523	18

Table 4. Historical (1922–2007) dissolved-solids concentrations and resistivity values from the three-dimensional model of the combined inverse modeling results of the direct-current resistivity and time-domain electromagnetic soundings in the surface geophysical subset area of the Mesilla Basin study area in Doña Ana County, New Mexico, and El Paso County, Texas.—Continued

[mm/dd/yyyy, month/day/year; ft, foot; mg/L, milligram per liter; 3D, three-dimensional; DC, direct-current; TDEM, time-domain electromagnetic; ohm-m, ohm-meter; --, not available; TWDB, Texas Water Development Board; USGS, U.S. Geological Survey; NMOSE, New Mexico Office of the State Engineer; NMBHO, New Mexico Office of Border Health; EPWU, El Paso Water Utilities]

Well identifier (fig. 16)	Sample date (mm/dd/yyyy)	Sample start time	Sample depth (ft)	Explanation of how sample depth was determined	Source of well information	Dissolved solids (mg/L)	Resistivity obtained from 3D model of DC resistivity and TDEM soundings (ohm-m)[1]
H124	07/24/1975	--	650	Reported	Wilson[2]	304	14
H125	07/24/1975	14:00	460	Reported	NMOSE	523	18
H126	07/24/1975	9:45	650	Reported	NMOSE	304	14
H127	11/05/2003	--	1,750	Reported	USGS	5,900	8
H128	05/04/1988	--	235	Bottom of well[4]	USGS	830	26
H129	10/18/1984	--	200	Reported	TWDB	930	17
H129	10/18/1984	--	350	Reported	TWDB	938	14
H129	11/04/1987	--	700	Reported	TWDB	1,261	12
H129	09/20/1983	11:15	771	Middle of open interval	TWDB	1,324	12
H130	07/24/1975	12:00	58	Reported	NMOSE	682	29
H131	05/30/1998	11:00	159	Middle of open interval[3]	TWDB	720	19
H131	08/05/1966	--	160	Reported	Wilson[2]	884	19
H132	11/06/2000	10:30	345	Middle of open interval[3]	TWDB	557	15
H133	10/05/1995	15:27	149	Middle of open interval	TWDB	1,376	14
H134	10/15/1956	--	482	Reported	TWDB	280	16
H134	12/04/2000	20:10	823	Middle of open interval	TWDB	405	20
H135	02/22/1988	--	45	Reported	TWDB	475	28
H135	02/27/1993	--	48	Middle of open interval	TWDB	781	27
H136	02/27/1993	--	152	Middle of open interval	TWDB	698	20
H137	02/27/1993	--	330	Middle of open interval	TWDB	556	17
H138	02/27/1993	--	799	Middle of open interval	TWDB	275	21
H138	02/22/1988	14:30	801	Reported	TWDB	331	21
H139	03/02/1993	--	43	Middle of open interval	TWDB	736	29
H140	08/31/2004	--	154	Reported	USGS	661	20
H141	09/01/2004	--	296	Reported	USGS	614	17
H142	09/01/2004	--	795	Reported	USGS	263	22
H143	02/15/1993	--	54	Middle of open interval	TWDB	668	31
H144	02/15/1993	--	154	Middle of open interval	TWDB	826	22
H145	02/15/1993	--	294	Middle of open interval	TWDB	481	17
H145	02/24/1988	12:30	1,294	Reported	TWDB	417	13
H146	02/25/1993	--	795	Middle of open interval	TWDB	332	24
H147	02/10/1993	--	55	Middle of open interval	TWDB	592	42
H148	02/09/1993	--	155	Middle of open interval	TWDB	1,151	22
H149	02/10/1993	--	295	Middle of open interval	TWDB	479	16
H150	02/23/1993	--	796	Middle of open interval	TWDB	306	23
H151	05/20/1958	--	287	Reported	Wilson[2]	190	17
H151	05/20/1958	--	500	Reported	Wilson[2]	267	24
H151	03/15/1980	--	526	Reported	TWDB	274	25
H151	05/18/1958	--	679	Reported	Wilson[2]	365	27
H151	12/07/1998	17:00	705	Middle of open interval	TWDB	436	27

Table 4. Historical (1922–2007) dissolved-solids concentrations and resistivity values from the three-dimensional model of the combined inverse modeling results of the direct-current resistivity and time-domain electromagnetic soundings in the surface geophysical subset area of the Mesilla Basin study area in Doña Ana County, New Mexico, and El Paso County, Texas.—Continued

[mm/dd/yyyy, month/day/year; ft, foot; mg/L, milligram per liter; 3D, three-dimensional; DC, direct-current; TDEM, time-domain electromagnetic; ohm-m, ohm-meter; --, not available; TWDB, Texas Water Development Board; USGS, U.S. Geological Survey; NMOSE, New Mexico Office of the State Engineer; NMBHO, New Mexico Office of Border Health; EPWU, El Paso Water Utilities]

Well identifier (fig. 16)	Sample date (mm/dd/yyyy)	Sample start time	Sample depth (ft)	Explanation of how sample depth was determined	Source of well information	Dissolved solids (mg/L)	Resistivity obtained from 3D model of DC resistivity and TDEM soundings (ohm-m)[1]
H151	05/18/1958	--	860	Reported	Wilson[2]	774	24
H151	05/18/1958	--	950	Reported	Wilson[2]	1,943	21
H152	09/21/1983	--	818	Middle of open interval	USGS	299	25
H153	10/20/1998	11:52	299	Middle of open interval	TWDB	592	17
H154	08/19/1986	--	468	Reported	USGS	460	49
H154	08/20/1986	--	712	Reported	USGS	564	31
H154	08/19/1986	--	806	Reported	USGS	648	27
H154	08/19/1986	--	1,576	Reported	USGS	319	17
H154	08/17/1986	--	1,792	Reported	USGS	1,300	14
H155	09/20/1983	--	152	Middle of open interval	TWDB	1,289	29
H156	10/20/1998	13:52	817	Middle of open interval	TWDB	274	28
H157	08/28/1957	--	418	Reported	Wilson[2]	345	31
H157	11/06/2000	10:20	421	Middle of open interval	TWDB	411	31
H158	11/12/1952	--	513	Middle of open interval	TWDB	1,098	119
H159	01/14/2000	11:25	905	Middle of open interval	TWDB	265	20
H160	11/06/1987	--	800	Reported	TWDB	291	23
H160	09/20/1983	--	901	Middle of open interval[3]	USGS	262	21
H161	12/14/1973	--	119	Middle of open interval	TWDB	1,810	33
H162	11/19/1976	--	230	Reported	TWDB	580	27
H162	11/19/1976	--	450	Reported	TWDB	536	21
H162	06/21/1977	--	510	Middle of open interval	USGS	442	20
H162	11/19/1976	--	520	Reported	TWDB	812	20
H162	11/19/1976	--	596	Reported	TWDB	815	19
H163	01/27/1998	12:50	747	Middle of open interval	TWDB	296	23
H163	10/15/1985	--	950	Reported	TWDB	286	21
H164	02/27/1960	--	103	Reported	Wilson[2]	619	26
H164	02/28/1960	--	197	Reported	Wilson[2]	607	23
H164	02/28/1960	--	288	Reported	Wilson[2]	771	21
H164	02/29/1960	--	407	Reported	Wilson[2]	686	20
H164	02/29/1960	--	526	Reported	Wilson[2]	428	19
H164	03/01/1960	--	636	Reported	Wilson[2]	506	19
H164	03/01/1960	--	752	Reported	Wilson[2]	418	18
H164	03/01/1960	--	858	Reported	Wilson[2]	405	18
H164	01/27/1998	13:15	915	Middle of open interval	TWDB	275	18
H164	03/03/1960	--	918	Reported	Wilson[2]	279	18
H164	03/02/1960	--	978	Reported	Wilson[2]	334	17
H164	03/02/1960	--	1,129	Reported	Wilson[2]	265	16
H165	01/27/1998	13:11	358	Middle of open interval	TWDB	631	20
H166	06/19/1975	17:00	96	Middle of open interval	NMOSE	649	38
H167	01/19/1987	--	412	Middle of open interval	TWDB	1,060	37

Table 4. Historical (1922–2007) dissolved-solids concentrations and resistivity values from the three-dimensional model of the combined inverse modeling results of the direct-current resistivity and time-domain electromagnetic soundings in the surface geophysical subset area of the Mesilla Basin study area in Doña Ana County, New Mexico, and El Paso County, Texas.—Continued

[mm/dd/yyyy, month/day/year; ft, foot; mg/L, milligram per liter; 3D, three-dimensional; DC, direct-current; TDEM, time-domain electromagnetic; ohm-m, ohm-meter; --, not available; TWDB, Texas Water Development Board; USGS, U.S. Geological Survey; NMOSE, New Mexico Office of the State Engineer; NMBHO, New Mexico Office of Border Health; EPWU, El Paso Water Utilities]

Well identifier (fig. 16)	Sample date (mm/dd/yyyy)	Sample start time	Sample depth (ft)	Explanation of how sample depth was determined	Source of well information	Dissolved solids (mg/L)	Resistivity obtained from 3D model of DC resistivity and TDEM soundings (ohm-m)[1]
H168	03/19/1995	--	310	Reported	USGS	280	21
H169	05/09/1981	--	300	Reported	TWDB	571	16
H169	05/09/1981	--	430	Reported	TWDB	386	16
H169	05/08/1981	--	490	Reported	TWDB	370	16
H169	05/31/1988	--	598	Middle of open interval	USGS	353	17
H169	05/08/1981	--	610	Reported	TWDB	388	17
H169	05/08/1981	--	740	Reported	TWDB	540	17
H170	10/27/1977	--	152	Middle of open interval	TWDB	1,608	21
H171	04/08/1966	--	241	Middle of open interval	TWDB	674	20
H172	08/02/1966	--	175	Middle of open interval	TWDB	585	15
H173	10/04/1989	--	215	Middle of open interval	USGS	818	44
H174	10/02/1953	--	190	Reported	Wilson[2]	918	50
H174	09/18/1953	--	383	Reported	Wilson[2]	1,110	29
H174	10/01/1953	--	598	Reported	Wilson[2]	992	18
H175	04/23/1986	--	20	Bottom of well[4]	USGS	1,190	15
H176	09/14/2007	16:00	470	Middle of open interval	TWDB	645	13
H176	03/10/1983	9:30	600	Reported	TWDB	560	13
H177	04/09/1973	--	400	Bottom of well[4]	NMOSE	1,060	--
H178	06/18/1985	--	1,050	Bottom of well[4]	USGS	465	--
H179	06/12/1975	--	52	Reported	Wilson[2]	1,260	--
H180	06/26/1956	--	73	Reported	Wilson[2]	1,430	42
H181	06/26/1956	--	141	Bottom of well[4]	Wilson[2]	1,970	--
H182	08/09/1972	--	650	Reported	Wilson[2]	499	--
H183	06/16/1975	--	150	Bottom of well[4]	Wilson[2]	1,050	--
H184	06/05/1965	--	224	Reported	Wilson[2]	894	--
H185	04/09/1974	--	300	Reported	Wilson[2]	1,060	--
H186	06/30/1953	--	76	Reported	Wilson[2]	682	40
H187	06/19/1975	--	106	Reported	Wilson[2]	649	37
H188	06/26/1956	--	86	Bottom of well[4]	Wilson[2]	1,290	30
H189	10/14/1953	--	279	Reported	Wilson[2]	724	18
H189	10/15/1953	--	407	Reported	Wilson[2]	601	18
H189	10/16/1953	--	554	Reported	Wilson[2]	360	19
H189	10/20/1953	--	737	Reported	Wilson[2]	354	19
H190	07/24/1975	--	58	Reported	Wilson[2]	682	29
H191	06/26/1959	--	146	Bottom of well[4]	Wilson[2]	790	26
H192	05/29/1956	--	78	Reported	Wilson[2]	857	30
H193	06/16/1953	--	84	Reported	Wilson[2]	857	38
H194	01/22/1959	--	421	Reported	Wilson[2]	714	62
H195	07/01/1953	--	77	Reported	Wilson[2]	857	22
H196	07/09/1953	--	91	Reported	Wilson[2]	886	26

Table 4. Historical (1922–2007) dissolved-solids concentrations and resistivity values from the three-dimensional model of the combined inverse modeling results of the direct-current resistivity and time-domain electromagnetic soundings in the surface geophysical subset area of the Mesilla Basin study area in Doña Ana County, New Mexico, and El Paso County, Texas.—Continued

[mm/dd/yyyy, month/day/year; ft, foot; mg/L, milligram per liter; 3D, three-dimensional; DC, direct-current; TDEM, time-domain electromagnetic; ohm-m, ohm-meter; --, not available; TWDB, Texas Water Development Board; USGS, U.S. Geological Survey; NMOSE, New Mexico Office of the State Engineer; NMBHO, New Mexico Office of Border Health; EPWU, El Paso Water Utilities]

Well identifier (fig. 16)	Sample date (mm/dd/yyyy)	Sample start time	Sample depth (ft)	Explanation of how sample depth was determined	Source of well information	Dissolved solids (mg/L)	Resistivity obtained from 3D model of DC resistivity and TDEM soundings (ohm-m)[1]
H197	06/09/1953	--	87	Reported	Wilson[2]	1,860	17
H198	07/09/1953	--	87	Bottom of well[4]	Wilson[2]	725	15
H199	03/15/1952	--	162	Reported	Wilson[2]	915	15
H199	03/18/1952	--	473	Reported	Wilson[2]	4,750	9
H199	03/19/1952	--	684	Reported	Wilson[2]	2,700	9
H199	03/21/1952	--	863	Reported	Wilson[2]	2,400	11
H200	02/05/1973	--	1,004	Bottom of well[4]	Wilson[2]	1,270	24
H201	01/11/1952	--	115	Reported	Wilson[2]	1,030	7
H201	01/09/1952	--	178	Reported	Wilson[2]	2,620	6
H201	06/08/1952	--	245	Reported	Wilson[2]	3,050	6
H202	08/01/1951	--	119	Reported	Wilson[2]	618	8
H202	08/01/1951	--	144	Reported	Wilson[2]	958	8
H202	08/01/1951	--	170	Reported	Wilson[2]	1,480	7
H202	08/01/1951	--	230	Reported	Wilson[2]	2,330	7
H203	08/01/1951	--	83	Bottom of well[4]	Wilson[2]	622	6
H204	07/23/1951	--	109	Reported	Wilson[2]	683	7
H204	07/23/1951	--	129	Reported	Wilson[2]	683	7
H204	07/23/1951	--	151	Reported	Wilson[2]	908	7
H204	07/23/1951	--	230	Reported	Wilson[2]	1,640	6
H205	07/09/1951	--	112	Reported	Wilson[2]	368	7
H205	07/10/1951	--	152	Reported	Wilson[2]	420	7
H205	07/10/1951	--	172	Reported	Wilson[2]	750	7
H205	07/11/1951	--	204	Reported	Wilson[2]	1,430	6
H205	07/12/1951	--	222	Reported	Wilson[2]	1,880	6
H206	06/26/1951	--	78	Reported	Wilson[2]	460	6
H206	06/27/1951	--	87	Reported	Wilson[2]	430	6
H206	06/28/1951	--	97	Reported	Wilson[2]	670	6
H206	06/28/1951	--	107	Reported	Wilson[2]	670	6
H206	06/29/1951	--	177	Reported	Wilson[2]	2,130	5
H206	06/30/1951	--	231	Reported	Wilson[2]	2,090	5
H207	08/01/1951	--	352	Reported	Wilson[2]	2,190	7
H207	08/01/1951	--	389	Reported	Wilson[2]	2,420	7
H208	05/29/1956	--	294	Bottom of well[4]	Wilson[2]	1,210	6
H209	08/20/1951	--	72	Reported	Wilson[2]	428	7
H209	08/20/1951	--	91	Reported	Wilson[2]	662	7
H209	08/21/1951	--	114	Reported	Wilson[2]	600	6
H209	08/21/1951	--	150	Reported	Wilson[2]	518	6
H209	08/22/1951	--	172	Reported	Wilson[2]	923	6
H209	08/22/1951	--	191	Reported	Wilson[2]	1,120	6
H210	08/17/1951	--	90	Reported	Wilson[2]	533	5

Table 4. Historical (1922–2007) dissolved-solids concentrations and resistivity values from the three-dimensional model of the combined inverse modeling results of the direct-current resistivity and time-domain electromagnetic soundings in the surface geophysical subset area of the Mesilla Basin study area in Doña Ana County, New Mexico, and El Paso County, Texas.—Continued

[mm/dd/yyyy, month/day/year; ft, foot; mg/L, milligram per liter; 3D, three-dimensional; DC, direct-current; TDEM, time-domain electromagnetic; ohm-m, ohm-meter; --, not available; TWDB, Texas Water Development Board; USGS, U.S. Geological Survey; NMOSE, New Mexico Office of the State Engineer; NMBHO, New Mexico Office of Border Health; EPWU, El Paso Water Utilities]

Well identifier (fig. 16)	Sample date (mm/dd/yyyy)	Sample start time	Sample depth (ft)	Explanation of how sample depth was determined	Source of well information	Dissolved solids (mg/L)	Resistivity obtained from 3D model of DC resistivity and TDEM soundings (ohm-m)[1]
H210	08/17/1951	--	110	Reported	Wilson[2]	585	5
H210	08/17/1951	--	132	Reported	Wilson[2]	1,140	5
H211	08/24/1956	--	274	Bottom of well[4]	Wilson[2]	910	4
H212	06/19/1951	--	70	Reported	Wilson[2]	2,460	4
H213	05/29/1951	--	20	Reported	Wilson[2]	2,900	2
H213	05/29/1951	--	50	Reported	Wilson[2]	7,550	2
H213	05/30/1951	--	134	Reported	Wilson[2]	14,400	2
H214	01/24/1951	--	55	Reported	Wilson[2]	775	4
H214	06/23/1950	--	160	Reported	Wilson[2]	3,400	5
H214	06/23/1951	--	230	Reported	Wilson[2]	3,500	5
H215	06/13/1951	--	420	Bottom of well[4]	Wilson[2]	1,910	76
H216	07/09/1951	--	393	Bottom of well[4]	Wilson[2]	10,300	--
H217	04/29/1996	8:30	80	Bottom of well[4]	NMBHO	554	26
H218	04/29/1996	12:45	94	Bottom of well[4]	NMBHO	832	25
H219	04/29/1996	9:50	100	Bottom of well[4]	NMBHO	688	26
H220	04/29/1996	14:00	84	Bottom of well[4]	NMBHO	1,630	25
H221	02/19/1996	8:30	80	Bottom of well[4]	NMBHO	2,000	25
H222	02/19/1996	11:50	118	Bottom of well[4]	NMBHO	478	26
H223	02/19/1996	14:20	120	Bottom of well[4]	NMBHO	638	26
H224	05/01/1996	15:00	72	Bottom of well[4]	NMBHO	504	24
H225	02/21/1996	14:15	108	Bottom of well[4]	NMBHO	434	22
H226	05/01/1996	15:00	84	Bottom of well[4]	NMBHO	1,330	30
H227	02/25/1996	15:00	230	Bottom of well[4]	NMBHO	1,760	20
H228	02/25/1996	17:30	40	Bottom of well[4]	NMBHO	652	13
H229	05/06/1996	8:30	90	Bottom of well[4]	NMBHO	1,520	18
H230	02/28/1996	16:00	130	Bottom of well[4]	NMBHO	1,370	15
H231	05/01/1996	9:00	60	Bottom of well[4]	NMBHO	454	--
H232	02/12/2007	--	21	Middle of open interval	EPWU	20,000	--
H233	02/14/2006	--	16	Middle of open interval	EPWU	7,300	3
H234	02/14/2006	--	7	Middle of open interval	EPWU	16,000	3
H235	02/14/2006	--	8	Middle of open interval	EPWU	12,000	3
H236	02/14/2006	--	17	Bottom of well[4]	EPWU	3,400	3
H237	02/14/2006	--	16	Bottom of well[4]	EPWU	5,300	3
H238	02/15/2006	--	17	Bottom of well[4]	EPWU	6,600	3
H239	02/14/2006	--	8	Middle of open interval	EPWU	14,000	3

[1]Combined inverse modeling results of the direct-current resistivity and time-domain electromagnetic soundings.

[2]Data compiled from Wilson and others (1981).

[3]Well contained multiple opening intervals; top of first opening interval and bottom of last opening interval reported.

[4]If no screened or open hole was reported for a well, the total depth of the well was used for the sampling depth.

Table 5. Wells from which geochemical data were collected in the Mesilla Basin study area in Doña Ana County, New Mexico, and El Paso, Texas, 2010.

[USGS, U.S. Geological Survey; ft, foot; NAVD 88, North American Vertical Datum of 1988; USF, upper part of the Santa Fe Group; MSF, middle part of the Santa Fe Group; RGA, Rio Grande alluvium; LSF, lower part of the Santa Fe Group]

Well identifier (fig. 20)	USGS station number	Latitude (decimal degrees)	Longitude (decimal degrees)	Land-surface altitude (ft) (NAVD 88)	Hydrogeologic unit
Q00	322320106551801	32.48600	106.92200	3,890	USF
Q01	322233106590901	32.37592	106.98634	4,256	MSF
Q02	322219106485001	32.37200	106.81400	3,547	MSF
Q03	322054106475201	32.34843	106.79834	3,715	USF
Q04	322024106463901	32.34000	106.77900	3,550	USF
Q05	321934106482601	32.32648	106.80778	3,366	MSF
Q06	321641106515401	32.27800	106.86500	3,273	MSF
Q07	321628106451501	32.27426	106.75417	3,370	MSF
Q08	321501106443801	32.25037	106.74445	3,554	USF
Q09	320939106441701	32.16093	106.73861	3,619	USF
Q10	320654106504201	32.11500	106.84500	3,352	MSF
Q11	320643106440401	32.11181	106.73448	3,319	MSF
Q12	320604107051201	32.10121	107.08723	3,867	MSF
Q13	320445106421001	32.07927	106.70333	3,695	USF
Q14	320253106364001	32.04800	106.61100	3,584	USF
Q15	320054106533901	32.01510	106.89473	3,774	USF
Q16	320040107054601	32.01121	107.09668	3,669	MSF
Q17	315955106362201	31.99649	106.60694	3,330	MSF
Q18	315940106372301	31.99444	106.62306	3,721	RGA
Q19	315940106372302	31.99444	106.62306	3,501	USF
Q20	315940106372303	31.99444	106.62306	3,001	MSF
Q21	315940106372304	31.99444	106.62306	2,501	LSF
Q22	315723106415201	31.95677	106.69833	3,625	MSF
Q23	315712106361802	31.95371	106.60583	3,628	USF
Q24	315712106361803	31.95371	106.60583	3,486	MSF
Q25	315712106361804	31.95371	106.60583	2,987	LSF
Q26	315646106374401	31.94611	106.62889	3,720	RGA
Q27	315646106374402	31.94611	106.62889	3,490	USF
Q28	315646106374403	31.94611	106.62889	2,990	MSF
Q29	315646106374404	31.94611	106.62889	2,480	LSF
Q30	315519106593101	31.92200	106.99200	3,661	MSF
Q31	315245106380601	31.87927	106.63555	3,583	MSF
Q32	315245106380602	31.87927	106.63555	3,355	LSF
Q33	315114106414901	31.85400	106.69700	3,454	MSF
Q34	315013106362601	31.83705	106.60777	3,599	USF
Q35	315013106362602	31.83705	106.60777	3,461	MSF
Q36	315013106395301	31.83705	106.66527	3,520	MSF
Q37	315006106354601	31.83500	106.59600	3,705	RGA
Q38	314932106493401	31.82594	106.82527	3,607	MSF
Q39	314908106371201	31.81900	106.62000	3,517	MSF
Q40	314817106325801	31.80483	106.54999	3,674	USF
Q41	314817106325802	31.80483	106.54999	3,589	MSF
Q42	314746106353601	31.79622	106.59388	3,559	MSF
Q43	314717106404401	31.78800	106.67900	3,619	MSF

Table 6. Major-ion, nutrient, trace-element, and selected pesticide analyses for equipment-blank samples and field-blank samples collected in association with groundwater samples in the Mesilla Basin study area in Doña Ana County, New Mexico, and El Paso County, Texas, 2010.

[USGS, U.S. Geological Survey; mm/dd/yyyy, month/day/year; mg/L, milligram per liter; AFH, Austin Field Headquarters; --, not available; µg/L, microgram per liter; M, presence verified but not quantified; CFC, chlorofluorocarbon. Laboratory reporting levels are indicated for values preceded by less than symbols (<) for a given analysis; laboratory reporting levels are subject to change, and more than one laboratory reporting level for a given constituent was common]

Well identifier (fig. 20)	USGS station number	Sample date (mm/dd/yyyy)	Sample start time	Blank type	Calcium, water, filtered (mg/L)	Magnesium, water, filtered (mg/L)	Potassium, water, filtered (mg/L)	Sodium, water, filtered (mg/L)	Bromide, water, filtered (mg/L)	Chloride, water, filtered (mg/L)	Fluoride, water, filtered (mg/L)	Silica, water, filtered (mg/L)	Sulfate, water, filtered (mg/L)
AFH01	302009097405901	10/07/2010	11:08	Equipment	--	--	--	--	--	--	--	--	--
AFH02	302009097405901	10/15/2010	14:08	Equipment	--	--	--	--	--	--	--	--	--
Q02	322219106485001	11/03/2010	12:05	Field	<0.04	<0.016	<0.06	<0.10	<0.02	<0.12	<0.08	<0.06	<0.18
Q04	322024106463901	11/16/2010	16:07	Field	--	--	--	--	--	--	--	--	--
Q05	321934106482601	11/16/2010	10:05	Field	--	--	--	--	--	--	--	--	--
Q33	315114106414901	11/03/2010	16:04	Field	<0.02	<0.008	<0.02	<0.06	<0.01	<0.06	<0.04	<0.03	<0.09
Q36	315013106395301	11/04/2010	9:05	Field	--	--	--	--	--	--	--	--	--
Q43	314717106404401	11/03/2010	9:05	Field	--	--	--	--	--	--	--	--	--

Well identifier (fig. 20)	Ammonia, water, filtered (mg/L as nitrogen)	Ammonia, water, filtered (mg/L as ammonium ion NH_4)	Nitrite, water, filtered (mg/L)	Nitrite, water, filtered (mg/L as nitrogen)	Nitrate, water, filtered (mg/L)	Nitrate, water, filtered (mg/L as nitrogen)	Nitrate plus nitrite, water, filtered (mg/L as nitrogen)	Total nitrogen, water, filtered, analytically determined (mg/L)	Total nitrogen, water, filtered (mg/L)	Total nitrogen, water, unfiltered (mg/L)	Total nitrogen, water, unfiltered (mg/L as nitrate)	Organic nitrogen, water, filtered (mg/L)	Organic nitrogen, water, unfiltered (mg/L)
AFH01	<0.01	<0.013	<0.003	<0.001	<0.089	<0.02	<0.02	--	<0.05	--	--	<0.05	--
AFH02	<0.01	<0.013	<0.003	<0.001	<0.089	<0.02	<0.02	--	<0.05	--	--	<0.05	--
Q02	<0.02	<0.026	<0.007	<0.002	<0.177	<0.04	<0.04	--	<0.10	--	--	<0.10	--
Q04	--	--	--	--	--	--	--	--	--	--	--	--	--
Q05	--	--	--	--	--	--	--	--	--	--	--	--	--
Q33	<0.01	<0.013	<0.003	<0.001	<0.089	<0.02	<0.02	--	<0.05	--	--	<0.05	--
Q36	--	--	--	--	--	--	--	--	--	--	--	--	--
Q43	--	--	--	--	--	--	--	--	--	--	--	--	--

Table 6. Major-ion, nutrient, trace-element, and selected pesticide analyses for equipment-blank samples and field-blank samples collected in association with groundwater samples in the Mesilla Basin study area in Doña Ana County, New Mexico, and El Paso County, Texas, 2010.—Continued

[USGS, U.S. Geological Survey; mm/dd/yyyy, month/day/year; mg/L, milligram per liter; AFH, Austin Field Headquarters; --, not available; µg/L, microgram per liter; M, presence verified but not quantified; CFC, chlorofluorocarbon. Laboratory reporting levels are indicated for values preceded by less than symbols (<) for a given analysis; laboratory reporting levels are subject to change, and more than one laboratory reporting level for a given constituent was common]

Well identifier (fig. 20)	Organic phosphorus, water, filtered (mg/L)	Organic phosphorus, water, unfiltered (mg/L)	Ortho-phosphate, water, filtered (mg/L)	Ortho-phosphate, water, filtered (mg/L as phosphorus)	Phosphate, water, unfiltered (mg/L)	Hydrogen sulfide, water, unfiltered (mg/L)	Aluminum, water, filtered (µg/L)	Barium, water, filtered (µg/L)	Antimony, water, filtered (µg/L)	Beryllium, water, filtered (µg/L)	Arsenic, water, filtered (µg/L)	Boron, water, filtered (µg/L)
AFH01	--	--	<0.012	<0.004	--	--	<1.7	M	<0.03	<0.01	<0.02	<3
AFH02	--	--	<0.012	<0.004	--	--	3.3	<0.07	<0.03	<0.01	<0.02	<3
Q02	--	--	<0.025	<0.008	--	--	<3.4	<0.14	<0.05	<0.01	<0.04	<3
Q04	--	--	--	--	--	--	<1.7	<0.07	<0.03	<0.01	0.04	<3
Q05	--	--	--	--	--	--	--	--	--	--	--	--
Q33	--	--	<0.012	<0.004	--	--	<1.7	<0.07	<0.03	<0.01	<0.02	<3
Q36	--	--	--	--	--	--	--	--	--	--	--	--
Q43	--	--	--	--	--	--	--	--	--	--	--	--

Well identifier (fig. 20)	Cadmium, water, filtered (µg/L)	Chromium, water, filtered (µg/L)	Cobalt, water, filtered (µg/L)	Copper, water, filtered (µg/L)	Iron, water, filtered (µg/L)	Lead, water, filtered (µg/L)	Lithium, water, filtered (µg/L)	Manganese, water, filtered (µg/L)	Molybdenum, water, filtered (µg/L)	Nickel, water, filtered (µg/L)	Selenium, water, filtered (µg/L)	Silver, water, filtered (µg/L)	Thallium, water, filtered (µg/L)	Vanadium, water, filtered (µg/L)
AFH01	<0.02	0.08	0.07	<0.5	--	0.06	<0.2	0.9	0.10	1.8	<0.03	M	<0.01	<0.08
AFH02	<0.02	<0.06	0.05	<0.5	--	<0.01	<0.2	<0.1	<0.014	<0.09	<0.03	<0.005	<0.01	<0.08
Q02	<0.02	<0.12	0.01	<1.0	<6	<0.03	<0.4	<0.3	<0.028	<0.12	<0.04	<0.010	<0.02	<0.16
Q04	<0.02	<0.06	<0.02	<0.5	--	<0.01	<0.2	<0.1	<0.014	<0.09	0.07	<0.005	<0.01	<0.08
Q05	--	--	--	--	--	--	--	--	--	--	--	--	--	--
Q33	<0.02	<0.06	0.02	<0.5	<3	0.03	<0.2	<0.1	<0.014	<0.09	<0.03	<0.005	<0.01	<0.08
Q36	--	--	--	--	--	--	--	--	--	--	--	--	--	--
Q43	--	--	--	--	--	--	--	--	--	--	--	--	--	--

Table 6. Major-ion, nutrient, trace-element, and selected pesticide analyses for equipment-blank samples and field-blank samples collected in association with groundwater samples in the Mesilla Basin study area in Doña Ana County, New Mexico, and El Paso County, Texas, 2010.—Continued

[USGS, U.S. Geological Survey; mm/dd/yyyy, month/day/year; mg/L, milligram per liter; AFH, Austin Field Headquarters; --, not available; µg/L, microgram per liter; M, presence verified but not quantified; CFC, chlorofluorocarbon. Laboratory reporting levels are indicated for values preceded by less than symbols (<) for a given analysis; laboratory reporting levels are subject to change, and more than one laboratory reporting level for a given constituent was common]

Well identifier (fig. 20)	Zinc, water, filtered (µg/L)	Strontium, water, filtered (µg/L)	Uranium (natural), water, filtered (µg/L)	1,1-Dichloro-ethene, water, unfiltered (µg/L)	1,1-Dichloro-propene, water, unfiltered (µg/L)	1,2,3-Trichloro-benzene, water, unfiltered (µg/L)	1,2,3-Trichloro-propane, water, unfiltered (µg/L)	1,2,3-Trimethyl-benzene, water, unfiltered (µg/L)	1,2,4-Trichloro-benzene, water, unfiltered (µg/L)	1,2,4-Trimethyl-benzene, water, unfiltered (µg/L)	1,2-Dibromo-ethane, water, unfiltered (µg/L)	1,2-Dichloro-benzene, water, unfiltered (µg/L)
AFH01	<1.4	<0.20	<0.004	<0.02	<0.04	<0.1	<0.12	<0.1	<0.1	<0.03	<0.03	<0.03
AFH02	<1.4	<0.20	<0.004	<0.02	<0.04	<0.1	<0.12	<0.1	<0.1	<0.03	<0.03	<0.03
Q02	<2.8	<0.40	<0.01	--	--	--	--	--	--	--	--	--
Q04	<1.4	<0.20	0.02	--	--	--	--	--	--	--	--	--
Q05	--	--	--	<0.02	<0.04	<0.1	<0.12	<0.1	<0.1	<0.03	<0.03	<0.03
Q33	<1.4	<0.20	<0.004	--	--	--	--	--	--	--	--	--
Q36	--	--	--	<0.02	<0.04	<0.1	<0.12	<0.1	<0.1	<0.03	<0.03	<0.03
Q43	--	--	--	<0.02	<0.04	<0.1	<0.12	<0.1	<0.1	<0.03	<0.03	<0.03

Well identifier (fig. 20)	1,2-Dichloro-ethane, water, unfiltered (µg/L)	1,2-Dichlo-ropropane, water, unfil-tered (µg/L)	Acrylonitrile, water, unfiltered (µg/L)	Benzene, water, unfiltered (µg/L)	Bromo-benzene, water, unfiltered (µg/L)	Bromo-dichloro-methane, water, unfiltered (µg/L)	Bromo-chloro-methane, water, unfiltered (µg/L)	Bromo-ethene, water, unfiltered (µg/L)	Bromo-methane, water, unfiltered (µg/L)	Carbon disulfide, water, unfiltered (µg/L)	CFC-11, water, unfiltered (µg/L)	CFC-113, water, unfiltered (µg/L)
AFH01	<0.1	<0.03	<0.8	<0.03	<0.02	<0.03	<0.06	<0.1	<0.2	<0.08	<0.06	<0.03
AFH02	<0.1	<0.03	<0.8	<0.03	<0.02	<0.03	<0.06	<0.1	<0.2	<0.08	<0.06	<0.03
Q02	--	--	--	--	--	--	--	--	--	--	--	--
Q04	--	--	--	--	--	--	--	--	--	--	--	--
Q05	<0.1	<0.03	<0.8	<0.03	<0.02	<0.03	<0.06	<0.1	<0.2	<0.08	<0.06	<0.03
Q33	--	--	--	--	--	--	--	--	--	--	--	--
Q36	<0.1	<0.03	<0.8	<0.03	<0.02	<0.03	<0.06	<0.1	<0.2	<0.08	<0.06	<0.03
Q43	<0.1	<0.03	<0.8	<0.03	<0.02	<0.03	<0.06	<0.1	<0.2	<0.08	<0.06	<0.03

Table 6. Major-ion, nutrient, trace-element, and selected pesticide analyses for equipment-blank samples and field-blank samples collected in association with groundwater samples in the Mesilla Basin study area in Doña Ana County, New Mexico, and El Paso County, Texas, 2010.—Continued

[USGS, U.S. Geological Survey; mm/dd/yyyy, month/day/year; mg/L, milligram per liter; AFH, Austin Field Headquarters; --, not available; µg/L, microgram per liter; M, presence verified but not quantified; CFC, chlorofluorocarbon. Laboratory reporting levels are indicated for values preceded by less than symbols (<) for a given analysis; laboratory reporting levels are subject to change, and more than one laboratory reporting level for a given constituent was common]

Well identifier (fig. 20)	CFC-12, water, unfiltered (µg/L)	Ethyl metha-crylate, water, unfiltered (µg/L)	Ethyl methyl ketone, water, unfiltered (µg/L)	Ethyl-benzene, water, unfiltered (µg/L)	Hexachloro-butadiene, water, unfiltered (µg/L)	Hexachloro-ethane, water, unfiltered (µg/L)	Iodo-methane, water, unfiltered (µg/L)	Isobutyl methyl ketone, water, unfiltered (µg/L)	Isodurene, water, unfiltered (µg/L)	Isopropyl-benzene, water, unfiltered (µg/L)	meta-Xylene plus para-xylene, water, unfiltered (µg/L)	Methyl acrylate, water, unfiltered (µg/L)
AFH01	<0.1	<0.2	<1.6	<0.04	<0.1	<0.2	<0.26	<0.3	<0.1	<0.04	<0.08	<0.8
AFH02	<0.1	<0.2	<1.6	<0.04	<0.1	<0.2	<0.26	<0.3	<0.1	<0.04	<0.08	<0.8
Q02	--	--	--	--	--	--	--	--	--	--	--	--
Q04	--	--	--	--	--	--	--	--	--	--	--	--
Q05	<0.1	<0.2	<1.6	<0.04	<0.1	<0.2	<0.26	<0.3	<0.1	<0.04	<0.08	<0.8
Q33	--	--	--	--	--	--	--	--	--	--	--	--
Q36	<0.1	<0.2	<1.6	<0.04	<0.1	<0.2	<0.26	<0.3	<0.1	<0.04	<0.08	<0.8
Q43	<0.1	<0.2	<1.6	<0.04	<0.1	<0.2	<0.26	<0.3	<0.1	<0.04	<0.08	<0.8

Well identifier (fig. 20)	Styrene, water, unfiltered (µg/L)	t-1,4-Dichloro-2-butene, water, unfiltered (µg/L)	tert-Butyl ethyl ether, water, unfiltered (µg/L)	tert-Butyl-benzene, water, unfiltered (µg/L)	Tetrachloro-ethene, water, unfiltered (µg/L)	Tetrachloro-methane, water, unfiltered (µg/L)	Tetrahydro-furan, water, unfiltered (µg/L)	1,1,1,2-Tetra-chloro-ethane, water, unfiltered (µg/L)	1,1,1-Trichloro-ethane, water, unfiltered (µg/L)	1,1,2,2-Tetrachloro-ethane, water, unfiltered (µg/L)	1,1,2-Trichloro-ethane, water, unfiltered (µg/L)	1,1-Dichloro-ethane, water, unfiltered (µg/L)
AFH01	<0.04	<0.4	<0.03	<0.06	<0.03	<0.06	<1	<0.04	<0.03	<0.14	<0.03	<0.04
AFH02	<0.04	<0.4	<0.03	<0.06	<0.03	<0.06	<1	<0.04	<0.03	<0.14	<0.03	<0.04
Q02	--	--	--	--	--	--	--	--	--	--	--	--
Q04	--	--	--	--	--	--	--	--	--	--	--	--
Q05	<0.04	<0.4	<0.03	<0.06	<0.03	<0.06	<1	<0.04	<0.03	<0.14	<0.03	<0.04
Q33	--	--	--	--	--	--	--	--	--	--	--	--
Q36	<0.04	<0.4	<0.03	<0.06	<0.03	<0.06	<1	<0.04	<0.03	<0.14	<0.03	<0.04
Q43	<0.04	<0.4	<0.03	<0.06	<0.03	<0.06	<1	<0.04	<0.03	<0.14	<0.03	<0.04

Table 6. Major-ion, nutrient, trace-element, and selected pesticide analyses for equipment-blank samples and field-blank samples collected in association with groundwater samples in the Mesilla Basin study area in Doña Ana County, New Mexico, and El Paso County, Texas, 2010.—Continued

[USGS, U.S. Geological Survey; mm/dd/yyyy, month/day/year; mg/L, milligram per liter; AFH, Austin Field Headquarters; --, not available; µg/L, microgram per liter; M, presence verified but not quantified; CFC, chlorofluorocarbon. Laboratory reporting levels are indicated for values preceded by less than symbols (<) for a given analysis; laboratory reporting levels are subject to change, and more than one laboratory reporting level for a given constituent was common]

Well identifier (fig. 20)	1,3,5-Trimethylbenzene, water, unfiltered (µg/L)	1,3-Dichlorobenzene, water, unfiltered (µg/L)	1,3-Dichloropropane, water, unfiltered (µg/L)	1,4-Dichlorobenzene, water, unfiltered (µg/L)	2,2-Dichloropropane, water, unfiltered (µg/L)	2-Chlorotoluene, water, unfiltered (µg/L)	2-Ethyltoluene, water, unfiltered (µg/L)	3-Chloropropene, water, unfiltered (µg/L)	4-Chlorotoluene, water, unfiltered (µg/L)	4-Isopropyltoluene, water, unfiltered (µg/L)	Acetone, water, unfiltered (µg/L)	Chlorobenzene, water, unfiltered (µg/L)	Chloroethane, water, unfiltered (µg/L)
AFH01	<0.03	<0.02	<0.1	<0.03	<0.06	<0.03	<0.03	<0.08	<0.04	<0.06	<3	<0.03	<0.1
AFH02	<0.03	<0.02	<0.1	<0.03	<0.06	<0.03	<0.03	<0.08	<0.04	<0.06	<3	<0.03	<0.1
Q02	--	--	--	--	--	--	--	--	--	--	--	--	--
Q04	--	--	--	--	--	--	--	--	--	--	--	--	--
Q05	<0.03	<0.02	<0.1	<0.03	<0.06	<0.03	<0.03	<0.08	<0.04	<0.06	<3	<0.03	<0.1
Q33	--	--	--	--	--	--	--	--	--	--	--	--	--
Q36	<0.03	<0.02	<0.1	<0.03	<0.06	<0.03	<0.03	<0.08	<0.04	<0.06	<3	<0.03	<0.1
Q43	<0.03	<0.02	<0.1	<0.03	<0.06	<0.03	<0.03	<0.08	<0.04	<0.06	<3	<0.03	<0.1

Well identifier (fig. 20)	Chloromethane, water, unfiltered (µg/L)	cis-1,2-Dichloroethene, water, unfiltered (µg/L)	cis-1,3-Dichloropropene, water, unfiltered (µg/L)	Dibromochloromethane, water, unfiltered (µg/L)	Dibromochloropropane, water, unfiltered (µg/L)	Dibromomethane, water, unfiltered (µg/L)	Dichloromethane, water, unfiltered (µg/L)	Diethyl ether, water, unfiltered (µg/L)	Diisopropyl ether, water, unfiltered (µg/L)	Methyl acrylonitrile, water, unfiltered (µg/L)	Methyl methacrylate, water, unfiltered (µg/L)	Methyl tert-pentyl ether, water, unfiltered (µg/L)
AFH01	<0.1	<0.02	<0.1	<0.1	<0.4	<0.05	<0.04	<0.1	<0.06	<0.3	<0.2	<0.06
AFH02	<0.1	<0.02	<0.1	<0.1	<0.4	<0.05	<0.04	<0.1	<0.06	<0.3	<0.2	<0.06
Q02	--	--	--	--	--	--	--	--	--	--	--	--
Q04	--	--	--	--	--	--	--	--	--	--	--	--
Q05	<0.1	<0.02	<0.1	<0.1	<0.4	<0.05	<0.04	<0.1	<0.06	<0.3	<0.2	<0.06
Q33	--	--	--	--	--	--	--	--	--	--	--	--
Q36	<0.1	<0.02	<0.1	<0.1	<0.4	<0.05	<0.04	<0.1	<0.06	<0.3	<0.2	<0.06
Q43	<0.1	<0.02	<0.1	<0.1	<0.4	<0.05	<0.04	<0.1	<0.06	<0.3	<0.2	<0.06

Table 6. Major-ion, nutrient, trace-element, and selected pesticide analyses for equipment-blank samples and field-blank samples collected in association with groundwater samples in the Mesilla Basin study area in Doña Ana County, New Mexico, and El Paso County, Texas, 2010.—Continued

[USGS, U.S. Geological Survey; mm/dd/yyyy, month/day/year; mg/L, milligram per liter; AFH, Austin Field Headquarters; --, not available; µg/L, microgram per liter; M, presence verified but not quantified; CFC, chlorofluorocarbon. Laboratory reporting levels are indicated for values preceded by less than symbols (<) for a given analysis; laboratory reporting levels are subject to change, and more than one laboratory reporting level for a given constituent was common]

Well identifier (fig. 20)	Methyl tert-butyl ether, water, unfiltered (µg/L)	Naphthalene, water, unfiltered (µg/L)	n-Butyl methyl ketone, water, unfiltered (µg/L)	n-Butyl-benzene, water, unfiltered (µg/L)	n-Propyl-benzene, water, unfiltered (µg/L)	ortho-Xylene, water, unfiltered (µg/L)	Prehnitene, water, unfiltered (µg/L)	sec-Butyl-benzene, water, unfiltered (µg/L)	Toluene, water, unfiltered (µg/L)
AFH01	<0.1	<0.2	<0.4	<0.1	<0.04	<0.03	<0.1	<0.03	<0.02
AFH02	<0.1	<0.2	<0.4	<0.1	<0.04	<0.03	<0.1	<0.03	<0.02
Q02	--	--	--	--	--	--	--	--	--
Q04	--	--	--	--	--	--	--	--	--
Q05	<0.1	<0.2	<0.4	<0.1	<0.04	<0.03	<0.1	<0.03	<0.02
Q33	--	--	--	--	--	--	--	--	--
Q36	<0.1	<0.2	<0.4	<0.1	<0.04	<0.03	<0.1	<0.03	<0.02
Q43	<0.1	<0.2	<0.4	<0.1	<0.04	<0.03	<0.1	<0.03	<0.02

Well identifier (fig. 20)	trans-1,2-Dichloro-ethene, water, unfiltered (µg/L)	trans-1,3-Dichloro-propene, water, unfiltered (µg/L)	Tribromo-methane, water, unfiltered (µg/L)	Trichloro-ethene, water, unfiltered (µg/L)	Trichloro-methane, water, unfiltered (µg/L)	Vinyl chloride, water, unfiltered (µg/L)	Organic carbon, water, filtered (mg/L)	Total carbon, water, unfiltered (mg/L)
AFH01	<0.02	<0.14	<0.1	<0.02	<0.03	<0.1	--	--
AFH02	<0.02	<0.14	<0.1	<0.02	<0.03	<0.1	--	--
Q02	--	--	--	--	--	--	--	--
Q04	--	--	--	--	--	--	--	--
Q05	<0.02	<0.14	<0.1	<0.02	<0.03	<0.1	0.2	--
Q33	--	--	--	--	--	--	--	--
Q36	<0.02	<0.14	<0.1	<0.02	<0.03	<0.1	0.3	--
Q43	<0.02	<0.14	<0.1	<0.02	<0.03	<0.1	<0.1	--

Table 7. Relative percent differences between environmental and sequential-replicate samples analyzed for physicochemical properties, dissolved solids, major ions, nutrients, trace elements, and selected pesticides measured in groundwater samples collected from wells in the Mesilla Basin study area in Doña Ana County, New Mexico, and El Paso County, Texas, 2010.

[Note: Where a laboratory reporting level (LRL) was applicable, results are reported only where the concentrations in the environmental and replicate samples were both equal to or larger than the LRL. USGS, U.S. Geological Survey; mm/dd/yyyy, month/day/year; µS/cm at 25 °C, microsiemen per centimeter at 25 degrees Celsius; mg/L, milligram per liter; µg/L, microgram per liter; <, less than laboratory reporting level; --, not available; pCi/L; picocurie per liter]

Well identifier (fig. 20)	USGS station number	Sample date (mm/dd/yyyy)	Constituent[1]	Environmental result	Replicate result	Relative percent differences	Relative percent difference greater than 10 percent?
Q03	322054106475201	11/08/2010	pH, water, unfiltered, laboratory (standard units)	7.5	7.5	0.00	No
Q03	322054106475201	11/08/2010	Specific conductance, water, unfiltered, laboratory (µS/cm at 25 °C)	1,700	1,690	0.59	No
Q03	322054106475201	11/08/2010	Dissolved solids dried at 180 degrees Celsius, water, filtered (mg/L)	1,250	1,250	0.00	No
Q03	322054106475201	11/08/2010	Calcium, water, filtered (mg/L)	227	230	1.31	No
Q03	322054106475201	11/08/2010	Magnesium, water, filtered (mg/L)	41.5	42.0	1.20	No
Q03	322054106475201	11/08/2010	Potassium, water, filtered (mg/L)	15.9	16.5	3.70	No
Q03	322054106475201	11/08/2010	Sodium, water, filtered (mg/L)	76.6	77.7	1.43	No
Q03	322054106475201	11/08/2010	Hardness, water (mg/L as $CaCO_3$)	742	750	1.07	No
Q03	322054106475201	11/08/2010	Bromide, water, filtered (mg/L)	0.33	0.33	0.00	No
Q03	322054106475201	11/08/2010	Chloride, water, filtered (mg/L)	133	135	1.49	No
Q03	322054106475201	11/08/2010	Fluoride, water, filtered (mg/L)	0.20	0.19	5.13	No
Q03	322054106475201	11/08/2010	Silica, water, filtered (mg/L)	28.9	28.7	0.69	No
Q03	322054106475201	11/08/2010	Sulfate, water, filtered (mg/L)	469	479	2.11	No
Q03	322054106475201	11/08/2010	Ammonia, water, filtered (mg/L as nitrogen)	0.030	0.031	3.28	No
Q03	322054106475201	11/08/2010	Ammonia, water, filtered (mg/L as ammonium)	0.039	0.040	2.53	No
Q03	322054106475201	11/08/2010	Total nitrogen, water, filtered (mg/L)	0.14	0.14	0.00	No
Q03	322054106475201	11/08/2010	Orthophosphate, water, filtered (mg/L)	0.081	0.081	0.00	No
Q03	322054106475201	11/08/2010	Orthophosphate, water, filtered (mg/L as phosphorus)	0.026	0.026	0.00	No
Q03	322054106475201	11/08/2010	Barium, water, filtered (µg/L)	49	49	0.00	No
Q03	322054106475201	11/08/2010	Antimony, water, filtered (µg/L)	0.10	0.10	0.00	No
Q03	322054106475201	11/08/2010	Arsenic, water, filtered (µg/L)	1.9	1.9	0.00	No
Q03	322054106475201	11/08/2010	Boron, water, filtered (µg/L)	187	186	0.54	No
Q03	322054106475201	11/08/2010	Cadmium, water, filtered (µg/L)	0.03	0.03	0.00	No
Q03	322054106475201	11/08/2010	Chromium, water, filtered (µg/L)	<0.06	0.15	--	No
Q03	322054106475201	11/08/2010	Copper, water, filtered (µg/L)	1.3	1.3	0.00	No
Q03	322054106475201	11/08/2010	Lead, water, filtered (µg/L)	0.48	0.52	8.00	No
Q03	322054106475201	11/08/2010	Cobalt, water, filtered (µg/L)	0.68	0.67	1.48	No
Q03	322054106475201	11/08/2010	Lithium, water, filtered (µg/L)	113	116	2.62	No
Q03	322054106475201	11/08/2010	Manganese, water, filtered (µg/L)	915	918	0.33	No
Q03	322054106475201	11/08/2010	Molybdenum, water, filtered (µg/L)	8.00	8.10	1.24	No
Q03	322054106475201	11/08/2010	Nickel, water, filtered (µg/L)	1.0	1.1	9.52	No
Q03	322054106475201	11/08/2010	Thallium, water, filtered (µg/L)	0.34	0.33	2.99	No
Q03	322054106475201	11/08/2010	Vanadium, water, filtered (µg/L)	5.2	5.1	1.94	No
Q03	322054106475201	11/08/2010	Selenium, water, filtered (µg/L)	0.16	0.16	0.00	No
Q03	322054106475201	11/08/2010	Zinc, water, filtered (µg/L)	4.6	4.6	0.00	No

Table 7. Relative percent differences between environmental and sequential-replicate samples analyzed for physicochemical properties, dissolved solids, major ions, nutrients, trace elements, and selected pesticides measured in groundwater samples collected from wells in the Mesilla Basin study area in Doña Ana County, New Mexico, and El Paso County, Texas, 2010.—Continued

[Note: Where a laboratory reporting level (LRL) was applicable, results are reported only where the concentrations in the environmental and replicate samples were both equal to or larger than the LRL. USGS, U.S. Geological Survey; mm/dd/yyyy, month/day/year; µS/cm at 25 °C, microsiemen per centimeter at 25 degrees Celsius; mg/L, milligram per liter; µg/L, microgram per liter; <, less than laboratory reporting level; --, not available; pCi/L; picocurie per liter]

Well identifier (fig. 20)	USGS station number	Sample date (mm/dd/yyyy)	Constituent[1]	Environmental result	Replicate result	Relative percent differences	Relative percent difference greater than 10 percent?
Q03	322054106475201	11/08/2010	Organic carbon, water, filtered (mg/L)	2.2	2.2	0.00	No
Q03	322054106475201	11/08/2010	Radon-222, water, unfiltered (pCi/L)	2,180	2,310	5.79	No
Q03	322054106475201	11/08/2010	Strontium, water, filtered (µg/L)	2,790	2,780	0.36	No
Q03	322054106475201	11/08/2010	Uranium (natural), water, filtered (µg/L)	62.4	62.7	0.48	No
Q03	322054106475201	11/08/2010	1,2-Dichloropropane, water, unfiltered (µg/L)	0.14	0.14	0.00	No
Q17	315955106362201	11/15/2010	Specific conductance, water, unfiltered, laboratory (µS/cm at 25 °C)	1,030	1,030	0.00	No
Q17	315955106362201	11/15/2010	Alkalinity, water, filtered, inflection-point method, field (mg/L as $CaCO_3$)	99.1	98.7	0.40	No
Q17	315955106362201	11/15/2010	Bicarbonate, water, filtered, inflection-point method, field (mg/L)	121	120	0.83	No
Q17	315955106362201	11/15/2010	Arsenic, water, filtered (µg/L)	10.6	10.5	0.95	No
Q17	315955106362201	11/15/2010	Boron, water, filtered (µg/L)	190	186	2.13	No
Q17	315955106362201	11/15/2010	Cadmium, water, filtered (µg/L)	0.02	0.02	0.00	No
Q17	315955106362201	11/15/2010	Aluminum, water, filtered (µg/L)	2.9	2.5	14.81	Yes
Q17	315955106362201	11/15/2010	Barium, water, filtered (µg/L)	64	65	1.55	No
Q17	315955106362201	11/15/2010	Beryllium, water, filtered (µg/L)	0.01	0.01	0.00	No
Q17	315955106362201	11/15/2010	Cobalt, water, filtered (µg/L)	0.03	0.02	40.00	Yes
Q17	315955106362201	11/15/2010	Lithium, water, filtered (µg/L)	89.9	86.5	3.85	No
Q17	315955106362201	11/15/2010	Manganese, water, filtered (µg/L)	4.00	4.00	0.00	No
Q17	315955106362201	11/15/2010	Molybdenum, water, filtered (µg/L)	9.1	9.1	0.00	No
Q17	315955106362201	11/15/2010	Organic carbon, water, filtered (mg/L)	0.5	0.3	50.00	Yes
Q17	315955106362201	11/15/2010	Strontium, water, filtered (µg/L)	433	437	0.92	No
Q17	315955106362201	11/15/2010	Thallium, water, filtered (µg/L)	0.01	0.01	0.00	No
Q17	315955106362201	11/15/2010	Uranium (natural), water, filtered (µg/L)	0.50	0.50	0.00	No
Q17	315955106362201	11/15/2010	Vanadium, water, filtered (µg/L)	0.12	0.11	8.70	No
Q31	315245106380601	11/09/2010	pH, water, unfiltered, laboratory (standard units)	7.6	7.6	0.00	No
Q31	315245106380601	11/09/2010	Specific conductance, water, unfiltered, laboratory (µS/cm at 25 °C)	2,230	2,240	0.45	No
Q31	315245106380601	11/09/2010	Calcium, water, filtered (mg/L)	24.5	25.1	2.42	No
Q31	315245106380601	11/09/2010	Magnesium, water, filtered (mg/L)	37.5	38.5	2.63	No
Q31	315245106380601	11/09/2010	Potassium, water, filtered (mg/L)	7.48	7.62	1.85	No
Q31	315245106380601	11/09/2010	Sodium, water, filtered (mg/L)	436	446	2.27	No
Q31	315245106380601	11/09/2010	Alkalinity, water, filtered, inflection-point method, field (mg/L as $CaCO_3$)	871	877	0.69	No

Table 7. Relative percent differences between environmental and sequential-replicate samples analyzed for physicochemical properties, dissolved solids, major ions, nutrients, trace elements, and selected pesticides measured in groundwater samples collected from wells in the Mesilla Basin study area in Doña Ana County, New Mexico, and El Paso County, Texas, 2010.—Continued

[Note: Where a laboratory reporting level (LRL) was applicable, results are reported only where the concentrations in the environmental and replicate samples were both equal to or larger than the LRL. USGS, U.S. Geological Survey; mm/dd/yyyy, month/day/year; µS/cm at 25 °C, microsiemen per centimeter at 25 degrees Celsius; mg/L, milligram per liter; µg/L, microgram per liter; <, less than laboratory reporting level; --, not available; pCi/L; picocurie per liter]

Well identifier (fig. 20)	USGS station number	Sample date (mm/dd/yyyy)	Constituent[1]	Environmental result	Replicate result	Relative percent differences	Relative percent difference greater than 10 percent?
Q31	315245106380601	11/09/2010	Bicarbonate, water, filtered, inflection-point method, field (mg/L)	1,060	1,070	0.94	No
Q31	315245106380601	11/09/2010	Hardness, water (mg/L as $CaCO_3$)	217	222	2.28	No
Q31	315245106380601	11/09/2010	Bromide, water, filtered (mg/L)	0.24	0.23	4.26	No
Q31	315245106380601	11/09/2010	Chloride, water, filtered (mg/L)	84.8	85.5	0.82	No
Q31	315245106380601	11/09/2010	Fluoride, water, filtered (mg/L)	0.73	0.74	1.36	No
Q31	315245106380601	11/09/2010	Silica, water, filtered (mg/L)	63.8	66.8	4.59	No
Q31	315245106380601	11/09/2010	Sulfate, water, filtered (mg/L)	256	258	0.78	No
Q31	315245106380601	11/09/2010	Ammonia, water, filtered (mg/L as nitrogen)	0.097	0.098	1.03	No
Q31	315245106380601	11/09/2010	Ammonia, water, filtered (mg/L as ammonium)	0.125	0.127	1.59	No
Q31	315245106380601	11/09/2010	Total nitrogen, water, filtered (mg/L)	0.10	0.11	9.52	No
Q31	315245106380601	11/09/2010	Orthophosphate, water, filtered (mg/L)	0.275	0.262	4.84	No
Q31	315245106380601	11/09/2010	Orthophosphate, water, filtered (mg/L as phosphorus)	0.090	0.085	5.71	No
Q31	315245106380601	11/09/2010	Aluminum, water, filtered (µg/L)	4.0	4.6	13.95	Yes
Q31	315245106380601	11/09/2010	Barium, water, filtered (µg/L)	25	24	4.08	No
Q31	315245106380601	11/09/2010	Beryllium, water, filtered (µg/L)	0.04	0.06	40.00	Yes
Q31	315245106380601	11/09/2010	Cadmium, water, filtered (µg/L)	0.06	0.06	0.00	No
Q31	315245106380601	11/09/2010	Chromium, water, filtered (µg/L)	0.08	0.35	125.58	Yes
Q31	315245106380601	11/09/2010	Iron, water, filtered (µg/L)	108	112	3.64	No
Q31	315245106380601	11/09/2010	Lead, water, filtered (µg/L)	0.02	0.02	0.00	No
Q31	315245106380601	11/09/2010	Lithium, water, filtered (µg/L)	547	555	1.45	No
Q31	315245106380601	11/09/2010	Manganese, water, filtered (µg/L)	37.8	37.6	0.53	No
Q31	315245106380601	11/09/2010	Molybdenum, water, filtered (µg/L)	32.5	33.0	1.53	No
Q31	315245106380601	11/09/2010	Nickel, water, filtered (µg/L)	0.70	0.93	28.22	Yes
Q31	315245106380601	11/09/2010	Strontium, water, filtered (µg/L)	975	930	4.72	No
Q31	315245106380601	11/09/2010	Thallium, water, filtered (µg/L)	0.05	0.05	0.00	No
Q31	315245106380601	11/09/2010	Antimony, water, filtered (µg/L)	0.03	0.04	28.57	Yes
Q31	315245106380601	11/09/2010	Arsenic, water, filtered (µg/L)	116	113	2.62	No
Q31	315245106380601	11/09/2010	Boron, water, filtered (µg/L)	1,050	1,050	0.00	No
Q31	315245106380601	11/09/2010	Cobalt, water, filtered (µg/L)	0.18	0.24	28.57	Yes
Q31	315245106380601	11/09/2010	Dissolved solids dried at 180 degrees Celsius, water, filtered (mg/L)	1,480	1,480	0.00	No
Q31	315245106380601	11/09/2010	Uranium (natural), water, filtered (µg/L)	18.6	18.6	0.00	No

Table 7. Relative percent differences between environmental and sequential-replicate samples analyzed for physicochemical properties, dissolved solids, major ions, nutrients, trace elements, and selected pesticides measured in groundwater samples collected from wells in the Mesilla Basin study area in Doña Ana County, New Mexico, and El Paso County, Texas, 2010.—Continued

[Note: Where a laboratory reporting level (LRL) was applicable, results are reported only where the concentrations in the environmental and replicate samples were both equal to or larger than the LRL. USGS, U.S. Geological Survey; mm/dd/yyyy, month/day/year; µS/cm at 25 °C, microsiemen per centimeter at 25 degrees Celsius; mg/L, milligram per liter; µg/L, microgram per liter; <, less than laboratory reporting level; --, not available; pCi/L; picocurie per liter]

Well identifier (fig. 20)	USGS station number	Sample date (mm/dd/yyyy)	Constituent[1]	Environmental result	Replicate result	Relative percent differences	Relative percent difference greater than 10 percent?
Q37	315006106354601	11/18/2010	pH, water, unfiltered, laboratory (standard units)	7.6	7.5	1.32	No
Q37	315006106354601	11/18/2010	Specific conductance, water, unfiltered, laboratory (µS/cm at 25 °C)	3,360	3,350	0.30	No
Q37	315006106354601	11/18/2010	Calcium, water, filtered (mg/L)	172	169	1.76	No
Q37	315006106354601	11/18/2010	Magnesium, water, filtered (mg/L)	19.1	18.9	1.05	No
Q37	315006106354601	11/18/2010	Potassium, water, filtered (mg/L)	6.94	6.96	0.29	No
Q37	315006106354601	11/18/2010	Sodium, water, filtered (mg/L)	518	513	0.97	No
Q37	315006106354601	11/18/2010	Hardness, water (mg/L as $CaCO_3$)	510	503	1.38	No
Q37	315006106354601	11/18/2010	Bromide, water, filtered (mg/L)	0.59	0.59	0.00	No
Q37	315006106354601	11/18/2010	Chloride, water, filtered (mg/L)	631	629	0.32	No
Q37	315006106354601	11/18/2010	Fluoride, water, filtered (mg/L)	0.53	0.55	3.70	No
Q37	315006106354601	11/18/2010	Silica, water, filtered (mg/L)	36.8	36.6	0.54	No
Q37	315006106354601	11/18/2010	Sulfate, water, filtered (mg/L)	616	602	2.30	No
Q37	315006106354601	11/18/2010	Ammonia, water, filtered (mg/L as nitrogen)	0.160	0.161	0.62	No
Q37	315006106354601	11/18/2010	Ammonia, water, filtered (mg/L as ammonium)	0.206	0.208	0.97	No
Q37	315006106354601	11/18/2010	Orthophosphate, water, filtered (mg/L)	0.097	0.096	1.04	No
Q37	315006106354601	11/18/2010	Orthophosphate, water, filtered (mg/L as phosphorus)	0.032	0.031	3.17	No
Q37	315006106354601	11/18/2010	Total nitrogen, water, filtered (mg/L)	0.26	0.24	8.00	No
Q37	315006106354601	11/18/2010	Barium, water, filtered (µg/L)	39	39	0.00	No
Q37	315006106354601	11/18/2010	Beryllium, water, filtered (µg/L)	0.02	0.01	66.67	Yes
Q37	315006106354601	11/18/2010	Antimony, water, filtered (µg/L)	0.06	<0.05	--	No
Q37	315006106354601	11/18/2010	Arsenic, water, filtered (µg/L)	6.3	6.3	0.00	No
Q37	315006106354601	11/18/2010	Boron, water, filtered (µg/L)	502	491	2.22	No
Q37	315006106354601	11/18/2010	Cadmium, water, filtered (µg/L)	0.10	0.09	10.53	Yes
Q37	315006106354601	11/18/2010	Cobalt, water, filtered (µg/L)	0.19	0.05	116.67	Yes
Q37	315006106354601	11/18/2010	Iron, water, filtered (µg/L)	323	329	1.84	No
Q37	315006106354601	11/18/2010	Lead, water, filtered (µg/L)	0.20	0.20	0.00	No
Q37	315006106354601	11/18/2010	Lithium, water, filtered (µg/L)	207	211	1.91	No
Q37	315006106354601	11/18/2010	Manganese, water, filtered (µg/L)	531	529	0.38	No
Q37	315006106354601	11/18/2010	Molybdenum, water, filtered (µg/L)	25.5	25.3	0.79	No
Q37	315006106354601	11/18/2010	Nickel, water, filtered (µg/L)	0.25	0.22	12.77	Yes
Q37	315006106354601	11/18/2010	Vanadium, water, filtered (µg/L)	2.8	2.9	3.51	No
Q37	315006106354601	11/18/2010	Selenium, water, filtered (µg/L)	0.10	<0.06	--	No

Table 7. Relative percent differences between environmental and sequential-replicate samples analyzed for physicochemical properties, dissolved solids, major ions, nutrients, trace elements, and selected pesticides measured in groundwater samples collected from wells in the Mesilla Basin study area in Doña Ana County, New Mexico, and El Paso County, Texas, 2010.—Continued

[Note: Where a laboratory reporting level (LRL) was applicable, results are reported only where the concentrations in the environmental and replicate samples were both equal to or larger than the LRL. USGS, U.S. Geological Survey; mm/dd/yyyy, month/day/year; µS/cm at 25 °C, microsiemen per centimeter at 25 degrees Celsius; mg/L, milligram per liter; µg/L, microgram per liter; <, less than laboratory reporting level; --, not available; pCi/L; picocurie per liter]

Well identi-fier (fig. 20)	USGS station number	Sample date (mm/dd/yyyy)	Constituent[1]	Environ-mental result	Replicate result	Relative percent differences	Relative percent difference greater than 10 percent?
Q37	315006106354601	11/18/2010	Zinc, water, filtered (µg/L)	6.3	6.2	1.60	No
Q37	315006106354601	11/18/2010	Radon-222, water, unfiltered (pCi/L)	330	300	9.52	No
Q37	315006106354601	11/18/2010	Strontium, water, filtered (µg/L)	2,150	2,130	0.93	No
Q37	315006106354601	11/18/2010	Uranium (natural), water, filtered (µg/L)	0.84	0.73	14.01	Yes
Q37	315006106354601	11/18/2010	Organic carbon, water, filtered (mg/L)	2.0	2.0	0.00	No
Q37	315006106354601	11/18/2010	Dissolved solids dried at 180 degrees Celsius, water, filtered (mg/L)	2,180	2,170	0.46	No
Q37	315006106354601	11/18/2010	Ethyl methyl ketone, water, unfiltered (µg/L)	0.5	0.5	0.00	No

[1]Constituents reported where complete sample pairs were available.

Table 8. Concentrations of selected pesticides in unspiked and spiked environmental samples and percent recovery of selected pesticide compounds added to spiked environmental samples, Mesilla Basin study area in Doña Ana County, New Mexico, and El Paso County, Texas, 2010.

[USGS, U.S. Geological Survey; mm/dd/yyyy, month/day/year; µg/L, microgram per liter; <, less than laboratory reporting level or interim laboratory reporting level; E, estimated; DCPA, dimethyl tetrachloroterephthalate; EPTC, s-ethyl dipropylthiocarbamate; CFC, chlorofluorocarbon; MTBE, methyl tert-butyl ether]

Well identifier (fig. 20)	USGS station number	Sample date (mm/dd/yyyy)	Constituent	Concentration measured in unspiked environmental sample (µg/L)	Concentration added to replicate (split) environmental sample (µg/L)[1]	Concentration measured in spiked environmental sample (µg/L)	Percent recovery
Q14	320253106364001	11/15/2010	1-Naphthol, water, filtered (0.7 micron glass fiber filter)	<0.036	0.100	E0.053	53
Q14	320253106364001	11/15/2010	2,6-Diethylaniline, water, filtered (0.7 micron glass fiber filter)	<0.006	0.100	0.103	103
Q14	320253106364001	11/15/2010	2-Ethyl-6-methylaniline, water, filtered	<0.010	0.100	E0.105	105
Q14	320253106364001	11/15/2010	3,4-Dichloroaniline, water, filtered	<0.004	0.100	E0.084	84
Q14	320253106364001	11/15/2010	3,5-Dichloroaniline, water, filtered	<0.004	0.100	0.094	94
Q14	320253106364001	11/15/2010	4-Chloro-2-methylphenol, water, filtered	<0.005	0.100	E0.070	70
Q14	320253106364001	11/15/2010	Acetochlor, water, filtered	<0.010	0.100	0.094	94
Q14	320253106364001	11/15/2010	Alachlor 2nd amide, water, filtered	<0.010	0.100	0.098	98
Q14	320253106364001	11/15/2010	Alachlor, water, filtered	<0.008	0.100	0.094	94
Q14	320253106364001	11/15/2010	alpha-Endosulfan, water, filtered	<0.006	0.100	0.093	93
Q14	320253106364001	11/15/2010	Atrazine, water, filtered	<0.008	0.100	0.093	93
Q14	320253106364001	11/15/2010	Azinphos-methyl oxygen analog, water, filtered	<0.042	0.100	E0.048	48
Q14	320253106364001	11/15/2010	Azinphos-methyl, water, filtered (0.7 micron glass fiber filter)	<0.120	0.100	E0.076	76
Q14	320253106364001	11/15/2010	Benfluralin, water, filtered (0.7 micron glass fiber filter)	<0.014	0.100	0.075	75
Q14	320253106364001	11/15/2010	Carbaryl, water, filtered (0.7 micron glass fiber filter)	<0.060	0.100	E0.108	108
Q14	320253106364001	11/15/2010	Carbofuran, water, filtered (0.7 micron glass fiber filter)	<0.060	0.100	E0.111	111
Q14	320253106364001	11/15/2010	Chlorpyrifos oxygen analog, water, filtered	<0.060	0.100	E0.044	44
Q14	320253106364001	11/15/2010	Chlorpyrifos, water, filtered	<0.004	0.100	0.091	91
Q14	320253106364001	11/15/2010	deethylatrazine, water, filtered	<0.006	0.100	E0.100	100
Q14	320253106364001	11/15/2010	cis-Permethrin, water, filtered (0.7 micron glass fiber filter)	<0.010	0.100	0.076	76
Q14	320253106364001	11/15/2010	cis-Propiconazole, water, filtered	<0.008	0.100	E0.050	50
Q14	320253106364001	11/15/2010	Cyanazine, water, filtered	<0.022	0.100	0.108	108
Q14	320253106364001	11/15/2010	Cyfluthrin, water, filtered	<0.016	0.100	E0.075	75
Q14	320253106364001	11/15/2010	Cypermethrin, water, filtered	<0.020	0.100	E0.068	68
Q14	320253106364001	11/15/2010	DCPA, water, filtered (0.7 micron glass fiber filter)	<0.008	0.100	0.120	120
Q14	320253106364001	11/15/2010	Desulfinylfipronil amide, water, filtered	<0.029	0.100	E0.104	104
Q14	320253106364001	11/15/2010	Desulfinylfipronil, water, filtered	<0.012	0.100	0.108	108
Q14	320253106364001	11/15/2010	Diazinon, water, filtered	<0.006	0.100	0.098	98
Q14	320253106364001	11/15/2010	Diazoxon, water, filtered	<0.010	0.100	0.087	87

Table 8. Concentrations of selected pesticides in unspiked and spiked environmental samples and percent recovery of selected pesticide compounds added to spiked environmental samples, Mesilla Basin study area in Doña Ana County, New Mexico, and El Paso County, Texas, 2010.—Continued

[USGS, U.S. Geological Survey; mm/dd/yyyy, month/day/year; µg/L, microgram per liter; <, less than laboratory reporting level or interim laboratory reporting level; E, estimated; DCPA, dimethyl tetrachloroterephthalate; EPTC, s-ethyl dipropylthiocarbamate; CFC, chlorofluorocarbon; MTBE, methyl tert-butyl ether]

Well identifier (fig. 20)	USGS station number	Sample date (mm/dd/yyyy)	Constituent	Concentration measured in unspiked environmental sample (µg/L)	Concentration added to replicate (split) environmental sample (µg/L)[1]	Concentration measured in spiked environmental sample (µg/L)	Percent recovery
Q14	320253106364001	11/15/2010	Dichlorvos, water, filtered	<0.040	0.100	E0.048	48
Q14	320253106364001	11/15/2010	Dicrotophos, water, filtered	<0.080	0.100	E0.038	38
Q14	320253106364001	11/15/2010	Dieldrin, water, filtered	<0.008	0.100	0.109	109
Q14	320253106364001	11/15/2010	Dimethoate, water, filtered (0.7 micron glass fiber filter)	<0.006	0.100	E0.060	60
Q14	320253106364001	11/15/2010	Disulfoton sulfone, water, filtered	<0.014	0.100	0.089	89
Q14	320253106364001	11/15/2010	Disulfoton, water, filtered (0.7 micron glass fiber filter)	<0.040	0.100	E0.096	96
Q14	320253106364001	11/15/2010	Endosulfan sulfate, water, filtered	<0.016	0.100	0.081	81
Q14	320253106364001	11/15/2010	EPTC, water, filtered (0.7 micron glass fiber filter)	<0.006	0.100	0.103	103
Q14	320253106364001	11/15/2010	Ethion monoxon, water, filtered	<0.021	0.100	E0.095	95
Q14	320253106364001	11/15/2010	Ethion, water, filtered	<0.008	0.100	0.084	84
Q14	320253106364001	11/15/2010	Ethoprop, water, filtered (0.7 micron glass fiber filter)	<0.016	0.100	0.099	99
Q14	320253106364001	11/15/2010	Fenamiphos sulfone, water, filtered	<0.054	0.100	0.087	87
Q14	320253106364001	11/15/2010	Fenamiphos sulfoxide, water, filtered	<0.080	0.100	E0.013	13
Q14	320253106364001	11/15/2010	Fenamiphos, water, filtered	<0.030	0.100	E0.088	88
Q14	320253106364001	11/15/2010	Fipronil sulfide, water, filtered	<0.012	0.100	0.090	90
Q14	320253106364001	11/15/2010	Fipronil sulfone, water, filtered	<0.024	0.100	0.085	85
Q14	320253106364001	11/15/2010	Fipronil, water, filtered	<0.018	0.100	E0.110	110
Q14	320253106364001	11/15/2010	Fonofos, water, filtered	<0.005	0.100	0.088	88
Q14	320253106364001	11/15/2010	Hexazinone, water, filtered	<0.008	0.100	0.057	57
Q14	320253106364001	11/15/2010	Iprodione, water, filtered	<0.014	0.100	E0.050	50
Q14	320253106364001	11/15/2010	Isofenphos, water, filtered	<0.006	0.100	0.086	86
Q14	320253106364001	11/15/2010	lambda-Cyhalothrin, water, filtered	<0.010	0.100	E0.056	56
Q14	320253106364001	11/15/2010	Malaoxon, water, filtered	<0.022	0.100	E0.105	105
Q14	320253106364001	11/15/2010	Malathion, water, filtered	<0.016	0.100	0.086	86
Q14	320253106364001	11/15/2010	Metalaxyl, water, filtered	<0.014	0.100	0.101	101
Q14	320253106364001	11/15/2010	Methidathion, water, filtered	<0.012	0.100	0.084	84
Q14	320253106364001	11/15/2010	Methyl paraoxon, water, filtered	<0.014	0.100	E0.073	73
Q14	320253106364001	11/15/2010	Methyl parathion, water, filtered (0.7 micron glass fiber filter)	<0.008	0.100	0.089	89
Q14	320253106364001	11/15/2010	Metolachlor, water, filtered	<0.020	0.100	0.097	97

Table 8. Concentrations of selected pesticides in unspiked and spiked environmental samples and percent recovery of selected pesticide compounds added to spiked environmental samples, Mesilla Basin study area in Doña Ana County, New Mexico, and El Paso County, Texas, 2010.—Continued

[USGS, U.S. Geological Survey; mm/dd/yyyy, month/day/year; µg/L, microgram per liter; <, less than laboratory reporting level or interim laboratory reporting level; E, estimated; DCPA, dimethyl tetrachloroterephthalate; EPTC, s-ethyl dipropylthiocarbamate; CFC, chlorofluorocarbon; MTBE, methyl tert-butyl ether]

Well identifier (fig. 20)	USGS station number	Sample date (mm/dd/yyyy)	Constituent	Concentration measured in unspiked environmental sample (µg/L)	Concentration added to replicate (split) environmental sample (µg/L)[1]	Concentration measured in spiked environmental sample (µg/L)	Percent recovery
Q14	320253106364001	11/15/2010	Metribuzin, water, filtered	<0.012	0.100	0.089	89
Q14	320253106364001	11/15/2010	Molinate, water, filtered (0.7 micron glass fiber filter)	<0.004	0.100	0.104	104
Q14	320253106364001	11/15/2010	Myclobutanil, water, filtered	<0.010	0.100	0.082	82
Q14	320253106364001	11/15/2010	Oxyfluorfen, water, filtered	<0.006	0.100	0.073	73
Q14	320253106364001	11/15/2010	Pendimethalin, water, filtered (0.7 micron glass fiber filter)	<0.012	0.100	0.095	95
Q14	320253106364001	11/15/2010	Phorate oxygen analog, water, filtered	<0.027	0.100	E0.092	92
Q14	320253106364001	11/15/2010	Phorate, water, filtered (0.7 micron glass fiber filter)	<0.020	0.100	0.092	92
Q14	320253106364001	11/15/2010	Phosmet oxygen analog, water, filtered	<0.051	0.100	<0.051	51
Q14	320253106364001	11/15/2010	Phosmet, water, filtered	<0.140	0.100	E0.010	10
Q14	320253106364001	11/15/2010	Prometon, water, filtered	<0.012	0.100	0.088	88
Q14	320253106364001	11/15/2010	Prometryn, water, filtered	<0.006	0.100	0.089	89
Q14	320253106364001	11/15/2010	Propanil, water, filtered (0.7 micron glass fiber filter)	<0.010	0.100	0.095	95
Q14	320253106364001	11/15/2010	Propargite, water, filtered (0.7 micron glass fiber filter)	<0.020	0.100	0.095	95
Q14	320253106364001	11/15/2010	Propyzamide, water, filtered (0.7 micron glass fiber filter)	<0.004	0.100	0.094	94
Q14	320253106364001	11/15/2010	Simazine, water, filtered	<0.006	0.100	0.085	85
Q14	320253106364001	11/15/2010	Tebuconazole, water, filtered	<0.020	0.100	0.081	81
Q14	320253106364001	11/15/2010	Tebuthiuron, water, filtered (0.7 micron glass fiber filter)	<0.028	0.100	0.122	122
Q14	320253106364001	11/15/2010	Tefluthrin, water, filtered	<0.010	0.100	E0.071	71
Q14	320253106364001	11/15/2010	Terbufos oxygen analog sulfone, water, filtered	<0.045	0.100	0.0903	90
Q14	320253106364001	11/15/2010	Terbufos, water, filtered (0.7 micron glass fiber filter)	<0.018	0.100	0.080	80
Q14	320253106364001	11/15/2010	Terbuthylazine, water, filtered	<0.006	0.100	0.096	96
Q14	320253106364001	11/15/2010	Thiobencarb, water, filtered (0.7 micron glass fiber filter)	<0.016	0.100	0.101	101
Q14	320253106364001	11/15/2010	trans-Propiconazole, water, filtered	<0.010	0.075	E0.065	84
Q14	320253106364001	11/15/2010	Tribuphos, water, filtered	<0.018	0.100	E0.066	66
Q14	320253106364001	11/15/2010	Trifluralin, water, filtered (0.7 micron glass fiber filter)	<0.018	0.100	0.086	86
Q33	315114106414901	11/03/2010	1,1,1,2-Tetrachloroethane, water, unfiltered	<0.040	0.280	0.282	101
Q33	315114106414901	11/03/2010	1,1,1-Trichloroethane, water, unfiltered	<0.030	0.233	0.253	109
Q33	315114106414901	11/03/2010	1,1,2,2-Tetrachloroethane, water, unfiltered	<0.140	0.745	0.831	112
Q33	315114106414901	11/03/2010	1,1,2-Trichloroethane, water, unfiltered	<0.028	0.373	0.397	106

Table 8. Concentrations of selected pesticides in unspiked and spiked environmental samples and percent recovery of selected pesticide compounds added to spiked environmental samples, Mesilla Basin study area in Doña Ana County, New Mexico, and El Paso County, Texas, 2010.—Continued

[USGS, U.S. Geological Survey; mm/dd/yyyy, month/day/year; µg/L, microgram per liter; <, less than laboratory reporting level or interim laboratory reporting level; E, estimated; DCPA, dimethyl tetrachloroterephthalate; EPTC, s-ethyl dipropylthiocarbamate; CFC, chlorofluorocarbon; MTBE, methyl tert-butyl ether]

Well identifier (fig. 20)	USGS station number	Sample date (mm/dd/yyyy)	Constituent	Concentration measured in unspiked environmental sample (µg/L)	Concentration added to replicate (split) environmental sample (µg/L)[1]	Concentration measured in spiked environmental sample (µg/L)	Percent recovery
Q33	315114106414901	11/03/2010	1,1-Dichloroethane, water, unfiltered	<0.044	0.280	0.316	113
Q33	315114106414901	11/03/2010	1,1-Dichloroethene, water, unfiltered	<0.022	0.233	0.262	113
Q33	315114106414901	11/03/2010	1,1-Dichloropropene, water, unfiltered	<0.040	0.233	0.220	95
Q33	315114106414901	11/03/2010	1,2,3-Trichlorobenzene, water, unfiltered	<0.060	0.652	0.499	77
Q33	315114106414901	11/03/2010	1,2,3-Trichloropropane, water, unfiltered	<0.120	0.931	1.020	110
Q33	315114106414901	11/03/2010	1,2,3-Trimethylbenzene, water, unfiltered	<0.060	0.465	0.526	113
Q33	315114106414901	11/03/2010	1,2,4-Trichlorobenzene, water, unfiltered	<0.080	0.652	0.649	100
Q33	315114106414901	11/03/2010	1,2,4-Trimethylbenzene, water, unfiltered	<0.032	0.280	0.318	114
Q33	315114106414901	11/03/2010	1,2-Dibromoethane, water, unfiltered	<0.028	0.373	0.403	108
Q33	315114106414901	11/03/2010	1,2-Dichlorobenzene, water, unfiltered	<0.028	0.233	0.252	108
Q33	315114106414901	11/03/2010	1,2-Dichloroethane, water, unfiltered	<0.080	0.651	0.725	111
Q33	315114106414901	11/03/2010	1,2-Dichloropropane, water, unfiltered	<0.026	0.280	0.287	103
Q33	315114106414901	11/03/2010	1,3,5-Trimethylbenzene, water, unfiltered	<0.032	0.280	0.283	101
Q33	315114106414901	11/03/2010	1,3-Dichlorobenzene, water, unfiltered	<0.024	0.233	0.239	103
Q33	315114106414901	11/03/2010	1,3-Dichloropropane, water, unfiltered	<0.060	0.651	0.687	106
Q33	315114106414901	11/03/2010	1,4-Dichlorobenzene, water, unfiltered	<0.026	0.233	0.243	104
Q33	315114106414901	11/03/2010	2,2-Dichloropropane, water, unfiltered	<0.060	0.466	0.382	82
Q33	315114106414901	11/03/2010	2-Chlorotoluene, water, unfiltered	<0.028	0.279	0.296	106
Q33	315114106414901	11/03/2010	2-Ethyltoluene, water, unfiltered	<0.032	0.279	0.299	107
Q33	315114106414901	11/03/2010	3-Chloropropene, water, unfiltered	<0.080	0.652	E0.637	98
Q33	315114106414901	11/03/2010	4-Chlorotoluene, water, unfiltered	<0.042	0.279	0.297	106
Q33	315114106414901	11/03/2010	4-Isopropyltoluene, water, unfiltered	<0.060	0.465	0.468	101
Q33	315114106414901	11/03/2010	Acetone, water, unfiltered	<3.4	27.9	34.0	122
Q33	315114106414901	11/03/2010	Acrylonitrile, water, unfiltered	<0.80	6.51	7.59	117
Q33	315114106414901	11/03/2010	Benzene, water, unfiltered	<0.026	0.233	0.249	107
Q33	315114106414901	11/03/2010	Bromobenzene, water, unfiltered	<0.022	0.233	0.236	101
Q33	315114106414901	11/03/2010	Bromochloromethane, water, unfiltered	<0.060	0.466	0.540	116
Q33	315114106414901	11/03/2010	Bromoethene, water, unfiltered	<0.120	0.930	1.090	117
Q33	315114106414901	11/03/2010	Bromomethane, water, unfiltered	<0.200	1.395	E1.680	120

Table 8. Concentrations of selected pesticides in unspiked and spiked environmental samples and percent recovery of selected pesticide compounds added to spiked environmental samples, Mesilla Basin study area in Doña Ana County, New Mexico, and El Paso County, Texas, 2010.—Continued

[USGS, U.S. Geological Survey; mm/dd/yyyy, month/day/year; µg/L, microgram per liter; <, less than laboratory reporting level or interim laboratory reporting level; E, estimated; DCPA, dimethyl tetrachloroterephthalate; EPTC, s-ethyl dipropylthiocarbamate; CFC, chlorofluorocarbon; MTBE, methyl tert-butyl ether]

Well identifier (fig. 20)	USGS station number	Sample date (mm/dd/yyyy)	Constituent	Concentration measured in unspiked environmental sample (µg/L)	Concentration added to replicate (split) environmental sample (µg/L)[1]	Concentration measured in spiked environmental sample (µg/L)	Percent recovery
Q33	315114106414901	11/03/2010	Carbon disulfide, water, unfiltered	<0.080	0.280	0.365	130
Q33	315114106414901	11/03/2010	CFC-11, water, unfiltered	<0.060	0.465	0.584	126
Q33	315114106414901	11/03/2010	CFC-113, water, unfiltered	<0.034	0.372	0.405	109
Q33	315114106414901	11/03/2010	CFC-12, water, unfiltered	<0.100	0.651	E0.780	120
Q33	315114106414901	11/03/2010	Bromodichloromethane, water, unfiltered	<0.034	0.372	0.369	99
Q33	315114106414901	11/03/2010	Chlorobenzene, water, unfiltered	<0.026	0.233	0.233	100
Q33	315114106414901	11/03/2010	Chloroethane, water, unfiltered	<0.060	0.465	0.546	117
Q33	315114106414901	11/03/2010	Chloromethane, water, unfiltered	<0.140	0.930	E1.250	134
Q33	315114106414901	11/03/2010	cis-1,2-Dichloroethene, water, unfiltered	<0.022	0.280	0.300	107
Q33	315114106414901	11/03/2010	cis-1,3-Dichloropropene, water, unfiltered	<0.100	0.651	0.599	92
Q33	315114106414901	11/03/2010	Dibromochloromethane, water, unfiltered	<0.120	0.931	0.930	100
Q33	315114106414901	11/03/2010	Dibromochloropropane, water, unfiltered	<0.400	2.791	3.050	109
Q33	315114106414901	11/03/2010	Dibromomethane, water, unfiltered	<0.050	0.373	0.391	105
Q33	315114106414901	11/03/2010	Dichloromethane, water, unfiltered	<0.040	0.373	0.444	119
Q33	315114106414901	11/03/2010	Diethyl ether, water, unfiltered	<0.100	0.464	0.521	112
Q33	315114106414901	11/03/2010	Diisopropyl ether, water, unfiltered	<0.060	0.465	0.464	100
Q33	315114106414901	11/03/2010	Ethyl methacrylate, water, unfiltered	<0.200	1.395	1.360	97
Q33	315114106414901	11/03/2010	Ethyl methyl ketone, water, unfiltered	<1.600	9.302	9.290	100
Q33	315114106414901	11/03/2010	Ethylbenzene, water, unfiltered	<0.036	0.280	0.283	101
Q33	315114106414901	11/03/2010	Hexachlorobutadiene, water, unfiltered	<0.080	0.465	0.406	87
Q33	315114106414901	11/03/2010	Hexachloroethane, water, unfiltered	<0.220	0.930	0.788	85
Q33	315114106414901	11/03/2010	Iodomethane, water, unfiltered	<0.260	0.930	E1.070	115
Q33	315114106414901	11/03/2010	Isobutyl methyl ketone, water, unfiltered	<0.320	2.791	3.060	110
Q33	315114106414901	11/03/2010	Isodurene, water, unfiltered	<0.080	0.652	0.734	113
Q33	315114106414901	11/03/2010	Isopropylbenzene, water, unfiltered	<0.042	0.280	0.271	97
Q33	315114106414901	11/03/2010	meta- plus para-Xylene, water, unfiltered	<0.080	0.652	0.700	107
Q33	315114106414901	11/03/2010	Methyl acrylate, water, unfiltered	<0.800	4.651	4.760	102
Q33	315114106414901	11/03/2010	Methyl acrylonitrile, water, unfiltered	<0.260	2.326	2.600	112
Q33	315114106414901	11/03/2010	Methyl methacrylate, water, unfiltered	<0.220	2.326	2.200	95
Q33	315114106414901	11/03/2010	Methyl tert-pentyl ether, water, unfiltered	<0.060	0.465	0.473	102

Table 8. Concentrations of selected pesticides in unspiked and spiked environmental samples and percent recovery of selected pesticide compounds added to spiked environmental samples, Mesilla Basin study area in Doña Ana County, New Mexico, and El Paso County, Texas, 2010.—Continued

[USGS, U.S. Geological Survey; mm/dd/yyyy, month/day/year; µg/L, microgram per liter; <, less than laboratory reporting level or interim laboratory reporting level; E, estimated; DCPA, dimethyl tetrachloroterephthalate; EPTC, s-ethyl dipropylthiocarbamate; CFC, chlorofluorocarbon; MTBE, methyl tert-butyl ether]

Well identifier (fig. 20)	USGS station number	Sample date (mm/dd/yyyy)	Constituent	Concentration measured in unspiked environmental sample (µg/L)	Concentration added to replicate (split) environmental sample (µg/L)[1]	Concentration measured in spiked environmental sample (µg/L)	Percent recovery
Q33	315114106414901	11/03/2010	MTBE, water, unfiltered	<0.100	0.652	0.715	110
Q33	315114106414901	11/03/2010	Naphthalene, water, unfiltered	<0.180	1.396	1.540	110
Q33	315114106414901	11/03/2010	n-Butyl methyl ketone, water, unfiltered	<0.400	3.721	4.010	108
Q33	315114106414901	11/03/2010	n-Butylbenzene, water, unfiltered	<0.080	0.652	0.632	97
Q33	315114106414901	11/03/2010	n-Propylbenzene, water, unfiltered	<0.036	0.279	0.276	99
Q33	315114106414901	11/03/2010	o-Xylene, water, unfiltered	<0.032	0.280	0.289	103
Q33	315114106414901	11/03/2010	Prehnitene, water, unfiltered	<0.100	0.652	0.724	111
Q33	315114106414901	11/03/2010	sec-Butylbenzene, water, unfiltered	<0.034	0.279	0.289	104
Q33	315114106414901	11/03/2010	Styrene, water, unfiltered	<0.042	0.279	<0.042	15
Q33	315114106414901	11/03/2010	trans-1,4-Dichloro-2-butene, water, unfiltered	<0.360	4.651	E2.350	51
Q33	315114106414901	11/03/2010	tert-Butyl ethyl ether, water, unfiltered	<0.032	0.372	0.385	103
Q33	315114106414901	11/03/2010	tert-Butylbenzene, water, unfiltered	<0.060	0.465	0.490	105
Q33	315114106414901	11/03/2010	Tetrachloroethene, water, unfiltered	<0.026	0.233	0.326	140
Q33	315114106414901	11/03/2010	Tetrachloromethane, water, unfiltered	<0.060	0.373	0.323	87
Q33	315114106414901	11/03/2010	Tetrahydrofuran, water, unfiltered	<1.400	9.302	10.600	114
Q33	315114106414901	11/03/2010	Toluene, water, unfiltered	<0.018	0.233	0.256	110
Q33	315114106414901	11/03/2010	trans-1,2-Dichloroethene, water, unfiltered	<0.018	0.233	0.257	111
Q33	315114106414901	11/03/2010	trans-1,3-Dichloropropene, water, unfiltered	<0.140	0.931	0.742	80
Q33	315114106414901	11/03/2010	Tribromomethane, water, unfiltered	<0.100	0.838	0.873	104
Q33	315114106414901	11/03/2010	Trichloroethene, water, unfiltered	<0.022	0.233	0.233	100
Q33	315114106414901	11/03/2010	Trichloromethane, water, unfiltered	<0.030	0.465	0.268	58
Q33	315114106414901	11/03/2010	Vinyl chloride, water, unfiltered	<0.060	0.465	0.576	124

[1]Values are the sample fortification concentrations listed in Laboratory Schedules 2003 and 2020 by the National Water Quality Laboratory.

Table 9. Major-ion balances and saturation indexes calculated from constituent concentrations measured in groundwater samples collected in the Mesilla Basin study area in Doña Ana County, New Mexico, and El Paso County, Texas, 2010.

[USGS, U.S. Geological Survey; SI, saturation index; USF, upper part of the Santa Fe Group; MSF, middle part of the Santa Fe Group; RGA, Rio Grande alluvium; LSF, lower part of the Santa Fe Group, --, not available]

Well identifier (fig. 20)	USGS station number	Hydrogeologic unit	Major-ion balance	Major-ion balance percent error	Absolute major-ion balance percent error	SI calcite	SI dolomite	SI gypsum	SI anhydrite
Q00	322320106551801	USF	-0.00032	-1.20	1.20	0.06	-0.48	-1.40	-1.64
Q01	322233106590901	MSF	0.00000	-0.01	0.01	-0.08	-0.21	-1.53	-1.76
Q02	322219106485001	MSF	-0.00109	-4.65	4.65	0.01	-0.36	-1.55	-1.78
Q03	322054106475201	USF	-0.00031	-0.96	0.96	0.31	0.15	-0.71	-0.95
Q04	322024106463901	USF	-0.00010	-0.55	0.55	-0.01	-0.26	-1.51	-1.74
Q05	321934106482601	MSF	-0.00002	-0.19	0.19	0.15	-0.18	-1.95	-2.18
Q06	321641106515401	MSF	0.00008	0.79	0.79	0.30	0.00	-1.84	-2.07
Q07	321628106451501	MSF	-0.00012	-1.11	1.11	0.20	-0.05	-1.84	-2.07
Q08	321501106443801	USF	-0.00019	-1.58	1.58	0.16	-0.12	-1.83	-2.07
Q09	320939106441701	USF	-0.00088	-2.72	2.72	0.57	0.63	-0.72	-0.96
Q10	320654106504201	MSF	-0.00064	-3.46	3.46	0.15	-0.04	-2.05	-2.24
Q11	320643106440401	MSF	-0.00011	-1.26	1.26	0.27	-0.02	-2.09	-2.33
Q12	320604107051201	MSF	-0.00038	-1.87	1.87	0.07	0.38	-2.03	-2.25
Q13	320445106421001	USF	-0.00077	-1.84	1.84	0.48	0.54	-0.58	-0.82
Q14	320253106364001	USF	-0.00065	-1.45	1.45	0.06	-0.04	-1.28	-1.50
Q15	320054106533901	USF	-0.00030	-1.64	1.64	0.15	0.59	-2.26	-2.43
Q16	320040107054601	MSF	-0.00078	-3.40	3.40	0.15	0.11	-2.64	-2.85
Q17	315955106362201	MSF	-0.00034	-1.81	1.81	0.15	-0.91	-1.69	-1.88
Q18	315940106372304	RGA	0.00002	0.27	0.27	0.03	-1.31	-2.50	-2.71
Q19	315940106372303	USF	0.00000	0.04	0.04	0.08	-0.82	-2.36	-2.57
Q20	315940106372301	MSF	-0.00447	-5.05	5.05	0.14	0.21	-0.78	-1.00
Q21	315940106372302	LSF	-0.00076	-2.19	2.19	0.33	0.44	-1.43	-1.65
Q22	315723106415201	MSF	-0.00001	-0.09	0.09	0.30	0.35	-2.30	-2.51
Q23	315712106361803	USF	-0.00063	-3.70	3.70	0.21	-0.28	-1.60	-1.83
Q24	315712106361802	MSF	-0.00045	-2.29	2.29	0.24	0.05	-1.40	-1.64
Q25	315712106361804	LSF	-0.00023	-0.68	0.68	0.18	-1.87	-1.24	-1.46
Q26	315646106374401	RGA	-0.00221	-2.30	2.30	0.67	0.89	-0.29	-0.53
Q27	315646106374403	USF	0.00011	1.47	1.47	0.08	-1.09	-2.85	-3.07
Q28	315646106374404	MSF	0.00029	0.80	0.80	0.06	-1.50	-1.96	-2.17
Q29	315646106374402	LSF	0.00005	0.68	0.68	0.05	-0.97	-2.60	-2.82
Q30	315519106593101	MSF	0.00003	0.20	0.20	0.07	-0.06	-2.19	-2.40
Q31	315245106380602	MSF	-0.01904	-15.60	15.60	0.38	0.73	-1.30	-1.50
Q32	315245106380601	LSF	-0.00161	-3.43	3.43	0.02	0.56	-1.90	-2.12
Q33	315114106414901	MSF	-0.00094	-4.78	4.78	0.26	0.32	-2.18	-2.38
Q34	315013106362601	USF	-0.00103	-1.76	1.76	0.04	-1.17	-1.05	-1.27
Q35	315013106362602	MSF	0.00815	5.31	5.31	0.26	-0.37	-0.34	-0.54
Q36	315013106395301	MSF	-0.00047	-1.84	1.84	0.08	-0.10	-1.25	-1.46
Q37	315006106354601	RGA	-0.00246	-3.86	3.86	0.38	0.08	-0.78	-1.02
Q38	314932106493401	MSF	-0.00138	-5.58	5.58	0.11	0.17	-2.16	-2.36
Q39	314908106371201	MSF	-0.00032	-1.46	1.46	0.19	-0.71	-1.43	-1.63
Q40	314817106325802	USF	-0.05776	-5.89	5.89	0.17	0.57	0.04	-0.18
Q41	314817106325801	MSF	-0.02250	-3.94	3.94	0.44	0.86	0.05	-0.18
Q42	314746106353601	MSF	-0.00125	-2.85	2.85	0.13	-1.02	-0.81	-1.01
Q43	314717106404401	MSF	0.00000	0.05	0.05	0.09	-0.11	-2.21	-2.42

Well identifier (fig. 20)	SI anhydrite	SI aragonite	SI celestite	SI strontianite	SI halite	SI oxygen gas	SI carbon dioxide gas	SI quartz	SI chalcedony
Q00	-1.64	-0.09	-1.61	-1.35	-5.98	-1.90	-2.06	0.80	0.35
Q01	-1.76	-0.23	-1.29	-1.09	-5.89	-1.01	-2.43	1.10	0.66
Q02	-1.78	-0.13	-1.64	-1.32	-6.16	-1.59	-1.89	0.65	0.22
Q03	-0.95	0.16	-0.92	-1.11	-6.61	-2.36	-1.77	0.76	0.31
Q04	-1.74	-0.15	-1.37	-1.10	-6.47	-2.35	-2.24	0.71	0.27
Q05	-2.18	0.01	-2.15	-1.28	-7.13	-2.65	-2.63	0.71	0.26
Q06	-2.07	0.15	-2.06	-1.16	-7.14	-2.64	-2.78	0.68	0.24
Q07	-2.07	0.05	-2.02	-1.22	-7.13	-2.64	-2.62	0.65	0.21
Q08	-2.07	0.01	-1.96	-1.18	-7.09	-2.66	-2.51	0.76	0.31
Q09	-0.96	0.42	-0.88	-0.81	-6.48	-2.66	-2.14	0.74	0.29
Q10	-2.24	0.01	-1.93	-1.03	-6.60	-2.57	-2.26	0.75	0.34
Q11	-2.33	0.13	-2.24	-1.10	-7.40	-1.24	-2.86	0.65	0.20
Q12	-2.25	-0.08	-1.58	-0.74	-6.71	-0.90	-2.87	0.42	-0.01
Q13	-0.82	0.34	-0.78	-0.93	-6.14	-2.35	-1.83	0.77	0.32
Q14	-1.50	-0.08	-1.04	-0.96	-5.65	-2.31	-1.12	0.90	0.47
Q15	-2.43	0.01	-1.89	-0.80	-6.40	-2.55	-2.55	0.67	0.27
Q16	-2.85	0.01	-2.35	-0.83	-6.54	-2.30	-2.65	0.39	-0.04
Q17	-1.88	0.01	-1.96	-1.42	-6.16	-2.57	-2.81	0.65	0.24
Q18	-2.71	-0.11	-2.89	-1.63	-7.00	-2.60	-3.69	0.56	0.13
Q19	-2.57	-0.06	-2.56	-1.38	-7.07	-2.30	-3.61	0.70	0.27
Q20	-1.00	0.00	-0.66	-1.00	-4.94	--	-1.29	0.77	0.34
Q21	-1.65	0.18	-1.32	-0.81	-5.72	-2.33	-1.98	0.84	0.40
Q22	-2.51	0.16	-2.18	-0.85	-6.56	-2.30	-3.26	0.68	0.26
Q23	-1.83	0.07	-1.61	-1.03	-6.35	-2.63	-3.58	0.70	0.26
Q24	-1.64	0.09	-1.41	-1.00	-6.42	-2.65	-2.43	0.70	0.26
Q25	-1.46	0.03	-1.70	-1.55	-5.59	-2.62	-4.59	0.49	0.06
Q26	-0.53	0.52	-0.48	-0.74	-5.08	-2.35	-1.49	0.89	0.44
Q27	-3.07	-0.06	-3.32	-1.66	-7.19	-2.60	-4.31	0.76	0.33
Q28	-2.17	-0.08	-1.90	-1.16	-5.45	-2.59	-4.13	0.42	0.00
Q29	-2.82	-0.09	-2.78	-1.39	-7.13	-2.62	-3.97	0.69	0.26
Q30	-2.40	-0.08	-2.25	-1.26	-7.35	-1.40	-1.94	1.12	0.70
Q31	-1.50	0.24	-1.24	-0.84	-4.77	-1.81	-0.96	0.95	0.53
Q32	-2.12	-0.12	-1.59	-0.92	-6.06	-2.14	-1.32	1.03	0.60
Q33	-2.38	0.12	-2.15	-1.01	-6.68	-2.11	-2.54	0.79	0.37
Q34	-1.27	-0.10	-1.44	-1.61	-5.02	-2.31	-3.90	0.71	0.28
Q35	-0.54	0.12	-0.94	-1.62	-4.30	-2.58	-3.50	0.92	0.50
Q36	-1.46	-0.06	-1.27	-1.22	-6.06	-1.51	-2.96	0.77	0.35
Q37	-1.02	0.23	-0.98	-1.04	-5.13	-2.65	-2.13	0.86	0.41
Q38	-2.36	-0.03	-2.10	-1.12	-6.07	--	-2.09	0.92	0.51
Q39	-1.63	0.05	-1.84	-1.51	-6.04	-1.43	-3.58	0.62	0.21
Q40	-0.18	0.02	0.07	-1.06	-2.70	-1.96	-1.84	0.48	0.04
Q41	-0.18	0.29	0.11	-0.74	-3.20	-1.90	-1.46	0.88	0.44
Q42	-1.01	-0.01	-1.13	-1.48	-5.58	-2.58	-3.71	0.65	0.23
Q43	-2.42	-0.05	-2.20	-1.17	-7.04	-1.83	-3.18	0.71	0.28

Table 10. Summary of selected physicochemical properties measured in groundwater samples collected in the Mesilla Basin study area in Doña Ana County, New Mexico, and El Paso County, Texas, 2010.

[USGS, U.S. Geological Survey; mm/dd/yyyy, month/day/year; ft, foot; µS/cm at 25 °C, microsiemen per centimeter at 25 degrees Celsius; mg/L, milligram per liter; USF, upper part of the Santa Fe Group; --, not available; MSF, middle part of the Santa Fe Group; RGA, Rio Grande alluvium; LSF, lower part of the Santa Fe Group]

Well identifier (fig. 20)	USGS station number	Hydrogeo-logic unit	Sample date (mm/dd/yyyy)	Sample start time	Sample depth (ft)	pH, water, unfiltered, field (standard units)	Specific conductance, water, unfiltered (µS/cm at 25 °C)	Dissolved oxygen, water, unfiltered (mg/L)	Temperature, water (degrees Celsius)
Q00	322320106551801	USF	11/17/2010	15:00	--	7.4	1,420	0.6	16.6
Q01	322233106590901	MSF	11/17/2010	11:00	--	7.8	2,010	4.2	22.2
Q02	322219106485001	MSF	11/03/2010	13:00	--	7.3	1,270	1.1	22.6
Q03	322054106475201	USF	11/08/2010	17:00	--	7.2	1,540	0.2	18.7
Q04	322024106463901	USF	11/16/2010	16:00	--	7.5	993	0.2	20.3
Q05	321934106482601	MSF	11/16/2010	12:00	--	7.8	569	0.1	19.4
Q06	321641106515401	MSF	11/16/2010	15:00	--	7.9	574	0.1	21.4
Q07	321628106451501	MSF	11/03/2010	17:00	--	7.8	599	0.1	21.1
Q08	321501106443801	USF	11/08/2010	11:00	--	7.7	644	0.1	18.2
Q09	320939106441701	USF	11/11/2010	11:00	--	7.5	1,680	0.1	18.9
Q10	320654106504201	MSF	11/11/2010	12:00	--	7.8	971	0.1	31.1
Q11	320643106440401	MSF	11/08/2010	10:00	--	8.0	453	2.6	19.9
Q12	320604107051201	MSF	11/12/2010	13:00	--	8.2	1,150	5.2	23.9
Q13	320445106421001	USF	11/11/2010	16:00	--	7.3	2,190	0.2	19.1
Q14	320253106364001	USF	11/15/2010	15:00	--	6.8	2,320	0.2	24.8
Q15	320054106533901	USF	11/16/2010	10:00	--	8.0	932	0.1	34.5
Q16	320040107054601	MSF	11/10/2010	15:00	--	8.3	1,150	0.2	27.1
Q17	315955106362201	MSF	11/15/2010	10:00	46	7.9	1,050	0.1	30.4
Q18	315940106372301	RGA	11/06/2010	17:00	55	--	--	--	--
Q19	315940106372302	USF	11/06/2010	15:00	275	7.5	1,850	0.2	22.5
Q20	315940106372303	MSF	11/06/2010	13:00	280	8.5	441	0.2	26.0
Q21	315940106372304	LSF	11/17/2010	16:00	200	8.6	465	0.1	26.7
Q22	315723106415201	MSF	11/02/2010	17:00	--	8.5	812	0.2	27.1
Q23	315712106361802	USF	11/14/2010	16:00	145	7.7	1,050	0.1	19.9
Q24	315712106361803	MSF	11/15/2010	18:00	--	8.4	954	0.1	21.9
Q25	315712106361804	LSF	11/14/2010	18:00	100	8.8	1,900	0.1	24.0
Q26	315646106374401	RGA	11/08/2010	16:00	47	7.2	4,580	0.2	19.1
Q27	315646106374402	USF	11/10/2010	18:00	275	8.8	416	0.1	24.0
Q28	315646106374403	MSF	11/12/2010	15:00	275	9.1	399	0.1	26.7
Q29	315646106374404	LSF	11/06/2010	16:00	280	8.8	1,980	0.1	28.1
Q30	315519106593101	MSF	11/18/2010	10:00	--	7.5	752	1.6	25.5
Q31	315245106380601	MSF	11/09/2010	18:00	150	7.3	2,260	0.3	23.5
Q32	315245106380602	LSF	11/10/2010	12:00	275	7.2	5,360	0.6	27.3

Table 10. Summary of selected physicochemical properties measured in groundwater samples collected in the Mesilla Basin study area in Doña Ana County, New Mexico, and El Paso County, Texas, 2010.—Continued

[USGS, U.S. Geological Survey; mm/dd/yyyy, month/day/year; ft, foot; µS/cm at 25 °C, microsiemen per centimeter at 25 degrees Celsius; mg/L, milligram per liter; USF, upper part of the Santa Fe Group; --, not available; MSF, middle part of the Santa Fe Group; RGA, Rio Grande alluvium; LSF, lower part of the Santa Fe Group]

Well identifier (fig. 20)	USGS station number	Hydrogeo-logic unit	Sample date (mm/dd/yyyy)	Sample start time	Sample depth (ft)	pH, water, unfiltered, field (standard units)	Specific conductance, water, unfiltered (µS/cm at 25 °C)	Dissolved oxygen, water, unfiltered (mg/L)	Temperature, water (degrees Celsius)
Q33	315114106414901	MSF	11/03/2010	16:00	--	8.1	1,040	0.3	28.5
Q34	315013106362601	USF	11/05/2010	17:00	135	8.2	3,120	0.2	24.2
Q35	315013106362602	MSF	11/09/2010	12:00	270	7.9	7,020	0.1	27.6
Q36	315013106395301	MSF	11/04/2010	12:00	--	7.9	1,480	1.2	28.3
Q37	315006106354601	RGA	11/18/2010	10:00	--	7.5	3,360	0.1	19.4
Q38	314932106493401	MSF	11/09/2010	12:00	360	7.7	1,160	--	29.0
Q39	314908106371201	MSF	11/02/2010	12:00	--	8.3	1,140	1.4	29.4
Q40	314817106325801	USF	11/04/2010	11:00	47	7.0	26,500	0.5	21.7
Q41	314817106325802	MSF	11/05/2010	14:00	132	7.0	42,800	0.4	22.9
Q42	314746106353601	MSF	11/15/2010	11:00	--	8.2	2,340	0.1	28.8
Q43	314717106404401	MSF	11/03/2010	10:00	--	8.2	501	0.6	26.1

Table 11. Summary of water types and selected constituents measured in groundwater samples collected in the Mesilla Basin study area in Doña Ana County, New Mexico, and El Paso County, Texas, 2010.

[USGS, U.S. Geological Survey; mm/dd/yyyy, month/day/year; ft, foot; mg/L, milligram per liter; mol/L, mole per liter; USF, upper part of the Santa Fe Group; --, not available; Na, sodium; Cl, chloride; MSF, middle part of the upper part of the Santa Fe Group; SO_4, sulfate; HCO_3, bicarbonate; Ca, calcium; RGA, Rio Grande alluvium; LSF, lower part of the Santa Fe Group; <, less than laboratory reporting level; µg/L, microgram per liter; mmol/L, millimole per liter]

Well identifier (fig. 20)	Hydro-geologic unit	USGS station number	Sample date (mm/dd/yyyy)	Sample start time	Sample depth (ft)	Water type	Chloride, water, filtered (mg/L)	Chloride, water, filtered (mol/L)	Sulfate, water, filtered (mg/L)
Q00	USF	322320106551801	11/17/2010	15:00	--	Na-Cl	223	0.00629	170
Q01	MSF	322233106590901	11/17/2010	11:00	--	Na-SO_4	139	0.00392	544
Q02	MSF	322219106485001	11/03/2010	13:00	--	Na-Cl-HCO_3	180	0.00508	139
Q03	USF	322054106475201	11/08/2010	17:00	--	Ca-SO_4	133	0.00375	469
Q04	USF	322024106463901	11/16/2010	16:00	--	Na-SO_4-HCO_3	113	0.00319	165
Q05	MSF	321934106482601	11/16/2010	12:00	--	Ca-Na-HCO_3	53.9	0.00152	58.5
Q06	MSF	321641106515401	11/16/2010	15:00	--	Ca-Na-HCO_3	61.4	0.00173	64.0
Q07	MSF	321628106451501	11/03/2010	17:00	--	Ca-Na-HCO_3	56.1	0.00158	71.6
Q08	USF	321501106443801	11/08/2010	11:00	--	Ca-HCO_3	72.7	0.00205	64.6
Q09	USF	320939106441701	11/11/2010	11:00	--	Ca-SO_4	191	0.00539	441
Q10	MSF	320654106504201	11/11/2010	12:00	--	Na-HCO_3	56.1	0.00158	135
Q11	MSF	320643106440401	11/08/2010	10:00	--	Ca-Na-HCO_3	35.4	0.000999	45.2
Q12	MSF	320604107051201	11/12/2010	13:00	--	Na-SO_4	38.6	0.00109	242
Q13	USF	320445106421001	11/11/2010	16:00	--	Ca-SO_4	204	0.00575	639
Q14	USF	320253106364001	11/15/2010	15:00	--	Na-Cl-HCO_3	397	0.0112	185
Q15	USF	320054106533901	11/16/2010	10:00	--	Na-HCO_3	95.8	0.00270	116
Q16	MSF	320040107054601	11/10/2010	15:00	--	Na-HCO_3	46.8	0.00132	134
Q17	MSF	315955106362201	11/15/2010	10:00	46	Na-Cl	171	0.00482	145
Q18	RGA	315940106372301	11/06/2010	17:00	55	Na-Cl-SO_4	745	0.0210	938
Q19	USF	315940106372302	11/06/2010	15:00	275	Na-Cl	296	0.00835	199
Q20	MSF	315940106372303	11/06/2010	13:00	280	Na-SO_4-HCO_3	42.1	0.00119	70.0
Q21	LSF	315940106372304	11/17/2010	16:00	200	Na-SO_4	42.9	0.00121	74.5
Q22	MSF	315723106415201	11/02/2010	17:00	--	Na-HCO_3	69.9	0.00197	120
Q23	USF	315712106361802	11/14/2010	16:00	145	Na-Ca-SO_4	115	0.00324	195
Q24	MSF	315712106361803	11/15/2010	18:00	--	Na-SO_4-Cl	118	0.00333	218
Q25	LSF	315712106361804	11/14/2010	18:00	100	Na-Cl-SO_4	320	0.00903	412
Q26	RGA	315646106374401	11/08/2010	16:00	47	Na-Ca-SO_4	613	0.0173	1,380
Q27	USF	315646106374402	11/10/2010	18:00	275	Na-SO_4-HCO_3	34.0	0.000959	71.1
Q28	MSF	315646106374403	11/12/2010	15:00	275	Na-SO_4-HCO_3	29.6	0.000835	68.2
Q29	LSF	315646106374404	11/06/2010	16:00	280	Na-Cl-SO_4	377	0.0106	296
Q30	MSF	315519106593101	11/18/2010	10:00	--	Na-HCO_3	14.2	0.000401	57.8
Q31	MSF	315245106380601	11/09/2010	18:00	150	Na-HCO_3	84.8	0.00239	256
Q32	LSF	315245106380602	11/10/2010	12:00	275	Na-HCO_3	769	0.0217	912
Q33	MSF	315114106414901	11/03/2010	16:00	--	Na-HCO_3	42.3	0.00119	159
Q34	USF	315013106362601	11/05/2010	17:00	135	Na-Cl	836	0.0236	331
Q35	MSF	315013106362602	11/09/2010	12:00	270	Na-Cl	1,960	0.0553	1,090
Q36	MSF	315013106395301	11/04/2010	12:00	--	Na-SO_4-Cl	176	0.00496	357
Q37	RGA	315006106354601	11/18/2010	10:00	--	Na-Cl-SO_4	631	0.0178	616
Q38	MSF	314932106493401	11/09/2010	12:00	360	Na-Cl-SO_4	151	0.00426	111
Q39	MSF	314908106371201	11/02/2010	12:00	--	Na-SO_4-Cl	186	0.00525	268
Q40	USF	314817106325801	11/04/2010	11:00	47	Na-Cl	7,630	0.215	4,600
Q41	MSF	314817106325802	11/05/2010	14:00	132	Na-Cl	15,300	0.432	4,970
Q42	MSF	314746106353601	11/15/2010	11:00	--	Na-SO_4-Cl	305	0.00860	735
Q43	MSF	314717106404401	11/03/2010	10:00	--	Na-HCO_3	47.2	0.00133	68.9

Well identifier (fig. 20)	Hydro-geologic unit	Sulfate, water, filtered (mol/L)	Carbonate, water, filtered, inflection-point titration method, field (mg/L)	Bicarbonate, water, filtered, inflection-point titration method, field (mg/L)	Fluoride, water, filtered (mg/L)	Bromide, water, filtered (mg/L)	Nitrate plus nitrite, water, filtered (mg/L)	Sodium, water, filtered (mg/L)	Sodium, water, filtered (mol/L)
Q00	USF	0.00177	--	261	0.64	0.219	0.050	181	0.00787
Q01	MSF	0.00566	--	269	1.17	1.72	6.34	394	0.0171
Q02	MSF	0.00145	--	286	1.07	0.206	0.570	151	0.00657
Q03	USF	0.00488	--	325	0.20	0.328	<0.02	76.6	0.00333
Q04	USF	0.00172	--	205	0.61	0.172	<0.02	114	0.00496
Q05	MSF	0.000609	--	165	0.49	0.084	<0.02	49.9	0.00217
Q06	MSF	0.000666	--	145	0.28	0.095	<0.02	43.5	0.00189
Q07	MSF	0.000745	--	165	0.51	0.096	<0.02	48.9	0.00213
Q08	USF	0.000672	--	177	0.35	0.093	<0.02	41.0	0.00178
Q09	USF	0.00459	--	288	0.22	0.396	<0.02	72.2	0.00314
Q10	MSF	0.00141	--	332	0.63	0.069	<0.02	180	0.00783
Q11	MSF	0.000471	--	153	0.30	0.056	<0.02	40.0	0.00174
Q12	MSF	0.00252	--	--	1.70	0.466	8.38	197	0.00857
Q13	USF	0.00665	--	368	0.23	0.486	<0.02	151	0.00657
Q14	USF	0.00193	--	538	0.32	0.275	<0.02	244	0.0106
Q15	USF	0.00121	--	261	1.33	0.127	<0.02	168	0.00731
Q16	MSF	0.00139	--	465	2.81	0.666	0.080	246	0.0107
Q17	MSF	0.00151	--	121	0.52	0.147	<0.02	164	0.00713
Q18	RGA	0.00976	--	593	0.40	0.753	<0.02	745	0.0324
Q19	USF	0.00207	--	372	0.61	0.242	<0.02	267	0.0116
Q20	MSF	0.000729	6.1	70.7	0.81	0.059	<0.02	74.7	0.00325
Q21	LSF	0.000776	--	79.9	0.68	0.061	<0.02	85.2	0.00371
Q22	MSF	0.00125	--	182	1.44	0.117	<0.02	153	0.00666
Q23	USF	0.00203	--	212	0.64	0.198	<0.02	127	0.00552
Q24	MSF	0.00227	1.6	73.2	0.46	0.201	<0.02	146	0.00635
Q25	LSF	0.00429	2.2	18.5	0.28	0.514	<0.02	336	0.0146
Q26	RGA	0.0144	--	665	0.34	1.11	<0.02	657	0.0286
Q27	USF	0.000740	5.1	68.0	0.77	0.054	<0.02	77.7	0.00338
Q28	MSF	0.000710	9.0	61.1	1.03	0.052	<0.02	79.7	0.00347
Q29	LSF	0.00308	8.5	40.7	4.73	0.284	<0.02	401	0.0174
Q30	MSF	0.000602	--	373	1.47	0.188	3.41	121	0.00526
Q31	MSF	0.00266	--	1,060	0.73	0.240	<0.02	436	0.0190
Q32	LSF	0.00949	--	1,970	0.73	0.597	<0.02	1,130	0.0492
Q33	MSF	0.00166	--	366	1.49	0.286	0.030	197	0.00857
Q34	USF	0.00345	--	25.1	0.86	0.776	<0.02	508	0.0221
Q35	MSF	0.0113	--	33.3	1.23	0.776	<0.02	1,340	0.0583
Q36	MSF	0.00372	--	91.2	0.92	0.913	1.16	204	0.00887
Q37	RGA	0.00641	--	289	0.53	0.590	<0.02	518	0.0225
Q38	MSF	0.00116	--	--	1.48	0.390	<0.02	228	0.00992
Q39	MSF	0.00279	--	56.2	0.90	0.233	0.130	202	0.00879
Q40	USF	0.0479	--	521	0.26	4.82	<0.02	5,230	0.227
Q41	MSF	0.0517	--	238	0.51	7.92	<0.02	8,590	0.374
Q42	MSF	0.00765	--	35.7	0.84	0.533	0.260	384	0.0167
Q43	MSF	0.000717	--	108	1.21	0.310	0.620	72.0	0.00313

Table 11. Summary of water types and selected constituents measured in groundwater samples collected in the Mesilla Basin study area in Doña Ana County, New Mexico, and El Paso County, Texas, 2010.—Continued

[USGS, U.S. Geological Survey; mm/dd/yyyy, month/day/year; ft, foot; mg/L, milligram per liter; mol/L, mole per liter; USF, upper part of the Santa Fe Group; --, not available; Na, sodium; Cl, chloride; MSF, middle part of the upper part of the Santa Fe Group; SO_4, sulfate; HCO_3, bicarbonate; Ca, calcium; RGA, Rio Grande alluvium; LSF, lower part of the Santa Fe Group; <, less than laboratory reporting level; µg/L, microgram per liter; mmol/L, millimole per liter]

Well identifier (fig. 20)	Hydro-geologic unit	Calcium, water, filtered (mg/L)	Calcium, water, filtered (mol/L)	Mag-nesium, water, filtered (mg/L)	Silica, water, filtered (mg/L as silica)	Silica, water, filtered (mmol/L as silica)	Potassium, water, filtered (mg/L)	Ammonia, water, filtered (mg/L as nitrogen)	Aluminum, water, filtered (µg/L)	Aluminum, water, filtered (mmol/L)
Q00	USF	86.1	0.00215	12.8	29.8	1.06	21.6	0.086	<1.7	<0.000063
Q01	MSF	26.3	0.000656	11.9	72.1	2.57	27.6	<0.01	3.6	0.00013
Q02	MSF	70.5	0.00176	14.0	26.1	0.929	14.6	<0.01	<1.7	<0.000063
Q03	USF	227	0.00566	41.5	28.9	1.03	15.9	0.030	<1.7	<0.000063
Q04	USF	62.4	0.00156	18.5	27.5	0.979	10.3	<0.01	<1.7	<0.000063
Q05	MSF	48.4	0.00121	8.42	26.6	0.947	6.20	0.055	<1.7	<0.000063
Q06	MSF	58.4	0.00146	7.43	26.6	0.947	3.88	0.132	<1.7	<0.000063
Q07	MSF	52.6	0.00131	9.28	24.8	0.883	5.35	0.028	2.1	0.000078
Q08	USF	61.6	0.00154	12.6	28.4	1.01	8.70	0.017	<1.7	<0.000063
Q09	USF	235	0.00586	39.5	28.0	0.997	5.48	0.290	<1.7	<0.000063
Q10	MSF	19.7	0.000492	3.49	43.4	1.55	3.09	0.032	2.6	0.000096
Q11	MSF	41.3	0.00103	5.83	23.6	0.84	2.62	0.072	1.8	0.000067
Q12	MSF	12.8	0.000319	10.6	16.2	0.577	5.31	<0.01	2.2	0.000082
Q13	USF	263	0.00656	53.2	29.9	1.06	6.28	0.186	<1.7	<0.000063
Q14	USF	151	0.00377	45.8	49.5	1.76	45.5	<0.01	5.2	0.00019
Q15	USF	14.1	0.000352	10.1	40.8	1.45	11.5	0.035	2.1	0.000078
Q16	MSF	5.56	0.000139	1.49	16.9	0.602	3.46	<0.01	<1.7	<0.000063
Q17	MSF	43.1	0.00108	1.09	34.2	1.22	4.46	0.019	2.9	0.00011
Q18	RGA	152	0.00379	59.1	36.3	1.29	31.4	0.230	<3.4	<0.00013
Q19	USF	80.3	0.00200	23.7	39.5	1.41	8.82	0.044	4.8	0.00018
Q20	MSF	13.4	0.000334	0.610	34.1	1.21	2.96	0.018	3.1	0.00011
Q21	LSF	9.11	0.000227	0.166	25.5	0.908	2.08	0.017	12.1	0.00045
Q22	MSF	11.4	0.000284	2.72	33.8	1.2	2.22	0.015	2.6	0.000096
Q23	USF	70.1	0.00175	13.8	26.5	0.944	6.12	0.019	5.3	0.00020
Q24	MSF	35.2	0.000878	3.47	29.5	1.05	4.08	0.016	2.6	0.000096
Q25	LSF	61.0	0.00152	0.172	20.6	0.733	2.71	0.022	6.1	0.00023
Q26	RGA	393	0.00981	74.7	38.6	1.37	9.03	0.805	<3.4	<0.00013
Q27	USF	7.47	0.000186	0.293	32.8	1.17	1.35	0.040	8.7	0.00032
Q28	MSF	4.34	0.000108	0.104	46.1	1.64	0.830	0.053	42.8	0.0016
Q29	LSF	14.7	0.000367	0.149	20.6	0.733	2.40	0.041	12.4	0.00046
Q30	MSF	31.0	0.000773	8.75	85.1	3.03	20.4	<0.01	3.4	0.00013
Q31	MSF	24.5	0.000611	37.5	63.8	2.27	7.48	0.097	4.0	0.00015
Q32	LSF	53.9	0.00134	21.4	59.9	2.13	6.40	0.101	<5.1	<0.00019
Q33	MSF	13.1	0.000327	3.48	44.5	1.58	4.25	<0.01	2.5	0.000093
Q34	USF	147	0.00367	3.79	31.9	1.14	4.54	0.068	4.0	0.00015
Q35	MSF	515	0.0128	28.1	56.7	2.02	11.0	0.111	<6.8	<0.00025
Q36	MSF	64.5	0.00161	14.7	42.0	1.5	8.65	<0.01	2.1	0.000078
Q37	RGA	172	0.00429	19.1	36.8	1.31	6.94	0.160	<3.4	<0.00013
Q38	MSF	20.2	0.000504	7.47	60.6	2.16	13.3	<0.01	4.3	0.00016
Q39	MSF	49.2	0.00123	1.69	31.5	1.12	3.24	<0.01	2.8	0.00010
Q40	USF	785	0.0196	360	37.9	1.35	28.5	1.39	32.5	0.0012
Q41	MSF	962	0.0240	728	14.5	0.516	35.4	1.11	<25.5	<0.00095
Q42	MSF	124	0.00309	2.79	32.6	1.16	5.92	0.010	2.5	0.000093
Q43	MSF	20.6	0.000514	4.58	34.1	1.21	4.24	<0.01	2.3	0.000085

Well identifier (fig. 20)	Hydro-geologic unit	Arsenic, water, filtered (µg/L)	Barium, water, filtered (µg/L)	Iron, water, filtered (µg/L)	Lithium, water, filtered (µg/L)	Man-ganese, water, filtered (µg/L)	Strontium, water, filtered (µg/L)	Uranium (natural), water, filtered (µg/L)	Ratio of sulfate (mol/L) to chloride (mol/L)	Ratio of chloride (mg/L) to bromide (mg/L)	Ratio of calcium (mol/L) to sodium (mol/L)
Q00	USF	4.5	96.9	5.9	167	606	1,060	1.14	0.281	1,020	0.273
Q01	MSF	6.9	10.9	319	142	3.64	889	16.0	1.44	80.8	0.0384
Q02	MSF	1.6	28.6	7.5	151	0.39	1,130	10.4	0.285	874	0.268
Q03	USF	1.9	48.7	<3.2	113	915	2,790	62.4	1.30	405	1.70
Q04	USF	1.1	43.1	112	96.0	1.37	1,670	7.20	0.539	657	0.315
Q05	MSF	4.9	75.9	93.8	80.0	186	595	0.107	0.401	642	0.558
Q06	MSF	4.6	65.4	45.0	53.1	15.0	682	0.236	0.385	646	0.772
Q07	MSF	2.7	54.5	31.2	61.5	32.4	680	8.79	0.472	584	0.615
Q08	USF	3.2	53.8	177	43.9	262	912	0.065	0.328	782	0.865
Q09	USF	5.5	113	9.1	96.8	105	3,230	2.34	0.852	482	1.87
Q10	MSF	18.4	42.1	43.7	194	7.59	492	0.896	0.892	813	0.0628
Q11	MSF	4.4	46.6	33.0	37.3	13.0	574	0.552	0.471	632	0.592
Q12	MSF	8.3	24.2	<3.2	65.7	0.13	691	6.25	2.31	82.8	0.0372
Q13	USF	3.1	74.5	101	115	796	3,290	23.0	1.16	420	0.998
Q14	USF	0.8	51.2	78.2	265	80.5	5,080	30.6	0.172	1,440	0.356
Q15	USF	14.6	74.9	10.9	117	8.72	606	1.71	0.448	754	0.0482
Q16	MSF	10.5	42.7	65.2	89.5	4.89	203	2.02	1.05	70.3	0.0130
Q17	MSF	10.6	64.2	13.7	89.9	4.00	433	0.496	0.313	1,160	0.151
Q18	RGA	1.2	43.1	485	610	390	3,830	2.08	0.465	989	0.117
Q19	USF	13.6	29.5	69.0	251	36.6	1,990	2.22	0.248	1,220	0.172
Q20	MSF	10.5	15.1	<3.2	30.2	5.28	162	0.106	0.613	714	0.103
Q21	LSF	1.7	5.55	5.2	41.8	2.88	70.8	0.139	0.641	703	0.0612
Q22	MSF	20.0	36.0	20.9	133	8.01	282	1.76	0.635	597	0.0426
Q23	USF	6.9	62.4	6.0	114	22.5	1,340	4.61	0.627	581	0.317
Q24	MSF	10.3	68.7	6.0	54.6	13.4	676	0.084	0.682	587	0.138
Q25	LSF	3.1	68.2	<3.2	116	25.3	401	0.011	0.475	623	0.104
Q26	RGA	0.5	50.9	1,820	457	2,170	4,970	0.791	0.832	552	0.343
Q27	USF	25.0	18.9	4.7	16.4	2.61	93.1	0.273	0.772	630	0.0550
Q28	MSF	24.0	5.15	110	22.4	3.03	27.2	0.049	0.850	569	0.0311
Q29	LSF	64.7	19.5	<3.2	179	3.18	318	0.116	0.291	1,330	0.0211
Q30	MSF	25.5	59.4	3.7	59.1	0.13	524	3.96	1.50	75.5	0.147
Q31	MSF	116	24.6	108	547	37.8	975	18.6	1.11	353	0.0322
Q32	LSF	71.5	17.9	212	998	32.5	1,190	30.4	0.437	1,290	0.0272
Q33	MSF	34.6	30.6	11.8	100	0.73	260	23.5	1.39	148	0.0382
Q34	USF	12.7	37.0	9.6	130	30.3	1,150	0.203	0.146	1,080	0.166
Q35	MSF	16.7	24.5	27.4	522	56.9	2,410	0.062	0.204	2,530	0.220
Q36	MSF	12.2	22.3	20.1	98.7	0.49	1,160	4.51	0.750	193	0.182
Q37	RGA	6.3	39.3	323	207	531	2,150	0.836	0.360	1,070	0.191
Q38	MSF	21.1	53.4	294	130	84.8	444	29.3	0.272	387	0.0508
Q39	MSF	15.5	36.9	3.7	68.1	3.31	361	0.863	0.531	798	0.140
Q40	USF	2.7	18.1	2,580	897	1,950	17,500	5.13	0.223	1,580	0.0863
Q41	MSF	2.4	12.4	433	1,270	2,350	19,600	107	0.120	1,930	0.0642
Q42	MSF	12.3	20.4	22.3	131	21.1	1,110	0.121	0.890	572	0.185
Q43	MSF	16.2	50.4	<3.2	37.6	0.13	397	3.05	0.539	152	0.164

Table 12. Summary of water types from the analysis of major cations and anions measured in groundwater samples collected in the Mesilla Basin study area in Doña Ana County, New Mexico, and El Paso County, Texas, 2010.

[RGA, Rio Grande alluvium; USF, upper part of the Santa Fe Group; MSF, middle part of the Santa Fe Group; LSF, lower part of the Santa Fe Group; Ca, calcium; Na, sodium; HCO_3, bicarbonate; Cl, chloride; SO_4, sulfate; %, percent]

Class	Water type	Percentage of samples from wells with screened or open intervals in RGA	Percentage of samples from wells with screened or open intervals in USF	Percentage of samples from wells with screened or open intervals in MSF	Percentage of samples from wells with screened or open intervals in LSF	Percentage of samples from all wells within Mesilla Basin study area
Bases	Alkaline earths (Ca) exceed alkalies (Na)	0.0	30.8	16.7	0.0	18.2
	Alkalies exceed alkaline earths	100.0	69.2	83.3	100.0	81.8
Acids	Weak acids (HCO_3)[1] exceed strong acids ($Cl+SO_4$)[2]	0.0	0.0	25.0	0.0	13.6
	Strong acids exceed weak acids	100.0	100.0	75.0	100.0	86.4
Water type	Calcium-bicarbonate type	0.0	0.0	4.2	0.0	2.3
	Calcium-chloride-sulfate type	0.0	15.4	0.0	0.0	4.5
	Sodium-chloride-sulfate type	100.0	69.2	62.5	100.0	70.5
	Sodium-bicarbonate type	0.0	0.0	12.5	0.0	6.8
	Mixed type (no cation-anion exceeds 50%)	0.0	15.4	20.8	0.0	15.9
Cations	Sodium type	100.0	69.2	83.3	100.0	81.8
	Calcium type	0.0	23.1	4.2	0.0	9.1
	Magnesium type	0.0	0.0	0.0	0.0	0.0
	No dominant cation type	0.0	7.7	12.5	0.0	9.1
Anions	Chloride type	33.3	15.4	12.5	25.0	15.9
	Sulfate type	33.3	15.4	16.7	0.0	15.9
	Bicarbonate type	0.0	0.0	25.0	0.0	13.6
	No dominant anion type	33.3	69.2	45.8	75.0	54.5

[1]Through deprotonation, weak acid carbonic acid (H_2CO_3) disassociates to HCO_3^- and water (H_2O); HCO_3- can be further deprotonated to CO_3^{2-}.

[2]In aqueous solutions, Cl^- and SO_4^{2-} are protonated to form hydrochloric acid (HCl) and sulfuric acid (H_2SO_4), respectively, both of which are strong acids.

Table 13. Summary of isotopic results measured in groundwater samples collected in the Mesilla Basin study area in Doña Ana County, New Mexico, and El Paso County, Texas, 2010.

[USGS, U.S. Geological Survey; mm/dd/yyyy, month/day/year; ft, foot; δD, delta deuterium; $\delta^{18}O$, delta oxygen-18; $^{87}Sr/^{86}Sr$, strontium-87 per strontium-86; USF, upper part of the Santa Fe Group; --, not available; MSF, middle part of the Santa Fe Group; RGA, Rio Grande alluvium; LSF, lower part of the Santa Fe Group; pCi/L, picocurie per liter; TU, tritium unit; ^{14}C, carbon-14; pmc, percent modern carbon; BP, before present (1950); $\delta^{13}C$, delta carbon-13; M, presence verified but not quantified]

Well identifier (fig. 20)	USGS station number	Hydrogeo-logic unit	Sample date (mm/dd/yyyy)	Sample start time	Sample depth (ft)	δD, water, unfiltered (per mil)	$\delta^{18}O$, water, unfiltered (per mil)	$^{87}Sr/^{86}Sr$, water, unfiltered
Q00	322320106551801	USF	11/17/2010	15:00	--	-72.38	-8.53	0.71125
Q01	322233106590901	MSF	11/17/2010	11:00	--	-86.92	-11.26	0.71109
Q02	322219106485001	MSF	11/03/2010	13:00	--	-87.71	-11.34	0.71119
Q03	322054106475201	USF	11/08/2010	17:00	--	-73.53	-8.71	0.71078
Q04	322024106463901	USF	11/16/2010	16:00	--	-86.98	-11.25	0.70950
Q05	321934106482601	MSF	11/16/2010	12:00	--	-90.30	-11.79	0.71031
Q06	321641106515401	MSF	11/16/2010	15:00	--	-90.06	-11.74	0.70873
Q07	321628106451501	MSF	11/03/2010	17:00	--	-89.46	-11.60	0.71000
Q08	321501106443801	USF	11/08/2010	11:00	--	-88.84	-11.49	0.70958
Q09	320939106441701	USF	11/11/2010	11:00	--	-74.58	-8.95	0.70883
Q10	320654106504201	MSF	11/11/2010	12:00	--	-87.54	-11.71	0.70899
Q11	320643106440401	MSF	11/08/2010	10:00	--	-90.41	-11.79	--
Q12	320604107051201	MSF	11/12/2010	13:00	--	-66.42	-8.75	0.70790
Q13	320445106421001	USF	11/11/2010	16:00	--	-74.40	-8.89	0.70929
Q14	320253106364001	USF	11/15/2010	15:00	--	-75.16	-10.10	0.71227
Q15	320054106533901	USF	11/16/2010	10:00	--	-85.80	-11.36	0.70918
Q16	320040107054601	MSF	11/10/2010	15:00	--	-66.71	-9.20	0.70924
Q17	315955106362201	MSF	11/15/2010	10:00	46	-85.18	-11.43	0.71084
Q18	315940106372301	RGA	11/06/2010	17:00	55	-69.74	-8.04	0.71145
Q19	315940106372302	USF	11/06/2010	15:00	275	-83.41	-11.05	0.70992
Q20	315940106372303	MSF	11/06/2010	13:00	280	-84.76	-11.29	0.71049
Q21	315940106372304	LSF	11/17/2010	16:00	200	-85.33	-11.39	0.71052
Q22	315723106415201	MSF	11/02/2010	17:00	--	-85.60	-11.39	0.70806
Q23	315712106361802	USF	11/14/2010	16:00	145	-68.02	-7.97	0.71091
Q24	315712106361803	MSF	11/15/2010	18:00	--	-74.01	-8.96	0.71039
Q25	315712106361804	LSF	11/14/2010	18:00	100	-86.65	-11.49	0.71078
Q26	315646106374401	RGA	11/08/2010	16:00	47	-71.17	-8.57	0.70976
Q27	315646106374402	USF	11/10/2010	18:00	275	-93.96	-12.61	0.70843
Q28	315646106374403	MSF	11/12/2010	15:00	275	-94.73	-12.85	0.70948
Q29	315646106374404	LSF	11/06/2010	16:00	280	-89.75	-11.84	0.71029
Q30	315519106593101	MSF	11/18/2010	10:00	--	-59.36	-8.29	0.71005
Q31	315245106380601	MSF	11/09/2010	18:00	150	-89.32	-12.00	0.70890
Q32	315245106380602	LSF	11/10/2010	12:00	275	-72.09	-9.46	0.70853
Q33	315114106414901	MSF	11/03/2010	16:00	--	-84.06	-10.93	0.70922
Q34	315013106362601	USF	11/05/2010	17:00	135	-61.57	-7.20	0.70871
Q35	315013106362602	MSF	11/09/2010	12:00	270	-63.39	-7.51	0.70881
Q36	315013106395301	MSF	11/04/2010	12:00	--	-67.08	-7.74	0.70913
Q37	315006106354601	RGA	11/18/2010	10:00	--	-65.04	-7.67	0.70937
Q38	314932106493401	MSF	11/09/2010	12:00	360	-82.65	-10.94	0.71001
Q39	314908106371201	MSF	11/02/2010	12:00	--	-63.03	-7.89	0.70871
Q40	314817106325801	USF	11/04/2010	11:00	47	-65.41	-7.99	0.70996
Q41	314817106325802	MSF	11/05/2010	14:00	132	-68.74	-8.14	0.70962
Q42	314746106353601	MSF	11/15/2010	11:00	--	-67.42	-8.38	0.70946
Q43	314717106404401	MSF	11/03/2010	10:00	--	-63.50	-8.08	0.70892

Well identifier (fig. 20)	Tritium, water, unfiltered (pCi/L)	Tritium, water, unfiltered (TU)	^{14}C, water, filtered (pmc)	^{14}C counting error, water, filtered (pmc)	Apparent age, ^{14}C years BP	$\delta^{13}C$, water, unfiltered (per mil)
Q00	11.6	3.6	82.31	0.26	1,500	-8.51
Q01	0.0	0.0	16.41	0.10	14,000	-6.73
Q02	0.8	0.3	48.66	0.18	5,700	-6.87
Q03	26.3	8.1	114.60	0.38	[1]-1,100	-11.27
Q04	4.1	1.3	48.40	0.14	5,800	-8.12
Q05	0.3	0.1	64.35	0.24	3,500	-7.66
Q06	-0.4	-0.1	60.80	0.19	3,900	-7.63
Q07	0.9	0.3	69.55	0.25	2,900	-8.10
Q08	0.2	0.1	--	--	--	--
Q09	28.3	8.8	102.20	0.39	[1]-230	-10.76
Q10	0.1	0.0	4.67	0.06	25,000	-5.63
Q11	0.1	0.0	70.41	0.22	2,800	-8.07
Q12	0.0	0.0	8.84	0.08	19,000	-7.20
Q13	20.1	6.2	110.50	0.35	[1]-900	-12.31
Q14	0.2	0.1	2.61	0.06	29,000	-4.33
Q15	0.1	0.0	8.80	0.09	20,000	-5.70
Q16	-0.3	-0.1	7.65	0.07	21,000	-8.45
Q17	--	--	7.26	0.08	21,000	-6.66
Q18	14.8	4.6	101.10	0.33	[1]-150	-11.47
Q19	0.7	0.2	10.32	0.09	18,000	-5.47
Q20	0.1	0.0	9.47	0.08	19,000	-7.42
Q21	-0.1	0.0	8.25	0.08	20,000	-8.69
Q22	-0.1	0.0	6.20	0.09	22,000	-6.28
Q23	13.7	4.2	141.50	0.45	[1]-2,800	-8.29
Q24	33.2	10.3	50.12	0.22	5,500	-9.05
Q25	3.0	0.9	12.64	0.10	17,000	-9.64
Q26	24.2	7.5	106.50	0.33	[1]-560	-13.20
Q27	-0.2	-0.1	3.76	0.05	26,000	-7.84
Q28	-0.2	-0.1	2.39	0.04	30,000	-9.06
Q29	0.0	0.0	1.63	0.03	33,000	-8.13
Q30	0.0	0.0	6.43	0.10	22,000	-6.46
Q31	0.1	0.0	1.21	0.03	35,000	-3.66
Q32	M	M	0.26	0.02	48,000	-5.96
Q33	-0.1	0.0	4.09	0.06	26,000	-7.52
Q34	-0.3	-0.1	5.27	0.07	24,000	-7.24
Q35	M	M	4.11	0.06	26,000	-7.80
Q36	M	M	2.07	0.03	31,000	-8.08
Q37	--	--	99.77	0.30	[1]-40	-10.37
Q38	0.1	0.0	4.75	0.06	24,000	-7.02
Q39	0.4	0.1	4.08	0.09	26,000	-8.59
Q40	4.2	1.3	90.94	0.33	700	-13.78
Q41	0.2	0.1	--	--	--	--
Q42	0.2	0.1	4.20	0.06	25,000	-10.46
Q43	0.0	0.0	2.81	0.04	29,000	-8.66

[1]Negative apparent water age is a result of high ^{14}C concentrations in the atmosphere from atomic bomb testing (Plummer and others, 1994).

Table 14. Summary statistics for selected physicochemical properties, constituents, and isotopes measured in groundwater samples within each geochemical group determined in the Mesilla Basin study area in Doña Ana County, New Mexico, and El Paso County, Texas, 2010.

[µS/cm at 25 °C, microsiemen per centimeter at 25 degrees Celsius; mg/L, milligram per liter; <, less than laboratory reporting level; µg/L, microgram per liter; δD, delta deuterium; $\delta^{18}O$, delta oxygen-18; $^{87}Sr/^{86}Sr$, strontium-87 per strontium-86; pCi/L, picocurie per liter; TU, tritium unit; ^{14}C, carbon-14; pmc, percent modern carbon]

Geochemical group	Groundwater samples within group (fig. 45)	Summary statistic	Temperature, water (degrees Celsius)	Specific conductance, water, unfiltered (µS/cm at 25 °C)	Dissolved oxygen, water, unfiltered (mg/L)	pH, water, unfiltered, field (standard units)	Chloride, water, filtered (mg/L)	Sulfate, water, filtered (mg/L)	Bicarbonate, water, filtered, inflection-point titration method, field (mg/L)	Fluoride, water, filtered (mg/L)	Bromide, water, filtered (mg/L)	Nitrate plus nitrite, water, filtered (mg/L)
Ancestral Rio Grande	Q10, Q15, Q17, Q20, Q21, Q22, Q27, Q28, Q33	Minimum	24.0	399	0.1	7.8	29.6	68.2	61.1	0.52	0.052	<0.02
		Maximum	34.5	1,050	0.3	9.1	171	159	366	1.49	0.286	0.03
		Median	27.1	812	0.1	8.5	42.9	116	121	0.81	0.069	<0.02
		Mean	28.3	725	0.1	8.4	64.9	107	171	0.97	0.108	0.02
Modern Rio Grande	Q03, Q09, Q13, Q18, Q23, Q26, Q37	Minimum	18.7	1,050	0.1	7.2	115	195	212	0.20	0.198	<0.02
		Maximum	19.9	4,580	0.2	7.7	745	1,380	665	0.64	1.11	<0.02
		Median	19.1	1,940	0.2	7.4	204	616	325	0.34	0.486	<0.02
		Mean	19.2	2,400	0.2	7.4	376	668	391	0.37	0.552	<0.02
Mountain front	Q01, Q02, Q04, Q12, Q16, Q30, Q38, Q43	Minimum	20.3	501	0.2	7.3	14.2	57.8	108	0.61	0.172	<0.02
		Maximum	29.0	2,010	5.2	8.3	180	544	465	2.81	1.72	8.38
		Median	24.7	1,150	1.1	7.8	80.1	137	278	1.34	0.350	0.62
		Mean	24.6	1,120	1.9	7.8	91.2	183	284	1.44	0.515	2.43
Deep groundwater upwelling	Q14, Q29, Q31, Q32, Q34, Q35, Q40, Q41	Minimum	21.7	1,980	0.1	6.8	84.8	185	25.1	0.26	0.240	<0.02
		Maximum	28.1	42,800	0.6	8.8	15,300	4,970	1,970	4.73	7.92	<0.02
		Median	24.5	4,240	0.3	7.3	803	622	380	0.73	0.687	<0.02
		Mean	25.0	11,400	0.3	7.5	3,420	1,580	553	1.17	1.96	<0.02
Deep groundwater upwelling (excluding Q40 and Q41)	Q14, Q29, Q31, Q32, Q34, Q35	Minimum	23.5	1,980	0.1	6.8	84.8	185	25.1	0.32	0.240	<0.02
		Maximum	28.1	7,020	0.6	8.8	1,960	1,090	1,970	4.73	0.776	<0.02
		Median	26.1	2,720	0.2	7.6	583	314	289	0.80	0.441	<0.02
		Mean	25.9	3,680	0.3	7.7	737	512	611	1.43	0.491	<0.02
Unknown freshwater	Q05, Q06, Q07, Q08, Q11	Minimum	18.2	453	0.1	7.7	35.4	45.2	145	0.28	0.056	<0.02
		Maximum	21.4	644	2.6	8.0	72.7	71.6	177	0.51	0.096	<0.02
		Median	19.9	574	0.1	7.8	56.1	64.0	165	0.35	0.093	<0.02
		Mean	20.0	568	0.6	7.8	55.9	60.8	161	0.39	0.085	<0.02
Mixed water	Q00, Q19, Q24, Q25, Q36, Q39, Q42	Minimum	16.6	954	0.1	7.4	118	170	18.5	0.28	0.201	<0.02
		Maximum	29.4	2,340	1.4	8.8	320	735	372	0.92	0.913	1.16
		Median	24.0	1,480	0.2	8.2	223	268	73.2	0.64	0.242	0.09
		Mean	24.5	1,580	0.5	8.1	232	337	130	0.66	0.408	0.23

Table 14. Summary statistics for selected physicochemical properties, constituents, and isotopes measured in groundwater samples within each geochemical group determined in the Mesilla Basin study area in Doña Ana County, New Mexico, and El Paso County, Texas, 2010.—Continued

[µS/cm at 25 °C, microsiemen per centimeter at 25 degrees Celsius; mg/L, milligram per liter; <, less than laboratory reporting level; µg/L, microgram per liter; δD, delta deuterium; $\delta^{18}O$, delta oxygen-18; $^{87}Sr/^{86}Sr$, strontium-87 per strontium-86; pCi/L, picocurie per liter; TU, tritium unit; ^{14}C, carbon-14; pmc, percent modern carbon]

Geochemical group	Groundwater samples within group (fig. 45)	Summary statistic	Sodium, water, filtered (mg/L)	Calcium, water, filtered (mg/L)	Magnesium, water, filtered (mg/L)	Silica, water, filtered (mg/L as silica)	Potassium, water, filtered (mg/L)	Ammonia, water, filtered (mg/L as nitrogen)	Aluminum, water, filtered (µg/L)	Arsenic, water, filtered (µg/L)	Barium, water, filtered (µg/L)	Iron, water, filtered (µg/L)	Lithium, water, filtered (µg/L)
Ancestral Rio Grande	Q10, Q15, Q17, Q20, Q21, Q22, Q27, Q28, Q33	Minimum	74.7	4.34	0.104	25.5	0.83	0.010	2.1	1.7	5.15	<3.2	16.4
		Maximum	197	43.1	10.1	46.1	11.5	0.053	42.8	34.6	74.9	110	194
		Median	153	13.1	1.09	34.2	2.96	0.019	2.9	18.4	30.6	11.8	89.9
		Mean	131	15.1	2.45	37.2	3.64	0.023	8.8	17.7	32.5	14.3	82.7
Modern Rio Grande	Q03, Q09, Q13, Q18, Q23, Q26, Q37	Minimum	72.2	70.1	13.8	26.5	5.48	0.019	<1.7	0.48	39.3	<3.2	96.8
		Maximum	745	393	74.7	38.6	31.4	0.805	5.3	6.9	113	1,820	610
		Median	151	227	41.5	29.9	6.94	0.186	3.4	3.1	50.9	101	115
		Mean	335	216	43.0	32.1	11.6	0.246	2.9	3.63	61.7	155	245
Mountain front	Q01, Q02, Q04, Q12, Q16, Q30, Q38, Q43	Minimum	72.0	5.56	1.49	16.2	3.46	<0.01	<1.7	1.1	10.9	<3.2	37.6
		Maximum	394	70.5	18.5	85.1	27.6	<0.01	4.3	25.5	59.4	319	151
		Median	174	23.5	9.68	30.8	11.8	<0.01	2.3	9.4	42.9	65.2	92.8
		Mean	190	31.2	9.66	42.3	12.4	<0.01	2.2	11.4	39.1	101	96.4
Deep groundwater upwelling	Q14, Q29, Q31, Q32, Q34, Q35, Q40, Q41	Minimum	244	14.7	0.149	14.5	2.40	0.010	4.0	0.79	12.4	<3.2	130
		Maximum	8,590	962	728	63.8	45.5	1.39	32.5	116	51.2	2,580	1,270
		Median	819	149	32.8	43.7	9.24	0.099	5.2	14.7	22.0	108	535
		Mean	2,230	332	153	41.9	17.7	0.220	9.0	35.9	25.7	431	601
Deep groundwater upwelling (excluding Q40 and Q41)	Q14, Q29, Q31, Q32, Q34, Q35	Minimum	244	14.7	0.149	20.6	2.40	0.010	4.0	0.79	17.9	<3.2	130
		Maximum	1,340	515	45.8	63.8	45.5	0.111	12.4	116	51.2	212	998
		Median	472	100	24.8	53.1	6.94	0.083	5.2	40.7	24.6	78.2	394
		Mean	677	151	22.8	47.1	12.9	0.063	5.7	47.1	29.1	72.0	440
Unknown freshwater	Q05, Q06, Q07, Q08, Q11	Minimum	40.0	41.3	5.83	23.6	2.62	0.017	<1.7	2.7	46.6	31.2	37.3
		Maximum	49.9	61.6	12.6	28.4	8.70	0.132	2.1	4.9	75.9	177	80.0
		Median	43.5	52.6	8.42	26.6	5.35	0.055	1.7	4.4	54.5	45.0	53.1
		Mean	44.7	52.5	8.71	26.0	5.35	0.061	1.8	3.96	59.2	76.0	55.2
Mixed water	Q00, Q19, Q24, Q25, Q36, Q39, Q42	Minimum	146	35.2	0.172	20.6	2.71	0.010	<1.7	3.1	20.4	<3.2	54.6
		Maximum	384	124	23.7	42.0	21.6	0.086	6.1	15.5	96.9	69.0	251
		Median	204	64.5	3.47	31.5	5.92	0.019	2.6	12.2	36.9	6.0	116
		Mean	246	71.5	8.47	32.2	7.86	0.028	2.8	10.2	49.0	10.2	127

Table 14. Summary statistics for selected physicochemical properties, constituents, and isotopes measured in groundwater samples within each geochemical group determined in the Mesilla Basin study area in Doña Ana County, New Mexico, and El Paso County, Texas, 2010.—Continued

[µS/cm at 25 °C, microsiemen per centimeter at 25 degrees Celsius; mg/L, milligram per liter; <, less than laboratory reporting level; µg/L, microgram per liter; δD, delta deuterium; $\delta^{18}O$, delta oxygen-18; $^{87}Sr/^{86}Sr$, strontium-87 per strontium-86; pCi/L, picocurie per liter; TU, tritium unit; ^{14}C, carbon-14; pmc, percent modern carbon]

Geochemical group	Groundwater samples within group (fig. 45)	Summary statistic	Manganese, water, filtered (µg/L)	Strontium, water, filtered (µg/L)	Uranium (natural), water, filtered (µg/L)	δD, water, unfiltered (per mil)	$\delta^{18}O$, water, unfiltered (per mil)	$^{87}Sr/^{86}Sr$, water, unfiltered	Tritium, water, unfiltered (pCi/L)	Tritium, water, unfiltered (TU)	^{14}C, water, filtered (pmc)	^{14}C counting error, water, filtered (pmc)	Apparent age, ^{14}C years BP
Ancestral Rio Grande	Q10, Q15, Q17, Q20, Q21, Q22, Q27, Q28, Q33	Minimum	0.73	27.2	0.049	-94.73	-12.85	0.70806	-0.2	-0.06	2.39	0.04	19,000
		Maximum	8.72	606	23.5	-84.06	-10.93	0.71084	0.1	0.03	9.47	0.09	30,000
		Median	4.00	260	0.496	-85.60	-11.39	0.70922	-0.1	-0.03	6.20	0.08	22,000
		Mean	4.76	270	3.21	-87.44	-11.66	0.70947	-0.1	-0.02	6.10	0.07	23,000
Modern Rio Grande	Q03, Q09, Q13, Q18, Q23, Q26, Q37	Minimum	22.5	1,340	0.791	-74.58	-8.95	0.70883	13.7	4.24	99.77	0.30	[1]-2,900
		Maximum	2,170	4,970	62.4	-65.04	-7.67	0.71145	28.3	8.76	141.50	0.45	[1]-40
		Median	531	3,230	2.34	-71.17	-8.57	0.70976	22.2	6.86	106.50	0.35	[1]-560
		Mean	704	3,090	13.7	-70.93	-8.40	0.71006	21.2	6.57	110.88	0.36	[1]-840
Mountain front	Q01, Q02, Q04, Q12, Q16, Q30, Q38, Q43	Minimum	0.13	203	2.02	-87.71	-11.34	0.70790	-0.3	-0.09	2.81	0.04	5,700
		Maximum	84.8	1,670	29.3	-59.36	-8.08	0.71119	4.1	1.27	48.66	0.18	29,000
		Median	0.88	608	6.73	-74.68	-10.07	0.70976	0.0	0.00	8.25	0.09	20,000
		Mean	11.9	744	9.77	-75.03	-9.89	0.70974	0.6	0.18	17.99	0.10	18,000
Deep groundwater upwelling	Q14, Q29, Q31, Q32, Q34, Q35, Q40, Q41	Minimum	3.18	318	0.062	-89.75	-12.00	0.70853	-0.3	-0.09	0.26	0.02	700
		Maximum	2,350	19,600	107	-61.57	-7.20	0.71227	4.2	1.30	90.94	0.33	48,000
		Median	47.4	1,800	11.9	-70.42	-8.80	0.70926	0.2	0.05	2.61	0.06	29,000
		Mean	568	6,030	24.0	-73.18	-9.28	0.70964	0.7	0.23	15.15	0.09	28,000
Deep groundwater upwelling (excluding Q40 and Q41)	Q14, Q29, Q31, Q32, Q34, Q35	Minimum	3.18	318	0.062	-89.75	-12.00	0.70853	-0.3	-0.09	0.26	0.02	24,000
		Maximum	80.5	5,080	30.6	-61.57	-7.20	0.71227	0.2	0.06	5.27	0.07	48,000
		Median	35.2	1,170	9.40	-73.63	-9.78	0.70886	0.1	0.02	2.12	0.05	31,000
		Mean	40.2	1,850	13.3	-75.21	-9.69	0.70959	0.0	0.00	2.52	0.05	32,000
Unknown freshwater	Q05, Q06, Q07, Q08, Q11	Minimum	13.0	574	0.065	-90.41	-11.79	0.70873	-0.4	-0.12	60.80	0.19	2,800
		Maximum	262	912	8.79	-88.84	-11.49	0.71031	0.9	0.28	70.41	0.25	3,900
		Median	32.4	680	0.236	-90.06	-11.74	0.70979	0.2	0.06	66.95	0.23	3,200
		Mean	102	689	1.95	-89.81	-11.68	0.70966	0.2	0.07	66.28	0.23	3,300
Mixed water	Q00, Q19, Q24, Q25, Q36, Q39, Q42	Minimum	0.49	361	0.011	-86.65	-11.49	0.70871	0.2	0.06	2.07	0.03	1,500
		Maximum	606	1,990	4.51	-63.03	-7.74	0.71125	33.2	10.3	82.31	0.26	31,000
		Median	21.1	1,060	0.863	-72.38	-8.53	0.70992	1.9	0.57	10.32	0.09	18,000
		Mean	101	965	1.28	-73.43	-9.15	0.70995	8.2	2.53	23.68	0.12	18,000

[1]Negative apparent water age is a result of high ^{14}C concentrations in the atmosphere from atomic bomb testing (Plummer and others, 1994).

Table 15. Mean winter water-level altitudes (November 2010 through April 2011) used for constructing potentiometric-surface maps of the Rio Grande alluvium and Santa Fe Group hydrogeologic units in the Mesilla Basin study area in Doña Ana County, New Mexico, and El Paso County, Texas.

[USGS, U.S. Geological Survey; ft, foot; NAVD 88, North American Vertical Datum of 1988; NWIS, USGS National Water Information System; RGA, Rio Grande alluvium; --, not available; SF, Santa Fe Group]

Well identifier (figs. 46 and 47)	USGS station number	Latitude (decimal degrees)	Longitude (decimal degrees)	Land-surface altitude (ft) (NAVD 88)	Well depth (ft)	NWIS aquifer code	Hydro-geologic group	Number of water-level-altitude measure-ments for well	Minimum water-level altitude (ft)	Maximum water-level altitude (ft)	Average water-level altitude (ft) (value used to generate potentiometric-surface maps) (figs. 46 and 47)
L001	322540106525101	32.42798	106.88093	3,936	35	Quaternary alluvium	RGA	1	3,924.09	3,924.09	3,924.09
L002	322312106503601	32.38842	106.84390	3,940	--	Quaternary alluvium	RGA	1	3,927.84	3,927.84	3,927.84
L003	322311106415401	32.38628	106.69836	4,439	420	--	SF	1	4,079.67	4,079.67	4,079.67
L004	322047106505001	32.34676	106.84834	3,908	--	Quaternary alluvium	RGA	1	3,898.55	3,898.55	3,898.55
L005	322045106461001	32.34593	106.77000	4,064	596	Santa Fe Group	SF	1	3,842.76	3,842.76	3,842.76
L006	322040106485302	32.34481	106.81528	3,911	30	Quaternary alluvium	RGA	1	3,890.38	3,890.38	3,890.38
L007	322011106591901	32.33620	106.99807	4,459	300	Santa Fe Group	SF	1	4,273.87	4,273.87	4,273.87
L008	322011106473301	32.33620	106.79195	3,908	605	Santa Fe Group	SF	1	3,856.89	3,856.89	3,856.89
L009	321956106453101	32.33259	106.76000	4,062	751	Santa Fe Group	SF	1	3,843.51	3,843.51	3,843.51
L010	321945106595001	32.32787	107.00112	4,462	300	Santa Fe Group	SF	1	4,275.72	4,275.72	4,275.72
L011	321934106482601	32.32648	106.80778	3,891	617	Santa Fe Group	SF	1	3,873.49	3,873.49	3,873.49
L012	321914106462501	32.32065	106.77445	3,934	381	Santa Fe Group	SF	1	3,853.81	3,853.81	3,853.81
L013	321859106503101	32.31664	106.84201	3,891	34	Quaternary alluvium	RGA	1	3,879.06	3,879.06	3,879.06
L014	321853106452101	32.31537	106.75556	4,051	730	Santa Fe Group	SF	1	3,839.84	3,839.84	3,839.84
L015	321832106451301	32.30926	106.75556	4,006	700	Santa Fe Group	SF	1	3,834.95	3,834.95	3,834.95
L016	321828107000501	32.30870	107.00390	4,429	260	Santa Fe Group	SF	1	4,274.30	4,274.30	4,274.30
L017	321827106473501	32.30787	106.79389	3,891	629	Santa Fe Group	SF	1	3,848.79	3,848.79	3,848.79
L018	321819106445201	32.30537	106.74834	4,041	591	Santa Fe Group	SF	1	3,837.39	3,837.39	3,837.39
L019	321814107000401	32.31676	107.00362	4,442	300	Santa Fe Group	SF	1	4,272.53	4,272.53	4,272.53
L020	321806106461501	32.30148	106.77139	3,897	700	Santa Fe Group	SF	1	3,835.72	3,835.72	3,835.72
L021	321745106492503	32.29593	106.82417	3,891	41	Quaternary alluvium	RGA	4	3,883.32	3,886.47	3,885.10
L022	321745106492502	32.29593	106.82417	3,891	105	Santa Fe Group	SF	4	3,883.25	3,885.95	3,884.80
L023	321745106492501	32.29593	106.82417	3,891	305	Santa Fe Group	SF	4	3,880.29	3,880.89	3,880.68
L024	321745106492106	32.29620	106.82306	3,891	650	Santa Fe Group	SF	12	3,858.13	3,861.79	3,860.26
L025	321745106492103	32.29593	106.82306	3,891	40	Quaternary alluvium	RGA	7	3,881.95	3,883.79	3,882.70
L026	321745106492102	32.29593	106.82306	3,891	110	Santa Fe Group	SF	7	3,875.81	3,877.20	3,876.55
L027	321745106492101	32.29593	106.82306	3,891	310	Santa Fe Group	SF	7	3,861.95	3,864.59	3,863.53
L028	321740106481004	32.29482	106.80334	3,901	640	Santa Fe Group	SF	3	3,855.32	3,864.58	3,859.93
L029	321740106481003	32.29454	106.80334	3,883	50	Quaternary alluvium	RGA	3	3,849.14	3,849.81	3,849.55
L030	321740106481002	32.29454	106.80334	3,883	120	Santa Fe Group	SF	2	3,848.79	3,849.56	3,849.18

Table 15. Mean winter water-level altitudes (November 2010 through April 2011) used for constructing potentiometric-surface maps of the Rio Grande alluvium and Santa Fe Group hydrogeologic units in the Mesilla Basin study area in Doña Ana County, New Mexico, and El Paso County, Texas.—Continued

[USGS, U.S. Geological Survey; ft, foot; NAVD 88, North American Vertical Datum of 1988; NWIS, USGS National Water Information System; RGA, Rio Grande alluvium; --, not available; SF, Santa Fe Group]

Well identifier (figs. 46 and 47)	USGS station number	Latitude (decimal degrees)	Longitude (decimal degrees)	Land-surface altitude (ft) (NAVD 88)	Well depth (ft)	NWIS aquifer code	Hydro-geologic group	Number of water-level-altitude measure-ments for well	Minimum water-level altitude (ft)	Maximum water-level altitude (ft)	Average water-level altitude (ft) (value used to generate potentiometric-surface maps) (figs. 46 and 47)
L031	321740106481001	32.29454	106.80334	3,883	332	Santa Fe Group	SF	7	3,843.48	3,849.04	3,845.78
L032	321733106454301	32.29204	106.76250	3,885	685	Santa Fe Group	SF	1	3,844.73	3,844.73	3,844.73
L033	321703106464701	32.28426	106.78028	3,887	700	Santa Fe Group	SF	1	3,849.43	3,849.43	3,849.43
L034	321651106454301	32.28093	106.76223	3,885	712	Santa Fe Group	SF	1	3,842.43	3,842.43	3,842.43
L035	321650106451201	32.28037	106.75361	3,904	485	Santa Fe Group	SF	1	3,839.26	3,839.26	3,839.26
L036	321640106524601	32.27787	106.88001	4,190	645	Santa Fe Group	SF	1	3,872.77	3,872.77	3,872.77
L037	321637106444001	32.27648	106.74611	3,960	626	Santa Fe Group	SF	1	3,851.17	3,851.17	3,851.17
L038	321628106451501	32.27426	106.75417	3,911	766	Santa Fe Group	SF	1	3,837.75	3,837.75	3,837.75
L039	321624106460201	32.27398	106.76695	3,875	470	Santa Fe Group	SF	1	3,842.04	3,842.04	3,842.04
L040	321623106445601	32.27371	106.74945	3,929	525	Santa Fe Group	SF	1	3,840.50	3,840.50	3,840.50
L041	321615106531601	32.27148	106.88834	4,196	380	Santa Fe Group	SF	1	3,866.25	3,866.25	3,866.25
L042	321518106471701	32.25509	106.78861	3,881	35	Quaternary alluvium	RGA	1	3,853.29	3,853.29	3,853.29
L043	321342106452202	32.22843	106.75667	3,865	30	Quaternary alluvium	RGA	1	3,847.74	3,847.74	3,847.74
L044	321335106472101	32.22648	106.78945	3,862	370	Santa Fe Group	SF	1	3,848.86	3,848.86	3,848.86
L045	321332106443703	32.22565	106.74417	3,858	40	Quaternary alluvium	RGA	5	3,836.73	3,838.49	3,837.78
L046	321332106443702	32.22565	106.74417	3,858	120	Santa Fe Group	SF	5	3,825.33	3,837.15	3,833.69
L047	321332106443701	32.22565	106.74417	3,858	307	Santa Fe Group	SF	5	3,822.08	3,836.69	3,832.55
L048	321308106453801	32.21982	106.76167	3,862	464	Santa Fe Group	SF	1	3,844.07	3,844.07	3,844.07
L049	321307106452203	32.21843	106.75695	3,855	618	Santa Fe Group	SF	1	3,832.46	3,832.46	3,832.46
L050	321307106452202	32.21843	106.75667	3,855	312	Santa Fe Group	SF	1	3,839.20	3,839.20	3,839.20
L051	321304106451505	32.21732	106.75500	3,852	121	Santa Fe Group	SF	1	3,838.50	3,838.50	3,838.50
L052	321304106451504	32.21732	106.75500	3,852	310	Santa Fe Group	SF	1	3,836.91	3,836.91	3,836.91
L053	321304106451401	32.21787	106.75445	3,855	686	Santa Fe Group	SF	1	3,840.49	3,840.49	3,840.49
L054	321241106461603	32.21148	106.77167	3,859	50	Quaternary alluvium	RGA	5	3,848.99	3,851.46	3,850.10
L055	321241106461602	32.21148	106.77167	3,859	120	Santa Fe Group	SF	5	3,832.52	3,848.52	3,843.55
L056	321241106461601	32.21148	106.77167	3,859	319	Santa Fe Group	SF	5	3,817.13	3,845.89	3,836.40
L057	321239106444501	32.21121	106.74528	3,855	480	Santa Fe Group	SF	1	3,840.34	3,840.34	3,840.34
L058	321237106462003	32.21037	106.77278	3,854	45	Quaternary alluvium	RGA	6	3,843.58	3,846.46	3,844.80
L059	321237106462002	32.21037	106.77278	3,854	125	Santa Fe Group	SF	6	3,822.50	3,841.60	3,836.42
L060	321237106462001	32.21037	106.77278	3,854	320	Santa Fe Group	SF	6	3,812.57	3,840.39	3,832.61

Table 15. Mean winter water-level altitudes (November 2010 through April 2011) used for constructing potentiometric-surface maps of the Rio Grande alluvium and Santa Fe Group hydrogeologic units in the Mesilla Basin study area in Doña Ana County, New Mexico, and El Paso County, Texas.—Continued

[USGS, U.S. Geological Survey; ft, foot; NAVD 88, North American Vertical Datum of 1988; NWIS, USGS National Water Information System; RGA, Rio Grande alluvium; --, not available; SF, Santa Fe Group]

Well identifier (figs. 46 and 47)	USGS station number	Latitude (decimal degrees)	Longitude (decimal degrees)	Land-surface altitude (ft) (NAVD 88)	Well depth (ft)	NWIS aquifer code	Hydro-geologic group	Number of water-level-altitude measure-ments for well	Minimum water-level altitude (ft)	Maximum water-level altitude (ft)	Average water-level altitude (ft) (value used to generate potentiometric-surface maps) (figs. 46 and 47)
L061	321105106442101	32.18497	106.73935	3,845	34	Quaternary alluvium	RGA	1	3,835.67	3,835.67	3,835.67
L062	321104107001702	32.18398	107.00557	4,323	420	Santa Fe Group	SF	1	4,009.79	4,009.79	4,009.79
L063	320927106531201	32.15732	106.88723	4,212	400	Santa Fe Group	SF	1	3,842.51	3,842.51	3,842.51
L064	320924106531201	32.15676	106.88723	4,212	680	Santa Fe Group	SF	1	3,844.25	3,844.25	3,844.25
L065	320824106510801	32.14065	106.85389	4,192	1,650	Santa Fe Group	SF	1	3,838.07	3,838.07	3,838.07
L066	320638106440502	32.11065	106.73528	3,924	120	Santa Fe Group	SF	1	3,818.67	3,818.67	3,818.67
L067	320615106413302	32.10427	106.69305	3,820	21	Quaternary alluvium	RGA	1	3,810.31	3,810.31	3,810.31
L068	320612107003601	32.10333	107.00944	4,267	472	Santa Fe Group	SF	1	3,831.24	3,831.24	3,831.24
L069	320456106383001	32.09704	106.64527	3,816	--	Quaternary alluvium	RGA	1	3,806.95	3,806.95	3,806.95
L070	320425106565201	32.07426	106.94862	4,217	445	Santa Fe Group	SF	1	3,829.97	3,829.97	3,829.97
L071	320405106373104	32.06760	106.62722	3,811	75	Quaternary alluvium	RGA	1	3,797.48	3,797.48	3,797.48
L072	320405106373103	32.06760	106.62722	3,811	48	Quaternary alluvium	RGA	1	3,801.05	3,801.05	3,801.05
L073	320405106373101	32.06815	106.62694	3,811	26	Quaternary alluvium	RGA	1	3,801.33	3,801.33	3,801.33
L074	320404106385801	32.06782	106.64950	3,811	34	Quaternary alluvium	RGA	1	3,799.34	3,799.34	3,799.34
L075	320303106542401	32.05056	106.90611	4,216	510	Santa Fe Group	SF	1	3,826.07	3,826.07	3,826.07
L076	320230107013501	32.04149	107.02807	4,264	437	Santa Fe Group	SF	1	3,855.18	3,855.18	3,855.18
L077	320227106570801	32.04065	106.95278	4,212	1,000	Santa Fe Group	SF	1	3,824.65	3,824.65	3,824.65
L078	320141106390602	32.02816	106.65222	3,797	1,880	Santa Fe Group	SF	1	3,774.57	3,774.57	3,774.57
L079	320141106390601	32.02816	106.65222	3,797	700	Santa Fe Group	SF	1	3,787.44	3,787.44	3,787.44
L080	320128106371501	32.02482	106.61972	3,797	--	Quaternary alluvium	RGA	1	3,789.68	3,789.68	3,789.68
L081	320032106381501	32.00899	106.63722	3,793	215	Quaternary alluvium	RGA	1	3,781.36	3,781.36	3,781.36
L082	320032106381101	32.00871	106.63749	3,793	1,050	Santa Fe Group	SF	1	3,755.72	3,755.72	3,755.72
L083	315955106490301	31.99788	106.81889	4,163	500	Santa Fe Group	SF	1	3,802.39	3,802.39	3,802.39
L084	315955106362201	31.99649	106.60694	3,800	600	Mesilla Bolson aquifer	SF	1	3,747.92	3,747.92	3,747.92
L085	315953106403901	31.99816	106.67805	3,799	90	Santa Fe Group	SF	1	3,780.08	3,780.08	3,780.08
L086	315953106390601	31.99832	106.65167	3,795	34	Quaternary alluvium	RGA	1	3,782.94	3,782.94	3,782.94
L087	315941106505801	31.99427	106.84945	4,191	560	Santa Fe Group	SF	1	3,806.57	3,806.57	3,806.57
L088	315940106372304	31.99444	106.62306	3,791	1,310	Santa Fe Group	SF	2	3,745.34	3,745.41	3,745.37
L089	315940106372303	31.99444	106.62306	3,791	810	Santa Fe Group	SF	2	3,743.91	3,745.39	3,744.65
L090	315940106372302	31.99444	106.62306	3,791	310	Santa Fe Group	SF	2	3,767.71	3,773.53	3,770.62

Table 15. Mean winter water-level altitudes (November 2010 through April 2011) used for constructing potentiometric-surface maps of the Rio Grande alluvium and Santa Fe Group hydrogeologic units in the Mesilla Basin study area in Doña Ana County, New Mexico, and El Paso County, Texas.—Continued

[USGS, U.S. Geological Survey; ft, foot; NAVD 88, North American Vertical Datum of 1988; NWIS, USGS National Water Information System; RGA, Rio Grande alluvium; --, not available; SF, Santa Fe Group]

Well identifier (figs. 46 and 47)	USGS station number	Latitude (decimal degrees)	Longitude (decimal degrees)	Land-surface altitude (ft) (NAVD 88)	Well depth (ft)	NWIS aquifer code	Hydro-geologic group	Number of water-level-altitude measure-ments for well	Minimum water-level altitude (ft)	Maximum water-level altitude (ft)	Average water-level altitude (ft) (value used to generate potentiometric-surface maps) (figs. 46 and 47)
L091	315940106372301	31.99444	106.62306	3,791	90	Quaternary alluvium	RGA	2	3,783.02	3,783.90	3,783.46
L092	315918106391301	31.98760	106.65472	3,789	390	Santa Fe Group	SF	1	3,777.11	3,777.11	3,777.11
L093	315915106354701	31.98816	106.59749	3,823	336	Mesilla Bolson aquifer	SF	1	3,755.38	3,755.38	3,755.38
L094	315902107005501	31.98732	107.01529	4,202	406	Santa Fe Group	SF	1	3,816.04	3,816.04	3,816.04
L095	315901106355001	31.98371	106.59777	3,823	264	Mesilla Bolson aquifer	SF	1	3,762.83	3,762.83	3,762.83
L096	315856106382001	31.98205	106.63888	3,790	80	Rio Grande alluvium	RGA	1	3,779.54	3,779.54	3,779.54
L097	315835106402501	31.97677	106.67416	3,800	149	Santa Fe Group	SF	1	3,780.47	3,780.47	3,780.47
L098	315831106345401	31.97538	106.58221	3,904	500	Mesilla Bolson aquifer	SF	1	3,735.10	3,735.10	3,735.10
L099	315823106384001	31.97455	106.64777	3,788	--	Quaternary alluvium	RGA	1	3,776.70	3,776.70	3,776.70
L100	315817106352301	31.97149	106.59082	3,853	310	Mesilla Bolson aquifer	SF	1	3,747.10	3,747.10	3,747.10
L101	315811106490401	31.96972	106.81722	4,167	510	Santa Fe Group	SF	1	3,804.88	3,804.88	3,804.88
L102	315804106375901	31.96649	106.63360	3,786	--	Quaternary alluvium	RGA	1	3,777.75	3,777.75	3,777.75
L103	315803106364501	31.96732	106.61305	3,782	1,063	Mesilla Bolson aquifer	SF	1	3,687.25	3,687.25	3,687.25
L104	315754106372404	31.96500	106.62333	3,783	1,275	Santa Fe Group	SF	1	3,712.34	3,712.34	3,712.34
L105	315754106372403	31.96500	106.62333	3,783	895	Santa Fe Group	SF	1	3,710.85	3,710.85	3,710.85
L106	315754106372402	31.96500	106.62333	3,783	295	Santa Fe Group	SF	1	3,766.35	3,766.35	3,766.35
L107	315754106372401	31.96500	106.62333	3,783	76	Quaternary alluvium	RGA	1	3,772.32	3,772.32	3,772.32
L108	315720106415601	31.95482	106.70027	4,101	722	Santa Fe Group	SF	3	3,780.43	3,781.61	3,780.96
L109	315717106364001	31.95510	106.61166	3,780	1,072	Mesilla Bolson aquifer	SF	1	3,704.70	3,704.70	3,704.70
L110	315712106364304	31.95344	106.61277	3,779	800	Mesilla Bolson aquifer	SF	3	3,709.93	3,723.91	3,715.42
L111	315712106364303	31.95344	106.61277	3,779	299	Mesilla Bolson aquifer	SF	3	3,703.42	3,734.85	3,721.17
L112	315712106364302	31.95344	106.61277	3,779	159	Rio Grande alluvium	RGA	3	3,764.76	3,766.70	3,765.69
L113	315712106364301	31.95344	106.61277	3,779	59	Rio Grande alluvium	RGA	3	3,768.23	3,768.76	3,768.51
L114	315712106362304	31.95399	106.60694	3,782	799	Mesilla Bolson aquifer	SF	3	3,708.51	3,725.42	3,715.46
L115	315712106362303	31.95371	106.60721	3,782	298	Mesilla Bolson aquifer	SF	3	3,702.65	3,729.46	3,720.49
L116	315712106362302	31.95371	106.60721	3,782	158	Rio Grande alluvium	RGA	3	3,763.83	3,765.75	3,764.94
L117	315712106362301	31.95371	106.60721	3,782	58	Rio Grande alluvium	RGA	3	3,768.64	3,769.83	3,769.09
L118	315712106361804	31.95371	106.60583	3,781	799	Mesilla Bolson aquifer	SF	7	3,703.98	3,726.08	3,711.28
L119	315712106361803	31.95371	106.60583	3,781	300	Mesilla Bolson aquifer	SF	7	3,688.03	3,730.53	3,703.88
L120	315712106361802	31.95371	106.60583	3,781	158	Rio Grande alluvium	RGA	7	3,758.34	3,764.71	3,761.26

Table 15. Mean winter water-level altitudes (November 2010 through April 2011) used for constructing potentiometric-surface maps of the Rio Grande alluvium and Santa Fe Group hydrogeologic units in the Mesilla Basin study area in Doña Ana County, New Mexico, and El Paso County, Texas.—Continued

[USGS, U.S. Geological Survey; ft, foot; NAVD 88, North American Vertical Datum of 1988; NWIS, USGS National Water Information System; RGA, Rio Grande alluvium; --, not available; SF, Santa Fe Group]

Well identifier (figs. 46 and 47)	USGS station number	Latitude (decimal degrees)	Longitude (decimal degrees)	Land-surface altitude (ft) (NAVD 88)	Well depth (ft)	NWIS aquifer code	Hydro-geologic group	Number of water-level-altitude measure-ments for well	Minimum water-level altitude (ft)	Maximum water-level altitude (ft)	Average water-level altitude (ft) (value used to generate potentiometric-surface maps) (figs. 46 and 47)
L121	315712106361801	31.95371	106.60583	3,781	47	Rio Grande alluvium	RGA	6	3,770.07	3,772.52	3,770.76
L122	315712106361204	31.95371	106.60444	3,784	803	Mesilla Bolson aquifer	SF	4	3,707.59	3,726.22	3,714.38
L123	315712106361203	31.95371	106.60444	3,784	334	Mesilla Bolson aquifer	SF	4	3,692.10	3,731.01	3,714.48
L124	315712106361202	31.95371	106.60444	3,784	156	Rio Grande alluvium	RGA	4	3,754.91	3,761.73	3,758.93
L125	315712106361201	31.95371	106.60444	3,784	52	Rio Grande alluvium	RGA	4	3,769.71	3,772.78	3,770.92
L126	315711106354201	31.95316	106.59305	3,844	135	Mesilla Bolson aquifer	SF	1	3,736.66	3,736.66	3,736.66
L127	315656106350702	31.94889	106.58528	3,908	660	Santa Fe Group	SF	1	3,731.52	3,731.52	3,731.52
L128	315656106350701	31.94889	106.58528	3,908	300	Santa Fe Group	SF	1	3,740.48	3,740.48	3,740.48
L129	315646106374404	31.94611	106.62889	3,780	1,322	Santa Fe Group	SF	2	3,726.05	3,729.61	3,727.83
L130	315646106374403	31.94611	106.62889	3,780	912	Santa Fe Group	SF	2	3,727.17	3,730.26	3,728.71
L131	315646106374402	31.94611	106.62889	3,780	331	Santa Fe Group	SF	2	3,757.15	3,759.08	3,758.11
L132	315646106374401	31.94611	106.62889	3,780	81	Quaternary alluvium	RGA	2	3,767.76	3,768.71	3,768.23
L133	315639106380401	31.94427	106.63499	3,779	130	Quaternary alluvium	RGA	1	3,766.67	3,766.67	3,766.67
L134	315637106394801	31.94344	106.66860	3,846	--	Santa Fe Group	SF	1	3,770.29	3,770.29	3,770.29
L135	315627106363701	31.94149	106.61138	3,773	1,013	Mesilla Bolson aquifer	SF	1	3,758.66	3,758.66	3,758.66
L136	315622106391705	31.93955	106.65527	3,782	1,765	Santa Fe Group	SF	1	3,741.51	3,741.51	3,741.51
L137	315556106363101	31.93205	106.60944	3,772	200	Rio Grande alluvium	RGA	1	3,758.71	3,758.71	3,758.71
L138	315554106365701	31.93177	106.61666	3,773	545	Mesilla Bolson aquifer	SF	1	3,757.12	3,757.12	3,757.12
L139	315535106543602	31.92593	106.91084	4,101	475	Santa Fe Group	SF	1	3,815.16	3,815.16	3,815.16
L140	315515106392801	31.91927	106.65805	3,779	--	Quaternary alluvium	RGA	1	3,768.75	3,768.75	3,768.75
L141	315453106374701	31.91705	106.63333	3,773	--	Quaternary alluvium	RGA	1	3,760.96	3,760.96	3,760.96
L142	315401106363701	31.90038	106.61082	3,764	116	Rio Grande alluvium	RGA	1	3,756.27	3,756.27	3,756.27
L143	315349106585701	31.89843	106.98528	4,107	580	Santa Fe Group	SF	1	3,812.86	3,812.86	3,812.86
L144	315336106582801	31.89482	106.99084	4,114	580	Santa Fe Group	SF	1	3,808.39	3,808.39	3,808.39
L145	315326106592501	31.89066	106.99084	4,112	--	Santa Fe Group	SF	1	3,802.64	3,802.64	3,802.64
L146	315318106384301	31.88816	106.64555	3,771	--	Quaternary alluvium	RGA	1	3,761.36	3,761.36	3,761.36
L147	315308106361001	31.88566	106.60332	3,762	150	Rio Grande alluvium	RGA	1	3,755.54	3,755.54	3,755.54
L148	315245106380602	31.87927	106.63555	3,761	427	Santa Fe Group	SF	2	3,749.75	3,750.41	3,750.08
L149	315245106380601	31.87927	106.63555	3,761	198	Santa Fe Group	SF	2	3,747.14	3,747.30	3,747.22
L150	315238106392301	31.87872	106.65721	3,832	330	Santa Fe Group	SF	1	3,759.39	3,759.39	3,759.39

Table 15. Mean winter water-level altitudes (November 2010 through April 2011) used for constructing potentiometric-surface maps of the Rio Grande alluvium and Santa Fe Group hydrogeologic units in the Mesilla Basin study area in Doña Ana County, New Mexico, and El Paso County, Texas.—Continued

[USGS, U.S. Geological Survey; ft, foot; NAVD 88, North American Vertical Datum of 1988; NWIS, USGS National Water Information System; RGA, Rio Grande alluvium; --, not available; SF, Santa Fe Group]

Well identifier (figs. 46 and 47)	USGS station number	Latitude (decimal degrees)	Longitude (decimal degrees)	Land-surface altitude (ft) (NAVD 88)	Well depth (ft)	NWIS aquifer code	Hydro-geologic group	Number of water-level-altitude measure-ments for well	Minimum water-level altitude (ft)	Maximum water-level altitude (ft)	Average water-level altitude (ft) (value used to generate potentiometric-surface maps) (figs. 46 and 47)
L151	315212106420901	31.87122	106.70416	4,112	536	Santa Fe Group	SF	3	3,769.39	3,770.06	3,769.73
L152	315204106381601	31.87010	106.63888	3,760	148	Quaternary alluvium	RGA	1	3,752.41	3,752.41	3,752.41
L153	315152106371901	31.86455	106.62249	3,757	128	Quaternary alluvium	RGA	1	3,749.34	3,749.34	3,749.34
L154	315150106415801	31.86427	106.70249	4,111	--	Santa Fe Group	SF	2	3,770.05	3,770.70	3,770.38
L155	315144106394101	31.86288	106.66277	3,883	333	Santa Fe Group	SF	1	3,751.51	3,751.51	3,751.51
L156	315126106381801	31.85899	106.64277	3,805	245	Santa Fe Group	SF	1	3,748.76	3,748.76	3,748.76
L157	315124106410001	31.85844	106.68277	4,086	537	Santa Fe Group	SF	1	3,758.43	3,758.43	3,758.43
L158	315118106422601	31.85483	106.71083	4,114	552	Santa Fe Group	SF	2	3,775.32	3,775.76	3,775.54
L159	315110106371702	31.85288	106.62194	3,752	404	Santa Fe Group	SF	1	3,748.21	3,748.21	3,748.21
L160	315110106371701	31.85288	106.62194	3,752	222	Santa Fe Group	SF	1	3,743.51	3,743.51	3,743.51
L161	315101106410701	31.85122	106.68583	4,082	524	Santa Fe Group	SF	1	3,757.06	3,757.06	3,757.06
L162	315049106373601	31.84761	106.62749	3,787	254	Santa Fe Group	SF	1	3,737.89	3,737.89	3,737.89
L163	315046106403201	31.84538	106.67944	4,091	601	Santa Fe Group	SF	2	3,754.60	3,756.47	3,755.54
L164	315013106362602	31.83705	106.60777	3,747	306	Santa Fe Group	SF	2	3,740.72	3,741.55	3,741.14
L165	315013106362601	31.83705	106.60777	3,747	168	Santa Fe Group	SF	2	3,740.19	3,741.29	3,740.74
L166	315007106370201	31.83649	106.62110	3,823	300	Santa Fe Group	SF	1	3,748.81	3,748.81	3,748.81
L167	314932106493401	31.82594	106.82527	4,130	533	Santa Fe Group	SF	3	3,799.16	3,799.63	3,799.37
L168	314920106343801	31.82233	106.57777	3,742	48	Quaternary alluvium	RGA	1	3,734.13	3,734.13	3,734.13
L169	314918106464401	31.82177	106.77916	4,104	490	Santa Fe Group	SF	2	3,792.97	3,793.12	3,793.05
L170	314914106530501	31.82094	106.88639	4,132	--	Santa Fe Group	SF	2	3,803.40	3,803.57	3,803.48
L171	314817106325802	31.80483	106.54999	3,734	166	Santa Fe Group	SF	2	3,726.97	3,727.27	3,727.12
L172	314817106325801	31.80483	106.54999	3,734	75	Quaternary alluvium	RGA	2	3,728.10	3,728.40	3,728.25
L173	314816106325901	31.80466	106.54994	3,734	34	Quaternary alluvium	RGA	1	3,727.98	3,727.98	3,727.98
L174	314810106513601	31.80427	106.86166	4,127	565	Santa Fe Group	SF	2	3,800.76	3,800.85	3,800.81
L175	314723106420001	31.78927	106.69971	4,085	500	Santa Fe Group	SF	3	3,774.35	3,774.45	3,774.41

Table 16. Differences in water-level altitudes (Rio Grande alluvium minus Santa Fe Group) based on data collected between 1985 and 2012 for different well groups in the Mesilla Basin study area in Doña Ana County, New Mexico, and El Paso County, Texas.

[ft, foot; NAVD 88, North American Vertical Datum of 1988; USGS, U.S. Geological Survey; RGA, Rio Grande alluvium; SF, Santa Fe Group]

Well group identifier (fig. 49)	Latitude (decimal degrees)	Longitude (decimal degrees)	Land-surface altitude (ft) (NAVD 88)	USGS station number for each well in group	Well depth (ft)	Hydro-geologic group	Common data-collection period	Number of water-level measure-ments for well	Minimum water-level altitude (ft)	Maximum water-level altitude (ft)	Mean water-level altitude (ft)	Mean difference (Rio Grande alluvium minus Santa Fe Group) in water-level altitudes between shallowest and deepest wells within well group (ft)
CWF–4	31.95344	106.61277	3,779	315712106364301	59	RGA	12/1984–6/2011	289	3,766.22	3,774.54	3,771.06	50.65
				315712106364302	159	RGA		314	3,760.52	3,773.12	3,768.05	
				315712106364303	299	SF		290	3,690.95	3,767.17	3,722.67	
				315712106364304	800	SF		288	3,677.39	3,763.63	3,720.41	
ISC–1	31.99444	106.62306	3,791	315940106372301	90	RGA	3/2003–2/2011	5	3,783.02	3,784.78	3,783.61	32.71
				315940106372302	310	SF		5	3,773.53	3,776.51	3,775.23	
				315940106372303	810	SF		5	3,745.39	3,753.30	3,750.96	
				315940106372304	1,310	SF		5	3,745.34	3,753.25	3,750.90	
ISC–2	31.96500	106.62333	3,783	315754106372401	75.5	RGA	3/2003–2/2011	5	3,766.14	3,772.91	3,771.23	53.06
				315754106372402	295	SF		5	3,759.75	3,766.35	3,763.96	
				315754106372403	895	SF		5	3,707.01	3,727.95	3,716.68	
				315754106372404	1,275	SF		5	3,708.64	3,729.36	3,718.17	
ISC–3	31.94611	106.62889	3,780	315646106374401	80.5	RGA	3/2003–2/2011	5	3,767.76	3,769.16	3,768.39	35.70
				315646106374402	331	SF		5	3,756.65	3,759.91	3,758.73	
				315646106374403	911.5	SF		5	3,728.11	3,739.22	3,733.33	
				315646106374404	1,321.5	SF		5	3,727.51	3,738.59	3,732.69	
ISC–4	31.80480	106.54998	3,734	314816106325901	34.2	RGA	2/2009–3/2011	6	3,727.98	3,729.28	3,728.69	1.24
				314817106325801	75	RGA		3	3,727.95	3,728.42	3,728.16	
				314817106325802	165.5	SF		3	3,726.85	3,728.54	3,727.45	
				314817106325801	75	RGA	9/2007–2/2011	5	3,727.95	3,728.62	3,728.22	0.74
				314817106325802	165.5	SF		5	3,726.85	3,728.54	3,727.47	
ISC–5	31.83705	106.60777	3,747	315013106362601	168	SF	9/2007–2/2011	5	3,740.28	3,742.23	3,741.29	-0.06
				315013106362602	306	SF		5	3,740.10	3,742.57	3,741.36	
ISC–6	31.85288	106.62194	3,752	315110106371701	222	SF	9/2007–2/2011	5	3,743.51	3,748.83	3,744.88	-2.65
				315110106371702	403.5	SF		5	3,744.33	3,749.59	3,747.53	
ISC–7	31.87927	106.63555	3,761	315245106380601	198	SF	9/2007–2/2011	5	3,747.14	3,750.96	3,748.08	-2.00
				315245106380602	426.8	SF		5	3,747.52	3,751.56	3,750.08	

Table 16. Differences in water-level altitudes (Rio Grande alluvium minus Santa Fe Group) based on data collected between 1985 and 2012 for different well groups in the Mesilla Basin study area in Doña Ana County, New Mexico, and El Paso County, Texas.—Continued

[ft, foot; NAVD 88, North American Vertical Datum of 1988; USGS, U.S. Geological Survey; RGA, Rio Grande alluvium; SF, Santa Fe Group]

Well group identifier (fig. 49)	Latitude (decimal degrees)	Longitude (decimal degrees)	Land-surface altitude (ft) (NAVD 88)	USGS station number for each well in group	Well depth (ft)	Hydro-geologic group	Common data-collection period	Number of water-level measure-ments for well	Minimum water-level altitude (ft)	Maximum water-level altitude (ft)	Mean water-level altitude (ft)	Mean difference (Rio Grande alluvium minus Santa Fe Group) in water-level altitudes between shallowest and deepest wells within well group (ft)
LC–1	32.29593	106.82417	3,891	321745106492503	41	RGA	2/1991–5/2012	143	3,877.20	3,888.63	3,885.34	3.72
				321745106492502	105	SF		239	3,877.46	3,888.84	3,885.53	
				321745106492501	305	SF		145	3,875.94	3,883.65	3,881.62	
LC–2	32.29600	106.82306	3,891	321745106492103	40	RGA	6/2002–7/2012	138	3,876.00	3,886.56	3,884.26	20.92
				321745106492102	110	SF		234	3,871.01	3,883.87	3,880.65	
				321745106492101	310	SF		103	3,856.36	3,873.42	3,866.47	
				321745106492106	650	SF		108	3,852.46	3,871.40	3,863.35	
				321745106492103	40	RGA	2/1991–7/2012	138	3,876.00	3,886.56	3,884.26	16.08
				321745106492102	110	SF		234	3,871.01	3,883.87	3,880.65	
				321745106492101	310	SF		136	3,856.36	3,876.53	3,868.18	
LC–3	32.29454	106.80334	3,883	321740106481003	50	RGA	2/1991–7/2012	140	3,840.87	3,866.83	3,855.14	2.80
				321740106481002	120	SF		221	3,840.53	3,870.45	3,859.43	
				321740106481001	332	SF		142	3,837.25	3,864.58	3,852.35	
LMV–1	31.94889	106.58528	3,908	315656106350701	300	SF	7/2003–1/2011	11	3,740.48	3,743.45	3,742.51	9.96
				315656106350702	660	SF		11	3,728.06	3,736.97	3,732.54	
LMV–2	32.02816	106.65222	3,797	320141106390601	700	SF	7/2003–1/2011	12	3,779.80	3,789.20	3,786.67	10.42
				320141106390602	1,880	SF		11	3,770.90	3,778.50	3,776.25	
M–1	32.21037	106.77278	3,854	321237106462003	45	RGA	12/1983–5/2012	142	3,841.52	3,848.09	3,845.42	8.06
				321237106462002	125	SF		245	3,822.50	3,846.44	3,841.95	
				321237106462001	320	SF		144	3,812.57	3,844.58	3,837.36	
M–2	32.21148	106.77167	3,859	321241106461603	50	RGA	9/1991–5/2012	142	3,847.03	3,853.14	3,850.72	7.83
				321241106461602	120	SF		246	3,832.52	3,852.11	3,848.28	
				321241106461601	319	SF		144	3,817.13	3,850.15	3,842.88	

Table 16. Differences in water-level altitudes (Rio Grande alluvium minus Santa Fe Group) based on data collected between 1985 and 2012 for different well groups in the Mesilla Basin study area in Doña Ana County, New Mexico, and El Paso County, Texas.—Continued

[ft, foot; NAVD 88, North American Vertical Datum of 1988; USGS, U.S. Geological Survey; RGA, Rio Grande alluvium; SF, Santa Fe Group]

Well group identifier (fig. 49)	Latitude (decimal degrees)	Longitude (decimal degrees)	Land-surface altitude (ft) (NAVD 88)	USGS station number for each well in group	Well depth (ft)	Hydro-geologic group	Common data-collection period	Number of water-level measure-ments for well	Minimum water-level altitude (ft)	Maximum water-level altitude (ft)	Mean water-level altitude (ft)	Mean difference (Rio Grande alluvium minus Santa Fe Group) in water-level altitudes between shallowest and deepest wells within well group (ft)
M–3	32.21760	106.75483	3,855	321304106451406	35	RGA	2/1985–2/1998	14	3,842.42	3,843.95	3,843.30	-0.80
				321304106451505	121	SF		14	3,842.09	3,843.26	3,842.78	
				321304106451504	310	SF		14	3,838.43	3,842.74	3,841.34	
				321304106451503	599	SF		14	3,836.77	3,840.62	3,839.37	
				321304106451401	686	SF		14	3,841.66	3,845.57	3,844.10	
				321304106451406	35	RGA	2/1985–1/2003	18	3,842.42	3,846.27	3,843.52	-0.77
				321304106451505	121	SF		18	3,842.09	3,843.27	3,842.78	
				321304106451504	310	SF		18	3,838.43	3,842.74	3,841.35	
				321304106451401	686	SF		18	3,841.66	3,846.56	3,844.28	
				321304106451505	121	SF	2/1985–1/2012	27	3,833.99	3,843.27	3,841.20	-1.42
				321304106451504	310	SF		27	3,831.32	3,842.74	3,839.42	
				321304106451401	686	SF		27	3,835.23	3,846.56	3,842.63	
M–4	32.22565	106.74417	3,858	321332106443703	40	RGA	2/1991–5/2012	149	3,830.23	3,849.32	3,841.37	4.39
				321332106443702	120	SF		229	3,824.09	3,847.68	3,841.47	
				321332106443701	307	SF		147	3,822.08	3,846.33	3,836.98	
NM344	32.06760	106.62722	3,811	320405106373101	26	RGA	2/1985–2/1993	8	3,801.30	3,802.19	3,801.68	0.87
				320405106373102	36	RGA		9	3,800.89	3,801.76	3,801.24	
				320405106373103	48	RGA		8	3,800.93	3,802.06	3,801.29	
				320405106373104	75	RGA		7	3,800.38	3,801.52	3,800.95	
				320405106373105	150	SF		8	3,800.05	3,801.37	3,800.80	
				320405106373101	26	RGA	2/1985–1/1999	14	3,801.30	3,802.26	3,801.83	0.79
				320405106373102	36	RGA		15	3,800.89	3,801.94	3,801.43	
				320405106373103	48	RGA		14	3,800.93	3,802.06	3,801.45	
				320405106373104	75	RGA		13	3,800.38	3,801.52	3,801.04	
				320405106373101	26	RGA	2/1985–1/2012	27	3,799.87	3,802.26	3,801.46	1.50
				320405106373103	48	RGA		27	3,799.61	3,802.06	3,801.11	
				320405106373104	75	RGA		26	3,795.50	3,801.52	3,799.95	

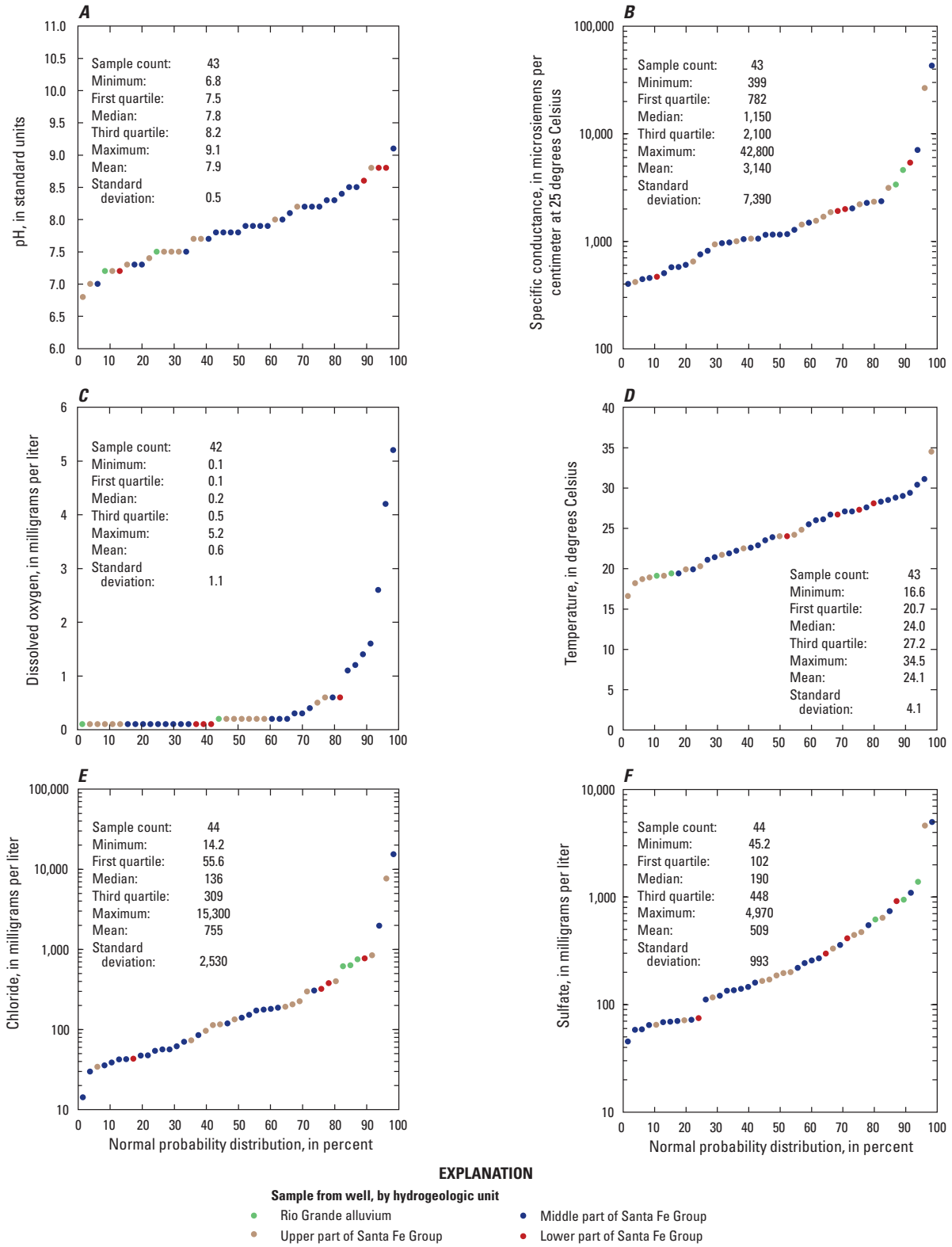

Figure 21. Selected constituent concentrations measured in groundwater samples collected in the Mesilla Basin study area in Doña Ana County, New Mexico, and El Paso County, Texas, 2010, grouped by hydrogeologic unit. *A*, pH. *B*, Specific conductance. *C*, Dissolved oxygen. *D*, Temperature. *E*, Chloride. *F*, Sulfate. *G*, Bicarbonate. *H*, Fluoride. *I*, Bromide. *J*, Nitrate plus nitrite. *K*, Sodium. *L*, Calcium. *M*, Magnesium. *N*, Silica. *O*, Potassium. *P*, Ammonia. *Q*, Aluminum. *R*, Arsenic. *S*, Barium. *T*, Iron. *U*, Lithium. V, Manganese. W, Strontium. *X*, Uranium. *Y*, Delta deuterium. *Z*, Delta oxygen-18. *AA*, Ratio of strontium-87 and strontium-86. *BB*, Tritium. *CC*, Carbon-14. *DD*, Apparent age.

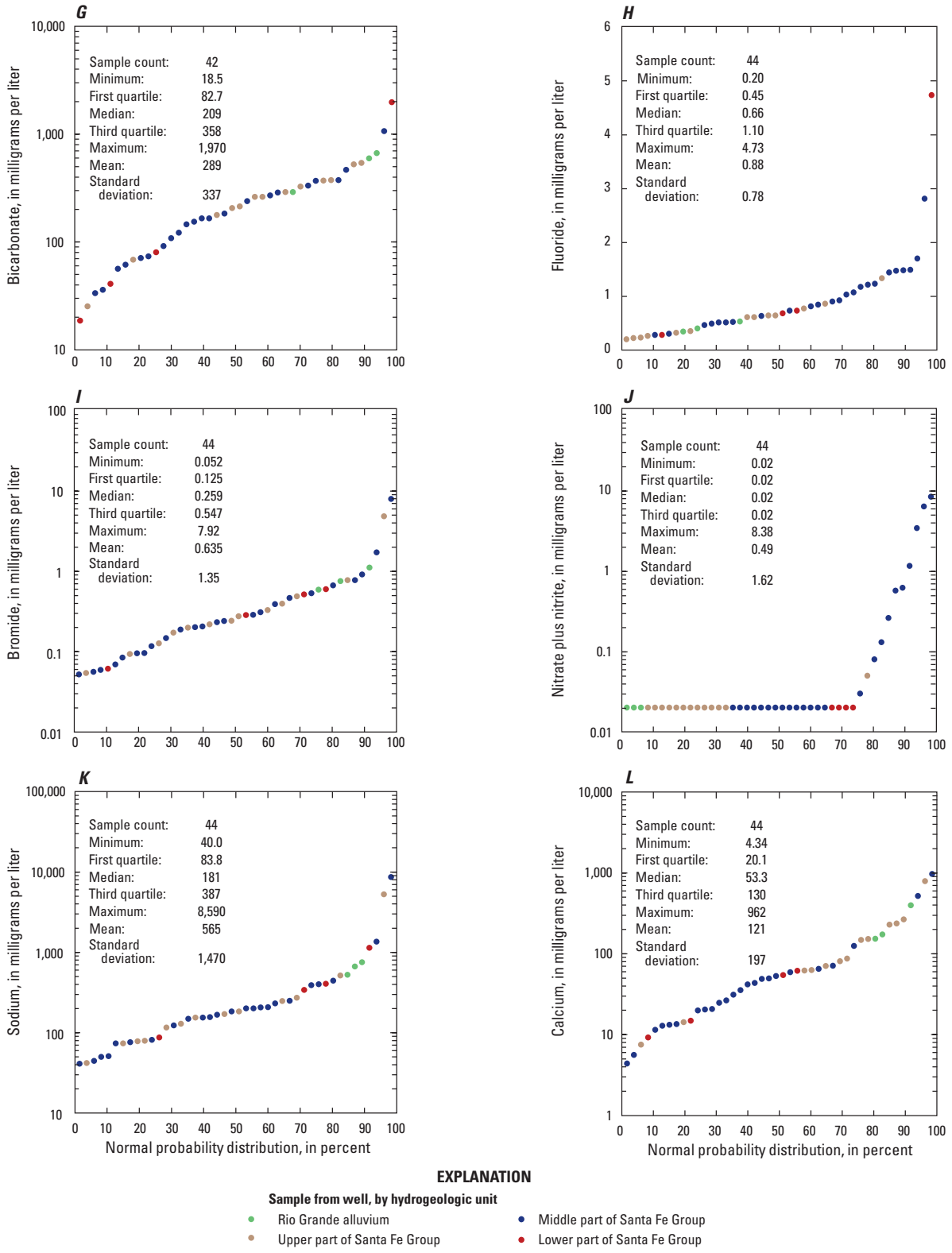

Figure 21. Selected constituent concentrations measured in groundwater samples collected in the Mesilla Basin study area in Doña Ana County, New Mexico, and El Paso County, Texas, 2010, grouped by hydrogeologic unit. *A*, pH. *B*, Specific conductance. *C*, Dissolved oxygen. *D*, Temperature. *E*, Chloride. *F*, Sulfate. *G*, Bicarbonate. *H*, Fluoride. *I*, Bromide. *J*, Nitrate plus nitrite. *K*, Sodium. *L*, Calcium. *M*, Magnesium. *N*, Silica. *O*, Potassium. *P*, Ammonia. *Q*, Aluminum. *R*, Arsenic. *S*, Barium. *T*, Iron. *U*, Lithium. V, Manganese. W, Strontium. *X*, Uranium. *Y*, Delta deuterium. *Z*, Delta oxygen-18. *AA*, Ratio of strontium-87 and strontium-86. *BB*, Tritium. *CC*, Carbon-14. *DD*, Apparent age.—Continued

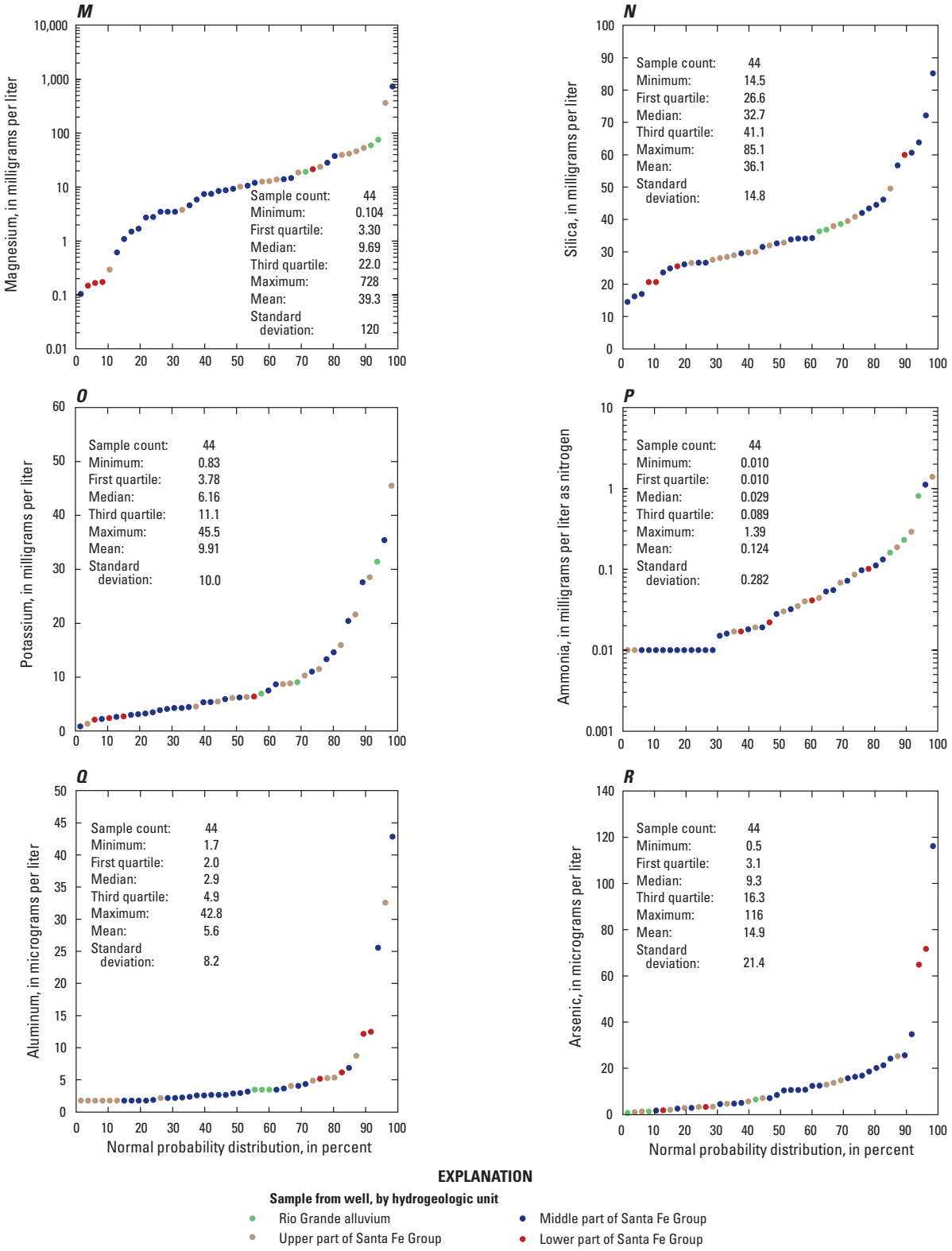

Figure 21. Selected constituent concentrations measured in groundwater samples collected in the Mesilla Basin study area in Doña Ana County, New Mexico, and El Paso County, Texas, 2010, grouped by hydrogeologic unit. *A*, pH. *B*, Specific conductance. *C*, Dissolved oxygen. *D*, Temperature. *E*, Chloride. *F*, Sulfate. *G*, Bicarbonate. *H*, Fluoride. *I*, Bromide. *J*, Nitrate plus nitrite. *K*, Sodium. *L*, Calcium. *M*, Magnesium. *N*, Silica. *O*, Potassium. *P*, Ammonia. *Q*, Aluminum. *R*, Arsenic. *S*, Barium. *T*, Iron. *U*, Lithium. V, Manganese. W, Strontium. *X*, Uranium. *Y*, Delta deuterium. *Z*, Delta oxygen-18. *AA*, Ratio of strontium-87 and strontium-86. *BB*, Tritium. *CC*, Carbon-14. *DD*, Apparent age.—Continued

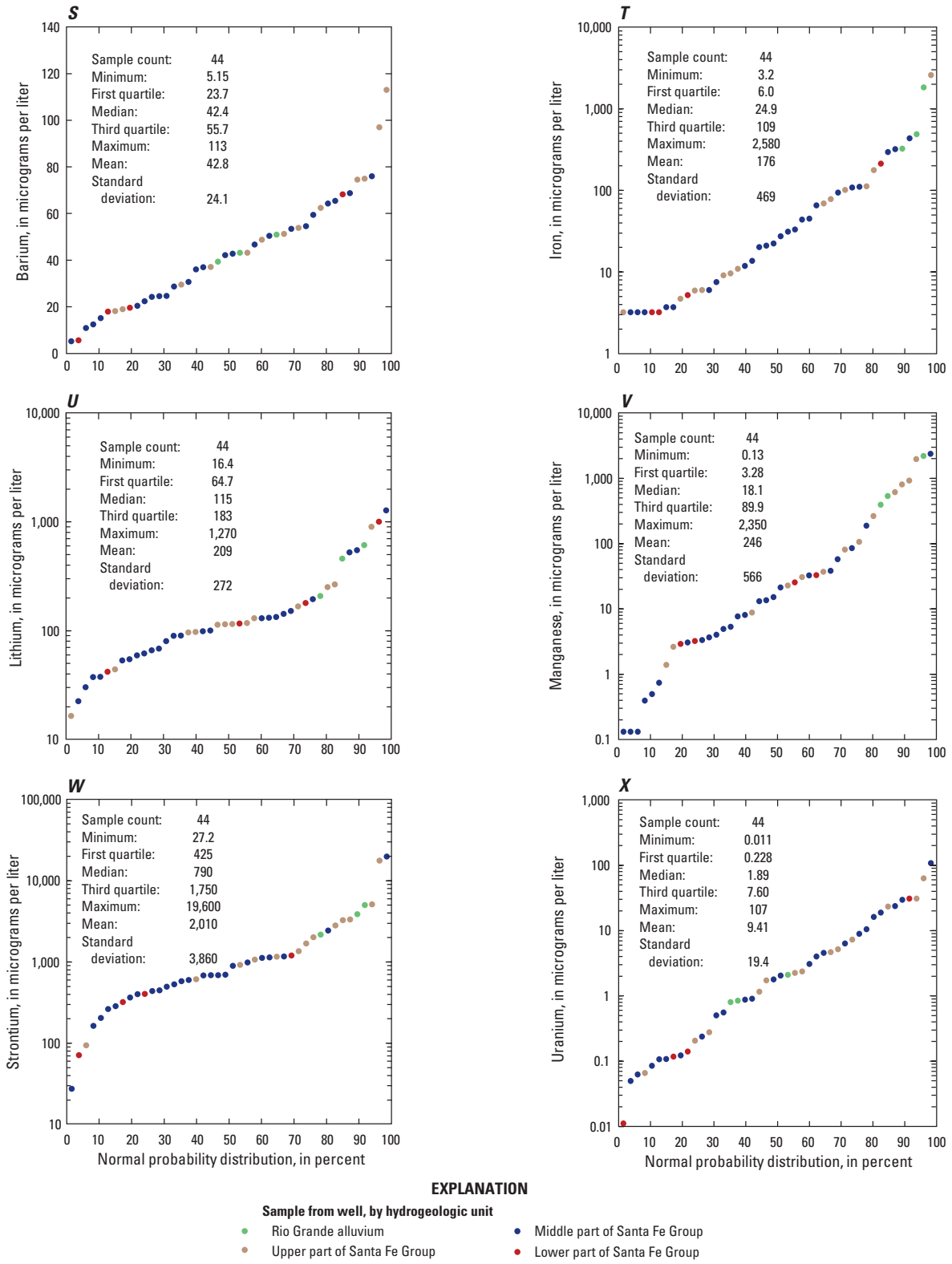

Figure 21. Selected constituent concentrations measured in groundwater samples collected in the Mesilla Basin study area in Doña Ana County, New Mexico, and El Paso County, Texas, 2010, grouped by hydrogeologic unit. *A*, pH. *B*, Specific conductance. *C*, Dissolved oxygen. *D*, Temperature. *E*, Chloride. *F*, Sulfate. *G*, Bicarbonate. *H*, Fluoride. *I*, Bromide. *J*, Nitrate plus nitrite. *K*, Sodium. *L*, Calcium. *M*, Magnesium. *N*, Silica. *O*, Potassium. *P*, Ammonia. *Q*, Aluminum. *R*, Arsenic. *S*, Barium. *T*, Iron. *U*, Lithium. V, Manganese. W, Strontium. *X*, Uranium. *Y*, Delta deuterium. *Z*, Delta oxygen-18. *AA*, Ratio of strontium-87 and strontium-86. *BB*, Tritium. *CC*, Carbon-14. *DD*, Apparent age.—Continued

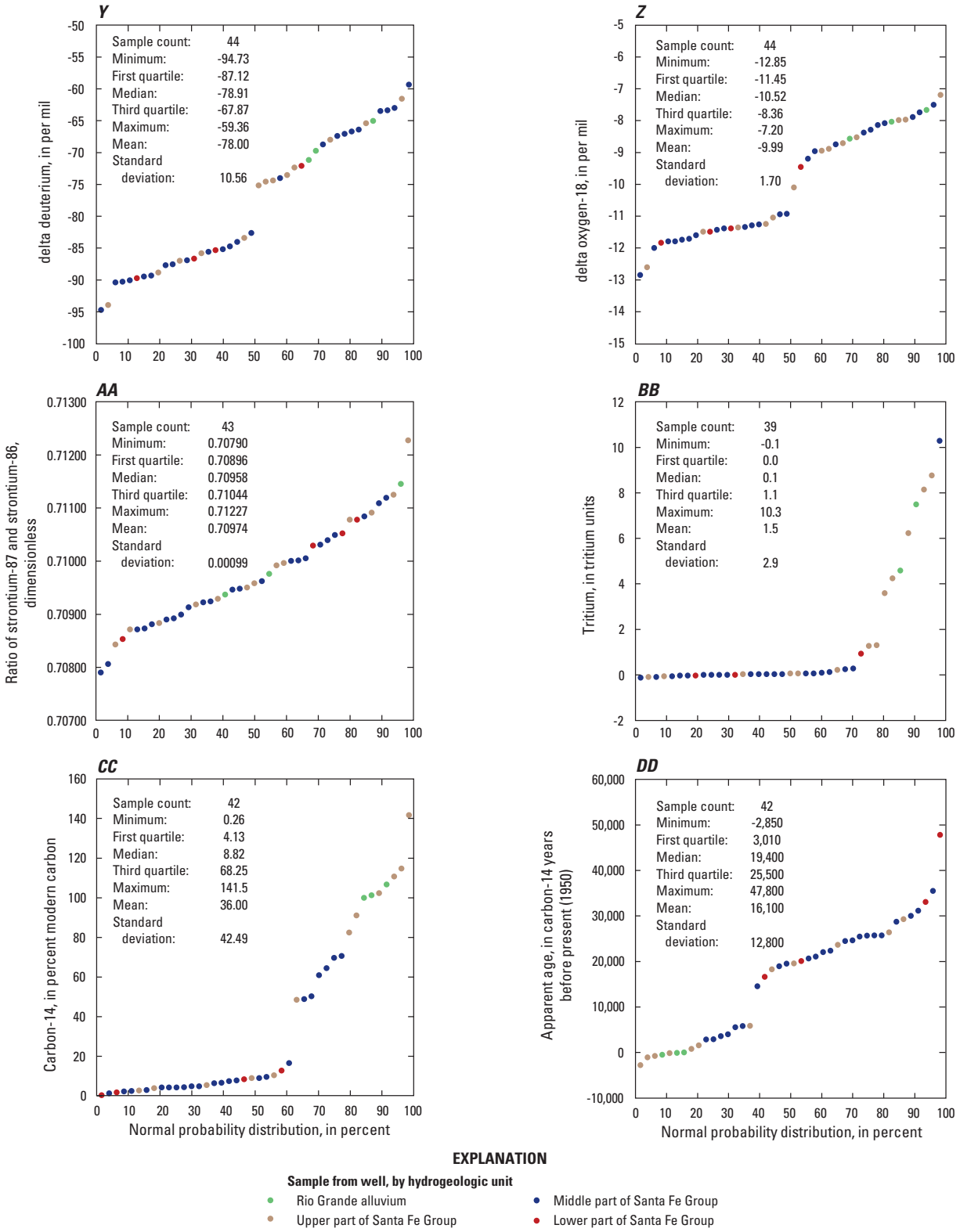

Figure 21. Selected constituent concentrations measured in groundwater samples collected in the Mesilla Basin study area in Doña Ana County, New Mexico, and El Paso County, Texas, 2010, grouped by hydrogeologic unit. *A*, pH. *B*, Specific conductance. *C*, Dissolved oxygen. *D*, Temperature. *E*, Chloride. *F*, Sulfate. *G*, Bicarbonate. *H*, Fluoride. *I*, Bromide. *J*, Nitrate plus nitrite. *K*, Sodium. *L*, Calcium. *M*, Magnesium. *N*, Silica. *O*, Potassium. *P*, Ammonia. *Q*, Aluminum. *R*, Arsenic. *S*, Barium. *T*, Iron. *U*, Lithium. V, Manganese. W, Strontium. *X*, Uranium. *Y*, Delta deuterium. *Z*, Delta oxygen-18. *AA*, Ratio of strontium-87 and strontium-86. *BB*, Tritium. *CC*, Carbon-14. *DD*, Apparent age.—Continued

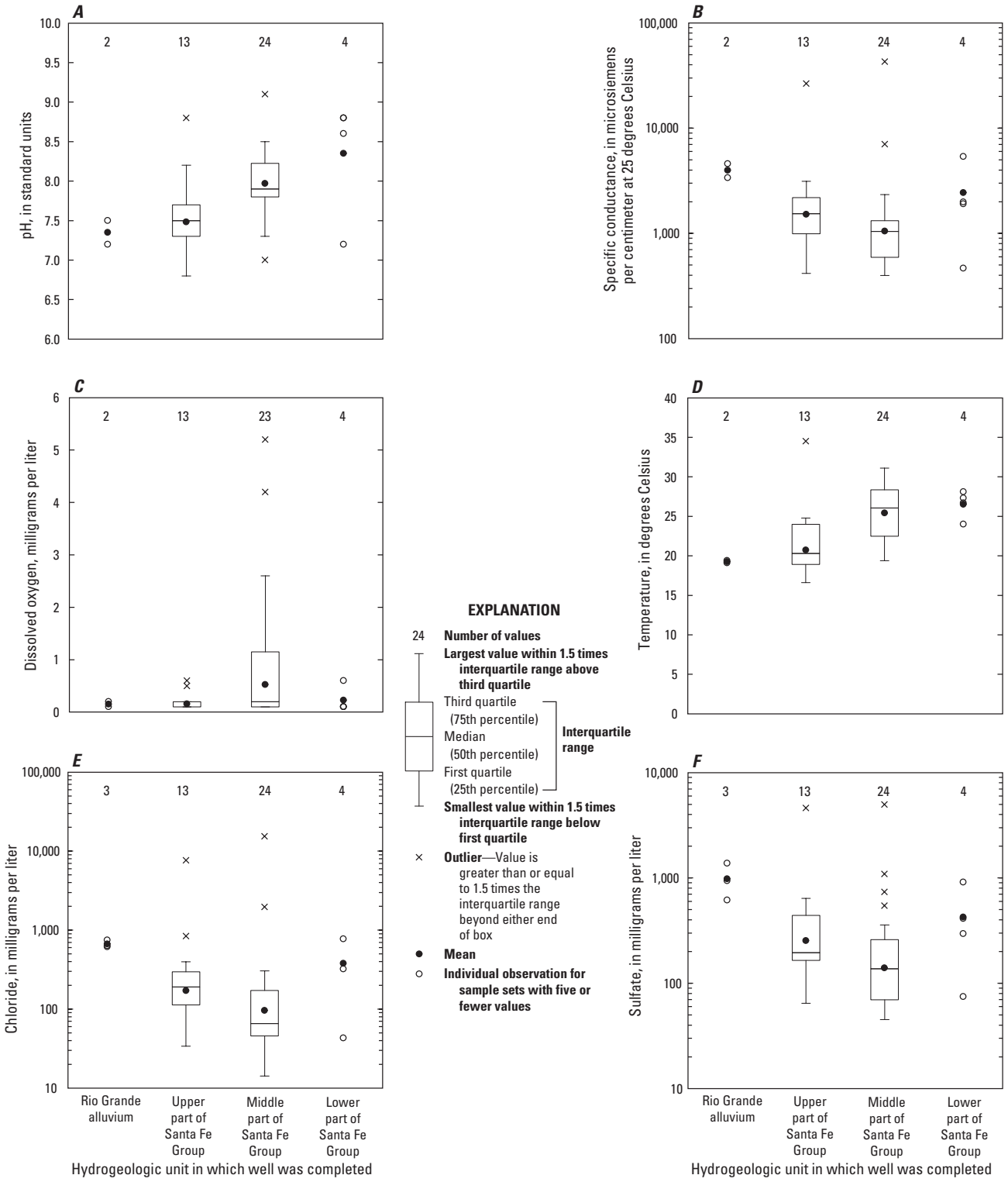

Note: See appendix 3 for discussion of boxplots of groundwater chemistry and isotopes.

Figure 22. Selected constituent concentrations measured in groundwater samples collected in the Mesilla Basin study area in Doña Ana County, New Mexico, and El Paso County, Texas, 2010, grouped by hydrogeologic unit. *A*, pH. *B*, Specific conductance. *C*, Dissolved oxygen. *D*, Temperature. *E*, Chloride. *F*, Sulfate. *G*, Bicarbonate. *H*, Fluoride. *I*, Bromide. *J*, Nitrate plus nitrite. *K*, Sodium. *L*, Calcium. *M*, Magnesium. *N*, Silica. *O*, Potassium. *P*, Ammonia. *Q*, Aluminum. *R*, Arsenic. *S*, Barium. *T*, Iron. *U*, Lithium. *V*, Manganese. *W*, Strontium. *X*, Uranium. *Y*, Delta deuterium. Z, Delta oxygen-18. *AA*, Ratio of strontium-87 and strontium-86. *BB*, Tritium. *CC*, Carbon-14. *DD*, Apparent age.

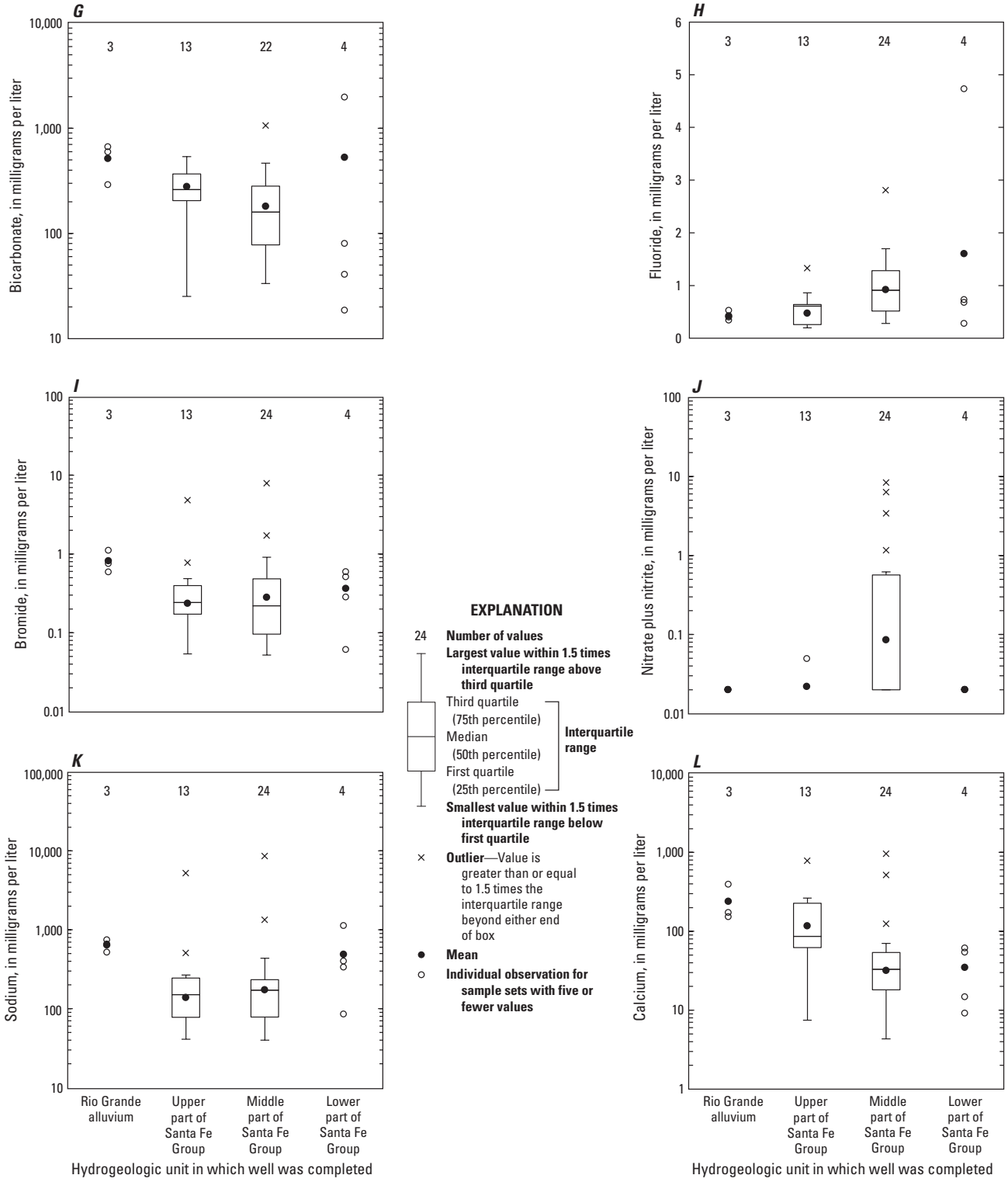

Note: See appendix 3 for discussion of boxplots of groundwater chemistry and isotopes.

Figure 22. Selected constituent concentrations measured in groundwater samples collected in the Mesilla Basin study area in Doña Ana County, New Mexico, and El Paso County, Texas, 2010, grouped by hydrogeologic unit. *A*, pH. *B*, Specific conductance. *C*, Dissolved oxygen. *D*, Temperature. *E*, Chloride. *F*, Sulfate. *G*, Bicarbonate. *H*, Fluoride. *I*, Bromide. *J*, Nitrate plus nitrite. *K*, Sodium. *L*, Calcium. *M*, Magnesium. *N*, Silica. *O*, Potassium. *P*, Ammonia. *Q*, Aluminum. *R*, Arsenic. *S*, Barium. *T*, Iron. *U*, Lithium. *V*, Manganese. *W*, Strontium. *X*, Uranium. *Y*, Delta deuterium. Z, Delta oxygen-18. *AA*, Ratio of strontium-87 and strontium-86. *BB*, Tritium. *CC*, Carbon-14. *DD*, Apparent age.—Continued

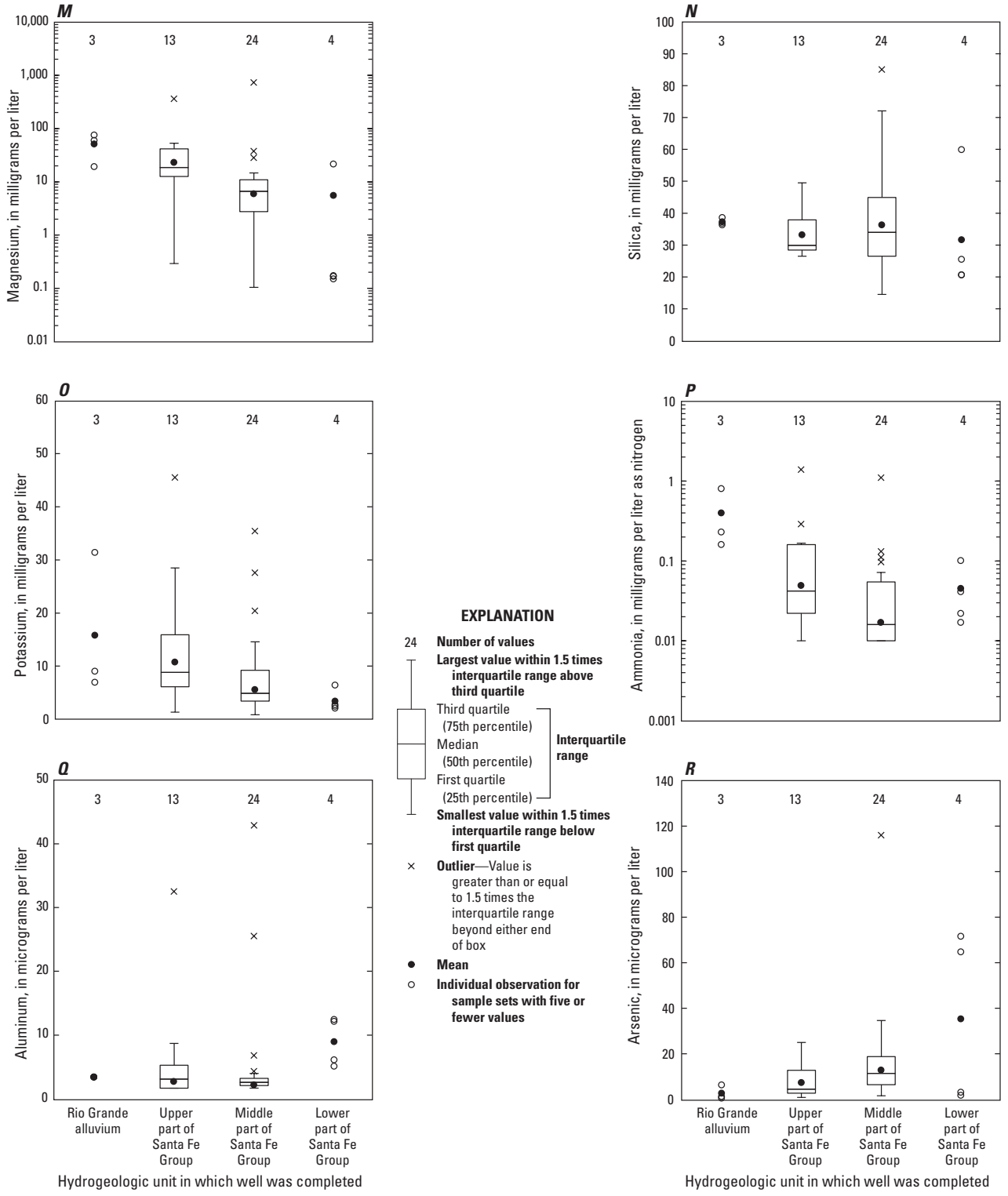

Note: See appendix 3 for discussion of boxplots of groundwater chemistry and isotopes.

Figure 22. Selected constituent concentrations measured in groundwater samples collected in the Mesilla Basin study area in Doña Ana County, New Mexico, and El Paso County, Texas, 2010, grouped by hydrogeologic unit. *A*, pH. *B*, Specific conductance. *C*, Dissolved oxygen. *D*, Temperature. *E*, Chloride. *F*, Sulfate. *G*, Bicarbonate. *H*, Fluoride. *I*, Bromide. *J*, Nitrate plus nitrite. *K*, Sodium. *L*, Calcium. *M*, Magnesium. *N*, Silica. *O*, Potassium. *P*, Ammonia. *Q*, Aluminum. *R*, Arsenic. *S*, Barium. *T*, Iron. *U*, Lithium. *V*, Manganese. *W*, Strontium. *X*, Uranium. *Y*, Delta deuterium. Z, Delta oxygen-18. *AA*, Ratio of strontium-87 and strontium-86. *BB*, Tritium. *CC*, Carbon-14. *DD*, Apparent age.—Continued

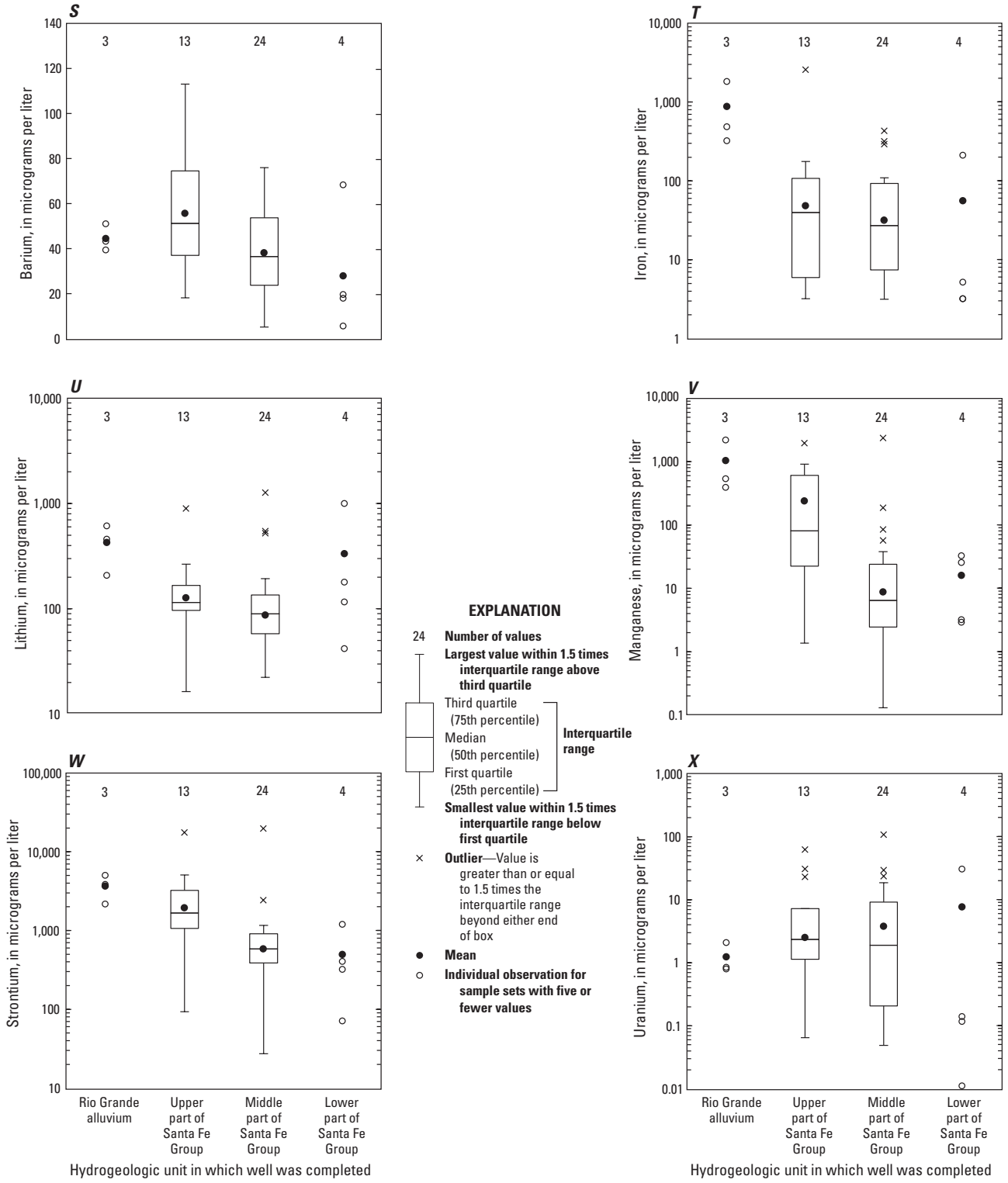

Note: See appendix 3 for discussion of boxplots of groundwater chemistry and isotopes.

Figure 22. Selected constituent concentrations measured in groundwater samples collected in the Mesilla Basin study area in Doña Ana County, New Mexico, and El Paso County, Texas, 2010, grouped by hydrogeologic unit. *A*, pH. *B*, Specific conductance. *C*, Dissolved oxygen. *D*, Temperature. *E*, Chloride. *F*, Sulfate. *G*, Bicarbonate. *H*, Fluoride. *I*, Bromide. *J*, Nitrate plus nitrite. *K*, Sodium. *L*, Calcium. *M*, Magnesium. *N*, Silica. *O*, Potassium. *P*, Ammonia. *Q*, Aluminum. *R*, Arsenic. *S*, Barium. *T*, Iron. *U*, Lithium. *V*, Manganese. *W*, Strontium. *X*, Uranium. *Y*, Delta deuterium. Z, Delta oxygen-18. *AA*, Ratio of strontium-87 and strontium-86. *BB*, Tritium. *CC*, Carbon-14. *DD*, Apparent age.—Continued

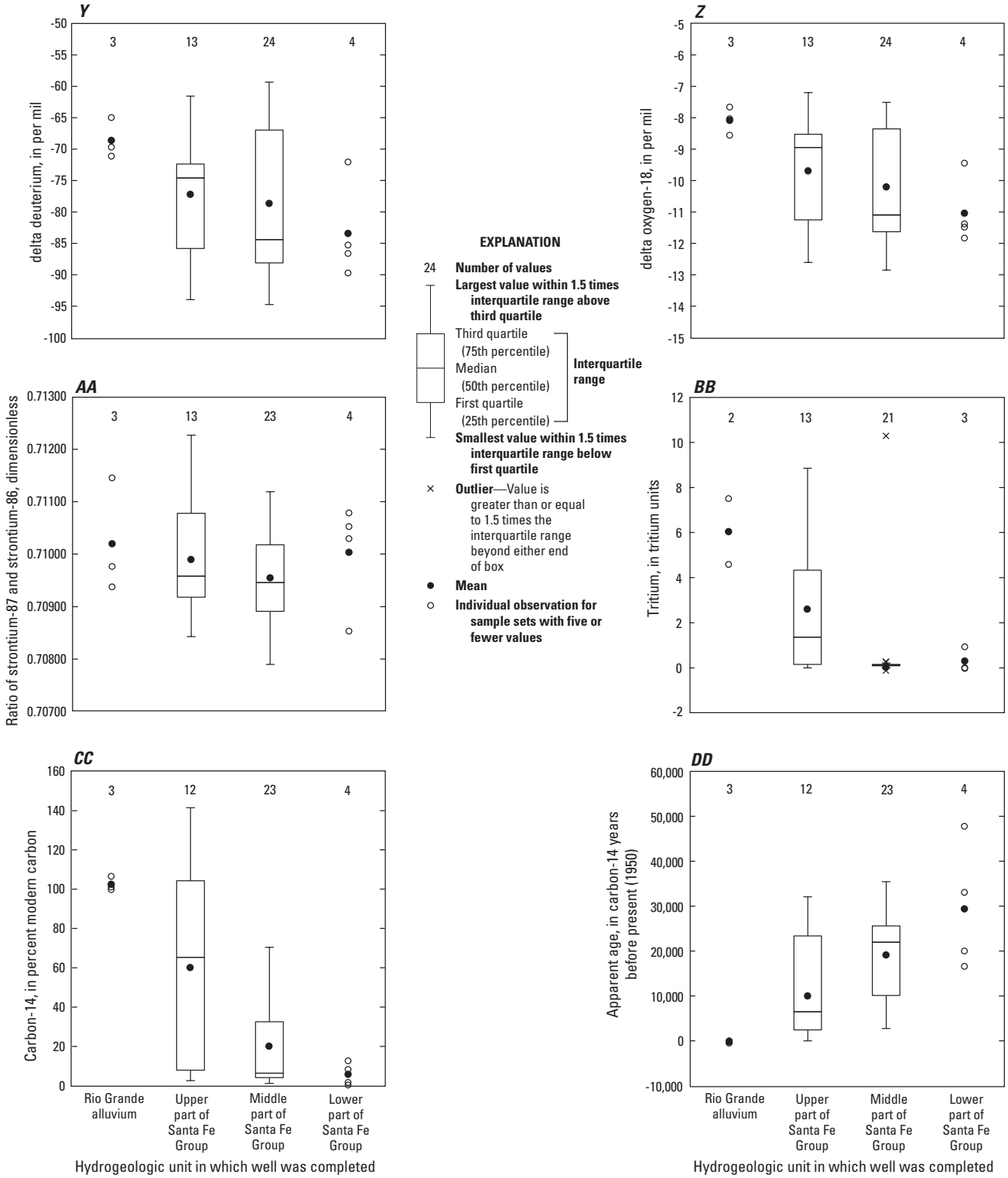

Note: See appendix 3 for discussion of boxplots of groundwater chemistry and isotopes.

Figure 22. Selected constituent concentrations measured in groundwater samples collected in the Mesilla Basin study area in Doña Ana County, New Mexico, and El Paso County, Texas, 2010, grouped by hydrogeologic unit. *A*, pH. *B*, Specific conductance. *C*, Dissolved oxygen. *D*, Temperature. *E*, Chloride. *F*, Sulfate. *G*, Bicarbonate. *H*, Fluoride. *I*, Bromide. *J*, Nitrate plus nitrite. *K*, Sodium. *L*, Calcium. *M*, Magnesium. *N*, Silica. *O*, Potassium. *P*, Ammonia. *Q*, Aluminum. *R*, Arsenic. *S*, Barium. *T*, Iron. *U*, Lithium. *V*, Manganese. *W*, Strontium. *X*, Uranium. *Y*, Delta deuterium. Z, Delta oxygen-18. *AA*, Ratio of strontium-87 and strontium-86. *BB*, Tritium. *CC*, Carbon-14. *DD*, Apparent age.—Continued

Appendix 1. Previously Published Data from United States Geological Survey Seepage Investigations

Appendix 1–1. Seepage measurement site locations in the Mesilla Basin study area in Doña Ana County, New Mexico, and El Paso County, Texas.

[Modified from Crilley and others, 2013; U.S. Geological Survey, 2017. USGS, U.S. Geological Survey; N. Mex., New Mexico; WWTP, wastewater treatment plant; Tex., Texas]

Site identifier (figs. 5 and 7)	USGS station number	USGS station name	Latitude (decimal degrees)	Longitude (decimal degrees)	River mile	Descrip-tion
S01	322841106551010	Rio Grande below Leasburg Dam, N. Mex.	32.4769	106.9197	1,312.3	Main stem
S02	322721106540810	Rio Grande near Leasburg, N. Mex.	32.4544	106.9017	1,310.2	Main stem
S03	322541106525110	Selden Drain at Levee Road near Leasburg, N. Mex.	32.4281	106.8814	1,307.6	Inflow
S04	322505106520110	Rio Grande near Hill, N. Mex.	32.4186	106.8672	1,306.3	Main stem
S05	322234106511710	Rio Grande at Shalem Bridge near Dona Ana, N. Mex.	32.3762	106.8553	1,302.7	Main stem
S06	322214106501410	Spillway Number 5 near Dona Ana, N. Mex.	32.3703	106.8381	1,301.2	Inflow
S07	322018106500910	Rio Grande near Picacho, N. Mex.	32.3383	106.8367	1,298.8	Main stem
S08	321745106492510	Rio Grande below Picacho Bridge near Las Cruces, N. Mex.	32.2964	106.8242	1,295.6	Main stem
S09	321735106492610	Las Cruces WWTP Outfall, Las Cruces, N. Mex.	32.2928	106.8247	1,295.4	Inflow
S10	321549106492910	Rio Grande at N. Mex.-359 Bridge near Mesilla, N. Mex.	32.2637	106.8253	1,293.1	Main stem
S10A	321448106490010	Rio Grande above Picacho Drain, N. Mex.	32.2468	106.8172	1,292.0	Inflow
S11	321434106485610	Picacho Drain above Mesilla Dam, N. Mex.	32.2422	106.8153	1,291.8	Inflow
S12	321430106484910	Rio Grande below Picacho Drain, N. Mex.	32.2419	106.8142	1,291.7	Main stem
S13	321317106471510	Rio Grande below Mesilla Dam near Santo Tomas, N. Mex.	32.2211	106.7886	1,289.5	Main stem
S14	321224106453210	Rio Grande at N. Mex.-28 Bridge near San Pablo, N. Mex.	32.2067	106.7597	1,287.3	Main stem
S15	321014106431410	Santo Tomas River Drain at Levee Road near San Miguel, N. Mex.	32.1707	106.7211	1,283.6	Inflow
S16	320943106425810	Rio Grande N. Mex.-192 Bridge near San Miguel, N. Mex.	32.162	106.7167	1,282.7	Main stem
S17	320648106400510	Rio Grande at N. Mex.-189 Bridge near Vado, N. Mex.	32.1136	106.6689	1,277.8	Main stem
S18	320610106393110	Del Rio Drain at Levee Road near Vado, N. Mex.	32.1029	106.6592	1,276.6	Inflow
S18A	320525106393410	Dona Ana Co South Central WWTP Outfall near Vado, N. Mex.	32.0903	106.66	1,275.7	Inflow
S19	320356106394510	Rio Grande at N. Mex.-226 Bridge near Berino, N. Mex.	32.0656	106.6633	1,273.8	Main stem
S20	320214106392510	La Mesa Drain at LeveeRoad near Chamberino, N. Mex.	32.0373	106.6575	1,271.6	Inflow
S21	320212106391810	Rio Grande below La Mesa Drain near Chamberino, N. Mex.	32.0369	106.6561	1,271.5	Main stem
S22	315958106380710	Rio Grande at N. Mex.-225 Bridge near Anthony, N. Mex.	31.9994	106.6361	1,268.5	Main stem
S23	315957106380610	Pipe Inflow at N. Mex.-225 Bridge near Anthony, N. Mex.	31.9992	106.6353	1,268.4	Inflow
S24	315807106361910	East Side Drain at Levee Road near Anthony, Tex.	31.9687	106.6058	1,265.4	Inflow
S25	315733106361610	Rio Grande at Vinton Bridge near Vinton, Tex.	31.9594	106.605	1,264.7	Main stem
S26	315454106360610	Rio Grande at Tex.-259 Bridge, Canutillo, Tex.	31.9153	106.6022	1,261.6	Main stem
S25C	315652106361710	Temporary Well-C Inflow below Vinton Bridge, near Vinton, Tex.	31.9479	106.6053	1,264.7	Inflow
S27	315309106355510	Rio Grande at Borderland Bridge near Borderland, Tex.	31.8861	106.5989	1,259.3	Main stem
S28	315046106361810	Rio Grande at Tex.-260 Bridge near Santa Teresa, N. Mex.	31.8464	106.6058	1,256.2	Main stem
S29	314824106345710	Rio Grande near Sunland Park, N. Mex.	31.8067	106.5828	1,252.8	Main stem
S30	314755106332510	Sunland Park WWTP Outfall, Sunland Park, N. Mex.	31.7986	106.5575	1,250.9	Inflow
S31	314756106331610	Rio Grande at Sunland Park Bridge, Sunland Park, N. Mex.	31.7989	106.555	1,250.3	Main stem
S32	314810106324610	Montoya Drain at Sunland Park, N. Mex.	31.8029	106.5467	1,250.3	Inflow
S32A	314812106324410	El Paso Electric Plant Wastewater Outfall, Sunland Park, Tex.	31.8036	106.5461	1,250.2	Inflow
S33	314818106323910	Keystone Reservoir Inlet, El Paso, Tex.	31.805	106.5444	1,250.1	Inflow
S33A	314813106322810	Side-Channel Inlet above Courchesne Bridge, El Paso, Tex.	31.8036	106.5417	1,250.0	Inflow
S34	08364000	Rio Grande at El Paso, Tex.	31.8029	106.5408	1,249.9	Main stem
S34A	314802106321710	Side-Channel Inlet below Courchesne Bridge, El Paso, Tex.	31.8007	106.5386	1,249.7	Inflow
S34B	314731106314510	Side-Channel Inflow above Executive Blvd, El Paso, Tex.	31.7921	106.5297	1,248.7	Inflow
S35	314718106313410	El Paso Water Utility Northwest WWTP Outfall, El Paso, Tex.	31.7884	106.5267	1,248.4	Inflow
S36	314713106313610	Rio Grande above American Dam, El Paso, Tex.	31.7871	106.5272	1,248.3	Main stem

Appendix 1–2. Yearly discharge measurements between 1988 and 2013 at seepage measurement sites in the Mesilla Basin study area in Doña Ana County, New Mexico, and El Paso County, Texas.

[Modified from Crilley and others, 2013; U.S. Geological Survey, 2017. --, not available]

Site identifier (figs. 5 and 7)	Discharge for respective year, in cubic feet per second									
	1988 (January 5–6)	1989 (January 10–11)	1990 (January 9–10)	1991 (January 8–9)	1992 (December 17–18 [1991])	1993 (January 26–27)	1995 (January 11–12)	1996 (January 23–24)	1997 (January 28–29)	1998 (January 27–28)
S01	95.1	33.1	37.8	38.4	43.2	189	52.2	313	331	326
S02	95.5	38.9	37.1	39.8	48.9	181	56.9	323	313	337
S03*	0.3	0.2	0.0	0.0	0.0	0.0	0.0	0.0	0.0	0.0
S04	98.9	48.8	49.7	48.5	55.3	184	64.2	353	312	354
S05	105	51.5	42.9	47.6	55.1	174	65	311	332	324
S06*	0.1	0.1	0.004	0.0	0.0	0.0	0.045	0.0	0.0	0.0
S07	102	54.5	44.9	57.4	58.5	178	65.1	342	329	344
S08	102	60.6	35.5	--	55.2	189	66.2	336	311	316
S09*	9.6	10	9.7	12.9	11.5	14.8	15.9	18	15.8	14.7
S10	113	55.1	48.7	54.7	59.4	193	74.1	288	331	318
S10A*	--	--	--	--	--	--	--	--	--	--
S11*	3.51	2.86	2.31	2.16	4.3	2.24	3.19	2.64	2.6	1.9
S12	115	33.4	45	45.5	52.8	183	70.6	341	328	323
S13	100	44.5	29	33.7	45.6	167	57.7	315	308	306
S14	103	43.3	29.9	31	46.1	166	62.2	297	290	306
S15*	--	0.0	0.0	0.0	--	0.0	0.0	0.0	0.0	0.0
S16	100	45	29.3	34.5	50.6	177	62.1	310	301	313
S17	91.2	50.4	26.2	30.4	46.2	155	66.3	297	285	283
S18*	36.4	33.2	27.4	26.2	31.2	29.4	30.2	25.6	22.4	25
S18A*	--	--	--	--	--	--	--	--	--	--
S19	131	70.1	54.9	53.4	78.7	185	85	337	294	316
S20*	12.6	12	9.77	9.47	16.6	11.1	11.8	8.84	8.72	9.24
S21	149	90.3	67.7	61.7	108	218	98.3	370	308	326
S22	163	80.6	65.5	73.9	103	201	98	338	314	336
S23*	--	--	0.05	0.1	0.22	0.02	0.09	0.1	0.23	0.021
S24*	11.2	8.59	5.56	6.77	8.56	7.66	7.74	7.35	4.79	9.37
S25	170	101	74.1	79.4	117	216	107	342	323	322
S26	171	105	66.8	71.6	107	200	105	330	311	338
S25C*	7.6	--	--	--	--	--	--	--	--	--
S27	160	91	65.1	71.7	94.2	213	96.2	286	314	343
S28	153	87.9	53.3	62.4	95.4	188	104	329	333	305
S29	139	82.3	55	61.6	91.2	197	92.5	323	285	333
S30*	0.14	0.9	0.9	0.75	0.61	0.77	1.1	2.17	1.18	0.94
S31	--	87.5	56.1	59.6	--	190	111	324	304	343
S32*	42.9	36.2	36.6	34.7	--	39.4	40.1	33.4	24.5	30.9
S32A*	--	--	--	--	--	--	--	--	--	--
S33*	0.2	0.035	0.0	0.08	4.25	0.3	1.2	0.0	1.81	1.0
S33A*	--	--	--	--	--	--	0.44	1.2	0.04	0.051
S34	194	122	94.6	88	--	230	130	354	335	339
S34A*	--	--	--	--	--	--	--	--	--	--
S34B*	--	--	--	--	--	--	--	--	--	--
S35*	--	--	--	--	--	--	--	--	--	--
S36	--	--	--	--	--	--	--	--	--	--

Appendix 1–2. Yearly discharge measurements between 1988 and 2013 at seepage measurement sites in the Mesilla Basin study area in Doña Ana County, New Mexico, and El Paso County, Texas.—Continued

[Modified from Crilley and others, 2013; U.S. Geological Survey, 2017. --, not available]

Site identifier (figs. 5 and 7)	Discharge for respective year, in cubic feet per second									
	2004 (February 24–25)	2005 (February 23/ March 4)	2006 (February 14–15)	2007 (February 13–14)	2008 (February 12–13)	2009 (February 10–11)	2010 (February 23)	2011 (February 15)	2012 (February 28)	2013 (February 26)
S01	2.12	14.9	6.67	28.7	17.7	31	--	--	1.31	0.7
S02	2.52	--	6.92	31	19.3	34.5	--	--	0.87	--
S03*	0.0	0.0	0.0	0.0	0.0	0.0	--	--	0.0	0.0
S04	3.93	16.4	11.1	31.8	21.3	38.2	--	--	0.0	0.0
S05	2.01	14	8.65	33.4	19.1	34.2	--	--	0.0	0.0
S06*	0.0	0.0	0.0	0.0	0.0	0.0	--	--	0.0	0.0
S07	0.0	13.7	5.57	18.2	15.8	34.9	--	--	0.0	0.0
S08	0.0	8.99	0.14	20.9	9.82	28.5	--	--	0.0	0.0
S09*	14.1	14.9	18.6	12.9	17	17.5	--	--	12.7	15.8
S10	7.85	17.6	10.7	33.5	19.4	39.4	--	--	4.37	2.77
S10A*	--	--	0.03	--	--	--	--	--	0.0	--
S11*	0.0	0.0	0.0	0.069	0.0	0.0	--	--	0.0	0.0
S12	0.0	4.85	--	30.3	13.6	34.9	--	--	0.0	0.0
S13	0.0	3.01	0.0	18.3	6.1	25.6	--	--	0.0	0.0
S14	0.0	1.21	0.0	18.1	6.89	24.6	--	--	0.0	0.0
S15*	0.0	0.0	0.0	0.0	0.0	0.0	--	--	0.0	0.0
S16	0.0	0.0	0.0	15	2.24	17.4	--	--	0.0	0.0
S17	0.0	0.069	0.09	13.9	0.2	18	--	--	0.0	0.0
S18*	0.16	2.84	5.32	4.86	4.69	4.16	--	--	0.0	0.0
S18A*	--	--	0.37	0.39	0.43	0.48	--	--	0.54	0.48
S19	0.46	3.6	5.77	16.3	5.75	17.9	--	--	0.0	0.0
S20*	0.0	0.0	4.05	0.001	2.43	4.5	--	--	0.0	0.0
S21	0.11	4.07	12.0	17.1	10.2	23.2	--	--	0.0	0.0
S22	0.025	3.65	12.3	18.8	10.4	25.9	12.5	5.14	0.0	0.0
S23*	0.19	0.045	0.004	0.01	0.09	0.025	0.021	0.01	0.09	0.025
S24*	2.01	0.91	2.28	3.31	2.85	3.27	2.11	0.89	0.0	0.0
S25	1.38	2.48	12.6	24.7	12	30.8	12.6	3.41	0.0	0.0
S26	0.0	0.0	8.66	21.4	9.77	26.6	11.3	0.0	0.0	0.0
S25C*	--	--	2.23	--	--	--	--	--	--	--
S27	0.0	0.0	6.14	19.3	7.31	23.5	9.8	0.0	0.0	0.0
S28	0.0	0.0	3.4	15.6	3.9	20.5	6.2	0.0	0.0	0.0
S29	0.0	0.0	2.41	12	0.89	14.1	3.6	0.0	0.0	0.0
S30*	2.79	2.4	2.54	3.01	2.77	2.42	2.11	2.21	2.14	2.77
S31	1.96	2.23	4.59	14.5	2.6	18.2	3.77	3.26	2.06	2.42
S32*	6.68	9.59	16.3	20.8	15.8	20	19.5	15.6	5.89	5.61
S32A*	0.9	0.61	0.57	0.6	0.13	0.0	0.0	0.0	0.0	0.0
S33*	0.0	0.057	0.076	0.56	0.29	0.58	0.73	0.53	0.41	0.36
S33A*	0.01	0.04	0.025	0.13	0.057	0.025	0.057	0.045	0.03	0.0
S34	9.75	13.6	22.1	38.4	23.5	34.5	27.7	17.6	8.12	8.64
S34A*	--	--	--	--	--	--	0.18	0.14	0.1	0.17
S34B*	--	--	--	--	--	--	1.4	--	--	--
S35*	--	--	--	--	--	--	8.31	24.8	15.3	11.2
S36	--	--	--	--	--	--	36.4	41.2	22.9	18.5

*Seepage measurement sites measuring inflows to the Rio Grande.

Appendix 1–3. Yearly gain or loss estimates at seepage measurement sites in the Mesilla Basin study area in Doña Ana County, New Mexico, and El Paso County, Texas.

[Modified from Crilley and others, 2013; U.S. Geological Survey, 2017. --, not available]

Site identifier (figs. 5 and 7)*	Gain or loss relative to the adjacent upstream station during the respective year, in cubic feet per second										
	1988 (January 5–6)	1989 (January 10–11)	1990 (January 9–10)	1991 (January 8–9)	1992 (Dec. 17–18 [1991])	1993 (January 26–27)	1995 (January 11–12)	1996 (January 23–24)	1997 (January 28–29)	1998 (January 27–28)	2004 (February 24–25)
S01	--	--	--	--	--	--	--	--	--	--	--
S02	0.4	5.8	-0.7	1.4	5.7	-8.0	4.7	10.0	-18.0	11.0	0.4
S04	3.1	9.7	12.6	8.7	6.4	3.0	7.3	30.0	-1.0	17.0	1.4
S05	6.1	2.7	-6.8	-0.9	-0.2	-10.0	0.8	-42.0	20.0	-30.0	-1.9
S07	-3.1	2.9	2.0	9.8	3.4	4.0	0.1	31.0	-3.0	20.0	-2.0
S08	0.0	6.1	-9.4	--	-3.3	11.0	1.1	-6.0	-18.0	-28.0	0.0
S10	1.4	-15.5	3.5	-15.6	-7.3	-10.8	-8.0	-66.0	4.2	-12.7	-6.3
S12	-1.5	-24.6	-6.0	-11.4	-10.9	-12.2	-6.7	50.4	-5.6	3.1	-7.9
S13	-15.0	11.1	-16.0	-11.8	-7.2	-16.0	-12.9	-26.0	-20.0	-17.0	0.0
S14	3.0	-1.2	0.9	-2.7	0.5	-1.0	4.5	-18.0	-18.0	0.0	0.0
S16	-3.0	1.7	-0.6	3.5	4.5	11.0	-0.1	13.0	11.0	7.0	0.0
S17	-8.8	5.4	-3.1	-4.1	-4.4	-22.0	4.2	-13.0	-16.0	-30.0	0.0
S19	3.4	-13.5	1.3	-3.2	1.3	0.6	-11.5	14.4	-13.4	8.0	0.3
S21	5.4	8.2	3.0	-1.2	12.7	21.9	1.5	24.2	5.3	0.8	-0.4
S22	14.0	-9.7	-2.2	12.2	-5.0	-17.0	-0.3	-32.0	6.0	10.0	-0.1
S25	-4.2	11.8	3.0	-1.4	5.2	7.3	1.2	-3.5	4.0	-23.4	-0.8
S26	1.0	4.0	-7.3	-7.8	-10.0	-16.0	-2.0	-12.0	-12.0	16.0	-1.4
S27	-18.6	-14.0	-1.7	0.1	-12.8	13.0	-8.8	-44.0	3.0	5.0	0.0
S28	-7.0	-3.1	-11.8	-9.3	1.2	-25.0	7.8	43.0	19.0	-38.0	0.0
S29	-14.0	-5.6	1.7	-0.8	-4.2	9.0	-11.5	-6.0	-48.0	28.0	0.0
S31	--	4.3	0.2	-2.8	--	-7.8	17.4	-1.2	17.8	9.1	-0.8
S34	11.8	-1.7	1.9	-6.4	--	0.3	-22.7	-4.6	4.6	-36.0	0.2
S36	--	--	--	--	--	--	--	--	--	--	--

Appendix 1–3. Yearly gain or loss estimates at seepage measurement sites in the Mesilla Basin study area in Doña Ana County, New Mexico, and El Paso County, Texas.—Continued

[Modified from Crilley and others, 2013; U.S. Geological Survey, 2017. --, not available]

Site identifier (figs. 5 and 7)*	Gain or loss relative to the adjacent upstream station during the respective year, in cubic feet per second									
	2005 (February 23/ March 4)	2006 (February 14–15)	2007 (February 13–14)	2008 (February 12–13)	2009 (February 10–11)	2010 (February 23)	2011 (February 15)	2012 (February 28)	2013 (February 26)	Median gain or loss for station
S01	--	--	--	--	--	--	--	--	--	--
S02	--	0.3	2.3	1.6	3.5	--	--	-0.4	--	1.5
S04	1.5	4.2	0.8	2.0	3.7	--	--	-0.9	-0.7	3.4
S05	-2.4	-2.5	1.6	-2.2	-4.0	--	--	0.0	0.0	-1.4
S07	-0.3	-3.1	-15.2	-3.3	0.7	--	--	0.0	0.0	0.0
S08	-4.7	-5.4	2.7	-6.0	-6.4	--	--	0.0	0.0	-3.3
S10	-6.3	-8.0	-0.3	-7.4	-6.6	--	--	-8.3	-13.0	-7.7
S12	-12.8	--	-3.3	-5.8	-4.5	--	--	-4.4	-2.8	-5.8
S13	-1.8	-10.7	-12.0	-7.5	-9.3	--	--	0.0	0.0	-11.3
S14	-1.8	0.0	-0.2	0.8	-1.0	--	--	0.0	0.0	0.0
S16	-1.2	0.0	-3.1	-4.7	-7.2	--	--	0.0	0.0	0.0
S17	0.1	0.1	-1.1	-2.0	0.6	--	--	0.0	0.0	-1.6
S19	0.7	0.0	-2.9	0.4	-4.7	--	--	-0.5	-0.5	0.1
S21	0.5	2.2	0.8	2.0	0.8	--	--	0.0	0.0	1.8
S22	-0.4	0.3	1.7	0.2	2.7	--	--	0.0	0.0	0.0
S25	-2.1	-2.0	2.6	-1.3	1.6	-2.0	-2.6	-0.1	0.0	-0.5
S26	-2.5	-3.9	-3.3	-2.2	-4.2	-1.3	-3.4	0.0	0.0	-2.9
S27	0.0	-4.8	-2.1	-2.5	-3.1	-1.5	0.0	0.0	0.0	-1.6
S28	0.0	-2.7	-3.7	-3.4	-3.0	-3.6	0.0	0.0	0.0	-2.9
S29	0.0	-1.0	-3.6	-3.0	-6.4	-2.6	0.0	0.0	0.0	-1.8
S31	-0.2	-0.4	-0.5	-1.1	1.7	-1.9	1.1	-0.1	-0.4	-0.3
S34	1.1	0.5	1.8	4.6	-4.3	3.6	-1.8	-0.3	0.3	0.3
S36	--	--	--	--	--	-1.2	-1.3	-0.6	-1.5	-1.3

*Seepage measurement sites measuring inflows to the Rio Grande were incorporated into the downstream gain or loss values.

References Cited

Crilley, D.M., Matherne, A.M., Thomas, Nicole, and Falk, S.E., 2013, Seepage investigations of the Rio Grande from below Leasburg Dam, Leasburg, New Mexico, to above American Dam, El Paso, Texas, 2006–13: U.S. Geological Survey Open-File Report 2013–1233, 34 p., accessed October 21, 2015, at http://pubs.usgs.gov/of/2013/1233/.

U.S. Geological Survey, 2017, U.S. Geological Survey National Water Information System: Accessed March 20, 2017, at http://dx.doi.org/10.5066/F7P55KJN.

Appendix 2. Methods for Constructing the Probability Plots of Groundwater Chemistry and Isotopes

Probability plots for selected geochemical constituents are presented in figure 21. Probability plots show the distribution of sample results found within the study area. The probability was calculated for these plots by ordering the sample constituent concentration from lowest to highest, numbering the samples incrementally from 1 at the lowest sample, and using the following equation:

$$P(z_i) = \begin{cases} 1 - 0.5^{1/n} \text{ for } i = 1 \\ \dfrac{i - 0.3175}{n + 0.365} \text{ for } 1 < i < n \\ 0.5^{1/n} \text{ for } i = n \end{cases}$$

where

$P(z_i)$	is the normal probability of sample i,
i	is the sample increment,
$<$	is less than, and
n	is the total number of samples.

Variations within the dataset can be observed by the slope of the data points within the plot. Outliers can be visually identified as data values less than the 10th percentile or greater than the 90th percentile values whose plotting positions vary substantially from the data values that plot between the 10th and 90th percentiles.

Appendix 3. Methods for Constructing the Boxplots of Groundwater Chemistry and Isotopes

Boxplots for selected geochemical constituents are presented in figure 22. Boxplots summarize the basic statistical values of a dataset. These statistical values include the minimum and maximum values; the first, second (median), and third quartiles; the mean; and outliers. The upper and lower limits for the dataset were calculated as one and a half times the interquartile range (the difference between the third quartile and the first quartile) and then subtracted from the first quartile for the lower limit and added to the third quartile for the upper limit. Any value outside these limits was considered an outlier, and the boxplot statistics were recalculated. Because the sample size for the Rio Grande alluvium and the lower Santa Fe were small (less than 5 samples), boxplots were not made and outliers were not determined for those HGUs. The explanation for the boxplots is as follows:

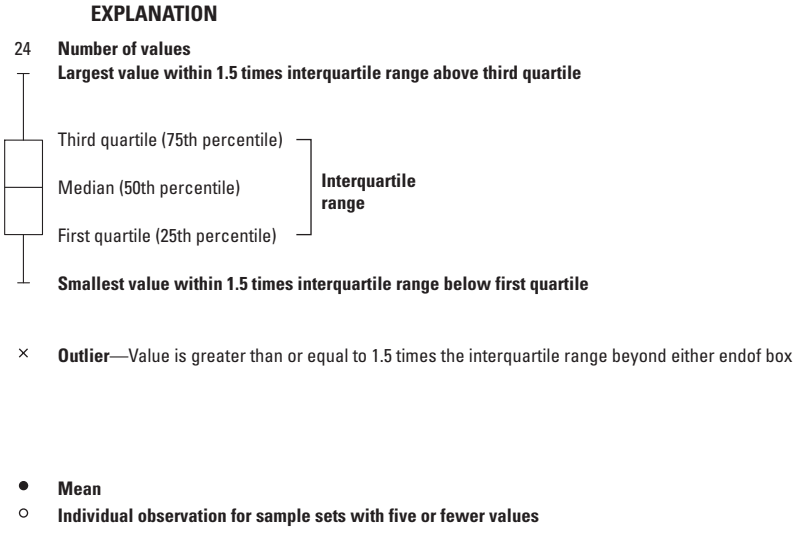

Publishing support provided by
Lafayette Publishing Service Center

Teeple—**Geophysics- and Geochemistry-Based Assessment of the Mesilla Basin, 2010–12**—SIR 2017–5028

ISSN 2328-0328 (online)
https://doi.org/10.3133/sir20175028